Fishing for molecular biomarkers -

Ecotoxicogenomic assessment of mode of action characteristic expression profiles in different aquatic non-target organisms

Dissertation
zur Erlangung des Doktorgrades
der Naturwissenschaften

vorgelegt beim Fachbereich Biowissenschaften
der Johann Wolfgang Goethe - Universität
in Frankfurt am Main

von
Hannes Reinwald
aus Neustadt a.d. Aisch

Frankfurt 2022
(D 30)

Vom Fachbereich 15 Biowissenschaften der Johann Wolfgang Goethe – Universität als Dissertation angenommen.

Dekan:	**Prof. Dr. Sven Klimpel** Goethe-Universität Frankfurt am Main Institut für Ökologie, Evolution und Diversität Integrative Parasitologie und Tierphysiologie Max-von-Laue-Str. 13, D-60438 Frankfurt am Main
1. Gutachter:	**Prof. Dr. Henner Hollert** Goethe-Universität Frankfurt am Main Institut für Ökologie, Evolution und Diversität Evolutionsökologie und Umwelttoxikologie Max-von-Laue-Str. 13, D-60438 Frankfurt am Main
2. Gutachter:	**Prof. Dr. Jörg Oehlmann** Goethe-Universität Frankfurt am Main Institut für Ökologie, Evolution und Diversität Aquatische Ökotoxikologie Max-von-Laue-Str. 13, D-60438 Frankfurt am Main

Datum der Disputation: _____

“The human race is challenged more than ever before

to demonstrate our mastery, not over nature but of ourselves.”

Rachel Carson (*1907 - †1964)

Mai 2022

TABLE OF CONTENTS

DANKSAGUNG III

ABSTRACT III

DEUTSCHE ZUSAMMENFASSUNG I

LIST OF PUBLICATIONS I

ABBREVIATIONS II

1. INTRODUCTION 1

1.1. WHY WE NEED TO EVOVLE CHEMICAL HAZARD ASESSEMENT 2

1.2. ECOTOXICOGENOMICS – A NEW HOPE FOR PREDICTIVE TOXICOLOGY 5

1.3. STUDY AIMS AND THESIS STRUCTURE 8

*1.3.1. Evaluating molecular fingerprints of endocrine and neuronal targeting chemicals in the zebrafish embryo model (**A1** - **A2**) 10*

*1.3.2. Sublethal immune toxicity short-term assay in zebrafish embryos using toxicogenomics (**A3**) 10*

*1.3.3. Transcriptomic profiling of neuronal targeting insecticides in Daphnia magna (**A4**) 11*

*1.3.4. Ecotoxicogenomic short term assay in the aquatic macrophyte model L. minor (**A5**) 12*

2. DISCUSSION 13

2.1. KEY FINDINGS OF THE PRESENT WORK 13

2.2. ECOTOXICOGENOMIC PROFILING 15

2.2.1. Molecular signature characteristics in the 96 hpf zebrafish embryo model 16

2.2.1a Thyroid system and signalling disruption 19

2.2.1b Nerve- and muscle-targeting insecticides 26

2.2.1c Cross-experiments functional profiles comparison 33

2.2.2. Transcriptomic immunosuppression signatures in early zebrafish embryos 38

2.2.3. Integrating omics in acute toxicity assessements for Daphnia magna and Lemna minor 43

2.2.3a Differentiating signatures of impaired GABA and ACh signalling in D. magna 46

2.2.3b The "lack of functional annotation"-problem and how to solve it 48

2.2.3c Differentiating molecular growth inhibitor effects in a shortened L. minor assay 51

2.3. CURRENT CHALLENGES AND FUTURE STEPS 54

2.4. CONCLUSION 59

3. SUPPLEMENTARY DISCUSSION FIGURES 62

4. REFERENCES 67

ANNEX 79

A1 TOXICOGENOMIC FIN(GER)PRINTS FOR THYROID DISRUPTION AOP REFINEMENT AND BIOMARKER IDENTIFICATION IN ZEBRAFISH EMBRYOS 80

A2 TOXICOGENOMIC PROFILING AFTER SUBLETHAL EXPOSURE TO NERVE- AND MUSCLE-TARGETING INSECTICIDES REVEALS CARDIAC AND NEURONAL DEVELOPMENTAL EFFECTS IN ZEBRAFISH EMBRYOS 94

A3 TRANSCRIPTOMIC PROFILING OF CLOBETASOL PROPIONATE-INDUCED IMMUNOSUPPRESSION IN CHALLENGED ZEBRAFISH EMBRYOS 112

A4 TOXICOGENOMIC DIFFERENTIATION OF FUNCTIONAL RESPONSES TO FIPRONIL AND IMIDACLOPRID IN *DAPHNIA MAGNA* 126

A5 A SHORT TERM TEST FOR TOXICOGENOMIC ANALYSIS OF ECOTOXIC MODES OF ACTION IN *LEMNA MINOR* 140

A6 CURICULUM VITAE 180

DANKSAGUNG

Hinter all den Stunden und Mühen die in diese Arbeit geflossen sind stehen auch immer eine Vielzahl an Personen, die direkt oder auch indirekt am Erfolg dieser Dissertation mitgewirkt haben. Diesen Menschen möchte im Folgenden meinen Dank aussprechen.

Allen voran Dr. Sebastian Eilebrecht als Betreuer vor Ort, für seine unvergleichlich herzliche Betreuung und die unerschöpfliche, stets motivierende Unterstützung während meiner gesamten Arbeitszeit am Fraunhofer IME. Auch möchte ich mich für das Vertrauen in mich bedanken und für die Aufnahme in die Attract Eco'n'OMICs Arbeitsgruppe. Gleichermaßen möchte ich mich bei Prof. Dr. Christoph Schäfers bedanken, für die Unterstützung des Fraunhofer IME durch eine herausragende technische Ausstattung und einzigartige Laborräume mit fantastischer Aussicht auf die Sauerländer Kulturwälder. Wenn auch nicht physisch Anwesend, gilt mein ganz besonderer Dank auch meinem Doktorvater Prof. Dr. Henner Hollert, dessen Motivations- und Begeisterungsfähigkeit für die Ökotoxikologie schier unendlich scheint. Dank seiner positiven und konstruktiven Unterstützung war es praktisch Unmöglich die Motivation für diese Dissertation zu verlieren. Realisierbar war dieses Forschungsprojekt dank der finanziellen Unterstützung des Fraunhofer Attract Förderprogramms.

So wichtig all die Professoren und Doktoren an solch einer Arbeit sind, genauso wichtig sind die Menschen die einem im Alltag den Rücken stärken oder dabei helfen die Laborarbeit zu meistern. Ganz besonders möchte ich hierbei Julia Alvincz für ihre phänomenale Labororganisation, exquisite musikalische Untermalung bei so mancher Pipettierarbeit im Labor und absolut fantastischen Bananenbrot-Back-Skills danken. Ihre herzliche Art und unser gemeinsames Engagement für eine tierleidfreie Ernährung haben meine Zeit in Schmallenberg nachhaltig positiv geprägt. Auch möchte ich mich bei Dr. Steve Ayobahan für seinen unermüdlichen Einsatz für eine funktionierende LC-MS bedanken. Ohne ihn wäre die Messung unserer *„little guys"* (Proteine) nicht möglich gewesen. Mein Dank gilt auch Stephanie Denzer, stellvertretend für alle Verantwortlichen der IME Fischhalterung. Außerdem danke ich ganz herzlich Fabian Essfeld, Alexandra Loll (*aka.* Lexi) und Julia Pfaff für ihre experimentelle Arbeit und der konstruktiven Forschungs-Zusammenarbeit.

Ich möchte mich auch bei den vielen Kolleginnen und Kollegen bedanken, welche über die Arbeit hinaus meine Zeit im Sauerland als unvergesslich gestaltet haben. Ich bedanke mich für die wundervollen Spaziergänge durch die nahgelegenen Wälder, schweißtreibende Klettersessions, sehr spaßige Koch-, Film-, und Spieleabende sowie den sonnigen Stunden (wenn die Sonne denn mal da war) im Mini-Skatepark, am Badesee oder mit Kaffee am Löschteich. Ein besonderer Dank geht auch an Anselm und Roland, meine treuen Calisthenics- und Turnbegleiter. Diese wundervollen Stunden mit euch halfen mir sehr dabei, meine Batterie immer wieder aufzufüllen.

Zum Abschluss möchte ich auch noch einmal ganz besonders meiner Familie und Lebenspartnerin für ihre unermüdliche Unterstützung danken. Besonders während der tristen und nassen Herbsttage im Sauerland war eine gelegentliche Aufmunterung durchaus notwendig. Auch wenn diese häufig nur aus der Ferne geschickt werden konnte, war sie dennoch wichtig für mich und hat mir geholfen trotz der grauen Tage weiterzumachen. Ohne eure Unterstützung wäre ich niemals so weit gekommen. Danke!

ABSTRACT

Regulatory required, classical toxicity studies for environmental hazard assessment are costly, time consuming, and often lack mechanistic insights about the toxic mode of action induced through a compound. In addition, classical toxicological non-human animal tests raise serious ethical concerns and are not well suited for high throughput screening approaches. Molecular biomarker-based screenings could be a suitable alternative for identifying particular hazardous effects (e.g. endocrine disruption, developmental neurotoxicity) in non-target organisms at the molecular level. This, however, requires a better mechanistic understanding of different toxic modes of action (MoA) to describe characteristic molecular key events and respective markers. Ecotoxicgenomics, which uses modern day *omic* technologies and systems biology approaches to study toxicological responses at the molecular level, are a promising new way for elucidating the processes through which chemicals cause adverse effects in environmental organisms. In this context, this PhD study was designated to investigate and describe MoA-characteristic ecotoxicogenomic signatures in three ecotoxicologically important aquatic model organisms of different trophic levels (*Danio rerio, Daphnia magna* and *Lemna minor*).

Applying non-target transcriptomic and proteomic methodologies post chemical exposure, the aim was to identify robust functional profiles and reliable biomarker candidates with potential predictive properties to allow for a differentiation among different MoA in these organisms. For the sublethal exposure studies in the zebrafish embryo model (96 hpf), the acute fish embryo toxicity test guideline (OECD 236) was used as conceptual framework. As different test compounds with known MoA, the thyroid hormone 3,3′,5-triiodothyronine (T3) and the thyrostatic 6-propyl-2-thiouracil (6-PTU), as well as six nerve- and muscle-targeting insecticides (abamectin, carbaryl, chlorpyrifos, fipronil, imidacloprid and methoxychlor) were evaluated. Furthermore, a novel sublethal immune challenge assay in early zebrafish embryos (48 hpf) was evaluated for its potential to assess immuno-suppressive effects at the gene expression level. Therefore, toxicogenomic profiles after an immune response inducing stimulus with and without prior clobetasol propionate (CP) treatment were compared. For the aquatic invertebrate *D. magna,* the study was performed with previously determined low effect concentrations (EC5 & EC20) of fipronil and imidacloprid according to the acute immobilization test in water flea (OECD 202). The aim was to compare toxicogenomic signatures of the GABA-gated chloride channel blocker (fipronil) and the nAChR agonist (imidacloprid). With similar low effect concentrations, a shortened 3 day version of the growth inhibition test with *L. minor* (OECD 221) was conducted to find molecular profiles

differentiating between photosynthesis and HMG-CoA reductase inhibitory effects. Here, the biological interpretation of the molecular stress response profiles in *L. minor* due to the lack of functional annotation of the reference genome was particularly challenging. Therefore, an annotation workflow was developed based on protein sequence homology predicted from the genomic reference sequences.

With this PhD work, it was shown how transcriptomic, proteomic and computational systems biology approaches can be coupled with aquatic toxicological tests, to gain important mechanistic insights into adverse effects at the molecular level. In general, for the different investigated adverse effects for the different organisms, biomarker candidates were identified, which describe a potential functional link between impaired gene expressions and previously reported apical effects. For the assessed chemicals in the zebrafish embryo model, biomarker candidates for thyroid disruption as well as developmental toxicity targeting the heart and central nervous system were described. The biomarkers derived from nerve- and muscle-targeting insecticides were associated with three major affected processes: (1) cardiac muscle cell development and functioning, (2) oxygen transport and hypoxic stress and (3) neuronal development and plasticity. To our knowledge, this is the first study linking neurotoxic insecticide exposure and affected expression of important regulatory genes for heart muscle (*tcap, actc2*) and forebrain (*npas4a*) development in a vertebrate model. The proposed immunosuppression assay found CP to affect innate immune induction by attenuating the response of genes involved in antigen processing, TLR signalling, NF-KB signalling, and complement activation. Overall, the herein presented findings not only provide mechanistic insights for the evaluated MoA in the respective model organisms, but also give further supportive evidence for the suitability of ecotoxicogenomic methods to identify early molecular MoA-pecific responses in different important model organisms for aquatic ecotoxicology. Comparing the transcriptomic profiles at the functional level revealed compound-specific fingerprints, suggesting a relationship between early affected molecular functions and a compound's MoA. These functional relationships can be further explored to identify targeted key pathways, which will improve the capability of differentiating hazardous MoA at the molecular level. Prospectively, this promotes the development of sensitive and informative biomarker-based *in vitro* assays for toxicological MoA prediction and AOP refinement. In the long run, the herein identified molecular fingerprints aim towards facilitating the development of biomarker-based high throughput screenings. Such next generation toxicology approaches could be used to efficiently predict a compound's hazardous MoA based on its ecotoxicogenomic signature.

DEUTSCHE ZUSAMMENFASSUNG

Die Belastung der Umwelt mit toxischen Chemikalien stellt ein erhebliches Risiko für die Gesundheit der dort lebenden Organismen dar und kann weitreichende negative Auswirkungen auf Populationen und ganze Ökosysteme haben. Als moderne Gesellschaft sind wir dennoch tagtäglich abhängig von einer Vielzahl an chemischen Stoffen. Um Umweltorganismen und damit Ökosysteme vor potenziell schädlichen Wirkungen zu schützen, müssen für die Registrierung und Zulassung einer Chemikalie ökotoxikologische Daten zur Umweltrisikobewertung von den Herstellern den Behörden zur Verfügung gestellt werden. Die von der EU-Gesetzgebung vorgeschriebenen Untersuchungen, z.B. im Rahmen von REACh, der Pflanzenschutzmittel-Verordnung, oder der Biozid-Verordnung, zur Bewertung der Umweltwirkung solcher Stoffe auf aquatische Ökosysteme umfassen neben Studien zur Bioakkumulation und Abbaubarkeit auch eine Reihe von Toxizitätstests mit aquatischen Modellorganismen verschiedener Trophiestufen (Algen, Krebstiere, Fische). Standardisierte Toxizitätstests erfassen quantitativ populationsrelevante Endpunkte nach definierten OECD Richtlinien. Diese klassischen ökotoxikologischen Untersuchungen sind jedoch kosten- und zeitintensiv, und nicht darauf ausgelegt, die primäre toxische Wirkungsweise (mode of action; MoA) eines Stoffes zu charakterisieren. In Bezug auf die Umweltrisikobewertung und Regulierung einer Chemikalie ist jedoch deren ökotoxikologische Wirkungsweise von entscheidender Bedeutung. So kann die Marktzulassung eines Wirkstoffes von z.B. Pflanzenschutzmitteln und Bioziden in der EU abgelehnt werden, wenn die primäre Wirkungsweise der Verbindung mutagene, fortpflanzungs-gefährdende oder endokrine Wirkungen auf Organismen zeigen. Darüber hinaus werfen klassische toxikologische Tierversuche ethische Bedenken auf und eignen sich schlecht für automatisierte Screening-Ansätze mit hohem Durchsatz. Die stetig steigende Zahl an neuen chemischen Substanzen und deren Bewertung stellt daher eine zunehmende Herausforderung für die Forschung als auch einen immer größer werdenden Kostenfaktor für die Industrie dar. Die Entwicklung neuer Verfahren ist daher erforderlich.

Eine mögliche neuartige Alternative zu klassischen Toxizitätstest stellen dabei auf molekularen Biomarkerprofilen basierende Screenings dar. Unter der Annahme, dass sich verschiedene toxische Wirkungsweisen (MoA) auf z.B. der Genexpressions-Ebene auflösen lassen, ließen sich mittels solcher Verfahren gefährliche Nebenwirkungen von Substanzen bereits auf molekularer Ebene vorhersagen und bewerten. Durch die regulatorischen Vorgaben und eine daraus resultierende mögliche Restriktion einer Substanz, ist es bereits während der

Chemikalien-Entwicklung von großem Interesse toxische Wirkungsweisen auf Organismen in der Umwelt frühzeitig zu identifizieren und zu verstehen. So ließen sich bereits frühzeitig eine funktionsbasierte Priorisierung von sichereren Vorläufersubstanzen etablieren. Allerdings erfordert die Entwicklung eines solchen Verfahrens ein besseres mechanistisches Verständnis verschiedener toxischer Wirkmechanismen, um charakteristische molekulare Schlüsselereignisse und zuverlässige Biomarker zu identifizieren.

Einen vielversprechenden Ansatz zur Überwindung dieser Herausforderungen stellen molekulare systembiologische Verfahren dar (*Omics*). Mit diesen Verfahren lässt sich die Expression zehntausender Gene (Transkriptom) und tausende ihrer Proteinprodukte (Proteom) aus einer einzigen Probe erfassen und quantifizieren. Der Forschungsbereich der Ökotoxikogenomik (*Ecotoxicogenomics*) nutzt diese modernsten Anwendungen, um die toxikologische Reaktion eines Organismus auf mögliche Umweltgifte systembiologisch auf molekularer Ebene zu erfassen. Der nicht-zielgerichtet Charakter von *Omics*-Methoden erlaubt darüber hinaus auch die Identifizierung neuer Biomarker-Kandidaten. Die Ökotoxikogenomik stellt daher einen neuen, vielversprechenden Weg zur Aufklärung molekularbiologischer Prozesse dar, durch die Chemikalien schädlich auf Umweltorganismen wirken. Dieses mechanistische Verständnis ist entscheidend für die Entwicklung von biomarkerbasierten Screenings zur Erfassung und Bewertung der Umweltwirkung von Stoffen. Ziel des Eco'n'OMICs Projekts am Fraunhofer-Institut für Molekularbiologie und Angewandte Oekologie IME ist die Erfassung von molekularen Daten zur Identifizierung und Aufklärung der Umweltwirkung von Wirkstoffen aus Pflanzenschutzmitteln, Bioziden, Arzneimitteln oder Kosmetika. Mittels Biomarker-Signaturen für stoffklassenspezifische Umweltwirkungen soll ein Screening zur Verfahrensbeschleunigung bei der Substanz- und Wirkstoffentwicklung entworfen werden. In diesem Kontext, war das Ziel dieser Doktorarbeit, molekulare ökotoxikogenomische Signaturen relevanter toxikologischer Wirkmechanismen in drei toxikologisch wichtigen aquatischen Modellorganismen unterschiedlicher Trophiestufen (*Danio rerio*, *Daphnia magna* und *Lemna minor*) zu erfassen und zu charakterisieren. Mit Hilfe von Transkriptom- und Proteom-Untersuchungen nach subletaler Wirkstoffexposition sollten systembiologische Profile funktional charakterisiert und zuverlässige Biomarker-Kandidaten mit potenzieller Vorhersagekraft relevanter MoA identifiziert werden. Als zentrale Frage galt es zu klären, ob eine Differenzierung unterschiedlicher MoA anhand molekularer Signaturen auf Genexpressionsebene möglich ist.

Zur Erfassung MoA-spezifischer toxikogenomischer Signaturen wurden verschiedene Referenzstoffe mit bekannter Wirkweise im Zielorganismus ausgewählt. Diese wurden in

verschiedenen subletalen Testkonzentrationen den Modellorganismen ausgesetzt, um anschließend Änderungen im Genexpressionsprofil zu erfassen und zu charakterisieren. Für alle drei Organismen wurde ein technischer Arbeitsablauf entwickelt, der die zeitgleiche Extraktion von RNA und Protein aus derselben biologischen Probe ermöglicht. Für die Expositionsstudien im Zebrafisch-Embryomodell (*D. rerio,* 96 Stunden nach Befruchtung) wurde die Prüfrichtlinie für den akuten Fischembryo-Toxizitätstest (OECD 236) als konzeptioneller Rahmen verwendet. Als Testsubstanzen mit bekannten MoA, wurden das Schilddrüsenhormon 3,3′,5-Trijodthyronin (T3) und das Thyreostatikum 6-Propyl-2-thiouracil (6-PTU), sowie sechs nerven- und muskelbetreffende Insektizide (Abamectin, Carbaryl, Chlorpyrifos, Fipronil, Imidacloprid und Methoxychlor) untersucht. Um weitere Anwendungsmöglichkeiten toxikogenomischer Signaturen auch im Bereich der Erfassung immunsuppressiver Wirkmechanismen zu ermöglichen, wurde ein subletaler Immunstimulationstest in frühen Zebrafischembryos (48 Stunden nach Befruchtung) durchgeführt. Damit sollte dessen Potenzial zur Bewertung immunsuppressiver Wirkungen auf Genexpressionsebene evaluiert werden. Hierzu wurden toxikogenomische Profile nach einem immunantwort-auslösenden Stimulus mit und ohne vorherige Exposition mit Clobetasolpropionat (CP) verglichen. CP ist auch in Fischen ein bekanntes Immunsuppressivum. Die Immunstimulation erfolgte durch Mikroinjektion von **P**athogen-**a**ssoziierten **m**olekularen Strukturen (***P****atterns*) (PAMPs). Zur Erfassung von ökotoxikogenomischen Expressionsprofilen neurotoxischer Substanzen im limnischen Frischwasserfloh *D. magna* wurden Expositionsstudien gemäß dem akuten Immobilisierungstest mit Wasserflöhen (OECD 202) durchgeführt. Hierzu wurden zunächst für Fipronil und Imidicaloprid niedrige Effektkonzentrationen ermittelt (EC5 und EC20) und anschließend die Genexpressionsprofile für diese Konzentrationen untersucht. Ziel war es, toxikogenomische Signaturen des GABA-gesteuerten Chloridkanalblockers (Fipronil) und des nAChR-Agonisten (Imidacloprid) zu vergleichen. Für die aquatische Makrophyte *L. minor* (Wasserkresse) wurde eine verkürzte 3-Tages-Version des Wachstumshemmungstests (OECD 221) durchgeführt. Dabei wurden auch hier niedrige Wirkungskonzentrationen (EC5 und EC20) zur Erstellung von möglichen stoffspezifischen Expressionsprofilen verwendet. Untersucht wurden das Herbizid und der Photosynthese-Inhibitor Bentazon sowie das Cholesterin-senkende Medikament Atorvastatin, welches die HMG-CoA-Reduktase hemmt. Die funktionale Interpretation der molekularen Stressreaktionsprofile in *L. minor* war dabei besonders herausfordernd. Grund hierfür war eine mangelnde funktionelle Annotation des Referenzgenoms. Aus diesem Grund wurde ein funktionelles Annotations-*R*-Package für diesen Organismus konstruiert, basierend auf Proteinsequenzhomologie zu entsprechenden Referenzpflanzen.

Im Rahmen dieser Doktorarbeit konnte gezeigt werden, wie anhand computergestützter systembiologischer Analysen von ökotoxikogenomischen Profilen, toxische Wirkmechanismen auf molekularer Ebene in *D. rerio, D. magna* und *L. minor* erfasst werden können. Im Allgemeinen erwiesen sich die ökotoxikogenomischen Ansätze als sensitiv. So waren signifikante Änderungen in den Genexpressionsprofilen bereits vor dem eintreten physiologischer Effekte oder in sehr geringen Wirkungskonzentrationen (EC5) ersichtlich. Es konnten mögliche MoA-spezifische Biomarker beschrieben werden, welche einen potenziellen molekularen Zusammenhang zu zum Teil bereits zuvor beschriebenen apikalen Effekten herstellen lassen. In Bezug auf die untersuchten thyroidal wirksamen Stoffe, konnten bereits zuvor beschriebene molekulare Biomarker für endokrine MoA validiert werden. Dies unterstreicht die Robustheit des entwickelten molekularbiologischen Ansatzes zur Erfassung toxikogenomischer Signaturen. Darüber hinaus wurde anhand der unterschiedlichen Transkriptomsignaturen von T3 und 6-PTU im 96 Stunden Fischembryo-Test zur Identifizierung von genetischen Biomarkern beigetragen, welche es ermöglichten, zwischen der T3 Synthese-inhibierenden Wirkung auf die Schilddrüse (*tg*, *tshba*) und aktivierende Wirkung auf das thyroidale Signalsystem (*dio3b*, *thraa*) der jeweiligen Substanz zu unterscheiden. Die Untersuchung neurotoxischer Insektizide auf die Genexpression im 96 Stunden Zebrafischembryo-Test identifizierte neben Markern von oxidativem Stress vor allem Indikatoren für entwicklungstoxische Mechanismen, welche mit Effekten auf Herzmuskelentwicklung (z.B. *tcap, actc2, desma, tnnt2c*) und Entwicklung des zentralen Nervensystems (z.B. *npas4a, egr1, btg2, ier2a, vgf*) in Zusammenhang gebracht werden konnten. Die Transkriptomprofile im frühen Zebrafischembryo-Test (48 Stunden) mit induzierter Immunantwort, deuten darauf hin, dass CP die angeborene Immuninduktion beeinträchtigt, indem es die Expression von Genen abschwächt, die an der Antigenprozessierung, der TLR-Signalübertragung, der NF-KB-Signalübertragung und der Komplementaktivierung beteiligt sind.

Ein Vergleich der molekularen Signaturen auf funktionaler Ebene der Gene ergab verbindungsspezifische molekulare Fingerabdrücke für die getesteten Substanzen verschiedener MoAs. Dies deutet darauf hin, dass die erfassten Signaturen einen MoA-spezifischen Charakter haben, welcher sich zur Vorhersage spezifischer toxischer Wirkmechanismen eignen könnte. In ähnlicher Weise wurden wirkstoffspezifische Genexpressionsprofile auch in den durchgeführten Studien mit dem Frischwasserkrebs *D. magna* und der aquatischen Makrophyte *L. minor* beobachtet. Durch die Untersuchung in *D. magna* und *L. minor* konnte gezeigt werden, dass die toxischen Wirkmechanismen

unterschiedlicher Substanzen, welche sich auf physiologischer Ebene nicht unterscheiden lassen, eine Differenzierung auf der Genexpressionsebene ermöglichen. Dies eröffnet neue Möglichkeiten zur Erfassung und Bewertung toxischer Wirkweisen in aquatischen Organismen auf molekularer Ebene. Obwohl die systembiologische Analyse für Organismen mit funktionell schlecht annotierten Referenzgenomen, insbesondere von *L. minor* oder *D. magna,* eine größere Herausforderung darstellte, konnte durch diese Doktorarbeit gezeigt werden, wie Forschende öffentlich verfügbare Informationen und bioinformatische Werkzeuge anwenden können, um diese Hürde zu überwinden. Das in dieser Arbeit für *L. minor* konstruierte Annotationspaket (*AnnotationDbi*) wurde öffentlich zur Verfügung gestellt (Zenodo: 6045874), um den Annotationsprozess in Zukunft für andere Forschende zu erleichtern. Das Paket lässt sich über die *R*-Befehlszeile implementieren und ermöglicht funktionelle *Gene Set Enrichment*- (GSEA) und *Over Representation*-Analysen (ORA) mit *L. minor*. Darüber hinaus ist der beschriebene Arbeitsablauf auch auf andere Organismen mit Referenzgenom ohne funktionelle Annotation erweiterbar, und kann so dabei helfen, toxikogenomische Forschung auch in anderen Nicht-Modellorganismen voran zu bringen.

Diese Doktorarbeit liefert nicht nur wichtige molekularbiologische Einblicke in verschiedene toxische Wirkmechanismen für verschiedene aquatische Modellorganismen, sondern stellt auch eine wichtige Datengrundlage für zukünftige *in silico* Untersuchungen bereit. Sie kann dazu verwendet werden, um essentielle Schlüssel-Stoffwechselwege und dazugehörige Biomarker zu identifizieren, die eine zuverlässige Differenzierung toxischer MoA auf molekularer Ebene ermöglichen. Die gewonnenen Erkenntnisse sind grundlegend für die Weiterentwicklung prädiktiver ökotoxikologischer Methoden der nächsten Generation mit denen sich gefährliche toxische MoA hervorsagen lassen. Langfristig zielen die hier identifizierten molekularen Fingerabdrücke darauf ab, die Entwicklung von biomarkerbasierten Hochdurchsatz-Screenings zu erleichtern. Solche Verfahren können prä-regulatorisch bereits während der Substanz- und Wirkstoffentwicklung zur Identifizierung und Priorisierung von umweltverträglicheren und sichereren Vorläufersubstanzen verwendet werden. Auch ermöglichen sie eine Erleichterung der Planung von höherstufigen Tier-Studien, was insgesamt die Zahl an Tierversuchen reduzieren könnte. Die Ökotoxikogenomik hat bei korrekter Anwendung das Potenzial, frühe molekulare Schlüsselereignisse und geeignete Biomarker hinter toxischen Mechanismen aufzudecken, was den Übergang zur chemischen Gefahrenbewertung der nächsten Generation mit höherem Informationsgehalt beschleunigen wird.

LIST OF PUBLICATIONS

A1 Reinwald H.*, König A.*, Ayobahan S. U., Alvincz J., Sipos L., Göckener B., Böhled G., Shomronie O., Hollert H., Salinas G., Schäfers C., Eilebrecht E. & Eilebrecht S. (2021). Toxicogenomic fin(ger)prints for thyroid disruption AOP refinement and biomarker identification in zebrafish embryos. *Science of the Total Environment,* **printed**

A2 Reinwald H., Alvincz J., Salinas G., Schäfers, C., Hollert, H. & Eilebrecht, S. (2021). Toxicogenomic profiling after sublethal exposure to nerve-and muscle-targeting insecticides reveals cardiac and neuronal developmental effects in zebrafish embryos. *Chemosphere*, **printed**

A3 Essfeld F., Reinwald H., Salinas G., Schäfers C., Eilebrecht E. & Eilebrecht S. (2022). Transcriptomic profiling of clobetasol propionate-induced immunosuppression in challenged zebrafish embryos. *Ecotoxicology and Environmental Safety*, **printed**

A4 Pfaff J., Reinwald H., Ayobahan S. U., Alvincz J., Göckener B., Shomroni O., Salinas G., Düring R., Schäfers C. & Eilebrecht S. (2021). Toxicogenomic differentiation of functional responses to fipronil and imidacloprid in *Daphnia magna*. *Aquatic Toxicology*, **printed**

SUBMITTED PUBLICATION †

A5 Loll A.*, Reinwald H.*, Ayobahan S., Shomroni O., Göckener B., Salinas G., Schäfers C., Schlich K., Hamscher G. & Eilebrecht S. (2022). A short term test for toxicogenomic analysis of ecotoxic modes-of-action in *Lemna minor. Environmental Science & Technology*, **submitted**

***:** Shared 1st authorship

†: This manuscript is submitted and not yet published. However, research efforts and findings from this work contribute significantly to the entity of this PhD thesis and are therefore also listed in the annex.

ABBREVIATIONS

ACh	acetylcholine
AO	adverse outcome
AOP	adverse outcome pathway
core DEG	common DEGs among multiple exposure concentrations of a test compound
DEG	differentially expressed gene
DGEA	differential gene expression analysis
GABA	gamma-aminobutyric acid
GO	gene ontology
GSEA	gene set enrichment analysis
HMGR	3-hydroxy-3-methyl-glutaryl-coenzyme A reductase
KE	key event
KEGG	Kyoto Encyclopedia of Genes and Genomes
MIE	molecular initating event
MoA	mode of action
nAChR	nicotinic acetylcholine receptor
NGS	next generation sequencing
ORA	overrepresentation analysis
PAMPs	pathogen Associated Molecular Patterns
PPP	plant protection product
REACH	registration, evaluation, quthorisation and restriction of chemicals
THR	thyroid hormone receptor
TPO	thyreoperoxidase

1. INTRODUCTION

Manufacturing, use and trade of chemicals are growing worldwide. In 2020, global chemical sales was valued at €3471 billion (CEFIC, 2022) and predictions forecast a double in chemical production by 2030 (European Commission, 2020). In the European Union, chemical manufacturing is the 4th largest industry with about 30 000 companies employing an estimate of 1.2 million people directly and 3.6 million indirectly (European Commission, 2020). From food production, packaging, cars, frying pans, cell phones, computer chips or therapeutics – chemicals are everywhere in our day to day life. A modern society heavily relies on a plethora of chemicals, e.g. for industrial use or as cosmetics, pharmaceuticals and pesticides. Chemicals and their production consequently have a high socioeconomic value for our society. However, this value comes with a cost. The unintentional or intentional release (e.g. pesticides) of hazardous chemicals poses a threat to environmental organisms, ecosystems and humans alike.

Biomonitoring studies in the EU revealed a growing number of hazardous compounds such as heavy metals, plasticizers, flame retardants or pesticides in human tissue and blood stream (Milieu Ltd et al., 2017). There are growing numbers of reports demonstrating how prenatal exposure to a mix of certain chemicals can lead to reduced foetal growth and lower birth rates in humans (European Commission, 2020). Further, the United Nations Human Rights Council concluded that the usage of pesticides conflicts with the very basic human right to a life with dignity, especially for children from low and middle-income countries. The prevailing and narrow focus on "food security"[1] leaves a massive blind spot for the negative consequences on environmental and human health as well as society as a whole (United Nations Human Rights Council, 2017). The ubiquitous release of pesticides to the environment used for crop protection is considered as one of the key drivers for the dramatic biodiversity loss observed in recent years (Brühl and Zaller, 2019). Aquatic ecosystems are especially susceptible to chemical contamination through agriculture run offs, sewage or flooding events (Johnson et al., 2020). Although improvements were achieved in recent years, still more than half of the EU water bodies are in poor ecological condition (EEA, 2018) while chemicals are increasingly reported in the surface and drinking waters of the EU (Baken et al., 2018; Escher et al., 2020). To safeguard non-target organisms and ecosystems from potential adverse effects, EU inquires ecotoxicological hazard assessment data from manufacturers for the registration and authorisation of a chemical.

[1] Approximately 77% of the world's agricultural land is used for feeding livestock while livestock itself only accounts for 18% of the global calorie supply (Ritchie and Roser, 2019). With these numbers in mind we should ask ourselves whether "food security" is really the problem or if it is rather a "diet security" debate.

1.1. WHY WE NEED TO EVOVLE CHEMICAL HAZARD ASESSEMENT

It is important to state that not all hazardous chemicals pose a direct risk to the environment or raise high concerns with respect to their adverse effects on living organisms. However certain chemicals or chemical groups can cause cancer or negatively affect the endocrine, reproductive, respiratory, cardiovascular and immune system (Milieu Ltd et al., 2017; Rehberger et al., 2017; Schrenk et al., 2020). The exposure to such harmful compounds threatens the health of an organism (including humans), which can have wide ranging adverse effects on ecosystems and populations alike (Persson et al., 2022). Consequently, novel compounds and materials should be inherently safe for us and the ecosystem, from manufacturing to their end of life. To achieve this ambitious goal, the EU has about 40 legislative tools at hand with the aim to ensure consumers and environmental safety of e.g. industrial chemicals, pharmaceuticals, cosmetics, biocides or plant protection products (PPP) (European Commission, 2020). Although the function of the different regulation frameworks is similar, their environmental protection goals and environmental risk assessment strategies differ (van Dijk et al., 2021). Depending on a chemicals use and/or annual tonnage production, different regulations apply. For active compounds which (a) have an annual production above 1 t, (b) are intentionally introduced to the environment (e.g. PPP) or (c) are indirectly introduced to the environment through usage (e.g. pharmaceuticals, cosmetics, biocides), EU legislation inquires environmental hazard data for chemical risk assessment (Directive 2001/83/EC; Reg (EC) No 1107/2009; Reg (EC) No 1223/2009; Reg (EC) No 1907/2006; Reg (EC) No 528/2012; Reg (EU) No 2019/6). Besides environmental fate, degradation and bioaccumulation studies, ecotoxicological hazard assessment also includes toxicity tests using a variety of non-target terrestrial and aquatic model organisms and test designs (Gourmelon et al., 2007; Kühnel and Nickel, 2014; Petersen et al., 2015). Although the current standardized *in-vivo* animal toxicity tests are essential for environmental safety assessments, they are also problematic for multiple reasons.

Firstly, such standardized non-human animal tests are often cost and time intensive. In consequence they cannot keep up with the pace at which novel compounds are invented (Persson et al., 2022; van Dijk et al., 2021). Out of the approximately 140 000 large scale commercialized synthetic compounds only a few thousand are considered as toxicologically 'well studied'[2], mainly pesticides and pharmaceuticals (Johnson et al., 2020). The bias towards these particular compound groups derives from the fact that by default they are designed for a target system. Therefore their effects on a living organism a far better investigated, in contrast

[2] The total number of compounds toxicologically assessed at all is considered between 10 and 20 thousand and mostly for acute and topical endpoints (Krewski et al., 2020).

to e.g. industrial chemicals. On top of that, for pesticides (EFSA regulation) and biocides (ECHA regulation), environmental risk assessment is always mandatory for the registration, as these compounds are actively introduced to the environment with the intention to harm specific target organisms. These studies are performed within a tiered testing framework, primarily focus on acute topical endpoints as the evaluation of chronic sublethal effects, as for the moment, requires highly cost intensive long term animal studies (e.g. OECD 229, 230, 234). To safeguard environmental safety, the continuously growing number of novel substances poses enormous financial and durational challenges upon industry and authorities relying on the currently implemented ecotoxicological animal tests (Canzler et al., 2020; Krewski et al., 2010).

Secondly, the resulting growing number of animal tests with sentient beings justifiably raises ethical concerns (Embry et al., 2010; Krewski et al., 2010). In 2018, an estimate of 2.76 million fish were sacrificed in animal tests in the EU. More than 1.9 million vertebrates alone were used in assessment studies to meet legislative requirements. From these sacrificed animals, 11.3 % (~220 000)[3] were used for toxicity and mainly ecotoxicity assessment of industrial chemicals, PPPs or biocides (European Comission, 2018). This staggering number of sacrificed sentient animal's lives stands in direct conflict with the "3R-principals" formulated by Russell and Burch in 1959, calling for a **r**eduction, **r**efinement and whenever possible **r**eplacement of animal test (Russell and Burch, 1959). Therefore, from both an ethical and economic perspective, it is crucial to reduce the number of these experiments whenever possible.

Additionally, many standard animal ecotoxicology tests are not designed to elucidate the mechanisms behind toxic effects, especially short term acute assays (Martyniuk and Simmons, 2016). For example, environmental hazard assessment of aquatic environments, implemented various standardized toxicity test guidelines for a variety of aquatic organisms from different trophic levels (e.g *Lemna sp.* Growth Inhibition Test (OECD 221), *Daphnia sp.* Acute Immobilisation Test (OECD 202), Fish Acute Toxicity Test (OECD 203)). These classical ecotoxicological toxicity tests primarily focus on answering the question: "What concentration level is toxic[4]?" and less often "Why is it toxic?". With respect to the regulation of a chemical, answering the latter is key, as the chemicals primary toxic mode of action is crucial for its legislative regulation in the European Union. Market authorization for an active compound in e.g. PPPs, biocides or cosmetics can be rejected if the compound's primary mode of action

[3] From this fraction, more than 100500 (45.7 %) vertebrates were sacrificed in studies listed as regulatory ecotoxicology studies and more than 86400 (39.3 %) in non-regulatory toxicology and ecotoxicology studies
[4] One or multiple adverse endpoints, which are considered as a toxic effect, are preliminary defined to the test.

(MoA) demonstrates mutagenic, reproductive or endocrine effects in environmental organisms[5] (van Dijk et al., 2021). As part of the European Green Deal's chemical strategy, the EU plans to extend this generic approach (hazard and not risk based) to chemical risk management in consumer products. Consequently, chemicals which are considered cancerogenic, mutagenic, endocrine active or toxic to reproduction could be rejected more often from authorisation in the future. Further, the level of protection granted to consumers shall be extended to professional users under REACH. Additionally, the EU commission formulated the goal to extend the generic approach to further harmful chemical properties, including immune, neurological and respiratory toxicity (European Commission, 2020).

It is therefore of great interest for the manufacturer to identify and understand a chemicals MoA to environmental non-target organisms early on during compound development. Having mechanistic insights from an early design stage on would allow the selection of safer preliminary compound candidates over hazardous ones. This idea is in line with the European green deal chemical strategy, promoting a pre-market sustainable-by-design approach for the development of environmentally safe chemicals (European Commission, 2020). Ideally, an early, non-target, high throughput compatible, non-animal hazard screening methodology would be at our disposal. Despite the importance for elucidating toxic mechanisms behind adverse effects for environmental safety assessments, to this point ecotoxicological research lacks high-throughput methodologies to detect, predict and reliably distinguish primary MoAs in non-target organisms. A promising alternative to overcome such limitations are molecular systems biology-based approaches which can be investigated in an untargeted manner via modern day *omic* technologies. Such molecular biology approaches require less resources and biomaterial than classical test assays while being highly sensitive and informative at the same time (Brinke and Buchinger, n.d.; Kim et al., 2015; Reid and Whitehead, 2016).

Moreover, mankind operates outside the safe planetary boundary with respect to novel entities[6] since, "annual production and releases are increasing at a pace that outstrips the global capacity for assessment and monitoring." (Persson et al., 2022). It is therefore crucial for safety for us as humans and the environment we are part of, that the scientific community explores and ultimately finds more effective ways for chemical risk assessments.

[5] "Unless the exposure of non-target organisms to that active substance in a plant protection product under realistic proposed conditions of use is negligible." (EU Regulation No 1107/2009)
[6] Expansion of the term chemical pollution which includes "chemicals and other new types of engineered materials or organisms not previously known to the Earth system as well as naturally occurring elements (e.g. heavy metals) mobilized by anthropogenic activities." (Steffen et al., 2015)

1.2. ECOTOXICOGENOMICS – A NEW HOPE FOR PREDICTIVE TOXICOLOGY

Through major advances in *omic* technologies in recent years, researchers nowadays can effort to quantify the response of thousands of genes and their products from a single sample simultaneously in an untargeted manner. The ability to detect molecular level changes on such a broad scale in response to chemical exposure, opens unprecedented opportunities for modern-day hazard assessment approaches (Cote et al., 2016).

'Ecotoxicogenomics' initially derives from 'toxicogenomics', which in the human health research context describes the expression analysis of genes in response to toxic exposures and elucidation of the toxic mechanisms per se. Similarly, yet intended for a broader scope of *omic* methods, 'ecotoxicogenomics' describes the application of transcriptomics, proteomics or metabolomics in the field of ecotoxicology and environmental hazard assessment. Ecotoxicogenomics is hereby defined as the non-target and wide scale expression study of genes, proteins or metabolites in non-target organisms in response to environmental toxicant exposure (Snape et al., 2004).

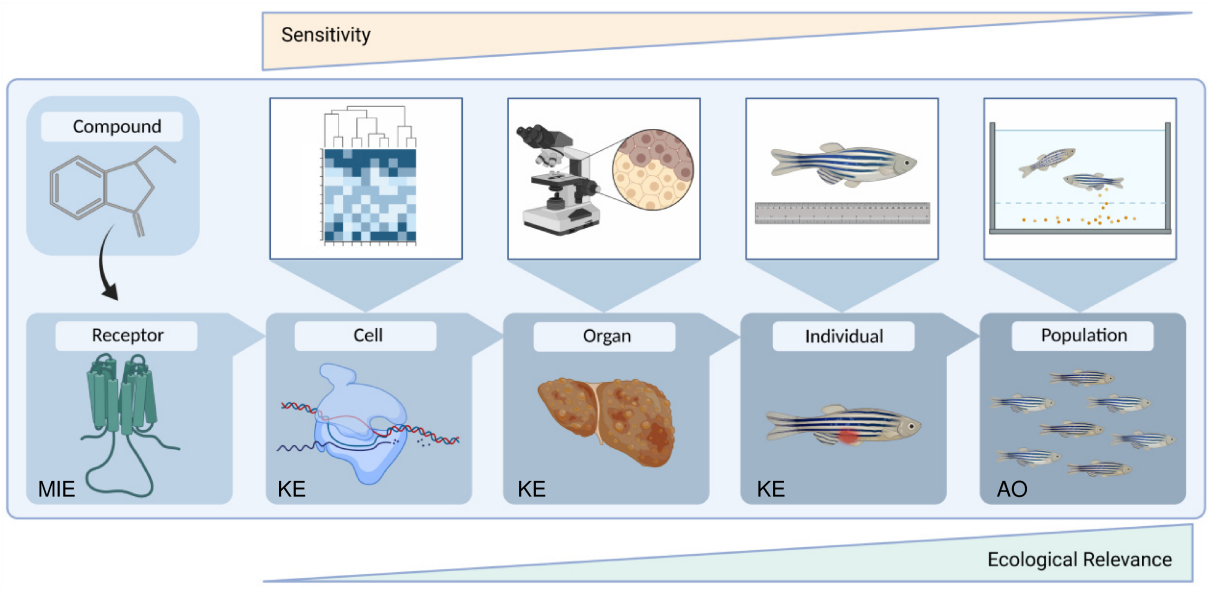

Figure 1: Conceptual illustration of the adverse outcome pathway (AOP) concept and how different biological organisational levels can be assessed toxicologically. An AOP links a molecular initiating event (MIE) to an adverse outcome (AO) of regulatory importance over multiple layers of biological organization via key events (KE). Different methodologies can be applied at different organizational levels. The assessment of cellular responses on the molecular level tend to have a higher sensitivity and require less bio-resources. On the other hand, assessment of endpoints on the individual physiology and population level have a higher ecological relevance, yet require more time and bio-resources.

The obtained molecular system biology data from such methods are in particularly valuable for the identification of molecular initiating events (MIE) and molecular key events (MKE) applicable in the adverse outcome pathway (AOP) framework (Brockmeier et al., 2017;

Heusinkveld et al., 2018; Ramaiahgari et al., 2019; Shankar et al., 2021) (**Figure 1**). As a conceptual construct, an AOP links existing knowledge beginning from a MIE to an adverse outcome (AO) at a higher biological organization level with relevance to chemical hazard assessment (e.g. organ, individual or population). The steps from MIE to AO across different biological organisational levels are linked by key events (KE) (Ankley et al., 2010; Conolly et al., 2017; LaLone et al., 2017) (https://aopwiki.org/aops). A fully described AOP allows for cross chemical extrapolation under the assumption that chemicals inducing identical MIEs will lead to similar AOs. One major goal of the AOP framework is therefore to identify MIEs or early MKE as indicators to predict specific apical adverse effects, which could facilitate regulatory chemical hazard assessment (Villeneuve et al., 2014a, 2014b). In human toxicology for example, the skin sensitization AOP is already successfully used for regulatory purposes. Thanks to such advances, skin sensitization can now be evaluated using molecular biomarkers in cell lines instead of animal test on mice (OECD, 2012a; Patlewicz et al., 2014; Wittwehr et al., 2017). However, the identification and definition of such biomarkers requires prior in depth mechanistic understanding of their biological function and how they might affect other important molecular regulators. Furthermore, the search for suitable biomarkers was tedious in the past as it was mostly based on targeted approaches (e.g. RT-qPCR) which made it impossible to analyse the response for tens of thousands of genes at once. This hurdle was overcome with the development of modern day full mRNA next generation sequencing or bottom-up shot gun proteomic LC-MS approaches. These transcriptomic and proteomic technologies enable non-targeted screenings for early molecular changes in a model organism in response to chemical exposure at the gene expression level. Consequently, the application of such methods can provide a deeper understanding about the early toxic mechanisms preceding adverse effects, which is fundamental for AOP refinement as well as novel AOP development. Further, the obtained high content datasets can be effectively screened for novel biomarker candidates and directly evaluated for their cross-regulation and biological functions.

Ecotoxicogenomics and the AOP framework have the potential to revolutionize classical hazard assessment of chemicals. The continuous development of these methods support the paradigm shift in ecotoxicological hazard assessment from descriptive to predictive assessment strategies. Improved molecular insights from applied transcriptomics or proteomics for a set of well characterized chemicals will help to facilitate the transition towards sensitive, informative and predictive biomarker based screening approaches. In the future, these methods and mechanistic insights derived from them will help to robustly characterize a chemical's primary MoA in non-target organisms under realistic sublethal exposure conditions. At Fraunhofer IME, the

Fraunhofer Attract Eco'n'OMICs research group aims towards a collective harmonized database combining ecotoxicogenomic profiles with prior knowledge of the tested compound, which could help in future to predict the MoA for newly developed compounds (**Figure 2**).

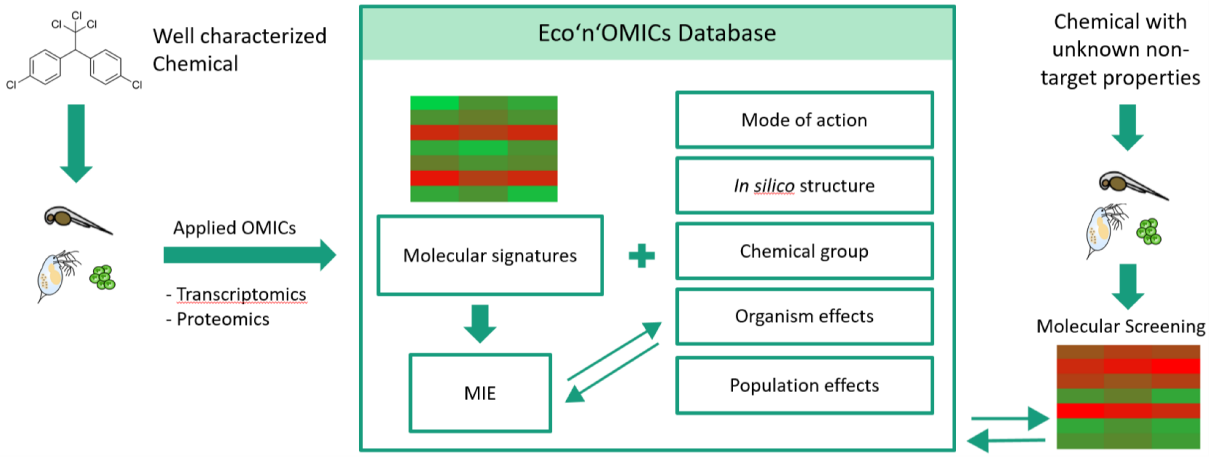

Figure 2: The vision of the attract eco'n'omics working group at fraunhofer IME. Ultimately the goal is to build database for various MoA specific compounds and their ecotoxicogenomic profiles. For multiple non-target organisms the compounds molecular fingerprint coupled with prior toxicological knowledge could be used to characterize adverse MoAs in newly developed compounds.

The current state of the art predictive toxicology models, such as the Verhaar scheme (Ellison et al., 2015; Verhaar et al., 1992) are purely *in silico* based and rely on the assumption that similar structured compounds induce similar toxic MoAs and on prior collected acute toxicity data. These models, well suited for a high throughput analysis of e.g. precursor compounds, solely consider a molecules structure for its acute toxicity predictions. Yet they are of limited use for predicting chronic and/or sublethal effects nor do they provide insights in the toxic MoA underlying adverse effects (Brockmeier et al., 2017). In this context, transcriptomics and proteomics have the potential to revolutionize predictive toxicology, by identifying and describing characteristic ecotoxicogenomic profiles as indicators for certain adverse MoA. Furthermore, potential molecular biomarkers can be identified with strong predictive characteristics for a chemicals MoA. This could enhance the development of ecotoxicological high throughput *in vitro* methods (e.g. fish cell cultures). This would not only speed up environmental hazard assessment and reduce the number of non-human animal tests. It would allow to build models which could link a chemicals toxicogenomic molecular signature to certain MIEs and apical AOs (Wang et al., 2021). Ecotoxicogenomic data ultimately facilitates the refinement of pre-existing AOPs and allows for the discovery of new AOPs with regulatory purposes (Wang et al., 2021; Wittwehr et al., 2017). However, such models must be built and trained on reliable pre-existing *omic* data first. Therefore, the required wide scale *omic* studies need to be performed by the scientific community in a transparent and reproducible manner,

which is a challenging task especially in *omic* studies (Harrill et al., 2021; Lange et al., 2008; Wilkinson et al., 2016).

1.3. STUDY AIMS AND THESIS STRUCTURE

As described above, system biology approaches have the potential to reveal mechanistic insights behind a compound's adverse effect on an early molecular level. This knowledge is vital for the development of biomarker based environmental hazard screenings in non-target organisms (**Figure 2**). In this context, the present thesis investigates the applicability of transcriptomic and proteomic methods to identify MoA related molecular signatures preceding adverse effects in three representative aquatic non-target organism of different trophic levels (*Danio rerio, Daphnia magna, Lemna minor)* (**Figure 3**). Based on the obtained ecotoxicogenomic signatures, robust functional profiles and reliable biomarker candidates should be identified with sufficient predictive properties to allow for a differentiation among regulatory relevant MoAs in non-target organism. Plant protection products and pharmaceuticals belong to the best studied chemicals (van Dijk et al., 2021) with known MoA, at least for the target system. Therefore, well characterized active compounds with known MoAs were tested at sublethal test concentrations to assess molecular changes in the organism's expression profiles using transcriptomics and proteomics. For each of the assessed organisms, the major tasks of the present thesis comprised of:

- Integration and optimization of *omic* methods in OECD wet-lab workflows which allow for simultaneous RNA and protein extraction from the same biological sample and ensure compatibility with downstream next generation sequencing (NGS) and LC-MS/MS shotgun proteomics.
- Development of fully automated *omic* raw data processing pipelines for high throughput analysis involving quality check (QC) steps to ensure the robustness and reliability of the downstream analysis results.
- Programming of automated downstream feature selection algorithms, identifying biomarker candidates, based on differential gene expression analysis (DGEA) and functional profiling based on over-representation analysis (ORA) and gene set enrichment analysis (GSEA).

The overarching goal is to address the following research questions:

- Is it possible to retrieve MoA specific ecotoxicogenomic profiles in different non-target organisms and if so, how specific are they?

- Can ecotoxicogenomic methods facilitate the assessment of regulatory relevant yet difficult/challenging hazards such as immune toxicity?
- How can we overcome functional analysis challenges due to limited annotation of an organism's reference genome (*D. magna* & *L. minor*) to still gain mechanistic insight?

The findings presented in this thesis constitute out of five manuscripts (**A1 – A5**) covering different experimental setups and study aims as shown in **Figure 3.**

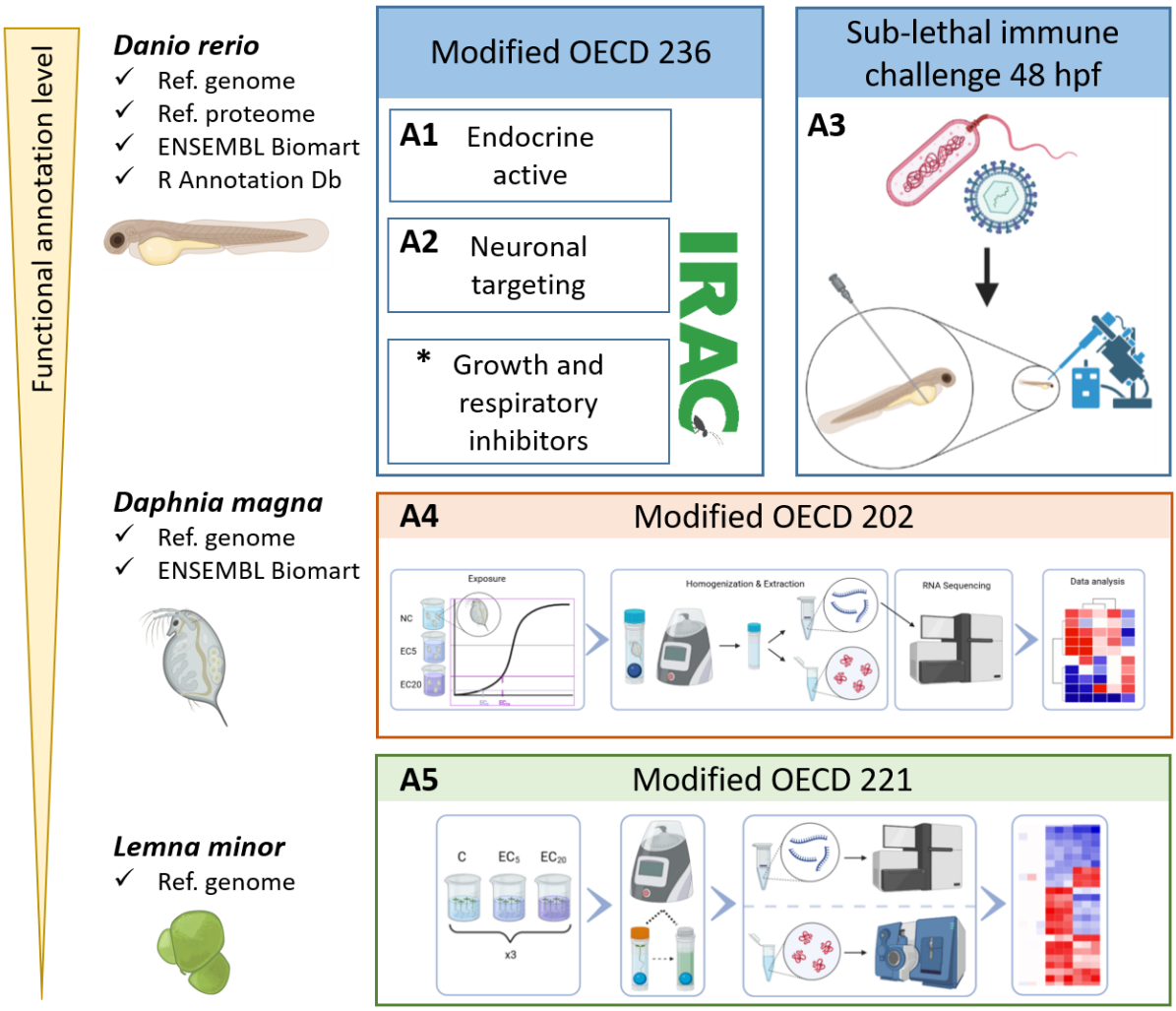

Figure 3: Schematic overview about major PhD project working blocks. Letters A1 – 5 refer to the respective manuscript (provided in the annex) for this work. Overall, for three different aquatic non-target organisms (*Danio rerio, Daphnia magna, Lemna minor*) compounds with different MoAs were tested to retrieve ecotoxicogenomic signatures for the respective MoA and organism. For A1 & A2 compounds were tested by a modified version of the fish embryo toxicity (FET) test (OECD 236). In A3 a novel sublethal immune challenge approach in zebrafish embryos at 48 hpf was evaluated to see if transcriptomics can help to identify immune suppressive effects. A4 & A5 again were tests following modified OECD guidelines for transcriptomic and/or proteomic profiling post pesticide exposure. The main challenge for *L. minor* and *D. magna* as poorly annotated test organisms, was to build a custom annotation from the reference genome inferred by sequence homology for each protein coding transcript.

1.3.1. Evaluating molecular fingerprints of endocrine and neuronal targeting chemicals in the zebrafish embryo model (**A1** - **A2**)

The zebrafish embryo is an ideal model from both ecotoxicological and systems biology perspectives. It was extensively utilized for toxicological studies in recent years (Belanger et al., 2013; Embry et al., 2010; McCollum et al., 2011) and is increasingly gaining popularity as model organism for human health research, due to the high level of conserved molecular functions among vertebrates (Hason and Bartůněk, 2019; Patton et al., 2021). Due to its importance as a model organism, a fully assembled and in depth annotated reference genome is available. Further, *D. rerio* is supported by Ensembl's Biomart annotation databases and various functional analysis R packages such as clusterProfiler (Durinck et al., 2009; Wu et al., 2021), which facilitates automated functional downstream analysis. As part of a kick-off study, the zebrafish embryo model was applied to study changes in gene expression profiles post sublethal exposure to thyroidal active compounds (**A1**) and well characterized nerve and muscle targeting insecticides (**A2**) (**Figure 3 A1 & A2**). The aim was a non-target analysis for MoA related ecotoxicogenomic profiles and affected biological processes for thyroid hormone signalling and neuronal development. A modified version of the fish embryo toxicity (FET) test (OECD 236) was used for this purpose. For the first study (**A1**), the thyroid hormone 3,3′,5-triiodothyronine (T3) and the thyrostatic 6-propyl-2-thiouracil (6- PTU) were selected as reference substances to capture two interrelated effects. For the later study (**A2**) six nerve- and muscle-targeting insecticides (abamectin, carbaryl, chlorpyrifos, fipronil, imidacloprid and methoxychlor) from five different pre-defined MoAs were evaluated. The insecticides MoA in the target system were pre-defined by the IRAC classification system (Sparks and Nauen, 2015).

1.3.2. Sublethal immune toxicity short-term assay in zebrafish embryos using toxicogenomics (**A3**)

Chemical exposure, even at low and sublethal concentration levels, can lead to immune system dysfunction in humans and wildlife such as fish (Hidasi et al., 2017; Koller, 2001). In their chemical strategy paper, the EU considers immunotoxicity as an adverse effect of concern for which a generic risk assessment approach could be justified e.g. under REACH (European Commission, 2020). Despite its regulatory relevance and importance for an organism's health, there are still no standardized test methods that allow the specific evaluation of immunotoxic MoA to be included in the environmental hazard assessment of chemicals (Rehberger et al., 2017). This issue has been increasingly addressed by the scientific community in the recent

years (Kataoka and Kashiwada, 2021; Luebke, 1997).Therefore as a follow up study on the previously established workflow for zebrafish embryos, the objective of this study **(A3)** was to apply transcriptome analysis to explore immunomodulatory MoAs at the gene expression level. This was performed through a sublethal immune challenge experiment in zebrafish embryos, with and without exposure to an immunosuppressive compound, and subsequent transcriptomic profile characterization and biomarker candidate selection (**Figure 3 A3**). Fertilized eggs were exposed to the corticosteroid and known immunosuppressant clobetasol propionate (CP) (Hidasi et al., 2017) as model compound. 48 hpf, the embryos immune system was challenged by pathogen-associated molecular patterns (PAMPs) through microinjection and total RNA was extracted 3 hours post injection. Using full mRNA-sequencing and functional transcriptomic analysis, differences in immune response related gene expression profiles with and without CP treatment were evaluated. Further, this study assessed in general the applicability of sublethal immune system stimulation in early zebrafish embryos to study immunosuppressive effects on the molecular level.

1.3.3. Transcriptomic profiling of neuronal targeting insecticides in *Daphnia magna* (**A4**)

To enable molecular marker based MoA characterization of chemicals on lower trophic levels than zebrafish and therefore for a wider ecotoxicological context, it is crucial to explore the application of ecotoxicogenomics in other relevant non-target test organisms. The challenge hereby is that, in contrast to zebrafish, most of the lower trophic aquatic test organisms (e.g. *Daphnia magna* or *Lemna minor*) are not necessarily standard model organisms in molecular biology. Consequently, if a reliable reference genome is available at all, it often lacks essential functional annotations. This makes bioinformatic up- as well as downstream analysis cumbersome and hampers biological interpretation and understanding of the obtained molecular data.

In ecotoxicology, *D. magna* is a commonly used model organism to assess acute or chronic toxicity of chemicals in aquatic invertebrates (OECD 202 & 211). Hereby, the small freshwater crustacean resembles an intermediate trophic level as primary consumer. As the standard endpoints of these tests are restricted to immobility or reproduction, they provide very limited insights into a chemicals MoA. The aim for this study **(A4)** was therefore, to explore ways to expand ecotoxicogenomic non-target screenings in the fresh water crustacean *Daphnia magna*. A special focus was put on developing *in silico* methods to link the crustacean's molecular profiles with biological processes for functional analysis with biologically interpretable results. Here (**Figure 3 A4**), transcriptomic profiling was combined with a modified version of the

D. magna acute immobilization test (OECD 202) to characterize gene expression profiles altered through the nicotinic acetylcholine receptor (nAChR) agonist imidacloprid and the GABA-gated chloride channel blocker fipronil.

1.3.4. Ecotoxicogenomic short term assay in the aquatic macrophyte model *L. minor* (**A5**)

In chemical hazard assessment, aquatic plant toxicity is often evaluated with the aquatic macrophyte *Lemna minor*, resembling the lowest trophic level as a primary producer. Its sensitivity to a variety of xenobiotics and simple cultivation promotes *L. minor* to an important bioassay organism (Aliferis et al., 2009). The standardized *Lemna* sp. grwoth inhibition test (OECD 221) evaluates the number of fronds, frond area and dry weight as endpoints post seven day chemical exposure. However, such endpoints do not provide mechanistic insights into the toxic MoA. Further, the long test duration of seven days is not well suited for quick short term screenings which would facilitate high throughput toxicity tests. Consequently, the aim for this study (**A5**) was to evaluate the sensitivity and applicability of a modified short term version of the *Lemna* sp. growth inhibition test using transcriptomic and proteomic non-target analysis. As model compounds with defined MoA, the photosynthesis inhibitor bentazon (herbicide) and the HMG-CoA reductase inhibitor atorvastatin (pharmaceutical) were tested at preliminarily defined low effect concentrations (EC5 & EC 20) (**Figure 3 A5**). Despite the importance of *L. minor* as model organism in ecotoxicology, the functional annotation of its reference genome is very poor up to this date, which hampers functional interpretation of obtained ecotoxicogenomic profiles and identification of relevant affected biological processes. Therefore, a major task in this study was to build a reliable functional annotation for *L. minor*, which is easily accessible and reusable for the scientific community and allows enrichment analysis for biological processes, molecular functions or cellular components.

2. DISCUSSION

In the subsequent section, first the overarching findings of this PhD thesis are briefly presented in section *2.1* before the publication and manuscript results are elaborated in more detail and put into context in section *2.2*. Further, the obtained insights from the different and partly novel ecotoxicogenomic approaches are discussed with respect to their implications for chemical hazard assessment. The corresponding publications and manuscripts are listed in the annex. An in depth discussion on the individual research results of the different studies and information on the distinct experimental setups are provided in the respective annex section (**A1-A5**). In section *2.3*, experienced general challenges of ecotoxicogenomic are addressed and the outlook for required future research is given. Lastly, a final conclusion is drawn from the obtained insights from this PhD study in section *2.4*.

2.1. KEY FINDINGS OF THE PRESENT WORK

- Transcriptomic and proteomic approaches can be implemented in standard OECD toxicity tests for relevant aquatic model organisms (*D. rerio, D. magna, L. minor*) to provide important mechanistic insights behind adverse effects at the molecular level. This mechanistic understanding is fundamental to progress further in the field of predictive ecotoxicology and novel AOP development.
- On both, the transcriptomic and biological functional level, the identified compound specific fingerprints suggest a relationship between early affected molecular functions and pathways and a compound's MoA. These functional relationships can be further explored to identify targeted key pathways, which will improve the capability of differentiating hazardous MoAs at the molecular level.
- With respect to the evaluation of molecular signatures for thyroid disrupting chemicals in zebrafish embryos, the developed transcriptomic workflow was able to identify previously defined thyroid disrupting biomarkers in fish, verifying the robustness of the established method. Further, transcriptomic and proteomic signatures demonstrated very distinct patterns which allowed the identification of biomarker candidates suitable for thyroid disruption hazard screening approaches.
- Our findings provide a better understanding about early molecular events in response nerve and muscle targeting MoAs of insecticides for aquatic non-target organisms (*D. magna* and *D.rerio*). For *D. rerio* embryos, respective biomarker candidates were identified for the

three major affected processes: (1) cardiac muscle cell development and functioning, (2) oxygen transport and hypoxic stress and (3) neuronal development and plasticity.

- To our knowledge, this is the first study linking neurotoxic insecticide exposure and affected expression of important regulatory genes for heart muscle (*tcap, actc2*) and forebrain (*npas4a*) development in a vertebrate model. The discussed gene sets represent early warning biomarker candidates for developmental toxicity affecting the heart and brain of aquatic vertebrates.
- A novel, sublethal immune challenge assay in early (48 hpf) zebrafish embryo was proposed for the mechanistic assessment of immunosuppressive effects at the gene expression level. The proposed approach was not only able to identify clearly immune response related processes but also to identify alternatively regulated processes and pathways with and without prior immunosuppressive treatment. Hence, it was shown as a powerful method for detecting biomarker candidates for immunosuppressive MoAs in fish.
- Custom developed functional annotation package for the *L. minor* reference genome allowed for the characterisation and description of genes and enable the analysis of ecotoxicogenomic signatures from a shortened 3 days *L. minor* growth inhibition test. The custom built annotation package was capable of identifying MoA associated biological processes and molecular functions for the assessed model compounds, supporting the validity of the built annotation package.
- In general, ecotoxicogenomic approaches were shown to be highly sensitive, as significant changes in gene expression profiles were observable in in the absence of morphological observable effects or very low effect concentrations as low as EC5. In some cases of the zebrafish embryo toxicity test (OECD 236), expression changes were detected even below previously reported NOEC values.
- Throughout all assessed substances in *D. rerio* (**Table 1**, p. 18), *D. magna* and *L. minor*, observed ecotoxicgenomic profiles responded in a concentration-response-like manner. This means, the number of differently expressed genes increase with the exposure concentrations. Also the level of regulation (log_2-fold change) was overall stronger in higher exposure conditions compared to lower exposures. These observations support the idea that ecotoxicogenomics could at some point determine quantitative endpoints in next generation risk assessment.

2.2. ECOTOXICOGENOMIC PROFILING

As described in the introduction section *1.2*, within the field of chemical hazard assessment, there is a severe need for novel approaches to evaluate toxicity effectively for the continuously growing number of active compounds with finite resources. With the capacity to assess the response of thousands of genes and their products from a single biological sample in a non-targeted manner, transcriptomics and proteomics allow to address mechanistic questions of a chemical's adverse effect at an early molecular level (Brockmeier et al., 2017). High expectations are therefore put into high content o*mic* technologies, facilitating biomarker discovery which allow for the prediction of adverse outcomes in environmental and human toxicology alike (Heijne et al., 2005; Villeneuve et al., 2014b; Zurlinden et al., 2020). Although there are no regulatory implementations of ecotoxicogenomics yet (Harrill et al., 2021; Verheijen et al., 2022), ecotoxicological biomarker based assays still bare a great potential in pre-regulatory screenings e.g. during novel compound development. Such molecular signature based hazard assessment could identify early environmental risks at a mechanistic level. Consequently, this would help to prioritize the development of saver compounds over those with higher environmental hazardous potentials. Further it can provide a baseline for the prioritization of higher tier studies which could ultimately lead to a reduced usage of animal tests for regulatory purpose without sacrificing precautious principals (Martyniuk, 2018).

However, to build such cost effective and high throughput-suitable molecular based screenings, ecotoxicogenomic signatures of chemicals with presumably known MoAs need to be identified for a given model test system at first. The consistency of such a model system (e.g. exposure duration, organism developmental stage or age, incubation conditions, etc.) is fundamental to allow for a robust cross experiment comparison and cross interpretation of molecular signatures. As *omic* technologies track changes at the molecular level, they are highly sensitive towards any type of variance in the experimental setup (e.g different incubation temperature, organism handling, etc.) (Harrill et al., 2021). For example, the transcriptomic response in zebrafish embryos to the same concentrations of a xenobiotic can vary significantly among different developmental stages (Schüttler et al., 2019). It is therefore of great importance, to use standardized toxicity test methods and to carefully control for harmonized experimental and laboratory conditions. In this context, OECD guidelines for toxicity tests provide an excellent reference framework from which to build up on test extensions for the assessment ecotoxicogenomic signatures. Therefore, among other things, this work presents, how integrated transcriptome and proteome analysis can be coupled with the test guidelines OECD 236 with zebrafish embryos (**A1** & **A2**), OECD 202 with *Daphnia magna* (**A4**) and OECD 221

with *Lemna minor* (**A5**). All of these guideline tests are intended as acute short term tests for different trophic level organisms. The subsequent sections will briefly discuss the findings from published (**A1** – **A4**) and unpublished (e.g. **A5**) ecotoxicogenomic studies conducted for this doctoral research project.

In section *2.2.1*, the identified potential biomarkers from 96 hpf exposure studies in zebrafish embryos with thyroid disrupting chemicals (**A1**) and neuronal targeting insecticides (**A2**) will be elaborated. In addition to the datasets presented in **A1** and **A2**, unpublished transcriptomic datasets were included to allow for a comparative meta-analysis of affected molecular pathways. These additional datasets include transcriptomic profiles obtained from different endocrine active compounds and insecticides classified after IRAC as "growth and development targeting" and "respiratory inhibitor" in the target system (**Table 1**). Based on the obtained datasets and current observations, the question whether molecular fingerprints allow for a MoA specific differentiation shall be addressed. Section *2.2.2*, discusses the applicability of *omic*-based approaches for assessing immunotoxic effects via sublethal immune challenge in the early zebrafish embryo model, in the context of the research findings presented in the conceptual study **A3**. Finally the section *2.2.3*, will demonstrate how functional analysis of *omic* profiles can be performed to gain mechanistic insights into adverse effects for poorly annotated non-systems-biology model organisms *Daphnia magna* (**A4**) and *Lemna minor* (**A5**). Special attention is hereby given to the developed workflow, by which high content reference genome sequence data can be annotated with biological GO terms, allowing for functional interpretation of DGEA results. The robustness of this sequence homology-based annotation approach is demonstrated in detail by the research findings provided in **A5**.

2.2.1. Molecular signature characteristics in the 96 hpf zebrafish embryo model

With the establishment of the OCED test guideline 236 for fish embryo toxicity (FET) tests, exposure studies with fertilized *D. rerio* eggs became a popular approach for chemical hazard assessment (Ton et al., 2006). According to the new EU Directive 2010/63/EU on the protection of animals used for scientific purposes, studies with non-human animal earliest life-stages are not considered animal tests until the organism is capable of independent feeding. For the zebrafish embryo, this is considered to occur after 120 hpf (Strähle et al., 2012). Yet the embryo already hatches and becomes a freely swimming larvae around 72 hpf. At this post-hatched eleutheroembryo stage, important organs like eyes, brain, heart, liver, gills or the digestive tract are already functionally developed. The 96 to 120 hpf developmental stage therefore allows to study the effect of chemicals within a miniature system of high functional complexity and

organelle-to-organelle interaction without being subject to regulations for animal experimentation (Strähle et al., 2012).

For both of the published research papers **A1** and **A2** a modified version of the zebrafish embryo toxicity test (OECD 236, 2013) coupled with ecotoxicogenomic methods was applied to identify characteristic fingerprints at the molecular level for a set of reference compounds. The overarching goal was to identify early responsive biomarker candidates and to functionally characterize the molecular responses in a defined model organism. Despite the advances of *omic* technologies to generate high content informative biological data, there is no cohesive approach to incorporate molecular level measurements into ecological or human health risk assessment up to this point (Brockmeier et al., 2017; Verheijen et al., 2022). More than a decade ago, Fent and Sumpter (2011) already pointed out that one of the key challenges to apply this technology to its full potential, is the lack of reliable links between the molecular responses and specific adverse effects of regulatory meaningful endpoints. To overcome this hurdle, molecular changes must be clearly linked to apical endpoints.

One of the main goals for this PhD study was therefore to evaluate ecotoxicogenomic signatures for a set of reference chemicals (**Table 1**) in the zebrafish embryo model. To identify early and ideally MoA-specific molecular responses for a tested compound, special focus must be given to the selection of sublethal test concentrations. An optimal range of test concentrations covers (a) the first (early responsive) gene expression changes to (b) minor effects not related to systemic toxicity. Therefore, for the lower test concentrations (a) no physiologically observable effects should be present. To allow for the differentiation of different adverse effects at the molecular level, it is crucial that the test concentrations for exotoxicogenomic profiling do not induce systemic toxicity in the organism. As shown and discussed in **A2**, high exposure related stress levels could result in a more general stress response, which would not allow to differentiate primary molecular key events among the different tested reference chemicals.

To ensure that the exposure experiments were performed within the appropriate concentration range, first the preliminary acute toxicity data were collected from the United States Environmental Protection Agency (EPA) ECOTOXicology Knowledgebase (ECOTOX). Using *standaRtox* (Scharmüller et al., 2020), a novel harmonized ecotoxicological data mining tool, the ECOTOX database could be effectively screened for prior toxicity data (**S.Figure 1**). The tool is extremely versatile and allows to derive single aggregated toxicity values for a specified chemical-taxonomic-group test combination.

Table 1: Overview of active compounds and their associated MoA (with respect to the target system) for which ecotoxicogenomic profiles were obtained from 96 hpf zebrafish embryos in a modified version of the OECD 236 zebrafish embryo toxicity test described in publications **A1** and **A2**. The different sublethal nominal test concentrations are provided. In cases where less than 35 DEGs were identified in the low exposure treatment, middle range exposure samples were additionally sent for sequencing and subjected to DGEA. Substance tests marked with '*', represent additionally unpublished datasets for this PhD thesis.

					Nominal test concentrations [µg/L]		
Substance	**CAS**	**Target Group**	**MoA**	**Chem. Subgroup**	**Low**	**Mid**	**High**
Abamectin	71751-41-2	Neurotoxin (Insecticide)	Glutamate gated chloride channel modulator	Avermectin	110	220	440
Carbaryl	63-25-2	Neurotoxin (Insecticide)	AChE inhibitor	Carbamate	1 100	-	275
Chlorpyrifos	2921-88-2	Neurotoxin (Insecticide)	AChE inhibitor	Organophosphate	3 000	-	750
Imidacloprid	138261-41-3	Neurotoxin (Insecticide)	nAChR competitive modulator	Neonicotinoid	15 000	30 000	60 000
Methoxychlor	72-43-5	Neurotoxin (Insecticide)	Sodium channel modulator	Chlorinated diphenylmethane	180	20	60
Fipronil	120068-37-3	Neurotoxin (Insecticide)	GABA gated chloride channel antagonist	Phenylpyrazole	30	300	75
Fenazaquin*	120928-09-8	Respiratory inhib. (Insecticide)	Mitochondrial complex I inhibitor	Quinazolines	3	-	6
Fenbutatinoxide*	13356-08-6	Respiratory inhib. (Insecticide)	Mitochondrial ATP synthase inhibition	Organotin	225	450	900
Pyriproxyfen*	95737-68-1	Growth inhib. (Insecticide)	Juvenile hormone mimics	Pyridine	170	-	1 700
6-PTU	51-52-5	Thyreostaticum	Thyroid hormone synthesis inhibitor	Thiourea derivative	1 000	10 000	100 000
T3	6893-02-3	Thyreostaticum	Nuclear thyroid hormone receptor activator	Thyroid hormone	3,3	-	327
Ethinylestradiol*	57-63-6	Synthetic oestrogen	Oestrogen receptor agonist	Estrogenic hormone	20	-	200
Flutamid*	13311-84-7	Cytostaticum	Androgen receptor antagonism (anti-androgen)	Amide of propionic acid	200	-	2 000
Methyltestosterone*	58-18-4	Synthetic testosterone	Androgen receptor agonism	Androgenic hormone	1 600	-	3 200
Tamoxifen*	10540-29-1	Selective estrogen receptor modulation	Partial estrogen receptor agonist (mixed estrogenic & antiestrogenic activity)	Triphenylethylene	50	-	500

*: Additional yet unpublished datasets used for toxicogenomic signature comparison in **Figure 7** and **Figure 8**.

Based on this prior knowledge, preliminary range finding experiments were conducted to verify or, if necessary, adjust to appropriate sublethal test concentrations (**S.Figure 2**). The tested reference chemicals shown in **Table 1** resemble well studied active compounds with well-defined target sites in the system or specific pre-defined MoA. The zebrafish is hereby an ideal model organism to explore different *omic* application methodologies to its fullest potential. Thanks to the high level of conserved molecular functions to humans and mice, *D. rerio* also became a very popular model organism for developmental biology and human health research in recent years (Choi et al., 2021; Dooley, 2000; Patton et al., 2021; Phillips and Westerfield, 2014). This small aquatic vertebrate showed to be a reliable model for studying e.g. cancer (Feitsma and Cuppen, 2008; Hason and Bartůněk, 2019) and a variety of cardiovascular (Bowley et al., 2022; Giardoglou and Beis, 2019) or neurodegenerative diseases (Klarić et al., 2014; Pitchai et al., 2019).

This resulted in the comfortable situation where a well-established and thoroughly studied model organism in ecotoxicology comes with a complete and functionally excellently annotated reference genome and proteome. Further, this vertebrate species is largely supported by a variety of systems biology databases (e.g. KEGG Pathways, Reactome Pathways, Panther Gene Ontologies, …), which allows to study molecular interactions at a biologically better interpretable functional level. Therefore, the zebrafish embryo was the ideal system for a first proof-of-principle study, evaluating if ecotoxicogenomic methodologies can be used to identify and differentiate thyroid disrupting MoAs (**A1**). In a follow up study (**A2**) an identical experimental approach was applied to study molecular signatures of neuronal targeting compounds in this aquatic vertebrate non-target model. Both studies **A1** and **A2** addressed the question how the observed gene expression changes can explain apical endpoints described in previous literature. Ultimately, the generated ecotoxicogenomic profiles were screened for potential biomarkers with MoA-characteristic properties, which could predict known apical adverse effects.

2.2.1a Thyroid system and signalling disruption

In the kick-off study **A1**, during which most of the wet-lab workflow was developed, the goal was to identify toxicogenomic signatures for increased and decreased thyroid hormone signalling in zebrafish embryos. A variety of OECD test guidelines assessing thyroid disruption are currently applied to assess potential thyroid disrupting properties of a chemical in the well-studied amphibian model *Xenopus laevis* (@cite OECDs here). Nevertheless, there is an urgent demand for test systems assessing thyroid disruption in fish as illustrated by the Horizon

2020 ERGO project (https://ergo-project.eu/). In the long term, such novel test methods could be integrated e.g. in the Fish Early Life Stage test (FELS) (OECD 210), which is already requested by regulatory authorities for an assessment of chronic toxicity. Such an integration could therefore supersede the need for additional amphibian studies, which will significantly reduce the number of animal tests and consequently the time required for regulatory decision making. Hence, the investigation and establishment of reliable thyroid disrupting biomarkers in the zebrafish embryo model contributes important mechanistic insights for the development of thyroid disruption assays in fish.

For this purpose, the most active thyroid hormone 3,3′,5-triiodothyronine (T3) was selected as reference compound inducing enhanced thyroid hormone signalling (**Figure 4A & B**) (Gereben et al., 2008). On the opposite, 6-propyl-2-thiouracil (6-PTU), a known thyroid hormone synthesis inhibitor in mammals and aquatic vertebrates (Baumann et al., 2016; Davidson et al., 1978; Nogimori et al., 1986), was chosen as reference substance to capture molecular signatures related to interference with thyroid hormone production and subsequent impaired signalling.

Although both compounds target the thyroidal system in a broader sense, their mechanisms of action are fundamentally different form each other. There are two principal molecular mechanisms through which a chemical can interfere with the vertebrate thyroid system: a) thyroid hormone action disruption (Boas et al., 2012) or b) thyroid gland function disruption (Thienpont et al., 2011). Mechanism a) is associated with direct thyroid receptor ligand binding and the subsequent thyroid signalling activation. As exemplary compound for this MoA the active form of thyroid hormone, T3. In contrast, mechanism b) is driven by the disruption of thyroid hormone homeostasis, which involves inhibition of enzymes for thyroid hormone synthesis or iodine uptake as well as their excretion, circulatory transport, cellular uptake and degradation (Baumann et al., 2016). Exemplary for this MoA is 6-PTU, which was shown to reduce T3 serum levels in mammals and fish alike (Gereben et al., 2008; Nogimori et al., 1986; Stinckens et al., 2016).

For mammals it has been described that 6-PTU reduces production of thyroid hormones by irreversibly inhibiting the thyroperoxidase (TPO) (Manna et al., 2013). As illustrated in **Figure 4A,** this hinders the TPO-mediated iodination of thyroglobulin (TG)-bound tyrosine residues within the thyroid follicle's colloid (Carvalho and Dupuy, 2017). Hence, appropriate functioning of TPO and homeostatic TG expression are, among other regulating factors, essential for maintaining the thyroidal system in vertebrates. However, as Manna et. al (2013) pointed out, it is worth noting that the MoA of thionamide-based anti-thyroid drugs is not fully

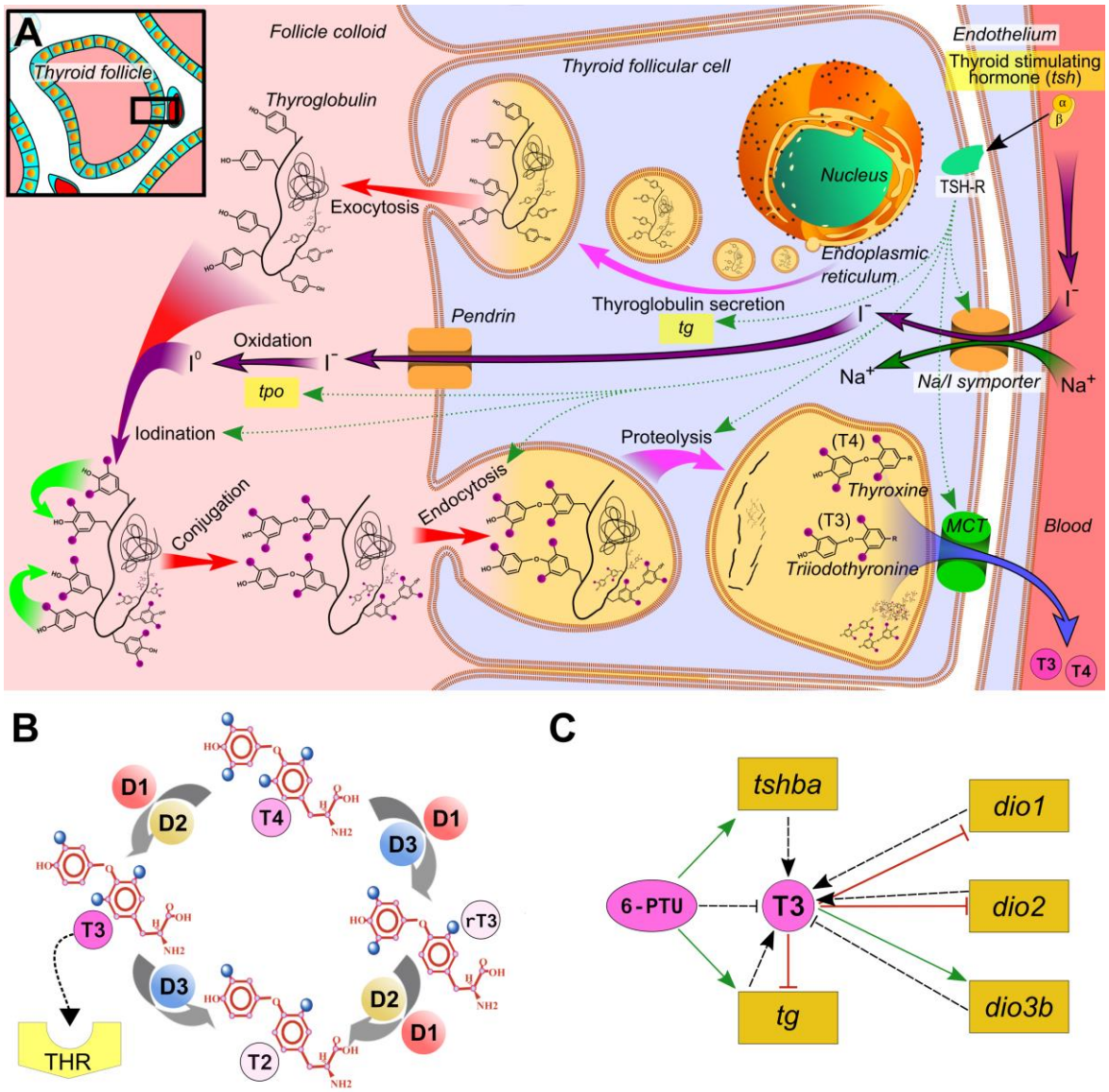

Figure 4: (A)[7] Thyroxine (T4) and triiodothyronine (T3) thyroid hormone synthesis process in thyroid follicle and regulating mechanisms of thyroid-stimulating-hormone receptor (TSH-R) (dashed green line = activation). Iodine from the bloodstream is imported into the thyroid follicular cell via Na/I-symporter complex and secreted into the follicle's colloid lumen where it is oxidized by thyroperoxidase (*tpo*). Thyroglobulin (*tg*) is transcribed and translated from the nucleus genome an secreted via exocytosis in into the colloid lumen as well. Oxidized iodine is then covalently bound to *tg* and the protein residues attached to the peptide chain are conjugated, forming the precursor version of thyroid hormone T3 and T4. Secreted into the blood stream, T3 induces thyroid hormone signalling cascades in the organism. **(B)**[8] Thyroid hormone transformation into different active states through deiodinase enzymes (DIO1 (D1), DIO2 (D2) and DIO3 (D3). The respective zebrafish orthologues are *dio1, dio2* and *dio3b*. D1 & D2 catalyse the mono-deiodination of T4 to T3, which is the most active thyroid hormone form, enhancing a variety of metabolic activities. The type 3 deiodinase (D3) catalyzes the deactivation of T3 into T2 or together with D1, the deactivation of T4 into reverse T3 (rT3). **(C)** Proposed gene expression regulation and interaction of T3 and 6-PTU in 96 hpf zebrafish embryos based on study A1. Colored lines show the observed interactions between the tested compounds and respective gene expression (Fig. 5). Dashed lines show interactions previously described in literature.

[7] Modified after: Walter and Boron (2003). Medical Physiology: A Cellular and Molecular Approaoch. p. 1300. ISBN 1-4160-2328-3

[8] Modified with permission from Bianco and Kim: J Clin Invest 116:2571–2579, 2006 (33). ©American Society for Clinical Investigation

understood yet. In consequence, the knowledge about 6-PTU's MoA in fish is even more limited than for mammals. Nevertheless, previous studies on juvenile zebrafish as young as 120 hpf do support the TPO inhibitory effect in fish (Baumann et al., 2016; Rehberger et al., 2018; Schmidt and Braunbeck, 2011; Stinckens et al., 2016). Therefore it was suggested that the observed decrease of T3 levels in zebrafish exposed to 6-PTU is the direct result of the fish's thyroperoxidase (*tpo*) inhibition. Stinckens et al. (2016) reported a decrease in whole body T3 serum levels while Rehberger et al. (2018) observed a concentration-dependent decrease in intrafollicular T3 and thyroxin (T4) in 120 hpf zebrafish embryos exposed to 6-PTU. Baumann et al. (2016) reported a significant upregulation of *tpo* transcripts in 120 hpf embryos exposed to sublethal 6-PTU concentrations. It was therefore concluded that, similar to mammals, 6-PTU decreases thyroid hormone levels in zebrafish by inhibiting *tpo* (Stinckens et al., 2020). This aligns with our RT-qPCR observations, which identified a significant upregulation of *tpo* expression for the highest exposure concentrations (8.39 mg/L 6-PTU) in 120 hpf embryos.

Interestingly, no corresponding ENSEMBL gene identifier for *tpo* (NCBI Gene ID: 569363) was found in the zebrafish ENSEMBL reference genome. Re-mapping of the raw sequencing files to NCBI's *Danio rerio* reference genome (GRCz11; RefSeq: GCF_000002035.6), containing *tpo*, returned a very low number of mapped reads to this transcript from the 96 hpf zebrafish embryo samples. In the control groups of study **A1** the count per million mapped reads (CPM) for *tpo* were well below 0.1 (mean: 0.083 ± 0.056; median: 0.075; n = 6). As low count numbers often co-occur with high relative signal variance which enhances the risk for a false-positive statistical result, it was previously suggested under the omics data analysis framework for regulatory application (R-ODAF) to exclude transcripts from the analysis with CPM < 1 (Verheijen et al., 2022). Under the R-ODAF, *tpo* would have been excluded from the transcriptomic dataset of 96 hpf embryos. Still, DGEA with *DESeq2*, did show a clear trend for the upregulation of *tpo* in the highest 96 hpf 6-PTU exposure condition (log2-fold change: 3.14±1.05; pvalue = 0.0002; padj (BH) = 0.0805), in accordance with our RT-qPCR results. These observed differences in detectability of *tpo* between the 96 and 120 hpf suggest that at 96 hpf the developing zebrafish does not express sufficiently high levels of *tpo* transcripts to be reliably analysed from whole embryo RNA extracts. The low *tpo* transcript abundance in 96 hpf stages cannot be explained by a lack of functionally developed thyroidal follicles as they form already at 55 hpf (Alt et al., 2006) and other thyroid follicle-specific transcripts such as thyroglobulin (*tg*) (Ma and Skeaff, 2014) (**Figure 4A**) were found in high copy numbers at 96 hpf across all RNA-sequence datasets (CPM mean: 21.2 ± 9.8; median: 20.2; n = 135). The

thyroid gland is considered fully functioning after the yolks sac has diminished and with it the maternal thyroid hormone supply which is usually around 120 hpf (Alt et al., 2006; Wendl et al., 2002). Hence, the lack of *tpo* expression in the 96 hpf compared to the 120 hpf stages might be related to this maturing process. Can the 96 hpf embryo model then still be considered as a sensitive and reliable model for assessing thyroid disruptive effects in an aquatic vertebrate? Based on the findings from study **A1**, as well as previous studies (Spaan et al., 2019), the answer is clearly yes.

Transcriptomic and proteomic analysis verified molecular signatures related to the thyroid regulating system. Important thyroid system-related genes (**Figure 5**) demonstrated significant differential expression in response to T3 and 6-PTU. Furthermore, molecular profiling showed distinguishable signatures at the transcriptomic (**A1 Figure 2**), proteomic (**A1 Figure 3**) as well as the functional systemic level (**Figure 7, Figure 8, A1 Figure 5**). At the individual molecular biomarker level, *tg* proves to be a promising candidate for predicting opposing thyroidal disrupting MoAs in zebrafish embryos. Thyroglobulin expression was found to be regulated in opposing direction in response to T3 and 6-PTU (**Figure 4C, Figure 5**). In mammals, thyroglobulin is considered a more sensitive biomarker for iodine deficiency than thyroidal hormones T3 and T4 (Carvalho and Dupuy, 2017; Ma and Skeaff, 2014). As illustrated in **Figure 4A**, *tg* transcripts are translated into the thyroglobulin glycoprotein, which is the precursor structure for thyroid hormone synthesis. The significant upregulation of *tg* and thyroid stimulating hormone subunit β (*thsba)* by 6-PTU verifies the embryos physiological response to low thyroid hormone levels. Thyroid stimulating hormones (TSH) are secreted from the anterior pituitary gland into the blood stream to regulate the endocrine function of the thyroid. It binds to the TSH receptor which induces a G-protein signalling cascade in the thyroid follicle cells enhancing thyroid hormone production and secretion (Szkudlinski et al., 2002). In accordance, T3 exposure consequently resulted in the opposite - a significantly decreased expression of *tg* (**Figure 5**). With this, the study A1 provides further weight-of-evidence for *tg* as sensitive biomarker in zebrafish for thyroid disruption as previously proposed by Spaan et al. (2019). Furthermore, *tg* has shown the capacity to differentiate different thyroid disrupting MoAs. Adverse effects leading to decreased T3 levels will result in an upregulation (demonstrated via 6-PTU), while enhanced T3 levels will lead to a downregulation of *tg* (**Figure 4C**).

Characteristic transcriptomic responses for low T3 levels were observed after 6-PTU exposure, without a considerable expression of *tpo* in 96 hpf embryos. This raised the question if thyroperoxidase inhibition is truly 6-PTU's primary MoA for decreased thyroid hormone levels

in fish. Most recently, attempts were made to describe molecular AOP frameworks for thyroid disruption in zebrafish based on compounds with presumably thyroperoxidase (*tpo*) and deiodinase inhibition potencies (Stinckens et al., 2020). It was suggested by the authors that 6-PTU leads to decreased whole body T3 concentrations, either through inhibition of thyroperoxidase-mediated thyroxine (T4) synthesis or via inhibition of deiodinase-mediated conversion of T4 to T3 via *dio1* and *dio2*. Deiodinases are essential thyroid hormone regulating enzymes, which convert thyroid hormones into different forms of activity (**Figure 4B**). For mammalian orthologues it is known that selenium containing DIO1 and DIO2 catalyse the removal of one iodine residue from T4 to form T3, the most active thyroid hormone (Gereben et al., 2008). On the other hand, DIO3 deactivates T3 into T2 or together with DIO1, catalyses the conversion of T4 to 3,3',5'-triiodothyronine, also known as reverse T3 (rT3) (Manna et al., 2013). The observed most sensitive deiodinase type marker to elevated T3 levels appeared to be *dio3b*, which was more than 16-fold increased in expression. Overall, T3 clearly regulated the expression of deiodinase genes (*dio1, dio2, dio3b*), to counteract high T3 hormone levels (**Figure 4B&C, Figure 5**). In contrast, 6-PTU did not induce any differential regulation of any deiodinase gene at 96 hpf. Yet *tg* and *tshba* were significantly upregulated (**Figure 5**) suggesting a lack of T3. Still, based on the RT-qPCR data from 120 hpf embryos a significant upregulation of *dio1* by 6-PTU was observed (**A1 – Fig.1C**). It was therefore concluded that the inhibition of *dio1* might not be the primary MoA of 6-PTU but rather a secondary response to low T3 levels.

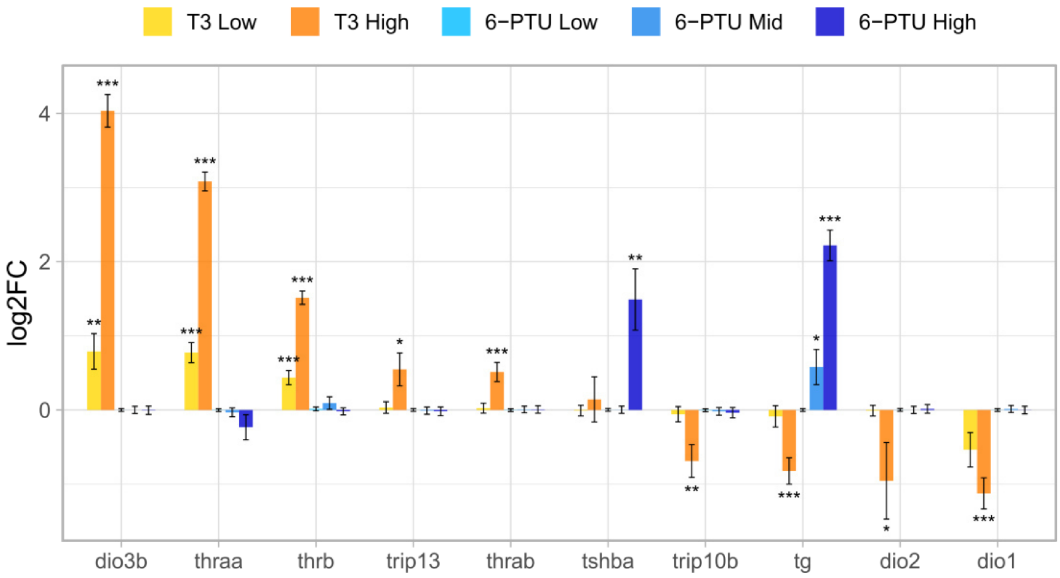

Figure 5: Expression changes (log2-fold change) of thyroid system related genes in 96 hpf zebrafish embryos exposed to sublethal concentrations of T3 (Low: 1.14 µg/L; High: 186.6 µg/L) and 6-PTU (Low: 1 mg/L, Mid: 8.39 mg/L; High: 108.81 mg/L). Statistically significant differentially expressed results with respect to the control group are indicated as follows: padj ≤ 0.001: ***; padj ≤ 0.01: **; padj ≤ 0.05: *. Thyroglobulin (*tg*) was the only thyroid related gene found to be significantly regulated in opposing directions for the two different tested thyroid disrupting MoAs.

To investigate molecular links between the obtained molecular thyroid disrupting signatures and physiological effects, an *upstream regulator* and *downstream effects analysis* (Qiagen Ingenuity Systems, 2014, 2011) was performed using the IPA® (Ingenuity Pathway Analysis) software. For the commonly targeted genes by T3 and 6-PTU (differentially expressed in at least one treatment condition), *upstream regulator analysis* identified T3 as the most relevant upstream regulator. This shows that the measured molecular fingerprints are not random patterns but can in fact be linked to a specific regulator. The IPA® model further predicted, among others, the thyroid hormone receptor beta (THRB) (**A1 Figure 5A**) to be an essential regulator for downstream effects. THRB was identified as upstream regulator for genes involved in muscle functioning and contraction. In fact, T3 induced the upregulation of three thyroid hormone receptor (THR) types: *thraa*, *thrb* and *thrab.* These findings align with recent findings from a toxicogenomic data mining approach, which identified THRB as core gene targeted by triphenyl phosphate, a potential endocrine disruptor affecting the thyroid system (Wang et al., 2021). The fact that no differential regulation of any thyroid hormone receptor appeared in the 6-PTU treatments, might explain why no impaired swim bladder development was observed in those treatments compared to T3 treatments at 120 hpf (**A1 – Fig.1B**).

In conclusion, the kick-off study **A1** provides evidence for primary thyroid hormone signalling targets in 4 days old zebrafish embryos. Based on the IPA® analysis, a considerable set of the compound-responsive genes is involved in muscle functioning and contraction, which aligns with previously proposed mechanisms for altered serum T3 levels leading to reduced swim bladder inflation (Robertson et al., 2007). Hence, the study provides weight-of-evidence for thyroid hormone-mediated impairment of genes involved in muscle functioning as a possible MKE for thyroid-related AOPs in fish based on the IPA's up- and downstream analysis predictions. However, overrepresentation analysis (ORA) for T3 and 6-PTU affected core DEGs did not find biological process GO terms directly associated with muscle contraction or development (**S.Figure 3**). In contrast, core DEG sets from neuronal targeting compounds such as fipronil or imidacloprid (**A2**) did show significantly enriched GO terms associated with muscle related processes (**S.Figure 3**).

The differences in the analysis results are most likely based on the different underlying databases and the type of analysis. IPA is a powerful and well established tool, performing data interpretation and predictions based on manually curated content of *Ingenuity Knowledge Base* (Qiagen Ingenuity Systems, 2014, 2011) optimized for human health research. Hence, the database compiles its information primarily from human- or mammal-related databases sources such as human Metabolome Database (HMDB), DrugBank, The Mouse Genome Database

(MGD) or humanCyc for metabolic pathway information. It is possible that IPA's database might contain more functionally described links which were not established yet for non-mammalian organisms in the gene ontology resource data banks (Carbon et al., 2019). Unfortunately, IPA is a non-open-source and time limited licenced software which results in annual high fees. The resulting expenses might be bearable in human health research areas but will exceed the cost-to-benefit ratio for less funded environmental research areas. As consequence and to further support science based on open-source tools, for the subsequent toxicogenomic profiling studies, functional enrichment or overrepresentation analysis were performed by the powerful *R* command line tools *clusterProfiler* (Wu et al., 2021; Yu et al., 2012) and *RecatomePA* (Yu and He, 2016). Using such freeware open-source tools does not only enhance the transparency and reproducibility of the data processing pipeline for other researchers, but also allows for high throughput data processing by the *R*-based programming language.

In summary, the study **A1** successfully demonstrated how ecotoxicogenomics can be applied to identify MoA specific biomarker candidates with the potential to differentiate among different thyroid disrupting MoAs. It was shown that the zebrafish embryo model is suitable for assessing thyroid disruption based on biomarker assays. The T3-induced signatures may be consulted to identify thyroid hormone receptor agonists, while 6-PTU-related molecular fingerprints can be assessed to identify substances directly interfering with thyroid hormone production. Limitations are that the primary target of 6-PTU in fish is not fully resolved yet. The study results suggest, that, similar to mammals, 6-PTU primarily targets the thyroid hormone production within the thyroid follicle. For future studies, directly decreased thyroid hormone signalling effects can be explored by toxicogenomic profiling of e.g. thyroid hormone receptor antagonists such as dronedarone or beraprost (Mackenzie, 2018). Molecular signatures for those proposed compounds will ultimately improve our mechanistic understanding further for the different types of thyroidal disruptive effects and will allow for the definition of robust biomarkers for a reliable differentiation of those MoAs. In the long term, such biomarker based improvements in early life-stage fish assays could replace previously used amphibian tests. This could reduce the total number of regulatory required animal tests as multiple critical endpoints might be evaluated with such biomarker based screenings.

2.2.1b Nerve- and muscle-targeting insecticides

To explore further MoA-related molecular signatures in the zebrafish embryo model, in the follow-up study toxicogenomic profiles of six nerve- and muscle targeting insecticides were

evaluated and potential neurotoxic biomarkers described (**A2**). In this study, the identical work-flow developed in A1, was applied to obtain compound-specific ecotoxicogenomic signatures after sublethal exposure to the six following insecticides: abamectin, carbaryl, chlorpyrifos, fipronil, imidacloprid and methoxychlor. With these compounds, the zebrafish embryo's ecotoxicogenomic profiles to glutamate-gated chloride channel (GluCls) modulation (abamectin), reversible and irreversible acetylcholine esterase inhibition (carbaryl and chlorpyrifos), GABA-gated chloride channel antagonism (fipronil) as well as nicotinic acetylcholine receptor (nAChR) (imidacloprid) and sodium channel modulation (methoxychlor) were compared. Although GluCls as direct target are only present in invertebrates, they are structurally highly similar to vertebrate glycine receptors (GlyRs) (Wolstenholme, 2012). Hence, the six compounds correspond to five different neuronal-signalling-targeting MoAs with respect to insects as the intended target system with possible similar target sites in vertebrates. The respective MoAs, pre-defined after the IRAC classification system (Sparks and Nauen, 2015), and nominal test concentrations are listed in **Table 1**. Furthermore, these reference compounds were selected, as previous studies demonstrated their neurotoxic effects in zebrafish (Glaberman et al., 2017; Gonçalves et al., 2020; Klüver et al., 2015).

Compounds affecting the nervous system are of particular concern as they pose significant risks to environmental organisms and humans alike. They have been associated with a variety of severe neuronal disorders in mammals (Amora and Giordani, 2018; Dörner and Plagemann, 2002; Iwaniuk et al., 2006; Rauh et al., 2015; Ton et al., 2006). Especially the early brain development and neurogenesis reflect a critically susceptible stage to neurotoxins in an organism's life (Perera and Herbstman, 2011). In contrast to that, zebrafish embryos were found to be less sensitive to neurotoxins with respect to acute lethal endpoints, compared to their adult life stage (Glaberman et al., 2017). This difference can be possibly explained by the fact that, in contrast to the adult life form, the embryo's oxygen supply can be still maintained through diffusion even when the circulatory oxygen transport is impaired (Klüver et al., 2015; Scholz et al., 2016). Hypoxic stress would be therefore much more lethal for adult organisms than for embryos. Hence, the determination of environmental safety levels for vulnerable early life stages based on acute lethal endpoints might not be sufficient. Previous studies demonstrated that the fish embryo model can be just as sensitive for sublethal endpoints (Klüver et al., 2015; Sanches et al., 2018). However, such sublethal neurotoxic developmental effects are still challenging to assess and to monitor as e.g. reliable biomarkers are still scarce. Therefore, the ecotoxicogenomic signatures in response to the five different nerve- and muscle-targeting MoA

were analysed to identify primarily affected biological processes from which biomarker candidates of neurotoxicity can be derived.

Similar to the kick-off study **A1**, although no physiological effects were visible in the lower exposure conditions to the insecticides (**S.Figure 2**), significant changes in embryo's gene expression profiles were observed. Also similar to **A1**, the number of DEGs as well as their effect size (log2-fold change) increased in a concentration-response like relationship with higher exposure levels. Across all investigate MoAs in study **A2**, more than 200 differentially expressed genes (DEGs) were identified in response to low levels of exposure (**Table 1**). From this set, a large fraction was found to be related to three major processes: (1) cardiac muscle cell development and functioning (*tcap, desma, bag3, hspb1, hspb8, flnca, myoz3a, mybpc2b, actc2, tnnt2c*), (2) oxygen transport and hypoxic stress (*alas2, hbbe1.1, hbbe1.3, hbbe2, hbae3, igfbp1a, hif1al*) and (3) neuronal development and plasticity (*npas4a, egr1, btg2, ier2a, vgf*) (**Figure 6**). Among those, essential regulatory genes for cardiac muscle (*tcap, actc2*) and forebrain development (*npas4a*) were frequently differentially expressed across all tested neurotoxic insecticide concentrations.

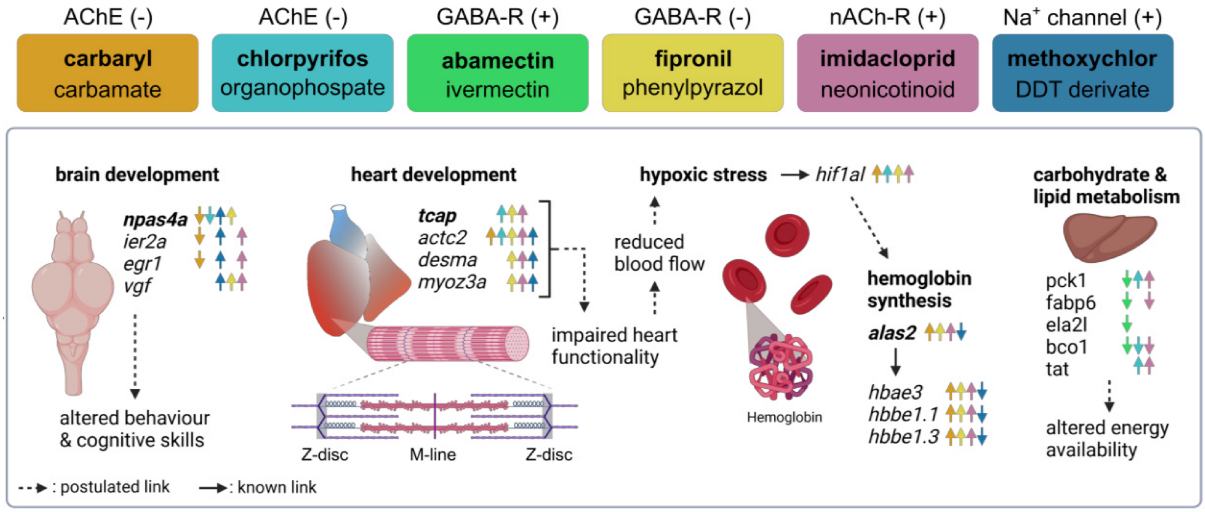

Figure 6: Selection of proposed early molecular biomarkers responsive to the exposure of the six nerve- and muscle targeting insecticides from study A2. The colored panels on top show the evaluated compounds while the respectively colored arrows next to the gene symbols indicate the observed significant up- or downregulation by the compound. Above the colored panels the compounds described targeted site with respect to the target organism is described. (+) resembles a receptor activation or channel opening. (-) resembles an inhibition or receptor blocking. Dashed arrows show the postulated links between differentially regulated gene sets and affected biological processes based on literature review. Solid arrows describe known well-established mechanistic links. The presented interactions could function as a baseline for developing novel AOPs.

Among the evaluated insecticides, abamectin showed the most diverging ecotoxicogenomic signature (**A2–Figure 2**) linked to metabolic and catabolic processes, especially in the context of lipid and olefinic compound processes (**A2–Figure 3**). As these processes are primarily

described for liver and kidney tissue (Hogstrand and Haux, 1991), the primary MoA of abamectin or its degradation products in the zebrafish embryo might be related to hepato- and nephro-toxic effects. This aligns with previous studies which demonstrated impaired kidney, liver and testis functioning in rats (Magdy et al., 2016) exposed to abamectin. Furthermore, a more recent study found ivermectin, a structurally highly similar compound, to reduce triglyceride accumulation and inhibition of lipogenesis related gene sets in human liver cells (Yang et al., 2019). The reported transcriptomic signatures post abamectin exposure could therefore provide potential biomarkers to identify hepatotoxic effects. However, this would require further studies in which transcriptomic signatures of particularly known hepatotoxic chemicals to the zebrafish must be evaluated and compared to those of abamectin.

Another interesting ecotoxicogenomic signature in 96 hpf zebrafish was observed for the neonicotinoid imidacloprid. A large fraction of imidacloprid's core DEG set as shown to be associated with immune and cytokine response processes as well as regulation of endopeptidase activity (**A2–Figure 3**). In insects, imidacloprid is designed to target the nicotinic acetylcholine receptor (nAChR) (Sparks and Nauen, 2015). In contrast to insects, where the cholinergic system is restricted to the central nervous system (Yamamoto, 1999), nAChRs in vertebrates are also found on the surface of immune system cells such as monocytes (Wang et al., 2003). There they were shown to function as important regulators in immune system homeostasis and inflammatory processes (Lu et al., 2014; Wang et al., 2003). Most recently, a novel nAChR with immune regulating functions was described in bivalves (Cao et al., 2021), suggesting a functional conservation across mammals, fish and aquatic molluscs alike. Hence, the presented differentially regulated immune and cytokine response-related gene sets can provide potential biomarkers to identify nAChR targeting MoAs in the zebrafish embryo model. It might be possible to expand such biomarkers for other vertebrates or even aquatic invertebrates. However the latter would require more in depth investigation on the level of nAChR signalling conservation between e.g. fish and bivales. In conclusion, the ecotoxicogenomic signatures of abamectin and imidacloprid in the 96 hpf zebrafish embryo demonstrated that pre-defined MoAs do not cover or describe all chemically induced effects for non-target organisms. Yet, these different, possibly adverse effects were identified on the ecotoxicogenomic level.

As described above, neurotoxic compounds are known to induce hypoxic stress in fish, for which the embryonic life stage is considered less sensitive with respect to acute lethal endpoints. However, the measured transcriptomic profiles (**A2**) did identify molecular responses to low oxygen levels after carbaryl, chlorpyrifos, imidacloprid and fipronil exposure. This suggests that for the tested sublethal test concentrations, the embryo is still experiencing

hypoxic stress, in the absence of physiological effects. In fact, gene set enrichment analysis (GSEA) verified a significant enrichment of biological process GO terms associated with oxygen transport and response to decreased oxygen levels for higher imidacloprid, fipronil and chlorpyrifos exposure levels. Despite, significant upregulation of classical hypoxic stress markers such as hypoxia inducible factor 1 subunit alpha like (*hif1al*) (Robertson et al., 2014) or insulin-like growth factor binding protein 1a (*igfbp1a*) (Kamei et al., 2008), a significant upregulation of embryonic haemoglobin (*hbbe1.3, hbbe1.1 & hbae3*) and aminolevulinate synthase 2 (*alas2*) coding genes was observed after the exposure to carbaryl, firponil and imidacloprid. While haemoglobins are essential for oxygen uptake and transport (Brownlie et al., 2003; Rombough and Drader, 2009), *alas2* is an enzyme involved in the haem biosynthetic pathway, primarily expressed in erythroid cells (Cox et al., 2004; Gardner et al., 1991). Interestingly, methoxychlor showed downregulated *alas2* transcript levels which consequently lead to downregulated haemoglobin transcript levels (**Figure 6**, **A2-Figure 2**). Hence, different nerve- and muscle targeting MoAs can have differing effects on the haemoglobin synthesis in 96 hpf zebrafish embryos. This could be potentially applied to differentiate such MoAs at the molecular level. Previous studies demonstrated an increase in haemoglobin in zebrafish embryos in response to extreme hypoxia (Rombough and Drader, 2009). As shown in **Figure 6**, a mechanistic link between the upregulation of classical hypoxia markers and the upregulation of haemoglobins in the zebrafish embryo as a response to neurotoxin-induced hypoxia was therefore proposed.

A plausible cause for insufficient oxygen supply in the developing zebrafish could be linked to an impaired circulation system. As discussed in **A2** in detail, a variety of previous studies in zebrafish, mammals and birds identified heart functioning and/or blood circulation impairment in response to the tested neurotoxic insecticides. This study provides molecular weight-of-evidence with potential molecular key events explaining these previously reported circulatory and cardiac effects. The compound specific core DEGs of especially chlorpyrifos, fipronil and imidacloprid, were associated with a large number of genes related to cardiac muscle cell development and functioning. For example, the human orthologues of *tcap, desma, bag3, hspb8, flnca, myoz3a, mybpc2b, actc2* (f.k.a. *zgc:86709*) and *tnnt2c* are all known biomarkers for hypertrophic and/or dilated cardiomyopathy (Dubińska-Magiera et al., 2020; Maron and Maron, 2013; Ojehomon et al., 2018; Vogel et al., 2009; Witjes et al., 2019). Among those, telethionin (*tcap*) expression was consistently significantly upregulated after all chlorpyrifos, fipronil and imidacloprid concentrations as well as high carbaryl and methoxychlor treatments. The human *TCAP* orthologue is localized in the Z-disc and interacts with muscle *LIM* protein

(*MLP*), which plays an essential role in stretch recognition of cardiomyocytes. Defects in this stretch recognition complex associated with heart failure (Knöll et al., 2002). Furthermore, *hspb8* and its interaction with co-chaperone BCL2-associated athanogene 3 *(bag3)* were shown to play a vital role in cardiac development in zebrafish similar to mammals (Dubińska-Magiera et al., 2020). Both *tcap* and *bag3* human orthologues are localized in the Z-disc of striated cardiac muscles where they play an essential role in stretch sensing for inducing heart contraction (Arimura et al., 2011; Domínguez et al., 2018). These observations suggest that the cardiac Z-disc structural development might be susceptible to a range of nerve- and muscle-targeting insecticides. Consequently, a dysfunctional Z-disk structure with impaired mechanical stretch sensing may impair the overall cardiac and blood circulatory function of the organism. If the cardiac development has been compromised due to chemical exposure during a vulnerable state, this can have long lasting effects even during adulthood. It was concluded that the observed upregulation of hypoxic stress markers and enhanced haemoglobin expression is a consequence of molecular key events leading to impaired myocardial development and function leading to a reduced blood flow. Consequently, the described cardiac-related biomarker candidates could be applied to identify possible heart development impairment as response to neurotoxic MoAs at an early molecular level and life-stage in the zebrafish. As these regulatory genes show high functional conservation among zebrafish and mammals (Bakkers, 2011; Bowley et al., 2022; Giardoglou and Beis, 2019; Narumanchi et al., 2021; Shi et al., 2018), it is possible that orthologues markers can be applied to other developing vertebrate models (e.g. birds) and for cross species comparison. A more detailed discussion on the above mentioned cardiac development and functioning biomarker candidates is provided in **A2**.

On top of the heart development related genes, many of the tested neurotoxic insecticides in study **A2** significantly altered the expression of important brain and neuronal development genes (**Figure 6**). Among those, *npas4a, egr1, btg2, ier2a* and *vgf* were identified as potential biomarkers for effects on the central nervous system in developing zebrafish. As discussed in **A2**, all of these genes, have crucial functions for neurogenesis and synaptic plasticity in the developing central nervous system. Furthermore, defects and altered expression levels for those genes were linked to altered organism behaviour in various previous studies (see discussion **A2**). The following will briefly cover *npas4a* and *vgf* due to their high levels of observed differential regulation among the tested insecticides as well as their molecular importance for brain development and functioning. A detailed discussion and functioning of those gene sets is provided in **A2**.

VGF nerve growth factor inducible (*vgf*) is a neuropeptide, which shows functional conservation across teleost, avian and mammal species and was recently reviewed as a neuroendocrine marker with major importance for seasonal energy balance regulation in multiple vertebrates (Helfer and Stevenson, 2020). It is induced through brain-derived neurotrophic and nerve growth factors. In humans, depression, schizophrenia and bipolar disorders were related to abnormal VGF levels in the brain, suggesting this gene to be a relevant contributor to the pathogenesis of mental illness (Alder et al., 2003; Bozdagi et al., 2008; Lin et al., 2015). Consequently, altered *vgf* levels in developing zebrafish could affect the animal's behaviour with possible long-term implications. The activity-dependent transcription factor neuronal PAS domain protein 4a (*npas4a*), was found in the core DEGs of methoxychlor, chlorpyrifos and carbaryl as well as higher fipronil exposure concentrations. As described in **A2**, multiple previous studies provide evidence that this gene is exclusively expressed in brain, where it functions as essential regulator of cerebral development, neurogenesis and synaptic plasticity in zebrafish and mammals. Human NPAS4A is considered a potential biomarker for forebrain development deficiencies and is functionally conserved between human, mouse and zebrafish orthologues (Klarić et al., 2014). The knockdown of *npas4a* was demonstrated to cause sensorimotor deficiencies and memory impairment, which were linked to abnormal forebrain development (Coutellier et al., 2012; Klarić et al., 2014; Lin et al., 2008; Ramamoorthi et al., 2011). More recently, altered *npas4a* expression levels in zebrafish were associated with differences in animal fear learning and behaviour (Baker and Wong, 2021; Torres-Hernández et al., 2016). Hence, an impairment of *npas4a* or *vgf* signalling during a vulnerable developmental stage through neurotoxic chemicals could lead to long-lasting effects at the organism as well as population level. Therefore *npas4a* and *vgf* were suggested as molecular biomarker for the zebrafish embryo model, to assess brain-related developmental neurotoxicity. In the study **A2**, *npas4a* demonstrated a significantly decrease expression in all AChE inhibitor (carbaryl and chlorpyrifos) treatments. In contrast, GABA-gated chloride channel inhibitor fipronil and sodium channel modulator methoxychlor led to its upregulation. Therefore, *npas4a* as neurotoxicity biomarker could even be applied to differentiate certain neurotoxic MoAs. As this is the first study to link altered *npas4a* expression levels to neurotoxic compound exposure, this proposal requires further investigation. Given their highly conserved functionality across teleost, avian, and mammalian species, these genes may represent suitable biomarkers for cross-species neurotoxicity assessment.

Despite the above suggested biomarker candidates for impaired heart and brain development, some of the potential biomarkers for altered thyroid hormone levels previously described in

study **A1** were also found to be differentially expressed. Significant upregulation of *dio3b* occurred in particular in all chlorpyrifos treatment groups as well as higher fipronil and imidacloprid exposures. In contrast, the middle and higher exposure concentrations of abamectin led to a depletion of *dio3b* expression. As elaborated above, (**Figure 4B**) *dio3b* is essential for the conversion of the active hormone signalling form T3 into less active T2. *dio3b* was found to respond highly sensitively to excessive T3 hormone levels with an upregulation (**Figure 5**), suggesting that chlorpyrifos, fipronil and imidacloprid might lead to enhanced T3 hormone levels or T3 hormone signalling. In fact, recent studies described molecular links between cholinergic signalling pathways and adverse thyroidal effects of chlorpyrifos in the zebrafish (Qiao et al., 2021). Furthermore, research findings in marine fish (Holzer et al., 2017) and mice (De Angelis et al., 2009) demonstrated a depletion of serum T3 levels post chlorpyrifos exposure. This suggests that the upregulation of *dio3b* is presumably a physiological response to elevated T3 hormone signalling. An enhanced *dio3b* consequently would counteract the serum T3 levels, explaining the observations by Holzer et al. (2017) and De Angelis et al. (2009). Furthermore, the expression of thyroid hormone receptor alpha (*thraa*) was also significantly enhanced in the higher chlorpyrifos treatments. Thyroid hormone receptors transcription factors activated through the binding of T3 (Vissenberg et al., 2015). In **A1**, the expression of *thraa* in zebrafish embryos was strongly upregulated by T3 exposure (**Figure 5**). A recent study found that a *thraa* mutation resulted in abnormal cardiac structure and overall impaired cardiac function in zebrafish (Han et al., 2021). This could be a functional link to the observed and previously discussed altered expression levels of heart development-related gene sets in the developing zebrafish. In conclusion, the study **A2** found thyroid disrupting biomarkers (*thraa* and *dio3b*) previously described in **A1** altered by different neuronal targeting insecticides. Deiodinase enzymes as well as thyroid hormone receptors are both essential proteins regulating cellular responses to T3 signalling in the organism's tissue outside the thyroid gland. Hence, the thyroid system-affecting property of chlorpyrifos is presumably based on thyroid hormone signalling disruption and not on thyroid gland disruption.

2.2.1c Cross-experiments functional profiles comparison

As demonstrated by study **A1** and **A2**, ecotoxicogenomics can provide molecular weight-of-evidence to explain physiological endpoints that were previously reported for the selected reference chemicals. Further, it could be shown that the applied *omic* methods coupled with the zebrafish embryo toxicity test allowed the identification of important biomarker candidates for certain adverse effects (e.g. thyroid signalling, heart development, brain development). The

developed bioinformatics workflow for DGEA and biomarker candidate selection was capable to identify previously described adverse effect-related biomarkers (e.g. *tg, vgf, tcap*), supporting the robustness of the workflow and analysed datasets. However, the final question to address here is if the overall high content ecotoxicogenomic data can be applied to differentiate compound-specific MoAs. Ideally, the generated molecular signatures can provide mechanistic insights into the toxic MoA and allow a chemical's hazard characterization.

To address this question, a cross experiment meta-analysis was performed to compare each reference substance's molecular signature at a biological functional level. In addition to the above discussed data sets, for this comparison also data from yet unpublished work was included to cover a wider range of investigated MoAs. Those transcriptomic datasets were generated analogous to the methods described in **A1** and **A2**. For the functional comparison, an overrepresentation analysis (ORA) was conducted based on the identified core DEGs from each of the reference substance shown in **Table 1**. These core DEG sets were tested for significantly enriched Reactome (**Figure 7**) and KEGG pathways (**Figure 8**) as well as GO terms for biological processes (**S.Figure 3**) and molecular functions (**S.Figure *4***) via *clusterProfiler* and *ReactomePA* as described in **A2**. The comparison for significantly overrepresented gene sets does not only facilitate the biological interpretability of expression data, but also allows to identify mechanistic similarities among different gene sets. As different genes can still affect the same biological process in a similar or closely related manner, such functional similarities could be missed at the gen or protein comparison level (Subramanian et al., 2005). Ideally such a comparison for enriched pre-defined functional terms would reflect a compounds MoA for the evaluated organism. Following this logic, one would expect to see more commonly shared enriched biological processes (GO BP), molecular functions (GO MF) or pathways (KEGG & Reactome) among compounds with more similar MoAs compared to those with more distant MoAs. For example, ACh signal targeting compounds would be expected to share more enriched terms with each other than with e.g. thyroid targeting compounds. However, there are two important constraints to this assumption.

Firstly, although sublethal test concentrations for ecotoxicogenomic profiling ideally reflect similar effect concentrations, the number of DEGs and consequently core DEGs can differ largely between different experiments. Different sizes in input gene lists for ORA will ultimately affect the overall number of significantly enriched terms. As shown in **Figure 7** and **Figure 8**, for substances with a very small number ($n < 15$) of identified core DEGs (e.g fenazaquin or pyriproxyfen), only very few pathways were found as significantly enriched. In contrast, a greater number of input genes for ORA does not automatically result in greater

numbers of significantly enriched terms (e.g. **Figure 7** flutamid vs imidacloprid). This difference could be explained by skewed annotation depths of different pathway or GO terms. Pathways / GO terms with important links to e.g. human diseases might be studied much more profoundly, leading to larger numbers of term-associated genes. Consequently, in turn such pathway or GO terms are more likely to be identified in an enrichment or overrepresentation analysis. Secondly, the pre-defined MoA may not necessarily be reflected in the test organism. Pharmaceuticals and especially insecticides were developed for a different target organism. Hence, the process-related ecotoxicogenomic signatures for the zebrafish embryo might differ from the intended MoA of the reference chemicals in the target organism.

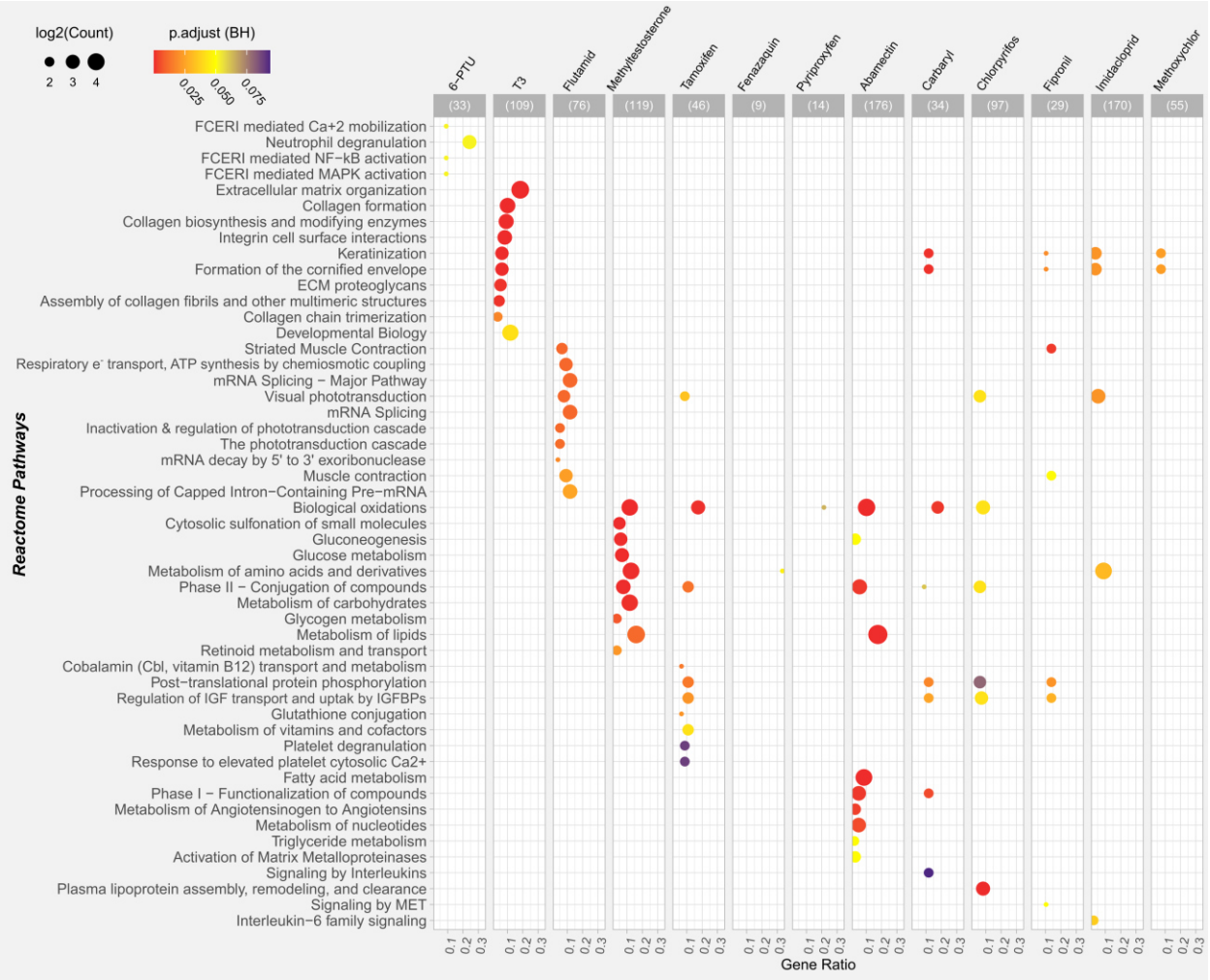

Figure 7: ORA results for significantly enriched reactome pathway terms from each compound's toxicogenomic core DEG set. In cases where DGEA was performed for more than two exposure conditions, the common DEGs among the two highest exposure conditions were chosen. For the representation, the top 10 most significantly expressed terms (BH padj < 0.1) from each compound were selected. If less than 10 terms were found significantly enriched only the significantly enriched are shown. If no terms were found enriched for a give compound, this compound is not presented in the figure. The x-axis of a dot plot shows the gene ratio for a given enriched term, while the dot size reflects the $\log_2$-transformed number of common genes between the input gene list and respective reactome pathway gene list. The dot colors correspond to the significance level of the result, showing highly

significant results in warmer colors (red) than less significant ones (blue). The numbers of above each panel give the total size of an input gene set for which the ORA was performed.

What can be observed throughout all ORA results for the different functional database types (Reactome, KEGG, GO-BP, GO-MF) is predominantly distinct sets of significantly enriched terms for each of the tested reference compounds. These compound-specific clusters are in particular prominent for significantly enriched biological process GO terms (**S.Figure 3**). Nevertheless, there are still some commonly affected processes among certain compounds, suggesting a more similar MoA in the zebrafish embryo for those. These commonly shared enriched term sets are especially prominent for the set of neuronal targeting compounds in the Reactome (**Figure 7**) and KEGG pathway (**Figure 8**) comparison. In contrast, the different endocrine active MoAs functional signatures show very little to none commonly affected pathways in the 96 hpf zebrafish embryo. E.g. T3, 6-PTU and methyltestosterone, an androgenic anabolic steroid, all display very distinct Reactome and KEGG pathway profiles. These observations suggest that a differentiation for different toxic MoA might be possible on the system functional level.

However, the observed distinctly affected functional profiles could also arise from systematic variance among different experiments. Although such a thought is worrisome, as it challenges the whole idea of applying ecotoxicogenomic signatures for chemical hazard assessment, it needs to be considered when interpreting the results. *Omic* methodologies are highly sensitive high-content measurements that can be dramatically influenced by various factors such as developmental stage of the organism (Schüttler et al., 2017), sample handling (Kellman et al., 2021) or data processing (Krassowski et al., 2020). When comparing multiple *omic* experiments one must be aware of such potential pitfalls and needs to ensure that sample handling and data processing was consistent throughout all comparison groups. For the comparison in this PhD thesis, all samples were obtained by the same consistent workflow. Therefore, the observed differences in affected molecular pathways were considered as a consequence of the different primary MoA and less as a result of experimental variability. This assumption aligns with most recently made observations, describing chemical group specific transcriptomic signatures for the zebrafish embryo model (Shankar et al., 2021). What further supports this assumption is that among the neuronal targeting compounds, especially carbaryl and chlorpyrifos share relatively large fraction of their enriched pathways. The MoA for both compounds in the target system is the acetyl choline esterase (AChE) inhibition. Interestingly, this similarity overlap is no longer present when comparing the significantly enriched GO terms for those two compounds. Consequently, this raises the question which functional comparison level (KEGG,

reactome, GO-MF, GO-BP) is the most suitable with the aim to differentiate adverse MoAs at the molecular signal level. The results presented here suggest, that KEGG and reactome pathways showed more shared enriched terms among functionally similar MoAs than biological process or molecular function GO terms. However, when it comes to returning significantly enriched results, it can be seen that KEGG and reactome comparisons are in a way "less sensitive". This means that fewer genes have associated reactome or KEGG pathways as compared to GO terms. Consequently, GO term-based comparisons will detect more enriched processes. However quantity is obviously not a measure for quality and one might need to consider carefully which database type to choose for their ORA.

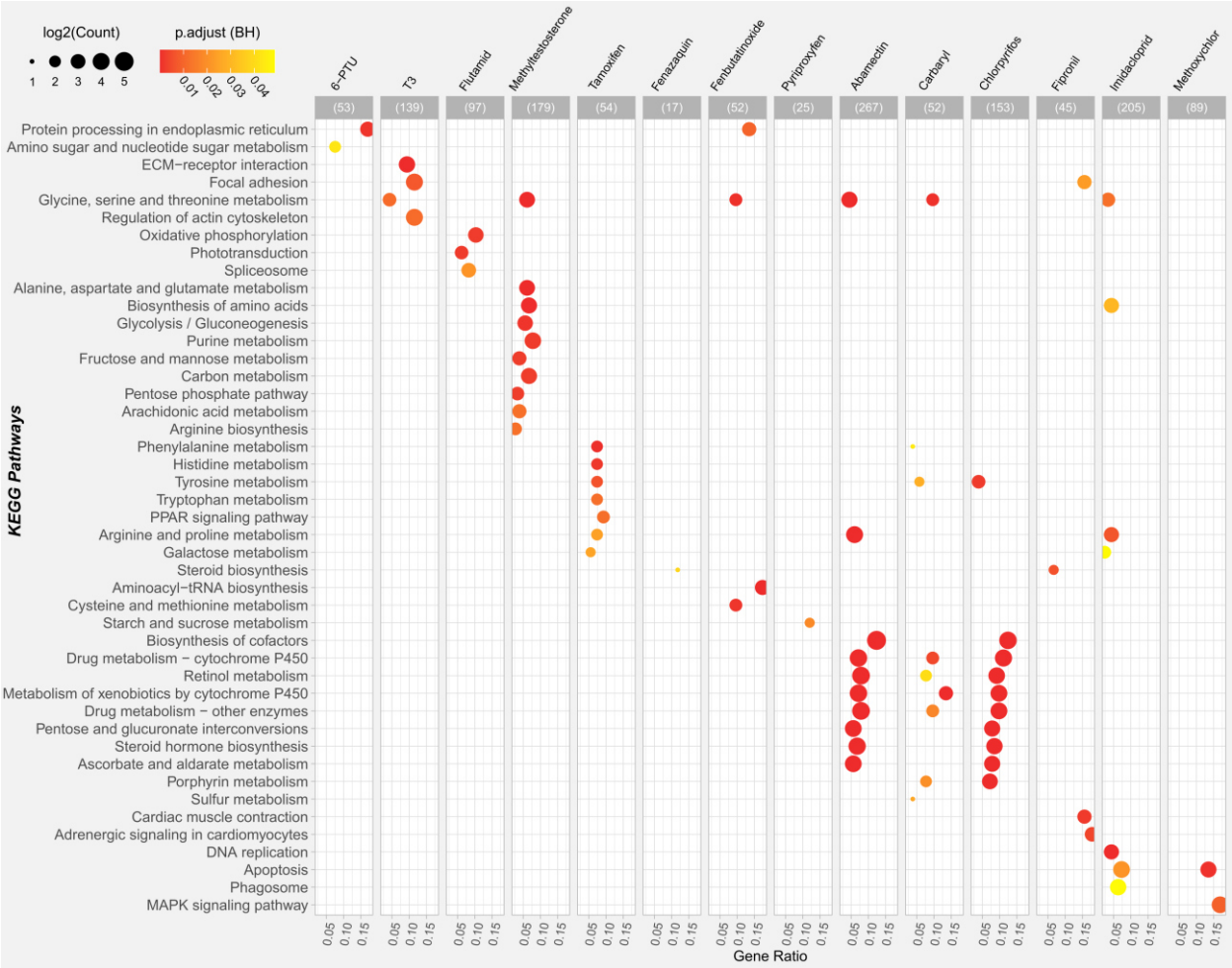

Figure 8: ORA results for significantly enriched KEGG pathway terms from each compound's toxicogenomic core DEG set. In cases where DGEA was performed for more than two exposure conditions, the common DEGs among the two highest exposure conditions were chosen. For the representation, the top 10 most significantly expressed terms (BH padj < 0.05) from each compound were selected. If less than 10 terms were found significantly enriched only the significantly enriched are shown. If no terms were found enriched for a give compound, this compound is not presented in the figure. The x-axis of a dot plot shows the gene ratio for a given enriched term, while the dot size reflects the $\log_2$-transformed number of common genes between the input gene list and respective KEGG pathway gene list. The dot colors correspond to the significance level of the result, showing highly significant results in warmer colors (red) than less significant ones (yellow). The numbers of above each panel give the total size of an input gene set for which the ORA was performed.

Overall, the tested substances displayed distinct functional profiles at the KEGG and reactome pathway level, with certain overlapping pathways for closely related MoAs (**Figure 7**, **Figure 8**). However, to ensure that these difference in pathway profiles actually arise from a compund's specific MoA and not from experimental differences, more data sets need to be generated and evaluated in a cross comparison. In particular more datasets for identical MoA would be required and ideally experiments should be repeated to verify that the obtained functional / pathways profiles are in fact reproducible and resemble robust MoA-specific signatures. Still, this is essential weight of evidence to further progress in the field of predictive toxicology. Future research can now use such ecotoxiocgenomic profiles to link this functional information with the chemical structure to build more informative and functional chemical hazard prediction models.

2.2.2. Transcriptomic immunosuppression signatures in early zebrafish embryos

Similar to endocrine or developmental toxicity, immunotoxicity represents a highly relevant adverse effect on an organism's health well below observable lethal endpoints. Immunotoxicity is defined as the adverse effects on the functioning of both local and systemic immune systems as a result of the exposure to toxic substances (Gulati and Ray, 2009). It is known now that certain environmental contaminating compounds have the potential to impair the immune system functioning of land mammals and organisms in the aquatic environment alike (Rehberger et al., 2017; Sánchez-Bayo and Goka, 2005; Selgrade, 2007). Chemical induced impairments on the immune system can lead to an enhanced risk for infectious, parasitic or neoplastic diseases (Sánchez-Bayo and Goka, 2005; Selgrade, 2007), which has far reaching consequences for a populations in any ecosystem. Despite its importance for the organism's health, immunotoxic hazard evaluations are rarely considered for ecotoxicological risk assessments (Rehberger et al., 2017). The EU Commission has acknowledged this issue and is eager to extend the generic risk assessment approach to immunotoxicity in the future (European Commission, 2020). However, the limiting factor for the EU's endeavour is that up to date there are no consistent approaches that allow a reliable evaluation of immune system impairments in aquatic vertebrates for ecotoxicoglocial hazard assessment. Further, there is a lack of clearly defined endpoints or robust markers, due to the complexity of the immune system coupled with a lack of understanding of its dynamics in ecotoxicological important model organisms (Rehberger et al., 2017). Hence, better mechanistic insights at the molecular level as well as robust immune system related biomarkers are desperately needed for a reliable screening of specific immunotoxic effects.

The study **A1** and **A2** in this work demonstrated that combining ecotoxicogenomic methods with standardized zebrafish embryo exposure experiments was a powerful method to identify molecular signatures and potential biomarkers related to a chemical's MoA. Experiences gained from these previous studies in optimal sample handling and appropriate bioinformatic data processing, gave us confidence that *omics* could be applied to identify specific mechanistic behind immunotoxic effects. These MoAs are however more challenging to assess as e.g. the evaluation of an immunosuppressive effect requires the activation of an immune system response to adequately quantify the level of impairment (Mottaz et al., 2017; Rehberger et al., 2017). Therefore in study **A3**, a novel experimental approach was developed to identify signatures for immune system impairment in early zebrafish embryos (48 hpf) on the gene expression level (**A3 – Figure 1**).

In mammals, four major MoA are distinguished through which a compound can induce immunotoxic effects: allergic reactions, auto-immune responses, developmental immunotoxicity and immunosuppressive reactions (Selgrade et al. 2008; Luster & Gerberick 2009). It was criticised by Rehberger et al. (2017) that in many previously perfomed fish immunotoxic assays, the rational for the choice of quantified parameters were not or only poorly reported. It was therefore often left unclear which of the suspected immunotoxic MoAs were associated with the studied chemical. Therefore it is pointed out here that, the experimental concept of study **A3** was based on the immune system-challenge approach, previously described by Hidasi et al. (2017) and Mottaz et al. (2017) to assess immunosuppressive effects in developing zebrafish. Their approach is based on a lethal hyper-stimulation of the innate immune response by bacterial lipopolysaccharides (LPS). When treated with an immuno-suppressant such as morphine or clobetasol propionate (CP), the mortality rate was shown to decrease in a concentration-dependent manner.

In contrast to the previous immune-challenge studies in zebrafish embryos (Hidasi et al., 2017; Mottaz et al., 2017), the approach presented in **A3** does not rely on quantifying survival rates and consequently no lethal hyper-stimulation. Instead, changes in the transcriptomic response to sublethal immune system stimulation with (CP^+) and without (CP^-) prior immunosuppressive CP treatment were analysed and compared. A major advantage of this ecotoxicogenomic study (**A3**) was that up to this point, potential biomarkers and molecular responses to chemical-induced immunosuppression in zebrafish have been limited to targeted gene analysis (Faltermann et al., 2020; Schmid and Fent, 2020; Willi et al., 2019). Using non-targeted transcriptomic analysis, allowed to investigate CP induced immunosuppressive effects in early

zebrafish much more profoundly under sub-lethal conditions. This enabled the detection of novel biomarker candidates critically involved in immunosuppression.

To induce a broader innate immune system response, organisms were challenged with pathogen-associated molecular patterns (PAMPs). These PAMPs reflect conserved motifs, associated with pathogen infection, which function as ligands for host pattern recognition molecules such as Toll-like receptors (Heise, 2014). Besides the broader immune response, another advantage of PAMPs over LPS is that it can be partially composed of synthetic compounds. This enhanced consistency in antigen motif composition is likely to improve the reproducibility and comparability of ecotoxicological immune challenge assays. The stimulation of the immune response in the early 48 hpf zebrafish embryos was induced via micro-injection of PAMPs into the blood stream. To control for the injection effect itself, all treatments were compared to a water injection CP free treatment (H_2O-CP^-). Transcriptomic profiling of immune challenge 48 hpf zebrafish embryos verified that PAMP injection (PAMP-CP^-) induced biological processes associated with innate immune system activity (van der Vaart et al., 2012; Yang et al., 2015). It is worth mentioning that this significant differences in gene expression profiles were quantifiable within few hours post PAMP injection. This underlines how fast-responsive molecular changes can occur on the gene expression level and how important it is therefore to rely on exact time intervals for sampling individuals for any ecotoxicogenomic study. The overall obtained expression patterns among all samples showed a clearly distinguishable clustering of sample groups, where the untreated control (NC) and the water injection control group (H_2O-CP^-) showed the least variance between their group centroids (**A3 – Figure 2A**). This demonstrated that the injection itself induced only minor effects in contrast to the CP treatment or PAMP injection. Interestingly, the differentially regulated genes between NC and H_2O-CP^- were associated with wound healing processes, underlining the robustness of the transcriptomic signatures in the obtained datasets.

Overall, a set of ten immune-regulating responsive biomarker candidates (*nr1d1, lyve1a, slc16a9b, mxc, c3a.6, olfm4, mfap4, lect2l, c3a.4 and cbln11*) were identified, which showed opposing regulation between the PAMP induced immune response (PAMP-CP^-) and only CP treatment (H_2O-CP^+). Among those, cerebellin 11 (*cbln11*), the complement proteins *c3a.4* and *ca3.6*, olfactomedin 4 (*olfm4*) and the myxovirus resistance C (*mxc*) gene are directly associated with relevant immune system processes in fish and other vertebrates (Coulthard and Woodruff, 2015; Liu and Rodgers, 2016; Lubbers et al., 2017; Mazurais et al., 2020). For example *mxc* gene has been reported to be strongly regulated in zebrafish of different life stages in response to viral RNA and thus has been used as positive control in studies dealing with viral infections

(Chen et al., 2015; García-Valtanen et al., 2014; Zhu et al., 2020). It is discussed in great detail in **A3**, how all of these ten genes play vital roles in immune defence regulating processes. In summary, the inversely regulated genes between PAMP-CP$^-$ and the H_2O-CP$^+$ resemble promising biomarker candidates at the gene expression level, which could allow to discriminate between an innate immune response and an immunosuppressive signature.

Compared to previous immune-challenge studies in the 96 hpf zebrafish embryo (Hidasi et al., 2017; Mottaz et al., 2017; Willi et al., 2019, 2018), our study used a much earlier developmental stage (48 hpf). Nevertheless, the observed gene expression patterns in response to CP exposure align well with previous findings as discussed in **A3**. For example the selected immune-system-related genes, *fkbp5, gilz, il17a, socs3, mmp9, per1a,* and *hsd11b2*, that were described as significantly upregulated in 96 hpf zebrafish by Willi et. al (2018), were also significantly upregulated in the 48 hpf stage of our study. This suggests that the innate immune response to an infection in the 48 hpf life-stage is functional and responds similar to as in 96 hpf zebrafish stages. The CP treatment alone (H_2O-CP$^+$) was also found be associated with immune system related processes (**A3 – Figure 3**), although some of the processes were significantly enriched exclusively in the PAMP-CP$^-$ treatments (e.g. MHC class antigen presentation, cytokine-mediated recognition). In general, only a small number of the infection responsive genes (PAMP-CP$^-$) were also differentially regulated by solely CP treated samples (H_2O-CP$^+$). These observations underline once more how important it is to consider immunosuppressive effects

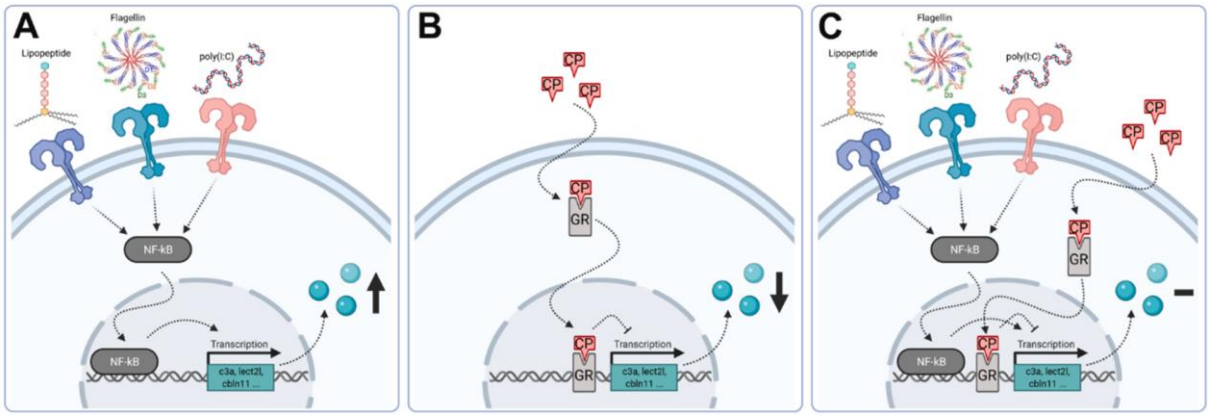

Figure 9: Conceptual model of clobetasol propionate (CP) effects on PAMP (pathogen associated molecular patterns) induced gene expression signalling in the zebrafish embryo, exemplarily shown for the observed NF-KB activation. NF-KB signalling is activated through antigen binding to an respective Toll-like receptor (TLR). Activated NF-KB migrates to the nucleus, where it binds to its recognition sites on DNA, where it activates the expression of immune-responsive genes. (B) Entering the cell, CP binds to and activates the glucocorticoid receptor (GR). The activated GR migrates to the nucleus, where it binds to its recognition sites on DNA, triggering a down-regulation of immune-responsive genes. (C) Activation of NF-KB by PAMPs and GR by CP leads to additive effects on their common immune-responsive target genes. For an opposing regulation by NF-KB and GR, the induced expression regulating effects act counter wise, leading to a net supressed expression of immune-responsive genes as shown in this figure. For cases of same-direction regulation, the effects were observed to be additively enhanced (not shown in figure).

in the context of an actual immune stimulation, which could be underestimated otherwise (Rehberger et al., 2017). This is why the study was also designed to investigate the transcriptomic effects of a PAMP induced immune signal under CP treatment (PAMP-CP$^+$), which is necessary to identify specifically the effects of a suppressed innate immune response after the CP treatment.

For this reason the 76 DEGs from the PAMP-CP$^-$ were investigated more closely by comparing the expression patterns in H_2O-CP$^+$ and PAMP-CP$^+$ (**A3- Figure 4**). Genes with an enhanced upregulation (log_2-fold change = lfc) prior CP treatment than by PAMP injection alone were defined as hyper-responsive to CP ($lfc_{PAMP\text{-}CP(+)}$ / $lfc_{PAMP\text{-}CP(-)} \geq 1.5$). Respectively, a suppressed regulation through CP in comparison to the PAMP treatment was defined as hypo-responsive to CP ($lfc_{PAMP\text{-}CP(-)}$ / $lfc_{PAMP\text{-}CP(+)} \geq 1.5$). The so identified hypo-responsive gene sets reflect the potential immunosuppressive mechanisms of CP. In almost all cases of these analysed 76 genes, the observed expression level in PAMP-CP$^+$ treatments appeared to be the result of an additive effect between the PAMP (PAMP-CP$^-$) and CP (H_2O-CP$^+$) conditions. As illustrated in **Figure 9**, this suggests independent regulatory mechanisms between CP and the innate immune response in zebrafish embryos, which can add-up to result in an adverse immune-related effect such as immunosuppression. Still our study shows that CP can also lead to an enhanced stimulation on the expression of certain infection responsive genes. However these particular gene sets were primarily associated with xenobiotic processing GO terms. In contrast, the identified hypo-responsive sets were significantly involved in immune and defence response to biotic stimuli (GO:0006952, GO:0006952, GO:0043207, GO:0009607) and in the antigen processing and presentation process (GO:0002474, GO:0048002, GO:0019882) (**A3 – Figure 5**). Interestingly, the common set of immune system related DEGs between PAMP-CP$^-$ and H20-CP$^+$ treatments, (*nr1d1, lyve1a, c3a.6, olfm4, c3a.4, cbln11* and *mfap4*), were all hypo-responsive (**A3** - Figure 4C). For *lyve1a* (lymphatic vessel endothelial hyaluronic receptor 1a) and *slc16a9b* (solute carrier family 16 member 9b) this additive effect was especially prominent and lead to an inverted expression by the CP treated PAMP stimulated groups (PAMP-CP$^+$). *lyve1a* is a homologue of the CD44 glycoprotein and mediates immune cell entry and trafficking in the lymphatic system (Johnson and Jackson, 2021). *slc16a9b* codes for a pH-sensitive creatine transporter (Futagi et al., 2020), while creatine metabolism has been previously shown to play multiple roles in the immune system (Kazak and Cohen, 2020). Hence, the identified

hypo-responsive gene sets are promising biomarker candidates for evaluating immunosuppressive effects in fish, which is discussed in further detail in **A3**.

In summary, study **A3** demonstrated that in zebrafish, the early 48 hpf life-stage is similarly suitable for assessing immunosuppressive effects on the molecular level compared to previously applied 96 hpf life-stages. Further it showed that the proposed sublethal immune-challenge approach coupled with ecotoxicogeomic methods is a powerful method for investigating molecular immunosuppression signatures and to derive sensitive MoA specific biomarker candidates. PAMP injection itself induced differential expression of genes associated with immune system activation while some of these genes were more differentially expressed upon prior exposure to CP than by immune induction alone, whereas others showed weaker or no differential regulation in response to the PAMP stimulus. Genes responding differently to PAMP post CP exposure showed additivity of PAMP- and CP-induced transcriptomic effects, indicating independent regulatory mechanisms as illustrated in **Figure 9**. The transcriptomic signatures suggest that CP's immunosuppressive effect on the innate immune response is primarily involved in antigen processing, TLR and NF-KB signalling as well as complement activation. Notably, our results argue for two independent mechanisms of gene expression regulation by PAMP stimulation and CP exposure rather than for an interconnection. Further, the study provided unprecedented mechanistic insights of additive chemical effects on the innate immune response for an early fish life-stage. These findings will help to improve and further develop currently established immunotoxicity assays based on molecular markers. Overall the described method in **A3** is a promising approach to improve our understanding of chemical effects on the fish's innate immune response and to identify immune-related biomarkers. Such biomarkers could help to establish assays capable of specifically predicting immunotoxic effects based on molecular signatures.

2.2.3. Integrating *omics* in acute toxicity assessements for *Daphnia magna* and *Lemna minor*

For a more holistic environmental hazards assessment approach, it is important to consider multiple trophic levels such as primary producers and primary consumers. The surface-floating macrophyte *Lemna minor* and the fresh water crustacean *Daphnia magna* are two exemplary organisms for such trophic levels and are well-established bioassay model organisms in aquatic ecotoxicology (Martins et al., 2007; Mkandawire et al., 2014). Toxicity tests with duckweeds (e.g. *Lemna* sp., *Spirodela* sp.) are one of the most standardized higher plant assays (Baudo et al., 2015; Mkandawire et al., 2014; Pietrini et al., 2022). In regulatory environmental hazard assessment for aquatic plants, an OECD-standardized 7-day growth inhibition test for the two

Lemna species *L. minor* and *L. gibba* is established (OECD 221, 2006). Adverse effects are evaluated based on frond number and frond area over the one week incubation time. On the other hand, two OECD guidelines are established for *Daphnia magna*, for the regulatory relevant aquatic invertebrate toxicity assessment of chemicals. One is the *Daphnia* sp. Acute Immobilization test (OECD 202, 2004) and the other the *D. magna* reproduction test (OECD 211, 2012). While the former assay evaluates acute toxicity after 48 hours of exposure based on immobility as a lethal endpoint, the latter test is applied to assess chronic toxicity over a period of 21 days using reproduction and lethality as endpoints. In both cases, the standard endpoints do not provide mechanistic insights on the observed adverse effects. For example, a quantified reduced frond area for *Lemna* sp. itself does not allow conclusions to be drawn about the underlying MoA of growth inhibition. Hence, these guideline tests are limited in terms of MoA classification of tests substances. Furthermore, the chronic toxicity test with *Daphnia* sp. as well as the growth inhibition test with *Lemna* sp. are both time-intensive bioassays, which hinders the development of high-throughput screening approaches. A possible solution in the future could be a molecular biomarker-based screening. It would allow for a more informative and quicker readout, compared to classical endpoints. The later aspect is especially relevant with respect to morphological endpoints in plants. Although *Lemna* sp. is fast growing compared to other aquatic macrophytes (Baudo et al., 2015), quantitative measures in plant morphology like frond area takes several days. Molecular stress responses such as altered gene expression can be detected within a few hours as shown in **A3**.

For developing molecular biomarker-based screenings with the capacity to differentiate different MoAs, one must first define suitable biomarker candidates for those aquatic invertebrate and plant model organisms. This requires the capability to functionally interpret and characterize molecular signatures, which can quickly become a challenging task if an organism is poorly annotated. In this context, study **A4** and **A5** were conducted to establish a methodology for assessing and functionally interpreting ecotoxicogenomic signatures in *D. magna* and *L. minor*. Despite the major relevance of *D. magna* and *L. minor* for aquatic ecotoxicology, it was only until recent years that the first draft genomes for those organisms were published (Orsini et al., 2016; Van Hoeck et al., 2015). Although having a reference genome is the first and probably most important step in transcriptomic or proteomic data analysis, it provides only very little biological insight if the genes have no or only very little functional annotation. As shown in **Table 2**, both organism and especially *L. minor* lack important descriptive or functional annotation. Without the linkage of a gene identifier with e.g. its associated pathways or GO terms it is impossible to perform functional enrichment or

overrepresentation analysis that would provide more biological relevant information. Fortunately, major technological advances were made in recent years which significantly facilitate functional gene annotation of unknown gene sets. A commonly used tool is EMBL's *eggNOG*-mapper[9] which performs functional annotation for large sequence sets based on phylogenetic orthology assignments (Huerta-Cepas et al., 2017). Since 2020, there is also a "all-in-one" cloud computational tool available called *Seq2Fun*[10] which enables researchers to quantify, functionally analyse and interpret their RNA-sequencing data without the need for a reference genome (Liu et al., 2021). However, given the novelty of this tool, *Seq2Fun* is neither widely used nor widely acknowledged in the scientific community yet.[11] Furthermore, it does not provide functional annotation support for proteomic data files. Therefore, the current state-of-the-art for functional systems biology analysis is to rely on curated available data base information (if available) or functionally annotate the reference genome e.g. based on sequence homology.

Table 2: Available features for transcriptomic/proteomic data analysis (e.g. reference genome or functional annotation types) for the three aquatic ecotoxicology model organisms investigate in this PhD study. Available features are marked with *x*. In study **A5** it is demonstrated how a custom reference proteome can be built from a reference genome for peptide spectra matching. Furthermore this study provides a detailed description for building a custom genome annotation package which allows for downstream functional analysis.

	Analysis feature	*Danio rerio*	*Daphnia magna*	*Lemna minor*
	Reference Genome	x	x	x
	Reference Proteome	x	x	custom
	Bioconductor AnnotationDbi OrgDb	x	custom	custom
	ENSEMBL Biomart	x	x	
	KEGG Pathway Db	x	x	
	Panther GO Db	x	x†	
	Reactome Db	x		
clusterProfiler ORA / GSEA	Gene Ontology (GO)	x	x*	x*
	KEGG Pathway	x		
	Reactome Pathway	x		

*: available through custom built annotation package †: only supports *D. pulex* but can be applied via gene orthologues

After the first release of the *Daphnia magna* reference genome in 2016, full RNA-sequencing transcriptomic studies gained popularity for this invertebrate, assessing molecular stress

[9] http://eggnog-mapper.embl.de/
[10] https://www.seq2fun.ca/
[11] A google schoolar search (30.3.2022) for the term "seq2fun" found 2 studies applying this tool in their work. In contrast, the term "eggNOG mapper" returned more than 2000 studies.

responses to insecticides, fungicides, anticancer drugs, or microplastics (Coady et al., 2020; Orsini et al., 2016; Poulsen et al., 2021; Russo et al., 2018). In contrast, since the release of the first draft genome of *L. minor* in 2015, only small number of studies used this resource for ecotoxicogenomic studies (Li et al., 2022; Wang et al., 2016). Presumably it is the lack of functional annotation for the *L. minor* reference genome (**Table 2**), which hinders functional characterisation and interpretation of systems biology data and discourages researchers from ecotoxicogenomically studying this organism. This underlines the importance of the two final studies **A4** and **A5**, which demonstrated how these challenges can be overcome with currently available information while using open source tools. Especially the developed annotation workflow and built annotation *R* package for *L. minor* (**Figure 11**) from study **A5** is considered a major contribution for ecotoxicogenomic research and the scientific community.

2.2.3a Differentiating signatures of impaired GABA and ACh signalling in D. magna

To characterize the molecular responses of two differing neurotoxic MoAs in *D. magna*, transcriptomic profiling was coupled with a modified version of the Acute Immobilization test (OECD 202, 2004) as described in **A4**. Daphnids were exposed to two different concentrations of the GABA-gated chloride channel blocker fipronil and the nAChR agonist imidacloprid. The selected exposure concentrations for transcriptomic profiling were based on preliminarily determined concentration-response relationships and correspond to the nominal EC5 and EC20 concentration (**S.Figure 5**) with immobility as endpoint. With the study **A4** the question was addressed if and how the different MoAs of fipronil and imidacloprid can be differentiated at the gene expression level. As discussed in **A4**, fipronil and imidacloprid both induce similar toxic effects through hyperexication in *D. magna.* However, these effects are triggered through different primary MoAs and consequently by different molecular initiating events. This makes these insecticides ideal model substances for our experimental approach to find MoA-characteristic molecular profiles which allow their differentiation.

The results showed that, although both insecticides induced similar observable paralytic effects in *D. magna*, the compound-specific transcriptomic signatures were distinct for each compound (**A4 – Figure 3**). For example, the gene orthologuous to the human dehydrogenase/reductase (SDR family) member 4 (DHRS4) was found significantly upregulated by imidacloprid and down-regulated by fipronil. In mammals, DHRS4 is known to be involved in retinoic acid synthesis (Endo et al., 2009), while the retinoic acid itself reduced GABA signalling (Sarti et al., 2013). More recently, a study with the honey bee *Apis mellifera* showed the effect of the neonicotinoid thiamethoxam on the retinoid system in bees (Gauthier et al., 2018). Hence, the

suppression of *dhrs4* by fipronil in *D. magna* could lead to decreased retinoic acid synthesis, which could be a physiological feedback mechanism to the GABA receptor blocking. These findings suggest that impaired ACh as well as impaired GABA signalling both affect the retinoic system in invertebrates. *dhrs4* was shown in this study as an opposing regulating biomarker candidate for *D. magna.*

A further detailed discussion of the study results is given in **A4**. In short, the majority of DEGs in the fipronil treatments were downregulated while imidacloprid preferably lead to an activation of the DEGs. This suggests that the observed toxicogenomic profiles could resemble MoA-specific signatures for the different targets involved in *D. magna.* To test this hypothesis, the obtained profiles were compared to previously described MoA related signatures (Fuertes et al., 2019; Orsini et al., 2016). Toxicogenomic fipronil signatures were compared to the positive allosteric modulator of GABA-gated chloride channels diazepam (Fuertes et al., 2019). In contrast to the negative modulation by fipronil, diazepam increases the GABA-gated chloride channel's conductivity for chloride ions, which inhibits further action potential signalling and results in a hypo-excitation state (Campo-Soria et al., 2006; Costa et al., 1978). On the other hand, imidacloprid signatures were compared to those reported by Orsini et al. (2016) for carbaryl. In this case, both compounds induce a similar effect of neuronal hyper-excitation through enhanced post-synaptic ACh signalling (Fukuto, 1990; IRAC, 2016; Matsuda et al., 2001). In accordance with their opposing MoAs, the comparison between fipronil and diazepam DEGs showed a negative correlation, while all upregulated DEGs by carbaryl were also upregulated for the imidacloprid treatments. Therefore, the identified gene sets in **A4** are likely to be specifically related to downstream effects of GABA-gated chloride channel blocking (fipronil) or activated acetylcholine signalling (imidacloprid) in *D. magna*. The distinct compound specific signature (core DEGs) was also reflected by specific molecular functions and pathways affected by the tested substances (**A4 – Figure 4**). As discussed in this study, a relevant proportion of impaired molecular functions and pathways identified as significantly enriched was consistent with the insecticde's MoA. Beyond the expected GABA-related signalling effects, the molecular signatures of fipronil suggested to affect lipid metabolism as well as moulting of the organism. These observations are in line with previous studies on physiological effects of fipronil on invertebrates (Al-Badran et al., 2018; Enell et al., 2010). For example it was shown that GABA can inhibit insulin signalling in *Drosophila melanogaster*. This provides a possible mechanistic link between GABA receptor blocking and lipid metabolic processes, as insulin was shown to play an important role in lipid metabolism (Saltiel and Kahn, 2001). While fipronil also interfered with molecular functions related to ATPase- coupled

transmembrane transport, imidacloprid predominantly affected oxidase and oxidoreductase activity related mechanisms. Again this aligns with previous observations of oxidative stress induction in *D. magna* (Jemec et al., 2007; Qi et al., 2018).

In conclusion, study **A4** provides important evidence that system biology approaches can be utilized to identify and differentiate chemical stressor MoAs in *D. magna*. Further, similar to the studies in zebrafish (**A1, A2, A3**), great emphasis was put on data transparency according to the FAIR data principals (Wilkinson et al., 2016). Hence, the generated transcriptomic datasets were made publicly available on ArrayExpress and reusable for the scientific community for comparative analysis or the development and refinement AOPs in *D. magna.*

2.2.3b The "lack of functional annotation"-problem and how to solve it

One of the major challenges in study **A4** was to find a suitable method for functional characterization of enriched gene sets, which improves the biological interpretation of *omic* data. A straight forward method was to use the web-based statistical enrichment test provided on the PANTHER classification system website[12] (Mi et al., 2019). Unfortunately, gene identifiers of *D. magna* are not supported by PANTHER in contrast to *D. pulex.* In consequence, orthologuous genes had to be mapped first from *D. magna* to the closely related *D. pulex*. As it turned out, the orthologues mapping via the *biomaRt R* package did not return similarity statistics for mapped orthologues, while the web-based ENSEMBL Biomart tool[13] did return a more comprehensive similarity statistic. Ultimately, an annotation table was generated to first map all *D. magna* genes to their orthologues *D. pulex* gene identifiers in all DGEA result tables before these files had to be manually uploaded onto PANTHER for GSEA. In consequence this approach is cumbersome and hinders high-throughput processing for large numbers of transcriptomic or proteomic datasets.

To perform ORA or GSEA for a large number of datasets, a command-line-suitable application would be preferable as it speeds up the analysis significantly and enhances reproducibility when source codes can be shared. For *R*-based analysis workflows, an *AnnotationDbi OrgDb* (Pagès et al., 2021) annotation package would be ideal as it allows an effective and fast command line-based annotation of gene identifiers with e.g. GO terms or gene descriptors. An *OrgDb* annotation data package is a SQLite-based object for *R,* which uses a central gene identifier for mappings between this identifier and other gene features (e.g. GO terms, other identifiers,

[12] http://pantherdb.org/
[13] http://mart.ensembl.org/biomart/martview/

descriptions, etc.). Currently, *OrgDb* annotation packages are available for only about 20 species (including *D.* rerio) [14]. Unfortunately, there are no *AnnotationDbi OrgDb* packages available neither for *D. magna* nor for *L. minor*. Without an *OrgDb* package, powerful command-line-based analysis tools such as *clusterProfiler* or *GOSemSim* (Yu, 2020) cannot be applied, as they require this database as backbone for their enrichment and overrepresentation analysis or for computing semantic similarities among GO terms. Hence, without an *OrgDb* annotation package, functional enrichment or overrepresentation analysis as demonstrated in **A2** with *D. rerio* cannot be applied. Therefore, the construction of a custom *OrgDb* annotation package for the organism of interest (**Figure 10**) highly facilitates the establishment of automated sample processing workflows. Further, the *OrgDb* package format can be easily distributed among researchers and simply installed in *R*, which enhances the reproducibility of analysis results. Once developed and installed, the *OrgDb* annotation package can be called into an *R* session whenever needed.

For *L. minor* there is nearly no functional genome or proteome annotation available. More than 22 300 genes are listed in the reference genome, for which approximately 15 000 expressed mRNA transcripts were observed (**A5 – S.Figure 7**). A Uniprot search for the taxon "*Lemna minor"* yielded only 157 described proteins (search date: 21.3.2022), which would only cover about 1 % of the expressed genes. This major lack of functional annotation and the fact that *L. minor* is neither supported by Biomart nor by PANTHER's GO database or KEGG pathways (**Table 2**), urged us to find a solution for a functional annotation of *L. minor*'s reference genome. Therefore, a reference genome annotation workflow was developed based on protein sequence homology predicted from the coding DNA regions (CDS). The workflow integrates two independent sequence alignment approaches using the protein basic local alignment search tool (*blastp*) algorithm (Camacho et al., 2009) and EMBL's fully automated *eggNOG*-mapper (Huerta-Cepas et al., 2017) (**Figure 10**). Both independent annotations, including the gene mapped GO terms, are integrated and used for the construction of an *OrgDb* annotation package for *R* via the *AnnotationForge* package (Carlson and Pagès, 2021). The integration of two independent search tools allows for a cross validation of the search results to enhance their reliability. The majority of the *blastp* search results for each predicted protein of the reference genome were associated with duckweed (79.02 %) or other plant related taxa (5.72 %). However, 15.26 % of the predicted mapped proteins were primarily associated with bacterial protein sequences, predominately for the genera of *Asticcacaulis* (Alphaproteobacteria), *Acinetobacter* and *Rhodanobacter* (Gammaproteobacteria) as well as

[14] https://bioconductor.org/packages/release/BiocViews.html#___OrgDb

Aquitalea (Betaproteobacteria) (**A5 – S.Figure 7 A1&A2**). This observation was also verified by the *eggNOG*-mapper search. All of these bacteria were previously reported as major bacterial community members and part of the microbiome living on or in close proximity to *L. minor* and other duckweeds (Acosta et al., 2020; Ishizawa et al., 2017). It is therefore likely, that these identified sequences in the reference genome reflect potential sequence contaminations from those microbiome-related prokaryotes. Alternatively, the endosymbiont theory might explain such highly bacteria-related sequences. As it cannot be differentiate, if a bacteria-mapped gene actually belongs to *L. minor* or corresponds to a contaminating sequence, it was decided to exclude these genes from the annotation. This will not have a relevant effect on downstream enrichment or overrepresentation analysis as the vast majority (99.52 %) of observed expressed genes from mRNA-sequencing (**A5**) were primarily related to duckweed (94.88 %; 14 548) or other plant (4.64 % ; 711) proteins (**A5 – S.Figure 7 B1&B2**). However, this duckweed-related

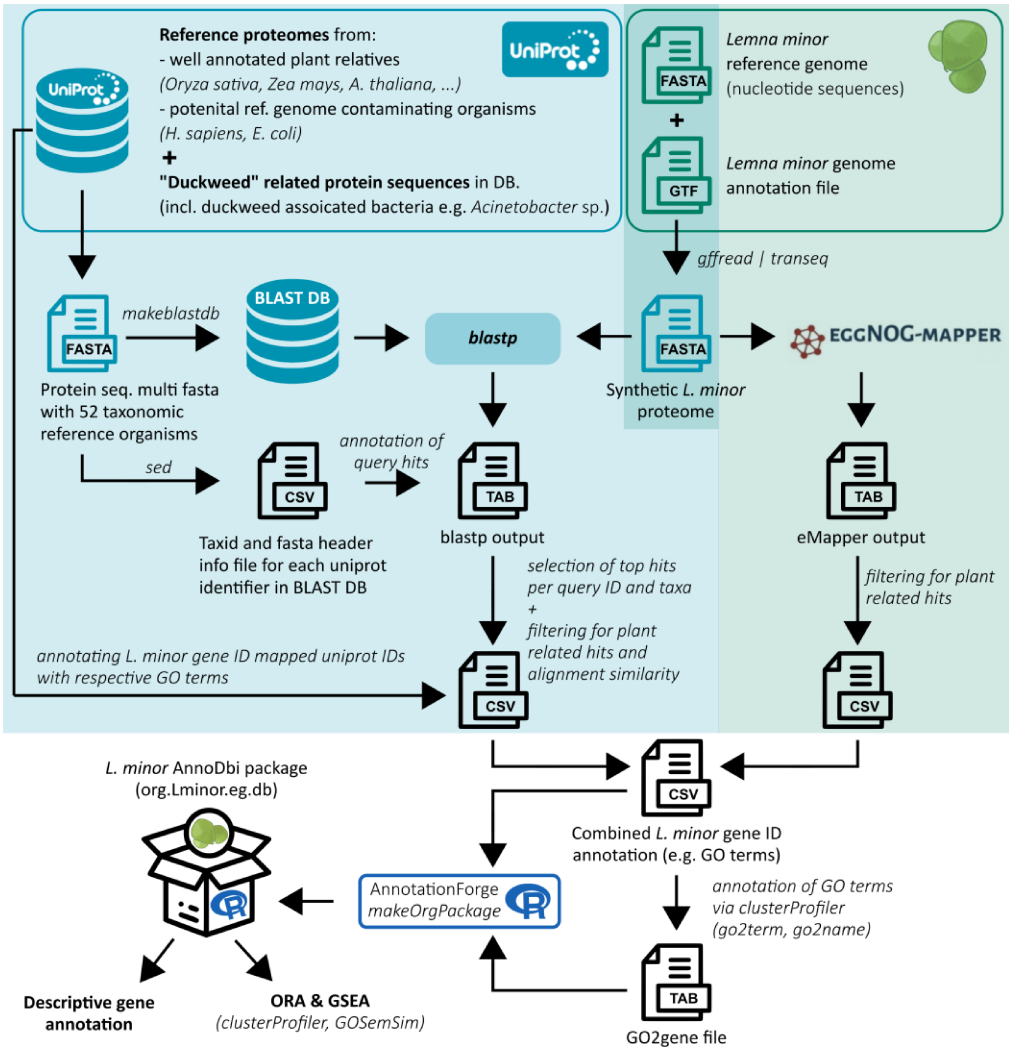

Figure 10: Custom functional annotation workflow to retrieve gene descriptions and related GO terms based on protein sequence homology. Two sequence mapping approaches are performed independently via *blastp* and *eggNOG*-mapper. Both search results can be cross validated before integrating their information for the construction of a Bioconductor *OrgDb* annotation package suitable for high-throughput downstream analysis in *R*. The here presented *org.Lminor.eg.db* package is publicly available on Zenodo under accession 6045874.

microbiota need to be considered when constructing a reference proteome, as these prokaryotes can contribute certain amount of proteins to the extracted *Lemna* protein sample.

Following the workflow shown in **Figure 10**, an annotation package (*org.Lminor.eg.db*) was built for *L. minor* and applied for the functional characterization of the ecotoxicogenomic signatures obtained in study **A5**. The only prerequisites for this workflow are 1) a reference genome, 2) a corresponding genome annotation file and 3) a set of well annotated reference organisms from which to retrieve functional annotation via *blastp* search. This package was able to annotate 99.8 % (15 278) of the quantified expressed genes in the transcriptomic datasets. Out of these, 93.4 % (14 267) were assigned to at least one GO term. Furthermore in this study (**A5**), the custom annotation database demonstrated its robustness in identifying clearly MoA-related biological processes and molecular functions for the tested compound's ecotoxicogenomic signatures (**Figure 11**). This underlines the robustness of the annotation approach and the applicability of this package for characterising transcriptomic or proteomic datasets at the biological process or molecular functional level. The *org.Lminor.eg.db* package, made publicly available (Zenodo: 6045874), will enable other research groups to functionally interpret ecotoxicogenomic datasets from *L. minor*. Further, the study **A5** provides a detailed description on how to build such an annotation package for poorly annotated model organisms. This blueprint may help bioinformatically experienced researchers to develop their own annotation package for their organism of interest.

2.2.3c Differentiating molecular growth inhibitor effects in a shortened L. minor assay

Similar to **A4**, the aim in study **A5** was to evaluate, whether ecotoxicogenomic profiling can also be applied in aquatic macrophytes to differentiate MoAs at the molecular level, which otherwise could not be differentiated with respect to classical endpoints. Relying on the *Lemna* sp. growth inhibition test (OECD 221) as framework for the standardized experimental setup, the additional goal was to assess if the bioassay can be abbreviated through the evaluation of molecular endpoints. As reference substances, the drug atorvastatin and the herbicide bentazon were first assessed via the standard 7 day growth inhibition test (OECD 221) to determine their EC5 and EC20 concentrations in *L. minor* (**A5 – Figure 1**, **A5 – Figure 2**). As quantitative measure and endpoint for these effect concentrations the frond area was evaluated. Subsequently, the determined effect concentrations were tested in a shortened 3 day exposure study to identify potential molecular key events leading to the observed impaired growth. Therefore, ecotoxicogenomic signatures were evaluated and characterized for their biological functions with the developed *org.Lminor.eg.db* annotation package. This allowed for a

differentiation of the different MoAs at the molecular functional level. While bentazon is a known herbicide designed to target the photosynthesis by inhibiting the photosystem II (PSII) (Mine and Matsunaka, 1975), atorvastatin is a statin (lipid-lowering) drug most commonly used in human medicine (Franzoni et al., 2003). Atorvastatin induces cholesterol- and lipid-lowering effects through the inhibition of 3-hydroxy-3-methyl-glutaryl-coenzyme A reductase (HMGR), which is a key enzyme in human cholesterol synthesis (Lennernäs, 2003). It was found that plants possess a functionally very similar HMGR which is involved in phytosterol synthesis through the mevalonic acid (MVA) pathway (Campos et al., 2014; Istvan, 2001). Previous studies already demonstrated a phytotoxic effect of atorvastatin in *L. gibba* (Brain et al., 2006). Interestingly, bentazon has also been associated with the inhibition of HMGR in the past (Grumbach and Bach, 1979).

It was demonstrated (**A5**) that both compounds induce growth inhibitory effects in *L. minor* through different molecular key mechanisms underlining the different primary MoAs of these compounds. Consistent with the findings of the previous studies (**A1**, **A2**, **A4**), a concentration-dependent increase of DEGs was observed. Again the common core DEGs were significantly positively correlated and showed generally greater changes in expression in response to the EC20 exposure compared to EC5. Two genes of the reference genome could be identified as possible HMGR orthologues in *L. minor*, Lminor_018294 and Lminor_013362. The predicted protein sequences for these genes showed high similarity levels with HMGR of the duckweed *Spirodela intermedia* A0A7I8KK04 (91.4 % and 88.5 % respectively). However, only Lminor_013362 was found as expressed based on the RNA-sequencing data with an average CPM of 65.8 ± 16.7 (median: 63.0; n = 18). Further, the expression of this gene was not significantly differentially regulated by the tested low effect concentration levels of atorvastatin or bentazon. Nevertheless, the *org.Lminor.eg.db* package enabled us to perform ORA with the identified core DEG sets of both compounds to characterize their associated biological processes and molecular functions.

As shown in **Figure 11**, the compound specific transcriptomic signature of both compounds showed very distinct affected biological processes and molecular functions. In accordance with its photosynthesis MoA, molecular signatures of bentazon were associated with biological processes related to light signalling and light response while atorvastatin demonstrated effects on the ethylene-activated or abscisic acid-activated signalling pathway as well as cellular lipid responses. The most significantly affected molecular functions by atorvastatin were lipase, phospholipase and oxidoreductase related functions, which is in line with the lipid-lowering MoA of the drug. In contrast, bentazon most significantly affected vitamin binding, electron

transfer or peptidase inhibitory activity related functions. How these observations align with previous research findings and support the robustness of the custom made annotation package for *L. minor* is discussed in great detail in **A5**.

Another important feature from this study for future ecotoxicogenomic studies on *L. minor* is the custom built and publicly available reference proteome (Zenodo: 6045874). It was constructed from the reference genome's predicted protein sequences and further included all "duckweed"-related search results from Uniprot as well as available protein sequences from duckweed associated microbiota (Acosta et al., 2020; Ishizawa et al., 2017). As it is technically challenging to extract protein from duckweed without simultaneous extraction of closely associated bacteria, the integrating of these prokaryotic protein sequences will help to differentiate the identified peptide spectra accordingly. This reduces the risk of falsely assigning a peptide spectrum obtained from a bacterial protein to a similar *L. minor* peptide spectrum. Further, as the reference proteome and the *org.Lminor.eg.db* annotation package share the same key identifiers it can be used to annotate proteomic and transcriptomic similarly. This allows a better harmonized *omics* dataset integration and consequently comparison. Up to this point, proteomic studies with *L. minor* were rather scarce, which is presumably due to the lack of functional annotation and a comprehensive reference proteome. A previous study by Su et al. (2019) investigated proteomic responses in *L. minor* aluminium stress. However, their protein spectra identification database was not designed from the reference genome and did not include prokaryotic sequences for a differentiation of identified proteins. In their case they used a compilation of available *Araceae* protein sequences. Unfortunately, in this manuscript the description of the database construction is insufficient and the developed database was not made publicly available. Therefore, the constructed *L. minor* reference proteome of this work (**A5**) is considered a major improvement for future proteomic studies in this important aquatic macrophyte.

In summary, study **A5** provides major contributions for studying ecotoxicogenomic responses in *L. minor*. Besides the development of an easy-to-use *R* annotation package, allowing researchers to perform powerful downstream enrichment and overrepresentation analysis with previously undescribed gene sets, this study also provides the research community with a suitable reference proteome for *L. minor*. Using these resources, a shortened three-day growth inhibition assay could be established, which allowed MoA characterization of test compounds based on gene expression signatures, which goes well beyond the classical endpoints of the OECD 221. As ecotoxicogenomic signatures were observed even at very low effect concentrations (EC5), study **A5** demonstrated once again the high sensitivity and informative

content of *omic* studies in ecotoxicology. The compound-specific molecular fingerprints were differentiated at a molecular mechanistic level enhancing our understanding behind different MoAs leading to impaired growth rates in aquatic macrophytes.

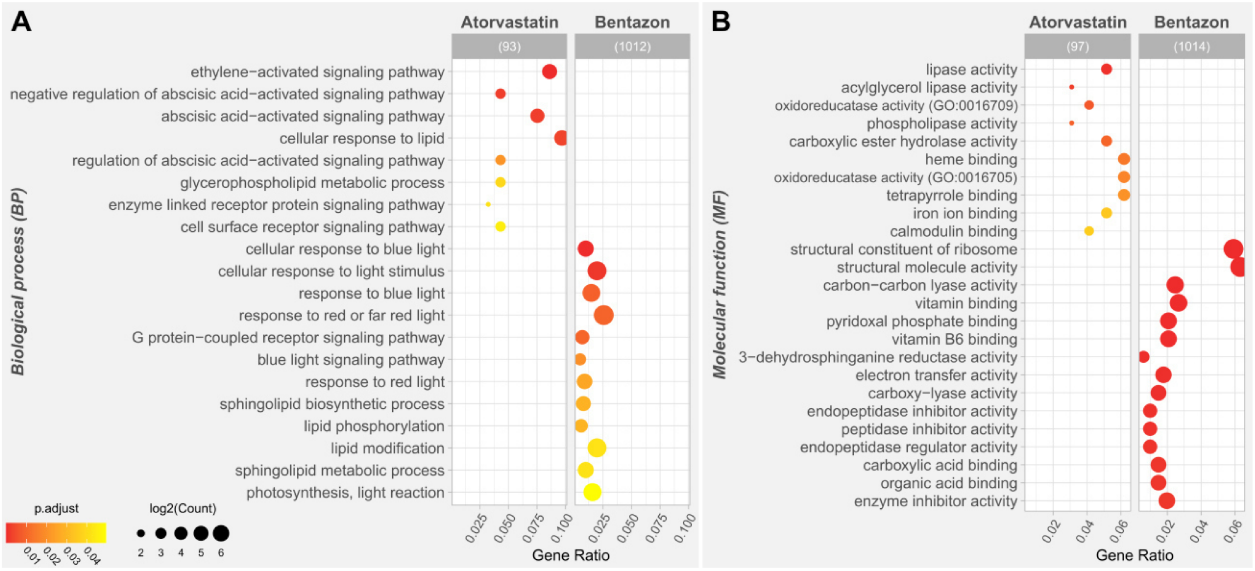

Figure 11: Significantly enriched GO terms (BH padj < 0.05) after overrepresentation analysis (ORA) with the core DEG sets of *Lemna minor* exposed to atorvastatin and bentazon. (A) shows affected biological processes, while (B) shows the affected molecular functions. For (A) the significant results were filtered for processes "light", "lipid" and "pathway" associated terms, while (B) shows the 15 most significantly enriched molecular functions for each compound. If less than 15 terms were significantly enriched, only those are shown. The x-axis shows the gene ratio for a given enriched term, while the dot size reflects the log2-transformed number of common genes between the input gene list and respective GO term related gene list. The dot colors correspond to the significance level of the result, showing highly significant results in warmer colors (red) than less significant ones (yellow). The numbers of above each panel give the total size of an input gene set for which the ORA was performed.

2.3. CURRENT CHALLENGES AND FUTURE STEPS

This PhD work has demonstrated the power of systems biology studies in ecotoxicology as a sensitive method to gain important mechanistic insights behind specific adverse effects. Despite their great potential, ecotoxicogenomic studies currently do not find any application in the regulatory context (Harrill et al., 2021). To transition from conceptual studies to harmonized study approaches suitable for regulatory or even pre-regulatory decision making, ecotoxicogenomics still has major challenges to overcome (Brockmeier et al., 2017; Buesen et al., 2017; Canzler et al., 2020; Harrill et al., 2021; Liang et al., 2020; Martyniuk, 2018; Verheijen et al., 2022). One of the main hurdles identified were the lack of: a) standardized minimum reporting guidelines to ensure accessibility and reusability of *omics* data (Harrill et al., 2021), b) a mutually agreed framework to quantitatively link the observed changes and

affected biological processes to key events (Brockmeier et al., 2017; Verheijen et al., 2022). From the latter, a third problem arises, which is the lack of transparency in bioinformatic data processing when converting raw data into biological interpretable and meaningful results (Harrill et al., 2021; Verheijen et al., 2022).

With respect to the lack of reporting guidelines for ecotoxicogenomic studies, the Organisation for Economic Co-operation and Development (OECD) Extended Advisory Group on Molecular Screening and Toxicogenomics (EAGMST) is currently working on a reporting framework compatible for regulatory use. Most recently, the first reporting guideline draft for describing the processing and analysis of transcriptomic (and metabolomic) data for regulatory toxicology was presented by Harrill et al.(2021). The studies presented in this PhD work (**A1** – **A5**) followed SETAC's reporting guidelines (SETAC, 2019) and the FAIR (**f**indable, **a**ccessible, **i**nteroperable & **r**eproducible) data principles (Wilkinson et al., 2016), which cover EAGMST's reporting recommendations for the data provider (Harrill et al., 2021). To provide reliable and useable information for potential future regulatory purpose, all three reporting principles should be considered when publishing the results. As there is currently no commonly agreed analysis framework for transcriptomic or proteomic data in ecotoxicology, it is especially important to make the raw data files from NGS or LC-MS measurements publically available. This allows a reanalysis of the data by the scientific community, once an analysis framework is agreed upon or for meta-analysis and comparative studies. For the reanalysis, however, the raw data files need to be findable. This means the data should be uploaded and made accessible through a searchable, well established and suitable database. This is why all transcriptomic datasets from this PhD study were made publicly available on ArrayExpress (Parkinson et al., 2007), while the proteomic datasets were uploaded on PRIDE (Proteomics Identification Database) (Martens et al., 2005). The respective accession numbers are provided in the subsequent publications (**A1** – **A5**). Both databases were developed and are maintained by the European Molecular Biology Laboratory (EMBL) and provide an excellent infrastructure for data mining and access through a command line interface. This allows an effective data download and management for a large number of datasets for comparative studies. Further, the upload process is supervised and manually checked by a curator to ensure sufficient meta-information is provided for each sample. This ensures the interpretability and reusability of the provided datasets by the scientific community. Future ecotoxicogenomic studies should therefore consider these databases for publishing their raw data.

How important it is to share the ecotoxicogenomic raw data in a findable and reusable way is demonstrated by the few numbers of datasets currently available on ArrayExpress

(https://www.ebi.ac.uk/arrayexpress/) for non-systems biology model organisms such as *D. magna* or *L. minor*. Although a variety of previous studies conducted RNA-sequencing experiments with *D. magna* (Coady et al., 2020; Fuertes et al., 2019; Orsini et al., 2016; Poulsen et al., 2021; Russo et al., 2018), the majority of entries are array-sequencing-based experiments. In fact, a search for "Daphnia magna*"* on ArrayExpress returned 39 entries, out of which only three were from mRNA-sequencing experiments (search date: 18.3.2022). From these three, two entries are the published datasets from study **A4**. The single other database entry is from the work published by Poulsen et al. (2021), investigation multigenerational effects of the fungicide prochloraz in *D. magna*. A search for "Lemna minor*"* or "Lemna" did not find any other entries on ArrayExpress. In contrast, the search for "Danio rerio" returned 758 entries out of which 276 were from NGS experiments. This demonstrates how important it is to conduct further studies and provide publicly accessible toxicogenomic profiles, especially for less well-studied organisms. More publicly findable and reusable information will allow for cross experiment comparisons to enhance our molecular understanding of adverse effects of chemicals for these aquatic organisms.

As much as findability and reusability of raw data from ecotoxicogenomic studies matters, also the reproducibility for such high content and complex *omic* datasets is important. Especially as there is currently no commonly agreed analysis framework (Harrill et al., 2021). When it comes to such complex datasets, the method descriptions in scientific publications are often insufficiently detailed, leading to the reproducibility crisis science is facing today (Baker, 2016). Hence, the full data analysis workflow itself must be described in the greatest detail possible. The best way of doing this is to provide the original source code for the respective analysis. Ideally it is a generic written script which handles any data of a specific structure (e.g. count matrix and respective sample annotation file) to perform an automated analysis. For this PhD work a variety of generic and stable bioinformatic analysis workflows were developed using bash, python and R programming. To provide these tools to other researchers as well as to enhance the transparency and consequently the reproducibility of this work, all scripts were made publicly available on github: https://github.com/hreinwal/zfeNeurotox.

While generally researchers are flexible to an extent in the way data is generated and analysed, this does not comply for the regulatory context where ideally an unambiguous answer, possibly later subject to legal scrutiny, is demanded. Therefore most recently, a potential trendsetting omics data analysis framework for regulatory application (R-ODAF) for the analysis of transcriptomic data was proposed by Verheijen et al. (2022). The R-ODAF has been built as an easy-to-use pipeline to analyse microarray or NGS data. The proposed workflow for RNA-

sequencing data provides robust overall sample quality thresholds (e.g. discarding samples which do not cluster with their sample group (variance > 20%), minimum mapped reads, etc.) as well as further statistical steps to remove false positive signals from the DGEA (Spurious spikes filter & 3rd quartile rule). To remove low abundant gene counts, they further proposed a relevance filter, which removes all genes which do not have at least 75% of their replicates expressed at 1 CPM in any one of the experimental conditions (Verheijen et al., 2022). Although, their proposed workflow for signal detection differs in certain statistical filter criteria (low abundant gene count removal, type of effect size shrinkage, p.adj (BH) cut-off), the proposed tools (e.g. STAR, DESeq2) for DGEA and overall workflow is highly similar to the performed analysis published in **A1** – **A5**. This suggested framework should be considered for future studies, especially with respect to the relevance and spurious spikes filter as well as the 3rd quartile rule. The two latter statistical filters were implemented to avoid an arbitrary effect size cut-off value, as it was demonstrated that such a parameter led to the loss of many true-positive signals (Verheijen et al., 2022). It is in agreement with our observations that high effect size thresholds (e.g. abs(log_2-fold change) > 1) lead to a significant loss of significantly regulated genes, with high expression values. Hence, while an effect size cut-off might be reasonable on normally distributed data, for the negative binomial distribution of sequencing read counts it overproportionally penalizes highly expressed genes, which tend to have much lower fold change values compared to lowly expressed genes (Verheijen et al., 2022).

In consequence, a too stringent effect size cut-off will most likely remove true-positive signals of genes which might be particularly interesting due to their high level of expression. For this reason a less stringent log_2-fold change cut-off (LFcut) was implemented in our studies which scales with the global variance in a transcriptomic dataset (see **A1** and **A2** for details). At first, LFcut was determined as the top 90% quantile of absolute log_2-fold changes. A comparative analysis with proteomic datasets (data not shown) showed that most of the detected proteins corresponded to highly expressed transcripts. To improve the signal coverage between transcriptomic and proteomic datasets, one must consider to avoid an effect size cut-off applying the additional methods proposed by Verheijen et al. (2022) or to further reduce the stringency of the effect size cut-off. For future ecotoxicogenomic studies, it is therefore suggested to implement the proposed spurious spikes filter and 3rd quartile rule in the workflow or a less stringent effect size cut-off (e.g. top 70% quantile of absolute log_2-fold changes).

In conclusion, ecotoxicogenomic methods are powerful, yet highly complex methodologies which require careful consideration with respect to the analysis steps. As there is no harmonized approach yet implemented for regulatory or pre-regulatory purpose, full transparency of the

workflows must be ensured and ideally only open access tools should be applied to ensure the availability of the applications to the whole scientific community. In contrast, the use of proprietary software will hinder transparency through uncommon access and might even lead to conflicts of interest (Verheijen et al., 2022).

There are still many open questions to solve in the field of ecotoxicogenomics before such methodologies can be acknowledged by regulatory authorities (Harrill et al., 2021). Nevertheless, the findings of this PhD work demonstrate how these methods can be implemented to identify biomarker candidates with the potential to differentiate between certain toxic MoA. Even though there is no regulatory application yet, these findings still provide valuable insight to further developed molecular marker-based hazard screenings. For example, such screenings could offer cost-effective qualitative hazard assessment opportunities in a pre-regulatory context for the industry during early compound development. This of course would require further investigation and verification of the presented biomarker candidates from this PhD study.

The aim of future studies should be to compare the here presented ecotoxicogenomic signatures with the signatures of other reference compounds from the same MoA. This way, the presented biomarker candidates could be evaluated for their MoA-specificity. Further, a global comparison of ecotoxicogenomic signatures with more replicates for a specific hazardous MoA could improve the selection of biomarker candidates with predictive properties. With more ecotoxicogenomic datasets available, further research attention should be also given to the identification of specific MoA-affected pathways, molecular functions or biological processes. As it was shown in this PhD study, there are multiple functional levels (Reactome & KEGG pathways, biological process GO, molecular function GO …) as well as statistical methods (e.g. GSEA or ORA) by which transcriptomic or proteomic signatures can be evaluated. Future *in silico* studies are needed to define which method and layer of comparison contributes most to the identification of a MoA-specific toxicant response. This knowledge will facilitate the identification of affected key pathways or molecular functions. Once identified, such a set of key pathways or molecular functions could be used to differentiate MoA fingerprints at the functional level. This enhances the biological interpretability of the high content over a gene level comparison. In the long run, once a larger set of robust biomarkers is identified with the potential to reliably differentiate hazardous MoA at the molecular level, the next steps would involve sample processing and signal read out automation. As molecular biomarker-based assays require very little biomaterial, the focus should be given to the miniaturization of the assay (e.g. micro well format). Ultimately, to fully replace the use of animal testing, the

transition to cell culture assays for biomarker-based hazard assessments is preferable and should be given sufficient research attention in the future.

2.4. CONCLUSION

This doctoral study was designated to investigate MoA-characteristic ecotoxicogenomic signatures in three important model organisms of aquatic toxicology of different trophic levels (*Danio rerio* embryo*, Daphnia magna, Lemna minor*). For all three organisms, a wet-lab workflow was established allowing for simultaneous RNA and protein extraction from the same biological sample for downstream full mRNA sequencing and LC-MS/MS shotgun proteomics. With the here presented studies, it was shown how transcriptomic and proteomic approaches can be coupled with toxicity tests, to obtain important mechanistic insights into adverse effects at the molecular level. In general, ecotoxicogenomic approaches were shown to be highly sensitive, as significant changes in gene expression profiles were detected in in the absence of morphological observable effects or very low effect concentrations as low as EC5. It was further shown how ecotoxicogenomics can be applied to identify potential MoA specific molecular biomarkers. For the 96 hpf zebrafish embryo model, ecotoxicogenomic signatures and MoA-specific biomarker candidates were described for two thyroid disrupting chemicals and six nerve- and muscle targeting insecticides. A meta-comparison between those and further, yet unpublished, ecotoxicogenomic profiles revealed compound-specific molecular fingerprints at the pathway and molecular functional level. Similarly, compound-specific functional profiles were observed in studies performed with the water flea *D. magna* and the aquatic macrophyte *L. minor*. Based on prior knowledge available for the reference compounds, the identified affected pathways and proposed biomarkers could be related to previously described physiological effects for the respective chemical's MoA. Overall, the findings presented here not only provide mechanistic insights into the evaluated MoAs in the respective model organisms, but also give further supportive evidence for the suitability of ecotoxicogenomic methods to identify early molecular MoA-specific responses in different model organisms in aquatic ecotoxicology.

Although, functional systems biology analysis were more challenging for organisms with poorly annotated reference genomes such as *L. minor* or *D. magna*, it was shown how publicly available information and bioinformatic tools can be applied to overcome this hurdle. To facilitate the annotation process for other researchers, a *L. minor* reference genome annotation package was built, which is now publicly available (Zenodo: 6045874) and can be easily implemented via the *R* command line. Overrepresentation analysis performed based on the

functional annotation in this package, clearly linked affected biological processes and molecular functions to the assessed compound's MoA, supporting the validity of the applied annotation workflow. Further, this allowed the differentiation of the two differing toxic MoAs leading to growth inhibition in aquatic macrophytes at the molecular level already after 3 days of exposure. When evaluating molecular changes, it is very likely that the exposure period could be further shortened (e.g. 1 – 2 days), as molecular responses to environmental stressors can be detected within hours. Molecular biomarker-based hazard screenings could therefore significantly enhance the throughput of such exposure studies and allow the differentiation among different hazardous MoAs.

Despite the standard exposure study experiments applied for ecotoxicogenomic profiling, this work also proposed a novel sublethal immune challenge assay in early (48 hpf) zebrafish embryo. The presented assay allowed the mechanistic assessment of immunosuppressive effects at the gene expression level. The proposed approach was not only able to identify immune response-related processes but also to identify alternatively regulated processes and pathways with and without prior immunosuppressive treatment. Overall, these findings will enhance the mechanistic understanding of immunosuppression in fish as well as they might open-up novel research opportunities needed for the immunotoxicity assessment in aquatic organisms.

Lastly, this doctoral research work provided an important high content data baseline for future *in silico* exploration methods to compare e.g. key targeted pathways or biomarkers, which could allow a reliable differentiation of hazardous MoAs at the molecular level. The mechanistic insights presented here at the gene expression level and proposed molecular links to previously reported apical adverse effects provide supportive evidence suitable for the refinement or development of novel AOPs. These mechanistic insights are fundamental to progress further in the field of predictive ecotoxicology. Ultimately, unravelling the mechanisms of chemical hazards will allow a better informed characterization of chemicals and their potential adverse effects.

In the long run, the herein identified molecular fingerprints aim towards facilitating the development of biomarker-based high throughput screenings. Such next generation toxicology approaches could be used to efficiently predict a compound's hazardous MoA based on its ecotoxicogenomic signature. Although, there are still many hurdles to take until such methods can be applied in the regulatory context, they could still be implemented in a pre-regulatory context e.g. during novel compound development. Informative biomarker-based assays can

help to prioritize precursor compounds for specific higher tier studies or even identify safer alternatives from an early stage on. Such an approach would align with the current EU's chemicals strategy and the proposed pre-market sustainable-by-design concept. To cope with the large number of annually developed novel compounds, it is imminent that ecotoxicological hazard assessment needs to evolve novel methodologies suitable for high throughput processing, ideally without the suffering of sentient organisms. Ecotoxicogenomics, if applied correctly, have the potential to unravel early molecular key events and suitable biomarkers behind toxic mechanism, which will accelerate the transition to next generation chemical hazard assessment of higher informative content.

3. SUPPLEMENTARY DISCUSSION FIGURES

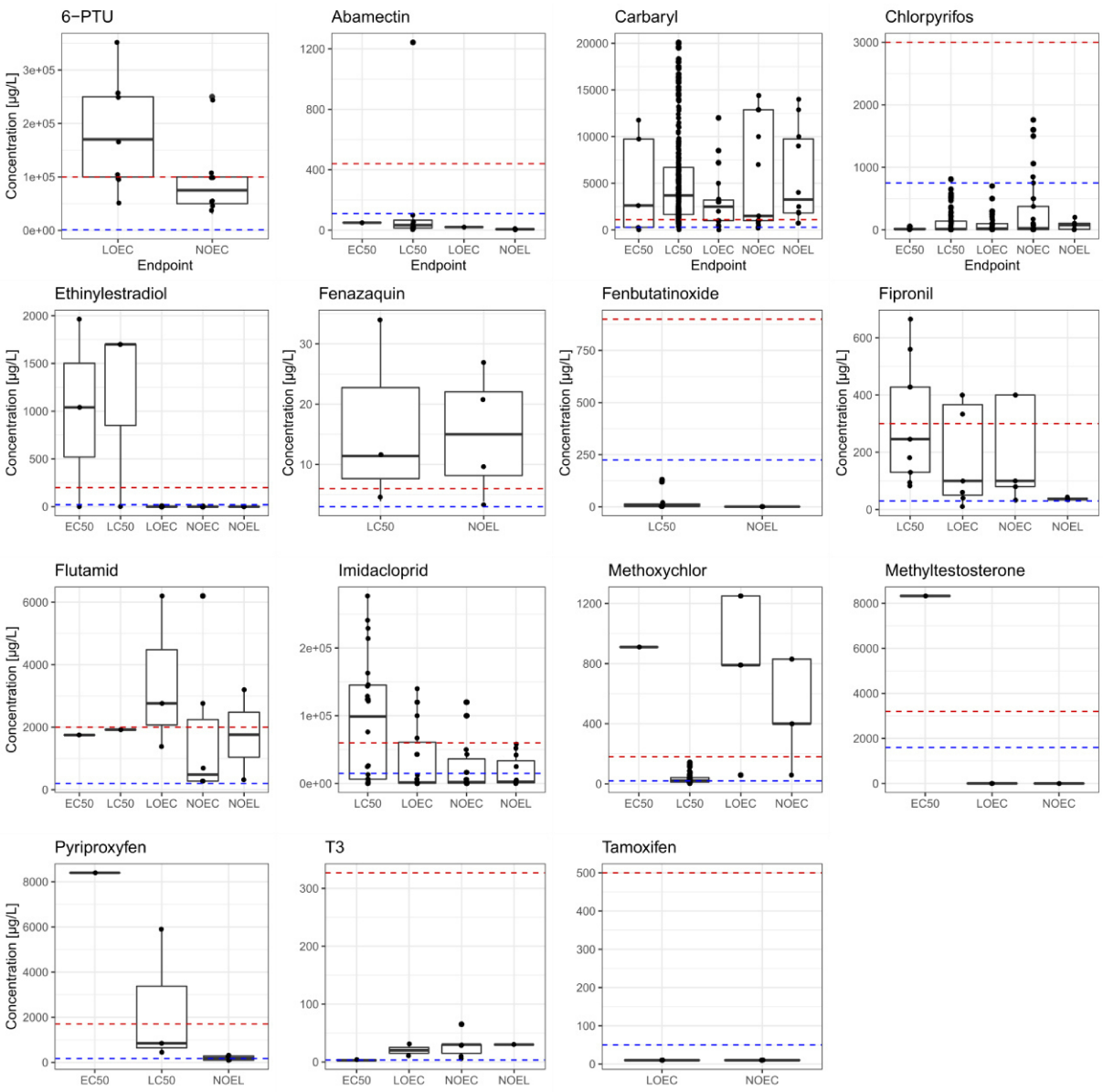

S.Figure 1: Boxplots visualizing publicly available toxicological data for different endpoints in cyprinidae and cypriniformes after 96 and 120 hours of exposure for the tested compounds. The highest and lowest nominal test concentration from which ecotoxicogenomic profiles were generated are indicated in a blue and red dashed line respectively. The data was compiled from the Environmental Protection Agency's (EPA) ECOTOXicology Knowledgebase (ECOTOX) using the StandaRtox R package (Scharmüller et al., 2020).

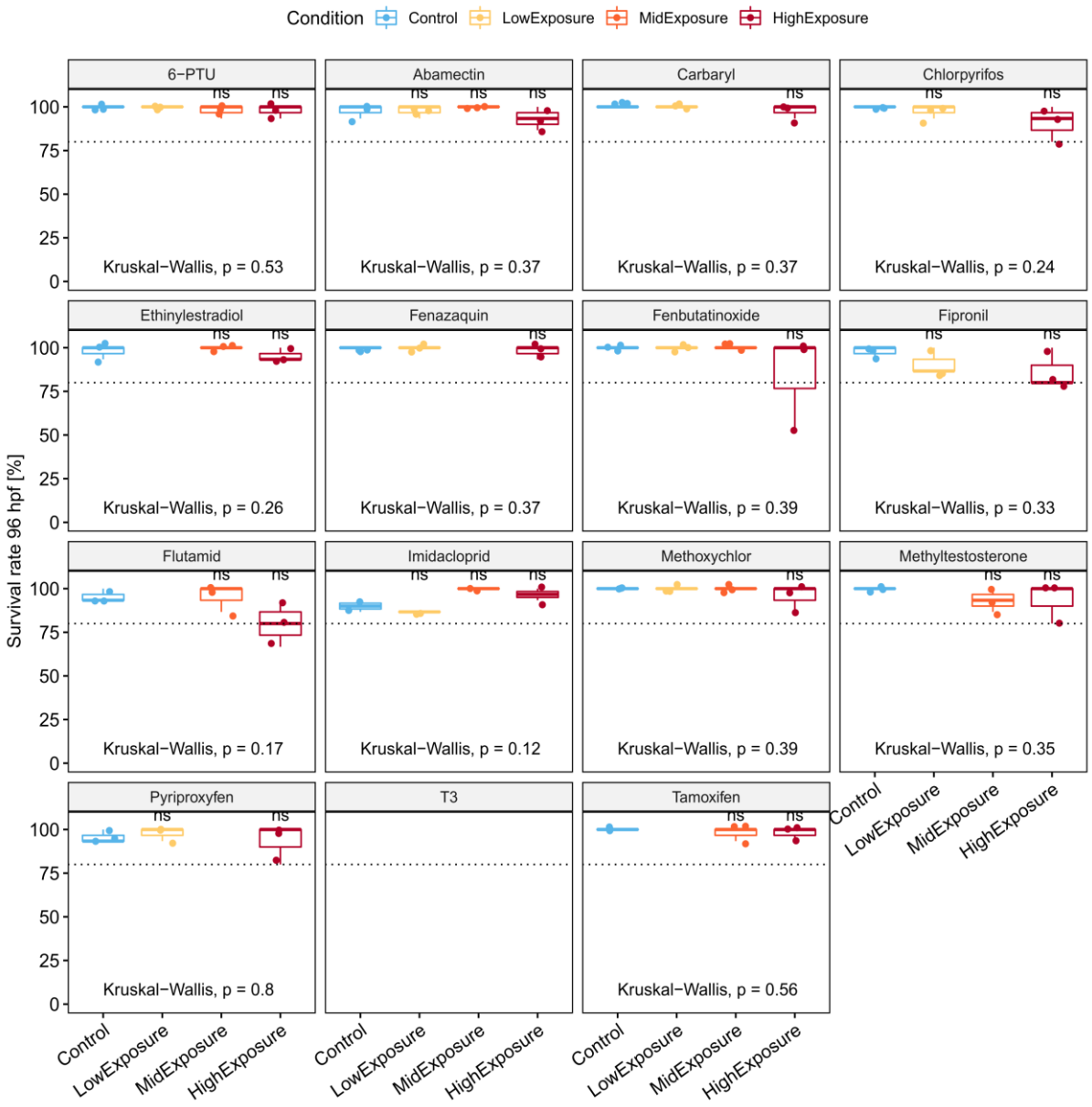

S.Figure 2: Survival rates of zebrafish embryos after 96 hours of chemical exposure. Each grid presents the results of an individually performed experiment for different test conditions reflected by the boxplot's color. Respective nominal exposure concentrations are given in Table 1. Dashed line shows 80 % survival threshold. Kruskal-Wallis test (one-way ANOVA on ranks) was conducted to test for statistically significant differences in sample distribution. Post-hoc pairwise t-test comparison was used to test for significant differences among sample means compared to control (ns = non significant). For T3, which was one of the first experiments conducted, no survival rate was documented.

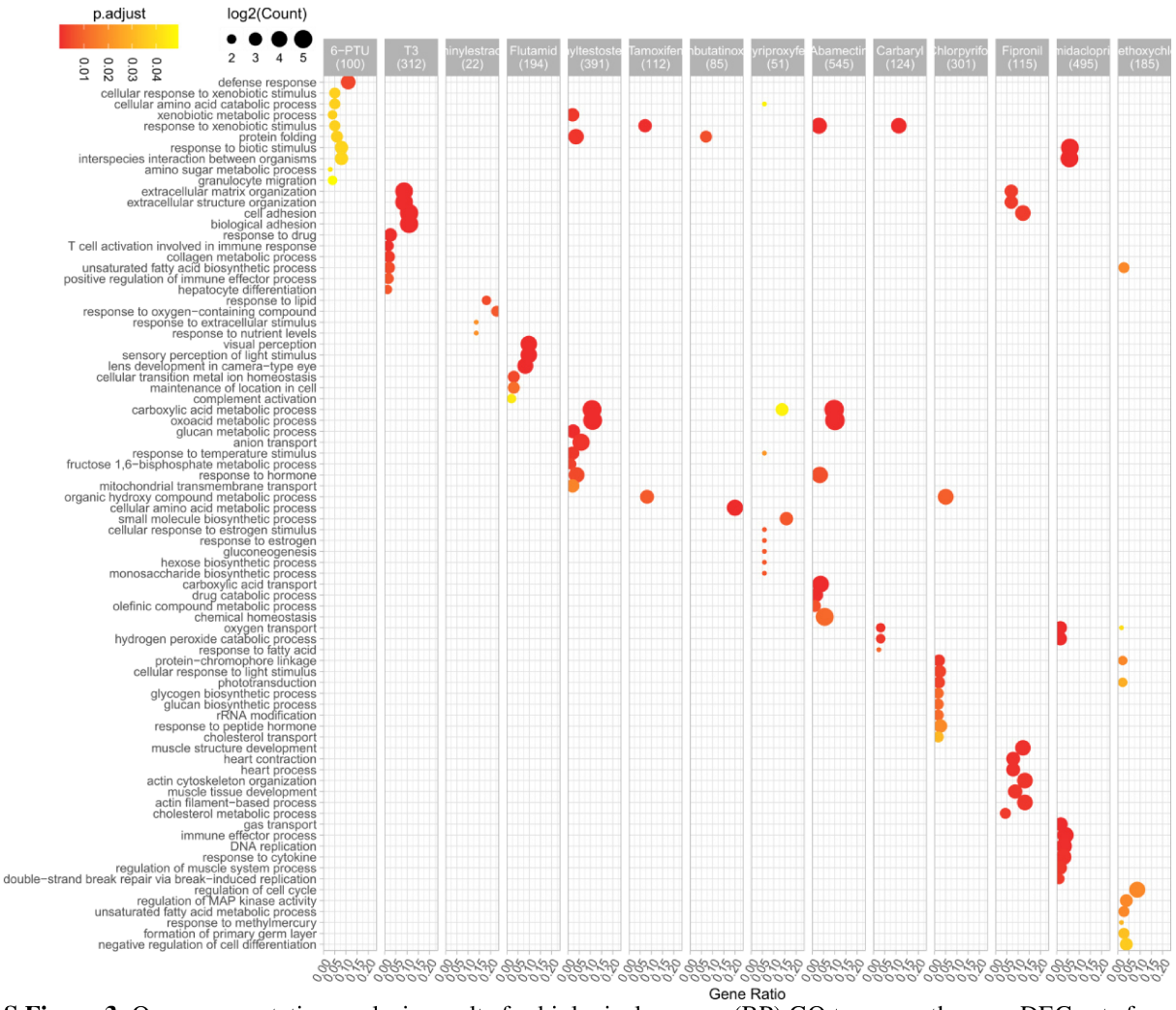

S.Figure 3: Overrepresentation analysis results for biological process (BP) GO terms on the core DEG sets from the different tested chemicals. The bubble plot shows the significantly enriched (p.adj < 0.05) terms. The colour of the bubbles reflect the significance level while the bubble size indicates the number of DEGs which are element of the enriched BP GO term gene set. The gene ratio is given on the x-axis. For each tested compound the top 10 most significantly enriched terms were selected and compiled for this figure. If less than then 10 BP GO terms were significantly enriched, only the significant results are shown. The plot, filtered for the top 10 results, shows 80 out of the 118 BP GO terms identified as significantly enriched across all tested substances.

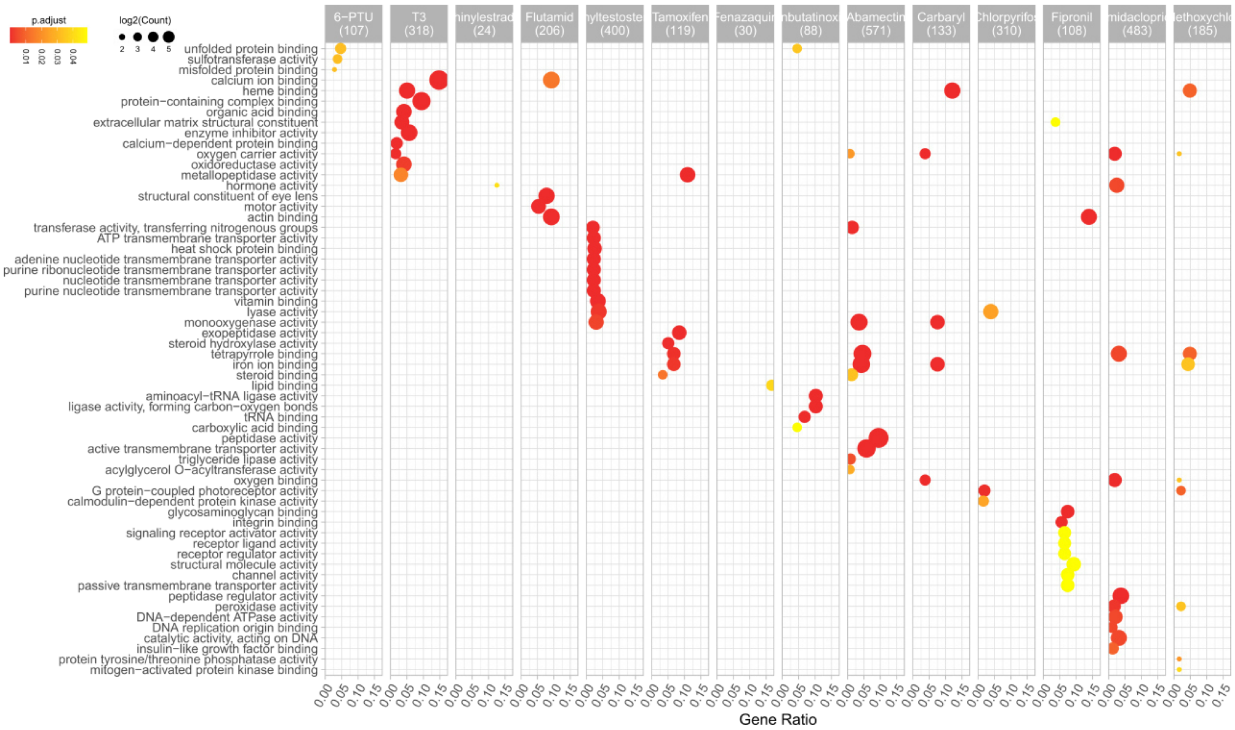

S.Figure 4: Overrepresentation analysis results for molecular function (MF) GO terms on the core DEG sets from the different tested chemicals. The bubble plot shows the significantly enriched (p.adj < 0.05) terms. The colour of the bubbles reflect the significance level while the bubble size indicates the number of DEGs which are element of the enriched MF GO term gene set. The gene ratio is given on the x-axis. For each tested compound the top 10 most significantly enriched terms were selected and compiled for this figure. If less than then 10 MF GO terms were significantly enriched, only the significant results are shown. The plot, filtered for the top 10 results, shows 60 out of the total 68 MF GO terms identified as significantly enriched across all tested substances.

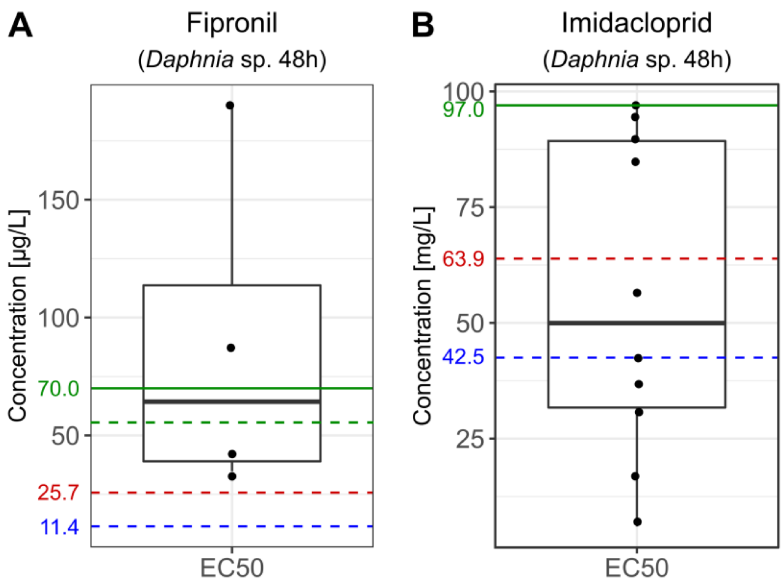

S.Figure 5: EC50 values (48 h exposure) of *Daphnia* sp. (includes data on *D. magna* and *D.* pulex) from the ECOTOXicology Knowledgebase (ECOTOX) for (A) fipronil and (B) imidacloprid. Dashed blue (low exposure ~ EC5) and red (high exposure ~ EC20) line indicate the analytically determined test concentrations for transcriptomic profiling in study **A4**. The solid green line shows the determined 48 h EC50 value from preliminary experiments, based on nominal concentrations. The dashed green line in (A) resembles a corrected EC50 (52.5 µg/L), as analytical quantification showed only 70-80 % recovery of fipronil in the main exposure study.

4. REFERENCES

Acosta, K., Xu, J., Gilbert, S., Denison, E., Brinkman, T., Lebeis, S., Lam, E., 2020. Duckweed hosts a taxonomically similar bacterial assemblage as the terrestrial leaf microbiome. PLoS One 15, e0228560. https://doi.org/10.1371/journal.pone.0228560

Al-Badran, A.A., Fujiwara, M., Gatlin, D.M., Mora, M.A., 2018. Lethal and sub-lethal effects of the insecticide fipronil on juvenile brown shrimp Farfantepenaeus aztecus. Sci. Rep. 8, 10769. https://doi.org/10.1038/s41598-018-29104-3

Alder, J., Thakker-Varia, S., Bangasser, D.A., Kuroiwa, M., Plummer, M.R., Shors, T.J., Black, I.B., 2003. Brain-Derived Neurotrophic Factor-Induced Gene Expression Reveals Novel Actions of VGF in Hippocampal Synaptic Plasticity. J. Neurosci. 23, 10800–10808. https://doi.org/10.1523/JNEUROSCI.23-34-10800.2003

Aliferis, K.A., Materzok, S., Paziotou, G.N., Chrysayi-Tokousbalides, M., 2009. Lemna minor L. as a model organism for ecotoxicological studies performing 1H NMR fingerprinting. Chemosphere 76, 967–73. https://doi.org/10.1016/j.chemosphere.2009.04.025

Alt, B., Reibe, S., Feitosa, N.M., Elsalini, O.A., Wendl, T., Rohr, K.B., 2006. Analysis of origin and growth of the thyroid gland in zebrafish. Dev. Dyn. 235, 1872–83. https://doi.org/10.1002/dvdy.20831

Amora, M., Giordani, S., 2018. The Utility of Zebrafish as a Model for Screening Developmental Neurotoxicity. Front. Neurosci. 12. https://doi.org/10.3389/fnins.2018.00976

Ankley, G.T., Bennett, R.S., Erickson, R.J., Hoff, D.J., Hornung, M.W., Johnson, R.D., Mount, D.R., Nichols, J.W., Russom, C.L., Schmieder, P.K., Serrrano, J.A., Tietge, J.E., Villeneuve, D.L., 2010. Adverse outcome pathways: A conceptual framework to support ecotoxicology research and risk assessment. Environ. Toxicol. Chem. https://doi.org/10.1002/etc.34

Arimura, T., Ishikawa, T., Nunoda, S., Kawai, S., Kimura, A., 2011. Dilated cardiomyopathy-associated BAG3 mutations impair Z-disc assembly and enhance sensitivity to apoptosis in cardiomyocytes. Hum. Mutat. 32, 1481–1491. https://doi.org/10.1002/humu.21603

Baken, K.A., Sjerps, R.M.A., Schriks, M., van Wezel, A.P., 2018. Toxicological risk assessment and prioritization of drinking water relevant contaminants of emerging concern. Environ. Int. 118, 293–303. https://doi.org/10.1016/j.envint.2018.05.006

Baker, M., 2016. Is there a reproducability crisis? Nature 533, 452–454. https://doi.org/10.1038/533452a

Baker, M.R., Wong, R.Y., 2021. Npas4a expression in the teleost forebrain is associated with stress coping style differences in fear learning. Sci. Rep. 11, 1–12. https://doi.org/10.1038/s41598-021-91495-7

Bakkers, J., 2011. Zebrafish as a model to study cardiac development and human cardiac disease. Cardiovasc. Res. 91, 279–288. https://doi.org/10.1093/cvr/cvr098

Baudo, R., Foudoulakis, M., Arapis, G., Perdaen, K., Lanneau, W., Paxinou, A.-C.M., Kouvdou, S., Persoone, G., 2015. History and sensitivity comparison of the Spirodela polyrhiza microbiotest and Lemna toxicity tests. Knowl. Manag. Aquat. Ecosyst. 23. https://doi.org/10.1051/kmae/2015019

Baumann, L., Ros, A., Rehberger, K., Neuhauss, S.C.F., Segner, H., 2016. Thyroid disruption in zebrafish (Danio rerio) larvae: Different molecular response patterns lead to impaired eye development and visual functions. Aquat. Toxicol. 172, 44–55. https://doi.org/10.1016/j.aquatox.2015.12.015

Belanger, S.E., Rawlings, J.M., Carr, G.J., 2013. Use of fish embryo toxicity tests for the prediction of acute fish toxicity to chemicals. Environ. Toxicol. Chem. https://doi.org/10.1002/etc.2244

Boas, M., Feldt-Rasmussen, U., Main, K.M., 2012. Thyroid effects of endocrine disrupting chemicals. Mol. Cell. Endocrinol. 355, 240–8. https://doi.org/10.1016/j.mce.2011.09.005

Bowley, G., Kugler, E., Wilkinson, R., Lawrie, A., van Eeden, F., Chico, T.J.A., Evans, P.C., Noël, E.S., Serbanovic-Canic, J., 2022. Zebrafish as a tractable model of human cardiovascular disease. Br. J. Pharmacol. 179, 900–917. https://doi.org/10.1111/bph.15473

Bozdagi, O., Rich, E., Tronel, S., Sadahiro, M., Patterson, K., Shapiro, M.L., Alberini, C.M., Huntley, G.W., Salton, S.R.J., 2008. The neurotrophin-inducible gene Vgf regulates hippocampal function and behavior through a brain-derived neurotrophic factor-dependent mechanism. J. Neurosci. 28, 9857–9869. https://doi.org/10.1523/JNEUROSCI.3145-08.2008

Brain, R.A., Reitsma, T.S., Lissemore, L.I., Bestari, K. (Jim), Sibley, P.K., Solomon, K.R., 2006. Herbicidal Effects of Statin Pharmaceuticals in Lemna gibba. Environ. Sci. Technol. 40, 5116–5123. https://doi.org/10.1021/es0600274

Brinke, A., Buchinger, S., n.d. Toxicogenomics in Environmental Science. Adv. Biochem. Eng. Biotechnol. 157, 159–186. https://doi.org/10.1007/10_2016_15

Brockmeier, E.K., Hodges, G., Hutchinson, T.H., Butler, E., Hecker, M., Tollefsen, K.E., Garcia-Reyero, N., Kille, P., Becker, D., Chipman, K., Colbourne, J., Collette, T.W., Cossins, A., Cronin, M., Graystock, P., Gutsell, S., Knapen, D., Katsiadaki, I., Lange, A., Marshall, S., Owen, S.F., Perkins, E.J., Plaistow, S., Schroeder, A., Taylor, D., Viant, M., Ankley, G., Falciani, F., 2017. The role of omics in the application of adverse outcome pathways for chemical risk assessment. Toxicol. Sci. 158, 252–262.

https://doi.org/10.1093/toxsci/kfx097
Brownlie, A., Hersey, C., Oates, A.C., Paw, B.H., Falick, A.M., Witkowska, H.E., Flint, J., Higgs, D., Jessen, J., Bahary, N., Zhu, H., Lin, S., Zon, L., 2003. Characterization of embryonic globin genes of the zebrafish. Dev. Biol. 255, 48–61. https://doi.org/10.1016/S0012-1606(02)00041-6
Brühl, C.A., Zaller, J.G., 2019. Biodiversity Decline as a Consequence of an Inappropriate Environmental Risk Assessment of Pesticides. Front. Environ. Sci. 7, 2013–2016. https://doi.org/10.3389/fenvs.2019.00177
Buesen, R., Chorley, B.N., da Silva Lima, B., Daston, G., Deferme, L., Ebbels, T., Gant, T.W., Goetz, A., Greally, J., Gribaldo, L., Hackermüller, J., Hubesch, B., Jennen, D., Johnson, K., Kanno, J., Kauffmann, H.M., Laffont, M., McMullen, P., Meehan, R., Pemberton, M., Perdichizzi, S., Piersma, A.H., Sauer, U.G., Schmidt, K., Seitz, H., Sumida, K., Tollefsen, K.E., Tong, W., Tralau, T., van Ravenzwaay, B., Weber, R.J.M., Worth, A., Yauk, C., Poole, A., 2017. Applying 'omics technologies in chemicals risk assessment: Report of an ECETOC workshop, in: Regulatory Toxicology and Pharmacology. Academic Press, pp. S3–S13. https://doi.org/10.1016/j.yrtph.2017.09.002
Camacho, C., Coulouris, G., Avagyan, V., Ma, N., Papadopoulos, J., Bealer, K., Madden, T.L., 2009. BLAST+: Architecture and applications. BMC Bioinformatics 10, 1–9. https://doi.org/10.1186/1471-2105-10-421
Campos, N., Arró, M., Ferrer, A., Boronat, A., 2014. Determination of 3-hydroxy-3-methylglutaryl CoA reductase activity in plants. Methods Mol. Biol. 1153, 21–40. https://doi.org/10.1007/978-1-4939-0606-2_3
Canzler, S., Schor, J., Busch, W., Schubert, K., Rolle-Kampczyk, U.E., Seitz, H., Kamp, H., von Bergen, M., Buesen, R., Hackermüller, J., 2020. Prospects and challenges of multi-omics data integration in toxicology. Arch. Toxicol. 94, 371–388. https://doi.org/10.1007/s00204-020-02656-y
Cao, Y., Tian, R., Jiao, Y., Zheng, Z., Wang, Q., Deng, Y., Du, X., 2021. Novel nicotinic acetylcholine receptor involved in immune regulation in pearl oyster (Pinctada fucata martensii). Comp. Biochem. Physiol. Part - B Biochem. Mol. Biol. 252, 110512. https://doi.org/10.1016/j.cbpb.2020.110512
Carbon, S., Douglass, E., Dunn, N., Good, B., Harris, N.L., Lewis, S.E., Mungall, C.J., Basu, S., Chisholm, R.L., Dodson, R.J., Hartline, E., Fey, P., Thomas, P.D., Albou, L.P., Ebert, D., Kesling, M.J., Mi, H., Muruganujan, A., Huang, X., Poudel, S., Mushayahama, T., Hu, J.C., LaBonte, S.A., Siegele, D.A., Antonazzo, G., Attrill, H., Brown, N.H., Fexova, S., Garapati, P., Jones, T.E.M., Marygold, S.J., Millburn, G.H., Rey, A.J., Trovisco, V., Dos Santos, G., Emmert, D.B., Falls, K., Zhou, P., Goodman, J.L., Strelets, V.B., Thurmond, J., Courtot, M., Osumi, D.S., Parkinson, H., Roncaglia, P., Acencio, M.L., Kuiper, M., Lreid, A., Logie, C., Lovering, R.C., Huntley, R.P., Denny, P., Campbell, N.H., Kramarz, B., Acquaah, V., Ahmad, S.H., Chen, H., Rawson, J.H., Chibucos, M.C., Giglio, M., Nadendla, S., Tauber, R., Duesbury, M.J., Del, N.T., Meldal, B.H.M., Perfetto, L., Porras, P., Orchard, S., Shrivastava, A., Xie, Z., Chang, H.Y., Finn, R.D., Mitchell, A.L., Rawlings, N.D., Richardson, L., Sangrador-Vegas, A., Blake, J.A., Christie, K.R., Dolan, M.E., Drabkin, H.J., Hill, D.P., Ni, L., Sitnikov, D., Harris, M.A., Oliver, S.G., Rutherford, K., Wood, V., Hayles, J., Bahler, J., Lock, A., Bolton, E.R., De Pons, J., Dwinell, M., Hayman, G.T., Laulederkind, S.J.F., Shimoyama, M., Tutaj, M., Wang, S.J., D'Eustachio, P., Matthews, L., Balhoff, J.P., Aleksander, S.A., Binkley, G., Dunn, B.L., Cherry, J.M., Engel, S.R., Gondwe, F., Karra, K., MacPherson, K.A., Miyasato, S.R., Nash, R.S., Ng, P.C., Sheppard, T.K., Shrivatsav Vp, A., Simison, M., Skrzypek, M.S., Weng, S., Wong, E.D., Feuermann, M., Gaudet, P., Bakker, E., Berardini, T.Z., Reiser, L., Subramaniam, S., Huala, E., Arighi, C., Auchincloss, A., Axelsen, K., Argoud, G.P., Bateman, A., Bely, B., Blatter, M.C., Boutet, E., Breuza, L., Bridge, A., Britto, R., Bye-A-Jee, H., Casals-Casas, C., Coudert, E., Estreicher, A., Famiglietti, L., Garmiri, P., Georghiou, G., Gos, A., Gruaz-Gumowski, N., Hatton-Ellis, E., Hinz, U., Hulo, C., Ignatchenko, A., Jungo, F., Keller, G., Laiho, K., Lemercier, P., Lieberherr, D., Lussi, Y., Mac-Dougall, A., Magrane, M., Martin, M.J., Masson, P., Natale, D.A., Hyka, N.N., Pedruzzi, I., Pichler, K., Poux, S., Rivoire, C., Rodriguez-Lopez, M., Sawford, T., Speretta, E., Shypitsyna, A., Stutz, A., Sundaram, S., Tognolli, M., Tyagi, N., Warner, K., Zaru, R., Wu, C., Chan, J., Cho, J., Gao, S., Grove, C., Harrison, M.C., Howe, K., Lee, R., Mendel, J., Muller, H.M., Raciti, D., Van Auken, K., Berriman, M., Stein, L., Sternberg, P.W., Howe, D., Toro, S., Westerfield, M., The Gene Ontology Consortium, 2019. The Gene Ontology Resource: 20 years and still GOing strong. Nucleic Acids Res. 47, D330–D338. https://doi.org/10.1093/nar/gky1055
Carlson, M., Pagès, H., 2021. AnnotationForge: Tools for building SQLite-based annotation data packages.
Carvalho, D.P., Dupuy, C., 2017. Thyroid hormone biosynthesis and release. Mol. Cell. Endocrinol. 458, 6–15. https://doi.org/10.1016/j.mce.2017.01.038
CEFIC, 2022. Facts and Figures of the European Chemical Industry [WWW Document]. URL https://cefic.org/a-pillar-of-the-european-economy/facts-and-figures-of-the-european-chemical-industry/
Chen, W.Q., Hu, Y.W., Zou, P.F., Ren, S.S., Nie, P., Chang, M.X., 2015. MAVS splicing variants contribute to the induction of interferon and interferon-stimulated genes mediated by RIG-I-like receptors. Dev. Comp. Immunol. 49, 19–30. https://doi.org/10.1016/j.dci.2014.10.017
Choi, T.Y., Choi, T.I., Lee, Y.R., Choe, S.K., Kim, C.H., 2021. Zebrafish as an animal model for biomedical research. Exp. Mol. Med. 53, 310–317. https://doi.org/10.1038/s12276-021-00571-5
Coady, K.K., Burgoon, L., Doskey, C., Davis, J.W., 2020. Assessment of Transcriptomic and Apical Responses

of Daphnia magna Exposed to a Polyethylene Microplastic in a 21-d Chronic Study. Environ. Toxicol. Chem. 39, 1578–1589. https://doi.org/10.1002/etc.4745

Conolly, R.B., Ankley, G.T., Cheng, W., Mayo, M.L., Miller, D.H., Perkins, E.J., Villeneuve, D.L., Watanabe, K.H., 2017. Quantitative Adverse Outcome Pathways and Their Application to Predictive Toxicology. Environ. Sci. Technol. 51, 4661–4672. https://doi.org/10.1021/acs.est.6b06230

Cote, I., Andersen, M.E., Ankley, G.T., Barone, S., Birnbaum, L.S., Boekelheide, K., Bois, F.Y., Burgoon, L.D., Chiu, W.A., Crawford-Brown, D., Crofton, K.M., Devito, M., Devlin, R.B., Edwards, S.W., Guyton, K.Z., Hattis, D., Judson, R.S., Knight, D., Krewski, D., Lambert, J., Maull, E.A., Mendrick, D., Paoli, G.M., Patel, C.J., Perkins, E.J., Poje, G., Portier, C.J., Rusyn, I., Schulte, P.A., Simeonov, A., Smith, M.T., Thayer, K.A., Thomas, R.S., Thomas, R., Tice, R.R., Vandenberg, J.J., Villeneuve, D.L., Wesselkamper, S., Whelan, M., Whittaker, C., White, R., Xia, M., Yauk, C., Zeise, L., Zhao, J., Dewoskin, R.S., 2016. The next generation of risk assessment multi-year study–highlights of findings, applications to risk assessment, and future directions. Environ. Health Perspect. https://doi.org/10.1289/EHP233

Coulthard, L.G., Woodruff, T.M., 2015. Is the Complement Activation Product C3a a Proinflammatory Molecule? Re-evaluating the Evidence and the Myth. J. Immunol. 194, 3542–3548. https://doi.org/10.4049/jimmunol.1403068

Coutellier, L., Beraki, S., Ardestani, P.M., Saw, N.L., Shamloo, M., 2012. Npas4: A Neuronal Transcription Factor with a Key Role in Social and Cognitive Functions Relevant to Developmental Disorders. PLoS One 7. https://doi.org/10.1371/journal.pone.0046604

Cox, T.C., Sadlon, T.J., Schwarz, Q.P., Matthews, C.S., Wise, P.D., Cox, L.L., Bottomley, S.S., May, B.K., 2004. The major splice variant of human 5-aminolevulinate synthase-2 contributes significantly to erythroid heme biosynthesis. Int. J. Biochem. Cell Biol. 36, 281–295. https://doi.org/10.1016/S1357-2725(03)00246-2

Davidson, B., Soodak, M., Neary, J.T., Strout, H. V, Kieffer, J.D., Mover, H., Maloof, F., 1978. The irreversible inactivation of thyroid peroxidase by methylmercaptoimidazole, thiouracil, and propylthiouracil in vitro and its relationship to in vivo findings. Endocrinology 103, 871–82. https://doi.org/10.1210/endo-103-3-871

De Angelis, S., Tassinari, R., Maranghi, F., Eusepi, A., Di Virgilio, A., Chiarotti, F., Ricceri, L., Venerosi Pesciolini, A., Gilardi, E., Moracci, G., Calamandrei, G., Olivieri, A., Mantovani, A., 2009. Developmental exposure to chlorpyrifos induces alterations in thyroid and thyroid hormone levels without other toxicity signs in CD-1 mice. Toxicol. Sci. 108, 311–319. https://doi.org/10.1093/toxsci/kfp017

Directive 2001/83/EC, 2001. Directive 2001/83/EC of the European Parliament and of the Council of 6 November 2001 on the Community code relating to medicinal products for human use. Off. J. Eur. Union L 311/67. https://doi.org/https://eur-lex.europa.eu/eli/dir/2001/83/oj

Domínguez, F., Cuenca, S., Bilińska, Z., Toro, Rocío, Villard, E., Barriales-Villa, R., Ochoa, J.P., Asselbergs, F., Sammani, A., Franaszczyk, M., Akhtar, M., Coronado-Albi, M.J., Rangel-Sousa, D., Rodriguez-Palomares, J.F., Jiménez-Jáimez, J., Garcia-Pinilla, José Manuel, Ripoll-Vera, T., Mogollón-Jiménez, M.V., Fontalba-Romero, A., Garcia-Medina, D., Palomino-Doza, J., de Gonzalo-Calvo, D., Cicerchia, M., Salazar-Mendiguchia, J., Salas, C., Pankuweit, S., Hey, T.M., Mogensen, J., Barton, P.J., Charron, P., Elliott, P., Garcia-Pavia, P., Eiskjær, H., Barriales, R., Fernández Fernández, X., Cicerchia, M., Monserrat, L., Ochoa, J.P., Salazar-Mendiguchia, J., Mogollón, M.V., Ripoll, T., Charron, P., Richard, P., Villard, E., Palomino Doza, J., Fontalba, A., Alonso-Pulpón, L., Cobo-Marcos, M., Domínguez, F., Garcia-Pavia, P., Gómez-Bueno, M., González-López, E., Hernández-Hernández, A., Hernández-Pérez, F.J., López-Sainz, Á., Restrepo-Córdoba, A., Segovia-Cubero, J., Toro, Rocio, de Gonzalo-Calvo, D., Rosa Longobardo, F., Limeres, J., Rodriguez-Palomares, J.F., Garcia-Pinilla, Jose Manuel, López-Garrido, M.A., Jiménez-Jaimez, J., Garcia-Medina, D., Rangel Sousa, D., Peña, M.L., Mogensen, J., Morris-Hey, T., Barton, P.J., Cook, S.A., Midwinter, W., Roberts, A.M., Ware, J.S., Walsh, R., Akhtar, M., Elliott, P.M., Rocha-Lopes, L., Savvatis, K., Syrris, P., Michalak, E., Ploski, R., Sobieszczanska-Malek, M., Bilińska, Z., Pankuweit, S., Asselbergs, F., Baas, A., Dooijes, D., Sammani, A., 2018. Dilated Cardiomyopathy Due to BLC2-Associated Athanogene 3 (BAG3) Mutations. J. Am. Coll. Cardiol. 72, 2471–2481. https://doi.org/10.1016/j.jacc.2018.08.2181

Dooley, K., 2000. Zebrafish: a model system for the study of human disease. Curr. Opin. Genet. Dev. 10, 252–256. https://doi.org/10.1016/S0959-437X(00)00074-5

Dörner, G., Plagemann, A., 2002. DDT in human milk and mental capacities in children at school age: An additional view on PISA 2000. Neuroendocrinol. Lett. 23, 427–431.

Dubińska-Magiera, M., Niedbalska-Tarnowska, J., Migocka-Patrzałek, M., Posyniak, E., Daczewska, M., 2020. Characterization of Hspb8 in Zebrafish. Cells 9. https://doi.org/10.3390/cells9061562

Durinck, S., Spellman, P.T., Birney, E., Huber, W., 2009. Mapping identifiers for the integration of genomic datasets with the R/ Bioconductor package biomaRt. Nat. Protoc. 4, 1184–1191. https://doi.org/10.1038/nprot.2009.97

EEA, 2018. European waters. https://doi.org/https://doi.org/10.2800/303664

Ellison, C.M., Madden, J.C., Cronin, M.T.D., Enoch, S.J., 2015. Investigation of the Verhaar scheme for

predicting acute aquatic toxicity: Improving predictions obtained from Toxtree ver. 2.6. Chemosphere 139, 146–154. https://doi.org/10.1016/j.chemosphere.2015.06.009

Embry, M.R., Belanger, S.E., Braunbeck, T.A., Galay-Burgos, M., Halder, M., Hinton, D.E., Léonard, M.A., Lillicrap, A., Norberg-King, T., Whale, G., 2010. The fish embryo toxicity test as an animal alternative method in hazard and risk assessment and scientific research. Aquat. Toxicol. 97, 79–87. https://doi.org/10.1016/j.aquatox.2009.12.008

Endo, S., Maeda, S., Matsunaga, T., Dhagat, U., El-Kabbani, O., Tanaka, N., Nakamura, K.T., Tajima, K., Hara, A., 2009. Molecular determinants for the stereospecific reduction of 3-ketosteroids and reactivity towards all-trans-retinal of a short-chain dehydrogenase/reductase (DHRS4). Arch. Biochem. Biophys. 481, 183–190. https://doi.org/10.1016/j.abb.2008.11.014

Enell, L.E., Kapan, N., Söderberg, J.A.E., Kahsai, L., Nässel, D.R., 2010. Insulin signaling, lifespan and stress resistance are modulated by metabotropic GABA receptors on insulin producing cells in the brain of Drosophila. PLoS One 5, e15780. https://doi.org/10.1371/journal.pone.0015780

Escher, B.I., Stapleton, H.M., Schymanski, E.L., 2020. Tracking complex mixtures of chemicals in our changing environment. Science (80-.). 367, 388–392. https://doi.org/10.1126/science.aay6636

European Comission, 2018. Summary Report on the statistics on the use of animals for scientific purposes in the Member States of the European Union and Norway in 2018. Com. Staff Work. Doc. https://doi.org/https://ec.europa.eu/environment/chemicals/lab_animals/pdf/SWD_%20part_A_and_B.pdf

European Commission, 2020. The EU chemical strategy for sustainability towards a toxic-free environment 25.

Faltermann, S., Hettich, T., Küng, N., Fent, K., 2020. Effects of the glucocorticoid clobetasol propionate and its mixture with cortisol and different class steroids in adult female zebrafish. Aquat. Toxicol. 218, 105372. https://doi.org/10.1016/j.aquatox.2019.105372

Feitsma, H., Cuppen, E., 2008. Zebrafish as a Cancer Model. Mol. Cancer Res. 6, 685–694. https://doi.org/10.1158/1541-7786.MCR-07-2167

Fent, K., Sumpter, J.P., 2011. Progress and promises in toxicogenomics in aquatic toxicology: is technical innovation driving scientific innovation? Aquat. Toxicol. 105, 25–39. https://doi.org/10.1016/j.aquatox.2011.06.008

Franzoni, F., Quiñones-Galvan, A., Regoli, F., Ferrannini, E., Galetta, F., 2003. A comparative study of the in vitro antioxidant activity of statins. Int. J. Cardiol. 90, 317–321. https://doi.org/10.1016/S0167-5273(02)00577-6

Fuertes, I., Campos, B., Rivetti, C., Piña, B., Barata, C., 2019. Effects of Single and Combined Low Concentrations of Neuroactive Drugs on Daphnia magna Reproduction and Transcriptomic Responses. Environ. Sci. Technol. 53, 11979–11987. https://doi.org/10.1021/acs.est.9b03228

Fukuto, T.R., 1990. Mechanism of action of organophosphorus and carbamate insecticides. Environ. Health Perspect. 87, 245–254. https://doi.org/10.1289/ehp.9087245

Futagi, Y., Narumi, K., Furugen, A., Kobayashi, M., Iseki, K., 2020. Molecular characterization of the orphan transporter SLC16A9, an extracellular pH- and Na+-sensitive creatine transporter. Biochem. Biophys. Res. Commun. 522, 539–544. https://doi.org/10.1016/j.bbrc.2019.11.137

García-Valtanen, P., Martinez-Lopez, A., Ortega-Villaizan, M., Perez, L., Coll, J.M., Estepa, A., 2014. In addition to its antiviral and immunomodulatory properties, the zebrafish β-defensin 2 (zfBD2) is a potent viral DNA vaccine molecular adjuvant. Antiviral Res. 101, 136–47. https://doi.org/10.1016/j.antiviral.2013.11.009

Gardner, L.C., Smith, S.J., Cox, T.M., 1991. Biosynthesis of δ-aminolevulinic acid and the regulation of heme formation by immature erythroid cells in man. J. Biol. Chem. 266, 22010–22018. https://doi.org/10.1016/s0021-9258(18)54738-4

Gauthier, M., Aras, P., Paquin, J., Boily, M., 2018. Chronic exposure to imidacloprid or thiamethoxam neonicotinoid causes oxidative damages and alters carotenoid-retinoid levels in caged honey bees (Apis mellifera). Sci. Rep. 8, 16274. https://doi.org/10.1038/s41598-018-34625-y

Gereben, B., Zavacki, A.M., Ribich, S., Kim, B.W., Huang, S.A., Simonides, W.S., Zeöld, A., Bianco, A.C., 2008. Cellular and Molecular Basis of Deiodinase-Regulated Thyroid Hormone Signaling1. Endocr. Rev. 29, 898–938. https://doi.org/10.1210/er.2008-0019

Giardoglou, P., Beis, D., 2019. On zebrafish disease models and matters of the heart. Biomedicines 7. https://doi.org/10.3390/biomedicines7010015

Glaberman, S., Padilla, S., Barron, M.G., 2017. Evaluating the zebrafish embryo toxicity test for pesticide hazard screening. Environ. Toxicol. Chem. 36, 1221–1226. https://doi.org/10.1002/etc.3641

Gonçalves, Í.F.S., Souza, T.M., Vieira, L.R., Marchi, F.C., Nascimento, A.P., Farias, D.F., 2020. Toxicity testing of pesticides in zebrafish—a systematic review on chemicals and associated toxicological endpoints. Environ. Sci. Pollut. Res. 27, 10185–10204. https://doi.org/10.1007/s11356-020-07902-5

Gourmelon, A., Ahtiainen, J., Organization for Economic Co-operation and Development, 2007. Developing Test Guidelines on invertebrate development and reproduction for the assessment of chemicals, including potential endocrine active substances- the OECD perspective. Ecotoxicology 16, 161–7. https://doi.org/10.1007/s10646-006-0105-1

Grumbach, K.H., Bach, T.J., 1979. The Effect of PS II Herbicides, Amitrol and SAN 6706 on the Activity of 3-Hydroxy-3-methylglutaryl-coenzyme-A-reductase and the Incorporation of [2-14C]Acetate and [2-3H]Mevalonate into Chloroplast Pigments of Radish Seedlings. Zeitschrift für Naturforsch. C 34, 941–943. https://doi.org/10.1515/znc-1979-1111

Gulati, K., Ray, A., 2009. Immunotoxicity, in: Handbook of Toxicology of Chemical Warfare Agents. Elsevier, pp. 595–609. https://doi.org/10.1016/B978-012374484-5.00040-7

Harrill, J.A., Viant, M.R., Yauk, C.L., Sachana, M., Gant, T.W., Auerbach, S.S., Beger, R.D., Bouhifd, M., O'Brien, J., Burgoon, L., Caiment, F., Carpi, D., Chen, T., Chorley, B.N., Colbourne, J., Corvi, R., Debrauwer, L., O'Donovan, C., Ebbels, T.M.D., Ekman, D.R., Faulhammer, F., Gribaldo, L., Hilton, G.M., Jones, S.P., Kende, A., Lawson, T.N., Leite, S.B., Leonards, P.E.G., Luijten, M., Martin, A., Moussa, L., Rudaz, S., Schmitz, O., Sobanski, T., Strauss, V., Vaccari, M., Vijay, V., Weber, R.J.M., Williams, A.J., Williams, A., Thomas, R.S., Whelan, M., 2021. Progress towards an OECD reporting framework for transcriptomics and metabolomics in regulatory toxicology. Regul. Toxicol. Pharmacol. 125, 105020. https://doi.org/10.1016/j.yrtph.2021.105020

Hason, M., Bartůněk, P., 2019. Zebrafish models of cancer-new insights on modeling human cancer in a non-mammalian vertebrate. Genes (Basel). 10, 1–30. https://doi.org/10.3390/genes10110935

Heijne, W.H., Kienhuis, A.S., van Ommen, B., Stierum, R.H., Groten, J.P., 2005. Systems toxicology: applications of toxicogenomics, transcriptomics, proteomics and metabolomics in toxicology. Expert Rev. Proteomics 2, 767–780. https://doi.org/10.1586/14789450.2.5.767

Heise, M.T., 2014. Viral Pathogenesis, in: Reference Module in Biomedical Sciences. Elsevier. https://doi.org/10.1016/B978-0-12-801238-3.00079-9

Helfer, G., Stevenson, T.J., 2020. Pleiotropic effects of proopiomelanocortin and VGF nerve growth factor inducible neuropeptides for the long-term regulation of energy balance. Mol. Cell. Endocrinol. 514, 110876. https://doi.org/10.1016/j.mce.2020.110876

Heusinkveld, H.J., Wackers, P.F.K., Schoonen, W.G., van der Ven, L., Pennings, J.L.A., Luijten, M., 2018. Application of the comparison approach to open TG-GATEs: A useful toxicogenomics tool for detecting modes of action in chemical risk assessment. Food Chem. Toxicol. 121, 115–123. https://doi.org/10.1016/j.fct.2018.08.007

Hidasi, A.O., Groh, K.J., Suter, M.J.-F., Schirmer, K., 2017. Clobetasol propionate causes immunosuppression in zebrafish (Danio rerio) at environmentally relevant concentrations. Ecotoxicol. Environ. Saf. 138, 16–24. https://doi.org/10.1016/j.ecoenv.2016.11.024

Hogstrand, C., Haux, C., 1991. Binding and detoxification of heavy metals in lower vertebrates with reference to metallothionein. Comp. Biochem. Physiol. Part C Comp. Pharmacol. 100, 137–141. https://doi.org/10.1016/0742-8413(91)90140-O

Holzer, G., Besson, M., Lambert, A., François, L., Barth, P., Gillet, B., Hughes, S., Piganeau, G., Leulier, F., Viriot, L., Lecchini, D., Laudet, V., 2017. Fish larval recruitment to reefs is a thyroid hormone-mediated metamorphosis sensitive to the pesticide chlorpyrifos. Elife 6, 1–22. https://doi.org/10.7554/eLife.27595

Huerta-Cepas, J., Forslund, K., Coelho, L.P., Szklarczyk, D., Jensen, L.J., Von Mering, C., Bork, P., 2017. Fast genome-wide functional annotation through orthology assignment by eggNOG-mapper. Mol. Biol. Evol. 34, 2115–2122. https://doi.org/10.1093/molbev/msx148

IRAC, 2016. Mode of Action Classification: The key to Insecticide Resistance Management 0, 2016.

Ishizawa, H., Kuroda, M., Morikawa, M., Ike, M., 2017. Evaluation of environmental bacterial communities as a factor affecting the growth of duckweed Lemna minor. Biotechnol. Biofuels 10, 62. https://doi.org/10.1186/s13068-017-0746-8

Istvan, E.S., 2001. Bacterial and mammalian HMG-CoA reductases: related enzymes with distinct architectures. Curr. Opin. Struct. Biol. 11, 746–51. https://doi.org/10.1016/s0959-440x(01)00276-7

Iwaniuk, A.N., Koperski, D.T., Cheng, K.M., Elliott, J.E., Smith, L.K., Wilson, L.K., Wylie, D.R.W., 2006. The effects of environmental exposure to DDT on the brain of a songbird: Changes in structures associated with mating and song. Behav. Brain Res. 173, 1–10. https://doi.org/10.1016/j.bbr.2006.05.026

Jemec, A., Tišler, T., Drobne, D., Sepčić, K., Fournier, D., Trebše, P., 2007. Comparative toxicity of imidacloprid, of its commercial liquid formulation and of diazinon to a non-target arthropod, the microcrustacean Daphnia magna. Chemosphere 68, 1408–1418. https://doi.org/10.1016/j.chemosphere.2007.04.015

Johnson, A.C., Jin, X., Nakada, N., Sumpter, J.P., 2020. Learning from the past and considering the future of chemicals in the environment. Science (80-.). 367, 384–387. https://doi.org/10.1126/science.aay6637

Johnson, L.A., Jackson, D.G., 2021. Hyaluronan and Its Receptors: Key Mediators of Immune Cell Entry and Trafficking in the Lymphatic System. Cells 10, 2061. https://doi.org/10.3390/cells10082061

Kataoka, C., Kashiwada, S., 2021. Ecological Risks Due to Immunotoxicological Effects on Aquatic Organisms. Int. J. Mol. Sci. 22, 8305. https://doi.org/10.3390/ijms22158305

Kellman, B.P., Baghdassarian, H.M., Pramparo, T., Shamie, I., Gazestani, V., Begzati, A., Li, S., Nalabolu, S., Murray, S., Lopez, L., Pierce, K., Courchesne, E., Lewis, N.E., 2021. Multiple freeze-thaw cycles lead to a loss of consistency in poly(A)-enriched RNA sequencing. BMC Genomics 22, 69.

https://doi.org/10.1186/s12864-021-07381-z
Kim, H.J., Koedrith, P., Seo, Y.R., 2015. Ecotoxicogenomic approaches for understanding molecular mechanisms of environmental chemical toxicity using aquatic invertebrate, Daphnia model organism. Int. J. Mol. Sci. 16, 12261–87. https://doi.org/10.3390/ijms160612261
Klarić, T., Lardelli, M., Key, B., Koblar, S., Lewis, M., 2014. Activity-dependent expression of neuronal PAS domain-containing protein 4 (npas4a) in the developing zebrafish brain. Front. Neuroanat. 8, 1–13. https://doi.org/10.3389/fnana.2014.00148
Klüver, N., König, M., Ortmann, J., Massei, R., Paschke, A., Kühne, R., Scholz, S., 2015. Fish embryo toxicity test: Identification of compounds with weak toxicity and analysis of behavioral effects to improve prediction of acute toxicity for neurotoxic compounds. Environ. Sci. Technol. 49, 7002–7011. https://doi.org/10.1021/acs.est.5b01910
Knöll, R., Hoshijima, M., Hoffman, H.M., Person, V., Lorenzen-Schmidt, I., Bang, M.L., Hayashi, T., Shiga, N., Yasukawa, H., Schaper, W., McKenna, W., Yokoyama, M., Schork, N.J., Omens, J.H., McCulloch, A.D., Kimura, A., Gregorio, C.C., Poller, W., Schaper, J., Schultheiss, H.P., Chien, K.R., 2002. The cardiac mechanical stretch sensor machinery involves a Z disc complex that is defective in a subset of human dilated cardiomyopathy. Cell 111, 943–955. https://doi.org/10.1016/S0092-8674(02)01226-6
Koller, L.D., 2001. A perspective on the progression of immunotoxicology. Toxicology 160, 105–110. https://doi.org/10.1016/S0300-483X(00)00434-0
Krassowski, M., Das, V., Sahu, S.K., Misra, B.B., 2020. State of the Field in Multi-Omics Research: From Computational Needs to Data Mining and Sharing. Front. Genet. https://doi.org/10.3389/fgene.2020.610798
Krewski, D., Acosta, D., Andersen, M., Anderson, H., Bailar, J.C., Boekelheide, K., Brent, R., Charnley, G., Cheung, V.G., Green, S., Kelsey, K.T., Kerkvliet, N.I., Li, A.A., McCray, L., Meyer, O., Patterson, R.D., Pennie, W., Scala, R.A., Solomon, G.M., Stephens, M., Yager, J., Zeise, L., Staff of Committee on Toxicity Test, 2010. Toxicity Testing in the 21st Century: A Vision and a Strategy. J. Toxicol. Environ. Heal. Part B 13, 51–138. https://doi.org/10.1080/10937404.2010.483176
Krewski, D., Andersen, M.E., Tyshenko, M.G., Krishnan, K., Hartung, T., Boekelheide, K., Wambaugh, J.F., Jones, D., Whelan, M., Thomas, R., Yauk, C., Barton-Maclaren, T., Cote, I., 2020. Toxicity testing in the 21st century: progress in the past decade and future perspectives, Archives of Toxicology. Springer Berlin Heidelberg. https://doi.org/10.1007/s00204-019-02613-4
Kühnel, D., Nickel, C., 2014. The OECD expert meeting on ecotoxicology and environmental fate--towards the development of improved OECD guidelines for the testing of nanomaterials. Sci. Total Environ. 472, 347–53. https://doi.org/10.1016/j.scitotenv.2013.11.055
LaLone, C.A., Ankley, G.T., Belanger, S.E., Embry, M.R., Hodges, G., Knapen, D., Munn, S., Perkins, E.J., Rudd, M.A., Villeneuve, D.L., Whelan, M., Willett, C., Zhang, X., Hecker, M., 2017. Advancing the adverse outcome pathway framework—An international horizon scanning approach. Environ. Toxicol. Chem. 36, 1411–1421. https://doi.org/10.1002/etc.3805
Lange, E., Tautenhahn, R., Neumann, S., Gröpl, C., 2008. Critical assessment of alignment procedures for LC-MS proteomics and metabolomics measurements. BMC Bioinformatics 9, 1–19. https://doi.org/10.1186/1471-2105-9-375
Lennernäs, H., 2003. Clinical pharmacokinetics of atorvastatin. Clin. Pharmacokinet. 42, 1141–60. https://doi.org/10.2165/00003088-200342130-00005
Li, R., Luo, C., Qiu, J., Li, Y., Zhang, H., Tan, H., 2022. Metabolomic and transcriptomic investigation of the mechanism involved in enantioselective toxicity of imazamox in Lemna minor. J. Hazard. Mater. 425, 127818. https://doi.org/10.1016/j.jhazmat.2021.127818
Liang, X., Martyniuk, C.J., Simmons, D.B.D., 2020. Are we forgetting the “proteomics” in multi-omics ecotoxicology? Comp. Biochem. Physiol. - Part D Genomics Proteomics 36, 100751. https://doi.org/10.1016/j.cbd.2020.100751
Lin, W.J., Jiang, C., Sadahiro, M., Bozdagi, O., Vulchanova, L., Alberini, C.M., Salton, S.R., 2015. VGF and its C-terminal peptide TLQP-62 regulate memory formation in hippocampus via a BDNF-TrkB-dependent mechanism. J. Neurosci. 35, 10343–10356. https://doi.org/10.1523/JNEUROSCI.0584-15.2015
Lin, Y., Bloodgood, B.L., Hauser, J.L., Lapan, A.D., Koon, A.C., Kim, T.K., Hu, L.S., Malik, A.N., Greenberg, M.E., 2008. Activity-dependent regulation of inhibitory synapse development by Npas4. Nature 455, 1198–1204. https://doi.org/10.1038/nature07319
Liu, P., Ewald, J., Galvez, J.H., Head, J., Crump, D., Bourque, G., Basu, N., Xia, J., 2021. Ultrafast functional profiling of RNA-seq data for nonmodel organisms. Genome Res. 31, 713–720. https://doi.org/10.1101/gr.269894.120
Liu, W., Rodgers, G.P., 2016. Olfactomedin 4 expression and functions in innate immunity, inflammation, and cancer. Cancer Metastasis Rev. 35, 201–212. https://doi.org/10.1007/s10555-016-9624-2
Lu, B., Kwan, K., Levine, Y.A., Olofsson, P.S., Yang, H., Li, J., Joshi, S., Wang, H., Andersson, U., Chavan, S.S., Tracey, K.J., 2014. α7 nicotinic acetylcholine receptor signaling inhibits inflammasome activation by preventing mitochondrial DNA release. Mol. Med. 20, 350–358.

https://doi.org/10.2119/molmed.2013.00117
Lubbers, R., van Essen, M.F., van Kooten, C., Trouw, L.A., 2017. Production of complement components by cells of the immune system. Clin. Exp. Immunol. 188, 183–194. https://doi.org/10.1111/cei.12952
Luebke, R., 1997. Aquatic Pollution-Induced Immunotoxicity in Wildlife Species,. Fundam. Appl. Toxicol. 37, 1–15. https://doi.org/10.1006/faat.1997.2310
Ma, Z.F., Skeaff, S.A., 2014. Thyroglobulin as a biomarker of iodine deficiency: a review. Thyroid 24, 1195–209. https://doi.org/10.1089/thy.2014.0052
Mackenzie, L.S., 2018. Thyroid Hormone Receptor Antagonists: From Environmental Pollution to Novel Small Molecules, 1st ed, Vitamins and Hormones. Elsevier Inc. https://doi.org/10.1016/bs.vh.2017.04.004
Magdy, B.W., Mohamed, F.E., Amin, A.S., Rana, S.S., 2016. Ameliorative effect of antioxidants (vitamins C and E) against abamectin toxicity in liver, kidney and testis of male albino rats. J. Basic Appl. Zool. 77, 69–82. https://doi.org/10.1016/j.jobaz.2016.10.002
Manna, D., Roy, G., Mugesh, G., 2013. Antithyroid drugs and their analogues: synthesis, structure, and mechanism of action. Acc. Chem. Res. 46, 2706–15. https://doi.org/10.1021/ar4001229
Maron, B.J., Maron, M.S., 2013. Hypertrophic cardiomyopathy. Lancet 381, 242–255. https://doi.org/10.1016/S0140-6736(12)60397-3
Martens, L., Hermjakob, H., Jones, P., Adamski, M., Taylor, C., States, D., Gevaert, K., Vandekerckhove, J., Apweiler, R., 2005. PRIDE: the proteomics identifications database. Proteomics 5, 3537–45. https://doi.org/10.1002/pmic.200401303
Martins, J., Oliva Teles, L., Vasconcelos, V., 2007. Assays with Daphnia magna and Danio rerio as alert systems in aquatic toxicology. Environ. Int. 33, 414–425. https://doi.org/10.1016/j.envint.2006.12.006
Martyniuk, C.J., 2018. Are we closer to the vision? A proposed framework for incorporating omics into environmental assessments. Environ. Toxicol. Pharmacol. https://doi.org/10.1016/j.etap.2018.03.005
Martyniuk, C.J., Simmons, D.B., 2016. Spotlight on environmental omics and toxicology: a long way in a short time. Comp. Biochem. Physiol. - Part D Genomics Proteomics 19, 97–101. https://doi.org/10.1016/j.cbd.2016.06.010
Matsuda, K., Buckingham, S.D., Kleier, D., Rauh, J.J., Grauso, M., Sattelle, D.B., 2001. Neonicotinoids: insecticides acting on insect nicotinic acetylcholine receptors. Trends Pharmacol. Sci. 22, 573–580. https://doi.org/10.1016/S0165-6147(00)01820-4
Mazurais, D., Servili, A., Noel, C., Cormier, A., Collet, S., Leseur, R., Le Roy, M., Vitré, T., Madec, L., Zambonino-Infante, J.-L., 2020. Transgenerational regulation of cbln11 gene expression in the olfactory rosette of the European sea bass (Dicentrarchus labrax) exposed to ocean acidification. Mar. Environ. Res. 159, 105022. https://doi.org/10.1016/j.marenvres.2020.105022
McCollum, C.W., Ducharme, N.A., Bondesson, M., Gustafsson, J.A., 2011. Developmental toxicity screening in zebrafish. Birth Defects Res. Part C Embryo Today Rev. 93, 67–114. https://doi.org/10.1002/bdrc.20210
Mi, H., Muruganujan, A., Huang, X., Ebert, D., Mills, C., Guo, X., Thomas, P.D., 2019. Protocol Update for large-scale genome and gene function analysis with the PANTHER classification system (v.14.0). Nat. Protoc. 14, 703–721. https://doi.org/10.1038/s41596-019-0128-8
Milieu Ltd, Ökopol, (RPA), R.& P.A., RIVM, 2017. Study for the strategy for a non-toxic environment of the 7th Environment Action Programme Final Report 1–132.
Mine, A., Matsunaka, S., 1975. Mode of action of bentazon: Effect on photosynthesis. Pestic. Biochem. Physiol. 5, 444–450. https://doi.org/10.1016/0048-3575(75)90017-6
Mkandawire, M., Teixeira da Silva, J.A., Dudel, E.G., 2014. The Lemna Bioassay: Contemporary Issues as the Most Standardized Plant Bioassay for Aquatic Ecotoxicology. Crit. Rev. Environ. Sci. Technol. 44, 154–197. https://doi.org/10.1080/10643389.2012.710451
Mottaz, H., Schönenberger, R., Fischer, S., Eggen, R.I.L., Schirmer, K., Groh, K.J., 2017. Dose-dependent effects of morphine on lipopolysaccharide (LPS)-induced inflammation, and involvement of multixenobiotic resistance (MXR) transporters in LPS efflux in teleost fish. Environ. Pollut. 221, 105–115. https://doi.org/10.1016/j.envpol.2016.11.046
Narumanchi, S., Wang, H., Perttunen, S., Tikkanen, I., Lakkisto, P., Paavola, J., 2021. Zebrafish Heart Failure Models. Front. Cell Dev. Biol. 9, 1–15. https://doi.org/10.3389/fcell.2021.662583
Nogimori, T., Braverman, L.E., Taurog, A., Fang, S.L., Wright, G., Emerson, C.H., 1986. A new class of propylthiouracil analogs: comparison of 5'-deiodinase inhibition and antithyroid activity. Endocrinology 118, 1598–605. https://doi.org/10.1210/endo-118-4-1598
OECD, 2019. Test No. 203: Fish, Acute Toxicity Test, Guidelines for the Testing of Chemicals, OECD Guidelines for the Testing of Chemicals, Section 2. OECD. https://doi.org/10.1787/9789264069961-en
OECD, 2013. Test No. 236: Fsh embryo toxicity (FET) test. Guidel. Test. Chem. 509–511. https://doi.org/10.3109/9781841848570-66
OECD, 2012a. The Adverse Outcome Pathway for Skin Sensitisation Initiated by Covalent Binding to Proteins. OECD Series on Testing and Assessment ENV/JM/MON, 1–59. https://doi.org/10.1787/9789264221444-en
OECD, 2012b. Test No. 211: Daphnia magna Reproduction Test. OECD Guidelines for the Testing of

Chemicals, Section 2. https://doi.org/10.1787/9789264185203-en
OECD, 2006. Test No. 221: Lemna sp. Growth Inhibition Test. Guidel. Test. Chem., OECD Guidelines for the Testing of Chemicals, Section 2 1–26. https://doi.org/10.1787/9789264016194-en
OECD, 2004. Test No. 202: Daphnia sp. Acute Immobilisation Test. Guidel. Test. Chem., OECD Guidelines for the Testing of Chemicals, Section 2 100, 327–341. https://doi.org/10.1787/9789264069947-en
OECD, 1992. Test No. 210: Fish, Early-Life Stage Toxicity Test. https://doi.org/https://doi.org/10.1787/9789264070103-en
Ojehomon, M., Alderman, S.L., Sandhu, L., Sutcliffe, S., Van Raay, T., Gillis, T.E., Dawson, J.F., 2018. Identification of the actc1c cardiac actin gene in zebrafish. Prog. Biophys. Mol. Biol. 138, 32–37. https://doi.org/10.1016/j.pbiomolbio.2018.06.007
Orsini, L., Gilbert, D., Podicheti, R., Jansen, M., Brown, J.B., Solari, O.S., Spanier, K.I., Colbourne, J.K., Rush, D., Decaestecker, E., Asselman, J., De Schamphelaere, K.A.C., Ebert, D., Haag, C.R., Kvist, J., Laforsch, C., Petrusek, A., Beckerman, A.P., Little, T.J., Chaturvedi, A., Pfrender, M.E., De Meester, L., Frilander, M.J., 2016. Daphnia magna transcriptome by RNA-Seq across 12 environmental stressors. Sci. Data. https://doi.org/10.1038/sdata.2016.30
Pagès, H., Carlson, M., Falcon, S., Li, N., 2021. AnnotationDbi: Manipulation of SQLite-based annotations in Bioconductor.
Parkinson, H., Kapushesky, M., Shojatalab, M., Abeygunawardena, N., Coulson, R., Farne, A., Holloway, E., Kolesnykov, N., Lilja, P., Lukk, M., Mani, R., Rayner, T., Sharma, A., William, E., Sarkans, U., Brazma, A., 2007. ArrayExpress--a public database of microarray experiments and gene expression profiles. Nucleic Acids Res. 35, D747-50. https://doi.org/10.1093/nar/gkl995
Patlewicz, G., Kuseva, C., Kesova, A., Popova, I., Zhechev, T., Pavlov, T., Roberts, D.W., Mekenyan, O., 2014. Towards AOP application – Implementation of an integrated approach to testing and assessment (IATA) into a pipeline tool for skin sensitization. Regul. Toxicol. Pharmacol. 69, 529–545. https://doi.org/10.1016/j.yrtph.2014.06.001
Patton, E.E., Zon, L.I., Langenau, D.M., 2021. Zebrafish disease models in drug discovery: from preclinical modelling to clinical trials. Nat. Rev. Drug Discov. 20, 611–628. https://doi.org/10.1038/s41573-021-00210-8
Perera, F., Herbstman, J., 2011. Prenatal environmental exposures, epigenetics, and disease. Reprod. Toxicol. 31, 363–373. https://doi.org/10.1016/j.reprotox.2010.12.055
Persson, L., Carney Almroth, B.M., Collins, C.D., Cornell, S., de Wit, C.A., Diamond, M.L., Fantke, P., Hassellöv, M., MacLeod, M., Ryberg, M.W., Søgaard Jørgensen, P., Villarrubia-Gómez, P., Wang, Z., Hauschild, M.Z., 2022. Outside the Safe Operating Space of the Planetary Boundary for Novel Entities. Environ. Sci. Technol. https://doi.org/10.1021/acs.est.1c04158
Petersen, E.J., Diamond, S.A., Kennedy, A.J., Goss, G.G., Ho, K., Lead, J., Hanna, S.K., Hartmann, N.B., Hund-Rinke, K., Mader, B., Manier, N., Pandard, P., Salinas, E.R., Sayre, P., 2015. Adapting OECD Aquatic Toxicity Tests for Use with Manufactured Nanomaterials: Key Issues and Consensus Recommendations. Environ. Sci. Technol. 49, 9532–47. https://doi.org/10.1021/acs.est.5b00997
Phillips, J.B., Westerfield, M., 2014. Zebrafish models in translational research: Tipping the scales toward advancements in human health. DMM Dis. Model. Mech. 7, 739–743. https://doi.org/10.1242/dmm.015545
Pietrini, F., Iannilli, V., Passatore, L., Carloni, S., Sciacca, G., Cerasa, M., Zacchini, M., 2022. Ecotoxicological and genotoxic effects of dimethyl phthalate (DMP) on Lemna minor L. and Spirodela polyrhiza (L.) Schleid. plants under a short-term laboratory assay. Sci. Total Environ. 806, 150972. https://doi.org/10.1016/j.scitotenv.2021.150972
Pitchai, A., Rajaretinam, R.K., Freeman, J.L., 2019. Zebrafish as an Emerging Model for Bioassay-Guided Natural Product Drug Discovery for Neurological Disorders. Medicines 6, 61. https://doi.org/10.3390/medicines6020061
Poulsen, R., De Fine Licht, H.H., Hansen, M., Cedergreen, N., 2021. Grandmother's pesticide exposure revealed bi-generational effects in Daphnia magna. Aquat. Toxicol. 236, 105861. https://doi.org/10.1016/j.aquatox.2021.105861
Qi, S., Wang, D., Zhu, L., Teng, M., Wang, C., Xue, X., Wu, L., 2018. Neonicotinoid insecticides imidacloprid, guadipyr, and cycloxaprid induce acute oxidative stress in Daphnia magna. Ecotoxicol. Environ. Saf. 148, 352–358. https://doi.org/10.1016/j.ecoenv.2017.10.042
Qiagen Ingenuity Systems, 2014. Ingenuity Upstream Regulator Analysis in IPA ®. Qiagen White Pap. 1–10. https://doi.org/http://pages.ingenuity.com/rs/ingenuity/images/0812%20upstream_regulator_analysis_whitepaper.pdf
Qiagen Ingenuity Systems, 2011. Ingenuity Downstream Effects Analysis in IPA. https://doi.org/http://pages.ingenuity.com/rs/ingenuity/images/0812 downstream_effects_analysis_whitepaper.pdf
Ramaiahgari, S.C., Auerbach, S.S., Saddler, T.O., Rice, J.R., Dunlap, P.E., Sipes, N.S., DeVito, M.J., Shah, R.R., Bushel, P.R., Merrick, B.A., Paules, R.S., Ferguson, S.S., 2019. The Power of Resolution:

Contextualized Understanding of Biological Responses to Liver Injury Chemicals Using High-throughput Transcriptomics and Benchmark Concentration Modeling. Toxicol. Sci. 169, 553–566. https://doi.org/10.1093/toxsci/kfz065

Ramamoorthi, K., Fropf, R., Belfort, G.M., Fitzmaurice, H.L., McKinney, R.M., Neve, R.L., Otto, T., Lin, Y., 2011. Npas4 Regulates a Transcriptional Program in CA3 Required for Contextual Memory Formation. Science (80-.). 334, 1669–1675. https://doi.org/10.1126/science.1208049

Rauh, V.A., Garcia, W.E., Whyatt, R.M., Horton, M.K., Barr, D.B., Louis, E.D., 2015. Prenatal exposure to the organophosphate pesticide chlorpyrifos and childhood tremor. Neurotoxicology 51, 80–86. https://doi.org/10.1016/j.neuro.2015.09.004

Reg (EC) No 1107/2009, 2009. Regulation (EC) No 1107/2009 of the European Parliament and of the Council of 21 October 2009 concerning the placing of plant protection products on the market and repealing Council Directives 79/117/EEC and 91/414/EEC. Off. J. Eur. Union L 309/1 91, 50. https://doi.org/https://eur-lex.europa.eu/eli/reg/2009/1107/oj

Reg (EC) No 1223/2009, 2009. Regulation (EC) No 1223/2009 of the European Parliament and of the Council of 30 November 2009 on cosmetic products. Off. J. Eur. Union L 342/59. https://doi.org/https://eur-lex.europa.eu/eli/reg/2009/1223/oj

Reg (EC) No 1907/2006, 2020. Commission Regulation (EU) 2020/507 of 7 April 2020 amending Regulation (EC) No 1907/2006 of the European Parliament and of the Council as regards the percentage of registration dossiers to be selected for compliance checking. Off. J. Eur. Union L 110/1. https://doi.org/https://eur-lex.europa.eu/eli/reg/2020/507/oj

Reg (EC) No 528/2012, 2012. Regulation (EU) No 528/2012 of the European Parliament and of the Council of 22 May 2012 concerning the making available on the market and use of biocidal products. Off. J. Eur. Union L 167/1. https://doi.org/https://eur-lex.europa.eu/eli/reg/2012/528/oj

Reg (EU) No 2019/6, 2018. Regulation (EU) 2019/6 of the European Parliament and of the Council of 11 December 2018 on veterinary medicinal products and repealing Directive 2001/82/EC. Off. J. Eur. Union L 4/43. https://doi.org/https://eur-lex.europa.eu/eli/reg/2019/6/oj

Rehberger, K., Baumann, L., Hecker, M., Braunbeck, T., 2018. Intrafollicular thyroid hormone staining in whole-mount zebrafish (Danio rerio) embryos for the detection of thyroid hormone synthesis disruption. Fish Physiol. Biochem. 44, 997–1010. https://doi.org/10.1007/s10695-018-0488-y

Rehberger, K., Werner, I., Hitzfeld, B., Segner, H., Baumann, L., 2017. 20 Years of fish immunotoxicology – what we know and where we are. Crit. Rev. Toxicol. 47, 509–535. https://doi.org/10.1080/10408444.2017.1288024

Reid, N.M., Whitehead, A., 2016. Functional genomics to assess biological responses to marine pollution at physiological and evolutionary timescales: toward a vision of predictive ecotoxicology. Brief. Funct. Genomics 15, 358–64. https://doi.org/10.1093/bfgp/elv060

Ritchie, H., Roser, M., 2019. Land Use. Our World Data.

Robertson, C.E., Wright, P.A., Köblitz, L., Bernier, N.J., 2014. Hypoxia-inducible factor-1 mediates adaptive developmental plasticity of hypoxia tolerance in zebrafish, Danio rerio. Proc. R. Soc. B Biol. Sci. 281. https://doi.org/10.1098/rspb.2014.0637

Rombough, P., Drader, H., 2009. Hemoglobin enhances oxygen uptake in larval zebrafish (Danio rerio) but only under conditions of extreme hypoxia. J. Exp. Biol. 212, 778–784. https://doi.org/10.1242/jeb.026575

Russell, W.M.S., Burch, R.L., 1959. The principles of humane experimental technique 238. https://doi.org/http://117.239.25.194:7000/jspui/bitstream/123456789/1342/1/PRILIMINERY%20%20AND%20%20CONTENTS.pdf

Russo, C., Isidori, M., Deaver, J.A., Poynton, H.C., 2018. Toxicogenomic responses of low level anticancer drug exposures in Daphnia magna. Aquat. Toxicol. 203, 40–50. https://doi.org/10.1016/j.aquatox.2018.07.010

Saltiel, A.R., Kahn, C.R., 2001. Insulin signalling and the regulation of glucose and lipid metabolism. Nature 414, 799–806. https://doi.org/10.1038/414799a

Sánchez-Bayo, F., Goka, K., 2005. Unexpected effects of zinc pyrithione and imidacloprid on Japanese medaka fish (Oryzias latipes). Aquat. Toxicol. 74, 285–293. https://doi.org/10.1016/j.aquatox.2005.06.003

Sarti, F., Zhang, Z., Schroeder, J., Chen, L., 2013. Rapid Suppression of Inhibitory Synaptic Transmission by Retinoic Acid. J. Neurosci. 33, 11440–11450. https://doi.org/10.1523/JNEUROSCI.1710-13.2013

Scharmüller, A., Schreiner, V.C., Schäfer, R.B., 2020. Standartox: Standardizing toxicity data. Data 5, 1–16. https://doi.org/10.3390/data5020046

Schmid, S., Fent, K., 2020. 17β-Estradiol and the glucocorticoid clobetasol propionate affect the blood coagulation cascade in zebrafish. Environ. Pollut. 259, 113808. https://doi.org/10.1016/j.envpol.2019.113808

Schmidt, F., Braunbeck, T., 2011. Alterations along the Hypothalamic-Pituitary-Thyroid Axis of the Zebrafish (Danio rerio) after Exposure to Propylthiouracil. J. Thyroid Res. 2011, 376243. https://doi.org/10.4061/2011/376243

Scholz, S., Klüver, N., Kühne, R., 2016. Analysis of the relevance and adequateness of using Fish Embryo Acute Toxicity (FET) Test Guidance (OECD 236) to fulfil the information requirements and addressing concerns

under REACH, European Chemicals Agency.
Schrenk, D., Bignami, M., Bodin, L., Chipman, J.K., del Mazo, J., Grasl-Kraupp, B., Hogstrand, C., Hoogenboom, L., Leblanc, J.C., Nebbia, C.S., Nielsen, E., Ntzani, E., Petersen, A., Sand, S., Vleminckx, C., Wallace, H., Barregård, L., Ceccatelli, S., Cravedi, J.P., Halldorsson, T.I., Haug, L.S., Johansson, N., Knutsen, H.K., Rose, M., Roudot, A.C., Van Loveren, H., Vollmer, G., Mackay, K., Riolo, F., Schwerdtle, T., 2020. Risk to human health related to the presence of perfluoroalkyl substances in food. EFSA J. 18. https://doi.org/10.2903/j.efsa.2020.6223
Schüttler, A., Altenburger, R., Ammar, M., Bader-Blukott, M., Jakobs, G., Knapp, J., Krüger, J., Reiche, K., Wu, G.M., Busch, W., 2019. Map and model-moving from observation to prediction in toxicogenomics. Gigascience 8, 1–22. https://doi.org/10.1093/gigascience/giz057
Schüttler, A., Reiche, K., Altenburger, R., Busch, W., 2017. The transcriptome of the zebrafish embryo after chemical exposure: A meta-analysis. Toxicol. Sci. 157, 291–304. https://doi.org/10.1093/toxsci/kfx045
Selgrade, M.K., 2007. Immunotoxicity - The risk is real. Toxicol. Sci. 100, 328–332. https://doi.org/10.1093/toxsci/kfm244
SETAC, 2019. Recommended Minimum Reporting Information for Environmental Toxicity Studies 1–3. https://doi.org/https://cdn.ymaws.com/www.setac.org/resource/resmgr/publications_and_resources/setac_tip_envtox_info.pdf
Shankar, P., McClure, R.S., Waters, K.M., Tanguay, R.L., 2021. Gene co-expression network analysis in zebrafish reveals chemical class specific modules. BMC Genomics 22, 1–21. https://doi.org/10.1186/s12864-021-07940-4
Shi, X., Chen, R., Zhang, Y., Yun, J., Brand-Arzamendi, K., Liu, X., Wen, X.Y., 2018. Zebrafish heart failure models: opportunities and challenges. Amino Acids 50, 787–798. https://doi.org/10.1007/s00726-018-2578-7
Snape, J.R., Maund, S.J., Pickford, D.B., Hutchinson, T.H., 2004. Ecotoxicogenomics: The challenge of integrating genomics into aquatic and terrestrial ecotoxicology. Aquat. Toxicol. 67, 143–154. https://doi.org/10.1016/j.aquatox.2003.11.011
Spaan, K., Haigis, A.-C., Weiss, J., Legradi, J., 2019. Effects of 25 thyroid hormone disruptors on zebrafish embryos: A literature review of potential biomarkers. Sci. Total Environ. 656, 1238–1249. https://doi.org/10.1016/j.scitotenv.2018.11.071
Sparks, T.C., Nauen, R., 2015. IRAC: Mode of action classification and insecticide resistance management. Pestic. Biochem. Physiol. https://doi.org/10.1016/j.pestbp.2014.11.014
Steffen, W., Richardson, K., Rockström, J., Cornell, S.E., Fetzer, I., Bennett, E.M., Biggs, R., Carpenter, S.R., de Vries, W., de Wit, C.A., Folke, C., Gerten, D., Heinke, J., Mace, G.M., Persson, L.M., Ramanathan, V., Reyers, B., Sörlin, S., 2015. Planetary boundaries: Guiding human development on a changing planet. Science (80-.). 347. https://doi.org/10.1126/science.1259855
Stinckens, E., Vergauwen, L., Blackwell, B.R., Ankley, G.T., Villeneuve, D.L., Knapen, D., 2020. Effect of Thyroperoxidase and Deiodinase Inhibition on Anterior Swim Bladder Inflation in the Zebrafish. Environ. Sci. Technol. 54, 6213–6223. https://doi.org/10.1021/acs.est.9b07204
Stinckens, E., Vergauwen, L., Schroeder, A.L., Maho, W., Blackwell, B.R., Witters, H., Blust, R., Ankley, G.T., Covaci, A., Villeneuve, D.L., Knapen, D., 2016. Impaired anterior swim bladder inflation following exposure to the thyroid peroxidase inhibitor 2-mercaptobenzothiazole part II: Zebrafish. Aquat. Toxicol. 173, 204–217. https://doi.org/10.1016/j.aquatox.2015.12.023
Strähle, U., Scholz, S., Geisler, R., Greiner, P., Hollert, H., Rastegar, S., Schumacher, A., Selderslaghs, I., Weiss, C., Witters, H., Braunbeck, T., 2012. Zebrafish embryos as an alternative to animal experiments-A commentary on the definition of the onset of protected life stages in animal welfare regulations. Reprod. Toxicol. 33, 128–132. https://doi.org/10.1016/j.reprotox.2011.06.121
Su, C., Jiang, Y., Yang, Y., Zhang, W., Xu, Q., 2019. Responses of duckweed (Lemna minor L.) to aluminum stress: Physiological and proteomics analyses. Ecotoxicol. Environ. Saf. 170, 127–140. https://doi.org/10.1016/j.ecoenv.2018.11.113
Szkudlinski, M.W., Fremont, V., Ronin, C., Weintraub, B.D., 2002. Thyroid-Stimulating Hormone and Thyroid-Stimulating Hormone Receptor Structure-Function Relationships. Physiol. Rev. 82, 473–502. https://doi.org/10.1152/physrev.00031.2001
Thienpont, B., Tingaud-Sequeira, A., Prats, E., Barata, C., Babin, P.J., Raldúa, D., 2011. Zebrafish eleutheroembryos provide a suitable vertebrate model for screening chemicals that impair thyroid hormone synthesis. Environ. Sci. Technol. 45, 7525–32. https://doi.org/10.1021/es202248h
Ton, C., Lin, Y., Willett, C., 2006. Zebrafish as a model for developmental neurotoxicity testing. Birth Defects Res. Part A - Clin. Mol. Teratol. 76, 553–567. https://doi.org/10.1002/bdra.20281
Torres-Hernández, B.A., Colón, L.R., Rosa-Falero, C., Torrado, A., Miscalichi, N., Ortíz, J.G., González-Sepúlveda, L., Pérez-Ríos, N., Suárez-Pérez, E., Bradsher, J.N., Behra, M., 2016. Reversal of pentylenetetrazole-altered swimming and neural activity-regulated gene expression in zebrafish larvae by valproic acid and valerian extract. Psychopharmacology (Berl). 233, 2533–2547. https://doi.org/10.1007/s00213-016-4304-z

United Nations Human Rights Council, 2017. Report of the Special Rapporteur on the right to food. Hum. Rights Counc. 34, 1–24.
van der Vaart, M., Spaink, H.P., Meijer, A.H., 2012. Pathogen Recognition and Activation of the Innate Immune Response in Zebrafish. Adv. Hematol. 2012, 1–19. https://doi.org/10.1155/2012/159807
van Dijk, J., Gustavsson, M., Dekker, S.C., van Wezel, A.P., 2021. Towards 'one substance – one assessment': An analysis of EU chemical registration and aquatic risk assessment frameworks. J. Environ. Manage. 280. https://doi.org/10.1016/j.jenvman.2020.111692
Van Hoeck, A., Horemans, N., Monsieurs, P., Cao, H.X., Vandenhove, H., Blust, R., 2015. The first draft genome of the aquatic model plant Lemna minor opens the route for future stress physiology research and biotechnological applications. Biotechnol. Biofuels 8, 1–13. https://doi.org/10.1186/s13068-015-0381-1
Verhaar, H.J.M., van Leeuwen, C.J., Hermens, J.L.M., 1992. Classifying environmental pollutants. Chemosphere 25, 471–491. https://doi.org/10.1016/0045-6535(92)90280-5
Verheijen, M.C., Meier, M.J., Asensio, J.O., Gant, T.W., Tong, W., Yauk, C.L., Caiment, F., 2022. R-ODAF: Omics data analysis framework for regulatory application. Regul. Toxicol. Pharmacol. 131, 105143. https://doi.org/10.1016/j.yrtph.2022.105143
Villeneuve, D.L., Crump, D., Garcia-Reyero, N., Hecker, M., Hutchinson, T.H., LaLone, C.A., Landesmann, B., Lettieri, T., Munn, S., Nepelska, M., Ottinger, M.A., Vergauwen, L., Whelan, M., 2014a. Adverse outcome pathway (AOP) development I: Strategies and principles. Toxicol. Sci. 142, 312–320. https://doi.org/10.1093/toxsci/kfu199
Villeneuve, D.L., Crump, D., Garcia-Reyero, N., Hecker, M., Hutchinson, T.H., LaLone, C.A., Landesmann, B., Lettieri, T., Munn, S., Nepelska, M., Ottinger, M.A., Vergauwen, L., Whelan, M., 2014b. Adverse outcome pathway development II: Best practices. Toxicol. Sci. 142, 321–330. https://doi.org/10.1093/toxsci/kfu200
Vissenberg, R., Manders, V.D., Mastenbroek, S., Fliers, E., Afink, G.B., Ris-Stalpers, C., Goddijn, M., Bisschop, P.H., 2015. Pathophysiological aspects of thyroid hormone disorders/thyroid peroxidase autoantibodies and reproduction. Hum. Reprod. Update 21, 378–387. https://doi.org/10.1093/humupd/dmv004
Vogel, B., Meder, B., Just, S., Laufer, C., Berger, I., Weber, S., Katus, H.A., Rottbauer, W., 2009. In-vivo characterization of human dilated cardiomyopathy genes in zebrafish. Biochem. Biophys. Res. Commun. 390, 516–522. https://doi.org/10.1016/j.bbrc.2009.09.129
Wang, Hong, Yu, M., Ochani, M., Amella, C.A., Tanovic, M., Susarla, S., Li, J.H., Wang, Haichao, Yang, H., Ulloa, L., Al-Abed, Y., Czura, C.J., Tracey, K.J., 2003. Nicotinic acetylcholine receptor α7 subunit is an essential regulator of inflammation. Nature 421, 384–388. https://doi.org/10.1038/nature01339
Wang, W., Li, R., Zhu, Q., Tang, X., Zhao, Q., 2016. Transcriptomic and physiological analysis of common duckweed Lemna minor responses to NH4+ toxicity. BMC Plant Biol. 16, 1–13. https://doi.org/10.1186/s12870-016-0774-8
Wang, X., Li, F., Chen, J., Ji, C., Wu, H., 2021. Integration of Computational Toxicology, Toxicogenomics Data Mining, and Omics Techniques to Unveil Toxicity Pathways. ACS Sustain. Chem. Eng. 9, 4130–4138. https://doi.org/10.1021/acssuschemeng.0c09196
Wendl, T., Lun, K., Mione, M., Favor, J., Brand, M., Wilson, S.W., Rohr, K.B., 2002. pax2.1 is required for the development of thyroid follicles in zebrafish. Development 129, 3751–3760. https://doi.org/10.1242/dev.129.15.3751
Wilkinson, M.D., Dumontier, M., Aalbersberg, Ij.J., Appleton, G., Axton, M., Baak, A., Blomberg, N., Boiten, J.W., da Silva Santos, L.B., Bourne, P.E., Bouwman, J., Brookes, A.J., Clark, T., Crosas, M., Dillo, I., Dumon, O., Edmunds, S., Evelo, C.T., Finkers, R., Gonzalez-Beltran, A., Gray, A.J.G., Groth, P., Goble, C., Grethe, J.S., Heringa, J., t Hoen, P.A.C., Hooft, R., Kuhn, T., Kok, R., Kok, J., Lusher, S.J., Martone, M.E., Mons, A., Packer, A.L., Persson, B., Rocca-Serra, P., Roos, M., van Schaik, R., Sansone, S.A., Schultes, E., Sengstag, T., Slater, T., Strawn, G., Swertz, M.A., Thompson, M., Van Der Lei, J., Van Mulligen, E., Velterop, J., Waagmeester, A., Wittenburg, P., Wolstencroft, K., Zhao, J., Mons, B., 2016. Comment: The FAIR Guiding Principles for scientific data management and stewardship. Sci. Data 3, 1–9. https://doi.org/10.1038/sdata.2016.18
Willi, R.A., Faltermann, S., Hettich, T., Fent, K., 2018. Active Glucocorticoids Have a Range of Important Adverse Developmental and Physiological Effects on Developing Zebrafish Embryos. Environ. Sci. Technol. 52, 877–885. https://doi.org/10.1021/acs.est.7b06057
Willi, R.A., Salgueiro-González, N., Carcaiso, G., Fent, K., 2019. Glucocorticoid mixtures of fluticasone propionate, triamcinolone acetonide and clobetasol propionate induce additive effects in zebrafish embryos. J. Hazard. Mater. 374, 101–109. https://doi.org/10.1016/j.jhazmat.2019.04.023
Witjes, L., Van Troys, M., Vandekerckhove, J., Vandepoele, K., Ampe, C., 2019. A new evolutionary model for the vertebrate actin family including two novel groups. Mol. Phylogenet. Evol. 141, 106632. https://doi.org/10.1016/j.ympev.2019.106632
Wittwehr, C., Aladjov, H., Ankley, G., Byrne, H.J., de Knecht, J., Heinzle, E., Klambauer, G., Landesmann, B., Luijten, M., MacKay, C., Maxwell, G., Meek, M.E.B., Paini, A., Perkins, E., Sobanski, T., Villeneuve, D.,

Waters, K.M., Whelan, M., 2017. How adverse outcome pathways can aid the development and use of computational prediction models for regulatory toxicology. Toxicol. Sci. 155, 326–336. https://doi.org/10.1093/toxsci/kfw207

Wu, T., Hu, E., Xu, S., Chen, M., Guo, P., Dai, Z., Feng, T., Zhou, L., Tang, W., Zhan, L., Fu, X., Liu, S., Bo, X., Yu, G., 2021. clusterProfiler 4.0: A universal enrichment tool for interpreting omics data. Innovation(China) 2, 100141. https://doi.org/10.1016/j.xinn.2021.100141

Yamamoto, I., 1999. Nicotine to Nicotinoids: 1962 to 1997, in: Nicotinoid Insecticides and the Nicotinic Acetylcholine Receptor. Springer Japan, Tokyo, pp. 3–27. https://doi.org/10.1007/978-4-431-67933-2_1

Yang, J.S., Qi, W., Farias-Pereira, R., Choi, S., Clark, J.M., Kim, D., Park, Y., 2019. Permethrin and ivermectin modulate lipid metabolism in steatosis-induced HepG2 hepatocyte. Food Chem. Toxicol. 125, 595–604. https://doi.org/10.1016/j.fct.2019.02.005

Yang, S., Marín-Juez, R., Meijer, A.H., Spaink, H.P., 2015. Common and specific downstream signaling targets controlled by Tlr2 and Tlr5 innate immune signaling in zebrafish. BMC Genomics 16, 547. https://doi.org/10.1186/s12864-015-1740-9

Yu, G., 2020. Gene ontology semantic similarity analysis using GOSemSim, in: Methods in Molecular Biology. Humana Press Inc., pp. 207–215. https://doi.org/10.1007/978-1-0716-0301-7_11

Yu, G., He, Q.-Y., 2016. ReactomePA: an R/Bioconductor package for reactome pathway analysis and visualization. Mol. Biosyst. 12, 477–479. https://doi.org/10.1039/c5mb00663e

Yu, G., Wang, L.-G., Han, Y., He, Q.-Y., 2012. ClusterProfiler: An R package for comparing biological themes among gene clusters. Omi. A J. Integr. Biol. 16, 284–287. https://doi.org/10.1089/omi.2011.0118

Zhu, J., Liu, X., Cai, X., Ouyang, G., Zha, H., Zhou, Z., Liao, Q., Wang, J., Xiao, W., 2020. Zebrafish prmt3 negatively regulates antiviral responses. FASEB J. 34, 10212–10227. https://doi.org/10.1096/fj.201902569R

Zurlinden, T.J., Saili, K.S., Rush, N., Kothiya, P., Judson, R.S., Houck, K.A., Hunter, E.S., Baker, N.C., Palmer, J.A., Thomas, R.S., Knudsen, T.B., 2020. Profiling the ToxCast Library With a Pluripotent Human (H9) Stem Cell Line-Based Biomarker Assay for Developmental Toxicity. Toxicol. Sci. 174, 189–209. https://doi.org/10.1093/toxsci/kfaa014

ANNEX

A1 Toxicogenomic fin(ger)prints for thyroid disruption AOP refinement and biomarker identification in zebrafish embryos

Declaration of author contributions to the publication:

Toxicogenomic fin(ger)prints for thyroid disruption AOP refinement and biomarker identification in zebrafish embryos

DOI: 10.1016/j.scitotenv.2020.143914
Status: Published
Journal: **Science of the Total Environment**

Contributing authors:
Reinwald H. (**RH**)*, König A.* (KA), Ayobahan S. U. (AS), Alvincz J. (AJ), Sipos L (SL)., Göckener B. (GB), Böhled G. (BG), Shomronie O. (SO), Hollert H. (HH), Salinas G. (SG), Schäfers C. (SC), Eilebrecht E. (EE) & Eilebrecht S. (ES)

(1) Concept and design

Doctoral candidate **RH**: 25% - Design and implementation of bioinformatic RNA-sequence read processing pipeline including sequence reads and alignment quality checks; sample management plan; public RNASeq database upload management
Co-author KA: 20%
Co-author ES, EE, SC: 55%

(2) Conducting tests and experiments

Doctoral candidate **RH**: 10% - Preliminary test for RNA and proteins extraction as well as TMT labelling protocol optimization
Co-author KA: 30% - Performance of toxicity tests for physiological endpoints; microscopic imaging
Co-author AJ: 15% - Performance of toxicity tests; RNA and protein extraction and molecular sample quality control
Co-author SL: 10% - TMT multiplex labelling of protein samples
Co-author AS: 10% - LC-MS/MS shotgun proteomic measurements
Co-author GS, SO: 5% - mRNA-Sequence library preparation and Illumina HiSeq NGS
Co-author BG: 10% - RT-qPCR
Co-author GB: 10% - Chemical analytics of tested substance concentrations

(3) Compilation of data sets and figures

Doctoral candidate **RH**: 50% - mRNA-Seq & PSM shotgun-proteomics data compilation; data QC plots (multiQC reports, dissimilarity matrix, tSNE & PCA clustering, p-value distribution, count library normalization plots …); biomarker selection for plotting venn diagrams and heatmaps; sample signal (log2FC) correlation plots; RNA-Seq log2FC expression bar plots
Co-author KA: 35% - Physiological effect imaging and image compilation; observed physiological effects dose-response curves (hatching delay, swim bladder width, relative pigmentation …)
Co-author ES: 15% - Upstream analysis plots; downstream effect analysis plots; visualization of suggestion for AOP refinement

(4) Analysis and interpretation of data

Doctoral candidate **RH**: 50% - RNASeq raw data processing and QC; design and programming of R scripts for differential gene expression analysis (DGEA) and multivariate data exploration for transcriptomic and proteomic datasets; DGEA data mining for potential biomarker discovery;
Co-author KA: 30% - dose-response calculations of physiological endpoints
Co-author AS: 10% - MS peptide spectra matching with proteome discoverer
Co-author ES: 10% - upstream analysis

(5) Drafting of manuscript

Doctoral candidate **RH**: 30%
Co-author KA: 30%
Co-author ES, EE, AS: 30%
Co-author SC, HH: 10% - Final draft comments

Science of the Total Environment 760 (2021) 143914

Contents lists available at ScienceDirect

Science of the Total Environment

journal homepage: www.elsevier.com/locate/scitotenv

Toxicogenomic fin(ger)prints for thyroid disruption AOP refinement and biomarker identification in zebrafish embryos

Hannes Reinwald [a,b,1], Azora König [a,1], Steve U. Ayobahan [a], Julia Alvincz [a], Levente Sipos [a], Bernd Göckener [c], Gisela Böhle [d], Orr Shomroni [e], Henner Hollert [b], Gabriela Salinas [e], Christoph Schäfers [d], Elke Eilebrecht [d], Sebastian Eilebrecht [a,*]

[a] Fraunhofer Attract Eco'n'OMICs, Fraunhofer Institute for Molecular Biology and Applied Ecology, Schmallenberg, Germany
[b] Department Evolutionary Ecology and Environmental Toxicology, Faculty Biological Sciences, Goethe University Frankfurt, Frankfurt, Germany
[c] Department Environmental and Food Analysis, Fraunhofer Institute for Molecular Biology and Applied Ecology, Schmallenberg, Germany
[d] Department Ecotoxicology, Fraunhofer Institute for Molecular Biology and Applied Ecology, Schmallenberg, Germany
[e] NGS-Services for Integrative Genomics, University of Göttingen, Göttingen, Germany

HIGHLIGHTS

- Toxicogenomic fingerprints of thyroid hormone signaling in zebrafish embryos
- Impaired thyroid hormone signaling dysregulates genes involved in muscle functioning.
- Mechanistic evidence for thyroid disruption AOP refinement in fish

GRAPHICAL ABSTRACT

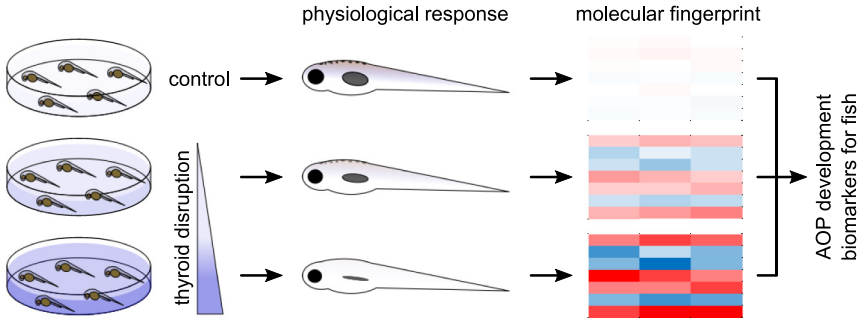

ARTICLE INFO

Article history:
Received 20 October 2020
Received in revised form 16 November 2020
Accepted 17 November 2020
Available online 10 December 2020

Editor: Damia Barcelo

Keywords:
Ecotoxicogenomics
Thyroid signaling
AOP refinement
Zebrafish embryo
Biomarkers

ABSTRACT

Endocrine disruption (ED) can trigger far-reaching effects on environmental populations, justifying a refusal of market approval for chemicals with ED properties. For the hazard assessment of ED effects on the thyroid system, regulatory decisions mostly rely on amphibian studies. Here, we used transcriptomics and proteomics for identifying molecular signatures of interference with thyroid hormone signaling preceding physiological effects in zebrafish embryos. For this, we analyzed the thyroid hormone 3,3′,5-triiodothyronine (T3) and the thyroid peroxidase inhibitor 6-propyl-2-thiouracil (6-PTU) as model substances for increased and repressed thyroid hormone signaling in a modified zebrafish embryo toxicity test. We identified consistent gene expression fingerprints for both modes-of-action (MoA) at sublethal test concentrations. T3 and 6-PTU both significantly target the expression of genes involved in muscle contraction and functioning in an opposing fashion, allowing for a mechanistic refinement of key event relationships in thyroid-related adverse outcome pathways in fish. Furthermore, our fingerprints identify biomarker candidates for thyroid disruption hazard screening approaches. Perspectively, our findings will promote the AOP-based development of in vitro assays for thyroidal ED assessment, which in the long term will contribute to a reduction of regulatory animal tests.

1. Introduction

Humans and environmental organisms can both be exposed to hormone-like substances, which enter the environment by different

* Corresponding author.
E-mail address: sebastian.eilebrecht@ime.fraunhofer.de (S. Eilebrecht).
[1] Equal contributions.

https://doi.org/10.1016/j.scitotenv.2020.143914

routes, e.g. pharmaceutical application or agricultural land use. This is of specific concern, as the hormonal system of humans and animals is well-balanced and therefore vulnerable to external stressors such as endocrine disruptors. From the 1990s on, scientists and the public became aware of endocrine disrupting chemicals (EDCs). However, it is only recently that a legal definition of EDCs was published for biocides (European Commission, 2017) and pesticides (European Commission, 2018) by the European Commission. This reflects the long-lasting uncertainty and the ongoing debate about how to address this important regulatory aspect. Consequently, a joint guidance document was issued by ECHA and EFSA in 2018 (European Chemica Agency, 2018), aiming at harmonizing the identification of EDCs in the context of regulations. The regulation of EDCs in the European Union is hazard based, i.e. solely intrinsic endocrine disrupting properties are considered, without taking into account substance exposure. While the main regulatory effort is focused on estrogen, androgen, and steroidal (EAS) modalities, chemicals interfering with the thyroid system, so called thyroid disruptors, increasingly gain attention (Du et al., 2013; Freyberger and Ahr, 2006; Godfrey et al., 2017; Hallinger et al., 2017; Leemans et al., 2019; Thambirajah et al., 2019). Moreover, there is increasing scientific evidence of close interactions between different endocrine axes (Bruggemann et al., 2018). The thyroid hormone system plays an essential role during vertebrate embryonic and juvenile development, including morphogenesis, metabolism, growth, and neurodevelopment. As the amphibian metamorphosis from tadpole to frog has been well studied over decades, OECD test guidelines for thyroid disruption have been developed using *Xenopus laevis* as the test organism. This includes the *Xenopus* Embryo Thyroid Signaling Assay (XETA) (OECD, 2019) the Amphibian Metamorphosis Assay (AMA) (OECD, 2009) and the Larval Amphibian Growth & Development Assay (LAGDA) (OECD, 2015). Therefore, the environmental hazard assessment of substances of potential goitrogenic concern requires large numbers of test animals, which strongly contrasts with the 3R principle of reduction, replacement and refinement of animal experiments (Russell, 1959). Global efforts made (e.g. by the Horizon 2020 ERGO project; https://ergo-project.eu/) illustrate the necessity for developing alternative approaches to assess thyroid disrupting chemicals in fish. In the long term, these approaches may be integrated into fish studies like the Fish Early Life Stage test (FELS) (OECD, 1992), which are already requested by regulatory authorities for an assessment of chronic toxicity. Such an integration would therefore supersede the need for additional amphibian studies, which would significantly reduce the number of animal tests for regulatory decision making. Furthermore, approaches for an assessment of thyroid disruption in fish could be utilized for hazard screening development using non-protected life stages like the zebrafish embryo (Busch et al., 2011; Strahle et al., 2012). For instance, Selderslaghs et al. have previously used a teratogenic index, calculated as the ratio of lethal to teratogenic effect concentrations, for developing a screening assay for teratogenicity and embryotoxicity in zebrafish embryos (Selderslaghs et al., 2009). In fact, the hypothalamus-pituitary-thyroid (HPT) axis is well explored in zebrafish and shows conserved mechanisms when compared to the mammalian system. Thyroid follicle maturation and the onset of thyroid hormone production takes place around 72 h post fertilization (hpf) (Porazzi et al., 2009). Thyroid hormones are involved in normal scale development and pigmentation, as well as in a number of essential developmental processes (Brown, 1997). Previous studies investigated the effects of thyroid disruptors on the early development of zebrafish, observing eye malformations, failure to hatch, retarded resorption of the yolk sac, or impaired swim bladder inflation (Delrue et al., 2016). In order to support regulatory decision making, an adverse outcome pathway (AOP) network of thyroid disruption in different species was established recently, including mammals, birds, reptiles, amphibians and fish (Noyes et al., 2019). Different AOPs for thyroid disruption in fish are currently under development (see aopwiki.org), representing a basis for alternative thyroid hormone disruption testing strategies (Ankley and Edwards, 2018; Delrue et al., 2016; Knapen et al., 2020; Stinckens et al., 2018; Stinckens et al., 2020). Starting from different molecular initiating events (MIEs), such as deiodinase 1 (DIO1, AOPs 157 and 158), deiodinase 2 (DIO2, AOPs 155 and 156) or thyroid peroxidase (TPO, AOP 159) inhibition, they all share the key events (KEs) of decreased T3 serum levels, reduced swim bladder inflation, reduced swimming performance, reduced young of year survival, finally leading to the adverse outcome (AO) of decreased population trajectory (Stinckens et al., 2020). In all these AOPs, the KE relationship between decreased T3 serum levels and reduced swim bladder inflation is of particular importance, as it connects changes at the molecular level with an observable physiological effect. While the correlation between these KEs has been proven in different previous studies (Cavallin et al., 2017; Nelson et al., 2016; Stinckens et al., 2018; Stinckens et al., 2020; Stinckens et al., 2016), the mechanism by which disturbed T3 serum levels result in an impaired swim bladder inflation still remains unclear.

The goal of our study was to provide toxicogenomic signatures of increased and decreased thyroid hormone signaling in zebrafish embryos for identifying biomarker candidates of thyroid disruption and for refining KE relationships of thyroid-related AOPs in fish. As a model substance for increased thyroid hormone signaling, we used the thyroid hormone 3,3′,5-triiodothyronine (T3), while 6-propyl-2-thiouracil (6-PTU) was selected as a reference substance to capture two interrelated effects: an interference with thyroid hormone production by inhibiting thyroid peroxidase (TPO) (Davidson et al., 1978) and a potential subsequent impairment in thyroid hormone signaling. While 6-PTU was shown to also potently inhibit iodothyronine deiodinases in mammals (Nogimori et al., 1986), previous studies primarily suggest a TPO inhibitory effect in zebrafish (Schmidt and Braunbeck, 2011; Stinckens et al., 2020). A recent study by Rehberger et al. observed a concentration-dependent decrease in intrafollicular T3 and T4 in zebrafish embryos after exposure to 6-PTU, which is in line with an interference with thyroid hormone production already at larval life stages (Rehberger et al., 2018). The obtained fingerprints are publically accessible, allowing datamining by the scientific community as a basis for hazard screening development and mechanistic weight-of-evidence for thyroidal AOP development and refinement.

2. Materials and methods

2.1. Test substances

T3 (3, 3′,5-Triiodo-L-thyronine, CAS 6893-02-3, ≥95% purity) and 6-PTU (6-propyl-2-sulfanylidene-1H-pyrimidin-4-one, CAS 51-52-5, ≥99% purity) were purchased from Merck KGgA (Darmstadt, Germany). T3 stock solution was prepared in 1 N NaOH. All test and control solutions were prepared using copper-reduced tap water containting the same final concentration of NaOH. For 6-PTU, an acetone stock solution was prepared. The same final volume of acetone was added to all vials of test and control solutions and evaporated by aeration. Test solutions were prepared in copper-reduced tap water. The pH of all test solutions was adjusted to 7.5.

2.2. Chemical analysis

Nominal test concentrations for T3 ranged from 1.0 μg/L to 330.0 μg/L, those for 6-PTU ranged from 0.1 mg/L to 100.0 mg/L. The actual concentrations of T3 and 6-PTU in the aqueous solutions were determined by chemical analysis (Table 1). A detailed description of the analytical method is given in the supporting information section. Briefly, the aqueous samples were diluted with methanol (T3) and acetonitrile (6-PTU) and were analyzed by ultra-high performance liquid chromatography coupled with tandem mass spectrometry (UHPLC-MS/MS). Both methods were validated according to the EU guideline SANCO/3029/99 at a limit of quantification (LOQ) of 0.2 μg/L (T3) and 20 μg/L (6-PTU).

Table 1
Nominal and measured T3 and 6-PTU concentrations. Substance, nominal concentrations and mean measured concentrations ± standard deviation are shown. LOQ: limit of quantification.

Substance	Nominal concentration	Mean measured concentration ± standard deviation
T3	Control (0.0 μg/L)	<LOQ
	1.0 μg/L	0.23 ± 0.01 μg/L
	3.3 μg/L	1.14 ± 0.18 μg/L
	10.0 μg/L	2.35 ± 0.20 μg/L
	330.0 μg/L	186.60 ± 1.54 μg/L
6-PTU	Control (0.0 mg/L)	<LOQ
	0.1 mg/L	0.06 ± 0.00 mg/L
	1.0 mg/L	1.00 ± 0.10 mg/L
	10.0 mg/L	8.39 ± 1.90 mg/L
	100.0 mg/L	108.81 ± 2.08 mg/L

2.3. Test organism

Parental zebrafish (*Danio rerio*), obtained from West Aquarium GmbH (Bad Lauterberg, Germany) and genetically identical to the European Zebrafish Resource Center's wild-type AB were maintained under flow-through conditions in 150 L tanks at 26 ± 2 °C at a 12:12 h light/dark cycle in a temperature-controlled room. Animals were fed daily with TetraMin® (Tetra Werke, Melle, Germany) main feed and nauplii of *Artemia salina* ad libitum. The day before test start, glass spawning-trays with artificial substrate were placed at the bottom of each tank. After spawning in the morning, freshly fertilized eggs were transferred from the spawning-trays into a sieve, rinsed with clean water and put into glass dishes. Fertilized eggs (early blastula stage) were then transferred into glass petri dishes filled either with test or control solutions.

2.4. Modified zebrafish embryo toxicity test (zFET)

A modified zFET (OECD, 2013) was performed for detecting substance-induced gene expression changes and thyroid-related physiological effects. Each treatment was performed in triplicate. The test was conducted at 27 ± 1 °C at a 14:10 h light/dark cycle in a light incubator with a thermostat (Schütt, Göttingen, Germany). Prior to test start, glass petri dishes were pre-saturated with each test solution. 15 freshly fertilized eggs per condition and replicate were placed in each of the saturated glass petri dishes containing 8 mL of fresh, aerated test solutions. At 24 h post fertilization (hpf), the eggs were inspected visually and, if present, single coagulated eggs were recorded and removed. At 24, 48, 60, 72 and 96 hpf, overall survival, hatching rate and morphological malformations were recorded (Tables S1 and S3). At 48 hpf, aged solutions were replaced by fresh, aerated test solutions. At 96 hpf, the embryos intended for gene expression profiling were immediately and simultaneously euthanized on ice, before being mechanically homogenized at 5 m/s for 40 s at room temperature using Lysing Matrix D© ceramic beads and a FastPrep-24© homogenizer (MP Biomedicals, Irvine, USA). Total RNA and total protein was isolated using an RNA/protein extraction kit as recommended by the manufacturer (Macherey&Nagel). RNA was quantified using a Nanodrop system (Thermo Fisher Scientific, Waltham, USA) and quality was assessed with a 2100 Bioanalyzer system (Agilent, Santa Clara, USA) prior to RNA-Seq library preparation. For the assessment of thyroid-related physiological effects, the test was extended to 120 hpf, allowing for a complete development of the posterior swim bladder in control embryos (Chang et al., 2012). Then, 30 embryos per condition and replicate were used for analysis of physiological effects. Another 30 embryos were immediately and simultaneously euthanized on ice and subjected to total RNA extraction using a RNeasy® PowerLyzer® Tissue & Cells kit as recommended by the manufacturer (Qiagen, Hilden, Germany). Total RNA was quantified using a Nanodrop system and subjected to gene expression analysis by RT-qPCR.

2.5. Analysis of physiological and hatching effects

For analysis of physiological effects, embryos were anesthetized by a 200 mg/L Tricaine solution and fixed on slides with 3% methylcellulose (Merck, Darmstadt, Germany). Embryo images were taken in lateral view using a Leica DMI6000B inverted microscope and a Leica DFC420 camera (Leica Microsystems, Wetzlar, Germany) in black/white mode using a 1.25-fold and 5-fold magnification. After microscopy, all embryos were euthanized in ice. Images were analyzed using ImageJ (Schindelin et al., 2012). Briefly, lateral length and swim bladder width were measured in pixels and then transformed into mm values. To determine head pigmentation, image coloring was inverted and the pigmented area from above the eye to the end of the swim bladder on the dorsal side was selected (Fig. S1). Then the total area size was measured in pixels and normalized to the control's mean as relative head pigmentation. Normality and variance homogeniety of data were tested by Shapiro-Wilk's test and Levene's test, respectively. A Williams *t*-test of three replicates of each condition, consisting of 30 individuals each, was used to assess significant concentration-response relationships. Hatching rates of each exposure concentration were plotted for each replicate against the time post fertilization. For each exposure concentration, a non-linear curve fit was performed to obtain time points of 50% hatching (Fig. S2 and Table S2). A relative hatching delay was calculated as the difference between the time point of 50% hatching of the respective exposure and the corresponding control. Statistically significant hatching delay was assessed by one sample *t*-test (Table S2).

2.6. RT-qPCR

For gene expression analysis, 500 ng of total RNA of each condition and replicate was reverse transcribed with the QuantiTect® Reverse Transcription kit as recommended by the manufacturer (Qiagen, Hilden, Germany). 50 ng cDNA per reaction served as a template for the quantitative polymerase chain reaction (qPCR) analysis performed with the FastStart Essential DNA Green Master kit (Roche, Mannheim, Germany) and a Lightcycler 96 System (Roche, Basel, Switzerland) as recommended by the manufacturers. The PCR program consisted of a pre-incubation at 95 °C for 600 s and 40 cycles of denaturing at 95 °C for 10 s, annealing at 60 °C for 10 s and elongation at 72 °C for 10 s. Primers for qPCR are listed in Table S4. Data were analyzed using the Δct method with β-actin and RPL8 as housekeeping genes (Schmittgen and Livak, 2008). One-way Anova followed by Dunnett's multiple comparisons test of three replicates of each condition was performed to detect statistically significant differences in gene expression.

2.7. Transcriptomics

For transcriptome library preparation, RNA samples with RIN > 9.0 were selected. Poly(A) + RNA was purified from total RNA and subjected to library preparation using the TruSeq RNA Library Prep Kit v2 as recommended by the manufacturer (Illumina, San Diego, USA). Libraries were sequenced on an Illumina HiSeq 4000 System (Illumina, San Diego, USA) in 50 bp single read mode, producing approximately 30 million raw reads per sample. Adapter sequences were removed from demultiplexed fastq files by trimmomatic (Bolger et al., 2014) and sequence quality was assured via FastQC (Andrews, 2010). Sequences were aligned to the *Danio rerio* reference genome (GRCz11) with STAR aligner v.2.5.2a (Dobin et al., 2013). Feature mapped reads were counted in feature-Counts v1.5.0-p1 (Liao et al., 2014). Mapped read tables were merged to a single count matrix for each substance and analyzed in R (R Core Team, 2019) via RStudio (Loraine et al., 2015). After removing genes with less than 9 counts across all analyzed samples, count normalization and differential expression analysis was

performed in DESeq2 v1.26.0 (Love et al., 2014). This was based on three biological replicates per condition applying pairwise Wald's *t*-test with independent hypothesis weighting (IHW) for *p*-value correction after Benjamini-Hochberg (Ignatiadis et al., 2016). To measure the effect between the conditions while controlling for fish tank differences, a multifactor model design was implemented, taking into account tank and condition. An effect size cut off was determined for each treatment comparison as the 90% quantile of the absolute non-shrunk $\log_2$-fold change values. Log_2-fold changes were then shrunk with apeglm and the final set of differentially expressed genes (DEGs) was selected after statistical significance (padj < 0.05) and the individual effect size cut off (Zhu et al., 2019). Raw and processed data have been deposited in the ArrayExpress database at EMBL-EBI (www.ebi.uk/arrayexpress) (Athar et al., 2019) under accession numbers E-MTAB-9054 (6-PTU) and E-MTAB-9056 (T3). Data quality assessment is shown in Figs. S3 to S6. The DEG analysis script is publicly available under: https://github.com/hreinwal/DESeq2Analysis.

2.8. Proteomics

Protein samples were adjusted to 100 mM TEAB containing 0.2% SDS and 2 M urea, before they were quantified via BCA protein assay kit (Thermo Fisher, Waltham, USA) and their quality was assessed through a 2100 Bioanalyzer system (Agilent, Santa Clara, USA). 100 μg of total protein were reduced with 200 mM TCEP and alkylated using 375 mM iodoacetamide, before being subjected to tryptic digestion (Thermo Fisher, Waltham, USA) at 37 °C over night. Peptide concentrations were detemined by quantitative colorimetric peptide assay (Thermo Fisher, Waltham, USA). 25 μg of peptides per replicate and condition were subjected to Tandem-Mass-Tag (TMT) labeling as recommended by the manufacturer (Thermo Fisher, Waltham, USA) (Table S5). Subsequently, peptide samples were pooled by experimental replicate and purified via C18 spin columns as recommended by the manufacturer (Thermo Fisher, Waltham, USA). Purified samples were resuspended in 2% acetonitrile and 0.1% formic acid. 500 ng of each combined sample were loaded on a C18 μPAC-trapping column (PharmaFluidics, Ghent, Belgium) connected to a nanoACQUITY UPLC (Waters, Massachusetts, USA). The samples were analyzed before being separated on a 50 cm μPAC™C18 nano-LC column (PharmaFluidics, Ghent, Belgium) using a linear gradient from 1 to 97.5% of 90% acetonitrile in 0.1% formic acid for 150 min with a flow rate of 300 nL/min. The separated peptides were ionized via nanospray ion source and detected with a Q Exactive™Hybrid-Quadrupol-Orbitrap mass spectrometer (MS) (Thermo Fisher, Waltham, USA) (Ayobahan et al., 2019; Ayobahan et al., 2020). LC-MS/MS raw data were processed using Proteome Discoverer™ software version 2.4 (Thermo Fisher, Waltham, USA). For peptide identification, MS data were matched to the Ensembl zebrafish database (version 12/2019 with 42,306 target sequences) using the SEQUEST algorithm (Moore et al., 2002). Differentially expressed proteins were identified in MSstatsTMT v1.5.4 on the basis of three technical replicate measurements of three biological replicates per condition (Choi et al., 2014). Differential expression with Benjamini-Hochberg-corrected *p*-values of padj ≤ 0.05 was considered as statistically significant. The mass spectrometry proteomics data have been deposited in the ProteomeXchange Consortium via the PRIDE (Perez-Riverol et al., 2019) partner repository with the dataset identifiers PXD019079 (6-PTU) and PXD019111 (T3). Data quality assessment is shown in Figs. S7 to S9.

2.9. Pathway analysis

Ingenuity Pathway Analysis (IPA®) was used for pathway analysis as recommended by the manufacturer (Qiagen, Hilden, Germany). For analysis with IPA, zebrafish ENSEMBL gene IDs were converted to their human homologues using ENSEMBL Biomart (Yates et al., 2020). IPA Downstream Effects Analysis was used to identify biological functions that are expected to increase or decrease based on the observed expression changes. This analysis is based on expected causal effects between molecules and functions derived from the literature compiled in the Ingenuity® Knowledge Base. IPA Upstream Regulator Analysis was used to identify upstream regulators that may be responsible for the gene expression changes observed. The p-values of overlap were calculated by a right-tailed Fisher's Exact Test. The IPA z-score algorithm was used to derive predictions (Kramer et al., 2014).

3. Results and discussion

3.1. Physiological endpoints of T3 and 6-PTU in zebrafish embryos

First, we assessed endpoints described for interference with the thyroid system in zebrafish, i.e. total length, swim bladder inflation and head pigmentation (Jomaa et al., 2014) (see Fig. 1A) as well as time to hatch and the expression of selected genes related to the thyroid system (Spaan et al., 2019). As posterior swim bladder development in zebrafish is completed only at 120 hpf, all the above-mentioned endpoints were assessed in an extended zFET (Chang et al., 2012). Based on previous studies in zebrafish, we selected nominal exposure concentrations of 1.0 μg/L, 3.3 μg/L and 10.0 μg/L for T3 and 0.1 mg/L, 1.0 mg/L and 10.0 mg/L for 6-PTU (Haggard et al., 2018; Jomaa et al., 2014; Liu et al., 2011; Schmidt and Braunbeck, 2011; van der Ven et al., 2006). Despite the pre-coating of glass surfaces as a preventive measure, the corresponding measured T3 exposure concentrations of 0.23 μg/L, 1.14 μg/L and 2.35 μg/L are likely to result from strong T3 adsorption to glass (Table 1). The measured 6-PTU exposure concentrations were 0.06 mg/L, 1.00 mg/L and 8.39 mg/L (Table 1). The exposure to 1.14 μg/L and 2.35 μg/L T3 resulted in a statistically significant decrease in lateral length of the embryos, a reduction of swim bladder width and a significant loss in head pigmentation. The exposure to 1.0 mg/L and 8.39 mg/L 6-PTU led to a statistically significant hatching delay (Fig. 1B and Table S6). The observed T3-mediated effects are in line with previous literature (Spaan et al., 2019) and a concentration-dependent hatching delay was previously reported in zebrafish embryos after exposure to the fungicide thiram, a suspected inhibitor of TPO (Chen et al., 2019). To verify thyroid-related molecular mechanisms for both substances, we further analyzed the expression of a set of thyroid-related genes, i.e. thyroglobulin (tg), deiodinase 1 (dio1), thyroid hormone receptor beta (thrbeta) and thyroid peroxidase (tpo) (Spaan et al., 2019). The expression of thyroid-related genes was affected more potently by T3 than by 6-PTU (Fig. 1C).

While all genes were differentially expressed in a statistically significant manner after exposure to all tested T3 concentrations, dio1 was significantly affected by 6-PTU concentrations of 1.00 mg/L and 8.39 mg/L and tg as well as tpo were significantly differentially expressed after exposure to 8.39 mg/L 6-PTU only (Fig. 1C). Notably, the expression of tpo was significantly increased after exposure to 6-PTU, which indicates a compensatory mechanism in response to TPO inhibition (Cooper, 2005). Three genes (tg, dio1 and tpo) showed opposing effects when comparing the test substances, being down-regulated by T3 and up-regulated by 6-PTU. Thrbeta was significantly up-regulated only by T3 treatments. These observations are predominantly in line with previous literature (Baumann et al., 2016) and may again reflect compensation of high (T3) and low endogenous (6-PTU) thyroid hormone levels.

3.2. Transcriptome response to T3 and 6-PTU

Given its high sensitivity and comprehensiveness, we used RNA-Seq for assessing transcriptome changes induced by each test substance in zebrafish embryos at 96 hpf, to comply with the OECD zFET workflow (OECD, 2013). To assure applicability of the identified signatures for hazard identification over a wide range of concentrations, we detected gene expression changes induced by a low and a high sublethal test

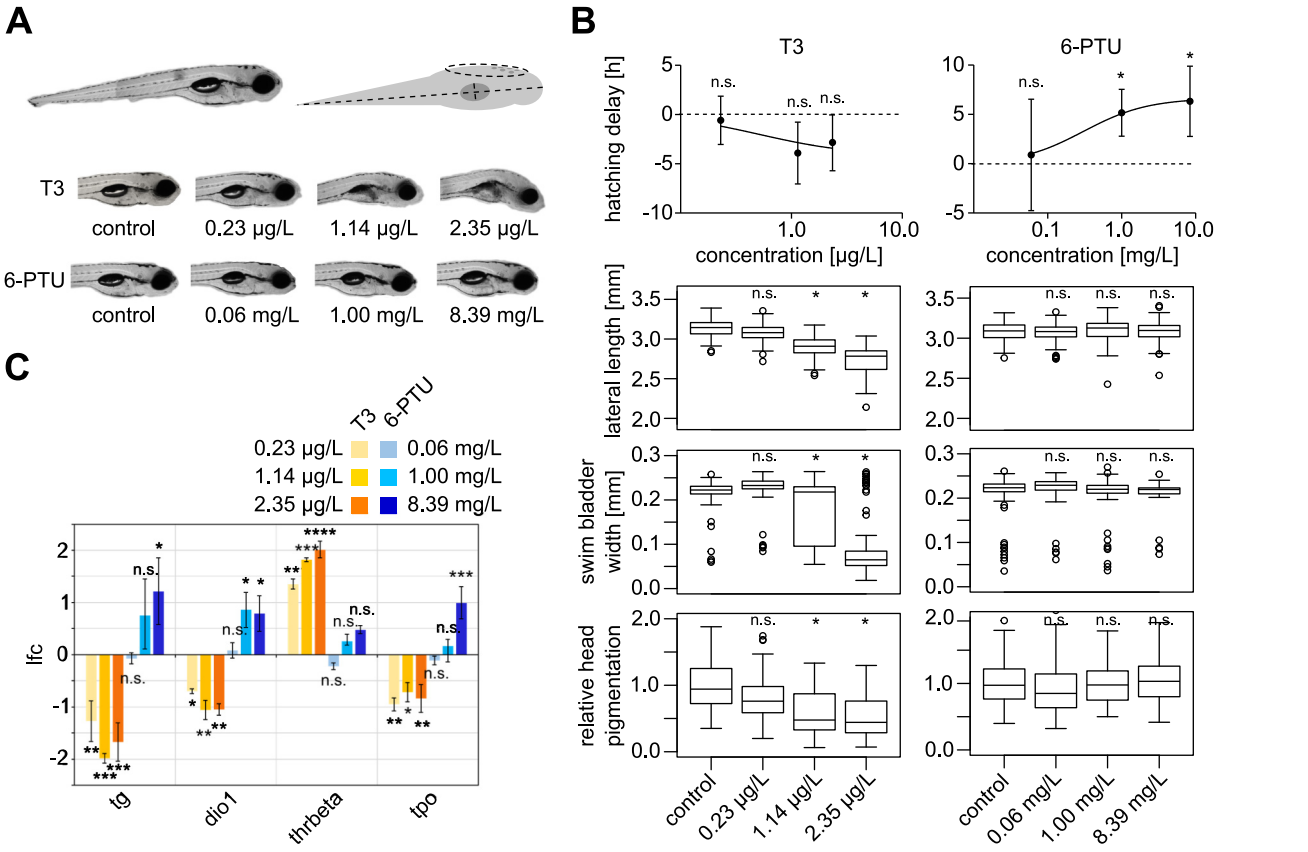

Fig. 1. Thyroid-related effects of T3 and 6-PTU in zebrafish embryos. (**A**) Physiological endpoints. Top: lateral view of a zebrafish embryo at 120 hpf (left). Lateral length, swim bladder width and head pigmentation measurements are indicated as dotted lines in the schematic view (right). Bottom: representative images of zebrafish embryos exposed to the indicated concentrations of T3 and 6-PTU as compared to non-treated controls. (**B**) Analysis of physiological endpoints upon exposure to different concentrations of T3 (left) and 6-PTU (right). Top: relative hatching delay compared to the control in hours. Statistical significance was assessed by a one sample *t*-test. Middle top: lateral length measurements in mm. Middle bottom: swim bladder width measurements in mm. Bottom: relative head pigmentation measurements. Statistical significance was assessed by William's t-test. N.s. not significant, $^{*}p \leq 0.05$. (**C**) RT-qPCR analysis of thyroid-related genes upon exposure to different concentrations of T3 and 6-PTU. The expression of tg, dio1, thrbeta and tpo upon exposure to the indicated concentrations of T3 and 6-PTU was compared to non-treated controls. Log_2-fold change (lfc) as compared to the non-treated controls are plotted. Statistical significance was assessed by one-way Anova followed by a Dunnett's multiple comparison test based on three biological replicates. N.s. not significant, *padj ≤ 0.05, **padj ≤ 0.01, ***padj ≤ 0.001, ****padj ≤ 0.0001.

concentration of each substance. Substance-specific signatures were defined as the common subset of DEGs after exposure to these two concentrations. For each substance, the low test concentration was selected as the lowest test concentration impairing physiological endpoints in a statistically significant manner, i.e. total length and swim bladder inflation for T3 and hatching for 6-PTU (Fig. 1). Notably, in the case of 6-PTU this concentration also represents the lower boundary of concentrations applied in amphibians for the validation of the AMA (OECD, 2007). The high nominal test concentration was set at a factor of 100 fold higher, resulting in measured concentrations of 186.6 µg/L in the case of T3 and 108.81 mg/L in the case of 6-PTU (Table 1). In both cases, exposure to the high test concentration did not induce lethality (Fig. S10).

In accordance with the observed thyroid-related physiological effects and in line with recent literature, T3 affected the transcriptome more potently than 6-PTU. A total set of 24,447 and 24,812 genes was analyzed for T3 and for 6-PTU, respectively, with a common set of 24,243 transcripts (see supplemental expression tables). Exposure to the high T3 test concentration resulted in 1056 DEGs (510 up, 547 down), while exposure to the low test concentration significantly affected the expression of 121 genes (93 up, 29 down) (Fig. 2A and supplemental expression table T3). 106 of these genes (88%) were in the common subset of both conditions. After exposure to the high 6-PTU test concentration, a total of 106 transcripts was identified as differentially expressed (27 up, 79 down) (Fig. 2A and supplemental expression table 6-PTU). 60 genes were significantly affected after exposure to the low 6-PTU test concentration (3 up, 57 down), of which 50 genes (83%) were in the common subset with the high exposure condition. For both substances, genes of the common subset of low and high exposure were concomitantly regulated in both exposure conditions without any exception, showing generally stronger regulation in the high exposure condition (Fig. 2B). Therefore, these genes respond to the corresponding model substance within a broad range of concentrations in a concentration-dependent fashion. Moreover, the expression of the remaining gene subsets of each exposure condition was highly positively correlated with respect to the other condition for each substance (Fig. 2B). A recent study by Haggard et al. identified a set of marker genes responsive to thyroid hormone receptor agonists in zebrafish embryos using microarray analyses (Haggard et al., 2018). Comparing the expression changes of these markers obtained by Haggard et al. with our results, we observed a highly concomitant regulation for T3 (Fig. S11), indicating that our approach is a reliable method for detection of substance-induced gene expression changes in zebrafish embryos. Against this background, we defined the common DEGs in high and low exposure as specific transcriptomic fingerprints for the tested substance (Fig. 2C).

These molecular signatures differentiate between the substances really well with only a single gene being part of both signatures, indicating a highly substance specific ecotoxicogenomic profile which cannot be explained by general stress signaling responses or systemic toxicity. When relaxing the constraints for signature definition to genes identified as DEG in at least the high exposure condition, we can increase

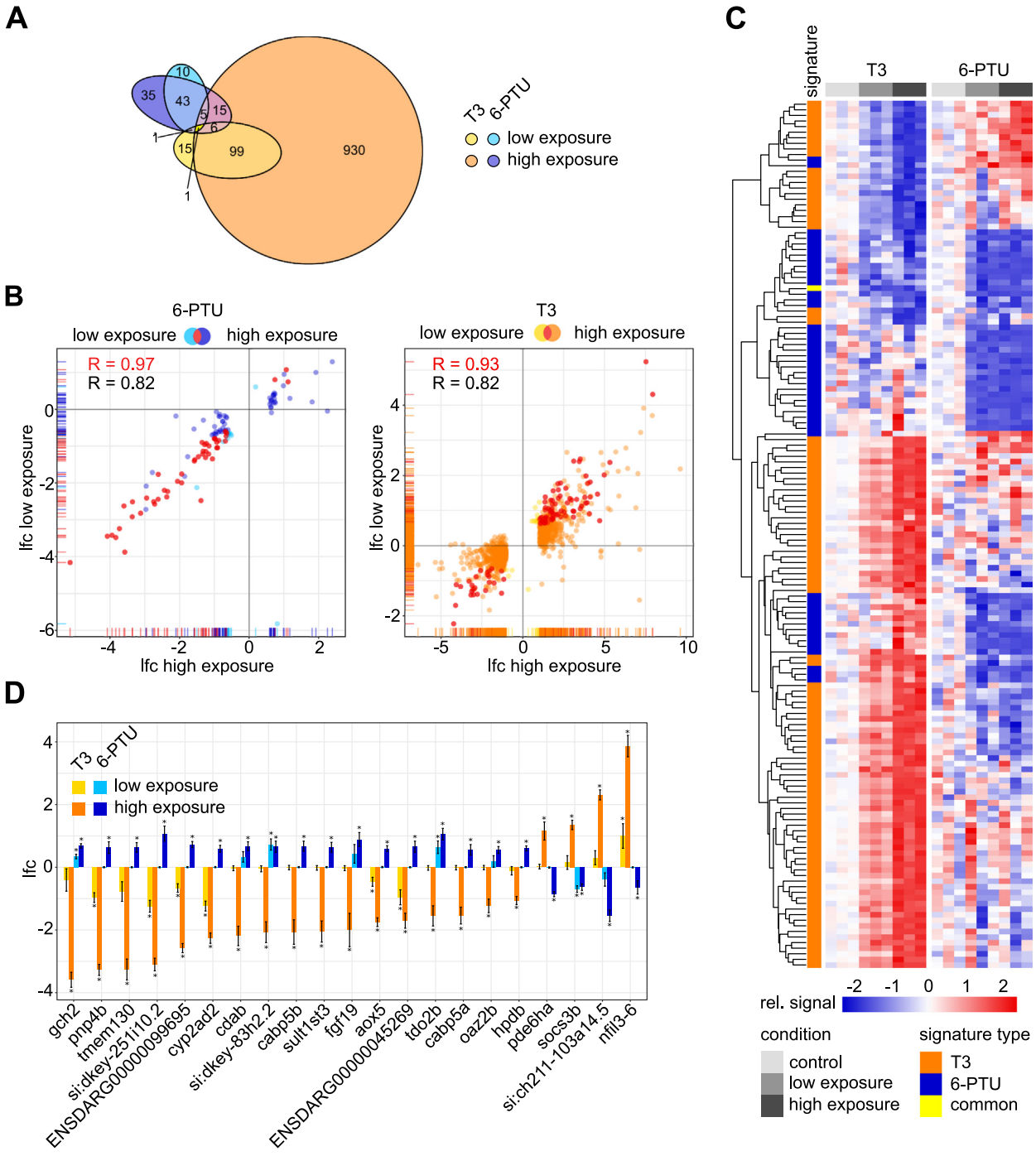

Fig. 2. Transcriptome response of zebrafish embryos to sublethal concentrations of T3 and 6-PTU at 96 hpf. (**A**) Venn diagram showing differentially expressed genes (DEGs) after exposure to 186.6 μg/L (high exposure, orange) and 1.14 μg/L (low exposure, yellow) T3 and to 108.81 mg/L (high exposure, dark blue) and 1.00 mg/L (low exposure, light blue) 6-PTU as compared to the non-treated controls. Displayed ellipses and intersection sizes correspond to the numbers of DEGs. (**B**) Scatter plots comparing ll $\log_2$-fold change (lfc) values of DEGs observed after low and high exposure to each corresponding substance. The common subset of both exposures is colored in red and considered as a substance-specific signature. (**C**) Heatmap containing the signature genes, which are indicated in red in the chart (B). The relative signal normalized to the control within each treatment of each gene (rows) is shown for each sample (columns). As compared to the mean of each non-treated control, an enhanced expression is indicated in red and a suppressed expression is indicated in blue. Genes are clustered after maximum distance measure with average linkage. The association with a T3 or a 6-PTU signature is indicated in orange and blue, respectively. Genes associated with both signatures are colored in yellow. (**D**) Lfc values of potential common marker genes for distinguishing T3 and 6-PTU responses. All genes were observed as DEGs in either low or high exposure condition after exposure to both substances and showed a counter-regulated response for T3 and 6-PTU. * indicates, in which treatment the corresponding gene was observed as a DEG. (For interpretation of the references to colour in this figure legend, the reader is referred to the web version of this article.)

the overlap between 6-PTU- and T3-responsive genes to 39, of which 31 (79%) are regulated in opposing directions when comparing 6-PTU and T3 (Fig. 2D). These genes represent promising biomarker candidates, which allow for a differentiation between enhanced thyroid signaling (T3) and the inhibition of thyroid hormone synthesis (6-PTU).

3.3. Proteome response to T3 and 6-PTU

Since valuable molecular biomarkers should be easily detectable, we further focused on robustly expressed gene products at the protein level. Consequently, we complemented transcriptomics by LC-MS/MS-

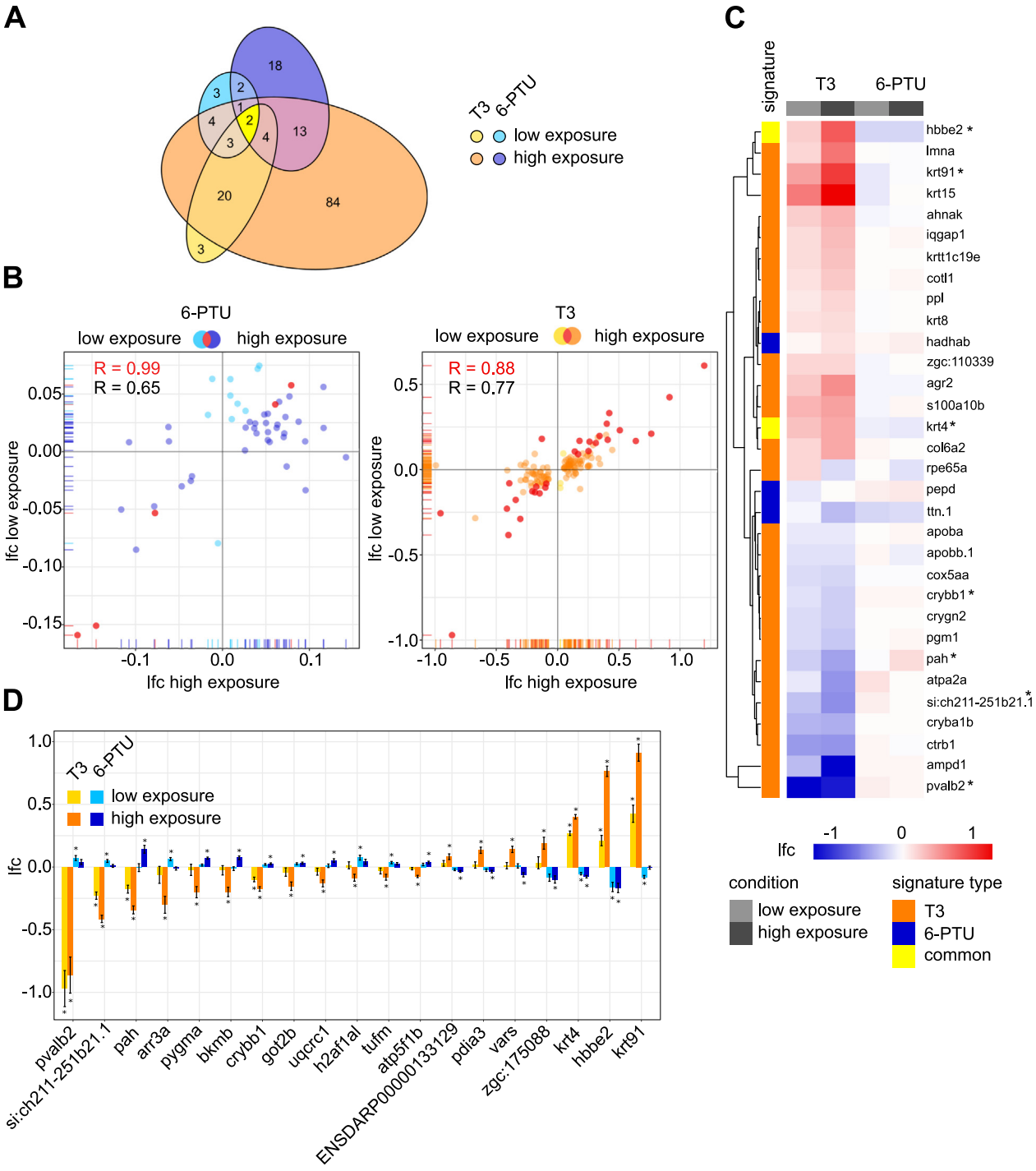

Fig. 3. Proteome response of zebrafish embryos to sublethal concentrations of T3 and 6-PTU at 96 hpf. (**A**) Venn diagram showing the statistically significantly (padj ≤ 0.05) differentially expressed proteins of the common set of detected proteins after exposure to 186.6 μg/L (high exposure, orange) and 1.14 μg/L (low exposure, yellow) T3 and to 108.81 mg/L (high exposure, dark blue) and 1.00 mg/L (low exposure, light blue) 6-PTU compared to control groups. Displayed ellipses and intersection sizes correspond to the numbers of proteins. (**B**) Scatter plots comparing the $\log_2$-fold change (lfc) values of differentially expressed proteins observed after low and high exposure to each corresponding substance. The common subset is colored in red. (**C**) Heatmap containing the proteins of the common subsets indicated in red in the chart (B). The lfc of each protein (rows) is shown for each sample (columns). Red heatmap colors represent an enhanced and blue a suppressed expression of the protein. Proteins are clustered after maximum distance measure with average linkage. The association with a T3 or a 6-PTU signature is indicated in orange and blue, respectively. Proteins associated with both signatures are colored in yellow. (**D**) Lfc values of potential common marker proteins for distinguishing T3 and 6-PTU responses. All proteins were observed as differentially expressed proteins in either low or high exposure condition after exposure to both substances and showed a counter-regulated response for T3 and 6-PTU. * indicates, in which treatment the corresponding protein was observed as differentially expressed. (For interpretation of the references to colour in this figure legend, the reader is referred to the web version of this article.)

based proteomics of total protein samples extracted simultaneously with the analyzed RNA samples. In exposure studies with T3 and 6-PTU, a total of 404 proteins was comprehensively detected at the proteomic level, which was further used for comparing the molecular responses of both substances. Reflecting the situation at the transcriptomic level, T3 also affects a larger set of proteins in comparison to 6-PTU (Fig. 3A). Exposure to the high T3 test concentration results in a significant differential expression of 131 proteins of the common detected set, while exposure to the low test concentration affects the expression of 32 proteins (Fig. 3A). 29 (90%) of these proteins

are in the common subset of both exposure conditions. In the case of 6-PTU, the expression of 40 proteins of the common detected set is significantly affected by exposure to the high test concentration and 15 proteins are differentially expressed after exposure to the low test concentration (Fig. 3A).

Five (33%) of these proteins are located in the common subset. As observed in transcriptomics, the proteins affected by low and high exposure conditions for both substances were also significantly co-regulated, in particular for the common comparable subset of both conditions (Fig. 3B). Remarkably, at the proteome level the high exposure condition also caused more pronounced effects than the low exposure condition. We defined the proteins in the common comparable subsets of both conditions as proteome fingerprint for each substance (Fig. 3C). When comparing T3 and 6-PTU, these fingerprints overlapped for two proteins (hbbe2 and krt4), and also showed contradictory regulation. As for the transcriptome profiles, relaxing the constraints for signature definition to proteins at least significantly differentially expressed in each high exposure condition increases the overlap between 6-PTU- and T3-responsive proteins to 20. Of these 13 proteins (65%) are regulated in opposing directions for each substance (Fig. 3D). These proteins expand the biomarker candidate set identified via transcriptomics by robustly expressed, and therefore easily detectable biomarkers for MoA differentiation.

3.4. Correlation of transcriptome and proteome responses

Integrating transcriptome and proteome results allowed us to detect those RNA signatures, which translate into functional protein responses. Furthermore, this approach helps differentiation between rapid responses at the RNA level and rather long-lasting effects at the level of protein. Despite the fact, that protein detection was limited to 404 total proteins, probably representing the most abundantly expressed genes, we observed a strong degree of concomitant regulation comparing DEGs at the transcriptome and the proteome level (Fig. 4A).

In particular, the common subset of DEGs at both levels was highly positively correlated ($R = 0.69$ for 6-PTU and $R = 0.84$ for T3), observing generally stronger regulation at the level of RNA, which is in line with previous literature (Perl et al., 2017). These effects are generally attributed to additional compensatory mechanisms by post-transcriptional regulation of proteins. Our approach allowed us to focus on genes, whose expression was significantly affected by both test substances in an opposing manner both at the level of RNA and protein. Such genes are particularly interesting, as they represent biomarker candidates, which allow for a differentiation of both MoAs via RNA or protein analysis techniques. Among these genes, we identified pkmb, pah, pyga, arr3a and pdia3 as a set of biomarker candidates, which have been previously shown to be involved in or affected by thyroid hormone signaling (Fig. 4B) (Baumann et al., 2016; Chu et al., 1985; Elkin et al., 1980; Hashimoto and Imaoka, 2013; Kato et al., 1989; Obata et al., 1988; Parkison et al., 1991; Reider and Connaughton, 2014; Wollenberger et al., 1964; Yu et al., 2018). After validation, an assessment of these biomarker candidates, in addition to established thyroid-related marker genes (Spaan et al., 2019), in a zFET-based screening approach (OECD, 2013) for thyroidal EDCs would promote a sustainable development of environmentally safe active substances.

3.5. Functional characterization of molecular signatures

As utilizing our data for thyroidal AOP refinement requires the extraction of functional information from the identified molecular responses, we performed downstream effect analyses using Ingenuity Pathway Analysis. For identifying MoA-specific physiological functions affected by each substance, we first analyzed each corresponding fingerprint separately on the basis of the transcriptome results. Reflecting the numbers of DEGs identified for each substance, we observed a more significant and comprehensive profile of affected physiological functions for T3 as compared to 6-PTU (Fig. S12). The 6-PTU signature was enriched for biological functions related to the immune system, such as activation of blood cells, generation and activation of leukocytes and generation, development and differentiation of t lymphocytes (Fig. S12A). An impact of thyroid hormone signaling on the immune system development in zebrafish was previously observed by Lam et al. (2005), who identified differential expression of immune-related genes after exposure to the TPO inhibitor methimazol. In another study, Quesada-Garcia et al. detected the expression of thyroid hormone receptors in immune organs and cells of rainbow trout, which were responsive to both T3 and 6-PTU (Quesada-Garcia et al., 2014). Therefore, the observed 6-PTU-mediated changes in immune-related functions may result from changes in thyroid hormone signaling in immune tissues and cells. In contrast, T3 predominantly affected biological functions associated with the formation of blood vessels, bone morphology and body size (Fig. S12B), the latter with the strongest observed z-score. While an impact of T3 on lateral length of the embryos was observed in our study (Fig. 1B), also previous studies have shown that

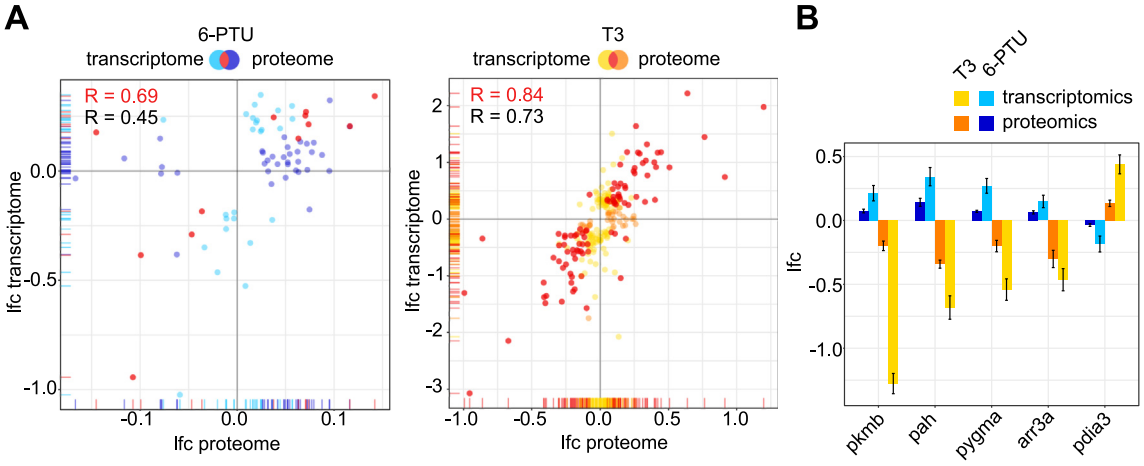

Fig. 4. Comparison of transcriptome and proteome responses to T3 and 6-PTU in zebrafish embryos. (**A**) Scatter plots comparing the $\log_2$-fold change (lfc) values of differentially expressed proteins observed after exposure to each corresponding substance at the levels of transcriptome (y-axis) and proteome (x-axis). The common subset of both methods is colored in red. Pearson correlation coeffcients are given for the common subset (red) and for the remaining proteins (black). (**B**) Lfc values of potential common marker proteins for distinguishing T3 and 6-PTU responses. All proteins were observed as statistically differentially expressed in transcriptome and proteome analysis after exposure to both substances and showed a counter-regulated response for T3 and 6-PTU. (For interpretation of the references to colour in this figure legend, the reader is referred to the web version of this article.)

thyroid hormone regulates skeletal growth in rainbow trout (Takagi et al., 1994) and morphogenesis and ossification in the majority of zebrafish bones (Keer et al., 2019).

To get a clear picture of direct, primary effects caused by enhanced (T3) and diminished thyroid hormone signaling (6-PTU), we took a closer look at the physiological functions targeted by both test substances.

For this, we performed an upstream regulator and a downstream effect analysis of the common target genes of T3 and 6-PTU. To obtain a sufficiently large gene set for analysis, these common target genes were defined as DEGs simultaneously observed in at least one exposure condition per substance, resulting in a total of 279 genes. Notably, 234 of these genes (84%) were regulated in an opposing fashion by the two test substances, an observation, which can be explained by the assumption that these genes are direct targets of thyroid hormone signaling. Upstream regulator analysis revealed T3 to be the most significant ($p \leq 9.41E\text{-}10$) and most comprehensive (z-score of ± 3.076) upstream regulator for this gene set via thyroid hormone receptor beta (THRB), the peroxisome proliferator-activated receptor (PPAR) signaling pathway (Hunter et al., 1996) or via retinoid X receptor alpha (RXRA) signaling (Zhang et al., 1992) (Fig. 5A). Besides energy homeostasis and cardiac functions, downstream effect analysis of the common target gene set showed muscle contraction and functioning to be most significantly impaired by T3 and 6-PTU (Fig. 5B and Fig. S13). Therefore, our results suggest that an impaired thyroid hormone signaling leads to a significant dysregulation of genes involved in muscle functioning and muscle contraction via THRB, PPAR and RXRA. Consequently, these functions may be impaired also at the physiological level. An impaired development of smooth muscle fibers was previously proposed as one possible mechanism, by which reduced T3 levels result in reduced swim bladder inflation (Stinckens et al., 2020). However, despite knowledge about an involvement of smooth muscle fibers in swim bladder inflation from a detailed study on swim bladder development and innervation in zebrafish (Robertson et al., 2007), the link between reduced T3 levels and muscle impairment still remains elusive to date. Our results provide a mechanistic link between impaired T3 signaling and impaired swim bladder inflation in zebrafish embryos, contributing to a deeper understanding of the relationship of the KEs of decreased T3 serum levels and reduced swim bladder inflation in fish (Fig. 5C). Furthermore, an impaired muscle functionality may result in impaired spontaneous movement of the embryos, explaining the observed hatching delay after TPO inhibition by 6-PTU (Fig. 1B). A similar effect was also observed in previous studies with the suspected TPO inhibitor thiram (Chen et al., 2019). While also a direct contribution of muscle impairment to a reduced swimming performance of juvenile fish is conceivable, recent studies observed clear correlations between swim bladder inflation and impaired swimming performance (Stinckens et al., 2020). The swimming distance of fish exposed to TPO and DIO

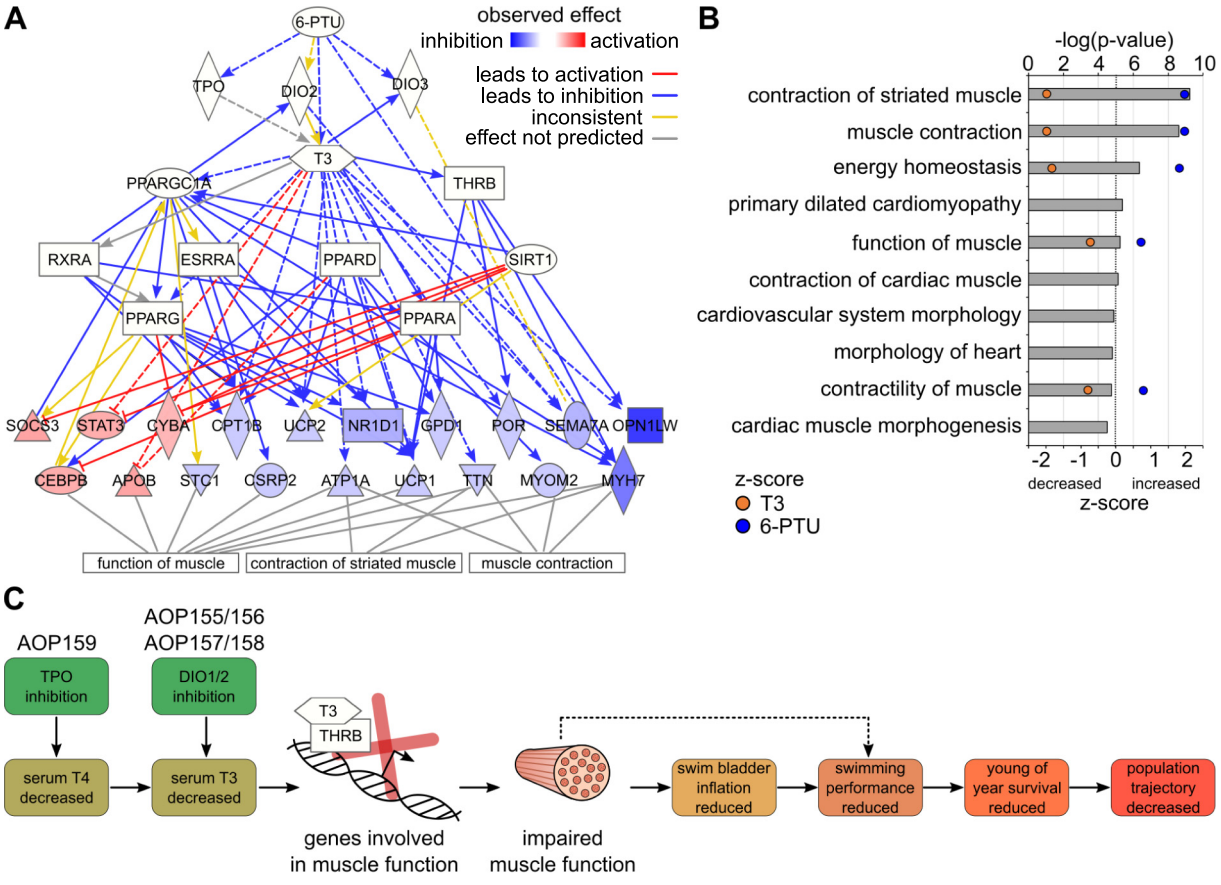

Fig. 5. Upstream regulator and downstream effect analysis of T3/6-PTU target genes. (**A**) Upstream regulator analysis of the common target gene set of T3 and 6-PTU indicates T3 signaling to be most significantly responsible for the observed gene expression changes. Direct and indirect T3/THRB signaling impacts the expression of different genes involved in muscle contraction and function. The observed up- (red) and down-regulation (blue) of genes is displayed as a colour code after exposure to T3. Functional connections are indicated as colored lines and arrows. For reasons of perceptibility, not all genes are shown. (**B**) Downstream effect analysis of the common target gene set of T3 and 6-PTU. The top ten statistically significantly enriched physiological functions are displayed ordered by their -log(*p*-value). The z-score indicates, whether a function is increased (positive) or decreased (negative value) after T3 (orange) and 6-PTU exposure (blue). (**C**) Proposed refinement of thyroid-related AOPs in fish. Both, induced thyroid signaling by exogenous T3 and reduced thyroid signaling by 6-PTU-mediated inhibition of TPO and DIO, significantly affect the expression of genes involved in muscle function and contraction via direct and indirect pathways shown in (B). The resulting impaired muscle function and contractility may directly affect swim bladder inflation and may indirectly also contribute to a reduced swimming performance. (For interpretation of the references to colour in this figure legend, the reader is referred to the web version of this article.)

inhibitors, which had inflated swim bladders, did not differ significantly from that of the control, conflicting with the hypothesis of a direct contribution of muscle impairment to reduced swimming performance.

4. Conclusion

Our study provides comprehensive transcriptomic and proteomic signatures of two model substances reported previously to interfere with thyroid hormone signaling in zebrafish embryos (Jomaa et al., 2014; Rehberger et al., 2018). All gene expression data obtained in this study as well as the analysis pipelines used are publically available, allowing datamining and reproduction of results by the scientific community. Covering a wide range of substance concentrations, our fingerprints can be utilized as for example custom gene panels for RT-qPCR or immunoblot arrays in zebrafish embryo-based short-term assays for thyroidal hazard screening of compounds. The gene expression fingerprints of each model substance separate well between their corresponding MoA. Thus, the T3 fingerprint may be consulted to identify thyroid hormone receptor agonists, while the 6-PTU-specific signature can be assessed to determine substances interfering with thyroid hormone production, in particular via TPO inhibition (Schmidt and Braunbeck, 2011; Stinckens et al., 2020). It is worth noting that the THR agonistic effects observed in our study have been induced by ectopic T3 concentrations and therefore do not reflect the physiological situation, but rather an induced ecotoxic incidence. The choice of 6-PTU as a model substance for an impaired thyroid hormone synthesis, subsequently leading to changes in thyroid hormone signaling, does not allow for a differentiation of the primary and the subsequent thyroidal effect. Effects of diminished thyroid hormone signaling only may be provided by an exposure to e.g. thyroid hormone receptor antagonists in future studies. However, besides their distinct molecular signatures, results of previous studies also demonstrate that both model substances should impact thyroid hormone signaling in an opposing fashion: exposure to exogenous T3 should increase thyroid hormone signaling, while TPO inhibition by 6-PTU should result in a reduced production of endogenous T3 (Rehberger et al., 2018), leading to decreased thyroid hormone signaling. Such a diminished endogenous thyroid hormone production after exposure to 6-PTU was observed in adult as well as in embryonic zebrafish in previous studies (Raldua and Babin, 2009; Rehberger et al., 2018; Stinckens et al., 2020; Thienpont et al., 2011). Therefore, the common target gene set of T3 and 6-PTU may be enriched for primary target genes of thyroid hormone signaling. Indeed, we observed that the vast majority (84%) of these genes was regulated in a contrary fashion by both substances. Furthermore, T3 was identified as a comprehensive upstream regulator of these genes via THRB, PPAR and RXRA signaling, providing further evidence for primary thyroid hormone signaling targets. A significant set of these genes is involved in muscle functioning and contraction. Besides an impaired anterior budding via altered Wnt and hedgehog signaling (Winata et al., 2009; Yin et al., 2011; Yin et al., 2012), an impaired muscle development (Robertson et al., 2007) belongs to previously proposed mechanisms for decreased serum T3 levels leading to reduced swim bladder inflation. However, to date this mechanism is only based on findings about the role of muscle fibers during swim bladder development (Robertson et al., 2007). Our study provides weight-of-evidence for thyroid hormone-mediated impairment in genes involved in muscle functioning, representing a possible mechanism for a central KE relationship of five thyroid-related AOPs in fish currently under development. Progress in the development and establishment of thyroid-related AOPs in fish will allow a development of zebrafish embryo-based or more preferably cell culture-based *in vitro* assays to detect thyroidal EDCs, complying with the recommendations given in the joint guidance document for the identification of EDCs by ECHA and EFSA (European Chemica Agency, 2018). In the long term, both, a biomarker-based assessment of thyroid disruption within the course of regulatory chronic fish tests and an AOP-based development of *in vitro* assays for thyroid disruption hazard assessment could replace the need for regulatory amphibian studies, which ultimately complies with the 3R principle (Russell, 1959).

Credit author statement

Hannes Reinwald and Azora König contributed equally to this study. Hannes Reinwald established and optimized the RNA and protein extraction method along with Julia Alvincz, programmed R scripts for automated differential gene expression and multivariate data analysis and visualization. He further performed the quality assessment and analysis of RNA-Seq data and contributed large parts to the manuscript writing. Azora König performed tests for the assessment of physiological endpoints, analyzed the corresponding data and contributed to manuscript writing. Steve Ayobahan performed proteomics measurements, analyzed the corresponding data and contributed to manuscript writing. Julia Alvincz performed the modified zebrafish embryo toxicity tests, RNA and protein extraction and sample quality assessment. Levente Sipos performed protein labelling for proteomics. Bernd Göckener performed chemical analysis of test substance concentrations. Gisela Böhle performed RT-qPCR analyses. Orr Shomroni performed RNA-Seq raw data processing and mapping. Henner Hollert contributed to manuscript writing. Gabriela Salinas supervised RNA sequencing. Christoph Schäfers contributed to study design and manuscript writing. Elke Eilebrecht designed the study and wrote the manuscript and Sebastian Eilebrecht designed and supervised the study and wrote the manuscript.

Funding

This work was supported by the Fraunhofer Internal Programs under Grant No. Attract 040-600300.

Declaration of competing interest

The authors declare that they have no known competing financial interests or personal relationships that could have appeared to influence the work reported in this paper.

Acknowledgements

The authors thank Terry Clark for language revision of this manuscript.

Appendix A. Supplementary data

The following files are available free of charge.

Supplemental_material_Reinwald_2020: supplemental materials and methods, supplemental tables, supplemental figures.

T3_DESeq2res.zip: DESeq2 result tables for T3 exposure including R session info.

6PTU_DESeq2res.zip: DESeq2 result tables for 6-PTU exposure including R session info.Supplementary data to this article can be found online at doi:https://doi.org/10.1016/j.scitotenv.2020.143914.

References

Andrews, S., 2010. FastQC: A Quality Control Tool for High Throughput Sequence Data.

Ankley, G.T., Edwards, S.W., 2018. The adverse outcome pathway: a multifaceted framework supporting 21(st) century toxicology. Curr Opin Toxicol 9, 1–7.

Athar, A., Fullgrabe, A., George, N., Iqbal, H., Huerta, L., Ali, A., Snow, C., Fonseca, N.A., Petryszak, R., Papatheodorou, I., Sarkans, U., Brazma, A., 2019. ArrayExpress update - from bulk to single-cell expression data. Nucleic Acids Res. 47, D711–D715.

Ayobahan, S.U., Eilebrecht, E., Kotthoff, M., Baumann, L., Eilebrecht, S., Teigeler, M., Hollert, H., Kalkhof, S., Schafers, C., 2019. A combined FSTRA-shotgun proteomics approach to identify molecular changes in zebrafish upon chemical exposure. Sci. Rep. 9, 6599.

Ayobahan, S.U., Eilebrecht, S., Baumann, L., Teigeler, M., Hollert, H., Kalkhof, S., Eilebrecht, E., Schafers, C., 2020. Detection of biomarkers to differentiate endocrine disruption from hepatotoxicity in zebrafish (Danio rerio) using proteomics. Chemosphere 240, 124970.

Baumann, L., Ros, A., Rehberger, K., Neuhauss, S.C., Segner, H., 2016. Thyroid disruption in zebrafish (Danio rerio) larvae: different molecular response patterns lead to impaired eye development and visual functions. Aquat. Toxicol. 172, 44–55.

Bolger, A.M., Lohse, M., Usadel, B., 2014. Trimmomatic: a flexible trimmer for Illumina sequence data. Bioinformatics 30, 2114–2120.

Brown, D.D., 1997. The role of thyroid hormone in zebrafish and axolotl development. Proc. Natl. Acad. Sci. U. S. A. 94, 13011–13016.

Bruggemann, M., Licht, O., Fetter, E., Teigeler, M., Schafers, C., Eilebrecht, E., 2018. Knotting nets: molecular junctions of interconnecting endocrine axes identified by application of the adverse outcome pathway concept. Environ. Toxicol. Chem. 37, 318–328.

Busch, W., Duis, K., Fenske, M., Maack, G., Legler, J., Padilla, S., Strahle, U., Witters, H., Scholz, S., 2011. The zebrafish embryo model in toxicology and teratology, September 2-3, 2010, Karlsruhe. Germany. Reproductive Toxicology 31, 585–588.

Cavallin, J.E., Ankley, G.T., Blackwell, B.R., Blanksma, C.A., Fay, K.A., Jensen, K.M., Kahl, M.D., Knapen, D., Kosian, P.A., Poole, S.T., Randolph, E.C., Schroeder, A.L., Vergauwen, L., Villeneuve, D.L., 2017. Impaired swim bladder inflation in early life stage fathead minnows exposed to a deiodinase inhibitor, iopanoic acid. Environ. Toxicol. Chem. 36, 2942–2952.

Chang, J., Wang, M., Gui, W., Zhao, Y., Yu, L., Zhu, G., 2012. Changes in thyroid hormone levels during zebrafish development. Zool. Sci. 29, 181–184.

Chen, X., Fang, M., Chernick, M., Wang, F., Yang, J., Yu, Y., Zheng, N., Teraoka, H., Nanba, S., Hiraga, T., Hinton, D.E., Dong, W., 2019. The case for thyroid disruption in early life stage exposures to thiram in zebrafish (Danio rerio). Gen. Comp. Endocrinol. 271, 73–81.

Choi, M., Chang, C.Y., Clough, T., Broudy, D., Killeen, T., MacLean, B., Vitek, O., 2014. MSstats: an R package for statistical analysis of quantitative mass spectrometry-based proteomic experiments. Bioinformatics 30, 2524–2526.

Chu, D.T., Shikama, H., Khatra, B.S., Exton, J.H., 1985. Effects of altered thyroid status on beta-adrenergic actions on skeletal muscle glycogen metabolism. J. Biol. Chem. 260, 9994–10000.

Cooper, D.S., 2005. Antithyroid drugs. N. Engl. J. Med. 352, 905–917.

Davidson, B., Soodak, M., Neary, J.T., Strout, H.V., Kieffer, J.D., Mover, H., Maloof, F., 1978. The irreversible inactivation of thyroid peroxidase by methylmercaptoimidazole, thiouracil, and propylthiouracil in vitro and its relationship to in vivo findings. Endocrinology 103, 871–882.

Delrue, N., Sachana, M., Sakuratani, Y., Gourmelon, A., Leinala, E., Diderich, R., 2016. The adverse outcome pathway concept: a basis for developing regulatory decision-making tools. Altern. Lab. Anim 44, 417–429.

Dobin, A., Davis, C.A., Schlesinger, F., Drenkow, J., Zaleski, C., Jha, S., Batut, P., Chaisson, M., Gingeras, T.R., 2013. STAR: ultrafast universal RNA-seq aligner. Bioinformatics 29, 15–21.

Du, G., Hu, J., Huang, H., Qin, Y., Han, X., Wu, D., Song, L., Xia, Y., Wang, X., 2013. Perfluorooctane sulfonate (PFOS) affects hormone receptor activity, steroidogenesis, and expression of endocrine-related genes in vitro and in vivo. Environ. Toxicol. Chem. 32, 353–360.

Elkin, R.G., Featherston, W.R., Rogler, J.C., 1980. Effects of dietary phenylalanine and tyrosine on circulating thyroid hormone levels and growth in the chick. J. Nutr. 110, 130–138.

European Chemica Agency, 2018. EFSA guidance for the identification of endocrine disruptors in the context of regulations (EU) No 1107/2009. EFSA J. 16.

European Commission, 2017. Setting Out Scientific Criteria for the Determination of Endocrine Disrupting Properties Pursuant to Regulation (EU) No 528/2012 of the European Parliament and Council. (ed^eds).

European Commission, 2018. Setting Out Criteria for the Determination of Endocrine Disrupting Properties. (ed^eds).

Freyberger, A., Ahr, H.J., 2006. Studies on the goitrogenic mechanism of action of N,N,N', N'-tetramethylthiourea. Toxicology 217, 169–175.

Godfrey, A., Hooser, B., Abdelmoneim, A., Horzmann, K.A., Freemanc, J.L., Sepulveda, M.S., 2017. Thyroid disrupting effects of halogenated and next generation chemicals on the swim bladder development of zebrafish. Aquat. Toxicol. 193, 228–235.

Haggard, D.E., Noyes, P.D., Waters, K.M., Tanguay, R.L., 2018. Transcriptomic and phenotypic profiling in developing zebrafish exposed to thyroid hormone receptor agonists. Reprod. Toxicol. 77, 80–93.

Hallinger, D.R., Murr, A.S., Buckalew, A.R., Simmons, S.O., Stoker, T.E., Laws, S.C., 2017. Development of a screening approach to detect thyroid disrupting chemicals that inhibit the human sodium iodide symporter (NIS). Toxicol. in Vitro 40, 66–78.

Hashimoto, S., Imaoka, S., 2013. Protein-disulfide isomerase regulates the thyroid hormone receptor-mediated gene expression via redox factor-1 through thiol reduction-oxidation. J. Biol. Chem. 288, 1706–1716.

Hunter, J., Kassam, A., Winrow, C.J., Rachubinski, R.A., Capone, J.P., 1996. Crosstalk between the thyroid hormone and peroxisome proliferator-activated receptors in regulating peroxisome proliferator-responsive genes. Mol. Cell. Endocrinol. 116, 213–221.

Ignatiadis, N., Klaus, B., Zaugg, J.B., Huber, W., 2016. Data-driven hypothesis weighting increases detection power in genome-scale multiple testing. Nat. Methods 13, 577–580.

Jomaa, B., Hermsen, S.A., Kessels, M.Y., van den Berg, J.H., Peijnenburg, A.A., Aarts, J.M., Piersma, A.H., Rietjens, I.M., 2014. Developmental toxicity of thyroid-active compounds in a zebrafish embryotoxicity test. ALTEX 31, 303–317.

Kato, H., Fukuda, T., Parkison, C., McPhie, P., Cheng, S.Y., 1989. Cytosolic thyroid hormone-binding protein is a monomer of pyruvate kinase. Proc. Natl. Acad. Sci. U. S. A. 86, 7861–7865.

Keer, S., Cohen, K., May, C., Hu, Y., McMenamin, S., Hernandez, L.P., 2019. Anatomical assessment of the adult skeleton of zebrafish reared under different thyroid hormone profiles. Anat Rec (Hoboken) 302, 1754–1769.

Knapen, D., Stinckens, E., Cavallin, J.E., Ankley, G.T., Holbech, H., Villeneuve, D.L., Vergauwen, L., 2020. Toward an AOP network-based tiered testing strategy for the assessment of thyroid hormone disruption. Environmental Science & Technology 54, 8491–8499.

Kramer, A., Green, J., Pollard Jr., J., Tugendreich, S., 2014. Causal analysis approaches in ingenuity pathway analysis. Bioinformatics 30, 523–530.

Lam, S.H., Sin, Y.M., Gong, Z., Lam, T.J., 2005. Effects of thyroid hormone on the development of immune system in zebrafish. Gen. Comp. Endocrinol. 142, 325–335.

Leemans, M., Couderq, S., Demeneix, B., Fini, J.B., 2019. Pesticides with potential thyroid hormone-disrupting effects: a review of recent data. Front Endocrinol (Lausanne) 10, 743.

Liao, Y., Smyth, G.K., Shi, W., 2014. featureCounts: an efficient general purpose program for assigning sequence reads to genomic features. Bioinformatics 30, 923–930.

Liu, C., Zhang, X., Deng, J., Hecker, M., Al-Khedhairy, A., Giesy, J.P., Zhou, B., 2011. Effects of prochloraz or propylthiouracil on the cross-talk between the HPG, HPA, and HPT axes in zebrafish. Environ Sci Technol 45, 769–775.

Loraine, A.E., Blakley, I.C., Jagadeesan, S., Harper, J., Miller, G., Firon, N., 2015. Analysis and visualization of RNA-Seq expression data using RStudio, bioconductor, and integrated genome browser. Methods Mol. Biol. 1284, 481–501.

Love, M.I., Huber, W., Anders, S., 2014. Moderated estimation of fold change and dispersion for RNA-seq data with DESeq2. Genome Biol. 15, 550.

Moore, R.E., Young, M.K., Lee, T.D., 2002. Qscore: an algorithm for evaluating SEQUEST database search results. J. Am. Soc. Mass Spectrom. 13, 378–386.

Nelson, K.R., Schroeder, A.L., Ankley, G.T., Blackwell, B.R., Blanksma, C., Degitz, S.J., Flynn, K.M., Jensen, K.M., Johnson, R.D., Kahl, M.D., Knapen, D., Kosian, P.A., Milsk, R.Y., Randolph, E.C., Saari, T., Stinckens, E., Vergauwen, L., Villeneuve, D.L., 2016. Impaired anterior swim bladder inflation following exposure to the thyroid peroxidase inhibitor 2-mercaptobenzothiazole part I: fathead minnow. Aquat. Toxicol. 173, 192–203.

Nogimori, T., Braverman, L.E., Taurog, A., Fang, S.L., Wright, G., Emerson, C.H., 1986. A new class of propylthiouracil analogs - comparison of 5′-deiodinase inhibition and antithyroid activity. Endocrinology 118, 1598–1605.

Noyes, P.D., Friedman, K.P., Browne, P., Haselman, J.T., Gilbert, M.E., Hornung, M.W., Barone, S., Crofton, K.M., Laws, S.C., Stoker, T.E., Simmons, S.O., Tietge, J.E., Degitz, S.J., 2019. Evaluating chemicals for thyroid disruption: opportunities and challenges with in vitro testing and adverse outcome pathway approaches. Environ Health Persp 127.

Obata, T., Kitagawa, S., Gong, Q.H., Pastan, I., Cheng, S.Y., 1988. Thyroid hormone down-regulates p55, a thyroid hormone-binding protein that is homologous to protein disulfide isomerase and the beta-subunit of prolyl-4-hydroxylase. J. Biol. Chem. 263, 782–785.

OECD, 1992. Test Guideline 210: Fish Early-Life Stage Toxicity Test. (ed^eds. Paris).

OECD, 2007. Final Report of the Validation of the Amphibian Metamorphosis Assay for the Detection of Thyroid Active Substances: Phase 1 - Optimization of the Test Protocol. (ed^eds. Paris).

OECD, 2009. Test Guideline 231: Amphibian Metamorphosis Assay. (ed^eds. Paris).

OECD, 2013. Test Guideline 236: Fish Embryo Acute Toxicity (FET) Test. (ed^eds. Paris).

OECD, 2015. Test Guideline 241: The Larval Amphibian Growth and Development Assay. (ed^eds. Paris).

OECD, 2019. Test Guideline 248: Xenopus Eleutheroembryonic Thyroid Assay. (ed^eds. Paris).

Parkison, C., Ashizawa, K., McPhie, P., Lin, K.H., Cheng, S.Y., 1991. The monomer of pyruvate kinase, subtype M1, is both a kinase and a cytosolic thyroid hormone binding protein. Biochem. Biophys. Res. Commun. 179, 668–674.

Perez-Riverol, Y., Csordas, A., Bai, J., Bernal-Llinares, M., Hewapathirana, S., Kundu, D.J., Inuganti, A., Griss, J., Mayer, G., Eisenacher, M., Perez, E., Uszkoreit, J., Pfeuffer, J., Sachsenberg, T., Yilmaz, S., Tiwary, S., Cox, J., Audain, E., Walzer, M., Jarnuczak, A.F., Ternent, T., Brazma, A., Vizcaino, J.A., 2019. The PRIDE database and related tools and resources in 2019: improving support for quantification data. Nucleic Acids Res. 47, D442–D450.

Perl, K., Ushakov, K., Pozniak, Y., Yizhar-Barnea, O., Bhonker, Y., Shivatzki, S., Geiger, T., Avraham, K.B., Shamir, R., 2017. Reduced changes in protein compared to mRNA levels across non-proliferating tissues. BMC Genomics 18, 305.

Porazzi, P., Calebiro, D., Benato, F., Tiso, N., Persani, L., 2009. Thyroid gland development and function in the zebrafish model. Mol. Cell. Endocrinol. 312, 14–23.

Quesada-Garcia, A., Valdehita, A., Kropf, C., Casanova-Nakayama, A., Segner, H., Navas, J.M., 2014. Thyroid signaling in immune organs and cells of the teleost fish rainbow trout (Oncorhynchus mykiss). Fish Shellfish Immunol 38, 166–174.

R Core Team, 2019. R: A Language and Environment for Statistical Computing. (ed^eds. Vienna, Austria).

Raldua, D., Babin, P.J., 2009. Simple, rapid Zebrafish larva bioassay for assessing the potential of chemical pollutants and drugs to disrupt thyroid gland function. Environmental Science & Technology 43, 6844–6850.

Rehberger, K., Baumann, L., Hecker, M., Braunbeck, T., 2018. Intrafollicular thyroid hormone staining in whole-mount zebrafish (Danio rerio) embryos for the detection of thyroid hormone synthesis disruption. Fish Physiol. Biochem. 44, 997–1010.

Reider, M., Connaughton, V.P., 2014. Effects of low-dose embryonic thyroid disruption and rearing temperature on the development of the eye and retina in zebrafish. Birth Defects Res B Dev Reprod Toxicol 101, 347–354.

Robertson, G.N., McGee, C.A.S., Dumbarton, T.C., Croll, R.P., Smith, F.M., 2007. Development of the swimbladder and its innervation in the zebrafish, *Danio rerio*. J Morphol 268, 967–985.

Russell, W.M.S., 1959. B.R.L. The Principles of Humane Experimental Technique. (ed^eds. Methuen).

Schindelin, J., Arganda-Carreras, I., Frise, E., Kaynig, V., Longair, M., Pietzsch, T., Preibisch, S., Rueden, C., Saalfeld, S., Schmid, B., Tinevez, J.Y., White, D.J., Hartenstein, V.,

Eliceiri, K., Tomancak, P., Cardona, A., 2012. Fiji: an open-source platform for biological-image analysis. Nat. Methods 9, 676–682.
Schmidt, F., Braunbeck, T., 2011. Alterations along the hypothalamic-pituitary-thyroid axis of the Zebrafish (Danio rerio) after exposure to propylthiouracil. J. Thyroid. Res. 2011, 376243.
Schmittgen, T.D., Livak, K.J., 2008. Analyzing real-time PCR data by the comparative C (T) method. Nat. Protoc. 3, 1101–1108.
Selderslaghs, I.W.T., Van Rompay, A.R., De Coen, W., Witters, H.E., 2009. Development of a screening assay to identify teratogenic and embryotoxic chemicals using the zebrafish embryo. Reprod. Toxicol. 28, 308–320.
Spaan, K., Haigis, A.C., Weiss, J., Legradi, J., 2019. Effects of 25 thyroid hormone disruptors on zebrafish embryos: a literature review of potential biomarkers. Sci. Total Environ. 656, 1238–1249.
Stinckens, E., Vergauwen, L., Schroeder, A.L., Maho, W., Blackwell, B.R., Witters, H., Blust, R., Ankley, G.T., Covaci, A., Villeneuve, D.L., Knapen, D., 2016. Impaired anterior swim bladder inflation following exposure to the thyroid peroxidase inhibitor 2-mercaptobenzothiazole part II: Zebrafish. Aquat. Toxicol. 173, 204–217.
Stinckens, E., Vergauwen, L., Ankley, G.T., Blust, R., Darras, V.M., Villeneuve, D.L., Witters, H., Volz, D.C., Knapen, D., 2018. An AOP-based alternative testing strategy to predict the impact of thyroid hormone disruption on swim bladder inflation in zebrafish. Aquat. Toxicol. 200, 1–12.
Stinckens, E., Vergauwen, L., Blackwell, B.R., Ankley, G.T., Villeneuve, D.L., Knapen, D., 2020. The effect of thyroperoxidase and deiodinase inhibition on anterior swim bladder inflation in the zebrafish. Environ. Sci. Technol. 54, 6213–6223.
Strahle, U., Scholz, S., Geisler, R., Greiner, P., Hollert, H., Rastegar, S., Schumacher, A., Selderslaghs, I., Weiss, C., Witters, H., Braunbeck, T., 2012. Zebrafish embryos as an alternative to animal experiments–a commentary on the definition of the onset of protected life stages in animal welfare regulations. Reprod. Toxicol. 33, 128–132.
Takagi, Y., Hirano, J., Tanabe, H., Yamada, J., 1994. Stimulation of skeletal growth by thyroid-hormone administrations in the rainbow-trout. Oncorhynchus-Mykiss. J Exp Zool 268, 229–238.
Thambirajah, A.A., Koide, E.M., Imbery, J.J., Helbing, C.C., 2019. Contaminant and environmental influences on thyroid hormone action in amphibian metamorphosis. Front Endocrinol (Lausanne) 10, 276.
Thienpont, B., Tingaud-Sequeira, A., Prats, E., Barata, C., Babin, P.J., Raldua, D., 2011. Zebrafish eleutheroembryos provide a suitable vertebrate model for screening chemicals that impair thyroid hormone synthesis. Environ Sci Technol 45, 7525–7532.
van der Ven, L.T.M., van den Brandhof, E.J., Vos, J.H., Power, D.M., Wester, P.W., 2006. Effects of the antithyroid agent propylthiouracil in a partial life cycle assay with zebrafish. Environmental Science & Technology 40, 74–81.
Winata, C.L., Korzh, S., Kondrychyn, I., Zheng, W.L., Korzh, V., Gong, Z.Y., 2009. Development of zebrafish swimbladder: the requirement of hedgehog signaling in specification and organization of the three tissue layers. Dev. Biol. 331, 222–236.
Wollenberger, A., Krause, E.G., Macho, L., 1964. Thyroid state and the activity of glycogen phosphorylase in Ischaemic myocardium. Nature 201, 789–791.
Yates, A.D., Achuthan, P., Akanni, W., Allen, J., Allen, J., Alvarez-Jarreta, J., Amode, M.R., Armean, I.M., Azov, A.G., Bennett, R., Bhai, J., Billis, K., Boddu, S., Marugan, J.C., Cummins, C., Davidson, C., Dodiya, K., Fatima, R., Gall, A., Giron, C.G., Gil, L., Grego, T., Haggerty, L., Haskell, E., Hourlier, T., Izuogu, O.G., Janacek, S.H., Juettemann, T., Kay, M., Lavidas, I., Le, T., Lemos, D., Martinez, J.G., Maurel, T., McDowall, M., McMahon, A., Mohanan, S., Moore, B., Nuhn, M., Oheh, D.N., Parker, A., Parton, A., Patricio, M., Sakthivel, M.P., Abdul Salam, A.I., Schmitt, B.M., Schuilenburg, H., Sheppard, D., Sycheva, M., Szuba, M., Taylor, K., Thormann, A., Threadgold, G., Vullo, A., Walts, B., Winterbottom, A., Zadissa, A., Chakiachvili, M., Flint, B., Frankish, A., Hunt, S.E., G, I.I., Kostadima, M., Langridge, N., Loveland, J.E., Martin, F.J., Morales, J., Mudge, J.M., Muffato, M., Perry, E., Ruffier, M., Trevanion, S.J., Cunningham, F., Howe, K.L., Zerbino, D.R., Flicek, P., 2020. Ensembl 2020. Nucleic Acids Res 48 (D682-D688).
Yin, A., Korzh, S., Winata, C.L., Korzh, V., Gong, Z.Y., 2011. Wnt signaling is required for early development of Zebrafish Swimbladder. PLoS One 6.
Yin, A., Korzh, V., Gong, Z.Y., 2012. Perturbation of zebrafish swimbladder development by enhancing Wnt signaling in Wif1 morphants. Bba-Mol Cell Res 1823, 236–244.
Yu, G., Sun, W., Shen, Y., Hu, Y., Liu, H., Li, W., Wang, Y., 2018. PKM2 functions as a potential oncogene and is a crucial target of miR-148a and miR-326 in thyroid tumorigenesis. Am. J. Transl. Res. 10, 1793–1801.
Zhang, X.K., Hoffmann, B., Tran, P.B.V., Graupner, G., Pfahl, M., 1992. Retinoid X-receptor is an auxiliary protein for thyroid-hormone and retinoic acid receptors. Nature 355, 441–446.
Zhu, A., Ibrahim, J.G., Love, M.I., 2019. Heavy-tailed prior distributions for sequence count data: removing the noise and preserving large differences. Bioinformatics 35, 2084–2092.

A2 Toxicogenomic profiling after sublethal exposure to nerve- and muscle-targeting insecticides reveals cardiac and neuronal developmental effects in zebrafish embryos

Declaration of author contributions to the publication:

Toxicogenomic profiling after sublethal exposure to nerve- and muscle-targeting insecticides reveals cardiac and neuronal developmental effects in zebrafish embryos

DOI: 10.1016/j.chemosphere.2021.132746
Status: Published
Journal: **Chemosphere**

Contributing authors:
Reinwald H. (**RH**), Alvincz J. (AJ), Salinas G. (SG), Hollert H. (HH), Schäfers C. (SC) & Eilebrecht S. (ES)

(1) Concept and design
Doctoral candidate **RH**: 65%
Co-author ES: 25%
Co-author SC: 10%

(2) Conducting tests and experiments
Doctoral candidate **RH**: 85% - Performance of preliminary and main toxicity tests; RNA and protein extraction and molecular sample quality control
Co-author AJ: 5% - Medium exchange over the weekends
Co-author GS: 10% - mRNA-Sequence library preparation and Illumina HiSeq NGS

(3) Compilation of data sets and figures
Doctoral candidate **RH**: 90% - mRNA-sequencing raw data processing and compilation for data QC plots (multiQC reports); Transcriptomic data plotting and data QC (dissimilarity matrix, tSNE & PCA clustering, p-value distribution, count library normalization plots …); biomarker selection for plotting venn diagrams and heatmaps; sample signal (log2FC) correlation plots; log_2-fold change expression bar plots
Co-author ES: 10% - Constructive feedback on figure structure and design

(4) Analysis and interpretation of data
Doctoral candidate **RH**: 90% - mRNA-sequencing raw data processing and QC (overall sequence quality, check for contaminating sequences, mapping quality, transcript integrity, gene body coverage, etc. …); design and programming of R scripts for differential gene expression analysis (DGEA) via DESeq2 and multivariate data exploration for transcriptomic datasets; DGEA data mining for potential biomarker discovery; gene set enrichment analysis (GSEA) as well as overrepresentation analysis (ORA) and network clustering by clusterProfiler; statistical evaluation of observed physiological effects (Kruskal-Wallis's ANOVA on ranks and post-hoc Wilcoxon signed-rank test)
Co-author ES: 10% - Constructive feedback on data analysis approaches

(5) Drafting of manuscript
Doctoral candidate **RH**: 70%
Co-author ES: 20%
Co-author SC, HH: 10% - Final draft comments

Chemosphere 291 (2022) 132746

Contents lists available at ScienceDirect

Chemosphere

journal homepage: www.elsevier.com/locate/chemosphere

Toxicogenomic profiling after sublethal exposure to nerve- and muscle-targeting insecticides reveals cardiac and neuronal developmental effects in zebrafish embryos

Hannes Reinwald [a,b], Julia Alvincz [a], Gabriela Salinas [c], Christoph Schäfers [d], Henner Hollert [b], Sebastian Eilebrecht [a,*]

[a] Fraunhofer Attract Eco'n'OMICs, Fraunhofer Institute for Molecular Biology and Applied Ecology, Schmallenberg, Germany
[b] Department Evolutionary Ecology and Environmental Toxicology, Faculty Biological Sciences, Goethe University Frankfurt, Frankfurt, Germany
[c] NGS-Services for Integrative Genomics, University of Göttingen, Göttingen, Germany
[d] Department of Ecotoxicology, Fraunhofer Institute for Molecular Biology and Applied Ecology, Schmallenberg, Germany

HIGHLIGHTS

- Transcriptomic profiles of nerve and muscle targeting insecticides were generated.
- We identified 222 early responsive protein coding genes in the zebrafish embryo.
- Among those were especially cardiac and neuronal development related genes.
- We propose forebrain development gene *npas4a* as potential neurotoxic marker.
- Abamectin primarily affected lipid and carbohydrate related processes.

GRAPHICAL ABSTRACT

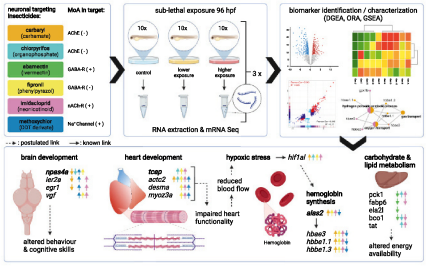

ARTICLE INFO

Handling Editor: Alvine C.Mehinto

Keywords:
Mode-of-action
Hazard assessment
Neurotoxicity
Transcriptomics
Toxicogenomics
Biomarkers

ABSTRACT

For specific primary modes of action (MoA) in environmental non-target organisms, EU legislation restricts the usage of active substances of pesticides or biocides. Corresponding regulatory hazard assessments are costly, time consuming and require large numbers of non-human animal studies. Currently, predictive toxicology of development compounds relies on their chemical structure and provides little insights into toxicity mechanisms that precede adverse effects. Using the zebrafish embryo model, we characterized transcriptomic responses to a range of sublethal concentrations of six nerve- and muscle-targeting insecticides with different MoA (abamectin, carbaryl, chlorpyrifos, fipronil, imidacloprid & methoxychlor). Our aim was to identify affected biological processes and suitable biomarker candidates for MoA-specific signatures. Abamectin showed the most divergent signature among the tested insecticides, linked to lipid metabolic processes. Differentially expressed genes (DEGs) after imidacloprid exposure were primarily associated with immune system and inflammation. In total, 222 early responsive genes to either MoA were identified, many related to three major processes: (1) cardiac muscle cell development and functioning (*tcap, desma, bag3, hspb1, hspb8, flnca, myoz3a, mybpc2b, actc2, tnnt2c*),

; MoA, Mode of action; AOP, Adverse outcome pathway; DEG, Differentially expressed gene; lfc, $\log_2$-fold change; LFcut, $\log_2$-fold change (effect size) cut off; DGEA, Differential gene expression analysis; GSEA, Gene set enrichment analysis; ORA, Overrepresentation analysis; RIN, RNA integrity number; BH, Benjamini-Hochberg p-value correction; GO, Gene Ontology.

* Corresponding author.
E-mail address: sebastian.eilebrecht@ime.fraunhofer.de (S. Eilebrecht).

https://doi.org/10.1016/j.chemosphere.2021.132746
Received 3 September 2021; Received in revised form 15 October 2021; Accepted 29 October 2021
Available online 5 November 2021

(2) oxygen transport and hypoxic stress (*alas2, hbbe1.1, hbbe1.3, hbbe2, hbae3, igfbp1a, hif1al*) and (3) neuronal development and plasticity (*npas4a, egr1, btg2, ier2a, vgf*). The thyroidal function related gene *dio3b* was upregulated by chlorpyrifos and downregulated by higher abamectin concentrations. Important regulatory genes for cardiac muscle (*tcap*) and forebrain development (*npas4a*) were the most frequently ifferentially expressed across all insecticide treatments. We consider the identified gene sets as useful early warning biomarker candidates, i.e. for developmental toxicity targeting heart and brain in aquatic vertebrates. Our findings provide a better understanding about early molecular events in response to the analyzed MoA. Perceptively, this promotes the development for sensitive and informative biomarker-based *in vitro* assays for toxicological MoA prediction and AOP refinement, without the suffering of adult fish.

1. Introduction

Modern day society relies on a plethora of chemicals, e.g. as cosmetics, pharmaceuticals or pesticides and the number of registered chemicals in the EU is continuously growing. In 2018 alone, over 7000 new substances were approved for the market for the first time (ECHA, 2018). With the exception of pharmaceuticals, EU legislation restricts the usage of active substances, e.g. of pesticides or biocides, for certain primary modes of action (MoA), such as endocrine activity. However, currently there is still a lack of systematic methodology to detect and reliably distinguish primary MoAs in non-target organisms. In addition, mandated hazard assessments still heavily rely on *in vivo* animal studies, which are costly and time consuming. From both an ethical and economic perspective, it is vital to reduce the number of these experiments whenever possible (Embry et al., 2010; Krewski et al., 2010; Russell and Burch, 1959). In the future, novel, high-throughput, non-animal screening approaches may enable an early focus on less environmentally harmful substances and thus reduce the number of regulatory required higher tier tests.

Predictive toxicology models, such as the *Verhaar* scheme (Ellison et al., 2015; Verhaar et al., 1992), are one way to characterize unknown substances and assign them with a primary MoA in a high throughput manner. However, these models function solely on the chemical structure of the relevant substance and on previously collected acute toxicity data. Hence, they are of limited use for predicting chronic and/or sublethal effects. In general, these models have limited value for interspecies extrapolation and do not yet provide insights into the toxicity mechanisms underlying adverse effects (Brockmeier et al., 2017).

A promising alternative to overcome these limitations are systems biology-based approaches, using OMICs profiles of model organisms to develop models with predictive power, i.e. for cardiotoxicity (Li et al., 2020). Thanks to major advances in OMICs technologies, researchers nowadays can quantify the response of thousands of genes and their products from a single sample simultaneously. These state-of-the-art methods for detecting changes in response to a specific chemical stressor at the molecular level (e.g. at the RNA or protein level), opens unprecedented opportunities for modern-day hazard assessment approaches (Cote et al., 2016). In particular in the context of development and refinement of adverse outcome pathways (AOPs), which requires a clearly defined molecular initiating event (MIE) and early key events (KE) (Ankley et al., 2010), OMICs data allow for a better understanding of toxicity mechanisms at low organizational levels (Villeneuve et al., 2014a, 2014b, 2014b). These improved molecular insights can deepen our understanding about the mechanisms leading to adverse effects, facilitating the transition towards more predictive and informative screening approaches. Such approaches, dealing with subacute exposure concentrations, will help in the future to answer the question of why a compound is toxic and how it acts in the non-target organism.

Compounds affecting the nervous system are of particular concern as they pose significant risks to both humans and environmental organisms and have been associated with neuronal disorders in humans (Amora and Giordani, 2018; Dörner and Plagemann, 2002; Iwaniuk et al., 2006; Rauh et al., 2015; Ton et al., 2006). Due to their MoA directed at the nerves in the target organism, neurotoxicity is a significant adverse effect of commonly used insecticides such as carbamates, organophosphates, phenylpyrazoles or neonicotinoids, which impair synaptic transmission and affect internal neurotransmitter levels with far-reaching effects on the homeostatic state of the organism (Gonçalves et al., 2020). Early brain development and neurogenesis reflect a critical developmental period in the life of an organism, making early life stages in particular sensitive to neurotoxic chemical exposure, e.g. from environmental contamination (Giussani, 2011; Perera and Herbstman, 2011).

In acute toxicity tests, it was found that zebrafish embryos, were less sensitive to neurotoxic chemicals than adults, which at first glance seems contradictory to the above (Glaberman et al., 2017). However, these conclusions mostly based on acute lethal endpoint assays and did not consider potential sublethal or chronic developmental effects. Previous studies showed that the fish embryo model can be just as sensitive when sublethal endpoints are evaluated (Klüver et al., 2015; Sanches et al., 2018). Consequently, the zebrafish embryo is a powerful toxicological vertebrate model to study early molecular responses to neurotoxic chemicals and developmental hazards, with great potential for cross vertebrate species extrapolation (Amora and Giordani, 2018; Tierney, 2011; Ton et al., 2006). Another major advantage of zebrafish is homology of important molecular signaling pathways or organ- and neurodevelopment to other vertebrates such as humans (Hason and Bartůně;k, 2019; Klarić et al., 2014). In recent years, this organism has gained increasing interest as *in vivo* model in human health research to investigate cancer (Feitsma and Cuppen, 2008) as well as cardiac (Huang et al., 2009) or neuronal diseases (Klarić et al., 2014). This opens up opportunities for comparison between disease-related phenotypes (e.g. knock out strains, lesion models, etc.) and responses to chemical stressors.

In this study, we applied full mRNA sequencing for functionally characterizing the responses of zebrafish embryos to different sublethal concentrations of six nerve- and muscle-targeting insecticides (abamectin, carbaryl, chlorpyrifos, fipronil, imidacloprid & methoxychlor) with five different pre-defined MoAs, as classified by the IRAC classification system (Sparks and Nauen, 2015). That way, we compared the ecotoxicogenomic profiles of glutamate-gated chloride channel (GluCls) modulation (abamectin), reversible and irreversible acetylcholine esterase inhibition (carbaryl and chlorpyrifos), GABA-gated chloride channel antagonism (fipronil) as well as nicotinic acetylcholine receptor (nAChR) (imidacloprid) and sodium channel modulation (methoxychlor). Although GluCls as direct target are only present in invertebrates, they are structurally highly similar to vertebrate glycine receptors (GlyRs) (Wolstenholme, 2012). In both cases the activation of the GluCls or GlyRs increase the permeability for Cl^- ions which leads to a hyperpolarization of the membrane potential, reducing signal transmission (Betz, 1991; Wolstenholme, 2012). Further, abamectin was shown to target GABA gated chloride channels of vertebrates as well (Wang et al., 2019). Organophosphates inhibit the enzymatic degradation of the neurotransmitter acetylcholine (ACh), prolonging the activated state of the postsynaptic cell, leading to an enhanced signal transmission. With a similar outcome but different target site, neonicotinoids target the nAChR, leaving the receptor activated even in the absence of ACh. Thus, because these MoAs are also present in non-target organisms such as

aquatic vertebrates, it is reasonable to assume that insecticides which target them will exert corresponding effects here as well.

By testing a series of well-characterized insecticides, we aimed to molecularly decipher MoA-based hazards rather than defining quantitative endpoints. Thus, the intent of our study was conceptual. Prior knowledge of these agents was used to investigate, compare, and link the hazards of specific MoAs to known adverse effects in the non-target organism in an aquatic vertebrate model under sublethal exposure conditions based on ecotoxicogenomic profiles. This involved the identification of key biological processes affected and appropriate candidate biomarkers, as well as the characterization of early warning signatures for these MoAs. Thus, our study aimed to establish bases for the development of pre-regulatory screening approaches which could predict MoA hazards in unknown development compounds based on the identified biomarkers.

Being aware of the arising challenges using OMICs approaches in ecotoxicological research, such as reproducibility issues due to the lack of standardized analysis approaches (Baker, 2016; Brockmeier et al., 2017), we complied to the best of our knowledge with the FAIR data principles (Wilkinson et al., 2016) and SETAC's minimum reporting guidelines for ecotoxicological research (SETAC, 2019). We provided full access to raw and processed data files as well as complete analysis scripts to maximize transparency, reproducibility and reusability of the obtained datasets for the scientific community.

2. Materials and methods

2.1. Test substances and test solution setup

Six compounds from different chemical groups, defined by the IRAC MoA classification system (Sparks and Nauen, 2015), namely abamectin, carbaryl, chlorpyrifos, fipronil, imidacloprid and methoxychlor, were chosen as test substances (Table 1). Chemicals were purchased from Merck KGgA (Darmstadt, Germany). To avoid interference with systemic toxicity, sublethal test concentrations (Table 1) were chosen based on literature review and/or preliminary experiments (Brown et al., 2015; Chow et al., 2013; Correia et al., 2019; Jacobson et al., 2010; Jin et al., 2015; Lin et al., 2007; McCollum et al., 2011; Padilla et al., 2012; Sanches et al., 2017, 2018; Scheil and Köhler, 2009; Selderslaghs et al., 2010; Stehr et al., 2006; Tišler et al., 2009; Tišler and Kožuh Eržen, 2006; Tufi et al., 2016; Versonnen et al., 2004; Wu et al., 2014, 2018; Yen et al., 2011). Low and mid exposure concentrations reflect levels, at which no physiological effects were observed for the respective insecticide.

Stock solutions were prepared one day prior to the start of the experiment. With the exceptions of carbaryl and imidacloprid (prepared with copper-reduced tap water), stock solutions were set up in acetone, from which solvent free test solutions were prepared as the following: Respective amounts of acetone stock solution were added to 250 mL screw cap bottles. The same final volume of acetone used for the high exposure solution was added to all other exposure and control solutions to ensure equal proportions of acetone among each prepared test solution. After solvent evaporation by aeration (30 min at RT), 200 mL copper-reduced tap water with an adjusted pH of 7.5 were added to each bottle and mixed with a magnetic stirrer for 4 h at RT in the dark. Test solutions were then stored at RT in the dark and used over the course of the experiment.

2.2. Modified zebrafish embryo toxicity test (ZFET)

A modified zebrafish embryo toxicity test (ZFET) (OECD236) was performed to identify substance-induced alterations at the level of the transcriptome after exposure to sublethal concentrations of the neuronal targeting insecticides for 96 hpf. Modifications compared to the OECD guideline test were made to integrate transcriptomics and mainly affected the number of eggs used, test volumes and sample processing at the end of the test (see below). Maintenance of parental wild-type AB zebrafish (*Danio rerio*), spawning procedure, egg collection and the modified ZFET are described in detail by Reinwald et al. (2021a, 2021b) and in the supplements. Briefly, each treatment and control was performed in three biological replicates at 27 ± 1 °C at a 14:10 h light/dark cycle in glass petri dishes. Every experiment was performed in a balanced test design. Each replicate comprised eggs from a different spawning group (fish tank). Prior to the test start, glass dishes were pre-saturated with each solution overnight. From each spawning tank, approximately 50 eggs were pre-picked for each condition in 10 mL of the respective test solution. Via stereomicroscopy, 15 fertilized eggs of the same early blastula stage (3–4 hpf) were selected and transferred into the pre-saturated glass dishes filled with 8 mL of fresh, aerated test solution. At 24 hpf, the eggs were inspected visually and, if present, single coagulated eggs were recorded and removed. Aged solutions were renewed with fresh aerated test solutions at 48 hpf. At 96 hpf, overall survival, hatching rates and morphological malformations were recorded (S.Fig. 1).

2.3. RNA extraction and library sequencing

For each biological replicate, 10 embryos were randomly selected and pooled in a 1.5 mL Eppendorf tube. All tubes were then immediately and simultaneously placed on ice, killing the larvae before RNA extraction for gene expression profiling. Total RNA was isolated with a filter aided NucleoSpin RNA/protein extraction kit (REF 740933.250 - MACHEREY-NAGEL, Düren, Germany) according to the manufacturer's protocol. In brief, the supernatant was removed from the pooled larvae and 350 µl RP1 lysis buffer, prepared with TCEP, were added to each sample. Mechanical homogenization was performed at 5 m/s for 40 s at room temperature with Lysing Matrix D© ceramic beads on a FastPrep-24© homogenizer (MP Biomedicals, Irvine, USA). RNA yields and sample purity were quantified via Nanodrop (Thermo Fisher Scientific, Waltham, USA). Total RNA integrity was assessed with a 2100 Bioanalyzer system (Agilent, Santa Clara, USA) using the RNA 6000 Nano Kit (5067–1511).

Only samples with a RNA integrity number (RIN) > 8 were considered for mRNA-Seq (S.Fig. 2). Library preparation and sequencing was

Table 1
List of investigated neuronal targeting insecticides in this study and their tested sublethal exposure concentrations (nominal) exposed to zebrafish embryos for 96 hpf. Environmental concentrations are given based on available literature (Bonifacio et al., 2017; Deiú et al., 2021; Frankel et al., 2020; Peterson et al., 1994; Thunnissen et al., 2020; Tišler and Kožuh Eržen, 2006). (*: Sum of B1a and B1b HPLC area).

Insecticide	CAS	Purity [%]	***Mode of Action (MoA)*** (IRAC classification)	***Environmental concentrations [µg/L]***	Exposure concentration [µg/L]		
					Low	Mid	High
Abamectin	71751-41-2	≥95*	Glutamate gated chloride channel modulator	0.011–18	110	220	440
Carbaryl	63-25-2	≥98	AChE inhibitor	≤4800	275	–	1100
Chlorpyrifos	2921-88-2	≥98	AChE inhibitor	≤10	750	–	3000
Fipronil	120068-37-3	≥99	GABA gated chloride channel antagonist	0.5–465	75	–	300
Imidacloprid	138261-41-3	≥98	nAChR competitive modulator	0.001–320	15000	30000	60000
Methoxychlor	72-43-5	≥98	Sodium channel modulator	0.02–50	20	60	180

conducted by NGS-Services for Integrative Genomics at the University of Göttingen, Germany. Samples were poly(A) (+) enriched (Rio et al., 2010) and subjected to library preparation using the TruSeq RNA Library Prep Kit v2 as recommended by the manufacturer (Illumina) before sequencing with Illumina HiSeq 4000 (Illumina) in 50 bp single read mode, with approximately 30 million raw reads per sample.

2.4. Bioinformatic data processing

Complying with the FAIR data principles (Wilkinson et al., 2016) and minimum reporting guidelines of the Society of Environmental Toxicology and Chemistry (SETAC, 2019), raw and processed data files and analysis scripts are made publicly available and free to use under the Creative Commons (CC) BY-SA 4.0 license. Raw sequencing files and processed gene counts of each experiment were deposited in the ArrayExpress database (Brazma et al., 2003) at EMBL-EBI (www.ebi.uk/arrayexpress) under the following accession numbers: E-MTAB-9852 (abamectin), E-MTAB-9855 (carbaryl), E-MTAB-9853(chlorpyrifos), E-MTAB-9854 (fipronil), E-MTAB-9859 (imidacloprid), E-MTAB-9860 (methoxychlor). All bioinformatic analysis scripts, including full conda (Grüning et al., 2018) environment descriptions and R package versions are available on github (https://github.com/hreinwal/zfeNeurotox). Sequence and alignment QC reports (MultiQC, Ewels et al., 2016) as well as annotated differential gene expression analysis (DGEA) and gene set enrichment analysis (GSEA) result tables are available on Zenodo (www.zenodo.org) under the accession number: 5218919 (Reinwald et al., 2021a). Details on library preparation, sequencing, raw read processing, sequence alignment and *in silico* data QC are described in the supplements. In brief, reads were mapped to the *Danio rerio* reference genome GRCz11 release version 100 (ENSEMBL, 2020) using STAR aligner v2.7.5b (Dobin et al., 2013) and counted via STAR's '*–quantMode GeneCounts*'.

2.4.1. Differential gene expression analysis (DGEA)

To identify differentially expressed genes (DEGs), read count tables for each tested substance were merged into a single count matrix and subjected to differential gene expression analysis (DGEA) with DESeq2 v1.28.1 (Love et al., 2014) in R v4.0.2 (R Core Team, 2021). Low abundant genes with less total counts per gene than the number of samples were removed prior DESeq2's median of ratios normalization (S.Fig. 3) and statistical testing. The total common set of analyzed genes was 24676, covering 95.2–98.6% of the individually analyzed gene sets for each exposure experiment. Unsupervised multivariate sample clustering methods were applied to check for the robustness of general underlying data patterns (Fig. 1A, S.Fig. 4 and S.Fig. 5). A multifactor model design considering tank and condition was implemented to control for the variance among fish tanks. With three biological replicates per condition, exposure treatments were compared in a pairwise fashion with respect to the control group, applying Wald's *t*-test. P-values were corrected for multiple testing with independent hypothesis weighting (IHW) (Ignatiadis et al., 2016) after Benjamini-Hochberg (BH). Biological effect size cut off (LFcut) was determined for each comparison as the 90% quantile of the absolute non-shrunk log2-fold change (lfc) values. Under the assumption that lfc values are equally distributed around 0, this scalable effect size cut off adjusts with the global lfc distribution. We pursued this approach, as we observed the global lfc distribution to widen with higher substance exposure levels, hence with higher organismal stress levels (S.Fig. 6). After determining LFcut, lfc values were shrunk using the *apeglm* method (Zhu et al., 2019). Finally, a gene was considered as differentially expressed when (a) its mean expression differed significantly from the control group (BH adjusted p (p.adj) $\leq$ 0.05) and (b) the absolute apeglm shrunk lfc was greater LFcut (abs [apeglm(lfc)] $\geq$ LFcut) (S.Fig. 7). The common set of identified differentially expressed genes (DEGs) across the different exposure conditions for each tested insecticide were defined as core DEG set (Fig. 1B) and evaluated by correlation analysis (S.Fig. 8). ENSEMBL gene identifiers

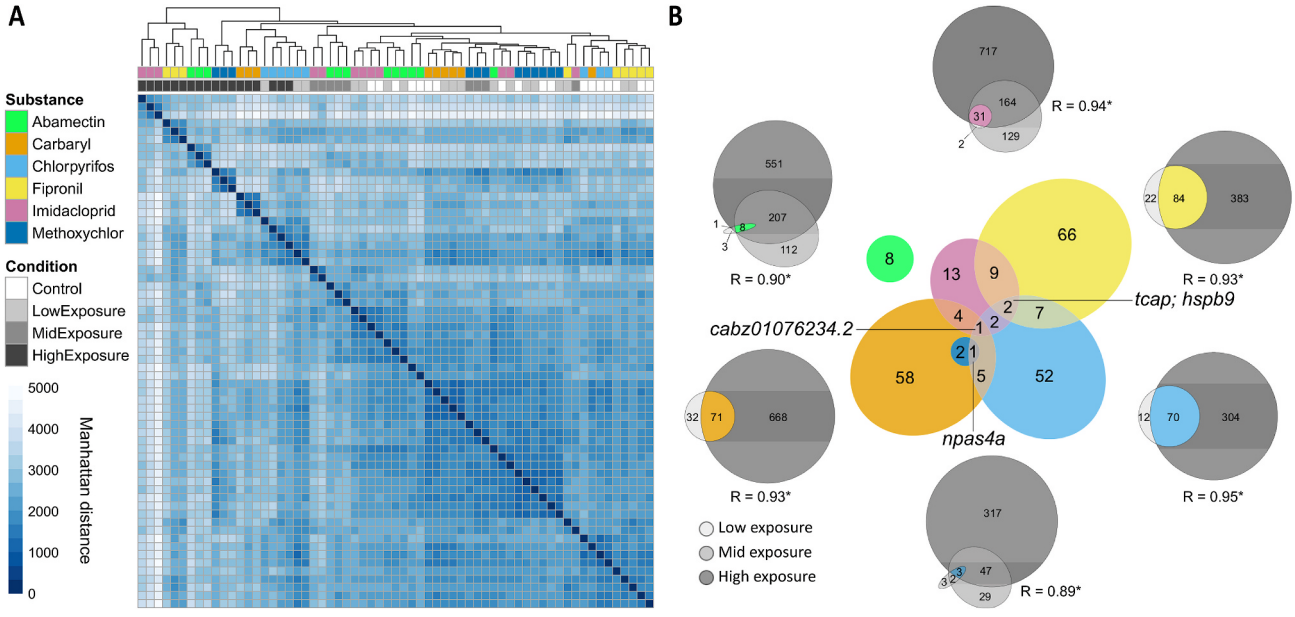

Fig. 1. Sample distance matrix and differentially expressed genes (DEGs) of different neuro-targeting MoA. (A) Global sample clustering shown in a dissimilarity matrix on normalized and variance-stabilized transformed gene counts for the 5000 most varying genes. Samples were clustered by Manhattan distances using Ward's D2 method. The color code below the hierarchical cluster describes the sample's association with the respective test substance and gray scales display the treatment condition for each substance (control, low exposure, mid exposure, high exposure). (B) Multiple venn diagram showing the number of identified differentially expressed genes (DEGs) in each condition for each substance. The outer venn plots display the DEGs for each treatment condition and each substance. The common DEG set among all treatments (core DEG) is colored for each test substance (color code identical to (A)). Pearson correlation coefficients (R) display the correlation of $\log_2$-fold change (lfc) values for the core DEG sets (*: $p < 0.001$ for one side (greater) Pearson correlation test) (S.Fig. 8). In the case of three treatment conditions, Pearson correlation coefficients were computed from the common DEGs among mid and high exposure. The inner venn plot shows the overlap for the different core DEG sets among the tested neurotoxic insecticides. (For interpretation of the references to color in this figure legend, the reader is referred to the Web version of this article.)

were annotated via biomaRt (Durinck et al., 2009) in R.

2.4.2. Overrepresentation analysis (ORA) on substance-specific gene clusters

To evaluate the functional properties of the identified substance-specific gene clusters, overrepresentation analysis (ORA) was performed for gene ontology (GO) terms (Carbon et al., 2019) as well as Reactome (Fabregat et al., 2018) and KEGG pathways (Kanehisa et al., 2008) in R using ClusterProfiler v3.18 (Yu et al., 2012) and ReactomePA v1.34 (Yu and He, 2016). To cover at least 50 genes for each substance-specific cluster, we selected the intersecting DEG sets between high and low exposure of carbaryl, chlorpyrifos, and fipronil and the high and mid exposure of abamectin, imidacloprid and methoxychlor as input for the ORA. Gene clusters were analyzed with *compareCluster()* default settings and BH p-value correction. To reduce redundancy within the significant enriched GO terms, semantic similarities were computed among them after Yu (2020) implemented in the clusterProfiler's *simplify()* function with a similarity cutoff of 0.5.

2.4.3. Gene set enrichment analysis (GSEA)

To evaluate the biological processes affected by the different neuronal targeting insecticides, gene set enrichment analysis (GSEA) (Subramanian et al., 2005) for Reactome pathways, KEGG pathways and GO of biological processes, was conducted in R. The obtained DESeq2's DGEA result tables were reduced to a set of 24676 commonly analyzed genes, sorted by their apeglm shrunk lfc values and subjected to GSEA via clusterProfiler v3.18 and ReactomePA v1.34 (Yu and He, 2016). For GSEA on KEGG and Reactome pathways, where ENTREZ gene identifiers are required as input, gene lists were sorted by their p-value before removing duplicated ENTREZ identifiers before the analysis. The obtained p-values, as a measure for the significance of an enriched GO term or pathway, were corrected for multiple testing after BH. Only gene sets with a p.adj $\leq$0.05 were considered as statistically significantly enriched.

3. Results and discussion

3.1. DGEA - transcriptomic profiles of neuronal targeting insecticides

To identify and evaluate differences and similarities across molecular responses to the tested neuronal targeting MoAs in the zebrafish embryo model, we performed a modified ZFET followed by DGEA using NGS of mRNA. In this approach, we applied a range of subsequent, sublethal exposure concentrations for each tested substance in order to minimize interfering responses of systemic toxicity. For each substance, sublethal low effect test concentrations were chosen based on literature review and range finding pre-tests. While for all tested insecticides, indeed none of the selected exposure concentrations induced statistically significant lethality as compared to the controls (S.Fig. 1A), solely the high exposure concentration of abamectin induced a statistically significant hatching delay (S.Fig. 1B). Consequently, all tested low and mid exposure conditions reflected concentration levels well below acute toxicity with no observed morphological changes in the embryo's development. Nevertheless, we identified significant changes in embryo's gene expression profiles throughout all exposure conditions for all substances, suggesting a higher sensitivity of a transcriptomic approach compared to observable physiological effects.

At the gene expression level, PCA and t-SNE clustering (S.Fig. 4) as well as the sample distance matrix (Fig. 1A) displayed an enhanced separation of conditions and controls with increasing exposure concentrations for each substance. Cross comparison of all samples showed adjacent clustering of the control groups in all exposure experiments (S. Fig. 5). We interpret this observation as an indicator for the stability of our test approach, since the exposure experiments for the different insecticides were conducted several months apart. Furthermore, this clustering supports the assumption that the variance among sample groups was primarily driven by the insecticide exposure and not by biological variance, i.e. by different spawning tanks (S.Figs. 4 and 5). With the exception of chlorpyrifos, the low exposure conditions clustered closely with the control groups, suggesting that the chosen concentration range covered very early gene expression changes, which likely were not a result of systemic effects (Fig. 1A). Hence, we conclude that the low exposure conditions for all tested insecticides reflected exposure levels in which transcriptomic changes are starting to emerge, reflecting an early molecular response to the chemical.

For all tested insecticides, the total number of DEGs increased with the exposure concentration, in a concentration-response-like relationship (Fig. 1B and S.Fig. 7). The combined subsets of DEGs identified between the lowest and highest exposure concentrations each covered a significant proportion of DEGs responding to the low exposure concentration, with 93% for imidacloprid, 85% for chlorpyrifos, 79% for fipronil, 75% for abamectin, and 69% for carbaryl (Fig. 1B). In the case of methoxychlor, where we observed the lowest number of DEGs responding to the low exposure concentration, the common DEG set with the high exposure concentration represented 38%, whereas the common DEG subset between medium and high exposure concentrations comprised 62% of DEGs responding to the medium exposure condition. The intercepts of DEGs from different exposure conditions each showed a strong positive correlation for their lfc values ($R \geq 0.89$, one-sided Pearson correlation test $p \leq 0.013$, Fig. 1B and S.Fig. 8). Hence, these common subsets of DEGs after low and the higher exposure conditions represented genes, which a) responded to very low sub-acute exposure levels of the tested insecticides and b) were differentially regulated in a comparable manner over a wide range of exposure concentrations. Therefore, we considered these genes as core DEG sets, representing biomarker candidates, which could allow for the discrimination of early molecular events specific for the respective MoA in our non-target model. The total set of core DEGs consisted of 230 genes (Fig. 1B), composed of 222 (96.5%) protein coding transcripts, six (2.6%) long intergenic non-coding RNAs (lincRNA) and two (0.9%) unprocessed pseudogenes (S.Fig. 9).

3.2. Functional characterization of neurotoxic insecticide responsive gene sets

Promising biomarker candidates should be robustly detectable and thus reliably expressed. To focus on such candidates, we selected from the total set of 222 core DEGs (S.Fig. 9) protein coding genes with an average normalized base-mean expression of 500 reads (67% top quantile) or higher, leaving a set of 88 genes presented in Fig. 2 and S. Fig. 10. While the majority of these robustly expressed core DEGs appeared to be compound-specific, some of the gene clusters shown were nevertheless differentially expressed with increasing exposure levels across the six insecticides tested.

As an example, the upregulated embryonic hemoglobin (hbbe & hbae) & aminolevulinate synthase 2 (alas2) cluster belongs to the core DEGs assigned to carbaryl. However, this cluster is also differentially expressed after exposure to higher concentrations of methoxychlor, imidacloprid and fipronil (Fig. 2 & S.Fig. 11). While exposure to carbaryl, imidacloprid and fipronil induced this gene cluster, methoxychlor exposure resulted in a repression. Alas2 is an enzyme involved in the heme biosynthetic pathway, which is primarily expressed in erythroid cells (Cox et al., 2004; Gardner et al., 1991). The embryonic hemoglobins *hbbe1.1*, *hbbe1.3, hbbe2*, and *hbae3* (S.Fig. 11) are essential for oxygen uptake and transport (Brownlie et al., 2003; Rombough and Drader, 2009). The upregulation of this hemoglobin cluster could represent a direct response to low oxygen levels in the embryo's tissue (Rombough and Drader, 2009). This assumption is further supported by the co-upregulation of hypoxic stress markers such as insulin-like growth factor binding protein 1a *igfbp1a* (Kamei et al., 2008) or hypoxia inducible factor 1 subunit alpha like (*hif1al*) (Fig. 2 & S.Fig. 11). The orthologue in human is HIF3A. HIF1 is a heterodimeric

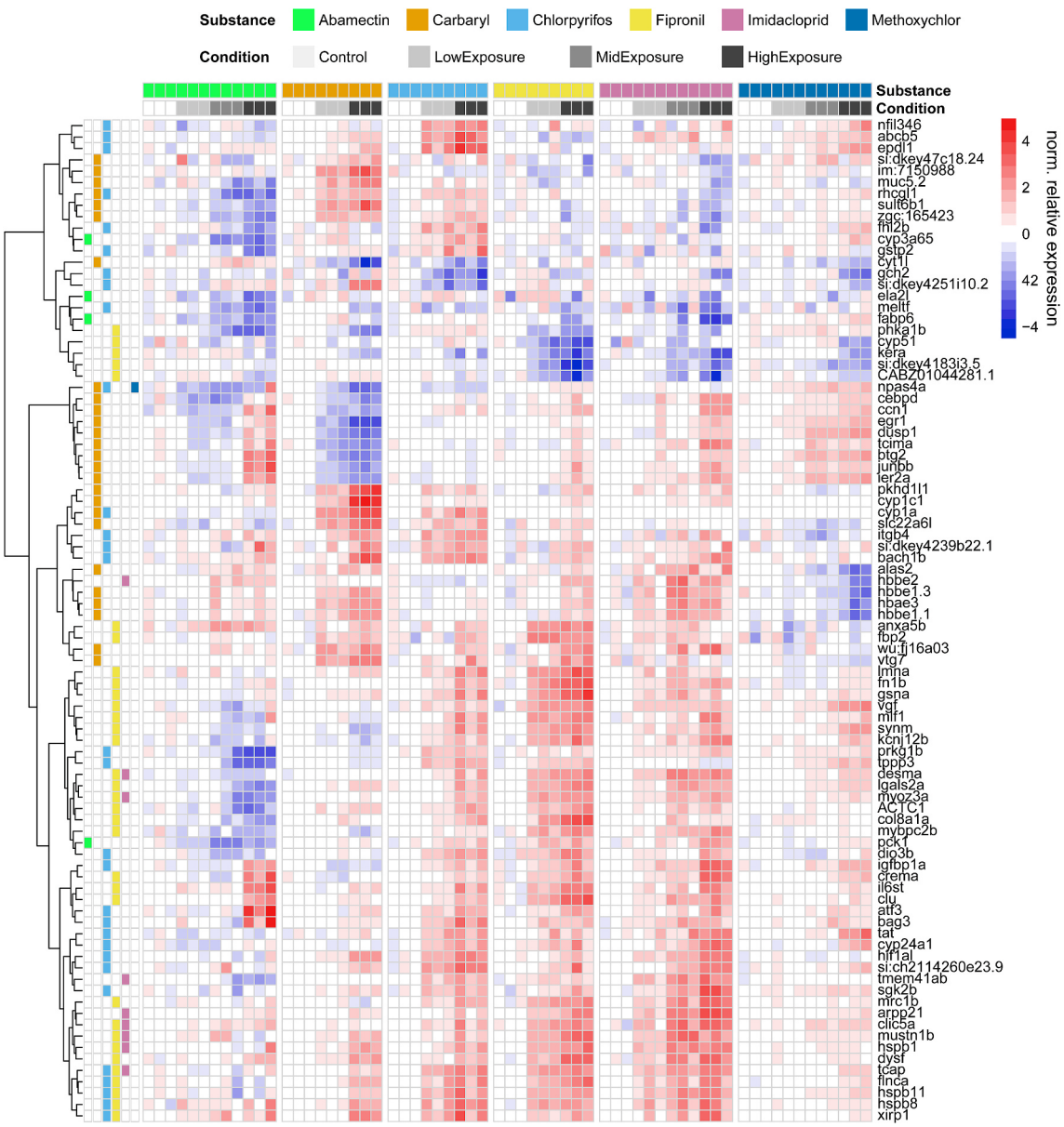

Fig. 2. Heatmap showing relative gene expression patterns of zebrafish embryos post exposure to sublethal concentrations of neurotoxic insecticides at 96 hpf. Presented is the selection of 88 protein coding core DEGs (Fig. 1B) (rows) across all samples (columns) with an average normalized gene count ≥500 (top 67% quantile). The expression profiles of all 222 protein coding core DEGs is shown in S.Fig. 9. Relative expression signal for each gene is the variance-transformed normalized counts, centered around the control group's mean and scaled by the global standard deviation. Red color indicates an enhanced and blue a suppressed expression relative to the global control's mean expression of a gene. Genes were clustered for Euclidean distance by ward.D2. The color code above each column describes the assignment of the sample to the respective test substance and exposure condition. The color code on the left hand side of the rows indicates, for which tested substance a gene was identified as core DEG. (For interpretation of the references to color in this figure legend, the reader is referred to the Web version of this article.)

transcription factor, activating a variety of genes in response to hypoxia, which is critical for the normal development of the cardiovascular system in vertebrates (Robertson et al., 2014). It enhances the transcription of vascular endothelial growth factor, glycolytic enzymes, glucose transporters and erythropoietin, an important growth factor for erythrocyte formation (Agani et al., 2000).

GSEA verified a significant enrichment of biological GO terms associated with oxygen transport and response to decreased oxygen levels for higher imidacloprid, fipronil and chlorpyrifos exposures (Supplementary data 5218919).

Fig. 3 shows a linked network based on the insecticide-specific gene set collection (see material and methods) for the 30 most significantly enriched biological process GO terms. Based on the selection of early responsive genes for each tested compound, we observe distinguishable enriched GO clusters for the tested insecticides. For example, the genes differentially regulated by abamectin exposure are primarily linked to metabolic and catabolic processes, especially in the context of lipid and olefinic compound processes. This suggest that lipid homeostasis might be affected by abamectin exposure in zebrafish embryos. Further, genes related to drug and xenobiotic metabolic processes were found significantly enriched as well. These biological processes occur especially in liver and kidney (Hogstrand and Haux, 1991). This suggests that abamectin's primary MoA in the fish could be due to hepato- and nephrotoxic effects. In fact, previous studies in rats demonstrated highly affected testis, kidney and liver functions after abamectin exposure (Magdy et al., 2016). Further, human liver cell lines exposed to

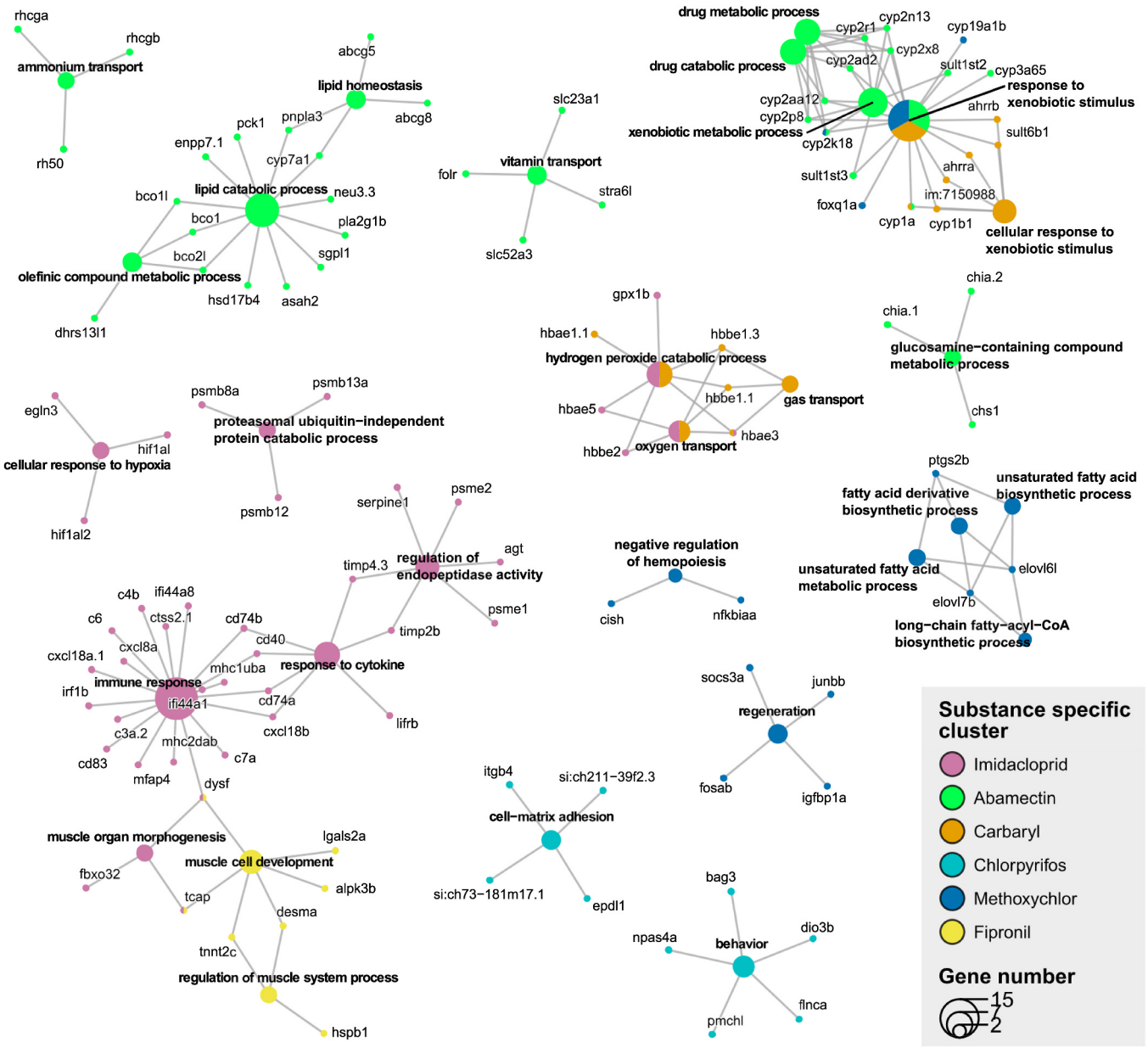

Fig. 3. Gene network cluster showing the top 30, most significantly (padj BH $\leq$ 0.1) enriched biological process GO terms from ORA linked with their associated genes. As input for the ORA, substance specific gene sets were selected based on the shared DEGs between higher and lower exposure condition. For abamectin, imidacloprid and methoxychlor, the common set between high and mid exposure was selected, to ensure a minimum gene set size of 50 for each ORA. GO term bubble size reflects the number of genes from the input gene set associated with this biological process. GO term bubble colors indicate for which substance's gene set the term was significantly enriched. To this term associated gene from the input set are colored respectively. (For interpretation of the references to color in this figure legend, the reader is referred to the Web version of this article.)

ivermectin, a structurally highly similar compound, demonstrated reduced triglyceride accumulation and inhibition of lipogenesis related gene sets (Yang et al., 2019).

In contrast, the network shows a large number of imidacloprid specific differential expressed genes associated with immune response and response to cytokines as well as the regulation of endopeptidase activity. As imidacloprid is designed to target the insect's nAChRs, this is not surprising as in vertebrates, nAChRs are important regulators in immune homeostasis and inflammatory processes (Cao et al., 2021; Lu et al., 2014; Wang et al., 2003). In contrast to insects, where the cholinergic system is restricted to the central nervous system (Yamamoto, 1999), nAChRs in vertebrates are also found on immune system cells such as monocytes, lymphocytes and macrophages (Wang et al., 2003). Most recently, a novel nAChR with immune regulating functions was described in bivalves (Cao et al., 2021), suggesting a functional conservation across mammals (Lu et al., 2014), fish (Toledo-Ibarra et al., 2013) and aquatic mollusks alike. In a study of medaka conducted by Sánchez-Bayo and Goka (2005), it was found that organisms exposed to imidacloprid were more susceptible to infections and parasitic infestations, suggesting a possible link between nAChR-targeting compounds and an impaired immune response. Although greater parasite infestation could be explained by a general increased stress level due to the test compound, the observed transcriptomic profiles after imidacloprid exposure suggest a possible direct link. Consequently, the enrichment of immune response related GO terms could eventually be a characteristic molecular fingerprint of chemicals targeting the nAChRs in aquatic organisms.

The early molecular responses to carbaryl and imidacloprid were

linked to oxygen transport. The network also shows the potential molecular link for the hemoglobin cluster downregulation through methoxychlor exposure by *nfkbiaa* and *cish,* which are associated with negative regulation of hematopoiesis (Frame et al., 2020; Lewis et al., 2014). As we observed an upregulation of *hif1al,* coherent with the upregulation of hemoglobin and aminolevulinate synthase, in embryos exposed to carbaryl, fipronil and imidacloprid, we suggest this as a molecular response to internal hypoxic stress.

Among the 88 biomarker candidates from the core DEG sets shown in Fig. 2, a large subset of up-regulated genes was linked with cardiac muscle cell development and functioning. *tcap, desma, bag3, hspb8, flnca, myoz3a, mybpc2b, actc2 (*f.k.a. *zgc:86709*) and *tnnt2c* (S.Fig. 11) are known biomarkers for hypertrophic cardiomyopathy in humans (Dubińska-Magiera et al., 2020; Maron and Maron, 2013; Ojehomon et al., 2018; Vogel et al., 2009; Witjes et al., 2019). All of these genes represented core DEGs, often shared between chlorpyrifos and fipronil or fipronil and imidacloprid in our study.

Cardiac troponin T *(tnnt2)* is known to regulate the interaction between actin and myosin in response to the Ca^{2+} wave (Parmacek and Solaro, 2004) and plays a crucial role in myofibrillogenesis in zebrafish and human alike (Huang et al., 2009). A depletion in *tnnt2* has been shown to lead to heart malformations and a silent heart in developing zebrafish and in mouse embryos (Nishii et al., 2008; Sehnert et al., 2002).

The intermediate filament protein desmin (*desma*) was observed to be downregulated after exposure to abamectin, while it was upregulated after chlorpyrifos, fipronil, imidacloprid and methoxychlor exposure. A recent study on desmin knockout zebrafish reported defects of heart calcium flux (Kayman Kürekçi et al., 2021), which was previously linked to an abnormal localization of ryanodine receptors (RyRs) (Ramspacher et al., 2015). RyRs are named after the neurotoxic insecticide ryanoide, which binds these receptors with high affinity (Rogers et al., 1948; Santulli and Marks, 2015). These receptors regulate Ca^{2+} signaling and are involved in modulating spontaneous heartbeat (Van Petegem, 2012; Wu et al., 2011) and musculoskeletal, cardiovascular, and nervous system differentiation in the developing zebrafish (Wu et al., 2011).

Most prominently, telethionin *(tcap)* showed an early and consistent significant upregulation after exposure to all chlorpyrifos, fipronil and imidacloprid concentrations as well as after exposure to the high carbaryl and methoxychlor treatments (S.Fig. 11). This gene is expressed in the skeletal muscle, myotome and the heart. In developing zebrafish, *tcap* is expressed from the 21-somite stage on and a reduction of its expression leads to deformed muscle structure and impaired swimming ability (Zhang et al., 2009). Human orthologues of *tcap* are associated with hypertrophic and dilated cardiomyopathy (Hayashi et al., 2004) as well as with limb-girdle muscular dystrophy 2G (Zhang et al., 2009). Molecular studies suggest that tcap, which is localized in the Z-disc and interacts with muscle LIM protein (MLP), plays an essential role in stretch recognition of cardiomyocytes. Defects in this stretch recognition complex have been associated with heart failure (Knöll et al., 2002).

Among the differentially expressed heat shock proteins in response to chlorpyrifos, fipronil and imidacloprid exposure in our study, *hspb1* (previously *hsp27)* and *hspb8* are known regulators of skeletal and cardiac cell development in fish, frogs and mice (Brown et al., 2007; Dubińska-Magiera et al., 2020; Middleton and Shelden, 2013). *hspb1* plays a crucial role in cardiomyocyte differentiation (Davidson and Morange, 2000). In developing zebrafish, the expression of *hsbp1* was reported to be highest in cardiac, ocular and craniofacial muscles (Middleton and Shelden, 2013). Recently, Dubińska-Magiera et al., 2020 and colleagues characterized hspb8 function during zebrafish development, observing changes in the heart area after morpholino-mediated *hspb8* knockdown and demonstrating an interaction of hspb8 with the co-chaperone Bcl2-associated athanogene 3 (*bag3*). These observations suggested that the hspb8/bag3 interaction may play a vital role in heart functioning of developing zebrafish, which appears to be evolutionarily conserved among vertebrates. Like *tcap,* also *bag3* is localized in the Z-disc of striated muscles and was linked to dilated cardiomyopathy in previous studies (Arimura et al., 2011; Domínguez et al., 2018). Thus, our observations indicate that the cardiac Z-disc structural development in zebrafish might be susceptible to a range of neuronal targeting insecticides. Consequently, a dysfunctional Z-disk structure with impaired mechanical stretch sensing may impair cardiac function of the organism, even in adulthood.

ORA showed that early toxicogenomic responses to fipronil exposure were in particular linked to muscle cell development and regulation of muscle system processes (Fig. 3). Also GSEA revealed that muscle cell differentiation and muscle structure development were among most significantly enriched terms occurring after chlorpyrifos, fipronil, imidacloprid and methoxychlor treatments (Fig. 4). Previous studies frequently reported cardiac malformations, impaired cardiac functionality and reduced heart rates in developing fish embryos exposed to AChE inhibiting carbamate and organophosphate insecticides (Jin et al., 2015; Kais et al., 2018; Lin et al., 2007; Schock et al., 2012; Solomon and Weis, 1979; Toledo-Ibarra et al., 2013; Watson et al., 2014; Weis and Weis, 1974). Heart developmental defects leading to reduced heart rate and developmental defects in cardiac looping as well as cardiac edema were previously described for developing zebrafish embryos exposed to carbaryl (Lin et al., 2007; Schock et al., 2012) and chlorpyrifos (Jin et al., 2015; Kais et al., 2018; Pérez et al., 2013; Watson et al., 2014). As a consequence, embryos often showed reduced or lacking blood circulation (Kais et al., 2018; Lin et al., 2007). Similarly, adverse effects on the early heart development and blood circulation in zebrafish were also reported for fipronil (Park et al., 2020), abamectin (Sanches et al., 2017) and the neonicotinoid imidacloprid (Vignet et al., 2019). Indicating conserved effects across different species, cardiac effects induced by imidacloprid or fipronil were also previously reported in birds. Imidacloprid lead to heart tube malformation in developing chickens (Gao et al., 2016), while fipronil caused abnormal cardiac muscle tissue formation in the Japanese quail (Khalil et al., 2019).

In general, we observed various molecular signatures linked to heart muscle development, which may precede severe heart failure and cardiac malformations reported for higher levels of exposure. Similar to human cardiomyopathy, fish may also be susceptible to sudden cardiac death under conditions of physical stress (e.g., escape from predators, territorial fights, mating), especially if cardiac development has been compromised due to chemical exposure in a vulnerable state. In this case, the observed induction of oxygen stress could be a consequence of molecular key events related to impaired myocardial development or function resulting in a reduced blood flow. In previous studies, the zebrafish embryo was reported to be less sensitive to neuronal targeting insecticides compared to juvenile or adult life stages (Glaberman et al., 2017). Impairment of the cardiovascular system as a major consequence of early chemical exposure and the resulting oxygen deficiency might be less severe for the embryo than for the adult organism because oxygen could be absorbed through the skin by diffusion (Klüver et al., 2015; Scholz et al., 2016). However, the here presented transcriptomic profiles suggest that the reported hypoxic stress might be a secondary toxic effect as a result of primarily impaired cardiac functioning. To enhance the sensitivity of fish embryo assays for these types of chemicals we, therefore, suggest to check for molecular markers related with heart development and functioning (i.e. *tcap* or *actc2)* and hemoglobin synthesis (i.e. *alas2*) along with hypoxic stress markers (i.e. *hif1l*) even in the absence of observable physiological effects.

As second major important group of DEGs, responsive to the tested compounds, we identified *npas4a, egr1, btg2, ier2a* and *vgf* (Fig. 2 & S. Fig. 11). For all of these genes, crucial functions for neurogenesis and synaptic plasticity in the developing central nervous system were reported (Bozdagi et al., 2008; Hong and Dawid, 2009; Kamaid and Giráldez, 2008; Klarić et al., 2014; Moriya et al., 2016; Takeuchi et al., 2018; Torres-Hernández et al., 2016; Zhang et al., 2013) and linked to altered organism behavior (Baker and Wong, 2021; Coutellier et al., 2012; Lopes et al., 2015; Malki et al., 2016; Mizoguchi et al., 2017;

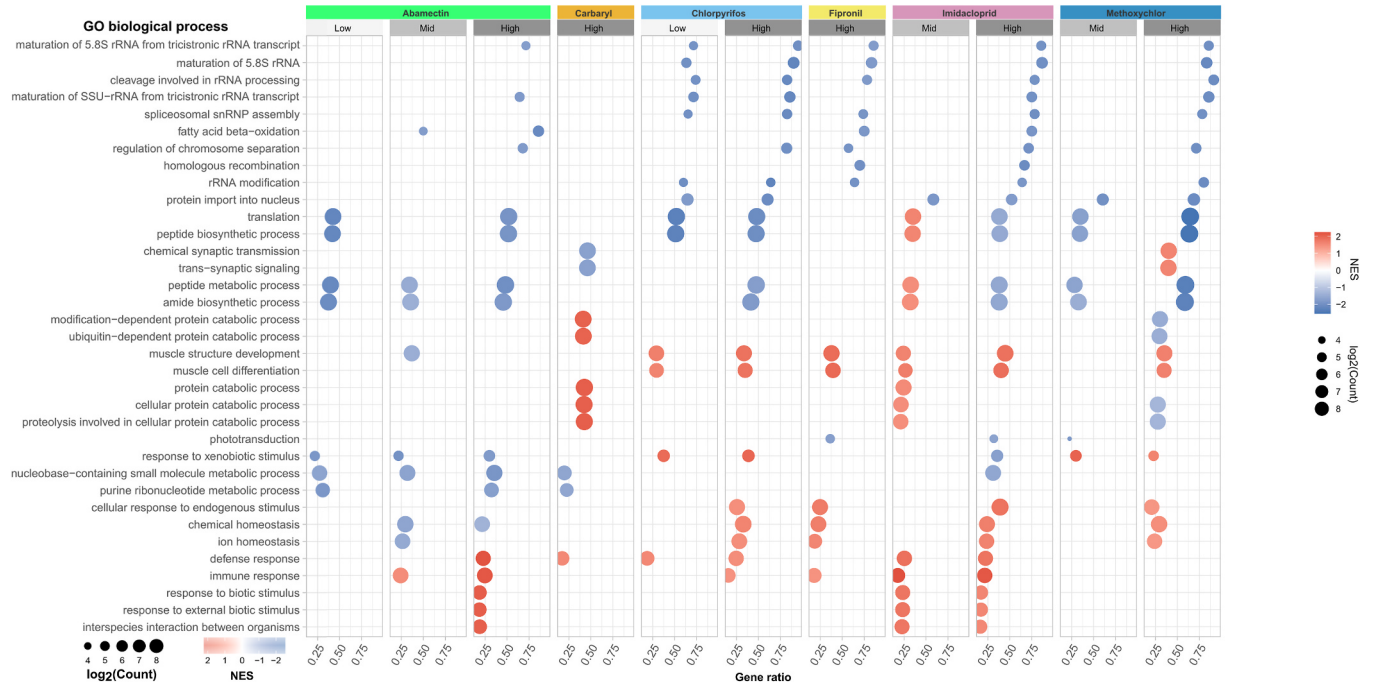

Fig. 4. Selection of the topmost significantly enriched biological processes GO terms post sublethal neurotoxic insecticide exposure in zebrafish embryos at 96 hpf. The selection consists of the common set of the top 5 (sorted by p-value) enriched pathways (y-axis) for each tested substance and condition. Each grid displays the GSEA results for a given experimental treatment (substance and condition). Bubbles are drawn for terms identified as statistically significantly enriched (BH adjusted $p \leq 0.05$) for the respective experimental treatment. Bubble size reflects the $\log_2$-transformed number of genes identified as enriched in a gene set (Count). The gene ratio (Count/gene set size) defines the bubble's position on the x-axis as a measure for how many genes in a gene set were enriched relative to set size. Bubble colors indicate a positive (red) or negative (blue) normalized enrichment score (NES). In cases where no GO terms were found statistically significantly enriched, no grid was drawn. Similar selections of significant enriched KEGG and Reactome pathways are shown in S.Fig. 12 and S.Fig. 13. (For interpretation of the references to color in this figure legend, the reader is referred to the Web version of this article.)

Torres-Hernández et al., 2016). While *npas4a, egr1, btg2*, and *ier2a* were downregulated by carbaryl exposure, the expression of these genes was induced by imidacloprid and methoxychlor in the high exposure condition, with *npas4a* being an exception (S.Fig. 11). These observations post carbaryl exposure align well with previous studies on neuronal development and behavior, which found co-regulation between *npas4a* and *btg2* (Lopes et al., 2015; Malki et al., 2016).

The activity-dependent transcription factor neuronal PAS domain protein 4a (*npas4a*) showed opposite regulation by the AChE inhibitors carbaryl and chlorpyrifos compared with the sodium channel modulator methoxychlor and the GABA-gated chloride channel inhibitor fipronil. *Npas4a* is exclusively expressed in brain, where it functions as essential regulator of brain development, neurogenesis and synaptic plasticity in mammals as well as in zebrafish (Baker and Wong, 2021; Bloodgood et al., 2013; Flavell and Greenberg, 2008; Kim et al., 2020; Klarić et al., 2014; Lopes et al., 2015; Maya-Vetencourt et al., 2012). Its expression is upregulated in response to calcium signaling-mediated neuronal activity, which is believed to induce GABAergic inhibitory synapses (Lin et al., 2008). Knockdown of *npas4a* has previously been shown to cause neurophysiological defects such as sensorimotor deficits and memory impairment, which are due to abnormal forebrain development (Coutellier et al., 2012; Klarić et al., 2014; Lin et al., 2008; Ramamoorthi et al., 2011). Recently, altered *npas4a* expression levels in zebrafish were linked to differences in animal fear learning and behavior (Baker and Wong, 2021; Torres-Hernández et al., 2016).

Like *npas4a*, also *egr1* is an inducible transcription factor with important regulatory functions in the brain linked to nerve cell growth and differentiation, synaptic plasticity and memory (Boyer et al., 2013; Calogero et al., 2004; Shafarenko et al., 2005). Previous studies demonstrated the importance of *egr1* for embryonic retina morphogenesis and glial cell development in developing birds (Bitzer and Schaeffel, 2002; Fischer et al., 2009), mammals (Hu et al., 2006) and fish (Busquet et al., 2014; Close et al., 2002). In zebrafish, *egr1* is expressed from the 40–48 hpf life stage on (Close et al., 2002) and its knockdown leads to reduced eye size with abnormal retinal lamination by suppressing the differentiation of retinal parvalbumin and GABA-positive amacrine and horizontal cells (Zhang et al., 2013).

Functionally equivalent human orthologues of *egr1* and the immediate early response 2a (*ier2a*, f.k.a *ier2*) (Hong and Dawid, 2009; Zhang et al., 2013) are part of a previously described set of 11 markers of prenatal arsenic exposure in human infants (Fry et al., 2007). In medaka, *ier2a* is primarily expressed in telencephalon, midbrain and the hypothalamus (Moriya et al., 2016). Decreasing expression of the ier2 orthologue has been observed in rats during aging (Fu et al., 2006), but also in response to neurotoxins (Ryan et al., 2010).

B-cell translocation gene 2 (*btg2*) and *ier2a* were both described as important regulators for neuronal development in vertebrates (Kamaid and Giráldez, 2008; Moriya et al., 2016). Previous studies linked *btg2* depletion with abnormal aggressive behavior in zebrafish and mice (Liu et al., 2020; Malki et al., 2016), indicating important roles of both genes for aggression-related brain functions.

In contrast to the neuronal-related genes mentioned above, the inducible nerve growth factor *vgf* was not differentially expressed after carbaryl exposure but was significantly upregulated after exposure to all test concentrations of fipronil and after exposure to higher concentrations of chlorpyrifos, imidacloprid, and methoxychlor. *Vgf* is a neuropeptide induced through brain-derived neurotrophic and nerve growth factors, which shows functional conservation across teleost, avian and mammal species (Helfer and Stevenson, 2020). It is involved in important neuronal functions such as synaptic plasticity, neurogenesis as well as brain neurite growth (Mizoguchi et al., 2017; Takeuchi et al., 2018) and has shown neuroprotective properties in retina ganglia cells (Takeuchi et al., 2018). In mice, *vgf* knockout resulted in enhanced depressive and asocial behavior coupled with lower brain weights and

memory impairments (Mizoguchi et al., 2017). In humans, depression, schizophrenia and bipolar disorders were related to abnormal *VGF* levels in the brain, suggesting this gene to be a relevant contributor to the pathogenesis of mental illness (Alder et al., 2003; Bozdagi et al., 2008; Lin et al., 2015). Recently, *vgf* was reviewed as a neuroendocrine marker with major importance for seasonal energy balance regulation in multiple vertebrate species (Helfer and Stevenson, 2020). Consequently, the here discussed genes related to important neuronal functions may represent early indicators of potential deleterious effects on neuronal development in the zebrafish embryo that translate into impaired behavior, memory, and even energy balance in the organism. Given their highly conserved functionality across teleost, avian, and mammalian species, these genes may represent suitable biomarker candidates for cross-species neurotoxicity.

We observed significant upregulation at all chlorpyrifos treatments and higher fipronil and imidacloprid exposures, as well as downregulation at the two highest abamectin concentrations of iodothyronine diiodinase 3b (*dio3b*). In fish, *dio3b* encodes an enzyme involved in thyroid hormone synthesis and has been shown to be particularly expressed in the developing central nervous system of zebrafish embryos (Alves et al., 2017; Baumann et al., 2016; Guo et al., 2014). Knockout of *dio3b* resulted in strong thyroid hormone-dependent growth restriction after 72 hpf (Guo et al., 2014), which may explain the severely impaired hatching rate in the high abamectin exposure treatments. Despite its neurotoxic properties, chlorpyrifos is considered an endocrine disruptor in both mammals and fish (Ubaid Ur Rahman et al., 2021). Chlorpyrifos has been described to alter thyroid hormone levels in mice (De Angelis et al., 2009) and marine fish (Holzer et al., 2017) and to have an inhibitory effect on testosterone synthesis in testicular and ovarian tissues of freshwater fish (Brandt et al., 2015). Similar to our observation, a recent study in zebrafish revealed molecular links between cholinergic signaling pathways and thyroid-damaging effects of chlorpyrifos (Qiao et al., 2021). Interestingly, mutation of thyroid hormone receptor alpha in zebrafish has been shown to result in abnormal cardiac structure and overall impaired cardiac function (Han et al., 2021). This may suggest that the altered expression of important genes related to heart development observed in our experiments may be associated with impaired thyroid pathways.

3.3. Challenges of biological functional profile comparison

We performed GSEA on the expression profiles for each treatment condition for biological process gene ontologies (BP GO) (Fig. 4) as well as KEGG (S.Fig. 12) and Reactome pathways (S.Fig. 13). This provides insights about affected biological functions and molecular pathways on a higher organizational level and facilitates biological data interpretability, compared to single gene comparison (Carbon et al., 2019; Subramanian et al., 2005).

From a selection of the most significantly enriched GO terms (Fig. 4) we see that, a) the number of affected biological processes increased with the exposure concentration and b) affected processes were often induced by both lower and higher exposure conditions. We would like to draw attention to the fact that in many cases an increasing number of enriched genes (increasing gene content) was observed in a given GO term set with increasing exposure concentration. This is also the case, for example, for amide and peptide biosynthetic processes or peptide metabolic processes. This suggests a concentration dependence of the number of enriched genes for a given gene set.

Although we identified DEGs in all low exposure concentration treatments for all test compounds (Fig. 1B & S.Fig. 7), we found no statistically significant (BH p.adj $\leq$0.05) enriched BP GO terms (Fig. 4) or Reactome pathways (S.Fig. 13) for those in carbaryl, fipronil, imidacloprid and methoxychlor. Similarly, no enriched KEGG pathways (S. Fig. 14) were detected after exposure to low concentrations of fipronil, methoxychlor or imidacloprid. This shows that the improved biological interpretability and dimension reduction of GSEA comes with the cost of sensitivity compared to the single gene level. On the other hand, GSEA can help identifying molecular functional similarities among transcriptomic profiles, which could be missed by single gene comparison, as different genes could still affect the same biological process in a similar or closely related manner (Subramanian et al., 2005). Therefore, to identify toxicological similarities between chemicals, comparison of GSEA results may be a more robust approach that takes into account conserved functionalities of adverse effects than comparison of individual genes.

Comparing the GSEA profiles of the tested substances, we found that chlorpyrifos, imidacloprid and methoxychlor in particular shared common GO terms. This was particularly striking when comparing the higher exposure concentrations. In the lower exposure conditions, the differences between the compounds were more pronounced, although not necessarily large. Therefore, to reliably distinguish between different MoAs, it is important to test low exposure concentrations, ideally in a region where early molecular events are just beginning. At higher exposure concentrations, the different profiles started to blur into each other. Thus, differentiation of molecular signatures is not possible in areas of systemic toxicity, where the breakdown of essential functions likely overrides the differentiable profiles. However, the observed similarity of the GSEA profiles of chlorpyrifos and imidacloprid is not surprising, as both chemicals target the cholinergic system, resulting in prolonged activation of the nAChR. Surprisingly, the two organophosphates tested (carbaryl and chlorpyrifos) did not show a high degree of functional similarity, although both compounds target the cholinergic system by inhibiting AChE. A major difference between the two organophosphates is that the inhibition of AChE by carbaryl is reversible, whereas that of chlorpyrifos is not. Imidacloprid, on the other hand, irreversibly activates nAChR (Mehlhorn et al., 1999; Sánchez-Bayo and Tennekes, 2020). Therefore, we hypothesize that the main differences in response profiles may be due to reversible and irreversible activation of the cholinergic system.

While in our study the investigation of lower exposure concentrations led to a stronger differentiability of functional gene expression responses, previous meta-analyses of toxicogenomic studies have shown that shorter exposure durations and thus the consideration of toxicokinetic parameters also provide an approach to distinguish different mechanisms of action (Schüttler et al., 2017). Thus, a long exposure duration could lead to incipient systemic effects, which could then override the specific gene expression changes. However, in our case, even at the high exposure concentrations, no systemic effects were evident at the physiological level. Moreover, our approach only considers the intersection of DEGs from low and high exposure concentrations as a specific signature, which excludes possible systemic effects at high exposure concentrations.

Our results show that there are shared as well as distinct responsive patterns among the most significantly enriched biological processes (Fig. 4). However, similar to the most significantly enriched GO terms from ORA shown in Fig. 3, we can only focus on a minor selection from the total dataset. Although GSEA and ORA help dramatically to reduce the dimensionality of the data, an in depth comparison becomes very tedious and cumbersome, especially for a larger number of datasets. To characterize and compare a large number of chemicals based on their molecular fingerprints would require an established method to quantify similarities among them. Most recently, a promising tool called *MegaGO* was published (Verschaffelt et al., 2021). Designed for the functional comparison of microbial communities, *MegaGO* measures semantic similarities for a list of GO terms between two datasets. We believe that such a tool, through its implementability in R, could also help in characterizing similarities between functional effects of chemicals, even with a large number of datasets. However, the applicability of MegaGO for this purpose needs to be explored and evaluated first. Despite the lower sensitivity compared to the gene level in detecting differences in transcriptome datasets, which is due to the dimension reduction, GSEA also have the advantages mentioned above. In the future, further research

will be needed to determine which method is best suited for functional characterization and classification of chemicals based on ecotoxicogenomic profiles. Recently, a promising systems biology approach based on a network model for predicting cardiotoxic effects from transcriptomic profiles in zebrafish larvae has been published (Li et al., 2020). We propose to use the data we have provided to further test and elaborate this model, as our observations suggest a potential cardiotoxic link for some of the MoAs evaluated.

It is often argued that the fish embryo models might be less sensitive as they could lack fully developed metabolic pathways compared to adults (Embry et al., 2010; Glaberman et al., 2017). However, we observed large numbers of insecticide affected metabolic and catabolic pathways (see GSEA result tables on Zenodo 5218919) in zebrafish embryos 96 hpf. This suggests that essential metabolism is present in the organism at that life stage. In contrast, an embryo model could be more sensitive to non-lethal developmental toxic effects, such as cardiac or neuronal development, which may be less severe in adult organisms. Overall, the sensitivity for sublethal endpoints in the embryo model can be enhanced for neurotoxins when screening for molecular parameters.

It is known that the response and sensitivity of molecular biomarkers can vary significantly between different life stages of the organism (Domingues et al., 2010, 2016; Schüttler et al., 2019; Zucchi et al., 2011). For a robust ecotoxicological characterization of chemicals, we, therefore, suggest to rely on a specific developmental stage or use consistent exposure conditions for cross substance ecotoxicogenomic profiling. For example, the here presented approach can be easily implemented as an extension of the standardized acute zebrafish embryo toxicity test OECD 236, which is an approved alternative to the acute adult fish test OECD 203 under REACH legislation for chemical registration. Perspectively, this allows for a more informative hazard assessment of the tested chemical based on ecotoxicogenomic profiles.

4. Conclusion

In our study, we identified biomarker candidates for a set of nerve- and muscle-targeting insecticides acting via five different MoAs in zebrafish embryos using transcriptomics. ORA and GSEA revealed shared as well as distinct affected biological processes by the tested insecticides. Abamectin appeared to primarily affect lipid metabolic processes while the nAChR inhibitor imidacloprid rather affected genes involved in immune system and inflammatory processes. From the total 222 core DEGs, 88 protein-coding transcripts with high expressions values (base mean count >500) were identified, which are related to three major processes: (1) cardiac muscle cell development and functioning (*tcap, desma, bag3, hspb1, hspb8, flnca, myoz3a, mybpc2b, actc2, tnnt2c*), (2) oxygen transport and hypoxic stress (*alas2, hbbe1.1, hbbe1.3, hbbe2, hbae3, igfbp1a hif1al*) and (3) neuronal development and plasticity (*npas4a, egr1, btg2, ier2a, vgf*). Further, we observed upregulation by chlorpyrifos and downregulation by abamectin of the thyroidal function related *dio3b*, which could be a link to endocrine activity in vertebrates. All of these genes are conserved in function across vertebrate species, opening the possibility of cross-species toxicity assessment. To our knowledge, this is the first report linking differential expression of important regulatory genes for heart muscle (*tcap*) and forebrain (*npas4a*) development in response to neurotoxic insecticide exposure in an aquatic vertebrate model. The here discussed gene sets represent early warning biomarker candidates for developmental toxicity affecting heart and brain of aquatic vertebrates. The substance-specific regulated genes can help to distinguish primary MoAs from each other. Our toxicogenomic profiles indicate that the nerve- and muscle-targeting insecticides analyzed in our study induced an impaired heart functioning, which may result in a reduced blood flow. We hypothesize that the observed regulation of markers of hypoxic stress is a consequence of reduced oxygen supply. Thus, our study contributes to previous proposals (Domingues et al., 2013; Sanches et al., 2018) to include sublethal parameters such as molecular biomarkers to promote more sensitive and informative fish embryo tests. We consider the here provided molecular insights crucial for improving the toxicological understanding of nerve- and muscle-targeting MoAs in non-target organisms. In accordance with the 3R principals, this will facilitate the development of sensitive and informative molecular based screening approaches, which has the potential to reduce the number of required animal test for chemical hazard assessment in the future.

Declaration of competing interest

The authors declare that they have no known competing financial interests or personal relationships that could have appeared to influence the work reported in this paper.

Acknowledgements

The Fraunhofer Internal Programs under Grant No. Attract 040-600300 supported and financed this work. Graphs and illustrations were generated with the help of the freeware tools R/R Studio and Inkscape. (www.inkscape.org). Graphical abstract illustration was generated using Biorender (www.biorender.com).

Appendix A. Supplementary data

Supplementary data to this article can be found online at https://doi.org/10.1016/j.chemosphere.2021.132746.

Supporting information available

The following files are available free of charge:

- Supplemental methods and figures (*Reinwald_2021_supplements.pdf)*
- Raw RNAseq data as well as processed and normalized gene count tables on ArrayExpress under the following accession numbers: E-MTAB-9852 (abamectin), E-MTAB-9855 (carbaryl), E-MTAB-9853 (chlorpyrifos), E-MTAB-9854 (fipronil), E-MTAB-9859 (imidacloprid), E-MTAB-9860 (methoxychlor)

- MultiQC summary reports of RNAseq quality statistics as well as DGEA, ORA and GSEA result tables are publicly available on ZENODO under accession 5218919(Reinwald et al., 2021a).
- R Session Info files, providing a list of applied R packages and respective version numbers (*R_SessionInfo_DESeq2.txt; R_SessionInfo_clusterProfiler.txt*)
- Data analysis scripts available on the Github repository: https://github.com/hreinwal/zfeNeurotox

Author contributions statement

Hannes Reinwald performed and designed the experiments, analyzed the data and wrote the manuscript. Julia Alvincz contributed to experimental work. Gabriela Salinas supervised RNA sequencing. Christoph Schäfers and Henner Hollert contributed to study design. Sebastian Eilebrecht designed and supervised the study and contributed to manuscript writing.

References

Agani, F.H., Pichiule, P., Chavez, J.C., LaManna, J.C., 2000. The role of mitochondria in the regulation of hypoxia-inducible factor 1 expression during hypoxia. J. Biol. Chem. 275, 35863–35867. https://doi.org/10.1074/jbc.M005643200.

Alder, J., Thakker-Varia, S., Bangasser, D.A., Kuroiwa, M., Plummer, M.R., Shors, T.J., Black, I.B., 2003. Brain-derived neurotrophic factor-induced gene rxpression reveals novel actions of VGF in hippocampal synaptic plasticity. J. Neurosci. 23, 10800–10808. https://doi.org/10.1523/JNEUROSCI.23-34-10800.2003.

Alves, R.N., Cardoso, J.C.R., Harboe, T., Martins, R.S.T., Manchado, M., Norberg, B., Power, D.M., 2017. Duplication of Dio3 genes in teleost fish and their divergent

expression in skin during flatfish metamorphosis. Gen. Comp. Endocrinol. 246, 279–293. https://doi.org/10.1016/j.ygcen.2017.01.002.
Amora, M., Giordani, S., 2018. The utility of zebrafish as a model for screening developmental neurotoxicity. Front. Neurosci. 12 https://doi.org/10.3389/fnins.2018.00976.
Ankley, G.T., Bennett, R.S., Erickson, R.J., Hoff, D.J., Hornung, M.W., Johnson, R.D., Mount, D.R., Nichols, J.W., Russom, C.L., Schmieder, P.K., Serrrano, J.A., Tietge, J. E., Villeneuve, D.L., 2010. Adverse outcome pathways: a conceptual framework to support ecotoxicology research and risk assessment. Environ. Toxicol. Chem. https://doi.org/10.1002/etc.34.
Arimura, T., Ishikawa, T., Nunoda, S., Kawai, S., Kimura, A., 2011. Dilated cardiomyopathy-associated BAG3 mutations impair Z-disc assembly and enhance sensitivity to apoptosis in cardiomyocytes. Hum. Mutat. 32, 1481–1491. https://doi.org/10.1002/humu.21603.
Baker, M., 2016. Is there a reproducability crisis? Nature 533, 452–454. https://doi.org/10.1038/533452a.
Baker, M.R., Wong, R.Y., 2021. Npas4a expression in the teleost forebrain is associated with stress coping style differences in fear learning. Sci. Rep. 11, 1–12. https://doi.org/10.1038/s41598-021-91495-7.
Baumann, L., Ros, A., Rehberger, K., Neuhauss, S.C.F., Segner, H., 2016. Thyroid disruption in zebrafish (*Danio rerio*) larvae: different molecular response patterns lead to impaired eye development and visual functions. Aquat. Toxicol. 172, 44–55. https://doi.org/10.1016/j.aquatox.2015.12.015.
Betz, H., 1991. Glycine receptors: heterogeneous and widespread in the mammalian brain. Trends Neurosci. 14, 458–461. https://doi.org/10.1016/0166-2236(91)90045-v.
Bitzer, M., Schaeffel, F., 2002. Defocus-induced changes in ZENK expression in the chicken retina. Invest. Ophthalmol. Vis. Sci. 43, 246–252.
Bloodgood, B.L., Sharma, N., Browne, H.A., Trepman, A.Z., Greenberg, M.E., 2013. The activity-dependent transcription factor NPAS4 regulates domain-specific inhibition. Nature 503, 121–125. https://doi.org/10.1038/nature12743.
Bonifacio, A.F., Ballesteros, M.L., Bonansea, R.I., Filippi, I., Amé, M.V., Hued, A.C., 2017. Environmental relevant concentrations of a chlorpyrifos commercial formulation affect two neotropical fish species, Cheirodon interruptus and Cnesterodon decemmaculatus. Chemosphere 188, 486–493.
Boyer, B., Ernest, S., Rosa, F., 2013. Egr-1 induction provides a genetic response to food aversion in zebrafish. Front. Behav. Neurosci. 7 https://doi.org/10.3389/fnbeh.2013.00051.
Bozdagi, O., Rich, E., Tronel, S., Sadahiro, M., Patterson, K., Shapiro, M.L., Alberini, C. M., Huntley, G.W., Salton, S.R.J., 2008. The neurotrophin-inducible gene Vgf regulates hippocampal function and behavior through a brain-derived neurotrophic factor-dependent mechanism. J. Neurosci. 28, 9857–9869. https://doi.org/10.1523/JNEUROSCI.3145-08.2008.
Brandt, C., Burnett, D.C., Arcinas, L., Palace, V., Gary Anderson, W., 2015. Effects of chlorpyrifos on in vitro sex steroid production and thyroid follicular development in adult and larval Lake Sturgeon, Acipenser fulvescens. Chemosphere 132, 179–187. https://doi.org/10.1016/j.chemosphere.2015.03.031.
Brazma, A., Parkinson, H., Sarkans, U., Shojatalab, M., Vilo, J., Abeygunawardena, N., Holloway, E., Kapushesky, M., Kemmeren, P., Lara, G.G., Oezcimen, A., Rocca-Serra, P., Sansone, S.A., 2003. ArrayExpress - a public repository for microarray gene expression data at the EBI. Nucleic Acids Res. 31, 68–71. https://doi.org/10.1093/nar/gkg091.
Brockmeier, E.K., Hodges, G., Hutchinson, T.H., Butler, E., Hecker, M., Tollefsen, K.E., Garcia-Reyero, N., Kille, P., Becker, D., Chipman, K., Colbourne, J., Collette, T.W., Cossins, A., Cronin, M., Graystock, P., Gutsell, S., Knapen, D., Katsiadaki, I., Lange, A., Marshall, S., Owen, S.F., Perkins, E.J., Plaistow, S., Schroeder, A., Taylor, D., Viant, M., Ankley, G., Falciani, F., 2017. The role of omics in the application of adverse outcome pathways for chemical risk assessment. Toxicol. Sci. https://doi.org/10.1093/toxsci/kfx097.
Brown, D.D., Christine, K.S., Showell, C., Conlon, F.L., 2007. Small heat shock protein Hsp27 is required for proper heart tube formation. Genesis 45, 667–678. https://doi.org/10.1002/dvg.20340.
Brown, D.R., Clark, B.W., Garner, L.V.T., Di Giulio, R.T., 2015. Zebrafish cardiotoxicity: the effects of CYP1A inhibition and AHR2 knockdown following exposure to weak aryl hydrocarbon receptor agonists. Environ. Sci. Pollut. Res. 22, 8329–8338. https://doi.org/10.1007/s11356-014-3969-2.
Brownlie, A., Hersey, C., Oates, A.C., Paw, B.H., Falick, A.M., Witkowska, H.E., Flint, J., Higgs, D., Jessen, J., Bahary, N., Zhu, H., Lin, S., Zon, L., 2003. Characterization of embryonic globin genes of the zebrafish. Dev. Biol. 255, 48–61. https://doi.org/10.1016/S0012-1606(02)00041-6.
Busquet, F., Strecker, R., Rawlings, J.M., Belanger, S.E., Braunbeck, T., Carr, G.J., Cenijn, P., Fochtman, P., Gourmelon, A., Hübler, N., Kleensang, A., Knöbel, M., Kussatz, C., Legler, J., Lillicrap, A., Martínez-Jerónimo, F., Polleichtner, C., Rzodeczko, H., Salinas, E., Schneider, K.E., Scholz, S., van den Brandhof, E.J., van der Ven, L.T.M., Walter-Rohde, S., Weigt, S., Witters, H., Halder, M., 2014. OECD validation study to assess intra- and inter-laboratory reproducibility of the zebrafish embryo toxicity test for acute aquatic toxicity testing. Regul. Toxicol. Pharmacol. https://doi.org/10.1016/j.yrtph.2014.05.018.
Calogero, A., Lombari, V., De Gregorio, G., Porcellini, A., Ucci, S., Arcella, A., Caruso, R., Gagliardi, F.M., Gulino, A., Lanzetta, G., Frati, L., Mercola, D., Ragona, G., 2004. Inhibition of cell growth by EGR-1 in human primary cultures from malignant glioma. Cancer Cell Int. 4, 1. https://doi.org/10.1186/1475-2867-4-1.
Cao, Y., Tian, R., Jiao, Y., Zheng, Z., Wang, Q., Deng, Y., Du, X., 2021. Novel nicotinic acetylcholine receptor involved in immune regulation in pearl oyster (Pinctada fucata martensii). Comp. Biochem. Physiol. B Biochem. Mol. Biol. 252, 110512. https://doi.org/10.1016/j.cbpb.2020.110512.
Carbon, S., Douglass, E., Dunn, N., Good, B., Harris, N.L., Lewis, S.E., Mungall, C.J., Basu, S., Chisholm, R.L., Dodson, R.J., Hartline, E., Fey, P., Thomas, P.D., Albou, L. P., Ebert, D., Kesling, M.J., Mi, H., Muruganujan, A., Huang, X., Poudel, S., Mushayahama, T., Hu, J.C., LaBonte, S.A., Siegele, D.A., Antonazzo, G., Attrill, H., Brown, N.H., Fexova, S., Garapati, P., Jones, T.E.M., Marygold, S.J., Millburn, G.H., Rey, A.J., Trovisco, V., Dos Santos, G., Emmert, D.B., Falls, K., Zhou, P., Goodman, J. L., Strelets, V.B., Thurmond, J., Courtot, M., Osumi, D.S., Parkinson, H., Roncaglia, P., Acencio, M.L., Kuiper, M., Lreid, A., Logie, C., Lovering, R.C., Huntley, R.P., Denny, P., Campbell, N.H., Kramarz, B., Acquaah, V., Ahmad, S.H., Chen, H., Rawson, J.H., Chibucos, M.C., Giglio, M., Nadendla, S., Tauber, R., Duesbury, M.J., Del, N.T., Meldal, B.H.M., Perfetto, L., Porras, P., Orchard, S., Shrivastava, A., Xie, Z., Chang, H.Y., Finn, R.D., Mitchell, A.L., Rawlings, N.D., Richardson, L., Sangradlror-Vegas, A., Blake, J.A., Christie, K.R., Dolan, M.E., Drabkin, H.J., Hill, D.P., Ni, L., Sitnikov, D., Harris, M.A., Oliver, S.G., Rutherford, K., Wood, V., Hayles, J., Bahler, J., Lock, A., Bolton, E.R., De Pons, J., Dwinell, M., Hayman, G.T., Laulederkind, S.J.F., Shimoyama, M., Tutaj, M., Wang, S. J., D'Eustachio, P., Matthews, L., Balhoff, J.P., Aleksander, S.A., Binkley, G., Dunn, B.L., Cherry, J.M., Engel, S.R., Gondwe, F., Karra, K., MacPherson, K.A., Miyasato, S.R., Nash, R.S., Ng, P.C., Sheppard, T.K., Shrivatsav Vp, A., Simison, M., Skrzypek, M.S., Weng, S., Wong, E.D., Feuermann, M., Gaudet, P., Bakker, E., Berardini, T.Z., Reiser, L., Subramaniam, S., Huala, E., Arighi, C., Auchincloss, A., Axelsen, K., Argoud, G.P., Bateman, A., Bely, B., Blatter, M.C., Boutet, E., Breuza, L., Bridge, A., Britto, R., Bye-A-Jee, H., Casals-Casas, C., Coudert, E., Estreicher, A., Famiglietti, L., Garmiri, P., Georghiou, G., Gos, A., Gruaz-Gumowski, N., Hatton-Ellis, E., Hinz, U., Hulo, C., Ignatchenko, A., Jungo, F., Keller, G., Laiho, K., Lemercier, P., Lieberherr, D., Lussi, Y., Mac-Dougall, A., Magrane, M., Martin, M.J., Masson, P., Natale, D.A., Hyka, N.N., Pedruzzi, I., Pichler, K., Poux, S., Rivoire, C., Rodriguez-Lopez, M., Sawford, T., Speretta, E., Shypitsyna, A., Stutz, A., Sundaram, S., Tognolli, M., Tyagi, N., Warner, K., Zaru, R., Wu, C., Chan, J., Cho, J., Gao, S., Grove, C., Harrison, M.C., Howe, K., Lee, R., Mendel, J., Muller, H.M., Raciti, D., Van Auken, K., Berriman, M., Stein, L., Sternberg, P.W., Howe, D., Toro, S., Westerfield, M., The Gene Ontology Consortium, 2019. The gene ontology resource: 20 years and still GOing strong. Nucleic Acids Res. 47, D330–D338. https://doi.org/10.1093/nar/gky1055.
Chow, W.S., Chan, W.K.L., Chan, K.M., 2013. Toxicity assessment and vitellogenin expression in zebrafish (Danio rerio) embryos and larvae acutely exposed to bisphenol A, endosulfan, heptachlor, methoxychlor and tetrabromobisphenol A. J. Appl. Toxicol. 33, 670–678. https://doi.org/10.1002/jat.2723.
Close, R., Toro, S., Martial, J.A., Muller, M., 2002. Expression of the zinc finger Egr1 gene during zebrafish embryonic development. Mech. Dev. 118, 269–272. https://doi.org/10.1016/S0925-4773(02)00283-6.
Correia, D., Almeida, A.R., Santos, J., Machado, A.L., Koba Ucun, O., Žlábek, V., Oliveira, M., Domingues, I., 2019. Behavioral effects in adult zebrafish after developmental exposure to carbaryl. Chemosphere 235, 1022–1029. https://doi.org/10.1016/j.chemosphere.2019.07.029.
Cote, I., Andersen, M.E., Ankley, G.T., Barone, S., Birnbaum, L.S., Boekelheide, K., Bois, F.Y., Burgoon, L.D., Chiu, W.A., Crawford-Brown, D., Crofton, K.M., Devito, M., Devlin, R.B., Edwards, S.W., Guyton, K.Z., Hattis, D., Judson, R.S., Knight, D., Krewski, D., Lambert, J., Maull, E.A., Mendrick, D., Paoli, G.M., Patel, C.J., Perkins, E.J., Poje, G., Portier, C.J., Rusyn, I., Schulte, P.A., Simeonov, A., Smith, M. T., Thayer, K.A., Thomas, R.S., Thomas, R., Tice, R.R., Vandenberg, J.J., Villeneuve, D.L., Wesselkamper, S., Whelan, M., Whittaker, C., White, R., Xia, M., Yauk, C., Zeise, L., Zhao, J., Dewoskin, R.S., 2016. The next generation of risk assessment multi-year study–highlights of findings, applications to risk assessment, and future directions. Environ. Health Perspect. https://doi.org/10.1289/EHP233.
Coutellier, L., Beraki, S., Ardestani, P.M., Saw, N.L., Shamloo, M., 2012. Npas4: a neuronal transcription factor with a key role in social and cognitive functions relevant to developmental disorders. PLoS One 7. https://doi.org/10.1371/journal.pone.0046604.
Cox, T.C., Sadlon, T.J., Schwarz, Q.P., Matthews, C.S., Wise, P.D., Cox, L.L., Bottomley, S. S., May, B.K., 2004. The major splice variant of human 5-aminolevulinate synthase-2 contributes significantly to erythroid heme biosynthesis. Int. J. Biochem. Cell Biol. 36, 281–295. https://doi.org/10.1016/S1357-2725(03)00246-2.
Davidson, S.M., Morange, M., 2000. Hsp25 and the p38 MAPK pathway are involved in differentiation of cardiomyocytes. Dev. Biol. 218, 146–160. https://doi.org/10.1006/dbio.1999.9596.
De Angelis, S., Tassinari, R., Maranghi, F., Eusepi, A., Di Virgilio, A., Chiarotti, F., Ricceri, L., Venerosi Pesciolini, A., Gilardi, E., Moracci, G., Calamandrei, G., Olivieri, A., Mantovani, A., 2009. Developmental exposure to chlorpyrifos induces alterations in thyroid and thyroid hormone levels without other toxicity signs in CD-1 mice. Toxicol. Sci. 108, 311–319. https://doi.org/10.1093/toxsci/kfp017.
Deiú, A.S., Miglioranza, K.S., Ondarza, P.M., Fernando, R., 2021. Exposure to environmental concentrations of fipronil induces biochemical changes on a neotropical freshwater fish. Environ. Sci. Pollut. Control Ser. 1–13.
Dobin, A., Davis, C.A., Schlesinger, F., Drenkow, J., Zaleski, C., Jha, S., Batut, P., Chaisson, M., Gingeras, T.R., 2013. STAR: ultrafast universal RNA-seq aligner. Bioinformatics 29, 15–21. https://doi.org/10.1093/bioinformatics/bts635.
Domingues, I., Oliveira, R., Lourenço, J., Grisolia, C.K., Mendo, S., Soares, A.M.V.M., 2010. Biomarkers as a tool to assess effects of chromium (VI): comparison of responses in zebrafish early life stages and adults. Comp. Biochem. Physiol. C Toxicol. Pharmacol. 152, 338–345. https://doi.org/10.1016/j.cbpc.2010.05.010.
Domingues, I., Oliveira, R., Musso, C., Cardoso, M., Soares, A.M.V.M., Loureiro, S., 2013. Prochloraz effects on biomarkers activity in zebrafish early life stages and adults. Environ. Toxicol. 28, 155–163. https://doi.org/10.1002/tox.20710.
Domingues, I., Oliveira, R., Soares, A.M.V.M., Amorim, M.J.B., 2016. Effects of ivermectin on *Danio rerio*: a multiple endpoint approach: behaviour, weight and

subcellular markers. Ecotoxicology 25, 491–499. https://doi.org/10.1007/s10646-015-1607-5.

Domínguez, F., Cuenca, S., Bilińska, Z., Toro, Rocío, Villard, E., Barriales-Villa, R., Ochoa, J.P., Asselbergs, F., Sammani, A., Franaszczyk, M., Akhtar, M., Coronado-Albi, M.J., Rangel-Sousa, D., Rodriguez-Palomares, J.F., Jiménez-Jáimez, J., Garcia-Pinilla, Manuel, José, Ripoll-Vera, T., Mogollón-Jiménez, M.V., Fontalba-Romero, A., Garcia-Medina, D., Palomino-Doza, J., de Gonzalo-Calvo, D., Cicerchia, M., Salazar-Mendiguchia, J., Salas, C., Pankuweit, S., Hey, T.M., Mogensen, J., Barton, P.J., Charron, P., Elliott, P., Garcia-Pavia, P., Eiskjær, H., Barriales, R., Fernández Fernández, X., Cicerchia, M., Monserrat, L., Ochoa, J.P., Salazar-Mendiguchia, J., Mogollón, M.V., Ripoll, T., Charron, P., Richard, P., Villard, E., Palomino Doza, J., Fontalba, A., Alonso-Pulpón, L., Cobo-Marcos, M., Domínguez, F., Garcia-Pavia, P., Gómez-Bueno, M., González-López, E., Hernández-Hernández, A., Hernández-Pérez, F.J., López-Sainz, Á., Restrepo-Córdoba, A., Segovia-Cubero, J., Toro, Rocio, de Gonzalo-Calvo, D., Rosa Longobardo, F., Limeres, J., Rodriguez-Palomares, J.F., Garcia-Pinilla, Manuel, Jose, López-Garrido, M.A., Jiménez-Jaimez, J., Garcia-Medina, D., Rangel Sousa, D., Peña, M.L., Mogensen, J., Morris-Hey, T., Barton, P.J., Cook, S.A., Midwinter, W., Roberts, A.M., Ware, J.S., Walsh, R., Akhtar, M., Elliott, P.M., Rocha-Lopes, L., Savvatis, K., Syrris, P., Michalak, E., Ploski, R., Sobieszczanska-Malek, M., Bilińska, Z., Pankuweit, S., Asselbergs, F., Baas, A., Dooijes, D., Sammani, A., 2018. Dilated cardiomyopathy due to BLC2-associated athanogene 3 (BAG3) mutations. J. Am. Coll. Cardiol. 72, 2471–2481. https://doi.org/10.1016/j.jacc.2018.08.2181.

Dörner, G., Plagemann, A., 2002. DDT in human milk and mental capacities in children at school age: an additional view on PISA 2000. Neuroendocrinol. Lett. 23, 427–431.

Dubińska-Magiera, M., Niedbalska-Tarnowska, J., Migocka-Patrzałek, M., Posyniak, E., Daczewska, M., 2020. Characterization of Hspb8 in zebrafish. Cells 9. https://doi.org/10.3390/cells9061562.

Durinck, S., Spellman, P.T., Birney, E., Huber, W., 2009. Mapping identifiers for the integration of genomic datasets with the R/Bioconductor package biomaRt. Nat. Protoc. 4, 1184–1191. https://doi.org/10.1038/nprot.2009.97.

ECHA, E.C.A., 2018. REACH 2018 Registration Statistics https://doi.org/https://echa.europa.eu/documents/10162/750652/reach_2018_deadline_statistics_en.pdf/ecfe225f-caf0-5bad-7c7f-ce57d2c8938f.

Ellison, C.M., Madden, J.C., Cronin, M.T.D., Enoch, S.J., 2015. Investigation of the Verhaar scheme for predicting acute aquatic toxicity: improving predictions obtained from Toxtree ver. 2.6. Chemosphere 139, 146–154. https://doi.org/10.1016/j.chemosphere.2015.06.009.

Embry, M.R., Belanger, S.E., Braunbeck, T.A., Galay-Burgos, M., Halder, M., Hinton, D. E., Léonard, M.A., Lillicrap, A., Norberg-King, T., Whale, G., 2010. The fish embryo toxicity test as an animal alternative method in hazard and risk assessment and scientific research. Aquat. Toxicol. 97, 79–87. https://doi.org/10.1016/j.aquatox.2009.12.008.

ENSEMBL, 2020. Danio rerio Genome Assembly GRCz11. ENSEMBL Release 100 https://doi.org/http://ftp.ensembl.org/pub/release-100/fasta/danio_rerio/dna/Danio_rerio.GRCz11.dna.toplevel.fa.gz.

Ewels, P., Magnusson, M., Lundin, S., Käller, M., 2016. MultiQC: summarize analysis results for multiple tools and samples in a single report. Bioinformatics 32, 3047–3048. https://doi.org/10.1093/bioinformatics/btw354.

Fabregat, A., Jupe, S., Matthews, L., Sidiropoulos, K., Gillespie, M., Garapati, P., Haw, R., Jassal, B., Korninger, F., May, B., Milacic, M., Roca, C.D., Rothfels, K., Sevilla, C., Shamovsky, V., Shorser, S., Varusai, T., Viteri, G., Weiser, J., Wu, G., Stein, L., Hermjakob, H., D'Eustachio, P., 2018. The reactome pathway knowledgebase. Nucleic Acids Res. 46, D649–D655. https://doi.org/10.1093/nar/gkx1132.

Feitsma, H., Cuppen, E., 2008. Zebrafish as a cancer model. Mol. Cancer Res. 6, 685–694. https://doi.org/10.1158/1541-7786.MCR-07-2167.

Fischer, A.J., Scott, M.A., Tuten, W., 2009. Mitogen-activated protein kinase-signaling stimulates Müller glia to proliferate in acutely damaged chicken retina. Glia 57, 166–181. https://doi.org/10.1002/glia.20743.

Flavell, S.W., Greenberg, M.E., 2008. Expression and plasticity of the nervous system. Annu. Rev. Neurosci. 563–590. https://doi.org/10.1146/annurev.neuro.31.060407.125631.Signaling.

Frame, J.M., Kubaczka, C., Long, T.L., Esain, V., Soto, R.A., Hachimi, M., Jing, R., Shwartz, A., Goessling, W., Daley, G.Q., North, T.E., 2020. Metabolic regulation of inflammasome activity controls embryonic hematopoietic stem and progenitor cell production. Dev. Cell 55, 133–149. https://doi.org/10.1016/j.devcel.2020.07.015 e6.

Frankel, T.E., Bohannon, M.E., Frankel, J.S., 2020. Assessing the impacts of methoxychlor exposure on the viability, reproduction, and locomotor behavior of the Seminole ramshorn snail (Planorbella duryi). Environ. Toxicol. Chem. 39 (1), 220–228.

Fu, C., Hickey, M., Morrison, M., McCarter, R., Han, E.S., 2006. Tissue specific and non-specific changes in gene expression by aging and by early stage CR. Mech. Ageing Dev. 127, 905–916. https://doi.org/10.1016/j.mad.2006.09.006.

Gao, L.R., Li, S., Zhang, J., Liang, C., Chen, E.N., Zhang, S.Y., Chuai, M., Bao, Y.P., Wang, G., Yang, X., 2016. Excess imidacloprid exposure causes the heart tube malformation of chick embryos. J. Agric. Food Chem. 64, 9078–9088. https://doi.org/10.1021/acs.jafc.6b03381.

Gardner, L.C., Smith, S.J., Cox, T.M., 1991. Biosynthesis of δ-aminolevulinic acid and the regulation of heme formation by immature erythroid cells in man. J. Biol. Chem. 266, 22010–22018. https://doi.org/10.1016/s0021-9258(18)54738-4.

Giussani, D.A., 2011. The vulnerable developing brain. Proc. Natl. Acad. Sci. U.S.A. 108, 2641–2642. https://doi.org/10.1073/pnas.1019726108.

Glaberman, S., Padilla, S., Barron, M.G., 2017. Evaluating the zebrafish embryo toxicity test for pesticide hazard screening. Environ. Toxicol. Chem. 36, 1221–1226. https://doi.org/10.1002/etc.3641.

Gonçalves, Í.F.S., Souza, T.M., Vieira, L.R., Marchi, F.C., Nascimento, A.P., Farias, D.F., 2020. Toxicity testing of pesticides in zebrafish—a systematic review on chemicals and associated toxicological endpoints. Environ. Sci. Pollut. Res. 27, 10185–10204. https://doi.org/10.1007/s11356-020-07902-5.

Grüning, B., Dale, R., Sjödin, A., Chapman, B.A., Rowe, J., Tomkins-Tinch, C.H., Valieris, R., Köster, J., 2018. Bioconda: sustainable and comprehensive software distribution for the life sciences. Nat. Methods 15, 475–476. https://doi.org/10.1038/s41592-018-0046-7.

Guo, C., Chen, X., Song, H., Maynard, M.A., Zhou, Y., Lobanov, A.V., Gladyshev, V.N., Ganis, J.J., Wiley, D., Jugo, R.H., Lee, N.Y., Castroneves, L.A., Zon, L.I., Scanlan, T. S., Feldman, H.A., Huang, S.A., 2014. Intrinsic expression of a multiexon type 3 deiodinase gene controls zebrafish embryo size. Endocrinology 155, 4069–4080. https://doi.org/10.1210/en.2013-2029.

Han, C.R., Wang, H., Hoffmann, V., Zerfas, P., Kruhlak, M., Cheng, S.-Y., 2021. Thyroid hormone receptor α mutations cause heart defects in zebrafish. Thyroid 31, 315–326. https://doi.org/10.1089/thy.2020.0332.

Hason, M., Bartůněk, P., 2019. Zebrafish models of cancer-new insights on modeling human cancer in a non-mammalian vertebrate. Genes 10, 1–30. https://doi.org/10.3390/genes10110935.

Hayashi, T., Arimura, T., Itoh-Satoh, M., Ueda, K., Hohda, S., Inagaki, N., Takahashi, M., Hori, H., Yasunami, M., Nishi, H., Koga, Y., Nakamura, H., Matsuzaki, M., Choi, B.Y., Bae, S.W., You, C.W., Han, K.H., Park, J.E., Knöll, R., Hoshijima, M., Chien, K.R., Kimura, A., 2004. Tcap gene mutations in hypertrophic cardiomyopathy and dilated cardiomyopathy. J. Am. Coll. Cardiol. 44, 2192–2201. https://doi.org/10.1016/j.jacc.2004.08.058.

Helfer, G., Stevenson, T.J., 2020. Pleiotropic effects of proopiomelanocortin and VGF nerve growth factor inducible neuropeptides for the long-term regulation of energy balance. Mol. Cell. Endocrinol. 514, 110876. https://doi.org/10.1016/j.mce.2020.110876.

Hogstrand, C., Haux, C., 1991. Binding and detoxification of heavy metals in lower vertebrates with reference to metallothionein. Comp. Biochem. Physiol. C Comp. Pharmacol. 100, 137–141. https://doi.org/10.1016/0742-8413(91)90140-O.

Holzer, G., Besson, M., Lambert, A., François, L., Barth, P., Gillet, B., Hughes, S., Piganeau, G., Leulier, F., Viriot, L., Lecchini, D., Laudet, V., 2017. Fish larval recruitment to reefs is a thyroid hormone-mediated metamorphosis sensitive to the pesticide chlorpyrifos. Elife 6, 1–22. https://doi.org/10.7554/eLife.27595.

Hong, S.K., Dawid, I.B., 2009. FGF-dependent left-right asymmetry patterning in zebrafish is mediated by Ier2 and Fibp1. Proc. Natl. Acad. Sci. U.S.A. 106, 2230–2235. https://doi.org/10.1073/pnas.0812880106.

Hu, C.-Y., Yang, C.-H., Chen, W.-Y., Huang, C.-J., Huang, H.-Y., Chen, M.-S., Tsai, H.-J., 2006. Egr1 gene knockdown affects embryonic ocular development in zebrafish. Mol. Vis. 12, 1250–1258. https://doi.org/10.1167/iovs.03-1046.

Huang, W., Zhang, R., Xu, X., 2009. Myofibrillogenesis in the developing zebrafish heart: a functional study of tnnt2. Dev. Biol. 331, 237–249. https://doi.org/10.1016/j.ydbio.2009.04.039.

Ignatiadis, N., Klaus, B., Zaugg, J.B., Huber, W., 2016. Data-driven hypothesis weighting increases detection power in genome-scale multiple testing. Nat. Methods 13, 577–580. https://doi.org/10.1038/nmeth.3885.

Iwaniuk, A.N., Koperski, D.T., Cheng, K.M., Elliott, J.E., Smith, L.K., Wilson, L.K., Wylie, D.R.W., 2006. The effects of environmental exposure to DDT on the brain of a songbird: changes in structures associated with mating and song. Behav. Brain Res. 173, 1–10. https://doi.org/10.1016/j.bbr.2006.05.026.

Jacobson, S.M., Birkholz, D.A., McNamara, M.L., Bharate, S.B., George, K.M., 2010. Subacute developmental exposure of zebrafish to the organophosphate pesticide metabolite, chlorpyrifos-oxon, results in defects in Rohon-Beard sensory neuron development. Aquat. Toxicol. 100, 101–111. https://doi.org/10.1016/j.aquatox.2010.07.015.

Jin, Y., Liu, Z., Peng, T., Fu, Z., 2015. The toxicity of chlorpyrifos on the early life stage of zebrafish: asurvey on the endpoints at development, locomotor behavior, oxidative stress and immunotoxicity. Fish Shellfish Immunol. 43, 405–414. https://doi.org/10.1016/j.fsi.2015.01.010.

Kais, B., Ottermanns, R., Scheller, F., Braunbeck, T., 2018. Modification and quantification of in vivo EROD live-imaging with zebrafish (*Danio rerio*) embryos to detect both induction and inhibition of CYP1A. Sci. Total Environ. 615, 330–347. https://doi.org/10.1016/j.scitotenv.2017.09.257.

Kamaid, A., Giráldez, F., 2008. Btg1 and Btg2 gene expression during early chick development. Dev. Dynam. 237, 2158–2169. https://doi.org/10.1002/dvdy.21616.

Kamei, H., Lu, L., Jiao, S., Li, Y., Gyrup, C., Laursen, L.S., Oxvig, C., Zhou, J., Duan, C., 2008. Duplication and diversification of the hypoxia-inducible IGFBP-1 gene in Zebrafish. PLoS One 3. https://doi.org/10.1371/journal.pone.0003091.

Kanehisa, M., Araki, M., Goto, S., Hattori, M., Hirakawa, M., Itoh, M., Katayama, T., Kawashima, S., Okuda, S., Tokimatsu, T., Yamanishi, Y., 2008. KEGG for linking genomes to life and the environment. Nucleic Acids Res. 36, 480–484. https://doi.org/10.1093/nar/gkm882.

Kayman Kürekçi, G., Kural Mangit, E., Koyunlar, C., Unsal, S., Saglam, B., Ergin, B., Gizer, M., Uyanik, I., Boustanabadimaralan Düz, N., Korkusuz, P., Talim, B., Purali, N., Hughes, S.M., Dincer, P.R., 2021. Knockout of zebrafish desmin genes does not cause skeletal muscle degeneration but alters calcium flux. Sci. Rep. 11, 1–15. https://doi.org/10.1038/s41598-021-86974-w.

Khalil, S.R., Mohammed, W.A., Zaglool, A.W., Elhady, W.M., Farag, M.R., El sayed, S.A. M., 2019. Inflammatory and oxidative injury is induced in cardiac and pulmonary tissue following fipronil exposure in Japanese quail: mRNA expression of the genes encoding interleukin 6, nuclear factor kappa B, and tumor necrosis factor-alpha. Environ. Pollut. 251, 564–572. https://doi.org/10.1016/j.envpol.2019.05.012.

Kim, S., Park, D., Kim, Jinhu, Lee, D., Kim, D., Kim, H., Hong, S., Jeon, J., Kim, Jaehoon, Cheong, E., Um, J.W., Ko, J., 2020. The Activity-dependent Transcription Factor

Npas4 Regulates IQSEC3 Expression in Somatostatin Interneurons to Mediate Anxiety-like Behavior. https://doi.org/10.1101/659805 bioRxiv.
Klarić, T., Lardelli, M., Key, B., Koblar, S., Lewis, M., 2014. Activity-dependent expression of neuronal PAS domain-containing protein 4 (npas4a) in the developing zebrafish brain. Front. Neuroanat. 8, 1–13. https://doi.org/10.3389/fnana.2014.00148.
Klüver, N., König, M., Ortmann, J., Massei, R., Paschke, A., Kühne, R., Scholz, S., 2015. Fish embryo toxicity test: identification of compounds with weak toxicity and analysis of behavioral effects to improve prediction of acute toxicity for neurotoxic compounds. Environ. Sci. Technol. 49, 7002–7011. https://doi.org/10.1021/acs.est.5b01910.
Knöll, R., Hoshijima, M., Hoffman, H.M., Person, V., Lorenzen-Schmidt, I., Bang, M.L., Hayashi, T., Shiga, N., Yasukawa, H., Schaper, W., McKenna, W., Yokoyama, M., Schork, N.J., Omens, J.H., McCulloch, A.D., Kimura, A., Gregorio, C.C., Poller, W., Schaper, J., Schultheiss, H.P., Chien, K.R., 2002. The cardiac mechanical stretch sensor machinery involves a Z disc complex that is defective in a subset of human dilated cardiomyopathy. Cell 111, 943–955. https://doi.org/10.1016/S0092-8674(02)01226-6.
Krewski, D., Acosta, D., Andersen, M., Anderson, H., Bailar, J.C., Boekelheide, K., Brent, R., Charnley, G., Cheung, V.G., Green, S., Kelsey, K.T., Kerkvliet, N.I., Li, A.A., McCray, L., Meyer, O., Patterson, R.D., Pennie, W., Scala, R.A., Solomon, G.M., Stephens, M., Yager, J., Zeise, L., Staff of Committee on Toxicity Test, 2010. Toxicity testing in the 21st century: a vision and a strategy. J. Toxicol. Environ. Health Part B 13, 51–138. https://doi.org/10.1080/10937404.2010.483176.
Lewis, R.S., Noor, S.M., Fraser, F.W., Sertori, R., Liongue, C., Ward, A.C., 2014. Regulation of embryonic hematopoiesis by a cytokine-inducible SH2 domain homolog in zebrafish. J. Immunol. 192, 5739–5748. https://doi.org/10.4049/jimmunol.1301376.
Li, R., Zupanic, A., Talikka, M., Belcastro, V., Madan, S., Dörpinghaus, J., Berg, C. vom, Szostak, J., Martin, F., Peitsch, M.C., Hoeng, J., 2020. Systems toxicology approach for testing chemical cardiotoxicity in larval zebrafish. Chem. Res. Toxicol. 33, 2550–2564. https://doi.org/10.1021/acs.chemrestox.0c00095.
Lin, C.C., Hui, M.N.Y., Cheng, S.H., 2007. Toxicity and cardiac effects of carbaryl in early developing zebrafish (*Danio rerio*) embryos. Toxicol. Appl. Pharmacol. 222, 159–168. https://doi.org/10.1016/j.taap.2007.04.013.
Lin, W.J., Jiang, C., Sadahiro, M., Bozdagi, O., Vulchanova, L., Alberini, C.M., Salton, S. R., 2015. VGF and its C-terminal peptide TLQP-62 regulate memory formation in hippocampus via a BDNF-TrkB-dependent mechanism. J. Neurosci. 35, 10343–10356. https://doi.org/10.1523/JNEUROSCI.0584-15.2015.
Lin, Y., Bloodgood, B.L., Hauser, J.L., Lapan, A.D., Koon, A.C., Kim, T.K., Hu, L.S., Malik, A.N., Greenberg, M.E., 2008. Activity-dependent regulation of inhibitory synapse development by Npas4. Nature 455, 1198–1204. https://doi.org/10.1038/nature07319.
Liu, Z.H., Li, Y.W., Hu, W., Chen, Q.L., Shen, Y.J., 2020. Mechanisms involved in tributyltin-enhanced aggressive behaviors and fear responses in male zebrafish. Aquat. Toxicol. 220, 105408. https://doi.org/10.1016/j.aquatox.2020.105408.
Lopes, J.S., Abril-De-Abreu, R., Oliveira, R.F., 2015. Brain transcriptomic response to social eavesdropping in zebrafish (*Danio rerio*). PLoS One 10, 1–21. https://doi.org/10.1371/journal.pone.0145801.
Love, M.I., Huber, W., Anders, S., 2014. Moderated estimation of fold change and dispersion for RNA-seq data with DESeq2. Genome Biol. 15, 1–21. https://doi.org/10.1186/s13059-014-0550-8.
Lu, B., Kwan, K., Levine, Y.A., Olofsson, P.S., Yang, H., Li, J., Joshi, S., Wang, H., Andersson, U., Chavan, S.S., Tracey, K.J., 2014. α7 nicotinic acetylcholine receptor signaling inhibits inflammasome activation by preventing mitochondrial DNA release. Mol. Med. 20, 350–358. https://doi.org/10.2119/molmed.2013.00117.
Magdy, B.W., Mohamed, F.E., Amin, A.S., Rana, S.S., 2016. Ameliorative effect of antioxidants (vitamins C and E) against abamectin toxicity in liver, kidney and testis of male albino rats. J. Basic Appl. Zool. 77, 69–82. https://doi.org/10.1016/j.jobaz.2016.10.002.
Malki, K., Du Rietz, E., Crusio, W.E., Pain, O., Paya-Cano, J., Karadaghi, R.L., Sluyter, F., de Boer, S.F., Sandnabba, K., Schalkwyk, L.C., Asherson, P., Tosto, M.G., 2016. Transcriptome analysis of genes and gene networks involved in aggressive behavior in mouse and zebrafish. Am. J. Med. Genet. Part B Neuropsychiatr. Genet. 171, 827–838. https://doi.org/10.1002/ajmg.b.32451.
Maron, B.J., Maron, M.S., 2013. Hypertrophic cardiomyopathy. Lancet 381, 242–255. https://doi.org/10.1016/S0140-6736(12)60397-3.
Maya-Vetencourt, J.F., Tiraboschi, E., Greco, D., Restani, L., Cerri, C., Auvinen, P., Maffei, L., Castrén, E., 2012. Experience-dependent expression of NPAS4 regulates plasticity in adult visual cortex. J. Physiol. 590, 4777–4787. https://doi.org/10.1113/jphysiol.2012.234237.
McCollum, C.W., Ducharme, N.A., Bondesson, M., Gustafsson, J.A., 2011. Developmental toxicity screening in zebrafish. Birth Defects Res. Part C Embryo Today - Rev. 93, 67–114. https://doi.org/10.1002/bdrc.20210.
Mehlhorn, H., Mencke, N., Hansen, O., 1999. Effects of imidacloprid on adult and larval stages of the flea Ctenocephalides felis after in vivo and in vitro application: a light- and electron-microscopy study. Parasitol. Res. 85, 625–637. https://doi.org/10.1007/s004360050607.
Middleton, R.C., Shelden, E.A., 2013. Small heat shock protein HSPB1 regulates growth of embryonic zebrafish craniofacial muscles. Exp. Cell Res. 319, 860–874. https://doi.org/10.1016/j.yexcr.2013.01.002.
Mizoguchi, T., Minakuchi, H., Ishisaka, M., Tsuruma, K., Shimazawa, M., Hara, H., 2017. Behavioral abnormalities with disruption of brain structure in mice overexpressing VGF. Sci. Rep. 7, 1–12. https://doi.org/10.1038/s41598-017-04132-7.
Moriya, S., Chourasia, D., Ng, K.W., Khel, N.B., Parhar, I.S., 2016. Cloning and localization of immediate early response 2 (ier2) gene in the brain of medaka. J. Chem. Neuroanat. 77, 24–29. https://doi.org/10.1016/j.jchemneu.2016.04.005.
Nishii, K., Morimoto, S., Minakami, R., Miyano, Y., Hashizume, K., Ohta, M., Zhan, D.Y., Lu, Q.W., Shibata, Y., 2008. Targeted disruption of the cardiac troponin T gene causes sarcomere disassembly and defects in heartbeat within the early mouse embryo. Dev. Biol. 322, 65–73. https://doi.org/10.1016/j.ydbio.2008.07.007.
Ojehomon, M., Alderman, S.L., Sandhu, L., Sutcliffe, S., Van Raay, T., Gillis, T.E., Dawson, J.F., 2018. Identification of the actc1c cardiac actin gene in zebrafish. Prog. Biophys. Mol. Biol. 138, 32–37. https://doi.org/10.1016/j.pbiomolbio.2018.06.007.
Padilla, S., Corum, D., Padnos, B., Hunter, D.L., Beam, A., Houck, K.A., Sipes, N., Kleinstreuer, N., Knudsen, T., Dix, D.J., Reif, D.M., 2012. Zebrafish developmental screening of the ToxCast™ Phase I chemical library. Reprod. Toxicol. https://doi.org/10.1016/j.reprotox.2011.10.018.
Park, H., Lee, J.Y., Park, S., Song, G., Lim, W., 2020. Developmental Toxicity of Fipronil in Early Development of Zebrafish (Danio rerio) Larvae: Disrupted Vascular Formation with Angiogenic Failure and Inhibited Neurogenesis, Journal of Hazardous Materials. Elsevier B.V. https://doi.org/10.1016/j.jhazmat.2019.121531.
Parmacek, M.S., Solaro, R.J., 2004. Biology of the troponin complex in cardiac myocytes. Prog. Cardiovasc. Dis. 47, 159–176. https://doi.org/10.1016/j.pcad.2004.07.003.
Perera, F., Herbstman, J., 2011. Prenatal environmental exposures, epigenetics, and disease. Reprod. Toxicol. 31, 363–373. https://doi.org/10.1016/j.reprotox.2010.12.055.
Pérez, J., Domingues, I., Monteiro, M., Soares, A.M.V.M., Loureiro, S., 2013. Synergistic effects caused by atrazine and terbuthylazine on chlorpyrifos toxicity to early-life stages of the zebrafish *Danio rerio*. Environ. Sci. Pollut. Res. 20, 4671–4680. https://doi.org/10.1007/s11356-012-1443-6.
Peterson, H.G., Boutin, C., Martin, P.A., Freemark, K.E., Ruecker, N.J., Moody, M.J., 1994. Aquatic phyto-toxicity of 23 pesticides applied at expected environmental concentrations. Aquat. Toxicol. 28 (3–4), 275–292.
Qiao, K., Hu, T., Jiang, Y., Huang, J., Hu, J., Gui, W., Ye, Q., Li, S., Zhu, G., 2021. Crosstalk of cholinergic pathway on thyroid disrupting effects of the insecticide chlorpyrifos in zebrafish (*Danio rerio*). Sci. Total Environ. 757, 143769. https://doi.org/10.1016/j.scitotenv.2020.143769.
R Core Team, 2021. R: A Language and Environment for Statistical Computing.
Ramamoorthi, K., Fropf, R., Belfort, G.M., Fitzmaurice, H.L., McKinney, R.M., Neve, R.L., Otto, T., Lin, Y., 2011. Npas4 regulates a transcriptional program in CA3 required for contextual memory formation. Science 80 (334), 1669–1675. https://doi.org/10.1126/science.1208049.
Ramspacher, C., Steed, E., Boselli, F., Ferreira, R., Faggianelli, N., Roth, S., Spiegelhalter, C., Messaddeq, N., Trinh, L., Liebling, M., Chacko, N., Tessadori, F., Bakkers, J., Laporte, J., Hnia, K., Vermot, J., 2015. Developmental alterations in heart biomechanics and skeletal muscle function in desmin mutants suggest an early pathological root for desminopathies. Cell Rep. 11, 1564–1576. https://doi.org/10.1016/j.celrep.2015.05.010.
Rauh, V.A., Garcia, W.E., Whyatt, R.M., Horton, M.K., Barr, D.B., Louis, E.D., 2015. Prenatal exposure to the organophosphate pesticide chlorpyrifos and childhood tremor. Neurotoxicology 51, 80–86. https://doi.org/10.1016/j.neuro.2015.09.004.
Reinwald, H., Alvincz, J., Hollert, H., Schäfers, C., Eilebrecht, S., 2021a. Toxicogenomic Profiles of Neuronal Targeting Insecticides in Zebrafish Embryos as Non-target Aquatic Vertebrate Mode [Zenodo: 5218919] [WWW Document]. Zenodo. https://zenodo.org/record/5218919.
Reinwald, H., König, A., Ayobahan, S.U., Alvincz, J., Sipos, L., Göckener, B., Böhle, G., Shomroni, O., Hollert, H., Salinas, G., Schäfers, C., Eilebrecht, E., Eilebrecht, S., 2021b. Toxicogenomic fin(ger)prints for thyroid disruption AOP refinement and biomarker identification in zebrafish embryos. Sci. Total Environ. 760 https://doi.org/10.1016/j.scitotenv.2020.143914.
Rio, D.C., Ares, M., Hannon, G.J., Nilsen, T.W., 2010. Enrichment of poly(A)+ mRNA using immobilized oligo(dT). Cold Spring Harb. Protoc. 5, 2010–2013. https://doi.org/10.1101/pdb.prot5454.
Robertson, C.E., Wright, P.A., Köblitz, L., Bernier, N.J., 2014. Hypoxia-inducible factor-1 mediates adaptive developmental plasticity of hypoxia tolerance in zebrafish, *Danio rerio*. Proc. R. Soc. B Biol. Sci. 281 https://doi.org/10.1098/rspb.2014.0637.
Rogers, E.F., Koniuszy, F.R., Shavel, J., Folkers, K., 1948. Plant insecticides. I. Ryanodine, A new alkaloid from ryania speciosa vahl. J. Am. Chem. Soc. 70, 3086–3088. https://doi.org/10.1021/ja01189a074.
Rombough, P., Drader, H., 2009. Hemoglobin enhances oxygen uptake in larval zebrafish (*Danio rerio*) but only under conditions of extreme hypoxia. J. Exp. Biol. 212, 778–784. https://doi.org/10.1242/jeb.026575.
Russell, W.M.S., Burch, R.L., 1959. The Principles of Humane Experimental Technique 238 https://doi.org/http://117.239.25.194:7000/jspui/bitstream/123456789/1342/1/PRILIMINERY%20%20AND%20%20CONTENTS.pdf.
Ryan, J.C., Morey, J.S., Bottein, M.Y.D., Ramsdell, J.S., Van Dolah, F.M., 2010. Gene expression profiling in brain of mice exposed to the marine neurotoxin ciguatoxin reveals an acute anti-inflammatory, neuroprotective response. BMC Neurosci. 11 https://doi.org/10.1186/1471-2202-11-107.
Sanches, A.L.M., Daam, M.A., Freitas, E.C., Godoy, A.A., Meireles, G., Almeida, A.R., Domingues, I., Espíndola, E.L.G., 2018. Lethal and sublethal toxicity of abamectin and difenoconazole (individually and in mixture) to early life stages of zebrafish. Chemosphere 210, 531–538. https://doi.org/10.1016/j.chemosphere.2018.07.027.
Sanches, A.L.M., Vieira, B.H., Reghini, M.V., Moreira, R.A., Freitas, E.C., Espíndola, E.L. G., Daam, M.A., 2017. Single and mixture toxicity of abamectin and difenoconazole to adult zebrafish (*Danio rerio*). Chemosphere 188, 582–587. https://doi.org/10.1016/j.chemosphere.2017.09.027.

Sánchez-Bayo, F., Goka, K., 2005. Unexpected effects of zinc pyrithione and imidacloprid on Japanese medaka fish (Oryzias latipes). Aquat. Toxicol. 74, 285–293. https://doi.org/10.1016/j.aquatox.2005.06.003.

Sánchez-Bayo, F., Tennekes, H.A., 2020. Time-cumulative toxicity of neonicotinoids: experimental evidence and implications for environmental risk assessments. Int. J. Environ. Res. Publ. Health 17. https://doi.org/10.3390/ijerph17051629.

Santulli, G., Marks, A., 2015. Essential roles of intracellular calcium release channels in muscle, brain, metabolism, and aging. Curr. Mol. Pharmacol. 8, 206–222. https://doi.org/10.2174/1874467208666150507105105.

Scheil, V., Köhler, H.R., 2009. Influence of nickel chloride, chlorpyrifos, and imidacloprid in combination with different temperatures on the embryogenesis of the Zebrafish Danio rerio. Arch. Environ. Contam. Toxicol. 56, 238–243. https://doi.org/10.1007/s00244-008-9192-8.

Schock, E.N., Ford, W.C., Midgley, K.J., Fader, J.G., Giavasis, M.N., McWhorter, M.L., 2012. The effects of carbaryl on the development of zebrafish (*Danio rerio*) embryos. Zebrafish 9, 169–178. https://doi.org/10.1089/zeb.2012.0747.

Scholz, S., Klüver, N., Kühne, R., 2016. Analysis of the Relevance and Adequateness of Using Fish Embryo Acute Toxicity (FET) Test Guidance (OECD 236) to Fulfil the Information Requirements and Addressing Concerns under REACH. European Chemicals Agency.

Schüttler, A., Altenburger, R., Ammar, M., Bader-Blukott, M., Jakobs, G., Knapp, J., Krüger, J., Reiche, K., Wu, G.M., Busch, W., 2019. Map and model-moving from observation to prediction in toxicogenomics. GigaScience 8, 1–22. https://doi.org/10.1093/gigascience/giz057.

Schüttler, A., Reiche, K., Altenburger, R., Busch, W., 2017. The transcriptome of the zebrafish embryo after chemical exposure: a meta-analysis. Toxicol. Sci. 157 (2), 291–304.

Sehnert, A.J., Huq, A., Weinstein, B.M., Walker, C., Fishman, M., Stainier, D.Y.R., 2002. Cardiac troponin T is essential in sarcomere assembly and cardiac contractility. Nat. Genet. 31, 106–110. https://doi.org/10.1038/ng875.

Selderslaghs, I.W.T., Hooyberghs, J., De Coen, W., Witters, H.E., 2010. Locomotor activity in zebrafish embryos: a new method to assess developmental neurotoxicity. Neurotoxicol. Teratol. 32, 460–471. https://doi.org/10.1016/j.ntt.2010.03.002.

SETAC, 2019. Recommended Minimum Reporting Information for Environmental Toxicity Studies 1–3 (https://doi.org/https://cdn.ymaws.com/www.setac.org/resource/resmgr/publications_and_resources/setac_tip_envtox_info.pdf).

Shafarenko, M., Liebermann, D.A., Hoffman, B., 2005. Egr-1 abrogates the block imparted by c-Myc on terminal M1 myeloid differentiation. Blood 106, 871–878. https://doi.org/10.1182/blood-2004-08-3056.

Solomon, H.M., Weis, J.S., 1979. Abnormal circulatory development in medaka caused by the insecticides carbaryl, malathion and parathion. Teratology 19, 51–62. https://doi.org/10.1002/tera.1420190109.

Sparks, T.C., Nauen, R., 2015. IRAC: mode of action classification and insecticide resistance management. Pestic. Biochem. Physiol. https://doi.org/10.1016/j.pestbp.2014.11.014.

Stehr, C.M., Linbo, T.L., Incardona, J.P., Scholz, N.L., 2006. The developmental neurotoxicity of fipronil: notochord degeneration and locomotor defects in zebrafish embryos and larvae. Toxicol. Sci. 92, 270–278. https://doi.org/10.1093/toxsci/kfj185.

Subramanian, A., Tamayo, P., Mootha, V.K., Mukherjee, S., Ebert, B.L., Gillette, M.A., Paulovich, A., Pomeroy, S.L., Golub, T.R., Lander, E.S., Mesirov, J.P., 2005. Gene set enrichment analysis: a knowledge-based approach for interpreting genome-wide expression profiles. Proc. Natl. Acad. Sci. U.S.A. 102, 15545–15550. https://doi.org/10.1073/pnas.0506580102.

Takeuchi, H., Inagaki, S., Morozumi, W., Nakano, Y., Inoue, Y., Kuse, Y., Mizoguchi, T., Nakamura, S., Funato, M., Kaneko, H., Hara, H., Shimazawa, M., 2018. VGF nerve growth factor inducible is involved in retinal ganglion cells death induced by optic nerve crush. Sci. Rep. 8, 1–13. https://doi.org/10.1038/s41598-018-34585-3.

Thunnissen, N.W., Lautz, L.S., van Schaik, T.W.G., Hendriks, A.J., 2020. Ecological risks of imidacloprid to aquatic species in The Netherlands: measured and estimated concentrations compared to species sensitivity distributions. Chemosphere 254, 126604.

Tierney, K.B., 2011. Behavioural assessments of neurotoxic effects and neurodegeneration in zebrafish. Biochim. Biophys. Acta (BBA) - Mol. Basis Dis. 1812, 381–389. https://doi.org/10.1016/j.bbadis.2010.10.011.

Tišler, T., Jemec, A., Mozetič, B., Trebše, P., 2009. Hazard identification of imidacloprid to aquatic environment. Chemosphere 76, 907–914. https://doi.org/10.1016/j.chemosphere.2009.05.002.

Tišler, T., Kožuh Eržen, N., 2006. Abamectin in the aquatic environment. Ecotoxicology 15, 495–502. https://doi.org/10.1007/s10646-006-0085-1.

Toledo-Ibarra, G.A., Rojas-Mayorquín, A.E., Girón-Pérez, M.I., 2013. Influence of the cholinergic system on the immune response of teleost fishes: potential model in biomedical research. Clin. Dev. Immunol. https://doi.org/10.1155/2013/536534, 2013.

Ton, C., Lin, Y., Willett, C., 2006. Zebrafish as a model for developmental neurotoxicity testing. Birth Defects Res. Part A Clin. Mol. Teratol. 76, 553–567. https://doi.org/10.1002/bdra.20281.

Torres-Hernández, B.A., Colón, L.R., Rosa-Falero, C., Torrado, A., Miscalichi, N., Ortíz, J. G., González-Sepúlveda, L., Pérez-Ríos, N., Suárez-Pérez, E., Bradsher, J.N., Behra, M., 2016. Reversal of pentylenetetrazole-altered swimming and neural activity-regulated gene expression in zebrafish larvae by valproic acid and valerian extract. Psychopharmacology 233, 2533–2547. https://doi.org/10.1007/s00213-016-4304-z.

Tufi, S., Leonards, P., Lamoree, M., De Boer, J., Legler, J., Legradi, J., 2016. Changes in neurotransmitter profiles during early zebrafish (*Danio rerio*) development and after pesticide exposure. Environ. Sci. Technol. 50, 3222–3230. https://doi.org/10.1021/acs.est.5b05665.

Ubaid Ur Rahman, H., Asghar, W., Nazir, W., Sandhu, M.A., Ahmed, A., Khalid, N., 2021. A comprehensive review on chlorpyrifos toxicity with special reference to endocrine disruption: evidence of mechanisms, exposures and mitigation strategies. Sci. Total Environ. 755, 142649. https://doi.org/10.1016/j.scitotenv.2020.142649.

Van Petegem, F., 2012. Ryanodine receptors: structure and function. J. Biol. Chem. 287, 31624–31632. https://doi.org/10.1074/jbc.R112.349068.

Verhaar, H.J.M., van Leeuwen, C.J., Hermens, J.L.M., 1992. Classifying environmental pollutants. Chemosphere 25, 471–491. https://doi.org/10.1016/0045-6535(92)90280-5.

Verschaffelt, P., Van Den Bossche, T., Gabriel, W., Burdukiewicz, M., Soggiu, A., Martens, L., Renard, B.Y., Schiebenhoefer, H., Mesuere, B., 2021. MegaGO: a fast yet powerful approach to assess functional gene ontology similarity across meta-omics data aets. J. Proteome Res. 20, 2083–2088. https://doi.org/10.1021/acs.jproteome.0c00926.

Versonnen, B.J., Roose, P., Monteyne, E.M., Janssen, C.R., 2004. Estrogenic and toxic effects of methoxychlor on zebrafish (*Danio rerio*). Environ. Toxicol. Chem. 23, 2194–2201. https://doi.org/10.1897/03-228.

Vignet, C., Cappello, T., Fu, Q., Lajoie, K., De Marco, G., Clérandeau, C., Mottaz, H., Maisano, M., Hollender, J., Schirmer, K., Cachot, J., 2019. Imidacloprid induces adverse effects on fish early life stages that are more severe in Japanese medaka (*Oryzias latipes*) than in zebrafish (*Danio rerio*). Chemosphere 225, 470–478. https://doi.org/10.1016/j.chemosphere.2019.03.002.

Villeneuve, D.L., Crump, D., Garcia-Reyero, N., Hecker, M., Hutchinson, T.H., LaLone, C. A., Landesmann, B., Lettieri, T., Munn, S., Nepelska, M., Ottinger, M.A., Vergauwen, L., Whelan, M., 2014a. Adverse outcome pathway (AOP) development I: strategies and principles. Toxicol. Sci. 142, 312–320. https://doi.org/10.1093/toxsci/kfu199.

Villeneuve, D.L., Crump, D., Garcia-Reyero, N., Hecker, M., Hutchinson, T.H., LaLone, C. A., Landesmann, B., Lettieri, T., Munn, S., Nepelska, M., Ottinger, M.A., Vergauwen, L., Whelan, M., 2014b. Adverse outcome pathway development II: best practices. Toxicol. Sci. 142, 321–330. https://doi.org/10.1093/toxsci/kfu200.

Vogel, B., Meder, B., Just, S., Laufer, C., Berger, I., Weber, S., Katus, H.A., Rottbauer, W., 2009. In-vivo characterization of human dilated cardiomyopathy genes in zebrafish. Biochem. Biophys. Res. Commun. 390, 516–522. https://doi.org/10.1016/j.bbrc.2009.09.129.

Wang, Hong, Yu, M., Ochani, M., Amella, C.A., Tanovic, M., Susarla, S., Li, J.H., Wang, Haichao, Yang, H., Ulloa, L., Al-Abed, Y., Czura, C.J., Tracey, K.J., 2003. Nicotinic acetylcholine receptor α7 subunit is an essential regulator of inflammation. Nature 421, 384–388. https://doi.org/10.1038/nature01339.

Wang, X., O Reilly, A.O., Williamson, M.S., Puinean, A.M., Yang, Y., Wu, S., Wu, Y., 2019. Function and pharmacology of glutamate-gated chloride channel exon 9 splice variants from the diamondback moth Plutella xylostella. Insect Biochem. Mol. Biol. 104, 58–64. https://doi.org/10.1016/j.ibmb.2018.12.005.

Watson, F.L., Schmidt, H., Turman, Z.K., Hole, N., Garcia, H., Gregg, J., Tilghman, J., Fradinger, E.A., 2014. Organophosphate pesticides induce morphological abnormalities and decrease locomotor activity and heart rate in *Danio rerio* and *Xenopus laevis*. Environ. Toxicol. Chem. 33, 1337–1345. https://doi.org/10.1002/etc.2559.

Weis, P., Weis, J.S., 1974. Cardiac malformations and other effects due to insecticides in embryos of the killifish, *Fundulus heteroclitus*. Teratology 10, 263–267. https://doi.org/10.1002/tera.1420100308.

Wilkinson, M.D., Dumontier, M., Aalbersberg, IjJ., Appleton, G., Axton, M., Baak, A., Blomberg, N., Boiten, J.W., da Silva Santos, L.B., Bourne, P.E., Bouwman, J., Brookes, A.J., Clark, T., Crosas, M., Dillo, I., Dumon, O., Edmunds, S., Evelo, C.T., Finkers, R., Gonzalez-Beltran, A., Gray, A.J.G., Groth, P., Goble, C., Grethe, J.S., Heringa, J., t Hoen, P.A.C., Hooft, R., Kuhn, T., Kok, R., Kok, J., Lusher, S.J., Martone, M.E., Mons, A., Packer, A.L., Persson, B., Rocca-Serra, P., Roos, M., van Schaik, R., Sansone, S.A., Schultes, E., Sengstag, T., Slater, T., Strawn, G., Swertz, M. A., Thompson, M., Van Der Lei, J., Van Mulligen, E., Velterop, J., Waagmeester, A., Wittenburg, P., Wolstencroft, K., Zhao, J., Mons, B., 2016. Comment: the FAIR guiding principles for scientific data management and stewardship. Sci. Data 3, 1–9. https://doi.org/10.1038/sdata.2016.18.

Witjes, L., Van Troys, M., Vandekerckhove, J., Vandepoele, K., Ampe, C., 2019. A new evolutionary model for the vertebrate actin family including two novel groups. Mol. Phylogenet. Evol. 141, 106632. https://doi.org/10.1016/j.ympev.2019.106632.

Wolstenholme, A.J., 2012. Glutamate-gated chloride channels. J. Biol. Chem. 287, 40232–40238. https://doi.org/10.1074/jbc.R112.406280.

Wu, H., Gao, C., Guo, Y., Zhang, Y., Zhang, J., Ma, E., 2014. Acute toxicity and sublethal effects of fipronil on detoxification enzymes in juvenile zebrafish (*Danio rerio*). Pestic. Biochem. Physiol. 115, 9–14. https://doi.org/10.1016/j.pestbp.2014.07.010.

Wu, H.H.T., Brennan, C., Ashworth, R., 2011. Ryanodine receptors, a family of intracellular calcium ion channels, are expressed throughout early vertebrate development. BMC Res. Notes 4. https://doi.org/10.1186/1756-0500-4-541.

Wu, S., Li, X., Liu, X., Yang, G., An, X., Wang, Q., Wang, Y., 2018. Joint toxic effects of triazophos and imidacloprid on zebrafish (*Danio rerio*). Environ. Pollut. 235, 470–481. https://doi.org/10.1016/j.envpol.2017.12.120.

Yamamoto, I., 1999. Nicotine to nicotinoids: 1962 to 1997. In: Nicotinoid Insecticides and the Nicotinic Acetylcholine Receptor. Springer Japan, Tokyo, pp. 3–27. https://doi.org/10.1007/978-4-431-67933-2_1.

Yang, J.S., Qi, W., Farias-Pereira, R., Choi, S., Clark, J.M., Kim, D., Park, Y., 2019. Permethrin and ivermectin modulate lipid metabolism in steatosis-induced HepG2 hepatocyte. Food Chem. Toxicol. 125, 595–604. https://doi.org/10.1016/j.fct.2019.02.005.

Yen, J., Donerly, S., Levin, E.D., Linney, E.A., 2011. Differential acetylcholinesterase inhibition of chlorpyrifos, diazinon and parathion in larval zebrafish. Neurotoxicol. Teratol. 33, 735–741. https://doi.org/10.1016/j.ntt.2011.10.004.

Yu, G., 2020. Gene ontology semantic similarity analysis using GOSemSim. In: Methods in Molecular Biology. Humana Press Inc., pp. 207–215. https://doi.org/10.1007/978-1-0716-0301-7_11

Yu, G., He, Q.-Y., 2016. ReactomePA: an R/Bioconductor package for reactome pathway analysis and visualization. Mol. Biosyst. 12, 477–479. https://doi.org/10.1039/c5mb00663e.

Yu, G., Wang, L.-G., Han, Y., He, Q.-Y., 2012. ClusterProfiler: an R package for comparing biological themes among gene clusters. OMICS A J. Integr. Biol. 16, 284–287. https://doi.org/10.1089/omi.2011.0118.

Zhang, L., Cho, J., Ptak, D., Leung, Y.F., 2013. The role of egr1 in early zebrafish retinogenesis. PLoS One 8, 1–11. https://doi.org/10.1371/journal.pone.0056108.

Zhang, R., Yang, J., Zhu, J., Xu, X., 2009. Depletion of zebrafish Tcap leads to muscular dystrophy via disrupting sarcomere-membrane interaction, not sarcomere assembly. Hum. Mol. Genet. 18, 4130–4140. https://doi.org/10.1093/hmg/ddp362.

Zhu, A., Ibrahim, J.G., Love, M.I., 2019. Heavy-Tailed prior distributions for sequence count data: removing the noise and preserving large differences. Bioinformatics 35, 2084–2092. https://doi.org/10.1093/bioinformatics/bty895.

Zucchi, S., Blüthgen, N., Ieronimo, A., Fent, K., 2011. The UV-absorber benzophenone-4 alters transcripts of genes involved in hormonal pathways in zebrafish (*Danio rerio*) eleuthero-embryos and adult males. Toxicol. Appl. Pharmacol. 250, 137–146. https://doi.org/10.1016/j.taap.2010.10.001.

A3 Transcriptomic profiling of clobetasol propionate-induced immunosuppression in challenged zebrafish embryos

Declaration of author contributions to the publication:

Transcriptomic profiling of clobetasol propionate-induced immunosuppression in challenged zebrafish embryos

DOI: 10.1016/j.ecoenv.2022.113346
Status: Published
Journal: **Ecotoxicology and Environmental Safety**

Contributing authors:
Essfeld F., (EF), Reinwald H. (**RH**), Salinas G. (SG), Schäfers C. (SC), Eilebrecht E. (EE) & Eilebrecht S. (ES)

(1) Concept and design

Doctoral candidate **RH**: 20% - suggested suitable type of sample group comparison for the study
Co-author EF: 35%
Co-author ES: 30%
Co-author SC, EE: 15%

(2) Conducting tests and experiments

Co-author EF: 90% - Exposure study / microinjection; RNA extraction; *In vitro* sample quality check
Co-author GS: 10% - mRNA-Sequence library preparation and Illumina HiSeq NGS

(3) Compilation of data sets and figures

Doctoral candidate **RH**: 15% - Compilation of raw sequencing data for downstream processing; coding support for figure generation and data visualization
Co-author EF: 65% - Main data visualization; graphical abstract illustration; Network illustration and plotting of DGEA (heatmap, correlation plots, venn diagrams)
Co-author ES: 20% - Constructive feedback on figure structure and additive molecular effects illustration

(4) Analysis and interpretation of data

Doctoral candidate **RH**: 45% - Raw sequencing data processing and data QC; providing source code for downstream analysis and technical support during data analysis steps; support for data interpretation
Co-author EF: 50% - Differential gene expression analysis; feature selection; data interpretation; overrepresentation analysis and network clustering
Co-author ES: 5% - Constructive feedback on data analysis approaches

(5) Drafting of manuscript

Doctoral candidate **RH**: 15%
Co-author EF: 55%
Co-author ES: 25%
Co-author SC, EE: 5% - Final draft comments

Ecotoxicology and Environmental Safety 233 (2022) 113346

Contents lists available at ScienceDirect

Ecotoxicology and Environmental Safety

journal homepage: www.elsevier.com/locate/ecoenv

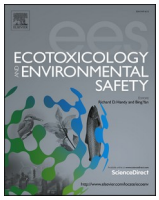

Transcriptomic profiling of clobetasol propionate-induced immunosuppression in challenged zebrafish embryos

Fabian Essfeld [a,b], Hannes Reinwald [a,c], Gabriela Salinas [d], Christoph Schäfers [e], Elke Eilebrecht [e], Sebastian Eilebrecht [a,*]

[a] Fraunhofer Attract Eco'n'OMICs, Fraunhofer Institute for Molecular Biology and Applied Ecology, Schmallenberg, Germany
[b] Computational Biology, Faculty of Biology, Bielefeld University, Bielefeld, Germany
[c] Department Evolutionary Ecology and Environmental Toxicology, Faculty Biological Sciences, Goethe University Frankfurt, Frankfurt, Germany
[d] NGS-Services for Integrative Genomics, University of Göttingen, Göttingen, Germany
[e] Department Ecotoxicology, Fraunhofer Institute for Molecular Biology and Applied Ecology, Schmallenberg, Germany

ARTICLE INFO

Edited by: Dr. Caterina Faggio

Keywords:
Immune challenge
Biomarkers
Immunosuppression
Immunotoxicity
Hazard assessment

ABSTRACT

In the ecotoxicological hazard assessment of chemicals, the detection of immunotoxicity is currently neglected. This is mainly due to the complexity of the immune system and the consequent lack of standardized procedures and markers for the comprehensive assessment of immunotoxic modes of action. In this study, we present a new approach applying transcriptome profiling to an immune challenge with a mixture of pathogen-associated molecular patterns (PAMPs) in zebrafish embryos, analyzing differential gene expression during acute infection with and without prior exposure to the immunosuppressive drug clobetasol propionate (CP). While PAMP injection itself triggered biological processes associated with immune activation, some of these genes were more differentially expressed upon prior exposure to CP than by immune induction alone, whereas others showed weaker or no differential regulation in response to the PAMP stimulus. All of these genes responding differently to PAMP after prior CP exposure showed additivity of PAMP- and CP-induced effects, indicating independent regulatory mechanisms. The transcriptomic profiles suggest that CP impaired innate immune induction by attenuating the response of genes involved in antigen processing, TLR signaling, NF-KB signaling, and complement activation. We propose this approach as a powerful method for detecting gene biomarkers for immunosuppressive modes of action, as it was able to identify alternatively regulated processes and pathways in a sublethal, acute infection zebrafish embryo model. This allowed to define biomarker candidates for immune-mediated effects and to comprehensively characterize immunosuppression. Ultimately, this work contributes to the development of molecular biomarker-based environmental hazard assessment of chemicals in the future.

1. Introduction

The anthropogenic use of chemicals such as pesticides, biocides and pharmaceuticals inevitably leads to their active ingredients being released into the environment, either directly or indirectly. In particular in aquatic ecosystems, non-target organisms are exposed and can be seriously harmed, depending on the hazard potential of the substance. Due to their exposure pathway via gill breathing, fish are often particularly affected and adverse effects can have serious consequences for entire populations and ecosystems (Rosi-Marshall and Royer, 2012; Mahmood et al., 2016). To avoid particularly harmful effects of active substances on populations, such as endocrine disruption, substance approval is subject to strict regulations, with the exception of pharmaceuticals. In order to take account of the EU chemicals strategy for sustainability towards a toxic-free environment, the EU Commission is endeavoring to extend the generic approach, which applies to endocrine disruptors, to other harmful modes of action such as immunotoxicity in the future (European Commission, 2020). However, despite a large number of studies with field observations of immune responses impaired by chemicals in wild fish (Luebke et al., 1997), no consistent approaches exist to date for considering immune parameters in ecotoxicological hazard assessment (reviewed by Rehberger et al., 2017). While the complexity of the immune system and the resulting lack of defined endpoints are one aspect of this, a major reason is the lack of immune

* Corresponding author.
E-mail address: Sebastian.eilebrecht@ime.fraunhofer.de (S. Eilebrecht).

https://doi.org/10.1016/j.ecoenv.2022.113346
Received 2 December 2021; Received in revised form 18 February 2022; Accepted 21 February 2022
Available online 25 February 2022

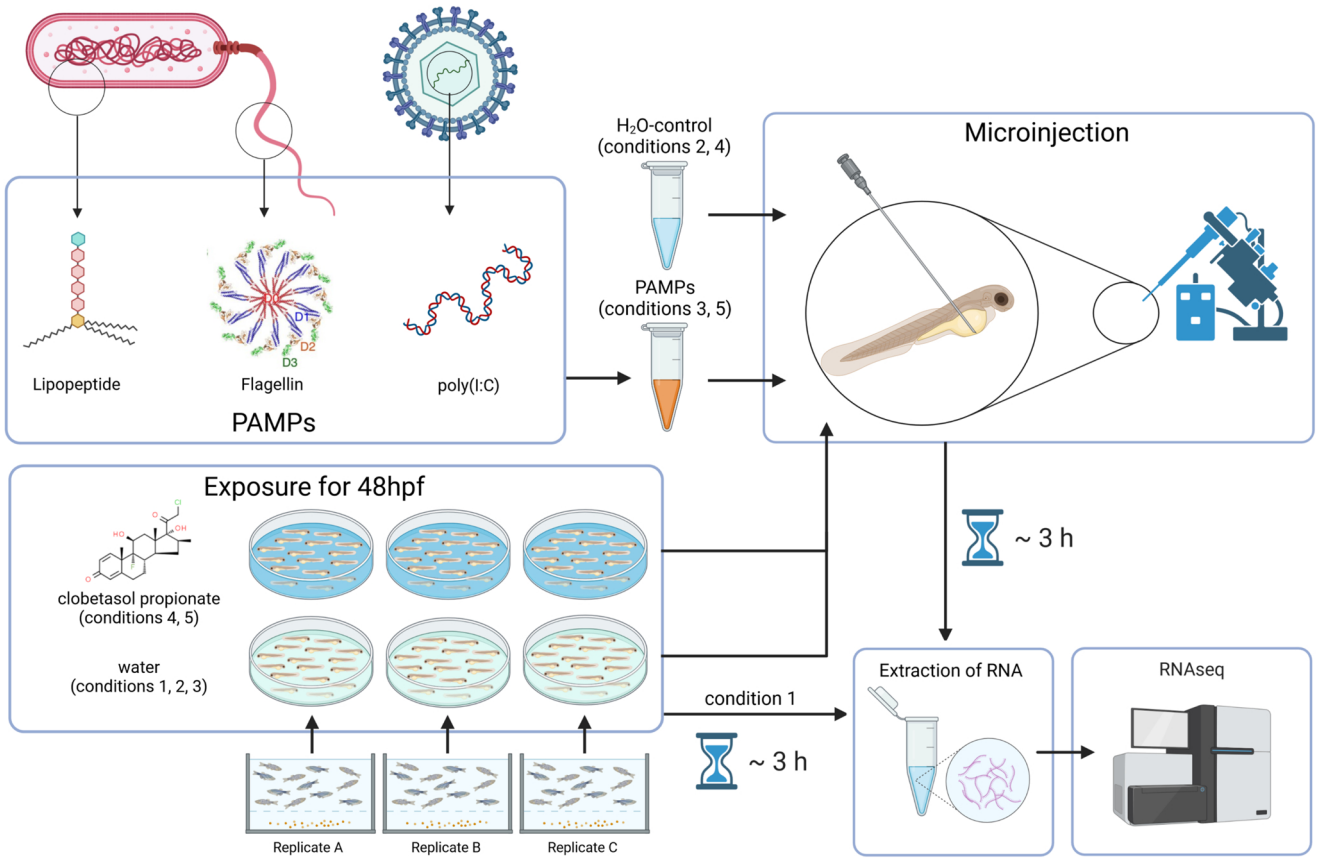

Fig. 1. Experimental design. Zebrafish embryos derived from three different spawning groups were exposed to either test substance or water as control for 48 hpf. The immune system was triggered by injection of a mix of different pathogen associated molecular patterns (PAMPs) consisting of bacterial flagellin, synthetic Pam3CSK4 mimicking bacterial lipopeptides and poly(I:C) mimicking viral dsRNA. Pure water was injected as injection control. Total RNA was extracted 3 h after injection and subsequently subjected to RNA-seq. All conditions mentioned in the text are indicated.

parameters and corresponding markers that allow reliable screening of immunotoxic modes of action. Detailed knowledge of changes at the molecular level triggered by immune induction or by immunomodulatory substances will additionally contribute to the identification of molecular initiating events and early key events of immunotoxic mechanisms of action. This increased knowledge at lower levels of biological organization will contribute to the development and establishment of immunotoxicologically relevant adverse outcome pathways (AOP) (Ankley et al., 2010; Ankley and Edwards, 2018), the development of which has not yet progressed much in this particular field (Neagu et al., 2021).

Zebrafish embryos have proven to be ideal research subjects for understanding immunity, as they rapidly develop a functional innate immune system within 24 hours post fertilization (hpf) (Herbomel et al., 1999; Traver et al., 2003). This life stage is also an established test organism in the assessment of environmental hazards from chemicals, for example, an OECD test guideline exists for acute toxicity testing (FET, OECD No. 236 (2013)). Moreover, the ability to perform high-throughput screenings without sacrificing complexity and the classification as non-protected life stage makes the zebrafish embryo an ideal model organism for immuntoxicity research (Caballero and Candiracci, 2018; Strähle et al., 2012). Recent studies by Mottaz et al. (2017) and Hidasi et al. (2017) described an approach to detect immunotoxicity by challenging zebrafish embryos with bacterial lipopolysaccharides (LPS) to elicit a strong exuberant immune response that is lethal to the majority of individuals. When the embryos were previously treated with an immunosuppressant such as morphine or clobetasol propionate (CP), the mortality rate in this assay decreased in a concentration-dependent manner, as a consequence of immune suppression. In addition, supporting gene expression analysis of selected marker genes was performed using RT-qPCR. The same method was applied by Schmid and Fent (2020), Willi et al. (2019) and Faltermann et al. (2020), who studied the effect of CP in combination with other steroidal compounds. Despite the existence of such promising approaches to study compound-induced impairments of innate immune responses in the zebrafish embryo, the differentiation of molecular mechanisms of action as well as the detection of novel, informative molecular biomarkers at the gene expression level has so far been limited by the targeted analysis of selected genes.

This limitation can be overcome by the application of methods such as next-generation sequencing that allow scientists to examine expression changes of thousands of genes simultaneously in a non-targeted manner. Such approaches not only allow the identification of mechanism-specific signatures and biomarkers of immunotoxicity, but they also enable to draw functional conclusions based on transcriptome-wide differences in gene expression, for example, by identifying signaling pathways affected by immunotoxic chemicals. A number of previous studies aimed at gaining mechanistic insights into immune responses in zebrafish by assessing the effects of infections with *Salmonella* (Stockhammer et al., 2009), mycobacteria (Rougeot et al., 2019), *Vibrio parahaemolyticus* (Zhang et al., 2018), *Edwardsiella tarda*, *Salmonella typhimurium* or *Mycobacterium marinum* (van der Vaart et al., 2012) using transcriptomics. Other studies used this approach to assess the immunotoxic effect of environmental chemicals, such as glufosinate-ammonium (Xiong et al., 2019) or beclomethasone (Xie et al., 2019).

This study aimed to establish a sublethal immune challenge approach in the zebrafish embryo and combine it with transcriptome

analysis to identify immunomodulatory modes of action at the gene expression level. For functional transcriptomics profiling, we used an analysis pipeline developed in our laboratory for ecotoxicological analysis of zebrafish embryos (Reinwald et al., 2021, 2022). By investigating the corticosteroid and immunosuppressant CP as a reference compound, this study aimed to identify informative biomarker candidates for immunosuppressive modes of action in fish. Future extension of the here presented approach to other immunotoxic mechanisms of action could pave the way for consideration of immunotoxicity in environmental hazard assessment of chemicals.

2. Materials and methods

2.1. Experimental design

The experimental setting was designed to determine transcriptomic effects of the immunosuppressant clobetasol propionate (CP) in zebrafish embryos in the presence and the absence of an immune challenge, i.e. an artificially activated immune response (Fig. 1). For this, a modified zebrafish embryo toxicity test was combined with an immune challenge experiment. Briefly, an artificial immune response was achieved via microinjection of a mixture of different pathogen-associated molecular patterns (PAMPs), namely Pam3CSK4, a synthetic lipopeptide, bacterial flagellin and a synthetic double stranded RNA called poly(I:C). To consider the injection injury effect, the respective control group was injected with ultrapure endotoxin-free water. Additionally, both types of injections were also performed on embryos that were previously exposed to CP. In order to estimate the effect of the injection itself, one group of embryos exposed to water only was not injected, serving as an untreated control. In summary, the following five conditions were used to analyze the immunosuppressive effect of CP: 1) a control condition exposed to water without injection (hereinafter referred to as 'untreated'), 2) a control condition exposed to water injected with water ('water'), 3) a condition exposed to water injected with PAMPs ('PAMP'), 4) a condition exposed to CP injected with water ('water_CP') and 5) a condition exposed to CP injected with PAMPs ('PAMP_CP'). Each of the conditions was performed in biological triplicates (see also Fig. 1).

2.2. Test substance and PAMPs

Clobetasol propionate (CP) (CAS 25122–46–7, $\geq$ 98% purity) was purchased from Merck KGgA (Darmstadt, Germany). A 5 mM stock solution and a 250 μM pre-dilution were prepared in acetone. In order to obtain 500 mL of a 250 nM test solution, 500 μL of the predilution was added to a flask. After complete evaporation of the acetone, the substance was re-dissolved in 500 mL copper-reduced tap water, from now on referred to as embryo water, by sonication (Sonorex RK 100 H, Bandelin, Germany) for 30 min.

Standard flagellin from *Bacillus subtilis* ($\approx$ 10% purity), Pam3CSK4 ($\geq$ 98% purity) and poly(I:C) HMW (high molecular weight) were purchased from InvivoGen SAS (Toulouse, France). Stock solutions (1 mg/mL for poly(I:C) and Pam3CSK4; 0.1 mg/mL for flagellin) were individually prepared in provided endotoxin-free water, aliquoted and stored according to the manufacturer's instructions until further use.

2.3. Test organism

Adult zebrafish (*Danio rerio*) of the wild-type strain AB, originally obtained from West Aquarium GmbH (Bad Lauterberg, Germany), were continuously bred for several generations at Fraunhofer IME. They were maintained under flow-through conditions in 150 L tanks at 26 $\pm$ 2 °C and a 12:12 light/dark cycle. Daily main feed was TetraMin® (Tetra Werke, Melle, Germany) regularly supplemented with nauplii of *Artemia salina*. For embryo collection, spawning trays equipped with stimulating spawning substrate were put into the tanks the day before test start. Directly after spawning in the morning, the trays were removed from the tanks. The eggs were rinsed in a sieve to remove dirt and feces. Clean eggs were kept in canning jars until they were transferred into petri dishes filled with test solutions as soon as possible.

2.4. Modified zebrafish embryo toxicity test with immune challenge

In order to detect effects of CP in zebrafish embryos at the transcriptomic level, particularly in relation to the immune system, a modified zFET (OECD, 2013) was performed. First, an appropriate sublethal CP test concentration that had no visible effect on the embryos but did affect immune-related gene expression was determined by pre-tests with two different CP concentrations using RT-qPCR analysis of selected genes as an indicator (Fig. S1).

After saturating petri dishes with the corresponding test solution overnight, freshly fertilized zebrafish eggs were split into five petri dishes with 20 eggs each for each replicate originating from a particular spawning group. Two dishes per replicate were then filled with 8 mL of 250 nM of aerated CP test solution and three with the same volume of aerated embryo water. The eggs were incubated at 27 $\pm$ 1 °C and a 14:10 h light/dark cycle using an IPP 400 incubator (Memmert, Buechenbach, Germany) equipped with an LED light source. At 24 h post fertilization (hpf), half of the test solution volumes were renewed. At 47 hpf, the embryos were manually dechorinated using two pointed forceps. For microinjection, PAMPs mixture was freshly prepared by mixing 10 μL of each stock solution.

The device for microinjection was set up using FemtoTip II injection needles with a complementary universal capillary holder (Eppendorf, Hamburg, Germany), connected to an IM-300 microinjector (Narishige, London, United Kingdom). Volume calibration was performed according to Sive et al. (2010) using a micrometer slide with 1/100 mm scale (Bresser, Rhede, Germany). Briefly, the needles were backfilled with 10 μL PAMP mixture or ultra-pure water. Injections for volume calibration were made into a drop of immersion oil purred on the micrometer slide, the output pressure was constantly kept at 10 psi, while the time of injection was adjusted until an injected drop had a diameter of approximately 250 μm. Assuming a perfectly sphere shaped droplet, the volume corresponds to 8 nL.

The procedure described below was performed for each of the five conditions in turn, treating the three replicates simultaneously. In order to anaesthetize the embryos, tricaine (Sigma Aldrich Taufkirchen, Germany) stock solution (4 mg/mL in 21 mM Tris pH 9) was added to the petri dishes to a final concentration of 200 μg/mL. The immobilized embryos were transferred onto a 1% agarose plate, which was divided into segments, one for each replicate. Excess liquid was removed, keeping the embryos in place by surface tension. Desiccation was prevented by adding liquid, if needed. To ensure a quick injection procedure, the embryos were aligned in a way that their dorsal sides pointed in the same direction. The injection was made on the dorsal side of the yolk sac and the needle was advanced through the yolk until it reached the yolk sac circulation valley on the ventral side of the embryo, where the injection was made directly into the bloodstream. After all replicates of a certain condition were processed and the integrity of the embryos was ensured by visual inspection, they were rinsed back into the corresponding dish containing renewed test solution. After further incubation for about three hours, total RNA was extracted from the ten embryos of each condition and replicate. For this, ten embryos of each sample were transferred into 1.5 mL reaction tubes. The liquid was removed completely before the embryos were snap-frozen in liquid nitrogen. Extraction was performed using a NucleoSpin RNA/Protein kit from Macherey-Nagel (Düren, Germany) as recommended by the manufacturer. Briefly, the frozen embryos were transferred into screw cap tubes filled with Lysing Matrix D ceramic beads (MP Biomedicals, Irvine, USA) and the lysis buffer from the kit. Homogenization was achieved by using a FastPrep-24 (MP Biomedicals, Irvine, USA) device at 5 m/s for 45 s. Further steps of the extraction protocol were made

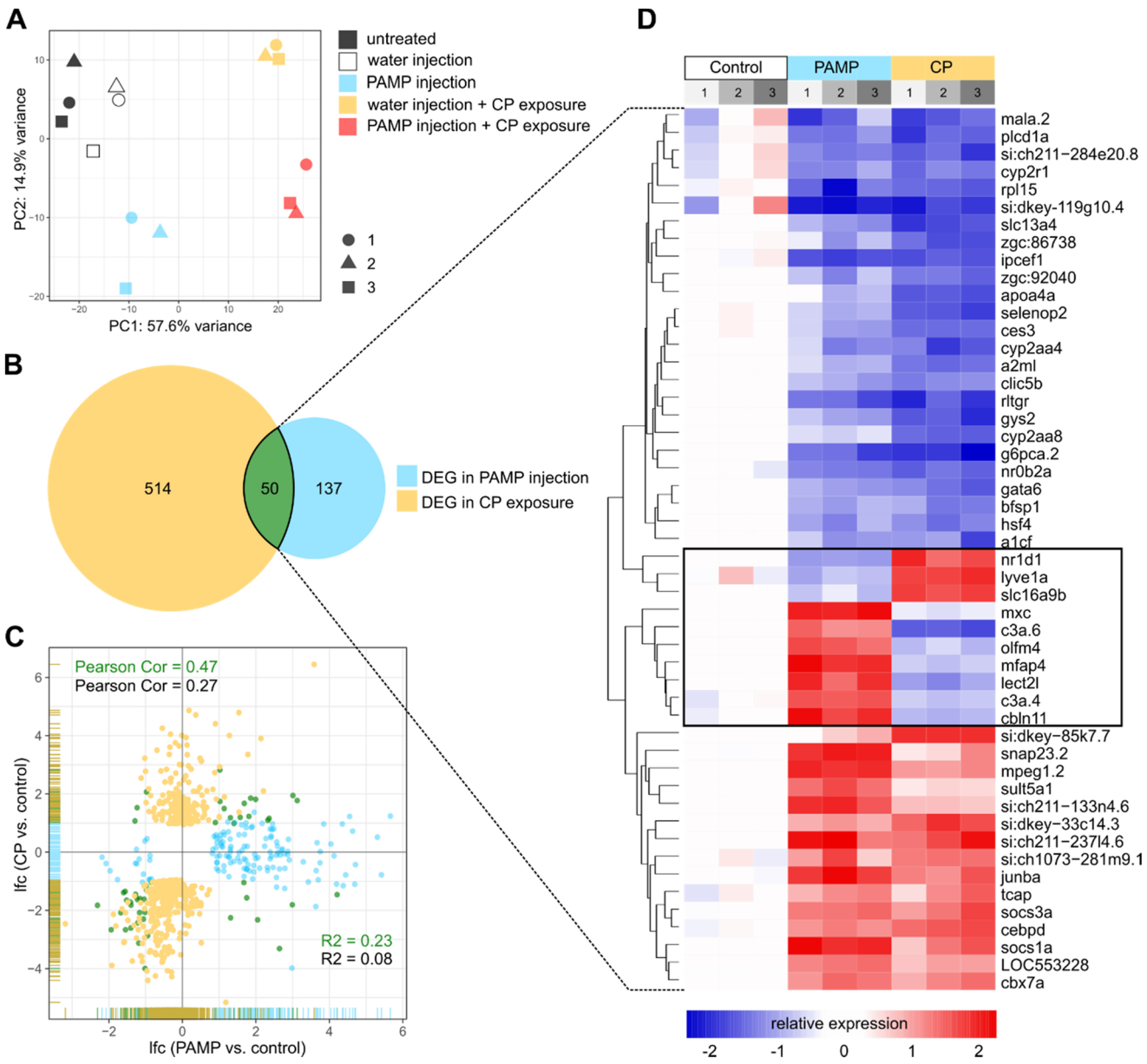

Fig. 2. Transcriptome changes in response to activation of the innate immune system and CP exposure in 51 hpf zebrafish embryos. Activation of the immune system was triggered by PAMP injection at 48 hpf, while effects of CP were analyzed after exposure to 250 nM CP preceding a water injection. The injection of water served as a control for both conditions. (A) PCA plot based on rlog normalized gene counts, showing variances between different conditions distinguished by colors. Symbols represent different biological replicates. (B) Venn diagram showing the number of statistically significant (padj $\leq$ 0.01) differentially expressed genes (DEGs) of each condition as well as the intersection. (C) Scatter plot comparing log2-fold change (lfc) values of DEGs observed in each condition. The coloring is the same as in the venn diagram. (D) Heatmap containing the 50 DEGs present in the common subset of both conditions. The relative expression signals of both conditions were normalized to the control. An enhanced expression is indicated in red and a suppressed expression is indicated in blue. Biological replicates are indicated above as different gray colored boxes. Genes are clustered after maximum distance measure with average linkage, while individual samples are clustered after Canberra method with average linkage. Those 10 genes showing an opposing expression when comparing both conditions (also represented in the scatter plot C), are highlighted by a box.

according to the manufacturer's instructions. Purity and concentration of total RNA was assessed using a NanoDrop 2000 system (Thermo Scientific, Waltham, USA), RNA integrity Numbers (RIN) were determined by RNA 6000 Nano assay on a Bioanalyzer 2100 device (Agilent, Santa Clara, USA).

2.5. RT-qPCR

RT-qPCR was performed on five exemplary immune system related target genes (*ccl34a, Il-1β, cxcl8, ifnγ, tnfα)*, which were chosen based on literature research. Relevant sources and the primer sequences used are listed in the supplemental material (Tables S2 and S3). Primers were purchased from Metabion (Planegg, Germany). For each sample 1 μg of high quality total RNA was subjected to reverse transcription using the SensiFAST cDNA Synthesis Kit (BioLine, London, UK) according to the manufacturer's instructions. The qPCR reactions with a total volume of 10 μL each were set up in white 96 well plates (Cat. No.: 72.1982.202; Sarstedt, Nuembrecht, Germany) using 4.2 μL of 5x diluted cDNA as template and 5.8 μL master mix. The master mix was prepared by mixing 5 μL 2x SensiFAST SYBR No-ROX Mix (BioLine, London, UK) with 0.4 μL of forward and reverse primers (10 μM each) for each reaction. The PCR reactions, which were performed as technical duplicates on a

LightCycler96 (Roche, Basel, Switzerland), started with a pre incubation for 120 s at 95 °C followed by amplification in 35 cycles (95 °C for 5 s, 60 °C for 10 s, 72 °C for 10 s). High resolution melting curves were recorded by heating from 65 °C to 97 °C with a temperature transition rate of 0.2 °C/s. Relative gene expression was calculated according to the $\Delta\Delta c_t$-method (Livak and Schmittgen, 2001) using *rpl8* as housekeeping gene.

2.6. RNA-seq and data processing

High quality RNA samples with RINs of at least 8.8 were normalized to 100 ng/μL and introduced to mRNA purification and library preparation using TruSeq RNA library Prep Kit v2 as recommended by the manufacturer (Illumina, San Diego, USA). Sequencing in 50 bp single read mode was performed on an Illumina HiSeq 4000 System (Illumina). Adapter sequences of demultiplexed FASTQ files were trimmed using trimmomatic v0.39 (Bolger et al., 2014) and an overall read and alignment quality check was performed using FastQC v0.11.5 (Andrews, 2010), samtools (Li et al., 2009) and RSeQC with bowtie2 (Langmead and Salzberg, 2012). FASTQ files were checked for potential contaminating sequences using FastQ Screen (Wingett and Andrews, 2018). STAR v2.5.2a (Dobin et al., 2013) was used for alignment to the *Danio rerio* reference genome assembly GRCz11 and for counting gene-mapped reads using the built *in –quantMode GeneCounts* function, which corresponds to the HTSeq algorithm with default settings (Anders et al., 2015). Overall, analysis QC reports were integrated using MultiQC (Ewels et al., 2016), which is provide on Zenodo under the accession 5750053 in the Supplemental materials section (www.zenodo.org). Read counts were merged to a single count matrix using R v4.0.3 (R Core Team, 2019). All downstream analysis were conducted in RStudio v.1.2.5033 (RStudio Team, 2020). A list of all packages used can be found in the session information file in the supplemental material. Differential gene expression analysis was performed using DESeq2 v1.30.1 (Love et al., 2014) as briefly described below. Low abundant genes with an average of less than one read per sample were excluded in advance. The gene counts were normalized using the negative binomial distribution model of DESeq2, with a parametric fit type applied to the dispersion estimation model. A multifactor model design was applied, considering condition and spawning group (i.e. biological replicates) as factors. Walds t-test was used to calculate p-values, which were corrected using independent hypothesis weighting (IHW) after Benjamini-Hochberg (Ignatiadis et al., 2016; Wald, 1943; Hochberg and Benjamini, 1990). An effect size cut-off (LFCcut) was defined for each comparison as the top 10% quantile of the absolute log2-fold change (LFC) values. Subsequently, LFC values were shrunk using apeglm v1.12.0 (approximate posterior estimation for generalized linear models; Zhu et al., 2019). Finally, a gene was considered as differentially expressed (DEG) for adjusted p-values ≤ 0.01 and with an absolute apgelm shrunk LFC $>$ LFCcut. ENSEMBL gene IDs were annotated using AnnotationDbi v1.52.0 (Pagès et al., 2017) and the org.Dr.eg.db v1.4.2 package (Team TBD, 2019). The background gene set for ORA, was defined by all genes tested for differential expression. Calculated p values were corrected according to Benjamini-Hochberg, subsequently only ontologies with adjusted p values ≤ 0.05 were regarded as significantly enriched. A deposit of raw and processed data is available in the ArrayExpress database at EMBL-EBI under accession number E-MTAB-11092. Result tables from DGEA and ORA are available on Zenodo (accession: 5750053). Results of data quality check can be found in the supplemental material (Figs. S2 to S6) and the MultiQC report (Zenodo accession 5750053). The R script used for identification of DEGs in this study are available under: https://github.com/hreinwal/-DESeq2Analysis/blob/master/DESeq2_multifactor_PairwiseWalds_v2.R.

3. Results and discussion

A driving force for our study was the insufficient data on markers and methods to assess immunotoxicity in fish. This results in the fact that immunotoxic effects have so far not been considered in environmental hazard assessment (Rehberger et al., 2017). Furthermore, there is a lack of robust approaches to define and record such markers.

In our study, we established a sublethal immune challenge in the zebrafish embryo as an aquatic vertebrate model organism and combined it with transcriptome analysis to identify potential marker genes for immunosuppression. The experimental approach thus combined the advantages of whole-organism testing of unprotected life stages with maximal readout at the level of gene expression. Previous immune challenge approaches in this model have targeted lethality through immune system overactivation as an endpoint to detect immunosuppression (Hidasi et al., 2017; Mottaz et al., 2017). Thus, such approaches were not suitable for comprehensive detection of gene expression changes to distinguish immunotoxic mechanisms of action, as lethality would override the molecular effects of specific drug mechanisms at the transcriptome level.

3.1. PAMP- and CP-induced gene expression changes and related functions

First, we examined the molecular effects of immune challenge and exposure to CP in zebrafish embryos. To provoke an immune response, a mixture of different PAMPs was injected into the embryos' bloodstream. An initial analysis of DEGs was performed in order to confirm that the experimental design was suitable to generate an artificial innate immune response, and thus, to mimic an acute infection. To evaluate the effects of CP, embryos were exposed to 250 nM CP, a sublethal concentration of the test compound that in preliminary experiments showed significant modulation of the responsiveness of selected immune-related genes to PAMP injection (Fig. S1). This CP concentration was previously shown to induce mild but significant physiological changes, regulation of selected immune-related genes, and borderline inhibition of macrophage activation (Willi et al., 2018; Hidasi et al., 2017). After exposure for 48 hpf, the corresponding transcriptomic changes were examined. In all cases the injection of ultrapure water served as reference condition (Fig. 2).

Principle component analysis (PCA) performed on all five test conditions for the total common set of 23.349 genes analyzed revealed that 72.5% of the data's variance were explained by PC1 and PC2 (Fig. 2A). At a glance, the individual conditions clustered clearly and the biological replicates accounted for a comparatively small proportion of the variation in each case. In addition, CP exposure accounted for a greater proportion of the variation than PAMP injection. To get an estimate of how much of the variance was due to the injection alone, the water injection was compared to an untreated control. Remarkably, these two control conditions clustered close to each other in the PCA, suggesting that the injection itself had only a minor contribution to gene expression changes.

PAMP injection resulted in 187 DEGs (↑142; ↓45), whereas the exposure to CP altered the expression of 564 genes (↑216; ↓348), with a total of 50 DEGs in the common subset of both conditions (Fig. 2B). The observed tendency for more genes being up-regulated than down-regulated after stimulation of an immune response was consistent with observations made in previous studies: Ordas et al. (2011) and Stockhammer et al. (2010) infected zebrafish embryos with *Salmonella typhimurium* and found the vast majority of DEGs up-regulated using multiple transcriptomic methods. The same tendency was observed by Wu et al. (2010), who profiled the transcriptome of adult zebrafish infected with *Streptococcus suis*. Furthermore, van der Vaart et al. (2012) have shown that DEGs are predominantly up-regulated in zebrafish embryos and adults following infection with different pathogens (*S. typhimurium*, *Edwardsiella tarda* and *Mycobacterium marinum*). In a

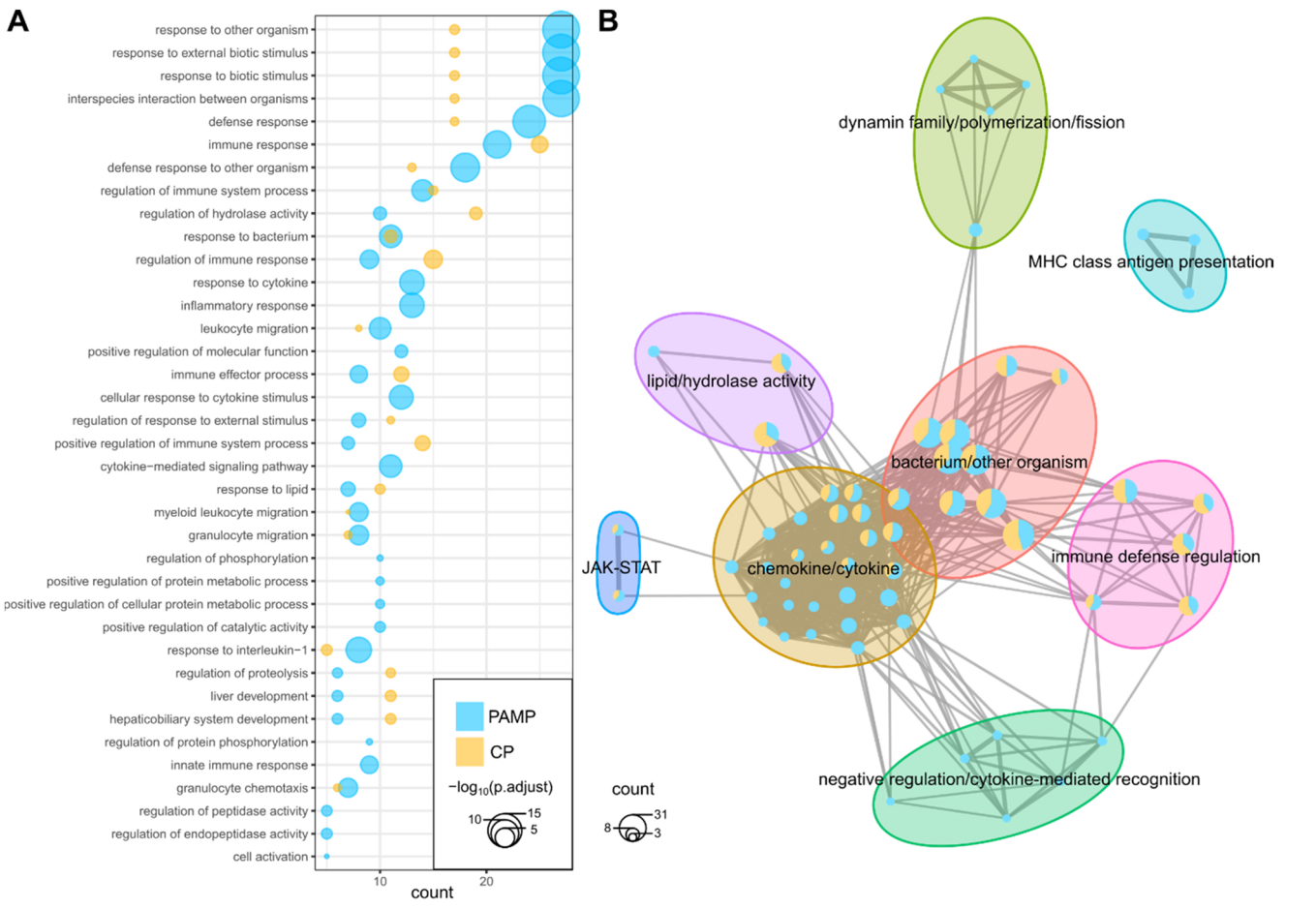

Fig. 3. Top most over represented biological processes from the Gene Ontology data base upon PAMP injection and CP exposure. DEGs used as input for the R package clusterProfiler are defined as genes with padj < 0.01 and by applying the condition-dependent LFC cutoff, which is based on the top 10% of genes ranked by LFC. (A) Bubbleplot showing over represented GO terms selected by applying a p-value cutoff of 0.05. Colors indicate the presence of one or both conditions in the respective terms. The position on the x-axis gives the number of genes present in each ontology, while the dot size represents the –log10 of the adjusted p-values. (B) Clustered network plot created using clusterProfilers function emapplot_cluster with the same input as in A. The dots are small pie charts showing in color from which condition the involved genes originate, while the size represents to total gene count in both conditions. The naming of the encircled clusters was conducted manually.

study by Yang et al. (2015), transcriptome profiling of zebrafish embryos was performed after injection of either the specific Toll-like receptor 2 (Tlr2) agonist Pam3CSK4 or the Tlr5-specific agonist flagellin. Although the time between injection and RNA isolation (1 h), the time point of injection (27 hpf), and the injected reagents (either Pam3CSK4 or flagellin) differed from our approach in this study, we observed highly significant positive correlations when comparing the expression changes of our and the previous study for the common subsets of DEGs (Fig. S7). These results suggest that the induced innate immune response at the gene expression level was robust and stable with respect to early developmental stages and inducing reagents, making the immune challenge a promising tool for identifying immune-related biomarkers.

It was apparent that the majority of DEGs appeared to be specific for the corresponding condition, as the common subset represented only 27% (PAMP) and 9% (CP) of the DEGs responding to the respective treatment. A comparative view on the direction of regulation of these gene sets revealed that the vast majority (80%) of the common subset was regulated in the same direction in both conditions (Fig. 2C). Consequently, 20% of the common DEGs showed an opposing regulation when comparing both conditions, i.e. they were up-regulated in one condition and down-regulated in the other. Only a small number of direct target genes of an infection (PAMP targets) were regulated by CP in the absence of infection. These findings indicate that when evaluating the immunotoxicity of a particular substance, it is essential to also consider effects of and interference with immune stimulation. Otherwise, a possibly existing immunosuppressive effect would be overlooked or at least be underestimated. This particular issue has already been described as one of the major challenges in the assessment of immunotoxicity by Rehberger et al. (2017).

Of the 50 DEGs that were in the intersection of both conditions, the ten that were inversely regulated under both conditions (i.e. *nr1d1*, *lyve1a*, *slc16a9b*, *mxc*, *c3a.6*, *olfm4*, *mfap4*, *lect2l*, *c3a.4* and *cbln11*) in particular may provide useful information about the molecular mechanisms of induction of immune responses and immunosuppression, as their study, in contrast to the similarly regulated genes, allows discrimination of the two (Fig. 2D). Among those, cerebellin 11 (*cbln11),* the complement proteins *c3a.4* and *ca3.6,* olfactomedin 4 (*olfm4*) and the myxovirus resistance C (*mxc*) gene are directly associated with processes relevant to the immune system. *cbln11*, which is a member of the tumor necrosis factor-like superfamily, is suspected to have a function in immune processes in European sea bass (*Dicentrarchus labrax*) (Mazurais et al., 2020). *c3a.4* and *ca3.6* are parts of the complement system, which is an important component of innate immunity of vertebrates (Lubbers et al., 2017). It was shown that C3a can have both anti-inflammatory and pro-inflammatory functions (Coulthard and Woodruff, 2015), which is consistent with the observations made in our study. *olfm4* was shown previously to play important roles during innate immunity against bacterial infections, among other things by inhibiting bacteria-induced nuclear factor KB (NF-KB) signaling (Liu and Rodgers, 2016). The expression of the *mxc* gene has been reported to be strongly

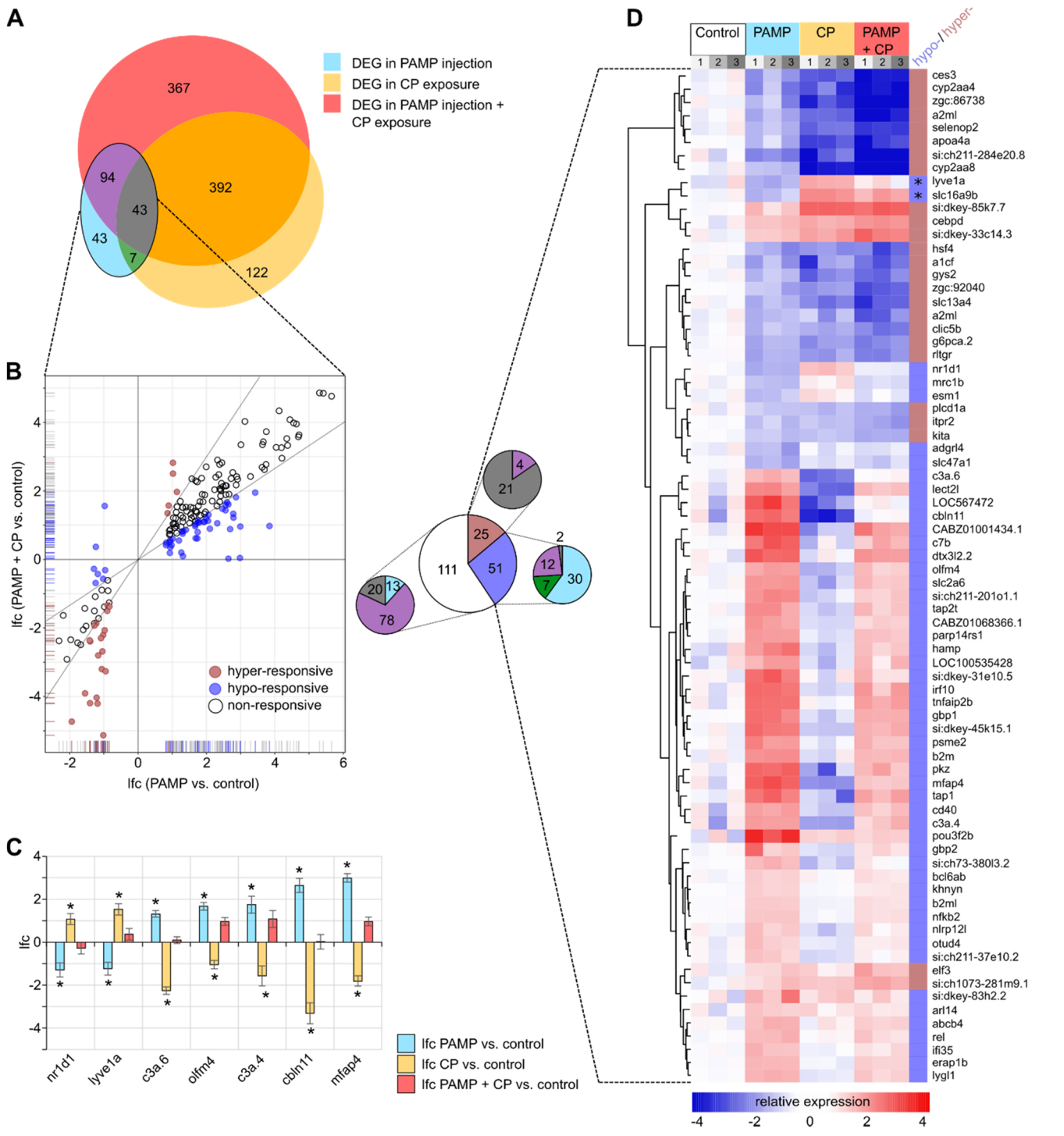

Fig. 4. Transcriptome response of zebrafish embryos to immune-induction with and without prior exposure to CP. (A) Venn diagram of DEGs induced by PAMP injection (blue), CP exposure (yellow) and PAMP injection following prior CP exposure (red). In all cases, DEGs were identified using the water injection condition as a control. (B) Left: Correlation plot for all PAMP-induced DEGs from (A), comparing their log2-fold change (lfc)-values after PAMP injection alone (x-axis) with their lfc-values after PAMP injection with prior CP exposure (y-axis). The definition of non-responsive genes is shown as a line. Non-responsive genes are shown in white, hyper-responsive genes in red and hypo-responsive genes in blue. Notably, the two genes regulated oppositely were assigned to the hypo-responsive genes. Right: pie chart showing the numbers of non-, hyper and hypo-responsive genes as well as their composition with respect to the DEGs shown in (A). (C) Biomarker candidates that are oppositely regulated when comparing PAMP injection and CP exposure and belong to the hypo-responsive PAMP DEGs. The change in expression (lfc) in each condition is indicated as a color code. Statistical significance (padj $\leq$ 0.01) is indicated by an asterisk. (D) Heatmap showing the relative expression of all 76 hyper- and hypo-responsive PAMP DEGs shown in (B). The relative signals normalized to the water injection control (white) are shown for each treatment (columns). As compared to the mean of control condition, an enhanced expression is indicated in red and a suppressed expression is indicated in blue. Biological replicates are indicated above as different gray colored boxes. Genes are clustered after maximum distance measure with average linkage. In the right column, the affiliation to the hyper- (red) or hypo-responsive (blue) genes is indicated. The two genes regulated in an opposite direction by PAMP and PAMP+CP are indicated by asterisks.

regulated in zebrafish of different life stages in response to viral RNA and thus has been used as positive control in studies dealing with viral infections (Chen et al., 2015; García-Valtanen et al., 2014; Zhu et al., 2020). *nr1d1* is a transcriptional regulator involved in the regulation of circadian rhythm (Harding and Lazar, 1993; Aninye et al., 2014). It has previously been shown to be regulated by glucocorticoids in mice (Torra et al., 2000) and essentially modulates innate immunity and inflammatory signaling (Baxter and Ray, 2020). The lymphatic vessel endothelial hyaluronan receptor 1 (*lyve1a*) is a homologue of the CD44 glycoprotein and mediates immune cell entry and trafficking in the lymphatic system (Johnson and Jackson, 2021). *slc16a9b* codes for a pH-sensitive creatine transporter (Futagi et al., 2019). Creatine metabolism has been previously shown to play multiple roles in the immune system (Kazak and Cohen, 2020) providing a link between *slc16a9b* and immune modulation. The leukocyte cell derived chemotaxin 2 (*lect2l*) was shown to act protective against bacterial infections by macrophage activation in previous studies (Lu et al., 2013; Wang et al., 2018). The microfibrillar-associated protein 4 (*mfap4*) was shown earlier to regulate hematopoiesis in zebrafish (Ong et al., 2020) and to be responsive to infections in catfish (Niu et al., 2011). Thus, while genes that were similarly regulated under both conditions also provide important insights into the modulation of the molecular immune response, in particular, genes that were oppositely regulated by immune induction and CP-induced immunosuppression are directly or indirectly related to immune function, and thus represent promising candidate markers at the gene level that allow discrimination between immune response induction and immunosuppression.

To identify biological processes associated with the DEGs responsive to PAMP injection and CP exposure, we performed overrepresentation analysis (ORA) for biological processes GO terms. ORA revealed that PAMP injection predominantly affected genes associated with GO terms related to the immune system, such as response and defense to other organism (GO:0051707, GO:0098542), immune and defense response (GO:0006955, GO:0050776, GO:0045087, GO:0050777), response to cytokine signaling (GO:0034097, GO:0019221, GO:0071345) or response to interleukin-1 (GO:0071347, GO:0070555) (Fig. 3A). Of note, some of the immune-related terms, such as response to cytokine (GO:0034097), inflammatory response (GO:0006954) or innate immune response (GO:0045088), were significantly enriched only in the PAMP condition. These predominantly belonged to ontology clusters related to chemokine signaling, antigen presentation and cytokine signaling (Fig. 3B). In other cases, such as response to other organism, defense and immune response, leukocyte migration (GO:0050900), granulocyte migration (GO:0097530), the significance of their enrichment was an order of magnitude greater in the PAMP condition than in the CP exposure condition. Those terms belonged to ontology clusters related to bacterial defense or immune regulation.

Previous studies have examined physiological effects and cellular immune responses in zebrafish embryos at various time points following exposure to CP concentrations similar to those used in our study (Willi et al., 2017; Hidasi et al., 2017). Willi et al. observed a decrease in spontaneous muscle contractions at 24 hpf, an increase in heart rate at 48 hpf, premature hatching at 72 hpf, and decreased swimming activity at 120 hpf after exposure to 246 nM CP. In addition, significant upregulation of selected immune-related genes such as *fkbp5*, *gilz*, *il17a*, *socs3*, *mmp9*, *per1a*, and *hsd11b2* was detected at 96 hpf in this study. Remarkably, we observed comparable significant upregulation of these genes even though our study was designed to end at 51 hpf (Fig. S8). Hidasi et al. analyzed the respiratory burst of macrophages in zebrafish embryos exposed to different CP concentrations at 120 hpf and found a statistically significant decrease in macrophage activation after exposure to 1000 nM CP, whereas exposure to 100 nM resulted in a decrease that was still not significant. The CP concentration in our study was intermediate between the NOEC and LOEC in view of the study by Hidasi et al. regarding the inhibition of macrophage activation.

Thus, our molecular and toxicogenomic data reflect, on the one hand, the induction of an innate immune response by PAMPs and, on the other hand, are consistent with previous studies showing the impairment of the immune response and inflammatory signaling cascades by glucocorticoids (Liberman et al., 2007; Cain and Cidlowski, 2017). Furthermore, our results can be linked to previously observed physiological changes and modulation of cellular immune responses as a result of CP exposure (Hidasi et al., 2017; Willi et al., 2018). This consistency with the existing literature demonstrated the robustness of the experiment and the validity of the control conditions.

3.2. *Effects of clobetasol propionate exposure and PAMP injection add up for a specific subset of immune-responsive genes*

We next sought to answer the question of whether and how CP exposure affects an induced innate immune response, i.e. the resistance capacity to pathogens, which is ultimately a measure of the organisms' ability to survive. To this end, we aimed to detect those genes that responded differently to PAMP-induced immune induction after CP exposure than under untreated conditions. Thus, we compared PAMP-regulated genes with CP-regulated genes in the presence and absence of PAMP injection, all using water injection as reference control (Fig. 4).

At the gene level, 43 genes (23%, blue) of the DEGs induced by PAMP injection were neither significantly differentially expressed by CP exposure alone nor by PAMP injection after prior exposure to CP (Fig. 4A). 94 genes (50% of the PAMP induced DEGs, purple) responded to PAMP irrespective of prior CP exposure and 7 genes (4% of the PAMP induced DEGs, green) were DEGs in the PAMP and the CP condition. A set of 43 genes (23%, grey) was identified as DEGs in all three conditions compared. To obtain information on whether and how each set of genes was affected by prior CP treatment, we compared their expression changes after PAMP injection upon prior CP treatment with those after PAMP injection alone (Fig. 4B). We categorized the PAMP-induced DEGs into either hyper-, hypo- or non-responsive to an additional prior CP exposure. Hyper-responsive DEGs were those 25 that were more strongly regulated by PAMP after prior CP exposure than by PAMP alone ($\log_2$-fold change (lfc)-ratio of PAMP_CP compared to PAMP ≥ 1.50, red). In contrast, hypo-responsive DEGs were those 49 that were less strongly regulated by PAMP after prior CP exposure than by PAMP alone (lfc-ratio of PAMP compared to PAMP_CP ≥ 1.50, blue). We observed a total of two DEGs, which were oppositely regulated by both conditions and which we considered as extreme cases of hypo-regulation (asterisks in Fig. 4D). The remaining 111 DEGs were considered non-responsive to prior CP treatment (white). While this set of non-responsive genes consisted predominantly of DEGs in the common subset of the PAMP and the PAMP_CP conditions, the majority of hyper-responsive genes were found in the intersection of all three conditions, and the hypo-responsive genes consisted mainly of DEGs in the PAMP condition alone and the intersection between the PAMP and CP conditions (Fig. 4B). Of note, all seven genes in the exclusive intersection of PAMP and CP conditions, *nr1d1*, *lyve1a*, *c3a.6*, *olfm4*, *c3a.4*, *cbln11 and mfap4*, were hypo-responsive (Fig. 4C). These genes were a subset of the previously discussed 10 DEGs that responded oppositely to PAMP injection and CP exposure, supporting their potential to serve as informative biomarkers of interference with the immune system. Plotting the expression changes of all hyper- and hypo-responsive genes in all test conditions as a heat map showed that the hyper- and hypo-responsiveness in the PAMP_CP condition was in almost all cases a result of additive effects of the individual PAMP and CP conditions (Fig. 4D). Whereas hypo-responsive genes were almost exclusively regulated in opposite directions in response to PAMP and CP, hyper-responsive genes were regulated in the same direction under both conditions. The additivity of the effects was further validated by comparing the calculated sum of the effects of PAMP and CP with the observed effects of the combined PAMP_CP condition (Fig. S9).

As mentioned earlier, Pam3CSK4 has been shown to specifically activate Tlr2 (Cheng et al., 2012) whereas the immune response to

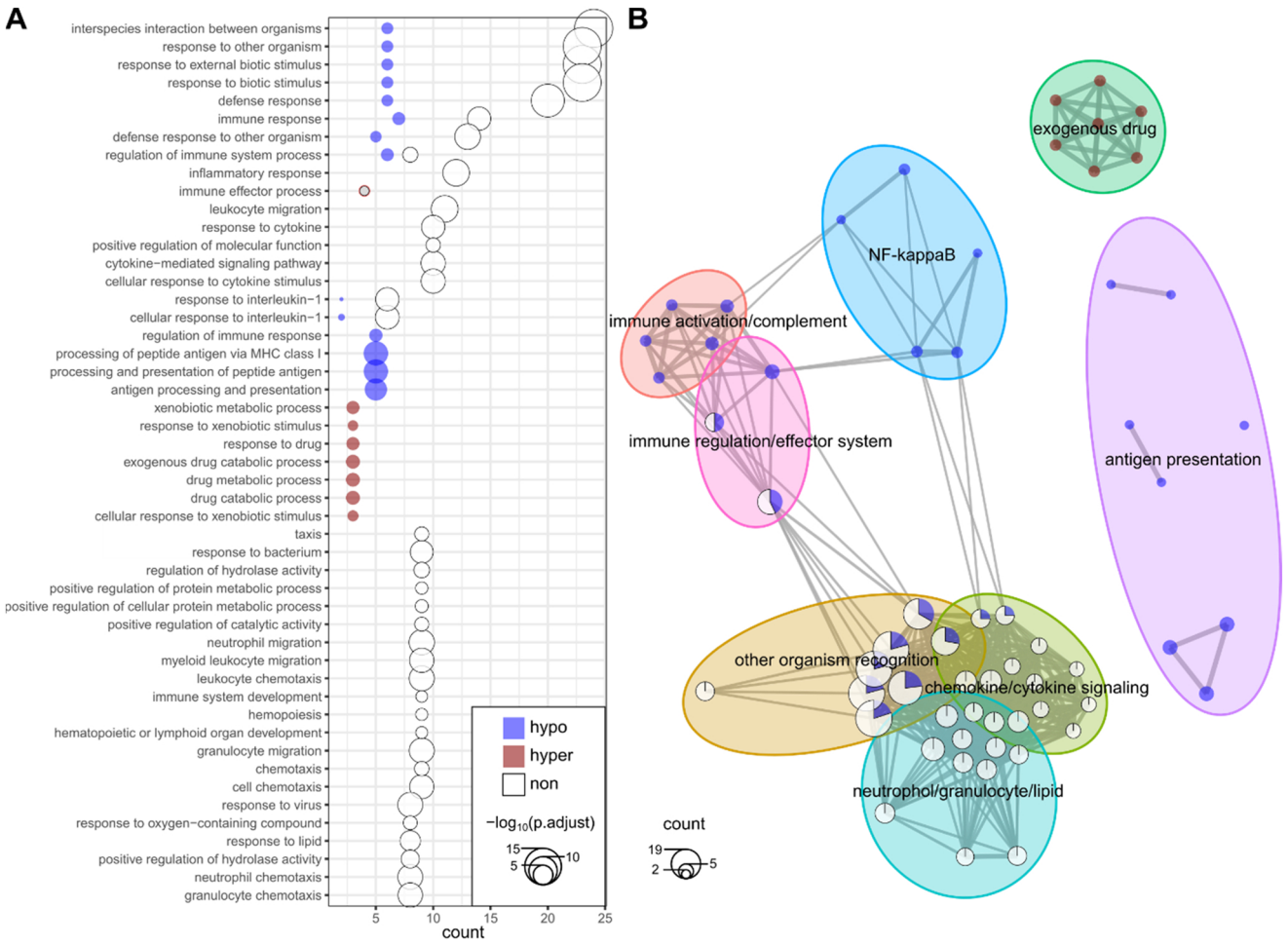

Fig. 5. Overrepresentation analysis (ORA) of GO biological processes using hyper-, hypo- and non-responsive genes previously defined as input for clusterProfiler. (A) Bubbleplot showing over represented GO terms selected by applying a p-value cutoff of 0.05. Colors indicate different gene sets. The position on the x-axis gives the number of genes present in each ontology, while the dot size represents the –log10 of the adjusted p-values. (B) Clustered network plot created using clusterProfilers' function emapplot_cluster with the same input as in A. The dots are small pie charts showing in color from which gene set the involved genes originate, while the size represents to total gene count in both conditions. The naming of the encircled clusters was manually adapted.

flagellin is mediated by Tlr5 (Hayashi et al., 2001) and the response to double-stranded RNA mimicked by poly(I:C) is triggered by Tlr3 (Matsumoto and Seya, 2008). Activation of Tlr2, Tlr3, and Tlr5 triggers different downstream signaling cascades that eventually lead to activation of transcription factors such as the NF-KB or the activator protein-1 (AP1), which trigger an innate immune response by regulating immune-related genes (Borrello et al., 2011; Karimi-Googheri and Arababadi, 2014; Sánchez de Medina et al., 2013; Akira and Takeda, 2004). The major pathways of NF-KB and AP1-mediated regulation of inflammatory genes are alteration of chromatin state through recruitment of chromatin modifiers or direct recruitment of transcription factors and parts of the transcription machinery to transcription regulatory regions via their respective DNA binding sites (Bhatt and Ghosh, 2014). Therefore, the PAMP-mediated changes in gene expression in our study may be primarily due to the activation of NF-KB and AP1, which has been shown to regulate the expression of cytokines and thereby inflammatory signaling (Kopp and Ghosh, 1995; Khalaf et al., 2010). The proposed predominant mechanism of action of CP is the activation of the glucocorticoid receptor (GR). Activated GR in turn can bind to its recognition sequences in the DNA, which often are located in transcription regulatory regions as well (Luisi et al., 1991; Beato and Miguel, 1989). Recent studies suggest that GR may also regulate a subset of inflammatory genes in a DNA-binding-dependent manner (Weikum et al., 2017; Surjit et al., 2011). In addition to this DNA-dependent mechanism, GR was previously shown to regulate gene expression also through DNA-independent mechanisms by tethering NF-KB and AP1 (Bosscher et al., 2003; Herrlich, 2001), which is currently the predominant model for GR-mediated suppression of inflammatory gene expression. Whereas the observed additivity of PAMP- and CP-induced effects in the case of hypo-responsive genes could be explained by DNA-independent regulation of NF-KB and AP1 by activated GR, the additivity observed in the case of hyper-responsive genes could rather be explained by a DNA-dependent mechanism. However, the high degree of additivity for both gene sets (Fig. S9) indicated one rather than two distinct mechanisms of action of CP, favoring the DNA-dependent mechanism, which in principle can explain the regulation of both gene sets. As the hypo- and hyper-responsive gene sets constituted immunosuppression-sensitive infection markers, they were considered as highly relevant for the key question of our study.

To gain insight into the immune-related processes that were either attenuated or enhanced by CP-induced immunosuppression, we performed ORAs for the hypo-, the hyper-, as well as the non-sensitive gene sets for biological process genes ontologies (Fig. 5). While processes such as cytokine signaling (GO:0034097, GO:0019221, GO:0071345), inflammatory response (GO:0006954, GO:0050727) or migration (GO:0050900, GO:1990266, GO:0097530, GO:0097529, GO:0072676, GO:0071674) and chemotaxis of immune cells (GO:0030595, GO:0030593, GO:0071621, GO:0060326) were not affected by

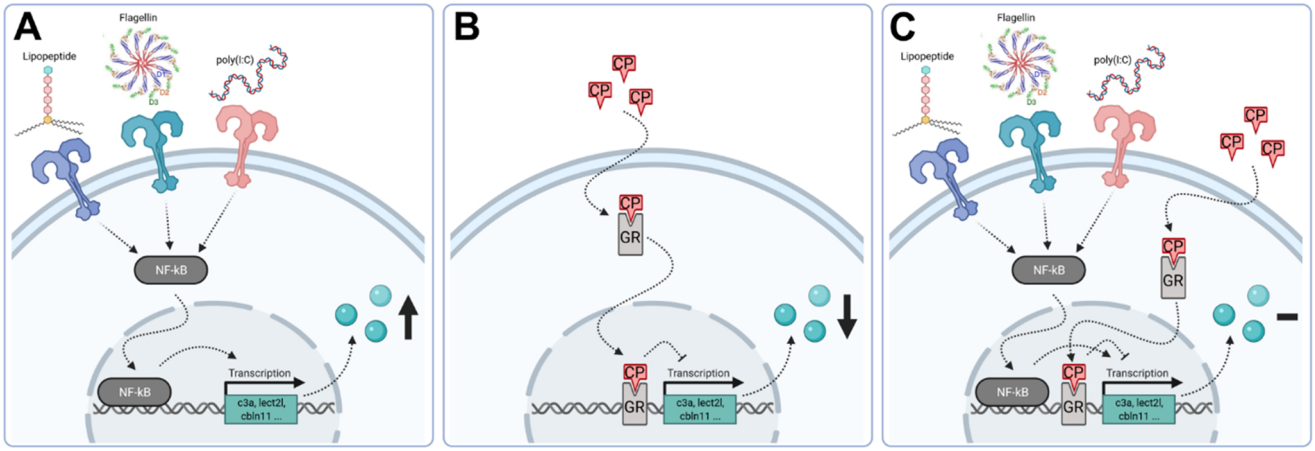

Fig. 6. Model of CP-mediated effects on PAMP-responsive genes. (A) PAMPs (lipopeptide, flagellin, and poly(I:C)) trigger NF-KB or AP1 (not shown) activation by binding to their respective Toll-like receptors (Tlrs). Activated NF-KB migrates to the nucleus, where it binds to its recognition sites on DNA, triggering activation of immune-responsive genes. (B) After entering the cell, CP binds to and activates the glucocorticoid receptor (GR). The activated GR migrates to the nucleus, where it binds to its recognition sites on DNA, triggering down-regulation of immune-responsive genes. (C) Activation of NF-KB by PAMPs and GR by CP leads to additive effects on their common immune-responsive target genes. In the case of opposing regulation by NF-KB and GR, the effects cancel each other out (as shown in this figure). In the case of same-direction regulation, the effects are additively enhanced (not shown in this figure).

immunosuppression, the hypo-responsive genes were significantly involved in immune and defense response to biotic stimuli (GO:0006952, GO:0006952, GO:0043207, GO:0009607) and in the antigen processing and presentation process (GO:0002474, GO:0048002, GO:0019882) (Fig. 5A). In contrast, the functions of the hyper-responsive genes were predominantly in drug response (GO:0042493) and the corresponding catabolic (GO:0042737, GO:0042738) and metabolic processes (GO:0017144). Network clustering of the over represented biological processes revealed that processes associated with the hypo-responsive genes were partially clustered separately from those associated with the non-responsive genes and were assigned to NF-KB, complement activation, and antigen presentation, whereas processes associated with the hypo-responsive genes were completely clustered separately and were associated with response to exogenous drugs (Fig. 5B).

Our findings therefore suggest, that immunosuppression by CP was triggered by CP-induced impairment of a subset of genes, which are differentially expressed in an immune response. A part of these genes are compounds of the complement system themselves. This is in line with previous studies, which have shown that glucocorticoids can modulate the expression of complement genes in human monocytes (Lappin and Whaley, 1991). Dampened activation of the complement cascade of the innate immune system would in turn lead to decreased stimulation of phagocytes and, consequently, impaired clearance of foreign material, ultimately leading to immunosuppression. A second major group of genes affected by CP exposure has critical functions in the antigen presentation pathway involving MHC class I. Previous studies have shown that corticosterone suppresses the formation of peptide-MHC class I complexes in dendritic cells in a GR-dependent manner, supporting our findings of glucocorticoid-mediated impairment of antigen presentation (Truckenmiller et al., 2005). Such impairment would subsequently lead to decreased activation of cytotoxic T cells and thus to an attenuated immediate immune response to non-self antigens.

4. Conclusion

Our approach allowed for a detection of molecular changes of an innate immune response at the gene as well as the functional level. Using the immunosuppressant CP, we demonstrated that gene expression changes after a single exposure to the drug differed significantly from those after additional immune activation. Thus, our study suggests that concurrent immune activation should be considered to detect and assess immunosuppressive effects. By molecular comparison of an immune challenge without and with previous exposure to CP, we identified immune-relevant genes and biological functions that were affected by this immunosuppressant and therefore represent promising marker candidates for assessing this mode of action. I.e. CP interfered with the pathogen-induced activation of complement expression and antigen presentation by dampening the induction of the corresponding gene sets involved. Notably, our results thereby argue for two independent mechanisms of gene expression regulation by PAMPs and CP rather than for an interconnection (Fig. 6). While these findings contribute to the establishment of key event relationships at the molecular level for AOP development (Ankley et al., 2010), the respective genes represent biomarker candidates for future studies and for environmental hazard assessments, which after validation can be used to detect immunosuppressive effects of substances. Application of our approach to additional model substances will allow to identify and validate appropriate biomarker candidates for a larger range of immunotoxic mechanisms of action, which will help to ensure that immunotoxicity issues can be increasingly addressed in the environmental hazard assessment of substances in the future using molecular markers.

CRediT authorship contribution statement

Fabian Essfeld performed the experiments, analyzed the data and wrote the manuscript. Hannes Reinwald contributed to bioinformatic data analysis. Gabriela Salinas supervised RNA sequencing. Christoph Schäfers and Elke Eilebrecht contributed to study design. Sebastian Eilebrecht designed and supervised the study and contributed to manuscript writing.

Declaration of competing interest

The authors declare that they have no known competing financial interests or personal relationships that could have appeared to influence the work reported in this paper.

Acknowledgements

This work was supported by the Fraunhofer Internal Programs under Grant No. Attract 040-600300. We especially thank Andrea Bräutigam, Computational Biology, Bielefeld University, for her valuable comments on this manuscript. Graphs and illustrations were generated with the

help of the freeware tools R / R Studio and Inkscape (www.inkscape.org). Graphical illustrations were generated using Biorender (www.biorender.com).

Appendix A. supporting information

Supplementary data associated with this article can be found in the online version at doi:10.1016/j.ecoenv.2022.113346.

References

Akira, Shizuo, Takeda, Kiyoshi, 2004. Toll-like receptor signalling. Nat. Rev. Immunol. 4 (7), 499–511. https://doi.org/10.1038/nri1391.

Anders, Simon, Pyl, Paul Theodor, Huber, Wolfgang, 2015. HTSeq—a Python framework to work with high-throughput sequencing data. ioinformatics. OXFORD ACADEMIC, pp. 166–169. https://doi.org/10.1093/bioinformatics/btu638.

Ankley, Gerald T., Edwards, Stephen W., 2018. The adverse outcome pathway: a multifaceted framework supporting 21st century toxicology. Curr. Opin. Toxicol. 9, 1–7. https://doi.org/10.1016/j.cotox.2018.03.004.

Ankley, Gerald T., Bennett, Richard S., Erickson, Russell J., Hoff, Dale J., Hornung, Michael W., Johnson, Rodney D., et al., 2010. Adverse outcome pathways: a conceptual framework to support ecotoxicology research and risk assessment. Environ. Toxicol. Chem. 29 (3), 730–741. https://doi.org/10.1002/etc.34.

Ewels, Philip, Magnusson, M.åns, Lundin, Sverker, Käller, Max, 2016. MultiQC: summarize analysis results for multiple tools and samples in a single report. Bioinformatics 32 (19), 3047–3048. https://doi.org/10.1093/bioinformatics/btw354.

Faltermann, Susanne, Hettich, Timm, Küng, Noemi, Fent, Karl, 2020. Effects of the glucocorticoid clobetasol propionate and its mixture with cortisol and different class steroids in adult female zebrafish. Aquat. Toxicol. 218, 105372 https://doi.org/10.1016/j.aquatox.2019.105372.

Futagi, Yuya; Narumi, Katsuya; Furugen, Ayako; Kobayashi, Masaki; Iseki, K. (2019): Molecular characterization of the orphan transporter SLC16A9, an extracellular pH- and Na+-sensitive creatine transporter. In undefined. Available online at https://www.ncbi.nlm.nih.gov/pubmed/31784090.

García-Valtanen, P., Martinez-Lopez, A., Ortega-Villaizan, M., Perez, L., Coll, J.M., Estepa, A., 2014. In addition to its antiviral and immunomodulatory properties, the zebrafish β-defensin 2 (zfBD2) is a potent viral DNA vaccine molecular adjuvant. Antivir. Res. 101, 136–147. https://doi.org/10.1016/j.antiviral.2013.11.009.

Harding, H.P., Lazar, M.A., 1993. The orphan receptor Rev-ErbA alpha activates transcription via a novel response element. Mol. Cell. Biol. 13 (5), 3113–3121. https://doi.org/10.1128/MCB.13.5.3113.

Hayashi, F., Smith, K.D., Ozinsky, A., Hawn, T.R., Yi, E.C., Goodlett, D.R., et al., 2001. The innate immune response to bacterial flagellin is mediated by Toll-like receptor 5. Nature 410 (6832), 1099–1103. https://doi.org/10.1038/35074106.

Herbomel, P. Thisse, B. Thisse, C. , 1999. Ontogeny and behaviour of early macrophages in the zebrafish embryo. In undefined. Available online at https://www.ncbi.nlm.nih.gov/pubmed/10433904.

Herrlich, P., 2001. Cross-talk between glucocorticoid receptor and AP-1. Oncogene 20 (19), 2465–2475. https://doi.org/10.1038/sj.onc.1204388.

Ignatiadis, Nikolaos, Klaus, Bernd, Zaugg, Judith, B., Huber, Wolfgang, 2016. Data-driven hypothesis weighting increases detection power in genome-scale multiple testing. Nat. Methods 13 (7), 577–580. https://doi.org/10.1038/nmeth.3885.

Johnson, Louise A., Jackson, David G., 2021. Hyaluronan and its receptors: key mediators of immune cell entry and trafficking in the lymphatic system. Cells 10 (8). https://doi.org/10.3390/cells10082061.

Karimi-Googheri, Masoud, Arababadi, Mohammad Kazemi, 2014. TLR3 plays significant roles against hepatitis B virus. Mol. Biol. Rep. 41 (5), 3279–3286. https://doi.org/10.1007/s11033-014-3190-x.

Kazak, Lawrence, Cohen, Paul, 2020. Creatine metabolism: energy homeostasis, immunity and cancer biology. Nat. Rev. Endocrinol. 16 (8), 421–436. https://doi.org/10.1038/s41574-020-0365-5.

Khalaf, Hazem, Jass, Jana, Olsson, Per-Erik, 2010. Differential cytokine regulation by NF-kappaB and AP-1 in Jurkat T-cells. BMC Immunol. 11, 26. https://doi.org/10.1186/1471-2172-11-26.

Kopp, Elizabeth B., Ghosh, Sankar, 1995. NF-κB and Rel Proteins in Innate Immunity. Adv. Immunol. 1–27.

Langmead, Ben, Salzberg, Steven L., 2012. Fast gapped-read alignment with Bowtie 2. Nat. Methods 9 (4), 357–359. https://doi.org/10.1038/nmeth.1923.

Lappin, D.F., Whaley, K., 1991. Modulation of complement gene expression by glucocorticoids. *Biochem. J.* 280 (Pt 1), 117–123. https://doi.org/10.1042/bj2800117.

Li, Heng, Handsaker, Bob, Wysoker, Alec, Fennell, Tim, Ruan, Jue, Homer, Nils, et al., 2009. The sequence alignment/map format and SAMtools. Bioinformatics 25 (16), 2078–2079. https://doi.org/10.1093/bioinformatics/btp352.

Liberman, Ana C., Druker, Jimena, Perone, Marcelo J., Arzt, Eduardo, 2007. Glucocorticoids in the regulation of transcription factors that control cytokine synthesis. Cytokine Growth Factor Rev. 18 (1–2), 45–56. https://doi.org/10.1016/j.cytogfr.2007.01.005.

Liu, Wenli, Rodgers, Griffin P., 2016. Olfactomedin 4 expression and functions in innate immunity, inflammation, and cancer. Cancer Metastas. Rev. 35 (2), 201–212. https://doi.org/10.1007/s10555-016-9624-2.

Livak, K.J., Schmittgen, T.D., 2001. Analysis of relative gene expression data using real-time quantitative PCR and the 2(-Delta Delta C(T)) Method. Methods 25 (4), 402–408. https://doi.org/10.1006/meth.2001.1262.

Love, Michael I., Huber, Wolfgang, Anders, Simon, 2014. Moderated estimation of fold change and dispersion for RNA-seq data with DESeq2. Genome Biol. 15 (12), 550. https://doi.org/10.1186/s13059-014-0550-8.

Lu, Xin-Jiang, Chen, Jiong, Yu, Chao-Hui, Shi, Yu-Hong, He, Yu-Qing, Zhang, Rui-Cheng, et al., 2013. LECT2 protects mice against bacterial sepsis by activating macrophages via the CD209a receptor. J. Exp. Med. 210 (1), 5–13. https://doi.org/10.1084/jem.20121466.

Lubbers, R., van Essen, M.F., van Kooten, C., Trouw, L.A., 2017. Production of complement components by cells of the immune system. Clin. Exp. Immunol. 188 (2), 183–194. https://doi.org/10.1111/cei.12952.

Luebke, R.W., Hodson, P.V., Faisal, M., Ross, P.S., Grasman, K.A., Zelikoff, J., 1997. Aquatic pollution-induced immunotoxicity in wildlife species. Fundam. Appl. Toxicol. 37 (1), 1–15. https://doi.org/10.1006/faat.1997.2310.

Luisi, B.F., Xu, W.X., Otwinowski, Z., Freedman, L.P., Yamamoto, K.R., Sigler, P.B., 1991. Crystallographic analysis of the interaction of the glucocorticoid receptor with DNA. Nature 352 (6335), 497–505. https://doi.org/10.1038/352497a0.

Mahmood, Isra, Imadi, Sameen Ruqia, Shazadi, Kanwal, Gul, Alvina, Hakeem, Khalid Rehman, 2016. Effects of Pesticides on Environment. In: Hakeem, Khalid Rehman, Akhtar, Mohd Sayeed, Abdullah, Siti Nor Akmar (Eds.), Plant, Soil and Microbes. Springer International Publishing, Cham, pp. 253–269.

Matsumoto, Misako, Seya, Tsukasa, 2008. TLR3: interferon induction by double-stranded RNA including poly(I:C). Adv. Drug Deliv. Rev. 60 (7), 805–812. https://doi.org/10.1016/j.addr.2007.11.005.

Mazurais, David, Servili, Arianna, Noel, Cyril, Cormier, Alexandre, Collet, Sophie, Leseur, Romane, et al., 2020. Transgenerational regulation of cbln11 gene expression in the olfactory rosette of the European sea bass (Dicentrarchus labrax) exposed to ocean acidification. Mar. Environ. Res. 159, 105022 https://doi.org/10.1016/j.marenvres.2020.105022.

Mottaz, H.élène, Schönenberger, Rene, Fischer, Stephan, Eggen, Rik I.L., Schirmer, Kristin, Groh, Ksenia J., 2017. Dose-dependent effects of morphine on lipopolysaccharide (LPS)-induced inflammation, and involvement of multixenobiotic resistance (MXR) transporters in LPS efflux in teleost fish. Environ. Pollut. 105–115. https://doi.org/10.1016/j.envpol.2016.11.046.

Neagu, Monica, Constantin, Carolina, Bardi, Giuseppe, Duraes, Luisa, 2021. Adverse outcome pathway in immunotoxicity of perfluoroalkyls. Curr. Opin. Toxicol. 25, 23–29. https://doi.org/10.1016/j.cotox.2021.02.001.

OECD, 2013. Test No. 236. Fish Embryo Acute Toxicity (FET) Test. OECD.

Andrews, Simon , 2010. FastQC. A quality control tool for high throughput sequence data. Available online at ⟨https://www.bioinformatics.babraham.ac.uk/projects/fastqc/⟩.

Aninye, Irene O., Matsumoto, Shunichi, Sidhaye, Aniket R., Wondisford, Fredric E., 2014. Circadian regulation of Tshb gene expression by Rev-Erbα (NR1D1) and nuclear corepressor 1 (NCOR1). J. Biol. Chem. 289 (24), 17070–17077. https://doi.org/10.1074/jbc.M114.569723.

Baxter, Matthew, Ray, David W., 2020. Circadian rhythms in innate immunity and stress responses. Immunology 161 (4), 261–267. https://doi.org/10.1111/imm.13166.

Beato, Miguel, 1989. Gene regulation by steroid hormones. Cell 56 (3), 335–344. https://doi.org/10.1016/0092-8674(89)90237-7.

Bhatt, Dev, Ghosh, Sankar, 2014. Regulation of the NF-κB-mediated transcription of inflammatory genes. Front. Immunol. 5, 71. https://doi.org/10.3389/fimmu.2014.00071.

Bolger, Anthony M., Lohse, Marc, Usadel, Bjoern, 2014. Trimmomatic: a flexible trimmer for Illumina sequence data. Bioinformatics 30 (15), 2114–2120. https://doi.org/10.1093/bioinformatics/btu170.

Borrello, S., Nicolò, C., Delogu, G., Pandolfi, F., Ria, F., 2011. TLR2: a crossroads between infections and autoimmunity? Int. J. Immunopathol. Pharmacol. 24 (3), 549–556. https://doi.org/10.1177/039463201102400301.

Bosscher, Karolien de, Vanden Berghe, Wim, Haegeman, Guy, 2003. The interplay between the glucocorticoid receptor and nuclear factor-kappaB or activator protein-1: molecular mechanisms for gene repression. Endocr. Rev. 24 (4), 488–522. https://doi.org/10.1210/er.2002-0006.

Caballero, Maria Virginia, Candiracci, Manila, 2018. Zebrafish as toxicological model for screening and recapitulate human diseases. JUMD 3 (2), 4. https://doi.org/10.20517/2572-8180.2017.15.

Cain, Derek W., Cidlowski, John A., 2017. Immune regulation by glucocorticoids. Nat. Rev. Immunol. 17 (4), 233–247. https://doi.org/10.1038/nri.2017.1.

Chen, Wen Qin, Hu, Yi. Wei, Zou, Peng Fei, Ren, Shi Si, Nie, Pin, Chang, Ming Xian, 2015. MAVS splicing variants contribute to the induction of interferon and interferon-stimulated genes mediated by RIG-I-like receptors. Dev. Comp. Immunol. 49 (1), 19–30. https://doi.org/10.1016/j.dci.2014.10.017.

Cheng, Kui, Wang, Xiaohui, Zhang, Shuting, Yin, Hang, 2012. Discovery of small-molecule inhibitors of the TLR1/TLR2 complex. Angew. Chem. Int. Ed. Engl. 51 (49), 12246–12249. https://doi.org/10.1002/anie.201204910.

Coulthard, Liam G., Woodruff, Trent M., 2015. Is the complement activation product C3a a proinflammatory molecule? Re-evaluating the evidence and the myth. J. Immunol. 194 (8), 3542–3548. https://doi.org/10.4049/jimmunol.1403068.

Dobin, Alexander, Davis, Carrie A., Schlesinger, Felix, Drenkow, Jorg, Zaleski, Chris, Jha, Sonali, 2013. STAR: ultrafast universal RNA-seq aligner. Bioinformatics 29 (1), 15–21. https://doi.org/10.1093/bioinformatics/bts635.

European Commission, 2020. Chemicals Strategy for Sustainability Towards a Toxic-Free Environment, 10/14/2020. ⟨https://ec.europa.eu/environment/pdf/chemicals/2020/10/Strategy.pdf⟩, checked on 2/18/2022.

Hidasi, Anita O., Groh, Ksenia J., Suter, Marc J.-F., Schirmer, Kristin, 2017. Clobetasol propionate causes immunosuppression in zebrafish (Danio rerio) at environmentally relevant concentrations. Ecotoxicol. Environ. Saf. 138, 16–24. https://doi.org/10.1016/j.ecoenv.2016.11.024.

Hochberg, Y., Benjamini, Y., 1990. More powerful procedures for multiple significance testing. Stat. Med. 9 (7), 811–818. https://doi.org/10.1002/sim.4780090710.

Niu, Donghong, Peatman, Eric, Liu, Hong, Lu, Jianguo, Kucuktas, Huseyin, Liu, Shikai, et al., 2011. Microfibrillar-associated protein 4 (MFAP4) genes in catfish play a novel role in innate immune responses. Dev. Comp. Immunol. 35 (5), 568–579. https://doi.org/10.1016/j.dci.2011.01.002.

Ong, Sheena L.M., Vos, Ivo J.H.M. de, Meroshini, M., Poobalan, Yogavalli, Dunn, N.Ray, 2020. Microfibril-associated glycoprotein 4 (Mfap4) regulates haematopoiesis in zebrafish. Sci. Rep. 10 (1), 11801. https://doi.org/10.1038/s41598-020-68792-8.

Ordas, Anita, Hegedus, Zoltan, Henkel, Christiaan V., Stockhammer, Oliver W., Butler, Derek, Jansen, Hans J., et al., 2011. Deep sequencing of the innate immune transcriptomic response of zebrafish embryos to Salmonella infection. Fish. Shellfish Immunol. 31 (5), 716–724. https://doi.org/10.1016/j.fsi.2010.08.022.

Pagès, Hervé; Carlson, Marc; Falcon, Seth; Nianhua, Li, 2017. AnnotationDbi: Bioconductor.

R Core Team, 2019. R: A Language and Environment for Statistical Computing. R Foundation for Statistical Computing,, Vienna, Austria. https://www.R-project.org/.

Rehberger, Kristina, Werner, Inge, Hitzfeld, Bettina, Segner, Helmut, Baumann, Lisa, 2017. 20 Years of fish immunotoxicology - what we know and where we are. Crit. Rev. Toxicol. 47 (6), 509–535. https://doi.org/10.1080/10408444.2017.1288024.

Reinwald, Hannes, König, Azora, Ayobahan, Steve U., Alvincz, Julia, Sipos, Levente, Göckener, Bernd, et al., 2021. Toxicogenomic fin(ger)prints for thyroid disruption AOP refinement and biomarker identification in zebrafish embryos. Sci. Total Environ. 760, 143914 https://doi.org/10.1016/j.scitotenv.2020.143914.

Reinwald, Hannes, Alvincz, Julia, Salinas, Gabriela, Schäfers, Christoph, Hollert, Henner, Eilebrecht, Sebastian, 2022. Toxicogenomic profiling after sublethal exposure to nerve- and muscle-targeting insecticides reveals cardiac and neuronal developmental effects in zebrafish embryos. Chemosphere 291 (Pt 1), 132746. https://doi.org/10.1016/j.chemosphere.2021.132746.

Rosi-Marshall, Emma J., Royer, Todd V., 2012. Pharmaceutical compounds and ecosystem function: an emerging research challenge for aquatic ecologists. Ecosystems 15 (6), 867–880. https://doi.org/10.1007/s10021-012-9553-z.

Rougeot, Julien, Torraca, Vincenzo, Zakrzewska, Ania, Kanwal, Zakia, Jansen, Hans J., Sommer, Frida, et al., 2019. RNAseq profiling of leukocyte populations in zebrafish larvae reveals a cxcl11 chemokine gene as a marker of macrophage polarization during mycobacterial infection. Front. Immunol. 10, 832. https://doi.org/10.3389/fimmu.2019.00832.

RStudio Team, 2020. RStudio: Integrated Development for R. In RStudio, PBC. Available online at http://www.rstudio.com/, checked on 9/14/2021.

Sánchez de Medina, Fermín, Ortega-González, Mercedes, González-Pérez, Raquel, Capitán-Cañadas, Fermín, Martínez-Augustin, Olga, 2013. Host-microbe interactions: the difficult yet peaceful coexistence of the microbiota and the intestinal mucosa. Br. J. Nutr. 109 (Suppl 2), S12–S20. https://doi.org/10.1017/S0007114512004035.

Schmid, Simon, Fent, Karl, 2020. 17β-Estradiol and the glucocorticoid clobetasol propionate affect the blood coagulation cascade in zebrafish. Environ. Pollut. https://doi.org/10.1016/j.envpol.2019.113808.

Sive, Hazel L., Grainger, Robert M., Harland, Richard M., 2010. Calibration of the injection volume for microinjection of Xenopus oocytes and embryos. pdb.prot5537. DOI Cold Spring Harb. Protoc. 2010 (12). https://doi.org/10.1101/pdb.prot5537, 17β-Estradiol and the glucocorticoid clobetasol propionate affect the blood coagulation cascade in zebrafish.

Stockhammer, Oliver W., Zakrzewska, Anna, Hegedûs, Zoltán, Spaink, Herman P., Meijer, Annemarie H., 2009. Transcriptome profiling and functional analyses of the zebrafish embryonic innate immune response to Salmonella infection. J. Immunol. 182 (9), 5641–5653. https://doi.org/10.4049/jimmunol.0900082.

Stockhammer, Oliver W., Rauwerda, Han, Wittink, Floyd R., Breit, Timo M., Meijer, Annemarie H., Spaink, Herman P., 2010. Transcriptome analysis of Traf6 function in the innate immune response of zebrafish embryos. Mol. Immunol. 48 (1–3), 179–190. https://doi.org/10.1016/j.molimm.2010.08.011.

Strähle, Uwe, Scholz, Stefan, Geisler, Robert, Greiner, Petra, Hollert, Henner, Rastegar, Sepand, et al., 2012. Zebrafish embryos as an alternative to animal experiments—a commentary on the definition of the onset of protected life stages in animal welfare regulations. Reprod. Toxicol. 33 (2), 128–132. https://doi.org/10.1016/j.reprotox.2011.06.121.

Surjit, Milan, Ganti, Krishna Priya, Mukherji, Atish, Ye, Tao, Hua, Guoqiang, Metzger, Daniel, et al., 2011. Widespread negative response elements mediate direct repression by agonist-liganded glucocorticoid receptor. Cell 145 (2), 224–241. https://doi.org/10.1016/j.cell.2011.03.027.

Team TBD, 2019. Full genome sequences for Danio rerio (UCSC version danRer11). Version 1.4.2. Available online at ⟨https://bioconductor.org/packages/3.14/data/annotation/html/BSgenome.Drerio.UCSC.danRer11.html⟩, checked on 11/26/2021.

Torra, I.P., Tsibulsky, V., Delaunay, F., Saladin, R., Laudet, V., Fruchart, J.C., et al., 2000. Circadian and glucocorticoid regulation of Rev-erbalpha expression in liver. Endocrinology 141 (10), 3799–3806. https://doi.org/10.1210/endo.141.10.7708.

Traver, D., Herbomel, P., Patton, E., Murphey, R., Yoder, J., Litman, G., Catic, A., Amemiya, C., Zon, L., Trede, N., et al., 2003. The Zebrafish as a Model Organism to Study Development of the Immune System. Adv. Immunol. 81, 253–330. https://doi.org/10.1016/S0065-2776(03)81007-6.

Truckenmiller, Mary E., Princiotta, Michael, F., Norbury, Christopher, C., Bonneau, Robert H., 2005. Corticosterone impairs MHC class I antigen presentation by dendritic cells via reduction of peptide generation. J. Neuroimmunol. 160 (1–2), 48–60. https://doi.org/10.1016/j.jneuroim.2004.10.024.

van der Vaart, Michiel, Spaink, Herman P., Meijer, Annemarie H., 2012. Pathogen recognition and activation of the innate immune response in zebrafish. Adv. Hematol. 2012, 159807 https://doi.org/10.1155/2012/159807.

Wald, Abraham, 1943. Tests of statistical hypotheses concerning several parameters when the number of observations is large. Trans. Am. Math. Soc. 54 (3), 426. https://doi.org/10.1090/S0002-9947-1943-0012401-3.

Wang, Zhiliang, Lu, Jiali, Li, Changzhi, Li, Qingwei, Pang, Yue, 2018. Characterization of the LECT2 gene and its protective effects against microbial infection via large lymphocytes in Lampetra japonica. Dev. Comp. Immunol. 79, 75–85. https://doi.org/10.1016/j.dci.2017.09.018.

Weikum, Emily R., Vera, Ian Mitchelle S. de, Nwachukwu, Jerome C., Hudson, William H., Nettles, Kendall W., Kojetin, Douglas J., Ortlund, Eric A., 2017. Tethering not required: the glucocorticoid receptor binds directly to activator protein-1 recognition motifs to repress inflammatory genes. Nucleic Acids Res. 45 (14), 8596–8608. https://doi.org/10.1093/nar/gkx509.

Willi, Raffael Alois, Faltermann, Susanne, Hettich, Timm, Fent, Karl, 2018. Active glucocorticoids have a range of important adverse developmental and physiological effects on developing zebrafish embryos. Environ. Sci. Technol. 52 (2), 877–885. https://doi.org/10.1021/acs.est.7b06057.

Willi, Raffael Alois, Salgueiro-González, Noelia, Carcaiso, Giulia, Fent, Karl, 2019. Glucocorticoid mixtures of fluticasone propionate, triamcinolone acetonide and clobetasol propionate induce additive effects in zebrafish embryos. J. Hazard. Mater. 374, 101–109. https://doi.org/10.1016/j.jhazmat.2019.04.023.

Wingett, Steven W., Andrews, Simon, 2018. FastQ screen: a tool for multi-genome mapping and quality control. F1000Research 7, 1338. https://doi.org/10.12688/f1000research.15931.2.

Wu, Zongfu, Zhang, Wei, Lu, Yan, Lu, Chengping, 2010. Transcriptome profiling of zebrafish infected with Streptococcus suis. Microb. Pathog. 48 (5), 178–187. https://doi.org/10.1016/j.micpath.2010.02.007.

Xie, Yufei, Tolmeijer, Sofie, Oskam, Jelle, M., Tonkens, Tijs, Meijer, Annemarie H., Schaaf, Marcel J.M., 2019. Glucocorticoids inhibit macrophage differentiation towards a pro-inflammatory phenotype upon wounding without affecting their migration. Dis. Models Mech. 12 (5) https://doi.org/10.1242/dmm.037887.

Xiong, Guanghua, Deng, Yunyun, Li, Jiali, Cao, Zigang, Liao, Xinjun, Liu, Yi, Lu, Huiqiang, 2019. Immunotoxicity and transcriptome analysis of zebrafish embryos in response to glufosinate-ammonium exposure. Chemosphere 236, 124423. https://doi.org/10.1016/j.chemosphere.2019.124423.

Yang, Shuxin, Marín-Juez, Rubén, Meijer, Annemarie, H., Spaink, Herman P., 2015. Common and specific downstream signaling targets controlled by Tlr2 and Tlr5 innate immune signaling in zebrafish. BMC Genom. 16 (1), 547. https://doi.org/10.1186/s12864-015-1740-9.

Zhang, Qinghua, Ji, Ce, Ren, Jianfeng, Zhang, Qiuyue, Dong, Xuehong, Zu, Yao, et al., 2018. Differential transcriptome analysis of zebrafish (Danio rerio) larvae challenged by Vibrio parahaemolyticus. J. Fish. Dis. 41 (7), 1049–1062. https://doi.org/10.1111/jfd.12796.

Zhu, Anqi, Ibrahim, Joseph, G., Love, Michael I., 2019. Heavy-tailed prior distributions for sequence count data: removing the noise and preserving large differences. Bioinformatics 35 (12), 2084–2092. https://doi.org/10.1093/bioinformatics/bty895.

Zhu, Junji, Liu, Xing, Cai, Xiaolian, Ouyang, Gang, Zha, Huangyuan, Zhou, Ziwen, et al., 2020. Zebrafish prmt3 negatively regulates antiviral responses. FASEB J. Off. Publ. Fed. Am. Soc. Exp. Biol. 34 (8), 10212–10227. https://doi.org/10.1096/fj.201902569R.

A4 Toxicogenomic differentiation of functional responses to fipronil and imidacloprid in *Daphnia magna*

Declaration of author contributions to the publication:

Toxicogenomic differentiation of functional responses to fipronil and imidacloprid in *Daphnia magna*

DOI: 10.1016/j.aquatox.2021.105927
Status: Published
Journal: **Aquatic Toxicology**

Contributing authors:
Pfaff J., (PJ), Reinwald H. (**RH**), Ayobahan S. (AS), Alvincz J. (AJ), Göckener B. (GB), Shomroni O. (SO), Salinas G. (SG), Düring R. (DR), Schäfers C. (SC) & Eilebrecht S. (ES)

(1) Concept and design

Doctoral candidate **RH**: 15% - design of RNA sequence raw processing pipeline; *D. magna* annotation concept
Co-author PJ: 30%
Co-author AS: 15%
Co-author ES: 30%
Co-author DR, SC: 10%

(2) Conducting tests and experiments

Doctoral candidate **RH**: 10% - Preliminary experiments for RNA extraction optimization
Co-author PJ: 70% - Exposure studies; RNA extraction; *in vitro* sample QC
Co-author SG,SO: 10% - mRNA-Sequence library preparation and Illumina HiSeq NGS
Co-author AJ,GB: 10% - Laboratory supervision; analytical chemistry

(3) Compilation of data sets and figures

Doctoral candidate **RH**: 20% - Compilation of raw sequencing data for downstream processing; coding support for figure generation and data visualization
Co-author PJ: 40% - Main manuscript figure illustration; exposure study data compilation
Co-author ES: 40% - Main manuscript figure illustration; concept and design; ORA figures

(4) Analysis and interpretation of data

Doctoral candidate **RH**: 35% - Raw sequencing data processing / mapping and corresponding data QC; providing source code for downstream analysis (DGEA) and technical support during data analysis steps; support for data interpretation and functional annotation
Co-author PJ: 30% - DGEA and feature selection; effect concentration determination; sample correlation analysis; sample clustering (PCA, t-SNE)
Co-author SA: 5% - Constructive feedback on data analysis approaches
Co-author GB: 10% - Chemical analytical quantification of tested substance concentrations
Co-author ES: 20% - Overrepresentation analysis via PANTHER web tool

(5) Drafting of manuscript

Doctoral candidate **RH**: 15%
Co-author PJ: 40%
Co-author ES: 35%
Co-author DR, SC: 10%

Aquatic Toxicology 238 (2021) 105927

Contents lists available at ScienceDirect

Aquatic Toxicology

journal homepage: www.elsevier.com/locate/aqtox

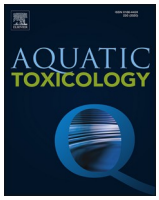

Toxicogenomic differentiation of functional responses to fipronil and imidacloprid in *Daphnia magna*

Julia Pfaff[a,b], Hannes Reinwald[a,c], Steve U. Ayobahan[a], Julia Alvincz[a], Bernd Göckener[d], Orr Shomroni[e], Gabriela Salinas[e], Rolf-Alexander Düring[b], Christoph Schäfers[f], Sebastian Eilebrecht[a,*]

[a] Fraunhofer Attract Eco'n'OMICs, Fraunhofer Institute for Molecular Biology and Applied Ecology, Schmallenberg, Germany
[b] Institute of Soil Science and Soil Conservation, Research Centre for BioSystems, Land Use and Nutrition (iFZ), Justus Liebig University Giessen, Giessen, Germany
[c] Department Evolutionary Ecology and Environmental Toxicology, Faculty Biological Sciences, Goethe University Frankfurt, Frankfurt, Germany
[d] Department Environmental and Food Analysis, Fraunhofer Institute for Molecular Biology and Applied Ecology, Schmallenberg, Germany
[e] NGS-Services for Integrative Genomics, University of Göttingen, Göttingen, Germany
[f] Department of Ecotoxicology, Fraunhofer Institute for Molecular Biology and Applied Ecology, Schmallenberg, Germany

ARTICLE INFO

Keywords:
Ecotoxicogenomics
D. magna
Neurotoxicity
Pathways
Biomarkers
Pesticides

ABSTRACT

Active substances of pesticides, biocides or pharmaceuticals can induce adverse side effects in the aquatic ecosystem, necessitating environmental hazard and risk assessment prior to substance registration. The freshwater crustacean *Daphnia magna* is a model organism for acute and chronic toxicity assessment representing aquatic invertebrates. However, standardized tests involving daphnia are restricted to the endpoints immobility and reproduction and thus provide only limited insights into the underlying modes-of-action. Here, we applied transcriptome profiling to a modified D. magna Acute Immobilization test to analyze and compare gene expression profiles induced by the GABA-gated chloride channel blocker fipronil and the nicotinic acetylcholine receptor (nAChR) agonist imidacloprid. Daphnids were expose to two low effect concentrations of each substance followed by RNA sequencing and functional classification of affected gene ontologies and pathways. For both insecticides, we observed a concentration-dependent increase in the number of differentially expressed genes, whose expression changes were highly significantly positively correlated when comparing both test concentrations. These gene expression fingerprints showed virtually no overlap between the test substances and they related well to previous data of diazepam and carbaryl, two substances targeting similar molecular key events. While, based on our results, fipronil predominantly interfered with molecular functions involved in ATPase-coupled transmembrane transport and transcription regulation, imidacloprid primarily affected oxidase and oxidoreductase activity. These findings provide evidence that systems biology approaches can be utilized to identify and differentiate modes-of-action of chemical stressors in *D. magna* as an invertebrate aquatic non-target organism. The mechanistic knowledge extracted from such data will in future contribute to the development of Adverse Outcome Pathways (AOPs) for read-across and prediction of population effects.

1. Introduction

Daphnia magna is used as a non-target aquatic invertebrate model species in guideline tests for ecotoxicological hazard and risk assessment of chemical compounds. These include active substances of plant protection products, biocides or pharmaceuticals, as well as industrial chemicals. The Organization for Economic Cooperation and Development (OECD) has developed two test guidelines using Daphnia as a test organism: the Daphnia sp. Acute Immobilization test (OECD TG 202) (OECD, 2004) and the D. magna reproduction test (OECD TG 211) (OECD, 2012). While the former test aims at the assessment of acute toxicity after 48 hours exposure using immobility as a lethal endpoint, the latter test is applied to identify chronic toxicity over a period of 21 days using reproduction and lethality as endpoints. Therefore, the readout of both guideline tests is limited in terms of mode-of-action classification of tests substances. This can be overcome by the

* Corresponding author.
E-mail address: sebastian.eilebrecht@ime.fraunhofer.de (S. Eilebrecht).

https://doi.org/10.1016/j.aquatox.2021.105927
Received 19 February 2021; Received in revised form 10 July 2021; Accepted 19 July 2021
Available online 27 July 2021

application of novel systems biology approaches, which enable a detection of gene expression changes at the whole transcriptome level. Recently, different studies combined acute or chronic toxicity testing in *D. magna* with gene expression profiling at the RNA level, either using *D. magna* custom microarrays or next generation sequencing of RNA in order to assess the molecular modes-of-actions of a variety of stressors. Song et al. (2016) (Song et al., 2016) used microarray-based transcriptomics to gain mechanistic insights into acute toxicity of the insecticide emamectin benzoate in *D. magna* and Poynton et al. (2012) (Poynton et al., 2012) applied a similar approach for the toxicity assessment of silver nanomaterials. More recently, Fuertes et al. (2019) analyzed the molecular effects of chronic exposures of single and combined neuroactive drugs in *D. magna*, including the positive allosteric modulator of GABA-gated chloride channels diazepam. In 2016, the *D. magna* reference transcriptome became available, allowing a detection of gene expression changes via next generation sequencing of RNA (Orsini et al., 2016). In the same study, differential gene expression induced by the acetylcholinesterase inhibitor carbaryl was assessed in *D. magna*. More recent studies applied RNA sequencing in *D. magna* for identifying toxicogenomic responses to anticancer drugs (Russo et al., 2018) and microplastics (Coady et al., 2020). Taken together, these previous studies contributed to the successful establishment of transcriptomics as a tool for toxicogenomic studies of chemical and environmental stressors in *D. magna*, which provides the basis for characterizing modes-of-action, identifying biomarkers, and developing and refining AOPs.

In this study, we aimed at answering the questions whether and how the modes-of-action of two different nerve- and muscle targeting insecticides can be distinguished at the molecular level by integrating RNA sequencing in a modified version of the D. magna Acute Immobilization test. We selected the widely used insecticides fipronil and imidacloprid as model substances in our study. Fipronil is an inhibitor of gamma-aminobutyric acid (GABA)-gated chloride channels, which causes reduced neuronal influx and finally results in a hyperexcitation of the nervous system, paralysis and death (Gunasekara et al., 2007; Wang et al., 2016). A study by Narahashi et al. (2010) has also identified fipronil as a blocker of glutamate-activated chloride channels in insects. In a recent study, Fuertes et al. (2019) analyzed gene expression changes in *D. magna* induced by the pharmaceutical diazepam. Diazepam is a positive allosteric modulator of GABA-gated chloride channels, whose interaction with the receptor promotes GABA binding, which in turn increases the receptor's conductivity for chloride ions and thereby results in hypoexcitation (Campo-Soria et al., 2006; Costa et al., 1978). Therefore, diazepam acts in an opposing manner when compared to fipronil both at the molecular level and at the level of resulting neurotransmission.

Unlike fipronil, the neonicotinoid imidacloprid acts as a competitive modulator of the nicotinic acetylcholine receptor (nAChR) (Matsuda et al., 2001). Since imidacloprid is not degraded by acetylcholinesterases, it acts more potently than the natural ligand acetylcholine (Cox, 2001; Nagata et al., 1998). The imidacloprid-nAChR interaction results in a permanent opening of the nAChR channel pore, which induces a permanent ion flux and thus causes membrane depolarization. The resulting excitatory post-synaptic potential finally leads to paralysis of the insect, and consequently to death. A recent study by Orsini et al. (2016) analyzed transcriptome-wide gene expression changes in *D. magna* after exposure to the insecticide carbaryl. Carbaryl belongs to the chemical class of carbamates, acting as a slowly reversible inhibitor of acetylcholinesterase (Fukuto, 1990). Such an inhibition interferes with the naturally rapid degradation of acetylcholine, resulting in an accumulation of the neurotransmitter. As a consequence, nAChRs are more frequently and longer activated than under normal physiological settings, which results in an excitatory post-synaptic potential. Thus, despite acting via different primary molecular mechanisms, carbaryl and imidacloprid both trigger an excitatory signaling as a downstream effect.

Fipronil and imidacloprid both induce similar adverse effects in *D. magna*, which are triggered by different molecular initiating events (MIEs), making these insecticides ideal model substances for our experimental approach. Previously published effects of diazepam and carbaryl, two compounds that target similar key molecular events as fipronil and imidacloprid, should add further weight of evidence to the current study. The ability to differentiate MIEs via gene expression fingerprints in a *D. magna* short term test would allow the identification of the primary mode-of-action of unknown test substances during environmental hazard assessment.

2. Materials and methods

2.1. Test substances

Fipronil (CAS 120068-37-3, $\geq$ 95 % purity) and imidacloprid (CAS 138261-41-3, $\geq$ 98 % purity) were purchased from Merck KGgA (Darmstadt, Germany). Imidacloprid test and control solutions were prepared using copper-reduced tap water. For fipronil, a stock solution was prepared in acetone. The same final volume of acetone was added to all vials of test and control solutions. Acetone was evaporated by aeration, before test and control solutions were prepared using copper-reduced tap water. The pH of all test solutions was 8.1 $\pm$ 0.1. Further analytical parameters of the tap water are listed in Table S1.

Data used for comparison of effects of diazepam and carbaryl were obtained from previous studies, which analyzed gene expression effects induced in juvenile *D. magna* after a four days exposure to 100 ng/L diazepam (CAS 439-14-5) (Fuertes et al., 2019) or a two days exposure to 8 µg/L carbaryl (CAS 63-25-2) (Orsini et al., 2016).

2.2. Test organism

The test organisms were 4 – 24 hours old, juvenile *D. magna*. Cladocerans were obtained from the German Federal Environment Agency, Institut für Wasser-, Boden- und Lufthygiene (Dessau, Germany). Adult daphnia were fed daily with an algal suspension (Desmodesmus subspicatus) and ArtemioFluid (JBL GmbH & Co. KG). Prior to test start, at least 3 weeks old adult daphnia were separated from the stock population by sieving, and batches of 30 to 50 animals were held at room temperature in approximately 1.8 L copper-reduced tap water. At test start, newborn *D. magna* were separated by sieving, and individuals applied in the test were transferred with a wide bore Pasteur pipette a few hours after sieving to ensure that only healthy organisms were used.

2.3. Test design

For detecting substance-induced gene expression changes at low effect concentrations, an Acute Immobilization Test with *D. magna* was performed similar to the corresponding OECD guideline test (OECD, 2004). To ensure sufficient material for downstream transcriptome analysis, the main difference to the guideline test was the use of 50 daphnids per replicate and three replicates per condition. In order to identify two low effect concentrations (approximately the EC5 and the EC20), range finding exposure experiments were performed in this setting for both test substances, based on published literature and the ECHA registration dossiers. For fipronil, previously reported EC50 values ranged from 14.6 to 190.0 µg/L (Chevalier et al., 2015b; Hayasaka et al., 2012; Stark and Vargas, 2005). The maximal acceptable toxicant concentration (the geometric mean of LOEC and NOEC) was reported as 14 µg/L (McNamara 1990a, b). For imidacloprid, previously reported EC50 values ranged from 43 to 94 mg/L (Chevalier et al., 2015b; Sanchez-Bayo and Goka, 2006; Tisler et al., 2009). The ECHA registration dossier reported a 48 hours NOEC of 42 mg/L. Concentration-response curves were obtained from the range finding exposure experiments by plotting the percentage of immobilized daphnids after 48 hours exposure against the test substance concentration

(Fig. S1). Data analysis and calculation of effect concentrations were performed by probit analysis using a linear maximum likelihood regression model (ToxRat v.3.0.0 software; ToxRat Solutions GmbH, Alsdorf, Germany). For the detection of gene expression changes induced by low effect concentrations of each test substance, the identified EC5 (low exposure, LE) and the EC20 (high exposure, HE) (see Fig. S1) as well as a non-treated (imidacloprid)/solvent-treated (fipronil) control per test substance were analyzed in triplicate.

The test was conducted at 21.0 ± 0.3°C with a 16:8 h light/dark cycle. Prior to test start, 250 mL glass beakers were pre-saturated with each test solution. Then 50 juvenile daphnids per condition and replicate were added to each of the saturated glass beakers containing 150 mL of fresh, aerated test solutions. At test start, the oxygen saturation of all test solutions was 97 ± 1 % (8.25 ± 0.16 mg/L). Further water quality parameters are listed in Table S1. The oxygen saturation at test end was 91 ± 3 % (7.67 ± 0.23 mg/L). During the test, all glass beakers were loosely covered with a plexiglass plate to minimize evaporation. At 24 and 48 hours after test start, immobile daphnids were removed and counted as well as abnormal behavior and appearance were recorded.

For the detection of substance-induced gene expression changes at 48 hours after test start, the mobile daphnids of each test condition were transferred to 1.5 mL reaction tubes containing a mixture of sterile glass beads of 1 and 5 mm diameter. The supernatant was removed and the daphnids were euthanized immediately in liquid nitrogen. After the addition of 350µl lysis buffer (RNA/protein extraction kit, Macherey&Nagel), the daphnids were homogenized mechanically at 5 m/s for 10 s at room temperature using a FastPrep-24© homogenizer (MP Biomedicals, Irvine, USA). Total RNA was isolated using an RNA/protein extraction kit as recommended by the manufacturer (Macherey&Nagel). RNA was quantified using a Nanodrop system (Thermo Fisher Scientific, Waltham, USA) and quality was assessed with a 2100 Bioanalyzer system (Fig. S2) on the basis of the 28S/18S ratio (Agilent, Santa Clara, USA) prior to RNA-Seq library preparation.

2.4. Chemical analysis

Nominal test concentrations for fipronil were 16 µg/L and 32 µg/L, those for imidacloprid were 42 mg/L and 64 mg/L, corresponding to the EC5 and EC20 of each compound, respectively. The measured concentrations of both test substances in the aqueous solutions were determined by chemical analysis (Table 1). A detailed description of the analytical method is given in the supporting information section. Briefly, the aqueous samples were diluted with acetonitrile and were analyzed by high performance liquid chromatography coupled with tandem mass spectrometry (HPLC-MS/MS). Both methods were successfully validated according to the EU guideline SANCO/3029/99 at a limit of quantification (LOQ) of 0.5 µg/L (fipronil) and 0.1 mg/L (imidacloprid), respectively (European Commission, 2000).

2.5. Transcriptomics

For transcriptome library preparation, RNA samples with a 28S/18S ratio > 2.0 were selected, assuring the analysis of high quality RNA. Poly (A)+ RNA was purified from total RNA and subjected to library preparation, using the TruSeq RNA Library Prep Kit v2 as recommended by the manufacturer (Illumina, San Diego, USA). Libraries were sequenced on an Illumina HiSeq 4000 System (Illumina, San Diego, USA) in 50 bp single read mode, producing approximately 30 million raw reads per sample. Adapter sequences were removed from demultiplexed fastq files by trimmomatic (Bolger et al., 2014), and sequence quality was assured via FastQC (Andrews, 2010). Sequences were aligned to the *D. magna* reference genome (daphmag2.4, GCA_001632505.1), containing a total of 27,350 genes, with STAR aligner v.2.5.2a (Dobin et al., 2013), resulting in alignment rates between 86.4% and 95.4%. Feature mapped reads were counted in feature-Counts v1.5.0-p1 (Liao et al., 2014). Mapped read tables were merged into a single count matrix for each substance and analyzed in R (R Core Team, 2019) via RStudio (Loraine et al., 2015). After removing genes with 0 counts in at least one of the analyzed samples, count normalization and differential expression analysis was performed in DESeq2 v1.26.0 (Love et al., 2014). This was based on three biological replicates per condition applying pairwise Wald's t-test with independent hypothesis weighting (IHW) (Ignatiadis et al., 2016). P-values were corrected after Benjamini-Hochberg. To measure the effect between the conditions while controlling replicate differences, a multifactor model design was used, including replicate as random factor to account for the variability among the independent biological replicates. Biological effect size cut off was determined for each treatment comparison as the 90 % quantile of the absolute non-shrunk $\log_2$-fold change values, focusing only on the top 10% with largest fold change values. $\log_2$-fold changes were then shrunk with apeglm (Zhu et al., 2019). The final set of differentially expressed genes (DEGs) was selected after statistical significance (padj < 0.05) and the individual effect size cut off. Raw and processed data have been deposited in the ArrayExpress database at EMBL-EBI (www.ebi.uk/arrayexpress) (Athar et al., 2019) under accession numbers E-MTAB-9829 (fipronil) and E-MTAB-9830 (imidacloprid). Data quality assessment is shown in Figs. S3–S5. The DEG analysis script is publicly available under: https://github.com/hreinwal/DESeq2Analysis (Reinwald et al., 2021).

Genes of the compound-specific signatures (common subsets of DEGs by LE and HE for each test compound) were functionally annotated using BLASTX (Sayers et al., 2021). Briefly, coding sequences from Ensembl Biomart (Howe et al., 2021) were subjected to a BLASTX search against the non-redundant protein sequence database. If available, the hit among the characterized proteins with the lowest E-score was assigned to the respective gene. Assigned protein hits were functionally annotated manually via literature research.

To compare the results of this study with previous data obtained by Orsini et al. (2016), we identified DEGs induced by carbaryl in *D. magna* by applying an analysis pipeline similar to the above mentioned one to the carbaryl data of the NCBI BioProject with the accession number PRJNA284518. For comparative assessment of data obtained in a previous study after exposure of *D. magna* to diazepam (Fuertes et al., 2019), statistically differentially ($p \leq 0.05$) expressed genes after diazepam exposure were identified by the GEO2R (Barrett et al., 2013) on the diazepam-treated and control samples of the GEO dataset with the accession number GSE131587 (Fuertes et al., 2019). Agilent-066414 D. magna 180k v2 microarray probe IDs were converted to *Daphnia pulex* gene IDs via the corresponding JGI IDs obtained from the Agilent-066414 D. magna 180k v2 microarray annotation file (Campos et al., 2018)(GEO accession number GPL22721). *Daphnia pulex* gene IDs were then converted to the corresponding uniquely mapped *D. magna* (daphmag2.4) homologues with high orthology confidence using ENSEMBL Biomart (Kinsella et al., 2011).

2.6. Gene set enrichment analysis for gene ontology and functional classification

For gene set enrichment analysis (GSEA) on gene ontology (GO) and functional classification, the PANTHER classification system (Mi et al., 2013, 2019) was used. As this system supports *Daphnia pulex* gene IDs, but not *D. magna* gene IDs, the latter ones (daphmag2.4) were first converted to the corresponding *D. pulex* (V1.0) homologues using ENSEMBL Biomart (Kinsella et al., 2011). Only genes with a one-to-one mapping and high orthology confidence (orthology confidence score = 1) between *D. magna* and *D. pulex* were considered for GSEA. This gene set contained a total of 10,323 genes. To obtain comparable results between both substances, only the common set of transcripts detected in both exposure experiments (fipronil & imidacloprid) were used for the analysis. GSEA was performed via the statistical enrichment test of the PANTHER classification system (Mi et al., 2013, 2019), using *Daphnia pulex* gene IDs and the corresponding DESeq2-generated apeglm shrunk

log_2-fold change values as input. The three main GO types biological process (BP), molecular function (MF), and cellular component (CC) were analyzed separately. P-values were corrected for multiple testing following Benjamini−Hochberg and ontologies considered as significantly enriched for padj ≤ 0.01. Ontologies and conditions were clustered by Euclidean distance in R (R Core Team, 2019) via RStudio (Loraine et al., 2015). Functional classification of gene sets was performed on the basis of the corresponding converted *Daphnia pulex* gene IDs, using the PANTHER classification system (Mi et al., 2013, 2019).

3. Results

3.1. Selection of low effect concentrations of fipronil and imidacloprid in D. magna

For fipronil, we obtained an EC50 of 70 μg/L, an EC20 of 32 μg/L and an EC5 of 16 μg/L (Fig. S1). Based on these effect concentrations, we selected nominal exposure concentrations of 32 μg/L and 16 μg/L as high (HE) and low exposure concentrations (LE) for gene expression profiling (measured concentrations of 25.7 μg/L (HE) and 11.4 μg/L (LE), respectively) (Table 1). For imidacloprid, we obtained an EC50 of 97 mg/L, an EC20 of 64 mg/L and an EC5 of 42 mg/L (Fig. S1). Therefore, we selected nominal exposure concentrations of 64 mg/L as HE and 42 mg/L as LE for gene expression profiling using imidacloprid (measured concentrations of 63.9 mg/L and 42.5 mg/L, respectively) (Table 1).

To validate the choice of low effect concentrations for both substances, we recorded immobility after 48 hours exposure for each test condition (Table 2). While the low exposure concentration in both cases did not induce immobility (one-way ANOVA) relative to the corresponding control condition, the high exposure concentration caused significant immobility by 15 and 19 percent in the case of fipronil and imidacloprid, respectively.

3.2. Transcriptome response to fipronil

Exposure to the LE of fipronil resulted in a total of 83 differentially expressed genes (DEGs, padj ≤ 0.05), of which 8 genes were up- and 75 genes were down-regulated, while the exposure to the HE caused 875 DEGs, of which 74 genes were up- and 801 genes were down-regulated (Fig. 1A). Seventy-nine genes (95% of DEGs after exposure to the LE) were statistically significantly dysregulated under both exposure conditions (Fig. 1B). Without exception, these genes were simultaneously dysregulated by exposure to the LE and HE, showing a strong positive correlation (R = 0.85) when comparing the log_2-fold change values for both conditions (Fig. 1C). For these reasons, we defined this common DEG subset of LE and HE as fipronil-specific gene expression signature in *D. magna*. Using BLASTX sequence homology searches for the coding sequences, 61 (77%) of these genes could be linked to known proteins (Table S2). Twenty of these (33%) were related to the cuticle and to proteins involved in chitin synthesis and metabolism, such as cuticular proteins (Marcu and Locke, 1998), endochitinase (Koga et al., 1983) or keratin-associated proteins. Eight proteins (13%) were linked to organelle and cellular architecture, including spidroin, extensin, cell wall components and the coiled-coil domain containing protein 9. Another larger proportion of 7 proteins (11%) was related to lipid metabolism, such as the SEC14 protein 2, phospholipase D1 or carboxylesterase 3. Smaller protein sets were involved in functions such as digestion, immune defense, RNA processing, gene expression regulation, acid-based regulation, movement, transport, and stress response. We identified 4-aminobutyrate aminotransferase, an enzyme involved in GABA catabolism, as a significantly down-regulated member of the annotated DEGs of the fipronil-specific signature (Madsen et al., 2008).

The remaining genes, affected in a statistically significant manner by only one of the exposure conditions, showed a high degree of positive correlation (R = 0.80), even though not statistically significantly regulated in the respective other condition. Globally, we observed a concentration-dependent regulation of DEGs, showing generally higher log_2-fold change values after exposure to the HE than after exposure to the LE (Fig. 1C). To identify biological processes affected by fipronil, we performed functional classification analyses with all fipronil-responsive genes. For this, we used only unique genes from both treatment groups. While 20.5% of the genes were assigned to general cellular processes, almost equal proportions ranging from 7.5 to 14.2% were assigned to multi-organism processes, biological regulation, response to stimulus, signaling, developmental processes, multicellular organismal processes, metabolic processes, and immune system processes (Fig. 1D). Only 1 and 2.4% of the genes were involved in cellular component organization or biogenesis and localization, respectively.

3.3. Transcriptome response to imidacloprid

In the case of imidacloprid, exposure to the LE resulted in a total of 35 DEGs, of which 32 genes were up- and 3 genes were down-regulated (Fig. 2A). Ninetyfour DEGs were observed after exposure to the HE, of which 66 genes were up- and 28 genes were down-regulated. Nineteen DEGs of the LE condition (54%) were also significantly differentially expressed after exposure to the HE (Fig. 2B). As it was the case for fipronil, the common subset of DEGs induced by the LE and the HE of imidacloprid – the imidacloprid-specific signature – was highly positively correlated (R = 0.96) (Fig. 2C). Three genes of this signature coded for known or putative proteins of the class of aminopeptidase N. BLASTX sequence homology searches revealed linkage to known proteins for 13 genes (68%) of the imidacloprid-specific signature (Table S3). Including the aminopeptidase N-related proteins, the largest set of five of these proteins was involved in digestive functions, while the smaller protein sets had functions involved in movement and immune defense. Imidacloprid exposure led to a significant up-regulation of neuropeptide-like protein 31, which belongs to a class of proteins involved in neuronal plasticity and immune regulation, among other functions (De Fruyt et al., 2020; Urbanski and Rosinski, 2018).

The remaining genes, representing DEGs in only one of the exposure conditions, were also highly positively correlated relative to the corresponding other condition (R = 0.88). For imidacloprid, the concentration-dependence of the log_2-fold change values was less pronounced than for fipronil. Reflecting the generally lower number of DEGs in comparison to fipronil, the imidacloprid target genes represented a lower number of biological processes (Fig. 2D). While the largest proportion of 28.6% of these genes was assigned to general cellular processes, almost equal fractions of 14.3 to 17.9% were involved in response to stimulus, signaling, metabolic processes, and biological regulation. Only 7.1% of the imidacloprid targets were assigned to processes associated with localization.

3.4. Differentiation of molecular changes induced by fipronil and imidacloprid

For assessing specificity at the gene expression level, we compared the identified gene expression signatures of each treatment for both test substances (Fig. 3A).

While the common subsets of LE and HE of each single substance were highly significant, there was no common subset of the LE treatments of both substances. As a consequence, the compound-specific signatures were unique. A minor set of 6 genes was located in the common subset of both HE treatments, of which 3 genes were also significantly affected in the LE treatment of imidacloprid. A set of 3 genes was also commonly regulated when comparing the HE treatment of fipronil and the LE treatment of imidacloprid. Of these 9 genes in the common subset of both substance exposures, 4 genes were regulated in a similar direction and 5 genes were regulated in an opposing direction when comparing fipronil and imidacloprid (Fig. S6). Seven genes (78%) of this intersection could be linked to known proteins using BLASTX

sequence homology searches (Table S4). Dehydogenase/reductase SDR family member 4 (dhrs4) was down-regulated under the HE condition of fipronil and up-regulated under the comparable condition of imidacloprid, whereas decaprenyl diphosphate synthase subunit 2 (pdss2) was down-regulated and C1q and tumor necrosis factor-related protein 3-like protein (ctrp3) was up-regulated in both cases. The transcription regulatory protein LGE1-like and the keratin-associated protein 19-2-like were both down-regulated under the HE condition of fipronil and up-regulated under the LE condition of imidacloprid. A cysteine-rich protein and mucin-2-like isoform X1 were up-regulated by both compounds.

Nevertheless, the vast majority of fipronil and imidacloprid target genes was either affected by the corresponding substance only, or the direction of regulation allowed for a discrimination between both substances. The compound-specific gene expression signatures, containing the intersecting DEGs of each LE and HE condition (79 genes for fipronil and 19 genes for imidacloprid), separated well between both substances (Fig. 3B).

Given the high degree of specificity of each gene expression signature, we further aimed at a functional classification of the observed responses. We performed a gene set enrichment (GSE) analysis of each treatment condition and each test substance for the gene ontology types, biological process (BP), molecular function (MF), cellular component (CC), as well as for PANTHER pathways.

As the organism *D. magna* is not supported in the PANTHER classification system (Mi et al., 2013, 2019), analysis was performed based on the converted uniquely mapping *D. pulex* gene orthologs. For all gene ontologies and for PANTHER pathways, we observed a significant agreement between up- and down-regulation when comparing LE and HE exposure for both test substances (Figs. 4 and S7). As for the gene expression signatures, the ontologies MF and BP and the PANTHER pathways allowed for a clear differentiation between the test substances (Figs. 4A and B and S7A), while the ontology CC did not discriminate between fipronil and imidacloprid, suggesting that both substances affect similar cellular components (Fig. S7B).

A prominent proportion of molecular functions affected by fipronil exposure was associated with DNA binding and transcription regulation (Fig. 4A). A second major fraction of fipronil-responsive molecular functions was involved in ATPase-coupled transmembrane transport of protons (Fig. 4A). In terms of pathway regulation, fipronil exposure affected a number of metabolic routes including ATP synthesis and cholesterol biosynthesis (Fig. 4B). Furthermore, fipronil exposure, significantly impaired metabotropic glutamate receptor signaling and a pathway associated with the Alzheimers disease-presenilin pathway in mammals (Fig. 4B).

In contrast, imidacloprid mainly impaired oxidase and oxidoreductase molecular functions as well as CoA ligase activity (Fig. 4A). Imidacloprid exposure also affected a number of metabolic pathways, which differed from those impaired by fipronil exposure (Fig. 4B). Among the most significantly repressed pathways were those associated with the Parkinson disease pathway and vasopressin synthesis in mammals. Furthermore, imidacloprid exposure also impaired GABA synthesis and aminobutyrate degradation (Fig. 4B).

3.5. Assessment of mode-of-action specificity using previously published results

For comparative gene expression analysis of fipronil and diazepam in *D. magna*, we identified DEGs ($p \leq 0.05$) after diazepam exposure by analyzing previous data obtained by Fuertes et al. (2019). Comparing these diazepam target genes with the target genes of the exposure to the HE of fipronil (padj ≤ 0.05), we observed a total of 20 assignable genes in the common subset of both substances (Fig. S8). Plotting their expression changes after exposure to each substance in a scatter plot reveals a negative correlation (QCR = -0.50) (Fig. S8).

For comparing imidacloprid- and carbaryl-induced gene expression changes, we identified DEGs (padj ≤ 0.05) after carbaryl exposure from data obtained in the study by Orsini et al. (2016), and compared them to DEGs observed after exposure to the HE of imidacloprid. Out of 58 carbaryl target genes, a highly significant (hypergeometric distribution p-value = 2.78E-8) proportion of 9 genes was also statistically significantly regulated by imidacloprid. Plotting their expression changes after exposure to each substance in a scatter plot revealed a highly positive correlation (QCR = 1.00) (Fig. S9).

4. Discussion

Our study aimed to determine whether an extension of the Acute Immobilization test with *D. magna* to include transcriptome analyses after exposure to low effect concentrations would allow characterization and differentiation of modes-of-action at the molecular level. Effect concentrations in our study were within the range of the ECHA registration dossier (EC50 = 85 mg/L) and previous literature (EC50 = 94 mg/L) (Chevalier et al., 2015a), especially for imidacloprid. In the case of fipronil, the EC50 value we determined was also in the range of some previous studies (88.3 µg/L) (Hayasaka et al., 2012), but on average higher than previously determined values (Chevalier et al., 2015a). This discrepancy may be related to the nominally determined effect concentrations in our study, since the measured fipronil concentrations in the main test were only about 70-80% of the nominal concentrations, while for imidacloprid measured and nominal concentrations matched well.

A first indication of differentiability of fipronil and imidacloprid with our approach was provided by the direction of regulation of the respective target genes. While in the case of fipronil the majority of genes were down-regulated, imidacloprid preferentially caused activation of its target genes, which could be explained by the downstream signaling of the respective receptors involved. Whereas fipronil blocks the GABA receptor, causing a prevention of GABA-induced downstream processes, imidacloprid permanently activates the nAChR and thus specifically triggers downstream signaling pathways.

Our results suggest that fipronil can induce early effects with potential consequences for molting, supporting previous studies, which reported fipronil-dependent effects on molting in the juvenile brown shrimp *Farfantepenaeus aztecus* (Al-Badran et al., 2018). Carbonic anhydrase 1 and 14, which play important neurophysiological roles in pH and ion regulation (Emameh et al., 2014), were dysregulated by fipronil exposure, representing a possible response to blocked chloride ion currents. Fipronil-induced changes in carboxylesterase 3 expression may represent a defense mechanism, as this enzyme has been previously shown to play a role in pesticide detoxification (Wheelock et al., 2005). A larger proportion of DEGs regulated by fipronil could be linked to lipid metabolism. A study by Enell et al. (2010) (Enell et al., 2010) has shown that GABA can inhibit insulin signaling in its regulation of metabolism, stress and life span in the brain of *Drosophila melanogaster*. This provides a possible linkage between GABA receptor blocking and lipid metabolic processes, as insulin was shown previously to play an important role in lipid metabolism (Saltiel and Kahn 2001). The observed downregulation of 4-aminobutyrate aminotransferase, an enzyme involved in the degradation of GABA, may represent a feedback mechanism designed to counteract the low activity of the blocked GABA receptors (Cocco et al., 2017; Zheng et al., 2021).

On the other hand, imidacloprid dysregulated the expression of aminopeptidase N and related proteins, which play roles in dietary protein digestion and as receptors during Cry toxin-induced pathogenesis (Ningshen et al., 2013). While the relationship between nAChR activation and aminopeptidase N expression still remains elusive, the observed imidacloprid-induced upregulation of neuropeptide-like protein 31 may represent a response to permanent activation of nAChRs, as certain neuropeptides have been shown to reduce acetylcholine release in humans (Herring et al., 2008; Wiley et al., 1990). Though some neuropeptides have also been identified and characterized in

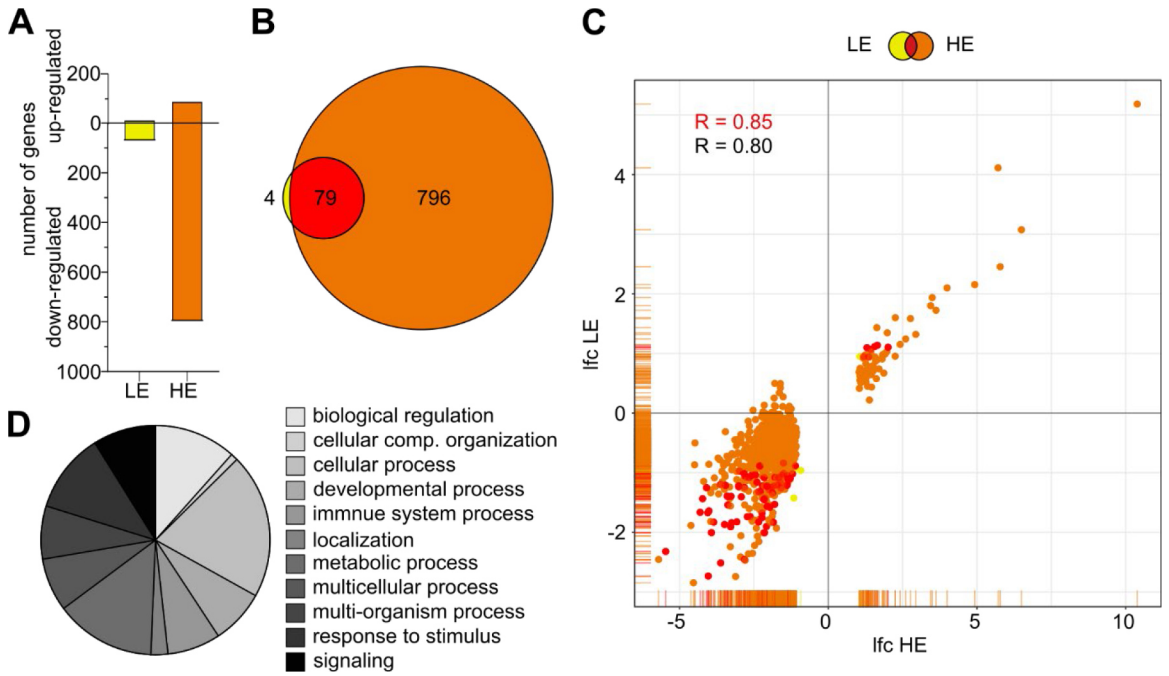

Fig. 1. Transcriptome response of *D. magna* to exposure to the LE and HE of fipronil after 48 hours. (A) Gene numbers of statistically significant (padj $\leq$ 0.05) up- and down-regulated genes after exposure to 11.4 µg/L (LE, yellow) and 25.7 µg/L (HE, orange). (B) Venn diagram showing differentially expressed genes (DEGs) after exposure to 11.4 µg/L (yellow) and 25.7 µg/L (orange) fipronil as compared to the non-treated controls. Displayed circles and the intersection size correspond to the numbers of DEGs. (C) Scatter plot comparing $\log_2$-fold change (lfc) values of DEGs observed after low and high exposure to fipronil. The common subset of both exposures is colored in red and considered as substance-specific signatures. (D) Circle plot showing a functional classification analysis of all fipronil-induced DEGs. Biological processes associated with these genes are indicated.

invertebrates (Xu et al., 2016), their physiological roles in *D. magna* require further research. A member of the imidacloprid target family of dhrs proteins is also a target of the ecdysone response in honeybee caste development (Guidugli et al., 2004), providing a linkage to impaired molting.

Among the few gene targets of both test substances, pdss2 was down- and ctrp3 was up-regulated in both cases. For defective mutations of pdss2, Parkinson's-like neuromuscular defects were observed in mice in

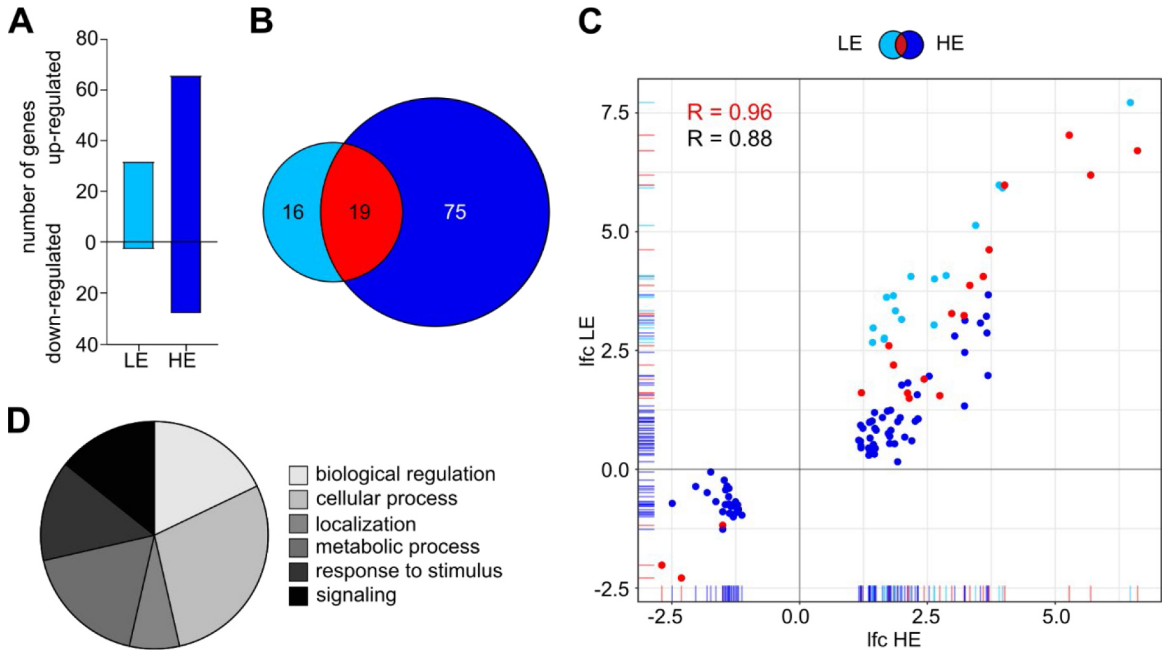

Fig. 2. Transcriptome response of *D. magna* to exposure to the LE and HE of imidacloprid after 48 hours. (A) Gene numbers of statistically significant (padj $\leq$ 0.05) up- and down-regulated genes after exposure to 42.5 mg/L (LE, light blue) and 63.9 mg/L (HE, dark blue). (B) Venn diagram showing differentially expressed genes (DEGs) after exposure to 42.5 mg/L (light blue) and 63.9 mg/L (dark blue) imidacloprid as compared to the non-treated controls. Displayed circles and the intersection size correspond to the numbers of DEGs. (C) Scatter plot comparing $\log_2$-fold change (lfc) values of DEGs observed after low and high exposure to imidacloprid. The common subset of both exposures is colored in red and considered as substance-specific signatures. (D) Circle plot showing a functional classification analysis of all imidacloprid-induced DEGs. Biological processes associated with these genes are indicated.

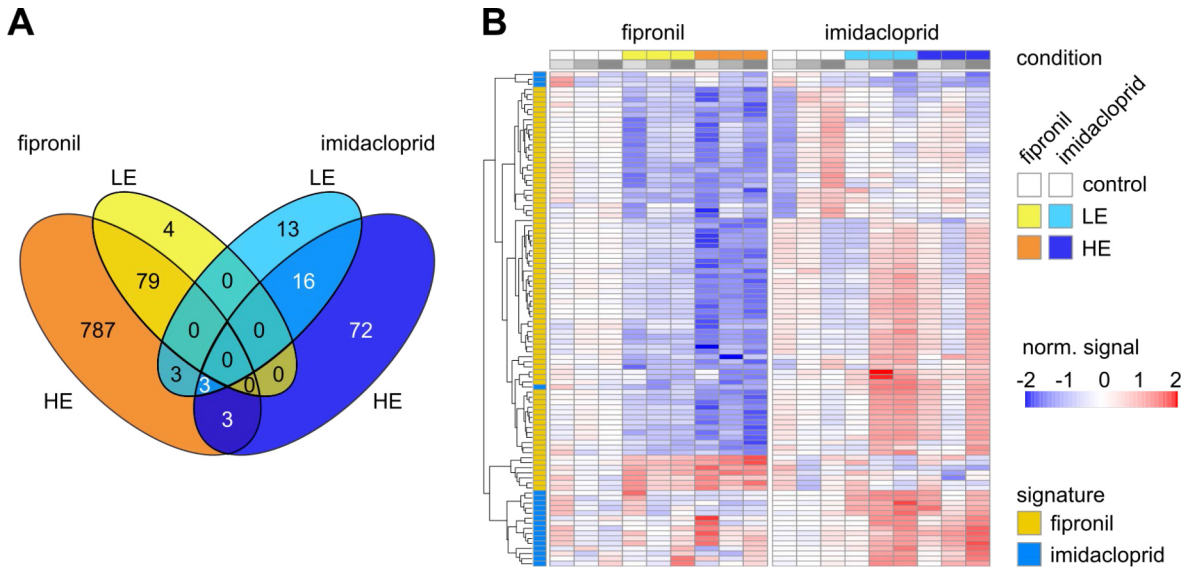

Fig. 3. Comparative functional genomics of fipronil and imidacloprid in *D. magna*. (A) Venn diagram of DEGs in the low (LE, yellow) and high exposure condition (HE, orange) for fipronil and the low (LE, light blue) and high exposure condition (HE, dark blue) for imidacloprid. Numbers indicate the DEG count for the corresponding common subset. (B) Heatmap containing the signature genes of each test substance, which are indicated in red in Figure 1 and Figure 2. The relative signal normalized to the control within each treatment of each gene (rows) is shown for each sample (columns). As compared to the mean of each non-treated control, an enhanced expression is indicated in red and a suppressed expression is indicated in blue. Genes are clustered after maximum distance measure with average linkage. The association with a fipronil or an imidacloprid signature is indicated in yellow and light blue, respectively.

a previous study (Ziegler et al., 2012), while ctrp3 has been previously associated with neuromuscular disorders in mice (Rehorst et al., 2019), directly linking both gene products to proper neuronal function in mammals. Dhrs4, which was down-regulated by fipronil and up-regulated by imidacloprid, is involved in retinoic acid synthesis in mammals (Endo et al., 2009). In line with these findings, neonicotinoid treatment has been previously shown to interfere with the retinoid system in bees (Gauthier et al., 2018), while Sarti et al. (2013) have shown that retinoic acid reduces GABA signaling in mammals by inducing receptor internalization (Sarti et al., 2013). In the case of fipronil, suppression of dhrs4 could lead to decreased retinoic acid synthesis, which could provide a feedback mechanism for GABA receptor blocking.

Taken together, at the gene level, the observed signatures for fipronil and imidacloprid separate well between both substances without major overlaps, and therefore, may be utilized in future ecotoxicogenomic studies to discriminate the corresponding modes-of-action in *D. magna*.

At the functional level, an interconnection of ligand-gated chloride channel activity with transcription regulatory pathways, such as the Wnt signaling pathway, was shown in previous studies in humans (Rapetti-Mauss et al., 2020). Therefore, fipronil-induced changes in transcription regulation may result from signaling cascades downstream of GABA-gated chloride channel activity, such as Wnt signaling, which is common in invertebrates and vertebrates (Holstein, 2012). We observed fipronil-induced effects in ATPase-coupled transmembrane transport of protons, which supports the results of a previous study, in which fipronil was shown to reduce mitochondrial activity by interfering with bioenergetic functioning in honeybees (Nicodemo et al., 2014). While effects on ATP synthesis are in line with the above mentioned interference with mitochondrial activity, fipronil-induced effects on cholesterol and saturated fatty acid synthesis have also been observed in a previous study in zebrafish embryos (Yan et al., 2016). Besides its antagonistic activity on GABA-gated chloride channels, fipronil has also been shown to sensitively block glutamate-activated chloride channels in insects (Narahashi et al., 2010), providing a link to glutamate signaling. GABA signaling has been previously discussed as a drug target for treatment of Alzheimer's disease in mammals (Solas et al., 2015), suggesting conserved mechanisms within the Alzheimer's disease pathway to be targeted by fipronil in *D. magna*.

Imidacloprid predominantly impaired oxidase and oxidoreductase function, which is in line with previous observations of oxidative stress induction in *D. magna* (Jemec et al. 2007; Qi et al., 2018). Acetyl-CoA ligases, whose expression was impaired by imidacloprid exposure in our study, are known to be involved in fatty acid synthesis (Wakil et al., 1983), and thus, our findings may explain chronic effects of imidacloprid on fatty acid synthesis, which were previously observed in bumblebees (Erban et al., 2019). Here, imidacloprid exposure also significantly impaired the expression of genes involved in the Parkinson's disease pathway and in vasopressin synthesis in mammals. In line with these observations, drugs targeting nAChRs have been previously suggested as a therapeutic treatment of Parkinson's disease (Quik and Wonnacott, 2011). Furthermore, an activation of vasopressin synthesis has been observed after activation of central nicotinic cholinergic receptors in humans (Cavun et al., 2004), which (once again) suggests common mechanisms in invertebrates. A study by Taylor-Wells et al. (2015) (Taylor-Wells et al., 2015) has shown antagonistic effects of imidacloprid on the fipronil-insensitive GABA receptor mutant Rdl in insects. Therefore, the observed effects on GABA synthesis and aminobutyrate degradation may possibly result from feedback mechanisms (Fig. 1 and Table 1).

Comparison of our data for fipronil with those previously recorded for the positive allosteric modulator of GABA-gated chloride channels diazepam (Fuertes et al., 2019) showed a negative correlation in expression changes between common target genes of both compounds, consistent with their opposing modes-of-action. A similar observation was made when comparing our data for imidacloprid with those previously published for the acetylcholinesterase inhibitor carbaryl (Orsini et al., 2016). This consistency, especially considering the different gene expression platforms and experimental settings used to obtain these results, underscores both the validity of our approach as well as of our results. In particular, these cross-platform and cross-substance consistent gene expression fingerprints likely contain genes that respond directly downstream of GABA-gated chloride channel blocking/activation (fipronil/diazepam) or activated/suppressed acetylcholine signaling (imidacloprid/carbaryl) and can be linked to the corresponding physiological changes. Thus, these are promising

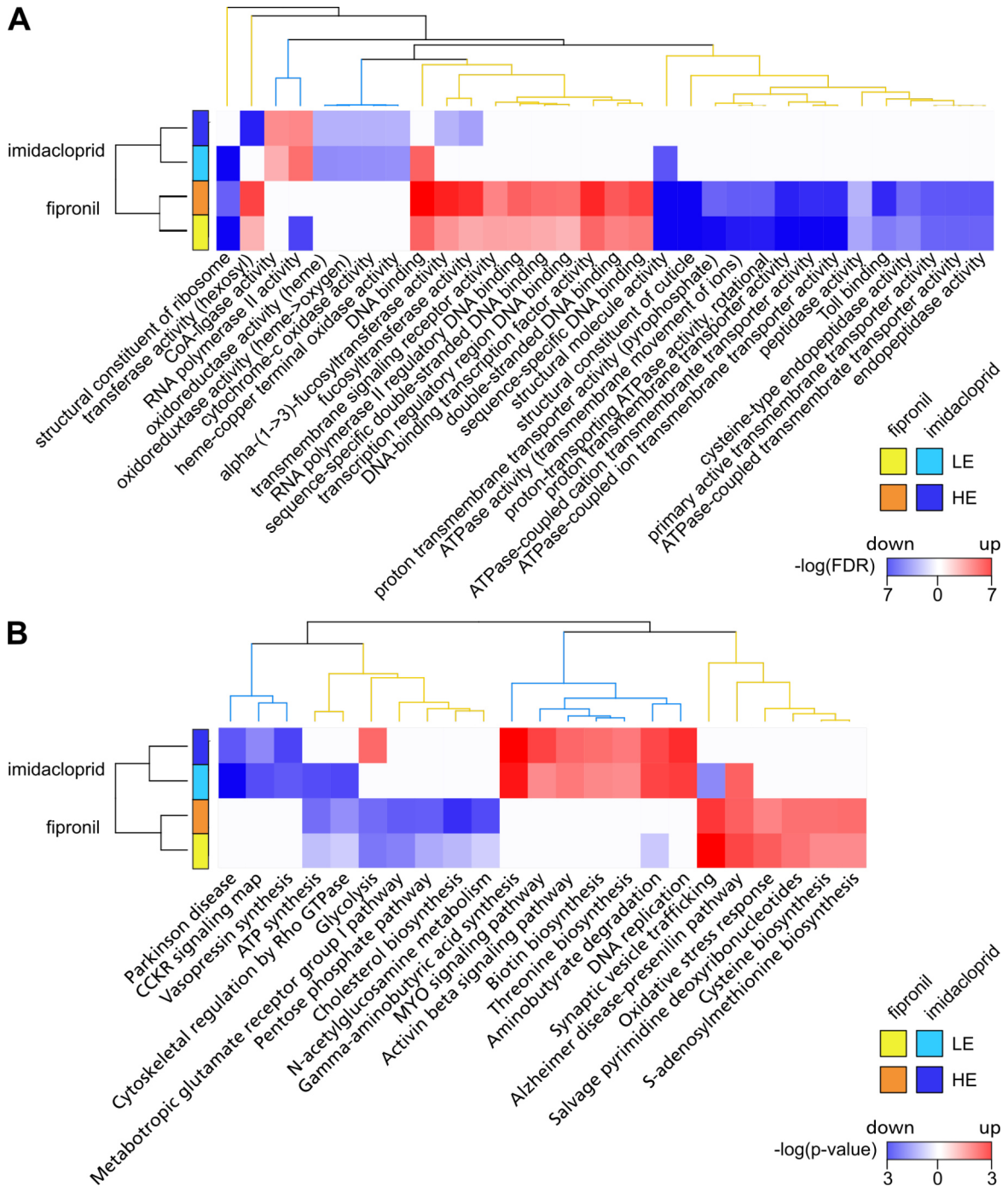

Fig. 4. GSE analysis after exposure to fipronil and imidacloprid based on the log_2-fold change values. (A) Heatmap of gene ontologies (molecular function) statistically significantly (FDR $\leq$ 0.01) enriched in the low and high exposure condition of each substance as identified by gene set enrichment analysis. –log(FDR) values are displayed as a color code. Up-regulation is indicated in red and down-regulation is indicated in blue. Non-significant as well as no regulation is colored in white. Gene ontologies and conditions are clustered by Euclidean distance based on the –log(FDR) change values. Clusters are colored by test substance as applied for signatures in panel B of Figure 3. (B) as in (A), but for PANTHER pathways statistically significantly (p-value $\leq$ 0.05) enriched in the low and high exposure condition. –log(p) values are displayed as a color code.

Table 1
Nominal and measured substance concentrations of fipronil and imidacloprid used for transcriptomics. Measured concentrations are given as the mean of fresh and aged (48 hours) solution. LOQ = limit of quantification.

	fipronil		imidacloprid	
condition	nominal concentration	measured concentration	nominal concentration	measured concentration
control	0 µg/L	< LOQ	0 mg/L	< LOQ
LE (~EC5)	16 µg/L	11.4 µg/L	42 mg/L	42.5 mg/L
HE (~EC20)	32 µg/L	25.7 µg/L	64 mg/L	63.9 mg/L

Table 2
Immobility observed in the different test conditions. For each exposure condition the immobility is given as the mean ± standard error of three replicates in %. Statistical significance compared with the control was calculated using a one-way ANOVA. n.s. = non statistically significant; * $p_{adj} \leq 0.05$

	fipronil		imidacloprid			
condition	concentration	immobility [%]	significance	concentration	immobility [%]	significance
control	0 µg/L	5 ± 1		0 mg/L	7 ± 3	
LE	11.4 µg/L	7 ± 2	n.s.	42.5 mg/L	13 ± 2	n.s.
HE	25.7 µg/L	15 ± 6	*	63.9 mg/L	19 ± 2	*

biomarker candidates that can be used in short-term ecotoxicological assays with *D. magna*, e.g., by RT-qPCR or other targeted approaches, to assess the appropriate mode-of-action. Future expansion of such toxicogenomic fingerprinting to a broader range of modes-of-action will strengthen weight-of-evidence approaches and facilitate prediction of environmental hazards of unknown chemicals to aquatic invertebrates in the future.

5. Conclusion

While high exposure concentrations of both test substances induced similar paralytic effects, exposure to the LE and HE of each substance in our study resulted in highly distinct gene expression patterns. Similarly, the expression of the common subset of fipronil target genes, with the previously obtained targets of the positive allosteric GABA-gated chloride channel modulator diazepam was significantly negatively correlated when comparing both substances. Given that fipronil and diazepam act in an opposing manner on GABA-gated chloride channels, this observation strongly suggests a highly specific and consistent gene expression signature of fipronil. Similarly, we found a positive correlation between imidacloprid targets and those observed previously for the acetylcholinesterase inhibitor carbaryl. In this case, the inhibition of acetylcholinesterase is believed to induce an accumulation of acetylcholine at presynaptic sites, which (in turn) results in a hyperactivation of nAChRs, similar to the direct activity of imidacloprid. Taking into account that our observed gene expression changes were specific for each test substance and consistent between exposure conditions, these target gene sets may be considered as biomarker candidates for the corresponding modes-of-action in *D. magna*.

Furthermore, by applying functional classification analysis to the identified gene sets, we identified specific molecular functions and pathways affected by each of the model substances, part of which validated previous studies. A significant proportion of impaired molecular functions and pathways was consistent with the substances's mode-of-action, which further validates the specificity of our findings. Therefore, our study proves that an integration of transcriptomics in a modified version of the D. magna Acute Immobilization test can be used to differentiate modes-of-action of test substances of interest when applying low effect concentrations. Prospectively, such a combination of systems biology methodologies with ecotoxicological test guidelines will help to understand the underlying molecular mechanisms of adverse effects on invertebrate organisms and populations, which will provide weight-of-evidence for ecotoxicological hazard assessment.

Authors' statement

Julia Pfaff performed the investigation and the formal analysis and contributed to manuscript writing. Hannes Reinwald wrote analysis scripts in R and contributed to formal data analysis and data curation. Steve U. Ayobahan contributed to formal data analysis. Julia Alvincz contributed to experimental investigation. Bernd Göckener performed chemical validation of test substance concentrations. Orr Shomroni performed formal RNA-Seq raw data analysis. Gabriela Salinas was involved in data curation for RNA sequencing data. Rolf-Alexander Düring and Christoph Schäfers contributed to study conceptualization. Sebastian Eilebrecht conceptualized and supervised the study, contributed to formal data analysis and wrote, reviewed and edited the original draft the manuscript.

Funding

This work was supported by the Fraunhofer Internal Programs under Grant No. Attract 040-600300.

Declaration of Competing Interest

The authors declare to have no competing interests.

Acknowledgement

The authors thank Terry Clark for language revision of this manuscript.

Supplementary materials

Supplementary material associated with this article can be found, in the online version, at doi:10.1016/j.aquatox.2021.105927.

References

Al-Badran, A.A., Fujiwara, M., Gatlin, D.M., Mora, M.A., 2018. Lethal and sub-lethal effects of the insecticide fipronil on juvenile brown shrimp *Farfantepenaeus aztecus*. Sci. Rep. 8, 1–12.
Andrews, S., 2010. FastQC: a Quality Control Tool for High Throughput Sequence Data.
Athar, A., Fullgrabe, A., George, N., Iqbal, H., Huerta, L., Ali, A., Snow, C., Fonseca, N.A., Petryszak, R., Papatheodorou, I., Sarkans, U., Brazma, A., 2019. ArrayExpress update - from bulk to single-cell expression data. Nucleic Acids Res. 47, D711–D715.
Barrett, T., Wilhite, S.E., Ledoux, P., Evangelista, C., Kim, I.F., Tomashevsky, M., Marshall, K.A., Phillippy, K.H., Sherman, P.M., Holko, M., Yefanov, A., Lee, H., Zhang, N.G., Robertson, C.L., Serova, N., Davis, S., Soboleva, A., 2013. NCBI GEO: archive for functional genomics data sets-update. Nucleic Acids Res. 41, D991–D995.
Bolger, A.M., Lohse, M., Usadel, B., 2014. Trimmomatic: a flexible trimmer for Illumina sequence data. Bioinformatics 30, 2114–2120.
Campo-Soria, C., Chang, Y., Weiss, D.S., 2006. Mechanism of action of benzodiazepines on GABAA receptors. Br. J. Pharmacol. 148, 984–990.
Campos, B., Fletcher, D., Pina, B., Tauler, R., Barata, C., 2018. Differential gene transcription across the life cycle in *Daphnia magna* using a new all genome custom-made microarray. BMC Genomics 19, 1–13.
Cavun, S., Savci, V., Ulus, I.H., 2004. Centrally injected CDP-choline increases plasma vasopressin levels by central cholinergic activation. Fund Clin. Pharmacol. 18, 71–77.
Chevalier, J., Harscoet, E., Keller, M., Pandard, P., Cachot, J., Grote, M., 2015a. Exploration of Daphnia behavioral effect profiles induced by a broad range of toxicants with different modes of action. Environ. Toxicol. Chem. 34, 1760–1769.
Chevalier, J., Harscoet, E., Keller, M., Pandard, P., Cachot, J., Grote, M., 2015b. Exploration of Daphnia behavioral effect profiles induced by a broad range of toxicants with different modes of action. Environ. Toxicol. Chem. 34, 1760–1769.
Coady, K.K., Burgoon, L., Doskey, C., Davis, J.W., 2020. Assessment of transcriptomic and apical responses of *Daphnia magna* exposed to a polyethylene microplastic in a 21-d chronic study. Environ. Toxicol. Chem. 39, 1578–1589.
Cocco, A., Ronnberg, A.M.C., Jin, Z., Andre, G.I., Vossen, L.E., Bhandage, A.K., Thornqvist, P.O., Birnir, B., Winberg, S., 2017. Characterization of the gamma-aminobutyric acid signaling system in the zebrafish (Danio Rerio Hamilton) central nervous system by reverse transcription-quantitative polymerase chain reaction. Neuroscience 343, 300–321.
Costa, E., Guidotti, A., Toffano, G., 1978. Molecular mechanisms mediating the action of diazepam on GABA receptors. Br. J. Psychiatry 133, 239–248.
Cox, C., 2001. Insecticide factsheet: imidacloprid. J. Pestic. Reform 21, 15–21.
De Fruyt, N., Yu, A.J., Rankin, C.H., Beets, I., Chew, Y.L., 2020. The role of neuropeptides in learning: insights from C. elegans. Int. J. Biochem. Cell Biol. 125, 105801.
Dobin, A., Davis, C.A., Schlesinger, F., Drenkow, J., Zaleski, C., Jha, S., Batut, P., Chaisson, M., Gingeras, T.R., 2013. STAR: ultrafast universal RNA-seq aligner. Bioinformatics 29, 15–21.

Emameh, R.Z., Barker, H., Hytonen, V.P., Tolvanen, M.E.E., Parkkila, S., 2014. Beta carbonic anhydrases: novel targets for pesticides and anti-parasitic agents in agriculture and livestock husbandry. Parasite Vector 7, 1–11.
Endo, S., Maeda, S., Matsunaga, T., Dhagat, U., El-Kabbani, O., Tanaka, N., Nakamura, K. T., Tajima, K., Hara, A., 2009. Molecular determinants for the stereospecific reduction of 3-ketosteroids and reactivity towards all-trans-retinal of a short-chain dehydrogenase/reductase (DHRS4). Arch. Biochem. Biophys. 481, 183–190.
Enell, L.E., Kapan, N., Soderberg, J.A., Kahsai, L., Nassel, D.R., 2010. Insulin signaling, lifespan and stress resistance are modulated by metabotropic GABA receptors on insulin producing cells in the brain of Drosophila. Plos One 5, e15780.
Erban, T., Sopko, B., Talacko, P., Harant, K., Kadlikova, K., Halesova, T., Riddellova, K., Pekas, A., 2019. Chronic exposure of bumblebees to neonicotinoid imidacloprid suppresses the entire mevalonate pathway and fatty acid synthesis. J. Proteomics 196, 69–80.
European Commission, 2000. SANCO/3029/99 rev.4 - Residues: Guidance for generating and reporting methods of analysis in support of pre-registration data requirements for Annex II (part A, Section 4) and Annex III (part A, Section 5) of Directive 91/414. Working document.
Fuertes, I., Campos, B., Rivetti, C., Pina, B., Barata, C., 2019. Effects of single and combined low concentrations of neuroactive drugs on *Daphnia magna* reproduction and transcriptomic responses. Environ. Sci. Technol. 53, 11979–11987.
Fukuto, T.R., 1990. Mechanism of action of organophosphorus and carbamate insecticides. Environ Health Persp 87, 245–254.
Gauthier, M., Aras, P., Paquin, J., Boily, M., 2018. Chronic exposure to imidacloprid or thiamethoxam neonicotinoid causes oxidative damages and alters carotenoid-retinoid levels in caged honey bees (*Apis mellifera*). Sci. Rep. 8, 16274.
Guidugli, K.R., Hepperle, C., Hartfelder, K., 2004. A member of the short-chain dehydrogenase/reductase (SDR) superfamily is a target of the ecdysone response in honey bee (*Apis mellifera*) caste development. Apidologie 35, 37–47.
Gunasekara, A.S., Truong, T., Goh, K.S., Spurlock, F., Tjeerdema, R.S., 2007. Environmental fate and toxicology of fipronil. J. Pesticide Sci. 32, 189–199.
Hayasaka, D., Korenaga, T., Suzuki, K., Sanchez-Bayo, F., Goka, K., 2012. Differences in susceptibility of five cladoceran species to two systemic insecticides, imidacloprid and fipronil. Ecotoxicology 21, 421–427.
Herring, N., Lokale, M.N., Danson, E.J., Heaton, D.A., Paterson, D.J., 2008. Neuropeptide Y reduces acetylcholine release and vagal bradycardia via a Y2 receptor-mediated, protein kinase C-dependent pathway. J. Mol. Cell Cardiol. 44, 477–485.
Holstein, T.W., 2012. The evolution of the Wnt pathway. Csh Perspect. Biol. 4, a007922.
Howe, K.L., Achuthan, P., Allen, J., Allen, J., Alvarez-Jarreta, J., Amode, M.R., Armean, I.M., Azov, A.G., Bennett, R., Bhai, J., Billis, K., Boddu, S., Charkhchi, M., Cummins, C., Da Rin Fioretto, L., Davidson, C., Dodiya, K., El Houdaigui, B., Fatima, R., Gall, A., Garcia Giron, C., Grego, T., Guijarro-Clarke, C., Haggerty, L., Hemrom, A., Hourlier, T., Izuogu, O.G., Juettemann, T., Kaikala, V., Kay, M., Lavidas, I., Le, T., Lemos, D., Gonzalez Martinez, J., Marugan, J.C., Maurel, T., McMahon, A.C., Mohanan, S., Moore, B., Muffato, M., Oheh, D.N., Paraschas, D., Parker, A., Parton, A., Prosovetskaia, I., Sakthivel, M.P., Salam, A.I.A., Schmitt, B.M., Schuilenburg, H., Sheppard, D., Steed, E., Szpak, M., Szuba, M., Taylor, K., Thormann, A., Threadgold, G., Walts, B., Winterbottom, A., Chakiachvili, M., Chaubal, A., De Silva, N., Flint, B., Frankish, A., Hunt, S.E., GR, I.I., Langridge, N., Loveland, J.E., Martin, F.J., Mudge, J.M., Morales, J., Perry, E., Ruffier, M., Tate, J., Thybert, D., Trevanion, S.J., Cunningham, F., Yates, A.D., Zerbino, D.R., Flicek, P.E., 2021. Ensembl 2021. Nucleic Acids Res. 49, D884–D891, 2021.
Ignatiadis, N., Klaus, B., Zaugg, J.B., Huber, W., 2016. Data-driven hypothesis weighting increases detection power in genome-scale multiple testing. Nat. Methods 13, 577–580.
Jemec, A., Tisler, T., Drobne, D., Sepcic, K., Fournier, D., Trebse, P., 2007. Comparative toxicity of imidacloprid, of its commercial liquid formulation and of diazinon to a non-target arthropod, the microcrustacean *Daphnia magna*. Chemosphere 68, 1408–1418.
Kinsella, R.J., Kahari, A., Haider, S., Zamora, J., Proctor, G., Spudich, G., Almeida-King, J., Staines, D., Derwent, P., Kerhornou, A., Kersey, P., Flicek, P., 2011. Ensembl BioMarts: a Hub for Data Retrieval Across Taxonomic Space. Database-Oxford.
Koga, D., Jilka, J., Kramer, K.J., 1983. Insect endochitinases - glycoproteins from molting fluid, integument and pupal hemolymph of Manduca-Sexta L. Insect Biochem. 13, 295–305.
Liao, Y., Smyth, G.K., Shi, W., 2014. featureCounts: an efficient general purpose program for assigning sequence reads to genomic features. Bioinformatics 30, 923–930.
Loraine, A.E., Blakley, I.C., Jagadeesan, S., Harper, J., Miller, G., Firon, N., 2015. Analysis and visualization of RNA-Seq expression data using RStudio, bioconductor, and integrated genome browser. Methods Mol. Biol. 1284, 481–501.
Love, M.I., Huber, W., Anders, S., 2014. Moderated estimation of fold change and dispersion for RNA-seq data with DESeq2. Genome Biol. 15, 550.
Madsen, K.K., Larsson, O.M., Schousboe, A., 2008. Regulation of excitation by GABA neurotransmission: focus on metabolism and transport. Results Probl. Cell Differ. 44, 201–221.
Marcu, O., Locke, M., 1998. A cuticular protein from the moulting stages of an insect. Insect Biochem. Mol. 28, 659–669.
Matsuda, K., Buckingham, S.D., Kleier, D., Rauh, J.J., Grauso, M., Sattelle, D.B., 2001. Neonicotinoids: insecticides acting on insect nicotinic acetylcholine receptors. Trends Pharmacol. Sci. 22, 573–580.
McNamara, P.C., 1990a. Acute Toxicity to Daphnids (*Daphnia magna*) During a 48-Hour Flow-Through Exposure. Springborn Laboratories, Inc., Wareham, Massachusetts.
McNamara, P.C., 1990b. The Chronic Toxicity of M&B 4630 to *Daphnia magna* Under Flow-Through Conditions. Springborn Laboratories, Inc., Wareham, Massachusetts.
Mi, H.Y., Muruganujan, A., Casagrande, J.T., Thomas, P.D., 2013. Large-scale gene function analysis with the PANTHER classification system. Nat. Protoc. 8, 1551–1566.
Mi, H.Y., Muruganujan, A., Huang, X.S., Ebert, D., Mills, C., Guo, X.Y., Thomas, P.D., 2019. Protocol update for large-scale genome and gene function analysis with the PANTHER classification system (v.14.0). Nat. Protoc. 14, 703–721.
Nagata, K., Song, J.H., Shono, T., Narahashi, T., 1998. Modulation of the neuronal nicotinic acetylcholine receptor-channel by the nitromethylene heterocycle imidacloprid. J. Pharmacol. Exp. Ther. 285, 731–738.
Narahashi, T., Zhao, X., Ikeda, T., Salgado, V.L., Yeh, J.Z., 2010. Glutamate-activated chloride channels: Unique fipronil targets present in insects but not in mammals. Pesticide Biochem. Physiol. 97, 149–152.
Nicodemo, D., Maioli, M.A., Medeiros, H.C.D., Guelfi, M., Balieira, K.V.B., De Jong, D., Mingatto, F.E., 2014. Fipronil and imidacloprid reduce honeybee mitochondrial activity. Environ. Toxicol. Chem. 33, 2070–2075.
Ningshen, T.J., Aparoy, P., Ventaku, V.R., Dutta-Gupta, A., 2013. Functional interpretation of a non-gut hemocoelic tissue aminopeptidase N (APN) in a lepidopteran insect pest *Achaea janata*. PLoS ONE 8, e1009463.
OECD, 2004. Test Guideline 202: Daphnia Sp. Acute Immobilisation Test. edˆeds, Paris.
OECD, 2012. Test Guideline 211: *Daphnia magna* Reproduction Test.
Orsini, L., Gilbert, D., Podicheti, R., Jansen, M., Brown, J.B., Solari, O.S., Spanier, K.I., Colbourne, J.K., Rush, D., Decaestecker, E., Asselman, J., De Schamphelaere, K.A.C., Ebert, D., Haag, C.R., Kvist, J., Laforsch, C., Petrusek, A., Beckerman, A.P., Little, T. J., Chaturvedi, A., Pfrender, M.E., De Meester, L., Frilander, M.J., 2016. *Daphnia magna* Transcriptome by RNA-Seq Across 12 Environmental Stressors. Sci Data, p. 3.
Poynton, H.C., Lazorchak, J.M., Impellitteri, C.A., Blalock, B.J., Rogers, K., Allen, H.J., Loguinov, A., Heckrnan, J.L., Govindasmawy, S., 2012. Toxicogenomic Responses of Nanotoxicity in *Daphnia magna* Exposed to Silver Nitrate and Coated Silver Nanoparticles. Environ Sci Technol 46, 6288–6296.
Qi, S.Z., Wang, D.H., Zhu, L.Z., Teng, M.M., Wang, C.J., Xue, X.F., Wu, L.M., 2018. Neonicotinoid insecticides imidacloprid, guadipyr, and cycloxaprid induce acute oxidative stress in *Daphnia magna*. Ecotox. Environ. Safe. 148, 352–358.
Quik, M., Wonnacott, S., 2011. Alpha 6 beta 2*and alpha 4 beta 2*nicotinic acetylcholine receptors as drug targets for Parkinson's disease. Pharmacol. Rev. 63, 938–966.
R Core Team, 2019. R: a Language and Environment for Statistical Computing edˆeds. Vienna, Austria.
Rapetti-Mauss, R., Berenguier, C., Allegrini, B., Soriani, O., 2020. Interplay between ion channels and the wnt/beta-catenin signaling pathway in cancers. Front. Pharmacol. 11 https://doi.org/10.3389/fphar.2020.525020.
Rehorst, W.A., Thelen, M.P., Nolte, H., Turk, C., Cirak, S., Peterson, J.M., Wong, G.W., Wirth, B., Kruger, M., Winter, D., Kye, M.J., 2019. Muscle regulates mTOR dependent axonal local translation in motor neurons via CTRP3 secretion: implications for a neuromuscular disorder, spinal muscular atrophy. Acta Neuropathol. Commun. 7, 154.
Reinwald, H., Konig, A., Ayobahan, S.U., Alvincz, J., Sipos, L., Gockener, B., Bohle, G., Shomroni, O., Hollert, H., Salinas, G., Schafers, C., Eilebrecht, E., Eilebrecht, S., 2021. Toxicogenomic fin(ger)prints for thyroid disruption AOP refinement and biomarker identification in zebrafish embryos. Sci. Total Environ. 760, 143914.
Russo, C., Isidori, M., Deaver, J.A., Poynton, H.C., 2018. Toxicogenomic responses of low level anticancer drug exposures in *Daphnia magna*. Aquat. Toxicol. 203, 40–50.
Saltiel, A.R., Kahn, C.R., 2001. Insulin signalling and the regulation of glucose and lipid metabolism. Nature 414, 799–806.
Sanchez-Bayo, F., Goka, K., 2006. Influence of light in acute toxicity bioassays of imidacloprid and zinc pyrithione to zooplankton crustaceans. Aquat Toxicol 78, 262–271.
Sarti, F., Zhang, Z., Schroeder, J., Chen, L., 2013. Rapid suppression of inhibitory synaptic transmission by retinoic acid. J. Neurosci. 33, 11440–11450.
Sayers, E.W., Beck, J., Bolton, E.E., Bourexis, D., Brister, J.R., Canese, K., Comeau, D.C., Funk, K., Kim, S., Klimke, W., Marchler-Bauer, A., Landrum, M., Lathrop, S., Lu, Z., Madden, T.L., O'Leary, N., Phan, L., Rangwala, S.H., Schneider, V.A., Skripchenko, Y., Wang, J., Ye, J., Trawick, B.W., Pruitt, K.D., Sherry, S.T., 2021. Database resources of the National Center for Biotechnology Information. Nucleic Acids Res. 49, D10–D17.
Solas, M., Puerta, E., Ramirez, M.J., 2015. Treatment options in Alzheimer's disease: the GABA story. Curr. Pharm. Des. 21, 4960–4971.
Song, Y., Rundberget, J.T., Evenseth, L.M., Xie, L., Gomes, T., Hogasen, T., Iguchi, T., Toleffsen, K.E., 2016. Whole-Organism Transcriptomic Analysis Provides Mechanistic Insight into the Acute Toxicity of Emamectin Benzoate in *Daphnia magna*. Environ Sci Technol 50, 11994–12003.
Stark, J.D., Vargas, R.I., 2005. Toxicity and hazard assessment of fipronil to Daphnia pulex. Ecotoxicol. Environ. Saf. 62, 11–16.
Taylor-Wells, J., Brooke, B.D., Bermudez, I., Jones, A.K., 2015. The neonicotinoid imidacloprid, and the pyrethroid deltamethrin, are antagonists of the insect Rdl GABA receptor. J Neurochem 135, 705–713.
Tisler, T., Jemec, A., Mozetic, B., Trebse, P., 2009. Hazard identification of imidacloprid to aquatic environment. Chemosphere 76, 907–914.
Urbanski, A., Rosinski, G., 2018. Role of neuropeptides in the regulation of the insect immune system - current knowledge and perspectives. Curr. Protein Pept. Sci. 19, 1201–1213.
Wakil, S.J., Stoops, J.K., Joshi, V.C., 1983. Fatty acid synthesis and its regulation. Annu. Rev. Biochem. 52, 537–579.
Wang, X., Martinez, M.A., Wu, Q.H., Ares, I., Martinez-Larranaga, M.R., Anadon, A., Yuan, Z.H., 2016. Fipronil insecticide toxicology: oxidative stress and metabolism. Crit. Rev. Toxicol. 46, 876–899.

Wheelock, C.E., Shan, G., Ottea, J., 2005. Overview of carboxylesterases and their role in the metabolism of insecticides. J. Pesticide Sci. 30, 75–83.
Wiley, J.W., Gross, R.A., Lu, Y.X., Macdonald, R.L., 1990. Neuropeptide-Y reduces calcium current and inhibits acetylcholine-release in nodose neurons via a pertussis toxin sensitive mechanism. J. Neurophysiol. 63, 1499–1507.
Xu, G., Gu, G.X., Teng, Z.W., Wu, S.F., Huang, J., Song, Q.S., Ye, G.Y., Fang, Q., 2016. Identification and expression profiles of neuropeptides and their G protein-coupled receptors in the rice stem borer *Chilo suppressalis*. Sci. Rep. 6, 1–15.
Yan, L., Gong, C.X., Zhang, X.F., Zhang, Q., Zhao, M.R., Wang, C., 2016. Perturbation of metabonome of embryo/larvae zebrafish after exposure to fipronil. Environ. Toxicol. Pharm. 48, 39–45.
Zheng, Q.Z., Bi, R., Xu, M., Zhang, D.F., Tan, L.W., Lu, Y.P., Yao, Y.G., 2021. Exploring the genetic association of the ABAT gene with Alzheimer's disease. Mol. Neurobiol. 58, 1894–1903.
Zhu, A., Ibrahim, J.G., Love, M.I., 2019. Heavy-tailed prior distributions for sequence count data: removing the noise and preserving large differences. Bioinformatics 35, 2084–2092.
Ziegler, C.G.K., Peng, M., Falk, M.J., Polyak, E., Tsika, E., Ischiropoulos, H., Bakalar, D., Blendy, J.A., Gasser, D.L., 2012. Parkinson's disease-like neuromuscular defects occur in prenyl diphosphate synthase subunit 2 (Pdss2) mutant mice. Mitochondrion 12, 248–257.

A5 A short term test for toxicogenomic analysis of ecotoxic modes of action in *Lemna minor*

Declaration of author contributions to the publication:

A short term test for toxicogenomic analysis of ecotoxic modes of action in *Lemna minor*

DOI:	n.a.
Status:	Review
Journal:	**Environmental Science and Technology**

Contributing authors:
Loll A. (LA)*, Reinwald H. (**RH**)*, Ayobahan S. (AS), Göckener B. (GB), Salinas G. (SG), Schäfers C. (SC), Schlich K. (SK), Hamscher G. (HG), & Eilebrecht S. (ES)

(1) Concept and design

Doctoral candidate **RH**:	30% - *In silico* workflow design (functional annotation to allow data interpretability)
Co-author LA:	30% - Laboratory workflow design
Co-author ES:	25%
Co-author SC, SK, HG:	5%

(2) Conducting tests and experiments

Co-author LA:	65% - Laboratory workflow design
Co-author AS:	15% - LC-MS/MS shotgun proteomic measurements
Co-author SG:	10% - mRNA-Sequence library preparation and Illumina HiSeq NGS
Co-author GB:	10% - Analytical chemistry to determine test concetrations

(3) Compilation of data sets and figures

Doctoral candidate **RH**: 65% - Raw mRNA-sequences and LC-MS shotgun-proteomics data compilation and QC plots; overrepresentation analysis plots; annotation package workflow illustration; correlation plots
Co-author LA: 30% - Dose-response-curves; heatmaps; venn diagrams; bar plots
Co-author ES: 5 % - Constructive feedback on figure structure

(4) Analysis and interpretation of data

Doctoral candidate **RH**: 60% - Transcriptomic and proteomic data processing; construction of functional annotation package for *L. minor;* overrepresentation analysis with clusterProfiler; DGEA and multivariate data exploration for transcriptomic and proteomic datasets;
Co-author LA: 30% - Dose-response-analysis; feature selection; data mining
Co-author AS: 10% - Peptide spectra identification with MaxQuant

(5) Drafting of manuscript

Doctoral candidate **RH**:	30%
Co-author LA:	30%
Co-author AS:	15%
Co-author ES:	20%
Co-author SC, SK, HG:	5% - Final draft comments

A short term test for toxicogenomic analysis of ecotoxic modes of action in *Lemna minor*

Alexandra Loll[†,1,2], Hannes Reinwald[†,1,3], Steve U. Ayobahan[1], Bernd Göckener[4], Gabriela Salinas[5], Christoph Schäfers[6], Karsten Schlich[6], Gerd Hamscher[2], Sebastian Eilebrecht[*,1]

[†] *A.L. and H.R. contributed equally to this paper (Shared 1st authorship)*

** Email: sebastian.eilebrecht@ime.fraunhofer.de*

[1] *Fraunhofer Attract Eco'n'OMICs, Fraunhofer Institute for Molecular Biology and Applied Ecology, Auf dem Aberg 1, 57392 Schmallenberg, Germany;*

[2] *Institute of Food Chemistry and Food Biotechnology, Justus Liebig University Giessen, Heinrich-Buff-Ring 17, 35392 Giessen, Germany*

[3] *Department Evolutionary Ecology and Environmental Toxicology, Goethe University Frankfurt, Max-von-Laue-Straße 9, 60438 Frankfurt am Main, Germany*

[4] *Department Environmental and Food Analysis, Fraunhofer Institute for Molecular Biology and Applied Ecology, Auf dem Aberg 1, 57392 Schmallenberg, Germany*

[5] *NGS-Services for Integrative Genomics, University of Göttingen, Transcriptome and Genome Analysis Laboratory, Justus von Liebig Weg 11, 37077 Göttingen, Germany*

[6] *Department Ecotoxicology, Fraunhofer Institute for Molecular Biology and Applied Ecology, Auf dem Aberg 1, 57392 Schmallenberg, Germany*

ABSTRACT

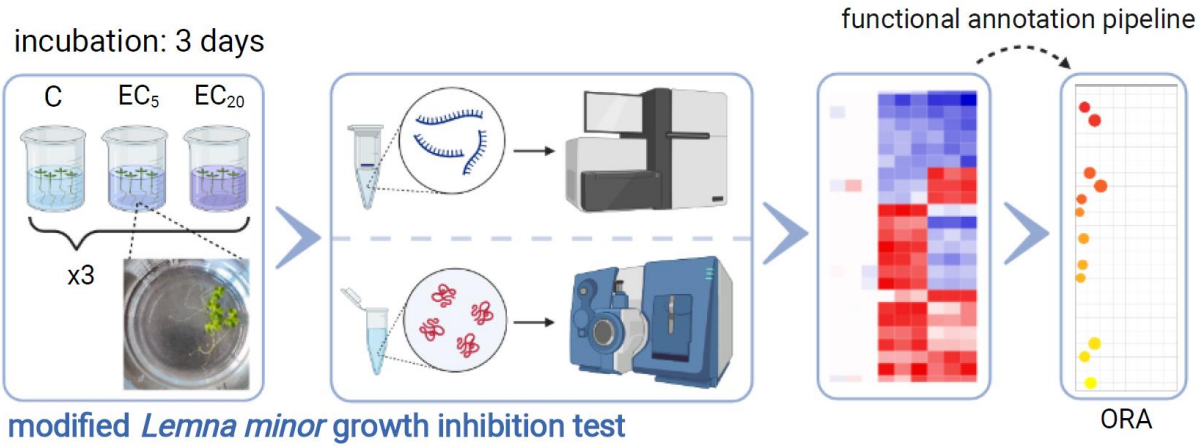

In the environmental risk assessment of substances, toxicity to aquatic plants is evaluated using, among other methods, the seven-day *Lemna sp.* growth inhibition test following the OECD TG 221. So far, the test is not applicable for short-term screening of toxicity, nor does it allow evaluation of toxic modes of action (MoA). The latter is also complicated by the lack of knowledge of gene functions in the test species. Using ecotoxicogenomics, we developed a time-shortened three-day assay in *Lemna minor* that allows discrimination of ecotoxic MoA. By examining the changes in gene expression induced by low effect concentrations of the pharmaceutical atorvastatin and the herbicide bentazon at the transcriptome and proteome levels, we were able to identify candidate biomarkers for the respective MoA. We developed a homology-based functional annotation pipeline for the reference genome of *L. minor*, which allowed overrepresentation analysis of the gene ontologies affected by both test compounds. Genes affected by atorvastatin mainly influenced lipid synthesis and metabolism, whereas the bentazon-responsive genes were mainly involved in light response. Our approach is therefore less time-consuming but sensitive and allows assessment of MoA in *L. minor*. Using this shortened assay, investigation of the identified candidate biomarkers may allow the development of MoA-specific screening approaches in the future.

INTRODUCTION

For the registration of a chemical under REACH (Registration, Evaluation, Authorisation of Chemicals) or of an active ingredient in pesticides, pharmaceuticals or biocides, the testing for effects on aquatic organisms is a registration requirement. Due to the increasing number of these anthropogenic substances on the market, the development of rapid and meaningful test systems to assess the potential hazard in the environment is becoming more and more important.[1] Standardized ecotoxicity tests for the environmental hazard assessment of xenobiotics have already been established for a variety of aquatic model organisms, including *Lemna minor*. However, they generally do not allow rapid screening or discrimination of harmful modes of action. The growth inhibition test in *L. minor* according to the Organization for Economic Cooperation and Development (OECD) Test Guideline (TG) No. 221, for example, captures changes in plant growth as an endpoint and takes seven days.[2]

Our study aimed to develop an abbreviated screening test that would allow discrimination of modes of action in *L. minor* beyond the classical endpoints. To this end, we developed an abbreviated version of the OECD TG 221 and combined it with the detection of compound-induced gene expression changes at the transcriptome and proteome levels. OMICs, as a non-target method, offer the possibility of comprehensive detection of molecular fingerprints and informative biomarker candidates.[3,4] Although a first draft genome for this species was published back in 2015, transcriptome methods have rarely been applied to *L. minor*.[5] For example, Wang et al. investigated molecular responses of *L. minor* to ammonia (NH_4^+)[6] and Li et al. recorded transcriptome changes after exposure to the EC_{50} of the pesticide imazamox[7]. Both studies used the seven-day OECD guideline test for this purpose. Proteomic studies on *L. minor* have been largely lacking. Moreover, due to the previously non-functionally annotated reference genome, it has been difficult to read out functional information from OMICs results, which may provide information on modes of action, for example.

We used the drug atorvastatin and the herbicide bentazon as reference substances to establish our abbreviated, mode of action-specific assay approach. Atorvastatin is one of the most commonly used statins in human medicine[8], which inhibits 3-hydroxy-3-methyl-glutaryl-coenzyme A reductase (HMGR), the key enzyme in human cholesterol synthesis, and thus has cholesterol- and lipid-lowering effects.[9] Plants also possess an HMGR very similar to humans, which is involved in phytosterol synthesis through the mevalonic acid (MVA) pathway.[10,11] A phytotoxic effect of atorvastatin has already been demonstrated in *L. gibba*, making it a promising candidate for our studies.[12] Bentazon is a herbicide that inhibits photosystem II (PSII)

and thus photosynthesis in plants.[13] In addition, bentazon has also been associated with inhibition of HMGR in a previous study.[14]

To achieve our aims a shortened *L. minor* growth inhibition assay integrating systems biology methods was established by testing these two reference substances. For this purpose, the gene expression profiles after shortened exposure to low effect concentrations of both substances was recorded, compared and functionally evaluated. A robust and comprehensible pipeline was established and applied for functional annotation of the *L. minor* reference genome. The assay approach was evaluated based on the identifiability of candidate biomarkers and on the distinguishability of the modes of action of both reference compounds.

MATERIALS AND METHODS

Test substances

The HMG-CoA reductase inhibitor atorvastatin calcium (CAS 134523-03-8, purity >95%) and the photosynthesis inhibitor bentazon (CAS 25057-89-0, purity ≥98%) were purchased from abcr and Sigma Aldrich, respectively. All test solutions and dilutions used were prepared with axenic Steinberg medium, made from a 10-fold concentrated stock solution according to OECD TG 221[2] the day before test start at pH 5.5±0.2. Solubilisation was done by stirring for two hours (atorvastatin) or one hour (bentazon) followed by 15 minutes in an ultrasonic bath. Preparation of atorvastatin-solutions was carried out taking into account that the substance is a calcium salt. All concentrations and effects therefore refer to the active substance. On the day of the test start, all test solutions were prepared as a dilution series of the highest test concentration in Steinberg medium.

Lemna minor culture and determination of effect concentrations

In order to identify suitable test concentrations for the modified *Lemna minor* growth inhibition test, effect concentrations (EC) were determined for both test substances in pretests, following OECD TG 221.[2] Briefly, *L. minor* were exposed to four successive concentrations of each test substance and an appropriate water control for seven days under static conditions. Pretest concentrations for each substance were chosen based on available literature.[12,15,16] Each test was performed with four replicates, while the control was performed with eight replicates, using a total volume of 150 mL per test vessel (**Figure 1**). Four healthy plants with three fronds each from a pre-culture of at least one week were used for each replicate. At the beginning and at the end of the pre- and modified inhibition test, the pH was measured for all samples,

(**Tables S2** and **S3**). Plants were exposed under continuous light (85-135 µE·m^{-2}·s^{-1}) at 24±2°C in a random arrangement using a Multitron Pro growth chamber (Infors HT) (**Table S3**).

At the beginning of the test and after 7 days, as well as at two time points in between, area and number of the fronds were measured, using a *Count & Classify v6.8* image analysis system (medeaLAB, Erlangen, Germany). Concentration-response curves were constructed by plotting the percent reduction in yield for both parameters after 7 days of exposure against the concentration of the test substance. Data analysis and calculation of effect concentrations were performed by probit analysis using a linear maximum likelihood regression model (ToxRat v.3.0.0 software; ToxRat Solutions GmbH, Alsdorf, Germany).

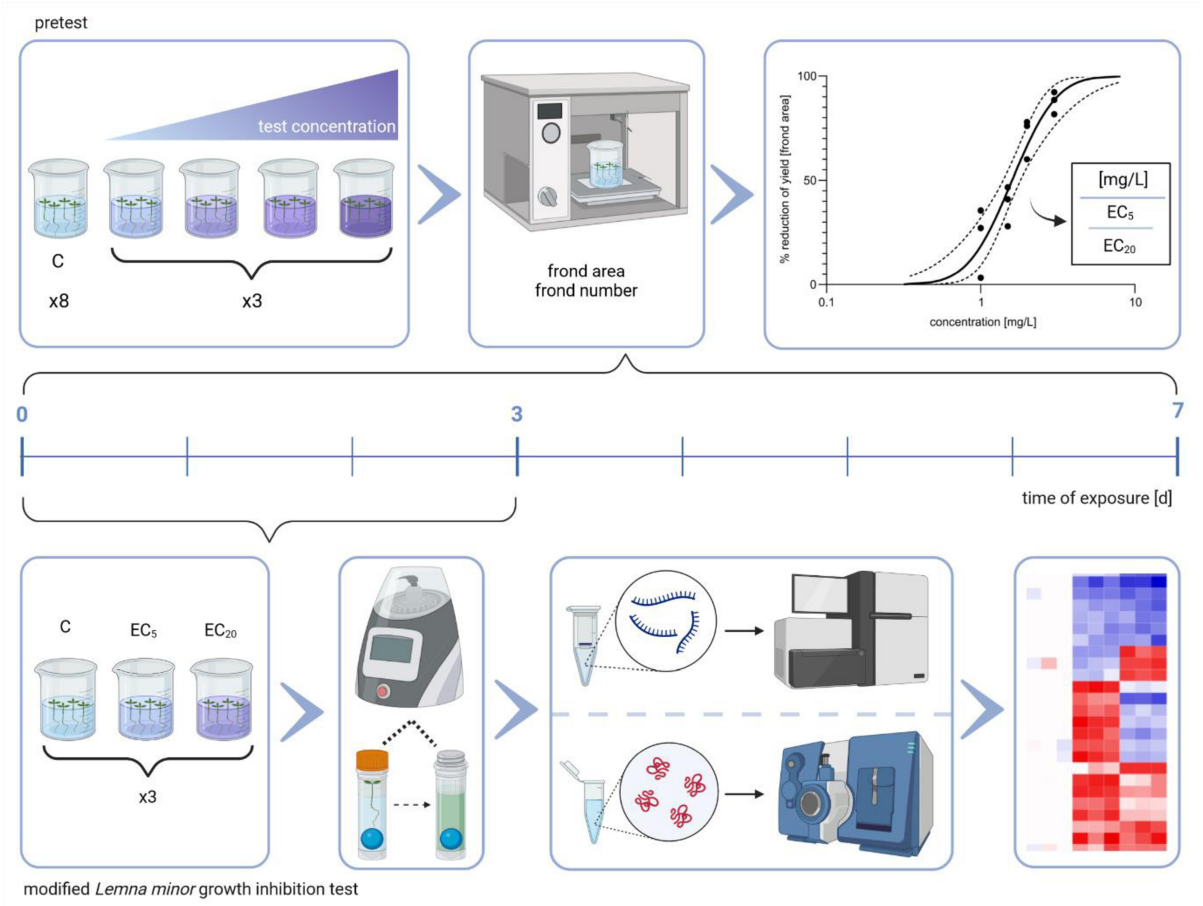

Figure 1. Schematic view and timelines of the pretest (top) and the modified *L. minor* growth inhibition test (bottom) workflows. The pretest followed the instructions of OECD TG 221 and was conducted with four test concentrations (3 replicates) and a control condition (8 replicates) over a period of 7 days. After measuring frond area and frond number, concentration-response-curves were generated. Subsequently, the EC_5 and EC_{20} were used as test conditions for the modified *L. minor* growth inhibition test, which was shortened to 3 days. At day 3, the plant material obtained was used for RNA and protein extraction for transcriptome and proteome analysis. Created with BioRender.com.

Modified short term Lemna minor growth inhibition test

For the early identification of substance-induced gene expression changes, a shortened version of the OECD TG 221[2] was performed with *L. minor* exposed to the EC_5 and the EC_{20} of each test substance identified in the pretests. . The shortened exposure lasted 72 h under static conditions and the test was conducted in three replicates per exposure condition and control (**Figure 1**). The incubation conditions were identical to those of the guideline and already described above. At the end of the test, the overgrown fronds were separated and the number and area of the fronds were determined as previously described, before total RNA and protein was extracted for subsequent transcriptome and proteome analysis.

Chemical analysis

The concentrations of atorvastatin and bentazon in Steinberg medium were determined by chemical analysis. A detailed description of the analytical method is provided in the supplemental information. Briefly, the aqueous samples were amended with methanol and further diluted if necessary. The samples were then directly analyzed by ultra-high performance liquid chromatography coupled with tandem mass spectrometry (UHPLC-MS/MS).

RNA extraction

For each sample, total RNA was isolated and purified from 25 mg of plant material following an optimized version of the manufacturer's protocol of the *RapidPURE RNA Plant Kit* (MP Biomedicals Illkirch, France). A detailed description is given in the supplements. The purity and concentration of the RNA was assessed using a Nanodrop 2000 instrument (Thermo Scientific) and RNA integrity was determined using a Bioanalyzer 2100 (Agilent Technologies). To assure high RNA quality, only samples with RNA Integrity Numbers (RIN) > 7.0 and a purity of $A_{260/230} > 1.6$ and $A_{260/280} > 2.0$ were selected for sequencing.

Transcriptomics

Poly(A)+ RNA was purified, fragmented, and transcribed into cDNA for library preparation using the *TruSeqRNA Library Prep Kit (v2)* (Illumina, UK) following the manufacturer's instructions. Sample libraries were sequenced on an Illumina HiSeq 4000 system in 50 bp single read mode with approximately 30 million raw reads per sample. A detailed description of the transcriptomic raw data processing workflow is provided in the supplements. In short, after adapter trimmed sequences quality and contamination checks via FastQC (v0.11.5)[17] and FastQ Screen (v0.14.1)[18], reads were mapped to *Lemna minor* reference genome 2019v2[5] (www.lemna.org) using STAR (v2.7.8a)[19] and respective genome annotation file.[20] A MultiQC[21] sequence reads and alignment quality report is provided in the supplement.

Reads were counted with featureCounts (v2.0.1).[22] Raw sequencing files and processed gene files were deposited in the ArrayExpress database under accession numbers E-MTAB-11459 (atorvastatin, reviewer access: Reviewer_E-MTAB-11459, password: Fbct211z) and E-MTAB-11460 (bentazon, reviewer access: Reviewer_E-MTAB-11460, password: ehet6zxx).[23]

Gene count library normalization and differential gene expression analysis (DGEA) were conducted in R[24] using DESeq2 (v1.30.0)[25]. Low abundant counts were removed prior DESeq2's median of ratios normalization and statistical testing for significant expression differences, using Wald's t-test and Benjamini-Hochberg (BH) correction with IHW for multiple testing.[26] To improve effect size signal-over-noise ratio, obtained $\log_2$-fold change (lfc) values were shrunk using the *apeglm* method.[27] For comparison of each treatment against the respective control group, an effect size cut off (LFcut) was determined as the top 25% quantile of absolute non-shrunk lfc values $LFcut = quantile(abs(lfc), 0.75)$. A gene was considered differentially expressed (DEG) when (a) statistical (padj ≤ 0.05) and (b) effect size cut off criteria ($abs(apeglm(lfc)) \geq LFcut$) were met, as described previously.[28]

Protein extraction, digestion and peptide labelling

Total protein was extracted simultaneously with RNA, using the *RapidPURE RNA Plant Kit* (MP Biomedicals Illkirch, France). For this, the protein-containing flow-through from RNA extraction was subjected to acetone precipitation. Precipitated proteins were resolubilized in 50 mM TEAB containing 4% CHAPS, 2 M thiourea and 6 M urea at pH 8.2, before buffer was exchanged to 100 mM TEAB containing 0.2% SDS and 2 M urea at pH 8.4 via 30 kDa molecular weight cut-off filters (Merck Darmstadt, Germany) for quantification, using the *Pierce BCA Protein Assay Kit* (Thermo Scientific, USA). The subsequent workflow for labelling tryptic digested protein samples TMT-6plex (Thermo Scientific, USA) followed the manufacturer's recommendations. Details about the workflow and sample label distribution are given in the supplements.

Proteomics

For quantitative proteomics, 500 ng combined TMT-labelled peptides were injected replicate wise onto a nanoACQUITY UPLC C18 Trap Column, before being separated on a nanoACQUITY reversed-phase analytical column (Waters, Massachusetts, USA) using a linear gradient from 3-97% (v/v) of 90% (v/v) acetonitrile in 0.1% (v/v) formic acid for 170 minutes with a flow rate of 300 nL/min. Eluted peptides were analyzed on a Thermo Fisher Q Exactive mass spectrometer (MS) (Thermo Fisher, Waltham, USA) as described previously.[29,30]

The resulting MS/MS data were processed using Maxquant search engine (v.2.0.1.0).[31] Tandem mass spectra were matched to a custom protein database with predicted protein sequence from the *L. minor* reference genome combined with duckweed related protein sequences (pro- and eukaryotic origin) obtained from Uniprot (search term "duckweed"). Further, a common lab contaminant protein list was provided for the PSM search. Differentially expressed proteins were identified using the MSstatsTMT R package (v.2.2.0)[32] on the basis of three technical replicate measurements of three biological replicates per condition. Statistical significance was assessed by comparing treatment to non-treated control using MSstatsTMT's implemented linear-mixed model with a moderated t-statistic. Proteins were considered statistically significantly regulated for BH-corrected p-values (padj) < 0.05[33] with degrees of freedom (DF) ≥ 6. The mass spectrometry proteomics data have been deposited in the ProteomeXchange Consortium via the PRIDE partner repository[34] with the dataset identifiers PXD031680 (atorvastatin, reviewer access: reviewer_pxd031680@ebi.ac.uk, password: uRtyStzZ) and PXD031679 (bentazon, reviewer access: reviewer_pxd031679@ebi.ac.uk, password: tRuIJdbC). A detailed description of the proteomics methodology can be found in the supplemental information.

Functional genome annotation and overrepresentation analysis (ORA)

A complementary approach using BLAST[35] and eggNOG[36] was applied to annotate the *L. minor* reference genome (2019v2) with gene ontology (GO) terms and gene descriptors based on protein sequence homology. A detailed workflow description is given in the supplements and a general overview is shown in **Figure 5**. Briefly, a multi fasta file listing the coding sequence per gene was extracted from the reference genome via the respective GTF file [Zenodo 6045874], and translated into amino acid sequences. For BLAST-based annotation, a local search database was created from the Uniprot database[37] containing peptide sequence information from closely related plant species as well as duckweed-associated microorganisms. Translated *L. minor* sequences were subjected to a BLASTP search against this local database and each gene was annotated with the Uniprot ID of the best hit scored by %-alignment for each reference species. Results were cleaned for non-plant related top hits as well as alignment lengths < 20 amino acids and alignment similarities < 35%. Each *L. minor* gene ID of these cleaned results was then annotated with the combined set of unique gene ontology (GO) terms associated with the matched plant related Uniprot IDs. Additionally, translated *L. minor* sequences were subjected to the eggNOG annotation with default settings.[38] All plant related matches were then combined in a single data frame with corresponding GO terms from which the *org.Lminor.eg.db* annotation package was constructed. Based on this custom built

annotation package, overrepresentation analysis (ORA) was performed in R using clusterProfiler v3.18[39] as described in the supplement.

RESULTS AND DISCUSSION

Identification of effect concentrations of atorvastatin and bentazon in L. minor

To determine low effect concentrations for ecotoxicogenomic assessment in a modified ecotoxicity test with *Lemna minor*, preliminary range-finding tests were performed. For each test substance, the effect of four concentrations was observed based on OECD TG 221, which were based on a literature review.[12,15,16]

Among the analyzed endpoints, frond area was found to be the most sensitive parameter (**Table 1** and **Table S1**), which was therefore used to determine effect concentrations for further ecotoxicogenomic test development. For atorvastatin (**Figure 2A**), the two highest and for bentazon (**Figure 2B**), all of the test concentrations resulted in statistically significant changes in frond area, as determined by Williams Multiple Sequential t-test. Concentration-response curves were generated (**Figure 2C** and **Figure 2D**), which were then used to calculate effect concentrations (**Table 1**). Whereas in the case of atorvastatin, effect concentrations were distributed over more than two orders of magnitude until a maximal effect was achieved (**Figure 2C**), in the case of bentazon, the maximal effect was achieved much more rapidly over a concentration range of less than one order of magnitude (**Figure 2D**). In contrast, atorvastatin effect concentrations (**Figure 2C** and **Table 1**) were by far lower than those of bentazon both in terms of mass concentration and molarity (**Figure 2D** and **Table 1**), indicating a significantly higher toxic potency of the pharmaceutical as compared to the herbicide.

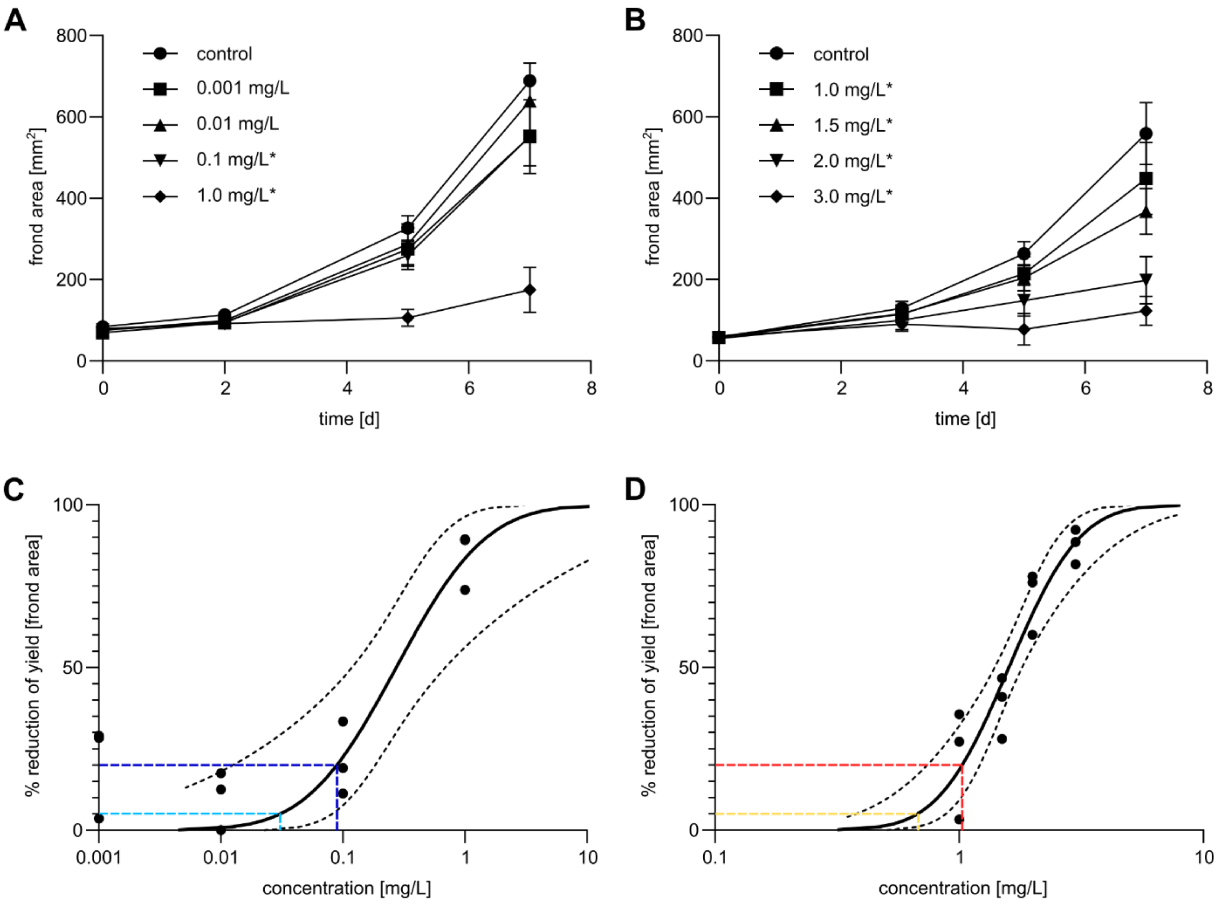

Figure 2. Pretest for detecting effect concentrations of atorvastatin and bentazon according to OECD TG 221. (A,B) Time-dependent course of the frond area at different exposure concentrations of atorvastatin (A) and bentazon (B). Statistically significant changes at day 7 compared to the control are indicated by an asterisk (Williams Multiple Sequential t-test). The standard deviation is given as error bar. (C,D) Concentration-response curve of frond area yield reduction after exposure to atorvastatin (C) and bentazon (D) on day 7. The EC_5 is colored in light blue and yellow and the EC_{20} is colored in dark blue and red.

Table 1. Obtained effect concentrations as mass concentration and molarity of each substance. [lower 95%-cI – higher 95%-cI]

Substance	EC_5	EC_{10}	EC_{20}	EC_{50}
Atorvastatin	0.03 mg/L [0.001 – 0.082] 0.027 µM [0.001 – 0.074]	0.05 mg/L [0.003 – 0.116] 0.045 µM [0.003 – 0.104]	0.09 mg/L [0.013 – 0.184] 0.081 µM [0.012 – 0.165]	0.27 mg/L [0.119 – 0.692] 0.242 µM [0.107 – 0.621]
Bentazon	0.69 mg/L [0.678 – 0.695] 2.875 µM [2.825 – 2.896]	0.83 mg/L [0.819 – 0.837] 3.458 µM [3.413 – 3.488]	1.04 mg/L [1.025 – 1.051] 4.333 µM [4.271 – 4.379]	1.60 mg/L [1.577 – 1.624] 6.667 µM [6.571 – 6.767]

By now, only one previous study investigated toxicity of atorvastatin in *L. minor*.[40] Klementová et al. found no significant effects up to a concentration of 200 mg/L, which is in contrast to the results of our study. Since the previous study also used OECD TG 221, possible explanations for the observed discrepancies could be the use of Swedish Standard growth medium and daylight exposure, whereas in our study Steinberg medium was used to prepare test solutions and controls and plants were constantly exposed to artificial light. However, our data in *L. minor* agree well with the phytotoxicity observed in the closely related species *Lemna gibba* in a previous study.[41] Brain et al. performed a toxicity test with atorvastatin according to the standards of the American Society for Testing and Materials (ASTM guideline E 1415-91), a guideline similar to OECD TG 221, and found an EC_{50} value of 0.24 mg/L for the frond number endpoint which is similar to our EC_{50} of 0.35 mg/L (**Table S1**).

For bentazon, several previous studies investigated toxicity in *L. minor*, predominantly according to the ISO 20079 standard, which has largely identical requirements to the OECD TG 221[2,42]. Munkegaard et al. observed an EC_{50} of 2.94 mg/L assessing the relative growth rate (RGR) of frond area.[15] Similarly, Cedergreen et al. identified an EC_{50} of 2.56 mg/L.[16] These previously identified effect concentrations were in the same order of magnitude as the EC_{50} observed in our study (**Table 1**), validating our experimental setting.

Gene expression signatures of atorvastatin and bentazon in L. minor

Since our study aimed to discriminate ecotoxic MoA based on gene expression profiles in a shortened *L. minor* growth inhibition assay, EC_5 and EC_{20} obtained with the regular OECD TG 221 were chosen as low effect concentrations to exclude systemic effects as much as possible. Thus, the shortened test was conducted with nominal concentrations of 0.03 (EC_5) and 0.09 mg/L (EC_{20}) for atorvastatin and 0.7 (EC_5) and 1.0 mg/L (EC_{20}) for bentazon. Chemical analysis employing UHPLC-MS/MS yielded recoveries between 90 and 103% of nominal test concentrations, so nominal concentrations are referenced below (**Table 2**). After a treatment period of three days gene expression changes were investigated by transcriptomics and proteomics.

For both test compounds, we observed a concentration-dependent behavior of gene expression, both in terms of the number of DEGs and the strength of their regulation (**Figure 3**), with more DEGs and generally higher lfc values in response to EC_{20} compared to EC_5.

Table 2. Nominal and measured concentrations of control and test solutions for both substances.

	Atorvastatin			Bentazon		
[µg a.s./L]	nominal	measured	recovery	nominal	measured	recovery
Control	0	-	-	0	-	-
EC_5	30.0	27. 1	90.3%	700.0	716.5	102.4%
EC_{20}	90.0	84.6	94.0%	1000.0	922.8	92.3%

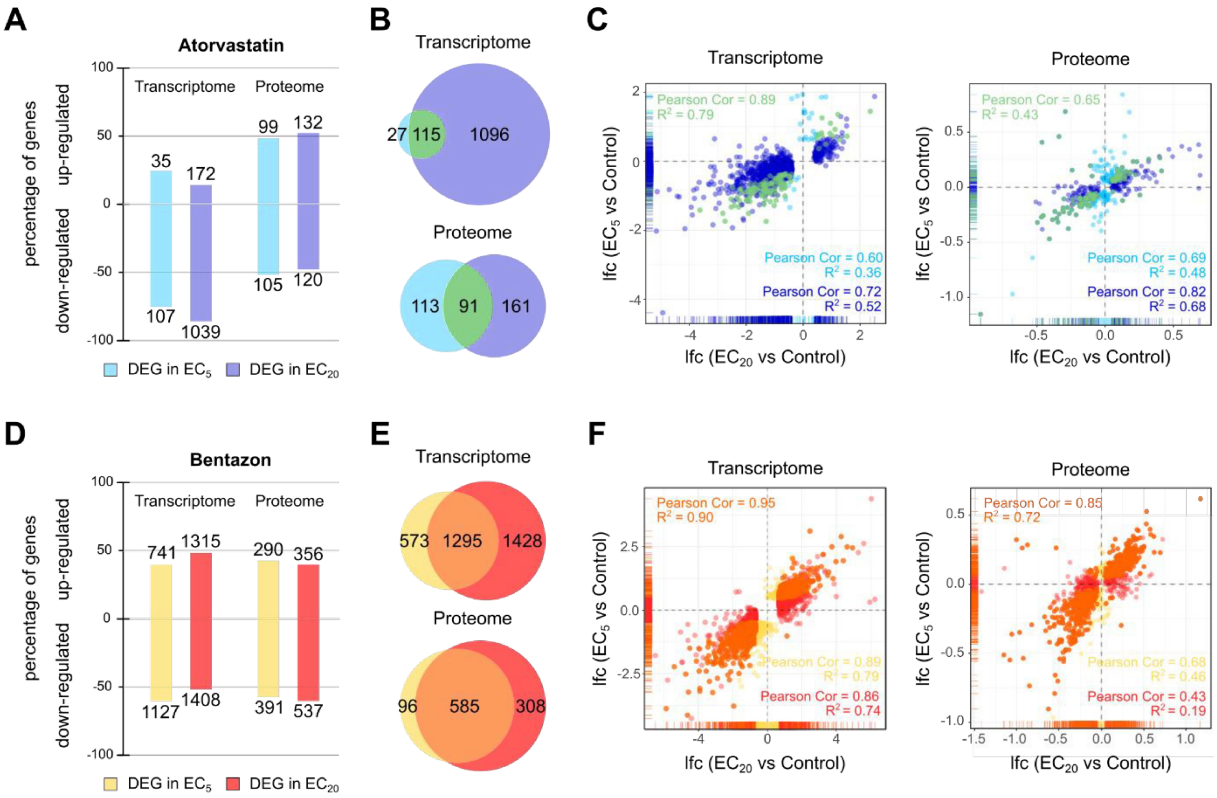

Figure 3. Gene expression changes in *L. minor* induced by exposure to EC_5 and EC_{20} of atorvastatin and bentazon after 3 days. (A) Percentages of the up- and downregulation of DEGs at the transcriptome and proteome level after exposure to EC_5 (light blue) and EC_{20} (dark blue) of atorvastatin compared to the control. The number of up- and downregulated genes is indicated as bar labels. (B) Venn diagrams showing the numbers of differentially expressed genes (DEGs) after exposure to EC_5 (light blue) and EC_{20} (dark blue) of atorvastatin and their intersection (green) at the transcriptome (top) and the proteome level (bottom). (C) Scatter plots showing the correlation of differential gene expression between exposure to the EC_5 and EC_{20} of atorvastatin at the transcriptome (left) and the proteome level (right) comparing their log_2-fold change (lfc) values. Coloring as in (B). (D) Percentages of the up- and downregulation of DEGs at the transcriptome and proteome level after exposure to EC_5 (yellow) and EC_{20} (red) of bentazon compared to the control. The number of up- and downregulated genes is indicated as bar labels. (E) Venn diagrams showing the numbers of differentially expressed genes (DEGs) after exposure to EC_5 (yellow) and EC_{20} (red) of bentazon and their intersection (orange) at the transcriptome (top) and the proteome level (bottom). (F) Scatter plots showing the correlation of differential gene expression between exposure to the EC_5 and EC_{20} of bentazon at the transcriptome (left) and the proteome level (right) comparing their lfc values. Coloring as in (E).

In the case of atorvastatin, 142 DEGs were detected at the transcriptome level by EC_5 and 1211 by EC_{20}, of which the majority (75% and 86%, respectively) were downregulated (**Figure 3A**). At the proteome level, 204 and 252 DEGs were identified in response to EC_5 and EC_{20}, respectively, of which half (51% and 48%, respectively) were downregulated. At the transcriptome level, 81% (115 genes) of DEGs responsive to EC_5 were also differentially expressed after exposure to EC_{20} (**Figure 3B**). At the proteome level, this intersection between EC_5 and EC_{20} consisted of 45% (91 genes) of the DEGs responding to EC_5. These common DEG sets of EC_5 and EC_{20} treatment conditions, representing early and consistently regulated genes, were defined as core DEG sets for each test compound. The lfc values induced by EC_5 and EC_{20} exposure showed a strong positive correlation for the atorvastatin core DEG sets, both at the transcriptome and proteome levels (Pearson correlation = 0.89 (transcriptome) and 0.65 (proteome)) (**Figure 3C**), making them a source for early biomarker candidates for inhibition of HMG-CoA reductase in *L. minor*.

In the case of bentazon, 1868 and 2723 DEGs were identified at the transcriptome level after exposure to EC_5 and EC_{20}, respectively, about half of which (60% and 52%, respectively) were downregulated (**Figure 3D**). At the proteome level, 681 and 893 DEGs were induced by EC_5 and EC_{20}, respectively, showing a comparable direction of regulation as in the transcriptome analyses (57% and 60% downregulation, respectively). A proportion of 69% (1295 genes) and 86% (585 genes) of the DEGs responding to EC_5 at the transcriptome and proteome levels, respectively, also responded to EC_{20} (**Figure 3E**).These core DEG sets of bentazon also showed strong positive correlations when comparing gene expression changes induced by EC_5 and EC_{20} (Pearson correlation = 0.95 (transcriptome) and 0.85 (proteome)) and therefore contain early biomarker candidates for photosynthesis inhibition (**Figure 3F**).

While few previous studies have analysed transcriptomic changes induced by various stressors in *L. minor*[5–7], proteomic data are notably lacking for molecular analysis in this species. Our data clearly demonstrate that both OMICs methods are applicable to a shortened growth inhibition assay in *L. minor* to generate core DEG sets affected by low effect concentrations as toxicogenomic fingerprints.

To assess whether these fingerprints of each compound could serve as a basis for MoA discrimination, we next compared the identified core DEG sets of atorvastatin and bentazon. While atorvastatin acts as an HMGR inhibitor in humans and plants[12], the herbicide bentazon interferes with photosynthesis by inhibiting plant PSII.[43] However, previous studies also suggested that bentazon has inhibitory properties related to HMGR activity.[14] In view of these potentially partially concordant MoA of both test substances, it was particularly interesting to

identify similarities and differences in their gene expression profiles. At the transcriptome level, the core DEG sets of atorvastatin and bentazon overlapped in a total of 48 genes, which accounted for 42% of the atorvastatin signature and 4% of the bentazon signature (**Figure 4A**). At the level of the proteome, the intersection of the core DEG sets totaled 44 genes, which corresponded to a 48% share of the atorvastatin signature and an 8% share of the bentazon signature. While in the case of the transcriptome, the genes that were jointly targeted by both compounds showed a positive correlation when comparing the two compounds (Pearson correlation = 0.57, $p \leq 0.0001$), the genes of the intersection were not significantly correlated at the proteome level (Pearson correlation = 0.15, $p = 0.3229$) (**Figure 4B**). Remarkably, the signatures of both substances that were not part of the intersection behaved in a substance-specific manner, i.e. their expression was predominantly not regulated by the respective other substance. Therefore, the common subset of core DEGs of both compounds at the transcriptome level may result from and indicate partial concordance in MoA, such as partial HMGR inhibition, whereas those of the intersection of core DEGs at the proteome level as well as compound-specific core DEG sets may allow discrimination of both MoA.

To provide a focus on robustly expressed biomarker candidates for both MoA, we extracted the top 50 from the core DEG sets of both compounds in terms of their expression levels in the control condition (**Figure 4C**). The resulting signatures allow clear discrimination of the molecular effects of atorvastatin and bentazon, and the shared gene clusters represent a minor proportion of each signature. Nevertheless, the common signatures show similar regulation in the vast majority of genes. Of particular interest for the selection of potential discriminatory biomarkers are genes that are differentially regulated by the two compounds. Examples of such promising biomarker candidates include the genes Lminor_013527, Lminor_000967, and Lminor_004696.

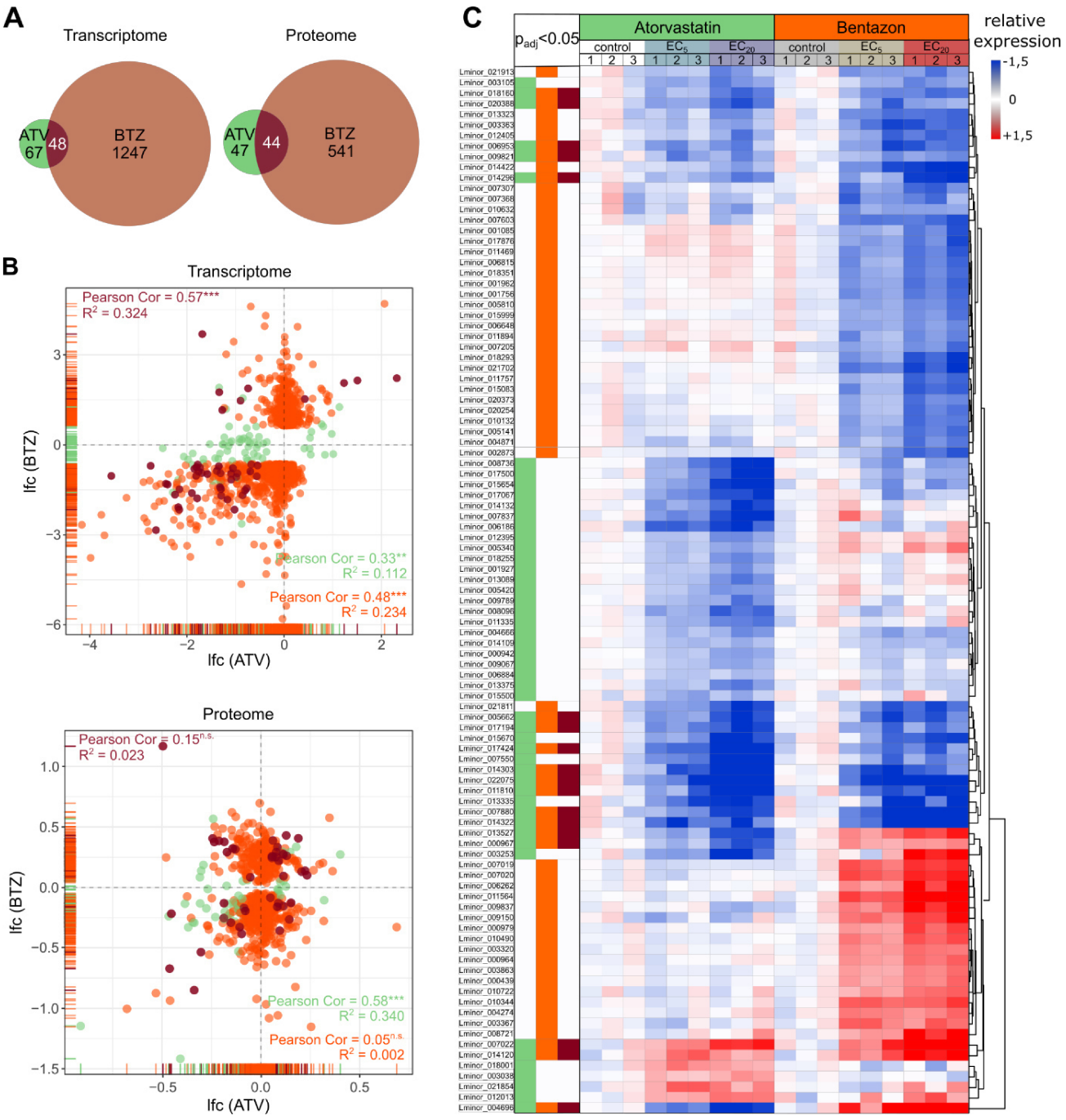

Figure 4. Comparison of gene expression signatures induced by atorvastatin and bentazon in *L. minor*. (A) Venn diagrams showing the numbers of DEGs in the intersections of EC_5 and EC_{20} exposures after atorvastatin (ATV, green) and bentazon (BTZ, orange) exposure at the transcriptome (left) and the proteome level (right). The intersections are colored in dark red. (B) Scatter plots comparing the lfc values of DEGs in the intersections of EC_5 and EC_{20} exposures after atorvastatin and bentazon exposure at the level of transcriptome (top) and proteome (bottom). Coloring as in (A). * $p < 0.05$, ** $p < 0.01$, *** $p < 0.001$, n.s. "not statistically significant". (C) Heatmap showing the relative expression of the top 50 DEGs in the intersections of EC_5 and EC_{20} exposures for both substances at the transcriptome level, based on their mean expression in the control condition. Red colour indicates upregulation and blue downregulation of a gene as compared to the control. The colour code on the top of each column illustrates the test condition. Columns indicate biological replicates (1-3) per condition. Genes were clustered by Euclidean distance. The color code on the left assigns the genes to the DEG sets defined in (A).

Functional classification of molecular effects of atorvastatin and bentazon

To gain insight into the functional processes affected by the two test compounds, we functionally annotated the *L. minor* reference genome to enable overrepresentation analysis of DEG sets with respect to gene ontologies such as biological processes, molecular functions, or cellular connections. To this end, we developed a homology-based bioinformatics workflow that allowed GO terms of closely related plant proteins to be mapped to the corresponding *L. minor* gene IDs (**Figure 5A**). About 99.5% of *L. minor* genes were assigned to duckweed-related taxa or other plants through our pipeline, whereas only a small fraction of 0.5% had the highest homology with bacterial proteins, which might be due to symbiotic living prokaryotes (**Figure S7**). Nevertheless, this clear assignability of genes demonstrates the robustness of our annotation approach, which is an important prerequisite for generating meaningful ORA results. The resulting *L. minor* AnnoDbi package was used for ORA analysis of the identified core DEG sets of atorvastatin and bentazon.

When we focused on lipid- and light-related biological processes, we identified a number of significantly impaired metabolic pathways by one or both test substances (**Figure 5B**). While light-related processes were predominantly affected by bentazon, different lipid-related processes were affected by either test substance, consistent with the partial agreement in MoA mentioned above.

Biological processes affected by atorvastatin were predominantly related to lipid metabolic processes, reflecting HMGR-inhibitory MoA leading to lipid and sterol deficiency. In particular, the cellular response to lipids, but also several biological processes related to signaling pathways activated by abisic acid (ABA), were significantly affected by atorvastatin exposure. These results are consistent with previous studies reporting ABA-mediated regulation of HMGR expression or activity.[44–46] ABA is an isoprenoid hormone synthesized via the chloroplastic 2-C-methyl-D-erythritol 4-phosphate (MEP) pathway. In addition to the MEP pathway, the mevalonate (MVA) pathway is the major metabolic pathway for the biosynthesis of isoprene precursors. One of the key enzymes of the MVA pathway is HMGR. MEP and MVA pathways operate in parallel and compensate for each other through intermediates such as isopentyl diphosphate (IPP).[12] Therefore, the observed changes in ABA-mediated signaling after atorvastatin exposure may represent a response to impaired synthesis of isoprene precursors due to HMGR inhibition by linking the MEP and MVA pathways. Such observations were previously made in *Arabidopsis thaliana* after lovastatin treatment, where carotenoid and chlorophyll content (MEP products) were impaired after HMGR inhibition.[47] Because carotenoids are precursors of ABA, increased carotenoid synthesis may also reflect ABA

content in the plant and ABA-related signaling pathways in general. Among the biological processes most affected was the ethylene-activated signaling pathway. Ethylene treatment was shown to upregulate HMGR expression in *Dioscorea zingiberensis*, suggesting a role for this enzyme in ethylene signaling and consistent with our results. In addition, atorvastatin also affected genes involved in a limited number of light-related processes such as light stimulus detection or red light phototransduction.

A previous study by Zheng et al. found a light-induced reduction in HMGR activity in grapevine, suggesting a direct or indirect role of HMGR in light sensing, which may also be reflected in our observations.[48]

However, the response to light was impaired, especially by bentazon. The biological processes most strongly regulated by bentazon were cellular response to blue light and light stimulus, response to red or far red light, and blue light signaling pathway. Bentazon is an inhibitor of PSII, which is the most light-sensitive component of the photosynthetic apparatus. Treatment of plants with PSII inhibitors thus causes them to die faster when exposed to light than in the dark.[49] However, the toxic mode of action of PSII herbicides is not directly triggered by light, but by damage to cells due to an excessive amount of non-released light energy. Normally, absorbed energy is transferred from chlorophyll to PSII within the electron transport chain of photosynthesis.[50] Since blocking PSII results in a break in this chain, the absorbed and short-lived energy must be dissipated by other means. Although excess energy is normally dissipated by carotenoids, in the case of PSII inhibition, the amount of energy is too high, resulting in the formation of lipid radicals that lead to lipid peroxidation of the membrane bilayer and ultimately to plant death.[49] These processes are also reflected in our ORA results, where bentazon caused changes in various lipid-related biological processes such as sphingolipid metabolism, lipid modification, or lipid phosphorylation. These results are also supported by recent studies by Czékus et al. where bentazon treatment caused increased lipid peroxidation and ion leakage in soybean and common ragweed.[43]

In summary, our study established a shortened three-day growth inhibition assay in *L. minor*, which allows an investigation of the mode of action of test compounds based on gene expression signatures beyond the endpoints of the OECD guideline assay. The functional annotation of the *L. minor* reference genome developed in our study allows ORA analyses to detect functional impairment and is transferable to other poorly or unannotated organisms. The shortened assay will help to develop future screening approaches for hazard assessment of compounds that can identify early modes of action in *L. minor* that lead to adverse effects.

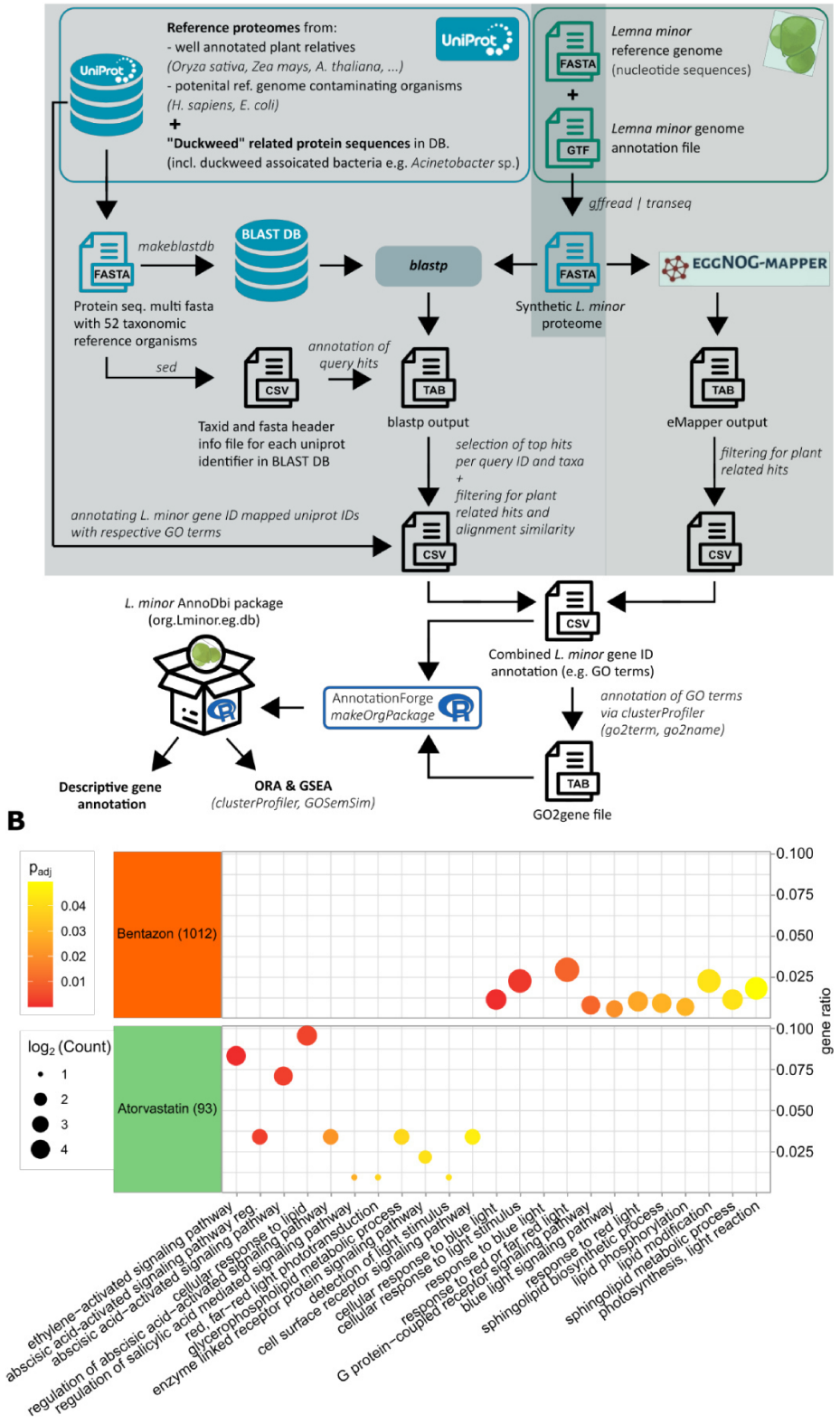

Figure 5. Functional analysis of gene expression responses induced by exposure to low effect concentrations of atorvastatin and bentazon in *L. minor*. (A) Bioinformatic pipeline for functional gene annotation in *L. minor*. A complementary approach applying BLAST[35] and eggNOG[36] was used to assign genes of the *L. minor* reference genome to gene ontology terms. Detailed information can be found in the materials and methods section as well as in the supplemental information. (B) Overrepresentation analysis of the DEGs in the intersections of EC_5 and EC_{20} exposure to atorvastatin (left) and bentazon (right) using the gene ontology biological function. The log_2-converted gene count for each ontology term is indicated as bubble size, the gene ratio (geneR) is plotted on the x-axis. P-values are given as a color code.

ASSOCIATED CONTENT

Supporting Information. Supplemental material contains additional experimental details, materials and methods including qualification schemes of RNA-Seq data, supplemental figures and tables (docx).

AUTHOR INFORMATION

Corresponding Author

*Sebastian Eilebrecht - Fraunhofer Attract Eco'n'OMICs, Fraunhofer Institute for Molecular Biology and Applied Ecology, Auf dem Aberg 1, 57392 Schmallenberg, Germany; Email: sebastian.eilebrecht@ime.fraunhofer.de

Authors

Alexandra Loll† – Fraunhofer Attract Eco'n'OMICs, Fraunhofer Institute for Molecular Biology and Applied Ecology, Auf dem Aberg 1, 57392 Schmallenberg, Germany; Institute of Food Chemistry and Food Biotechnology, Justus Liebig University Giessen, Heinrich-Buff-Ring 17, 35392 Giessen, Germany

Hannes Reinwald† – Fraunhofer Attract Eco'n'OMICs, Fraunhofer Institute for Molecular Biology and Applied Ecology, Auf dem Aberg 1, 57392 Schmallenberg, Germany; Department Evolutionary Ecology and Environmental Toxicology, Goethe University Frankfurt, Max-von-Laue-Straße 9, 60438 Frankfurt am Main, Germany

Steve Uwa Ayobahan – Fraunhofer Attract Eco'n'OMICs, Fraunhofer Institute for Molecular Biology and Applied Ecology, Auf dem Aberg 1, 57392 Schmallenberg

Bernd Göckener – Department Environmental and Food Analysis, Fraunhofer Institute for Molecular Biology and Applied Ecology, Auf dem Aberg 1, 57392 Schmallenberg, Germany

Gabriela Salinas – NGS-Services for Integrative Genomics, University of Göttingen, Transcriptome and Genome Analysis Laboratory, Justus von Liebig Weg 11, 37077 Göttingen, Germany

Christoph Schäfers – Department Ecotoxicology, Fraunhofer Institute for Molecular Biology and Applied Ecology, Auf dem Aberg 1, 57392 Schmallenberg, Germany

Karsten Schlich – Department Ecotoxicology, Fraunhofer Institute for Molecular Biology and Applied Ecology, Auf dem Aberg 1, 57392 Schmallenberg, Germany

Gerd Hamscher – Institute of Food Chemistry and Food Biotechnology, Justus Liebig University Giessen, Heinrich-Buff-Ring 17, 35392 Giessen, Germany

Author Contributions

The manuscript was written in collaboration with all authors. All authors have agreed to the final version of the manuscript. †: These authors contributed equally. Alexandra Loll performed experiments, contributed to data analysis and wrote the manuscript. Hannes Reinwald analyzed the data, developed the functional annotation pipeline and contributed to manuscript writing. Steve U. Ayobahan performed proteomics analysis. Bernd Göckener performed chemical analysis. Gabriela Salinas supervised RNA sequencing. Christoph Schäfers, and Gerd Hamscher contributed to study design. Karsten Schlich contributed to study design and supervision of the study. Sebastian Eilebrecht designed and supervised the study and contributed to manuscript writing.

ACKNOWLEDGMENT

This work was supported by the Fraunhofer Internal Programs under Grant No. Attract 040-600300. Graphs and illustrations were generated with the help of the freeware tools R / R Studio and Inkscape (www.inkscape.org). Graphical illustrations were generated using Biorender (www.biorender.com). We thank Julia Alvincz for introduction to laboratory methods, Stephan Hennecke for contributing to chemical analysis, Pamela Meyer for contributing to atorvastatin pretesting and Orr Shomroni for RNA-Seq raw data processing.

REFERENCES

(1) Ferrari, B.; Mons, R.; Vollat, B.; Fraysse, B.; Paxéus, N.; Lo Giudice, R.; Pollio, A.; Garric, J. Environmental Risk Assessment of Six Human Pharmaceuticals: Are the Current Environmental Risk Assessment Procedures Sufficient for the Protection of the Aquatic Environment? *Environ. Toxicol. Chem.* **2004**, *23* (5), 1344–1354. https://doi.org/10.1897/03-246.

(2) Organisation for Economic Co-operation and Development. OECD 221 Lemna Sp. Growth Inhibition Test. *Guidel. Test. Chem. Test. Chem.* **2006**, 1–26.

(3) Ge, Y.; Wang, D. Z.; Chiu, J. F.; Cristobal, S.; Sheehan, D.; Silvestre, F.; Peng, X.; Li, H.; Gong, Z.; Lam, S. H.; Wentao, H.; Iwahashi, H.; Liu, J.; Mei, N.; Shi, L.; Bruno, M.; Foth, H.; Teichman, K. Environmental OMICS: Current Status and Future Directions. *J. Integr. OMICS* **2013**, *3* (2), 75–87. https://doi.org/10.5584/jiomics.v3i2.141.

(4) Wheelock, C. E.; Goss, V. M.; Balgoma, D.; Nicholas, B.; Brandsma, J.; Skipp, P. J.; Snowden, S.; Burg, D.; D'Amico, A.; Horvath, I.; Chaiboonchoe, A.; Ahmed, H.; Ballereau, S.; Rossios, C.; Chung, K. F.; Montuschi, P.; Fowler, S. J.; Adcock, I. M.; Postle, A. D.; Dahleń, S. E.; Rowe, A.; Sterk, P. J.; Auffray, C.; Djukanović, R. Application of 'omics Technologies to Biomarker Discovery in Inflammatory Lung Diseases. *Eur. Respir. J.* **2013**, *42* (3), 802–825. https://doi.org/10.1183/09031936.00078812.

(5) Van Hoeck, A.; Horemans, N.; Monsieurs, P.; Cao, H. X.; Vandenhove, H.; Blust, R. The First Draft Genome of the Aquatic Model Plant Lemna Minor Opens the Route for Future Stress Physiology Research and Biotechnological Applications. *Biotechnol. Biofuels* **2015**, *8* (1), 1–13. https://doi.org/10.1186/s13068-015-0381-1.

(6) Wang, W.; Li, R.; Zhu, Q.; Tang, X.; Zhao, Q. Transcriptomic and Physiological Analysis of Common Duckweed Lemna Minor Responses to NH4+ Toxicity. *BMC Plant Biol.* **2016**, *16* (1), 1–13. https://doi.org/10.1186/s12870-016-0774-8.

(7) Li, R.; Luo, C.; Qiu, J.; Li, Y.; Zhang, H.; Tan, H. Metabolomic and Transcriptomic Investigation of the Mechanism Involved in Enantioselective Toxicity of Imazamox in Lemna Minor. *J. Hazard. Mater.* **2022**, *425* (September 2021), 127818. https://doi.org/10.1016/j.jhazmat.2021.127818.

(8) Franzoni, F.; Quiñones-Galvan, A.; Regoli, F.; Ferrannini, E.; Galetta, F. A Comparative Study of the in Vitro Antioxidant Activity of Statins. *Int. J. Cardiol.* **2003**, *90* (2–3), 317–321. https://doi.org/10.1016/S0167-5273(02)00577-6.

(9) Lennernäs, H. Clinical Pharmacokinetics of Atorvastatin. *Clin. Pharmacokinet.* **2003**, *42* (13), 1141–1160.

(10) Campos, N.; Arró, M.; Ferrer, A.; Boronat, A. Determination of 3-Hydroxy-3-Methylglutaryl CoA Reductase Activity in Plants. *Methods Mol. Biol.* **2014**, *1153*, 21–40. https://doi.org/10.1007/978-1-4939-0606-2.

(11) Istvan, E. S. Bacterial and Mammalian HMG-CoA Reductases: Related Enzymes with Distinct Architectures. *Curr. Opin. Struct. Biol.* **2001**, *11* (6), 746–751. https://doi.org/10.1016/S0959-440X(01)00276-7.

(12) Brain, R. A.; Reitsma, T. S.; Lissemore, L. I.; Bestari, K.; Sibley, P. K.; Solomon, K. R. Herbicidal Effects of Statin Pharmaceuticals in Lemna Gibba. *Environ. Sci. Technol.* **2006**, *40* (16), 5116–5123. https://doi.org/10.1021/es0600274.

(13) Herbicide Resistance Action Committee. HRAC Mode of Action Classification 2020 Poster www.hracglobal.com.

(14) Grumbach, K. H.; Bach, T. J. The Effect of PS II Herbicides, Amitrol and SAN 6706 on the Activity of 3-Hydroxy-3-Methylglutaryl-Coenzyme-A-Reductase and the Incorporation of [2-14C]Acetate and [2-3H]Mevalonate into Chloroplast Pigments of Radish Seedlings. *Zeitschrift fur Naturforsch. - Sect. C J. Biosci.* **1979**, *34*, 941–943.

(15) Munkegaard, M.; Abbaspoor, M.; Cedergreen, N. Organophosphorous Insecticides as Herbicide Synergists on the Green Algae Pseudokirchneriella Subcapitata and the Aquatic Plant Lemna Minor. *Ecotoxicology* **2008**, *17* (1), 29–35. https://doi.org/10.1007/s10646-007-0173-x.

(16) Cedergreen, N.; Streibig, J. C. The Toxicity of Herbicides to Non-Target Aquatic Plants and Algae: Assessment of Predictive Factors and Hazard. *Pest Manag. Sci.* **2005**, *61* (12), 1152–1160. https://doi.org/10.1002/ps.1117.

(17) Andrews, S. FastQC: A Quality Control Tool for High Throughput Sequence Data. 2010.

(18) Wingett, S. W.; Andrews, S. Fastq Screen: A Tool for Multi-Genome Mapping and Quality Control [Version 1; Referees: 3 Approved, 1 Approved with Reservations]. *F1000Research* **2018**, *7*, 1–14. https://doi.org/10.12688/f1000research.15931.1.

(19) Dobin, A.; Davis, C. A.; Schlesinger, F.; Drenkow, J.; Zaleski, C.; Jha, S.; Batut, P.; Chaisson, M.; Gingeras, T. R. STAR: Ultrafast Universal RNA-Seq Aligner. *Bioinformatics* **2013**, *29* (1), 15–21. https://doi.org/10.1093/bioinformatics/bts635.

(20) Genome Annotation File Lemna minor https://zenodo.org/record/6045874/files/Lminor_refGenome_GTF_CDS.7z?download=1.

(21) Ewels, P.; Magnusson, M.; Lundin, S.; Käller, M. MultiQC: Summarize Analysis Results for Multiple Tools and Samples in a Single Report. *Bioinformatics* **2016**, *32* (19), 3047–3048. https://doi.org/10.1093/bioinformatics/btw354.

(22) Liao, Y.; Smyth, G. K.; Shi, W. FeatureCounts: An Efficient General Purpose Program for Assigning Sequence Reads to Genomic Features. *Bioinformatics* **2014**, *30* (7), 923–930. https://doi.org/10.1093/bioinformatics/btt656.

(23) EMBL-EBI. ArrayExpress - functional genomics data https://www.ebi.ac.uk/arrayexpress/.

(24) Andy Bunn, M. K. An Introduction to DplR. *Ind. Commer. Train.* **2008**, *10* (1), 11–18.

(25) Love, M. I.; Anders, S.; Huber, W. Differential Analysis of Count Data - the DESeq2 Package. *Genome Biol.* **2014**, *15* (550), 10–1186.

(26) Ignatiadis, N.; Klaus, B.; Zaugg, J. B.; Huber, W. Data-Driven Hypothesis Weighting Increases Detection Power in Genome-Scale Multiple Testing. *Nat. Methods* **2016**, *13*, 577–580. https://doi.org/https://doi.org/10.1038/nmeth.3885.

(27) Zhu, A.; Ibrahim, J. G.; Love, M. I. Heavy-Tailed Prior Distributions for Sequence Count Data: Removing the Noise and Preserving Large Differences. *Bioinformatics* **2019**, *35* (12), 2084–2092. https://doi.org/10.1093/bioinformatics/bty895.

(28) Reinwald, H.; Alvincz, J.; Hollert, H.; Schäfers, C.; Eilebrecht, S. Toxicogenomic Profiles of Neuronal Targeting Insecticides in Zebrafish Embryos as Non-Target Aquatic Vertebrate Mode [Zenodo: 5218919]. *Zenodo* **2021**. https://doi.org/https://zenodo.org/record/5218919.

(29) Ayobahan, S. U.; Eilebrecht, E.; Kotthoff, M.; Baumann, L.; Eilebrecht, S.; Teigeler, M.; Hollert, H.; Kalkhof, S.; Schäfers, C. A Combined FSTRA-Shotgun Proteomics Approach to Identify Molecular Changes in Zebrafish upon Chemical Exposure. *Sci. Rep.* **2019**, *9* (1), 1–12. https://doi.org/10.1038/s41598-019-43089-7.

(30) Ayobahan, S. U.; Eilebrecht, S.; Baumann, L.; Teigeler, M.; Hollert, H.; Kalkhof, S.; Eilebrecht, E.; Schäfers, C. Detection of Biomarkers to Differentiate Endocrine Disruption from Hepatotoxicity in Zebrafish (Danio Rerio) Using Proteomics. *Chemosphere* **2020**, *240*, 1–12. https://doi.org/10.1016/j.chemosphere.2019.124970.

(31) Cox, J.; Mann, M. MaxQuant Enables High Peptide Identification Rates, Individualized p.p.b.-Range Mass Accuracies and Proteome-Wide Protein Quantification. *Nat. Biotechnol.* **2008**, *26* (12), 1367–1372. https://doi.org/10.1038/nbt.1511.

(32) Huang, T.; Choi, M.; Tzouros, M.; Golling, S.; Pandya, N. J.; Banfai, B.; Dunkley, T.; Vitek, O. MSstatsTMT: Statistical Detection of Differentially Abundant Proteins in Experiments with Isobaric Labeling and Multiple Mixtures. *Mol. Cell. Proteomics* **2020**, *19* (10), 1706–1723. https://doi.org/10.1074/mcp.RA120.002105.

(33) Diz, A. P.; Carvajal-Rodríguez, A.; Skibinski, D. O. F. Multiple Hypothesis Testing in Proteomics: A Strategy for Experimental Work. *Mol. Cell. Proteomics* **2011**, *10* (3), 1–10. https://doi.org/10.1074/mcp.M110.004374.

(34) Perez-Riverol, Y.; Csordas, A.; Bai, J.; Bernal-Llinares, M.; Hewapathirana, S.; Kundu, D. J.; Inuganti, A.; Griss, J.; Mayer, G.; Eisenacher, M.; Pérez, E.; Uszkoreit, J.; Pfeuffer, J.; Sachsenberg, T.; Yilmaz, Ş.; Tiwary, S.; Cox, J.; Audain, E.; Walzer, M.; Jarnuczak, A. F.; Ternent, T.; Brazma, A.; Vizcaíno, J. A. The PRIDE Database and Related Tools and Resources in 2019: Improving Support for Quantification Data. *Nucleic Acids Res.* **2019**, *47* (D1), D442–D450. https://doi.org/10.1093/nar/gky1106.

(35) Sayers, E. W.; Beck, J.; Bolton, E. E.; Bourexis, D.; Brister, J. R.; Canese, K.; Comeau, D. C.; Funk, K.; Kim, S.; Klimke, W.; Marchler-Bauer, A.; Landrum, M.; Lathrop, S.; Lu, Z.; Madden, T. L.; O'Leary, N.; Phan, L.; Rangwala, S. H.; Schneider, V. A.; Skripchenko, Y.; Wang, J.; Ye, J.; Trawick, B. W.; Pruitt, K. D.; Sherry, S. T. Database Resources of the National Center for Biotechnology Information. *Nucleic Acids Res.* **2021**, *49* (D1), D10–D17. https://doi.org/10.1093/nar/gkaa892.

(36) Cantalapiedra, C. P.; Hernández-Plaza, A.; Letunic, I.; Bork, P.; Huerta-Cepas, J. EggNOG-Mapper v2: Functional Annotation, Orthology Assignments, and Domain Prediction at the Metagenomic Scale. *Mol. Biol. Evol.* **2021**, *38* (12), 5825–5829. https://doi.org/10.1093/molbev/msab293.

(37) Bateman, A.; Martin, M. J.; Orchard, S.; Magrane, M.; Agivetova, R.; Ahmad, S.; Alpi, E.; Bowler-Barnett, E. H.; Britto, R.; Bursteinas, B.; Bye-A-Jee, H.; Coetzee, R.; Cukura, A.; Silva, A. Da; Denny, P.; Dogan, T.; Ebenezer, T. G.; Fan, J.; Castro, L. G.; Garmiri, P.; Georghiou, G.; Gonzales, L.; Hatton-Ellis, E.; Hussein, A.; Ignatchenko, A.; Insana, G.; Ishtiaq, R.; Jokinen, P.; Joshi, V.; Jyothi, D.; Lock, A.; Lopez, R.; Luciani, A.; Luo, J.; Lussi, Y.; MacDougall, A.; Madeira, F.; Mahmoudy, M.; Menchi, M.; Mishra, A.; Moulang, K.; Nightingale, A.; Oliveira, C. S.; Pundir, S.; Qi, G.; Raj, S.; Rice, D.; Lopez, M. R.; Saidi, R.; Sampson, J.; Sawford, T.; Speretta, E.; Turner, E.; Tyagi, N.; Vasudev, P.; Volynkin, V.; Warner, K.; Watkins, X.; Zaru, R.; Zellner, H.; Bridge, A.; Poux, S.; Redaschi, N.; Aimo, L.; Argoud-Puy, G.; Auchincloss, A.; Axelsen, K.; Bansal, P.; Baratin, D.; Blatter, M. C.; Bolleman, J.; Boutet, E.; Breuza, L.; Casals-Casas, C.; de Castro, E.; Echioukh, K. C.; Coudert, E.; Cuche, B.; Doche, M.; Dornevil, D.; Estreicher, A.; Famiglietti, M. L.; Feuermann, M.; Gasteiger, E.; Gehant, S.; Gerritsen, V.; Gos, A.; Gruaz-Gumowski, N.; Hinz, U.; Hulo, C.; Hyka-Nouspikel, N.; Jungo, F.; Keller, G.; Kerhornou, A.; Lara, V.; Le Mercier, P.; Lieberherr, D.; Lombardot, T.; Martin, X.; Masson, P.; Morgat, A.; Neto, T. B.; Paesano, S.; Pedruzzi, I.; Pilbout, S.; Pourcel, L.; Pozzato, M.; Pruess, M.; Rivoire, C.; Sigrist, C.; Sonesson, K.; Stutz, A.; Sundaram, S.; Tognolli, M.; Verbregue, L.; Wu, C. H.; Arighi, C. N.; Arminski, L.; Chen, C.; Chen, Y.; Garavelli, J. S.; Huang, H.; Laiho, K.; McGarvey, P.; Natale, D. A.; Ross, K.; Vinayaka, C. R.; Wang, Q.; Wang, Y.; Yeh, L. S.; Zhang, J. UniProt: The Universal Protein Knowledgebase in 2021. *Nucleic Acids Res.* **2021**, *49* (D1), D480–D489. https://doi.org/10.1093/nar/gkaa1100.

(38) Huerta-Cepas, J.; Forslund, K.; Coelho, L. P.; Szklarczyk, D.; Jensen, L. J.; Von Mering, C.; Bork, P. Fast Genome-Wide Functional Annotation through Orthology Assignment by EggNOG-Mapper. *Mol. Biol. Evol.* **2017**, *34* (8), 2115–2122. https://doi.org/10.1093/molbev/msx148.

(39) Yu, G.; Wang, L.-G.; Han, Y.; He, Q.-Y. ClusterProfiler: An R Package for Comparing Biological Themes among Gene Clusters. *Omi. A J. Integr. Biol.* **2012**, *16*, 284–287. https://doi.org/https://doi.org/10.1089/omi.2011.0118.

(40) Klementová, Š.; Petráňová, P.; Fojtíková, P. Photodegradation of Atorvastatin under Light Conditions Relevant to Natural Waters and Photoproducts Toxicity Assessment. *Open J. Appl. Sci.* **2021**, *10* (04), 489–499. https://doi.org/10.4236/ojapps.2021.104035.

(41) Brain, R. A.; Johnson, D. J.; Richards, S. M.; Hanson, M. L.; Sanderson, H.; Lam, M. W.; Young, C.; Mabury, S. A.; Sibley, P. K.; Solomon, K. R. Microcosm Evaluation of the Effects of an Eight Pharmaceutical Mixture to the Aquatic Macrophytes Lemna Gibba and Myriophyllum Sibiricum. *Aquat. Toxicol.* **2004**, *70* (1), 23–40. https://doi.org/10.1016/j.aquatox.2004.06.011.

(42) Deutsches Institut für Normung e.V. *DIN EN ISO 20079*; 2006.

(43) Czékus, Z.; Farkas, M.; Bakacsy, L.; Ördög, A.; Gallé, Á.; Poór, P. Time-Dependent Effects of Bentazon Application on the Key Antioxidant Enzymes of Soybean and Common Ragweed. *Sustain.* **2020**, *12* (9), 1–20. https://doi.org/10.3390/su12093872.

(44) Mansouri, H.; Asrar, Z. Effects of Abscisic Acid on Content and Biosynthesis of Terpenoids in Cannabis Sativa at Vegetative Stage. *Biol. Plant.* **2012**, *56* (1), 153–156. https://doi.org/10.1007/s10535-012-0033-2.

(45) Jing, F.; Zhang, L.; Li, M.; Tang, Y.; Wang, Y.; Wang, Y.; Wang, Q.; Pan, Q.; Wang, G.; Tang, K. Abscisic Acid (ABA) Treatment Increases Artemisinin Content in Artemisia Annua by Enhancing the Expression of Genes in Artemisinin Biosynthetic Pathway. *Biologia (Bratisl).* **2009**, *64* (2), 319–323. https://doi.org/10.2478/s11756-009-0040-8.

(46) Kochan, E.; Balcerczak, E.; Szymczyk, P.; Sienkiewicz, M.; Zielińska-Bliźniewska, H.; Szymańska, G. Abscisic Acid Regulates the 3-Hydroxy-3-Methylglutaryl CoA Reductase Gene Promoter and Ginsenoside Production in Panax Quinquefolium Hairy Root Cultures. *Int. J. Mol. Sci.* **2019**, *20* (6). https://doi.org/10.3390/ijms20061310.

(47) Laule, O.; Fürholz, A.; Chang, H. S.; Zhu, T.; Wang, X.; Heifetz, P. B.; Gruissem, W.; Lange, B. M. Crosstalk between Cytosolic and Plastidial Pathways of Isoprenoid Biosynthesis in Arabidopsis Thaliana. *Proc. Natl. Acad. Sci. U. S. A.* **2003**, *100* (11), 6866–6871. https://doi.org/10.1073/pnas.1031755100.

(48) Zheng, T.; Guan, L.; Yu, K.; Haider, M. S.; Nasim, M.; Liu, Z.; Li, T.; Zhang, K.; Jiu, S.; Jia, H.; Fang, J. Expressional Diversity of Grapevine 3-Hydroxy-3-Methylglutaryl-CoA Reductase (VvHMGR) in Different Grapes Genotypes. *BMC Plant Biol.* **2021**, *21* (1), 1–13. https://doi.org/10.1186/s12870-021-03073-8.

(49) Dan Hess, F. Light-Dependent Herbicides: An Overview. *Weed Sci.* **2000**, *48* (2), 160–170.

(50) Yoneyama, K.; Maejima, N.; Ogasawara, M.; Konnai, M.; Honda, I.; Nakajima, Y.; Asami, T.; Inoue, Y.; Yoshida, S. Photosystem II Inhibition by S-Triazines Having Hydrophilic Amino Groups. *Biosci. Biotechnol. Biochem.* **1995**, *59* (11), 2170–2171. https://doi.org/10.1271/bbb.59.2170.

SUPPLEMENT

A short term test for toxicogenomic analysis of ecotoxic modes-of-action in *Lemna minor*

Alexandra Loll[†,1,2], Hannes Reinwald[†,1,3], Steve U. Ayobahan[1], Bernd Göckener[4], Gabriela Salinas[5], Christoph Schäfers[6], Karsten Schlich[6], Gerd Hamscher[2], Sebastian Eilebrecht[1]

[†]: Shared 1st authorship

1 Supplemental Materials and Methods

1.1 Chemical analysis

The concentrations of atorvastatin and bentazon in the aqueous samples were determined by chemical analysis that was performed separately for both substances by ultra-high performance liquid chromatography coupled with tandem mass spectrometry (UHPLC–MS/MS).

For analysis of atorvastatin, samples of 5 mL volume were diluted with 1 mL methanol in glass tubes. Where necessary, samples were diluted with a mixture of the medium and methanol (5/1, v/v) to yield concentrations within the calibration range. Data were collected on a Waters Acquity UPLC H-Class system coupled to a Waters Xevo TQ-S tandem mass spectrometer operated in positive electrospray ionization (ESI) mode. Chromatographic separation was performed on a Waters UPLC BEH C18 column (1.7 µm, 50 mm x 2.1 mm) at a flow rate of 0.25 mL/min and a column temperature of 30 °C. The injection volume was 2 µL.

A mixture of water and methanol (95/5, v/v) with 2 mM ammonium acetate and 0.02% ammonium hydroxide was used as mobile phase (MP) A and methanol with 2 mM ammonium acetate and 0.02% ammonium hydroxide was used as MP B. The following linear gradient was applied for elution: 0 – 0.2 min: 0% MP B; 2.0 min: 20% MP B; 4.0 – 8.0 min: 100% MP B; 8.1 – 10 min: 0% MP B. The mass transition used for the quantification of atorvastatin was m/z 559.2 > m/z 440.1; the confirmation of the substance's identity was carried out via the mass transition m/z 559.2 > m/z 250.0.

A seven-point matrix calibration in a mixture of the medium and methanol (5/1, v/v) was used in a concentration range from 0.30 µg/L to 30 µg/L (referring to the aqueous part). The coefficient of determination (r2) of the linear calibration function was determined to be >0.998. The analytical method was successfully validated for the medium on two fortification levels (1.0 and 10 µg/L) according to the EU guideline SANTE/2020/12830[1] at a limit of quantification (LOQ) of 1.0 µg/L. The accuracy (overall mean recovery) was 99.2% and the precision was 0.90% (RSD of the recovery values).

Two quality control (QC) samples with concentrations of 2.0 and 20 µg/L were used for the ongoing verification of the matrix calibration. Recoveries of QC samples were within a range of 80 – 120%. Matrix-charged procedural blanks and controls were prepared and run with the samples to exclude possible cross-contaminations during laboratory work.

Chemical analysis of bentazon was conducted with a method similar as described above. 5 mL of the aqueous sample were amended with 1 mL of methanol. If necessary, samples were further diluted with a mixture of the medium and methanol (5/1, v/v) to yield concentrations within the

calibration range. A sample volume of 50 µL was directly injected into a Waters Acquity UPLC H-Class system coupled to a Waters Xevo TQ-D system. The same chromatographic column as mentioned above was used, but with a flowrate of 0.6 mL/min and a column temperature of 35 °C. As mobile phases, water (MP A) and acetonitrile (MP B) were acidified with 0.1% formic acid each. The linear gradient program was as follows. 0 min: 5% MP B; 0.5 min: 30% MP B; 3.0 – 4.0 min: 90% MP B; 4.0 – 5.0 min: 5% MP B. The mass transition used for the quantification of bentazon was m/z 239.2 > m/z 132.1. The mass transition m/z 239.2 > m/z 174.9 was used for confirmatory purposes.
A six-point matrix calibration with a concentration range from 1.0 µg/L to 10 µg/L (referring to the aqueous part) was prepared with the same solvent ratios as the samples. The coefficient of determination (r2) of the quadratic calibration function was determined to be >0.997.

1.2 RNA extraction

RNA extraction was performed according to RapidPURE RNA Plant Kit (REF 112722050 – MP Biomedicals Illkirch, France), with exceptions explained in the following. Since less plant material (25 mg) was used for extraction, the added amounts of Lysis Solution PS and ethanol were halved so that all lysate could subsequently be transferred to the spin filter in one step. The homogenization step after adding the Lysis Solution PS was performed at 5 m/s for one minute. Beyond that, the number of washing steps was optimized to three steps with Wash Buffer No. 1 and two steps of washing with Buffer No. 2. Subsequently, the samples were centrifuged at maximum speed for 2 min to eliminate any traces of ethanol.

1.3 Transcriptomics

Sequencing libraries were prepared for each sample (each normalized to 100 ng/µl total RNA) at the sequencing facility "NGS-Services for Integrative Genomics" at the University of Göttingen in Germany. According to their standard workflow, Poly(A)+ RNA was purified, fragmented, and transcribed into cDNA for library preparation using the TruSeqRNA Library Prep Kit (v2) (Illumina, UK) following the manufacturer's instructions. Libraries were validated using a Fragment Analyzer system (Agilent, Santa Clara, USA) before sequencing. Sample libraries were sequenced on an Illumina HiSeq 4000 system in 50 bp single read mode with approximately 30 million raw reads per sample.
Sequence images were transformed to BCL files with Illumina BaseCaller software and demultiplexed to fastq files via bcl2fastq (v2.17.1.14). Adapter sequences were removed using trimmomatic (v0.39) and sequencing quality of each sample was assessed using FastQC (v0.11.5). Additionally, reads were checked for potential contaminations by FastQ Screen (v0.14.1) using bowtie2 (v2.3.2) against the following organism's reference genomes: Oryzia latipes, Danio rerio, Oncorhynchus mykiss, Daphnia magna, Homo sapiens, Mus musculus, Drosophila melanogaster, Saccharomyces cerevisiae, Eschericia coli. For those organisms possible, pre-built Bowtie2 indices were directly downloaded from Babraham Bioinformatics with the built in function 'fastq_screen --get_genomes', which also included custom build human rRNA database.
Sequence reads were aligned to the Lemna minor reference genome 2019v2 (www.lemna.org) via STAR allowing for 2 mismatches within 50 bases. A respective genome annotation files in

GFF format was obtained from the CoGe database (www.genomevolution.org) under: https://genomevolution.org/coge/LoadGenome.pl?wid=47218 (requires CyVerse account for access). For better downstream analysis compatibility, the GFF annotation file was converted to GTF using the agat_convert_sp_gff2gtf.pl function from the AGAT toolkit [https://github.com/NBISweden/AGAT]. Contig headers in the reference genome fasta were harmonized to the respective annotation file. Final versions of compatible reference genome fasta and matching gtf annotation file used in this study are publicly accessible on Zenodo under the accession 6045874 [https://zenodo.org/record/6045874]. Alignment quality was evaluated via RSeQC, Qualimap and Samtools. Feature mapped reads were counted through featureCounts. A collective quality report summary on sequence reads, alignment and mapped features was generated using MultiQC. Subsequently, gene count library normalization and differential gene expression analysis (DGEA) was conducted as described in the main manuscript.

1.4 Protein extraction and peptide labelling

Protein extraction was fulfilled simultaneously to RNA extraction according to the manufacturer's protocol (*RapidPURE RNA Plant Kit*). In conclusion of the optimized volumina used for RNA extraction, less of the protein containing flow through was contained. Therefore, the solution was split into two equal amounts of about 280 µL and a threefold volume of ice-cold acetone as well as 350 µL of ice-cold ethanol (50%) were added for precipitation. Addition of acetone was followed by 10 min, addition of ethanol by 3 min of centrifugation at 13,400 g and 4°C.

The protein pellet was stored at -20°C until further processing. To this, 900 µL of a lysis buffer (6 M urea, 2 M thiourea, 4% CHAPS in 50 mM TEAB; pH = 8) were added and then incubated for 1 h at 4°C for resolubilization. Samples were then sonicated and centrifuged at 14,000 g for 15 min. In order to change the buffer, 450 µL were transferred to a MWCO filter (Amicon Ultra 3K, 0,5 mL, Merck). To this end, 450 µL of Cleanup Buffer (2 M urea, 0,2% SDS; pH = 8,4) and 100 mM TEAB were added sequentially. According to the manufacturer's recommendation, each concentration step was completed by centrifugation at 14,000 g for 30 min. Protein washing by addition of Cleanup Buffer was performed four times, and 100 mM TEAB was added twice. After that, the remaining sample volume of approximately 35 µL was briefly centrifuged at 1,000 g for one minute into a new tube. Protein quantification followed the manufacturer's instructions using the *Pierce BCA Protein Assay Kit* (REF 23225 – Thermo Scientific, USA). The subsequent workflow for labelling 25 µg of tryptic digested protein samples (1:40; trypsin : protein) with a *TMT-6plex* (Thermo Scientific, USA) was performed as recommended by the manufacturer. The workflow was modified after the protocol described in Ayobahan et al. 2019. Reduction, alkylation and acetone precipitation (overnight) was performed with 100 µL of protein samples normalized to a concentration of 1 µg/µL. Pellets were washed with 500 µL 70% ethanol and dried for 3 minutes before they were resuspended in 100 µL 50 mM TEAB with sonication for 20 s at 35 kHz and digested with 2.5 µg (2.5 µL) trypsin overnight at 37°C. Digested peptides were quantified using *BCA peptide quantification assay* (Thermo Scientific, USA) following the manufacturer's instructions. 25 µg of digested peptides were then subjected to TMT labelling (*TMT 6-plex kit*) with the

respective amount of labels (13.6 µL) as recommend by the manufacturer. The distribution of isobaric labels across the replicates per tested substance is given below:

	TMT-126 or TMT-129	TMT-127 or TMT-130	TMT-128 or TMT-131
Replicate 1	NC	LE	HE
Replicate 2	HE	NC	LE
Replicate 3	LE	HE	NC

After labelling, samples were combined and dried in a SpeedVac drier before being resuspended in 100 µL sample buffer (0.5% FA , 5% ACN in ultra-pure water) via sonication for 60 s at 35 kHz. Combined samples were cleaned from excessive TMT labels via C18 cleanup protocol as described by the manufacturer (Thermo Scientific, USA). After C18 cleanup, excessive ACN was removed by drying samples in a SpeedVac. Lastly, the dry pooled label peptide sample was dissolved in LC-MS buffer (2% ACN, 0.1% FA) by sonication for 60 s at 35 kHz. Peptide concentrations were measured via *BCA peptide quantification assay.* For LC-MS/MS measurement, pooled label peptide sample was adjusted to 500 ng/µL.

1.5 Proteomics

1.5.1 nanoLC-MS/MS analysis

The tryptic peptides were resuspended in 0.1% formic acid (solvent A) and analyzed on a Thermo Fisher Q Exactive mass spectrometer (MS) (Thermo Fisher, Waltham, USA) as described previously in Ayobahan et al2,3. The MS was equipped with a nanoflow ionization source and coupled to a nanoACQUITY UPLC (Waters, Massachusetts, USA). Data dependent acquisition was performed in a positive ion mode with the electrospray voltage set at 1.8 kV. For quantitative measurement, 500 ng of each replicate mixtures were injected onto nanoACQUITY UPLC packed 20 mm x 180 µm diameter C18 Trap Column, heated at 40 °C. Upon trapping, the peptides were eluted onto a nanoACQUITY reversed-phase analytical column (25-cm length, 75-µm i.d.) (Waters, Massachusetts, USA) using a linear gradient from 3-97% (v/v) of 90% (v/v) acetonitrile in 0.1% (v/v) formic acid (solvent B) for 170 minutes with a flow rate of 300 nL/min. The full MS survey scans were acquired at 375-1500 m/z range, using a resolving power of 70,000 at 200 m/z for the MS and 35,000 for MS2 scans. Fragmentation was triggered for the top 10 precursors of charge state ranging from 2+ to 7+ and intensity threshold above 2E4. Dynamic exclusion was set to exclude previous sequenced precursor ions for 30 seconds within a 10-ppm window. The automatic gain control and maximum injection time for MS2 spectra were set at 1E5 and 200 ms, respectively. MS2 scans were acquired in centroid mode. MS calibration was performed using the LTQ Velos ESI Positive Ion Calibration Solution (ThermoFisher, Waltham, USA).

1.5.2 Bioinformatics of proteome data

The resulting MS/MS data were processed using Maxquant search engine (v.2.0.1.0), at a peptide-spectrum match FDR of < 1 %. Tandem mass spectra were matched to a custom protein database with predicted protein sequence from the L. minor reference genome combined with

duckweed related protein sequences (including pro- and eukaryotic organism) obtained from Uniprot (search term “duckweed”). That way, protein sequences of bacteria with known duckweed association were also included in the PSM search database. Further, a common lab contaminant protein list was provided for the PSM search. Precursor mass tolerance of ±20 ppm and the integration of fully tryptic peptides with up to two missed cleavage sites were applied in the database search. Cysteine carbamidomethyl, peptide N-terminus TMT6plex and lysine TMT6plex were set as static modifications, whereas the acetylation of protein N-terminal and the oxidation of methionine were included as variable modifications. Only unique and razor peptides with no importation of missing values were considered. Differentially expressed proteins were identified using the MSstatsTMT R package version 2.2.0 on the basis of three technical replicate measurements of three biological replicates per condition4. The measured intensities of the isotope-labelled peptides were first log2-transformed. Thereafter, a reference channel-based normalization was applied by computing an average signal sum as the pseudo-reference channel, to remove any potential technical variation across runs. Proteins were tested for significant differences in expression to the non-treated control group using MSstatsTMT’s implemented linear-mixed model with a moderated t-statistic. Proteins were considered statistically significantly regulated for BH-corrected p-values (padj) < 0.055 with degrees of freedom (DF) ≥ 6. The mass spectrometry proteomics data have been deposited in the ProteomeXchange Consortium via the PRIDE partner repository6 with the dataset identifiers PXD031680 (atorvastatin) and PXD031679 (bentazon).

1.6 Functional L. minor genome annotation and overrepresentation analysis (ORA)

A complementary approach using BLAST32 and eggNOG33 was applied to annotate genes of the L. minor reference genome (2019v2) with gene ontology (GO) terms and gene descriptors based on protein sequence homology. A general workflow overview is shown in the main manuscript Figure 5. First, a multi fasta file listing all theoretical coding sequence (CDS) per gene was extracted from the reference genome with the corresponding GTF file [Zenodo 6045874] using cufflink’s gffread function, which also supports GTF format. The CDS were then translated into their respective amino acid sequences using transeq from the EMBOSS package.

For the BLAST-based annotation, first a local search database was created. Therefore, the reference proteomes of well annotated reference plant species (Arabidopsis thaliana, Sorghum bicolor, Phaleanopsis equestris, Oryza sativa, Triticum dicoccum, Zea mays) as well as all available protein sequence entries for duckweed species (e.g. Spirodela sp., Landolita sp., Wolffia sp., Lemna sp.) and duckweed-associated prokaryotes were downloaded from from the Uniprot database.34. Translated L. minor CDS sequences were then subjected to a blastp search against this database and each gene was matched with the Uniprot ID of the best hit scored by %-alignment for each reference plant species. The subsequent steps were performed in R. Results were cleaned from non-plant related top hits as well as alignment lengths < 20 amino acids and alignment similarities < 35%. Each L. minor gene ID from these cleaned results was then annotated with the combined set of unique GO terms associated with the matched Uniprot IDs across the plant taxa. GO terms for the filtered Uniprot ID blastp hits were obtained from Uniprot. For the eggNOG-based annotation, translated L. minor sequences were subjected to the eggNOG annotation pipeline with default settings.35 All non-plant related matches were

removed from the eggNOG annotation, before results were merged with filtered blastp search results. Hereby, GO terms from both searches were combined and the resulting gene2GO table (one gene mapped to multiple GO terms) was converted to a GO2gene format (one GO term mapped to multiple genes) using the topGO package function inverseList(). GO2gene table was filtered from deprecated GO terms while annotating the GO ids with GO term descriptions and ontology features (BP, MF or CC) using the clusterProfiler package36 functions go2term() and go2ont(). To allow for easy implementation of the GO term annotation for L. minor in the powerful enrichment analysis tool clusterProfiler, an custom AnnotationDbi organism package was built using the AnnotationForge package function makeOrgPackage(). The org.Lminor.eg.db package is publicly available under Zenodo accession 6045874 (www.zenodo.org).

Overrepresentation analysis (ORA) was conducted in R using clusterProfiler v3.1836 package via the enrichGO() function. ORA for significantly enriched biological process (BP) GO terms was performed for each of the tested substances with their core DEG set (genes both identified as differentially expressed in high and low exposure condition). The total universe background of 15278 genes were the common set of Lemna gene IDs among all count libraries after low gene counts removal. The orgDb parameter was specified as “org.Lminor.eg.db” with keyType=”GID”. p value adjustment method for multiple testing was performed after BH. Terms with p.adjust ≤ 0.05 were considered significantly enriched. To prepare GO terms for measuring semantic similarities among them, the godata() function from the GOSemSim package was used with the above specified OrgDb and keytype. To build significantly enriched network plots via emapplot() for data exploration purposes, semantic similarities between GO terms were computed after “Wang”.

2 Supplemental Results and Figures

2.1 Identification of effect concentrations of atorvastatin and bentazon in L. minor

In addition to the most sensitive endpoint "frond area", analogous data was collected for the number of fronds for both substances (**Figure S1**).

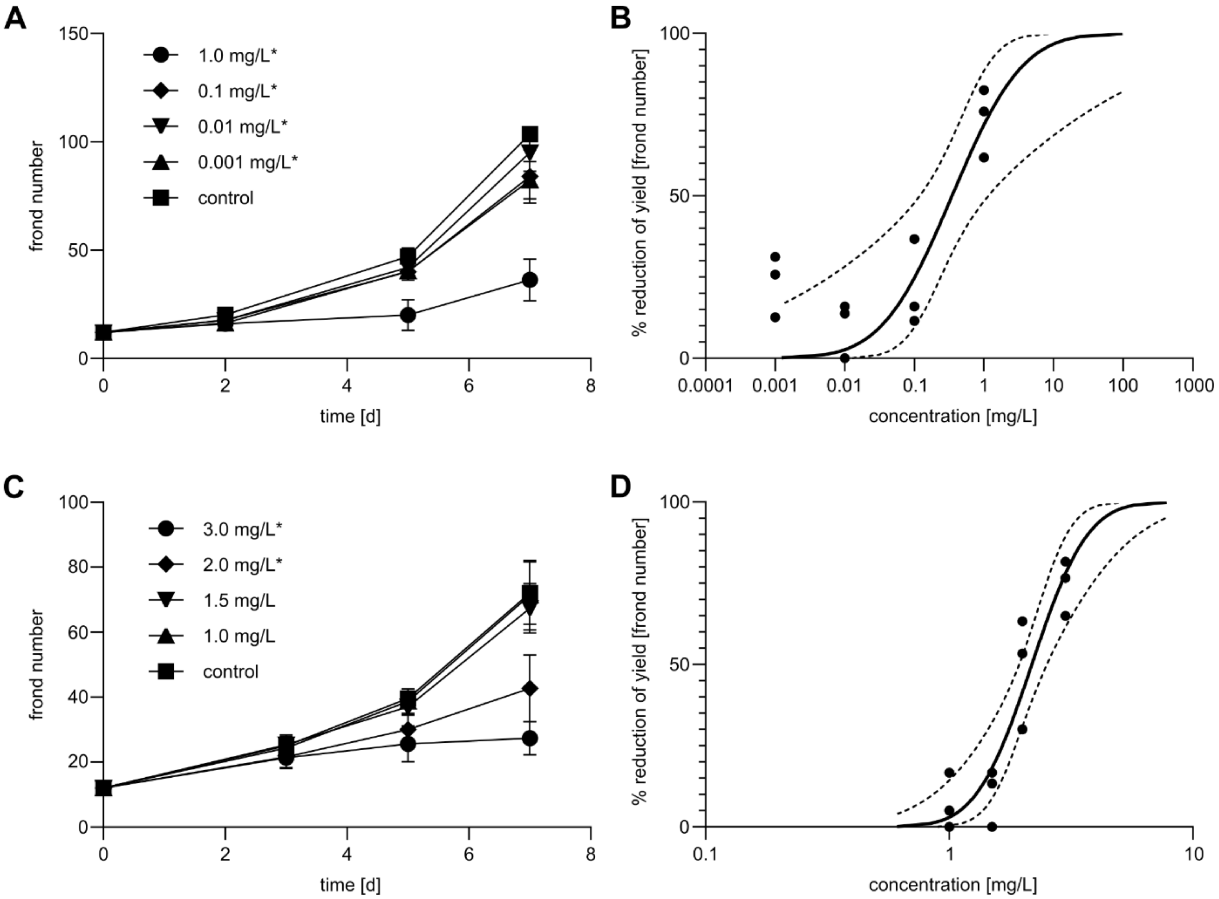

Figure S1. Pretest for detecting low effect concentrations of atorvastatin and bentazon according to OECD TG 221. (A) Time-dependent course of the frond number at different exposure concentrations of atorvastatin. Statistically significant changes compared to the control are indicated by an asterisk (Williams Multiple Sequential t-test). The standard deviation is given as error bar. (B) Concentration-response curve of frond number yield reduction after exposure to atorvastatin on day 7. (C) Time-dependent course of the frond number by different exposure concentrations to bentazon. Statistically significant changes compared to the control are indicated by an asterisk (Williams Multiple Sequential t-test). The standard deviation is given as error bar. (D) Concentration-response curve of frond number yield reduction after exposure to bentazon on day 7.

The corresponding concentration-response curves revealed effect concentrations, listed in **Table 1**. At the beginning and at the end of the test, pH value was measured for all test solutions. The results are shown in Table S2 for both substances. Table S3 contains analogously pH measurements as well as temperature and light conditions of the main tests, which were a shortened version of OECD TG 221.

Table S1. Obtained effect concentrations as mass concentration and molarity for the frond number of L. minor after treatment with atorvastatin and bentazon. [lower 95%-cI – higher 95%-cI]

substance	EC_5	EC_{10}	EC_{20}	EC_{50}
ATV	0.02 mg/L [0.000 – 0.067] 0.018 µM [0.000 – 0.060]	0.03 mg/L [0.000 – 0.104] 0.027 µM [0.000 – 0.093]	0.08 mg/L [0.003 – 0.186] 0.072 µM [0.003 – 0.167]	0.35 mg/L [0.120 – 1.161] 0.314 µM [0.108 – 1.041]
BTZ	1.11 mg/L [0.663 – 1.375] 4.620 µM [2.759 – 5.722]	1.29 mg/L [0.859 – 1.536] 5.369 µM [3.575 – 6.393]	1.54 mg/L [1.169 – 1.768] 6.409 µM [4.865 – 7.358]	2.19 mg/L [1.938 – 2.519] 9.114 µM [8.066 – 10.484]

Table S2. pH measurements of the pre-tests of atorvastatin and bentazon on test start and end.

pH	atorvastatin		bentazon	
	day 0	day 7	day 0	day 7
Control	5.67	6.55±0.07	5.57	6.63±0.06
c_1 (ATV: 0.001 mg/L; BTZ: 1.0 mg/L)	5.69	6.26±0.07	5.58	6.33±0.17
c_2 (ATV: 0.01 mg/L; BTZ: 1.5 mg/L)	5.74	6.36±0.20	5.58	6.28±0.21
c_3 (ATV: 0.1 mg/L; BTZ: 2.0 mg/L)	5.74	6.51±0.02	5.57	6.26±0.14
c_4 (ATV: 1.0 mg/L; BTZ: 3.0 mg/L)	5.75	6.11±0.03	5.57	6.14±0.25

Table S3. Light intensity, temperature and pH conditions of the start and end of the modified Lemna sp. Growth inhibition test with atorvastatin and bentazon.

parameter	atorvastatin		bentazon	
	day 0	day 3	day 0	day 3
light intenisty [µmol·m^{-2}·s^{-1}]	127.1	136.3	129.6	140.1
temperature [°C]	23.9	24.6	24.4	23.6
pH (Control)	5.70	5.83±0.05	5.74	6.03±0.15
pH (EC_5)	5.65	5.81±0.02	5.67	5.85±0.06
pH (EC_{20})	5.59	5.77±0.02	5.09	5.42±0.09

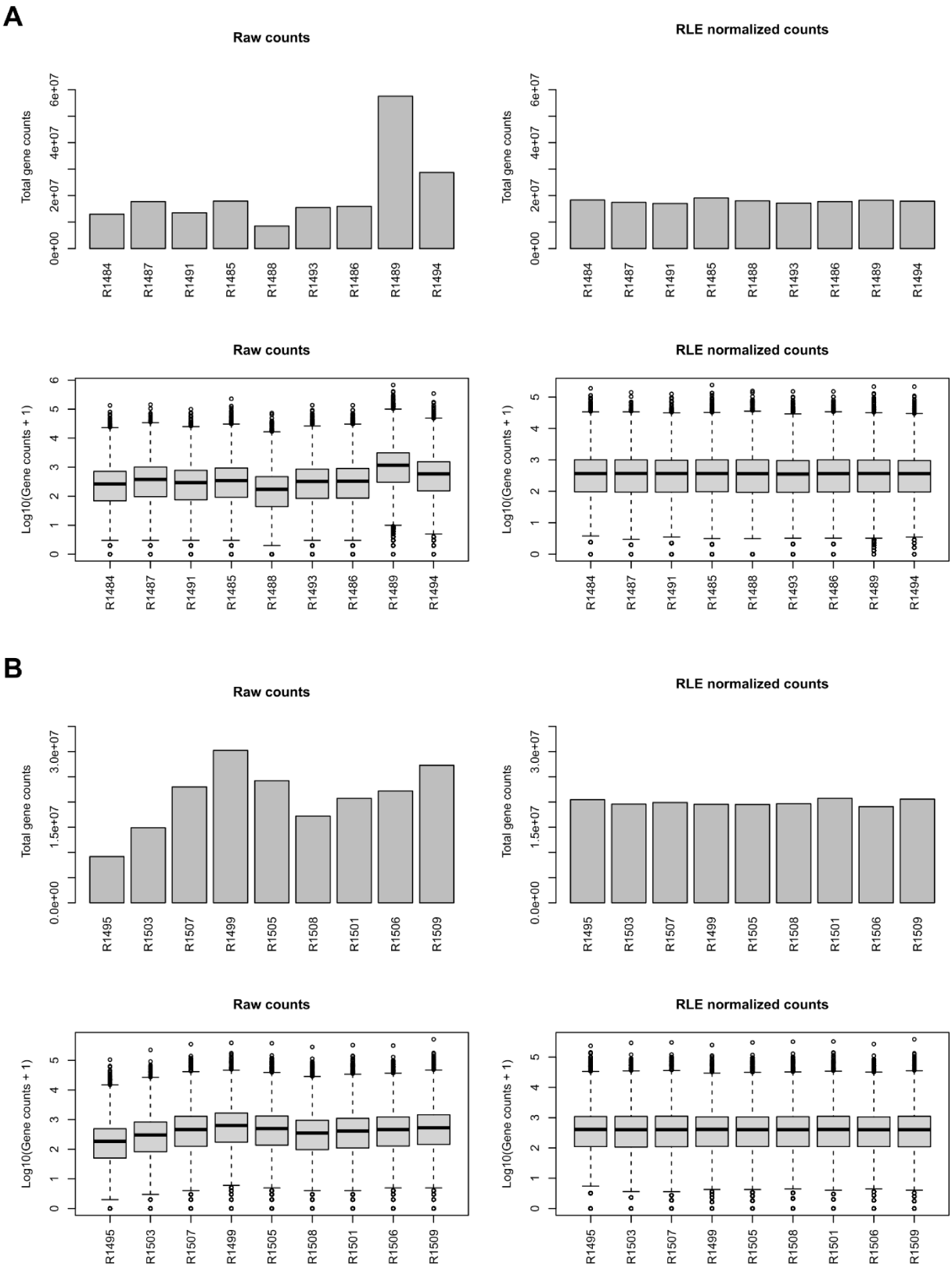

Figure S2. RNA-Seq read count normalization using DESeq2. (A) Raw and relative log expression (RLE) normalized read counts of atorvastatin treated samples (EC_5 and EC_{20}) and control samples. (B) Raw and relative log expression (RLE) normalized read counts of bentazon treated samples (EC_5 and EC_{20}) and control samples.

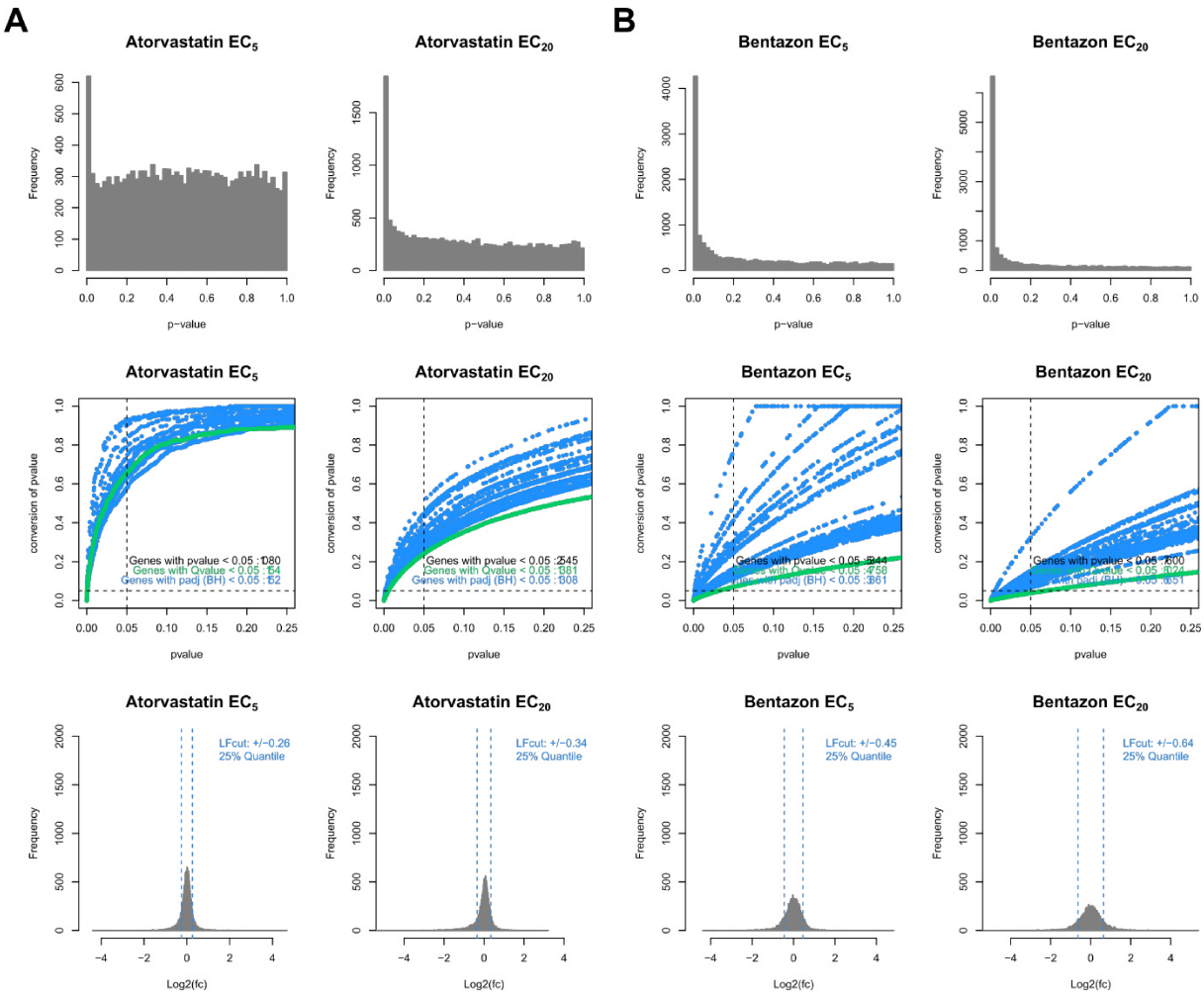

Figure S3. Distributions of p-values, p-value conversion and lfc distributions after exposure to atorvastatin and bentazon compared to the control as observed by gene expression data. (A) Top: Distribution of p-values of all genes after exposure to EC_5 (left) and EC_{20} (right) of atorvastatin. Centre: Conversion of p-values for all genes after exposure to EC_5 (left) and EC_{20} (right) of atorvastatin. Bottom: Distribution of lfc values of all genes after exposure to EC_5 (left) and EC_{20} (right) of atorvastatin. The lfc cut-off is indicated as dotted line. (B) Top: Distribution of p-values of all genes after exposure to EC_5 (left) and EC_{20} (right) of bentazon. Centre: Conversion of p-values for all genes after exposure to EC_5 (left) and EC_{20} (right) of bentazon. Bottom: Distribution of lfc values of all genes after exposure to EC_5 (left) and EC_{20} (right) of bentazon. The lfc cut-off is indicated as dotted line.

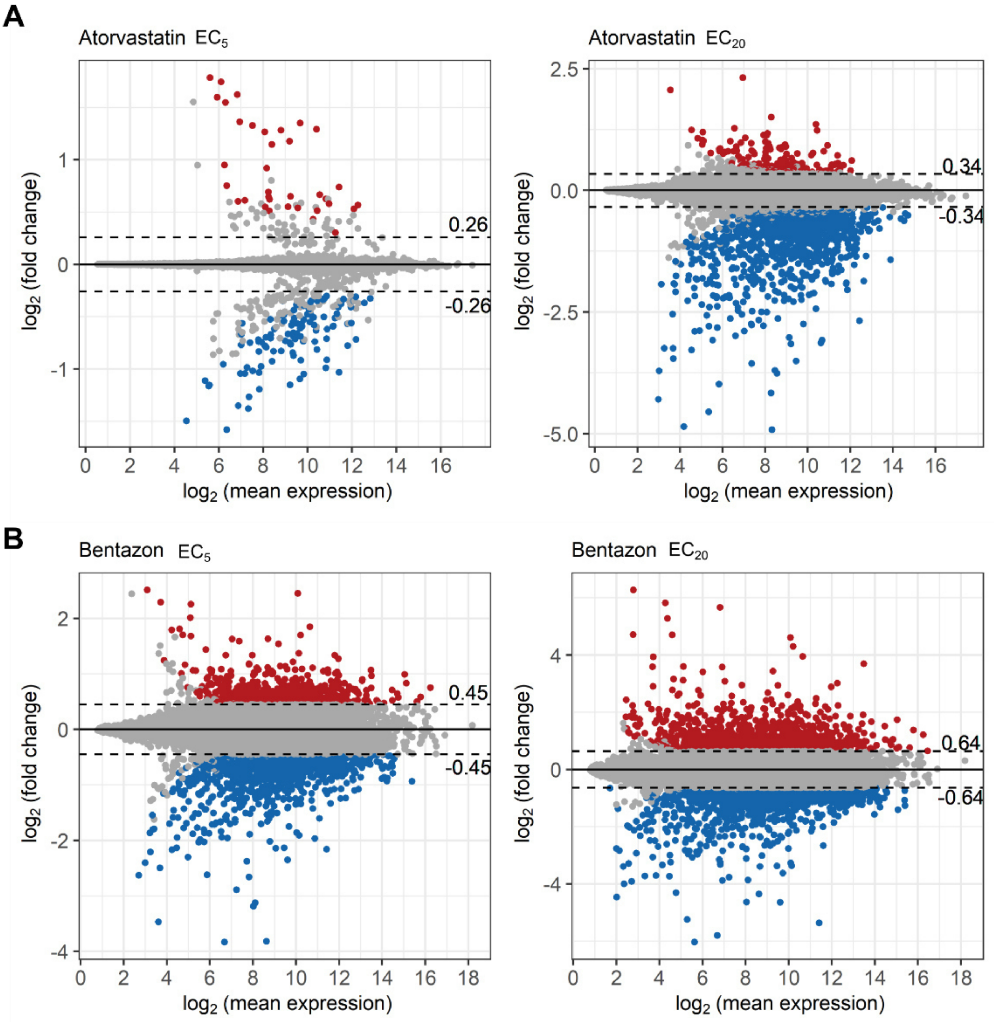

Figure S4. MA-plot illustration of the apeglm-shrunk lfc values for the genes of both conditions (EC_5 and EC_{20}) of atorvastatin (A) and bentazon (B) treatments.

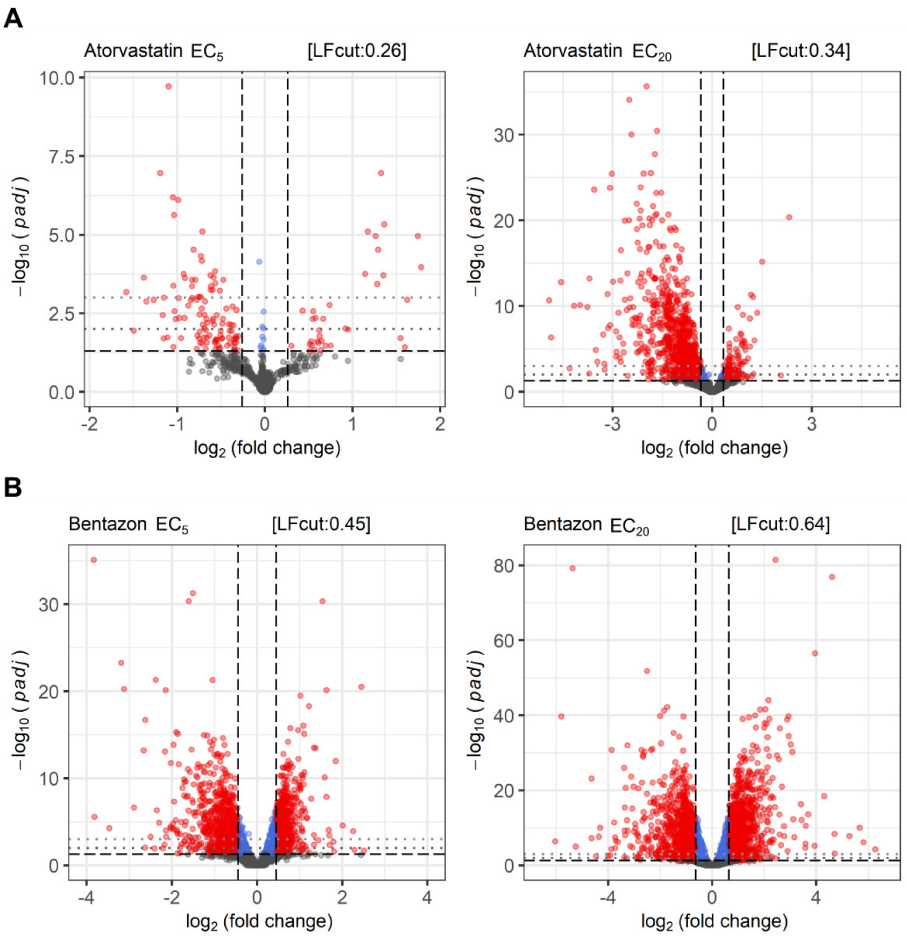

Figure S5. Vulcano plot illustration of the lfc values against the corresponding $-\log_{10}(p_{adj})$ values of genes that were differentially expressed after exposure of the EC_5 (left) and EC_{20} (right) of atorvastatin (A) and bentazon (B). The lfc value cut-off as well as the p_{adj} cut-off are indicated as dotted lines. Genes applying to both of them are coloured red.

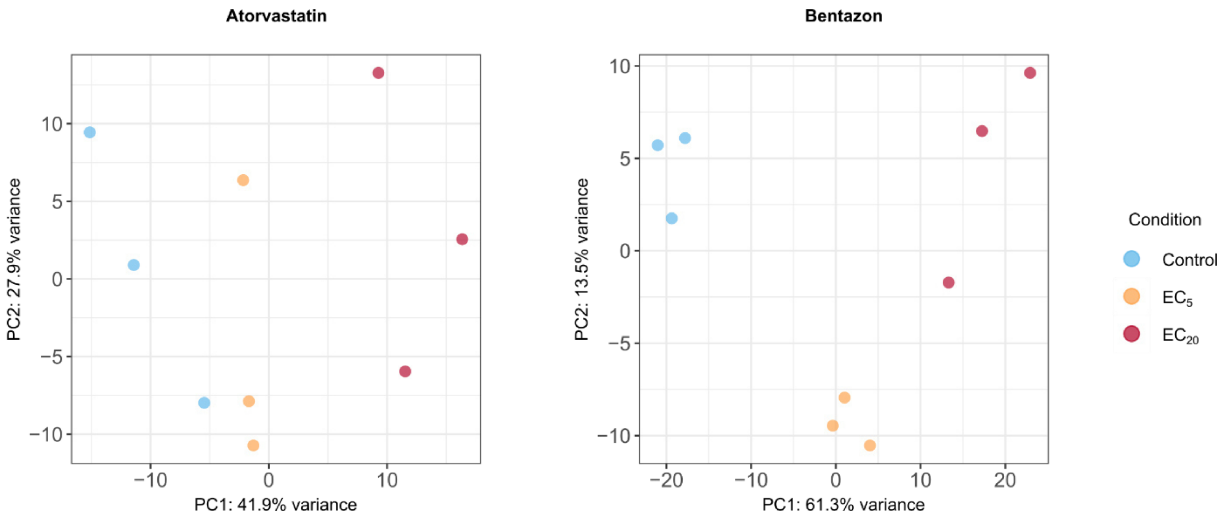

Figure S6. Principle component analysis (PCA) of control replicates and samples after treatment with EC_5 and EC_{20} of atorvastatin (left) and bentazon (right). Biological replicates are indicated as colour code.

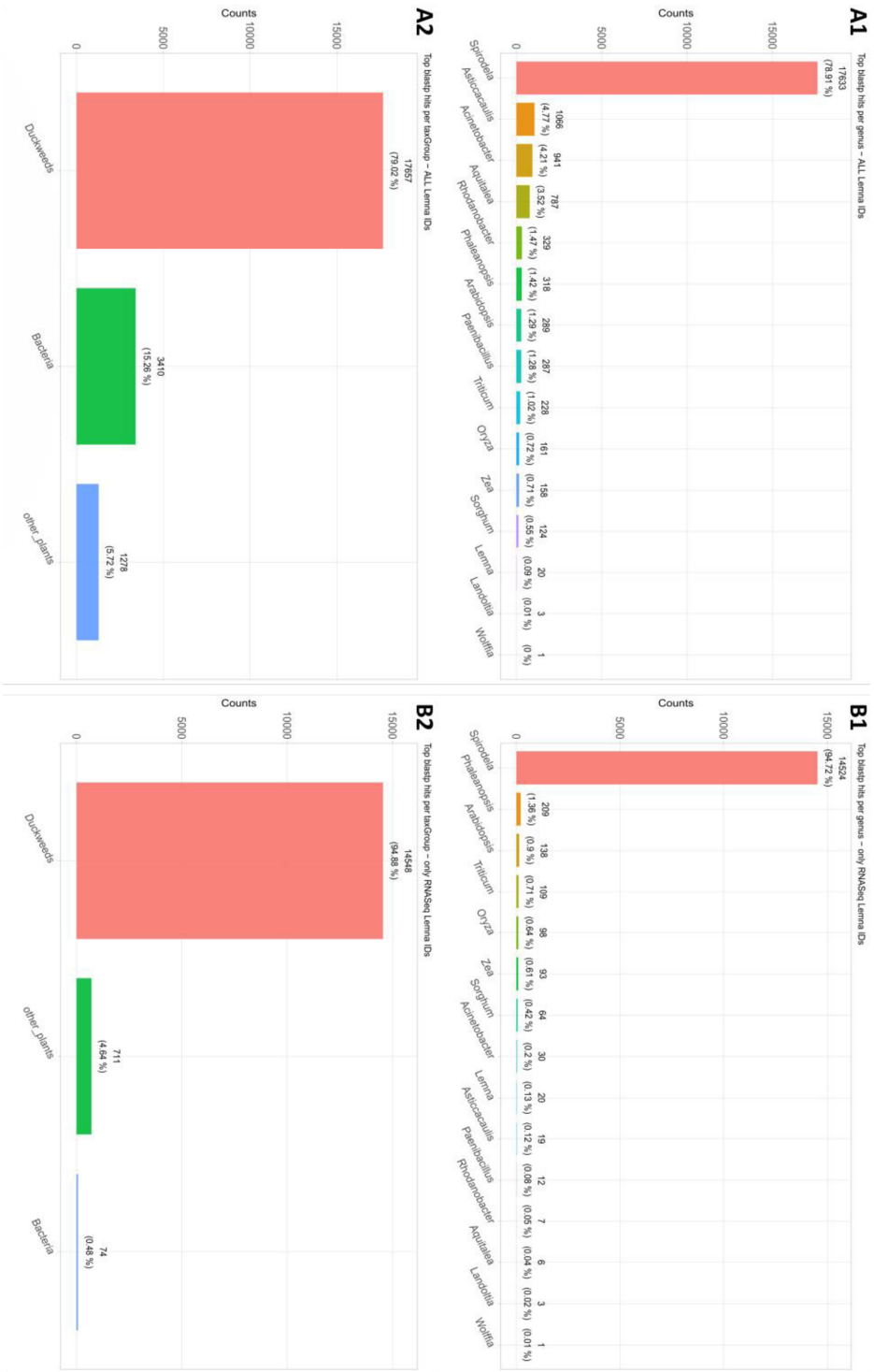

Figure S7: Total blastp top hit search results (1) per genus and (2) general taxa groups of "duckweeds", "other plants" and "bacteria". (A) panels show the top search result hits distribution across all 22345 Lemna minor gene IDs from the reference genome. (B) panels show the distribution only for 15333 Lemna minor gene IDs present in the RNA-Seq gene count libraries after removal of zero gene counts. Hence, B2 indicates how many of the gene IDs observed in our transcriptomic dataset match with a respective taxa group. We see that in the mRNA Seq data, 99.52% of gene IDs match with duckweed related taxa (94.88%) or other plants (4.64%). Only 0.48% in this set have a top hit with a bacteria related protein sequence. In contrast, in B1 of all matching IDs from the reference genome, a total of 15.26% has a top hit with bacteria related proteins. This suggests that the Leman minor reference genome still contains a relatively large fraction of contaminating bacterial sequences. This might derive from the fact that Lemna sp. lives in close relationship with prokaryotes such as Asticcacaulis sp., Acinetobacter sp., Aquitalea sp. or Rhodanobacter sp. The largest portion of top hits can be seen for Spirodela sp. This is not surprising, as Spirodela intermedia has by far the largest number of entries among all duckweeds in the Uniprot database. Unfortunately, the vast majority of these entries is not functionally annotated to any GO terms. Therefore we need to relay on functional annotations from 2nd best hits in a better studied reference plant species.

3 Supplemental References

(1) European Commission. Guidance Document on Pesticide Analytical Methods for Risk Assessment and Post-Approval Control and Monitoring Purposes. *Sante/2020/12830* **2021**, *Rev. 1*.

(2) Ayobahan, S. U.; Eilebrecht, E.; Kotthoff, M.; Baumann, L.; Eilebrecht, S.; Teigeler, M.; Hollert, H.; Kalkhof, S.; Schäfers, C. A Combined FSTRA-Shotgun Proteomics Approach to Identify Molecular Changes in Zebrafish upon Chemical Exposure. *Sci. Rep.* **2019**, *9* (1), 1–12. https://doi.org/10.1038/s41598-019-43089-7.

(3) Ayobahan, S. U.; Eilebrecht, S.; Baumann, L.; Teigeler, M.; Hollert, H.; Kalkhof, S.; Eilebrecht, E.; Schäfers, C. Detection of Biomarkers to Differentiate Endocrine Disruption from Hepatotoxicity in Zebrafish (Danio Rerio) Using Proteomics. *Chemosphere* **2020**, *240*, 1–12. https://doi.org/10.1016/j.chemosphere.2019.124970.

(4) Huang, T.; Choi, M.; Tzouros, M.; Golling, S.; Pandya, N. J.; Banfai, B.; Dunkley, T.; Vitek, O. MSstatsTMT: Statistical Detection of Differentially Abundant Proteins in Experiments with Isobaric Labeling and Multiple Mixtures. *Mol. Cell. Proteomics* **2020**, *19* (10), 1706–1723. https://doi.org/10.1074/mcp.RA120.002105.

(5) Diz, A. P.; Carvajal-Rodríguez, A.; Skibinski, D. O. F. Multiple Hypothesis Testing in Proteomics: A Strategy for Experimental Work. *Mol. Cell. Proteomics* **2011**, *10* (3), 1–10. https://doi.org/10.1074/mcp.M110.004374.

(6) Perez-Riverol, Y.; Csordas, A.; Bai, J.; Bernal-Llinares, M.; Hewapathirana, S.; Kundu, D. J.; Inuganti, A.; Griss, J.; Mayer, G.; Eisenacher, M.; Pérez, E.; Uszkoreit, J.; Pfeuffer, J.; Sachsenberg, T.; Yilmaz, Ş.; Tiwary, S.; Cox, J.; Audain, E.; Walzer, M.; Jarnuczak, A. F.; Ternent, T.; Brazma, A.; Vizcaíno, J. A. The PRIDE Database and Related Tools and Resources in 2019: Improving Support for Quantification Data. *Nucleic Acids Res.* **2019**, *47* (D1), D442–D450. https://doi.org/10.1093/nar/gky1106.